This publication is available free of charge from: https://doi.org/10.6028/NIST.IR.8271

NISTIR 8271 DRAFT SUPPLEMENT

Face Recognition Vendor Test (FRVT)

Part 2: Identification

Patrick Grother
Mei Ngan
Kayee Hanaoka
Information Access Division
Information Technology Laboratory

This document is a draft supplement of NIST Interagency Report 8271

2021/11/22

National Institute of Standards and Technology
U.S. Department of Commerce

This publication is available free of charge from: https://doi.org/10.6028/NIST.IR.8271

NISTIR 8271 DRAFT SUPPLEMENT

Face Recognition Vendor Test (FRVT)

Part 2: Identification

Patrick Grother
Mei Ngan
Kayee Hanaoka
Information Access Division
Information Technology Laboratory

This document is a draft supplement of NIST Interagency Report 8271

October 2021

U.S. Department of Commerce
Gina M. Raimondo, Secretary

National Institute of Standards and Technology
James K. Olthoff, Performing the Non-Exclusive Functions and Duties of the Under Secretary of Commerce for Standards and Technology & Director, National Institute of Standards and Technology

RELEASE NOTES

2021-11-22: The 1:N track of the FRVT remains open.

- This document is the twelfth draft update to NIST Interagency Report 8271. It includes results for algorithms recently submitted by three first-time participants Clearview AI, Griaule, and Mantra Softech India.
- This document and the 1:N results page also include results for algorithms from six returning developers: Acer Incorporated, Canon, Dermalog, Samsung S1, VisionLabs, and Veridas Digital Authentication.

2021-10-28: The 1:N track of the FRVT remains open.

- This document is the eleventh draft update to NIST Interagency Report 8271. It includes results for algorithms recently submitted by three first-time participants (20Face, Fujitsu Research and Development Center, and Vision-Box), and five returning participants (Alchera, Gorilla Technology, Tevian, Thales-Cogent, and Visidon). Visidon
- Both the main 1:N results page and the small-gallery paperless travel page have been updated.

2021-09-21: The 1:N track of the FRVT remains open. Three news items:

- This document is the tenth draft update to NIST Interagency Report 8271. It includes results for algorithms recently submitted by six first-time developers: Cubox, Fincore, HyperVerge, Qnap Security, Staqu Technologies, and Tripleize (Aize, 3-ize).
- It includes results also for four returning developers: Cognitec Systems, Incode Technologies, Innovatrics, Neurotechnology, and Rank One Computing.

2021-08-02: The 1:N track of the FRVT remains open. Three news items:

- This document is the nineth draft update to NIST Interagency Report 8271. It includes results for algorithms recently submitted by eight participants: Cyberlink Corp, NEC Corp, N-Tech Lab, Realnetworks Inc., Sensetime Group, Veridas Digital, Viettel Group, and Vigilant Solutions.
- Algorithms submitted since July 24 will be included in the next update scheduled for September 9, 2021.
- A new report, NIST Interagency Report 8381 - FRVT Part 7: Identification for Paperless Travel and Immigration, has been released [PDF, webpage]. It documents the use of FRVT 1:N algorithms in positive access control and immigration status update travel applications where the enrolled population size is as low as 420 people for aircraft boarding, and $42\,000$ for an airport security line. These population sizes are much smaller than those used in the main 1:N evaluation. Going forward, we will update the report and webpage with results for new algorithms.

2021-07-07: The 1:N track of the FRVT remains open. One update:

- This document is the eighth draft update to NIST Interagency Report 8271. It include results for an algorithm from one participant: Kakao Enterprises.

2021-06-22: The 1:N track of the FRVT remains open. Three updates:

- This is the seventh draft of the update to NIST Interagency Report 8271. It includes results for algorithms from three new participants: Line Corporation, Rendip, and Samsung S1 Corp.
- We have also added results for algorithms from five returning developers: Imagus Technology, Kneron, Tevian, Visidon, and Xforward AI Technology.

This publication is available free of charge from: https://doi.org/10.6028/NIST.IR.8271

- ▷ The algorithm-specific report cards (examples: 1, 2, and 3) now include figures showing how low threshold values can be used to reduce candidate list lengths for human review, while (usually) elevating miss rates (FNIR) only modestly. The reports also feature some minor additions and clarifications.

2021-03-26: The 1:N track of the FRVT remains open. Three updates:

- ▷ This is the sixth draft of the update to NIST Interagency Report 8271. It includes results for algorithms from three returning developers: Neurotechnology, Guangzhou Pixel Solutions, and Tech5 SA.
- ▷ We have added results on the webpage and in the report for a new ageing dataset in which border crossing photos are searched against a gallery of border crossing photos collected between 10 and 15 years prior to the mated search photos. See section 2 for a description of the images. Table 1 has a new entry describing the experiment.
- ▷ We will mostly discontinue running the mugshot ageing test, reserving it for algorithms that show high accuracy on the new border-crossing set.

2021-03-26: Regarding the fifth draft of the update to NIST Interagency Report 8271:

- ▷ In addition have added results for first algorithms from two new participants: Viettel Group and Veridas Digital Authentication Solutions.
- ▷ We have added results for algorithms from two returning developers: Idemia and Cognitec Systems.
- ▷ In addition to the report, the results page and its hyperlinked report cards have been updated.

2021-02-08: Regarding the fourth draft of the update to NIST Interagency Report 8271:

- ▷ We have added results for eight algorithms submitted by eight developers: Cyberlink, Dermalog, Imagus, Paravision, Sensetime, Trueface, Vigilant Solutions, and X-Forward AI. With the exception of Trueface, all of these developers have participated previously.
- ▷ We anticipate updating this report again in the first week of March 2021.
- ▷ The main results page has been revised with tabs for the investigative and lights-out identification tables, and a new tab dedicated to speed and resource consumption.
- ▷ The report cards (example here) hyperlinked from the results page have been revised to improve content and format.

2020-12-14: Regarding third draft of the update to NIST Interagency Report 8271:

- ▷ We have added results for fifteen algorithms submitted by thirteen developers. The four first-time participants are: Acer, Akurat Satu Indonesia, Canon, and Xforward AI Technology. The ten returning developers are: AllGoVision, Cyberlink Corp, Dahua Technology, Deepglint, Guangzhou Pixel Solutions, IIT Vision, Innovatrics, Rank One Computing, Scanovate, Sensetime Group, Synesis, and VisionLabs.
- ▷ We have added two new datasets to the evaluation: First a set of "visa-border" photos, representing search of an airport immigration lane photo against a database of closely ISO standard portraits; second a "visa-kiosk" set representing search of a photo collected in a registered traveller kiosk against the same ISO portrait gallery. The images are described in section 2.1.
- ▷ As in previous reports, we include results for searching mugshots against a mugshot gallery containing a single image of each of 12 million people. However we have suspending running searches against a gallery in which multiple lifetime photos per person are present, because this is computationally expensive. We retain a N = 3 million search test dedicated to ageing in which mugshots taken up to 18 years after the first photograph are searched - see Table 6.
- ▷ Tables containing computational resource information, Table 2. . ., now include duration of the finalization step, in which search algorithms can, at their option, build fast-search data structures.

This publication is available free of charge from: https://doi.org/10.6028/NIST.IR.8271

- ▷ We have linked revised per-algorithm PDF report cards from the main results page.
- ▷ We have regenerated all figures and tables to drop algorithms submitted before June 2018. Results for prior algorithms appear in archived editions of this report.
- ▷ Going forward, we anticipate producing more frequent updates to this report. Developers may submit one algorithm to this evaluation every four calendar months.

2020-03-24: Regarding the second draft of the update to NIST Interagency Report 8271:

- ▷ Adds results for three algorithms from three developers, Dermalog, Innovatrics, and Synesis.
- ▷ Adds Table 6 on ageing showing the increase in false negative rates with time elapsed between two photos. Some of the results were contained in graphs in prior editions of this report, but the table adds results for some newly submitted algorithms.
- ▷ Adjusts frontal mugshot results (for recent and lifetime consolidated galleries) to include the effect of removing some images that should not have been included in image test sets. These images were mostly profile views, images of tattoos containing faces, images of faces on tee shirts, and images of photographs on walls behind the intended subject. This affects many tables and reduces false negative identification rates for all algorithms. The reduction is larger for "recent" enrollments than for "lifetime consolidated" ones with the consequence that accuracy on recent images is now superior.

2020-02-26: Regarding the first draft of the update to NIST Interagency Report 8271:

- ▷ Adds results for 38 algorithms from 31 different developers, eleven of whom are entirely new to the 1:N track of FRVT. These are Allgovision, Cyberlink, Deepsea Tencent, Farbar F8, Imperial College London, Intsys MSU, Kedacom, Kneron, Pixelall, and Scanovate.

This publication is available free of charge from: https://doi.org/10.6028/NIST.IR.8271

DISCLAIMER

Specific hardware and software products identified in this report were used in order to perform the evaluations described in this document. In no case does identification of any commercial product, trade name, or vendor, imply recommendation or endorsement by the National Institute of Standards and Technology, nor does it imply that the products and equipment identified are necessarily the best available for the purpose.

This publication is available free of charge from: https://doi.org/10.6028/NIST.IR.8271

INSTITUTIONAL REVIEW BOARD

The National Institute of Standards and Technology's Research Protections Office reviewed the protocol for this project and determined it is not human subjects research as defined in Department of Commerce Regulations, 15 CFR 27, also known as the Common Rule for the Protection of Human Subjects (45 CFR 46, Subpart A).

ACKNOWLEDGMENTS

The authors are grateful for the support and collaboration of the the Department of Homeland Security's Science & Technology Directorate (S&T), Office of Biometric Identity Management (OBIM), and Customs and Border Protection (CBP).

Additionally, the authors are grateful to staff in the NIST Biometrics Research Laboratory for infrastructure supporting rapid evaluation of algorithms.

Executive Summary

This document is a draft revision of the September 2019 report NIST Interagency Report 8271. That report gave extensive documentation of face recognition applied to mugshots. This report extends that by adding more two more challenging datasets containing images with serious departures from canonical frontal image standards. The report also adds results for algorithms submitted to NIST since in 2019 and 2020. The algorithms, which implement one-to-many identification of faces appearing in two-dimensional images, are prototypes from the research and development laboratories of mostly commercial suppliers, and are submitted to NIST as compiled black-box libraries implementing a NIST-specified C++ test interface. The report therefore does not describe how algorithms operate. The report lists accuracy results alongside developer names and will therefore be useful for comparison of face recognition algorithms and assessment of absolute capability. The report is accompanied by a webpage with sortable results.

The evaluation uses six datasets: frontal mugshots, profile view mugshots, desktop webcam photos, visa-like immigration application photos, immigration lane photos, and registered traveler kiosk photos. These datasets are sequestered at NIST, meaning that developers do not have access to them for training or testing. This aspect is important because face recognition algorithms are very often deployed without the developer having access to the customers image data. A possible exception to this would be in a cloud-based application where the operational image data is uploaded to a cloud operated by a face recognition developer.

The major result in NIST IR 8271 was that massive gains in accuracy have been achieved in the years 2013 to 2018 and these far exceed improvements made in the prior period, 2010 to 2013. While the industry gains were broad - at least 30 developers' algorithms outperformed the most accurate algorithm from late 2013, there remains a wide range of capability. While this report shows accuracy gains only over the period 2018-2020, the most accurate algorithm reported here is substantially more accurate than anything reported in NIST IR 8271. This is evidence that face recognition development continues apace, and that FRVT reports are but a snapshot of contemporary capability.

From discussion with developers, the accuracy gains stem from the adoption of deep convolutional neural networks. As such, face recognition has undergone an industrial revolution, with algorithms increasingly tolerant of poorly illuminated and other low quality images, and poorly posed subjects. One related result is that a few algorithms correctly match side-view photographs to galleries of frontal photos, with search accuracy approaching that of the best c. 2010 algorithms operating on purely frontal images. The capability to recognize under a 90-degree change in viewpoint - pose invariance - has been a long-sought milestone in face recognition research.

With good quality portrait photos, the most accurate algorithms will find matching entries, when present, in galleries containing 12 million individuals, with rank one miss rates of approaching 0.1%. The remaining errors are in large part attributable to long-run ageing, facial injury and poor image quality. Given this impressive achievement - close to perfect recognition - an advocate might claim that cooperative face recognition is a solved problem, a statement that can be refuted with the following context and caveats:

- **Mugshots vs. less constrained captures:** The low error rates reported here are attained using mostly excellent cooperative live-capture mugshot images collected with an attendant present. Recognition in other circumstances, particularly those without a dedicated photographic environment and human or automated quality control checks, will lead to declines in accuracy. This is documented here for side-view images, poorer quality webcam images, and, particularly, for newly introduced ATM-style kiosk photos that were not originally intended for automated face recognition. In this case, recognition error rates are much higher, often in excess of 20% even with the more accurate algorithms which variously remain intolerant of face cropping (at image edge) and of large downward head pitch.

- **Algorithm accuracy spectrum:** Recognition accuracy is very strongly dependent on the algorithm and, more

This publication is available free of charge from: https://doi.org/10.6028/NIST.IR.8271

This publication is available free of charge from: https://doi.org/10.6028/NIST.IR.8271

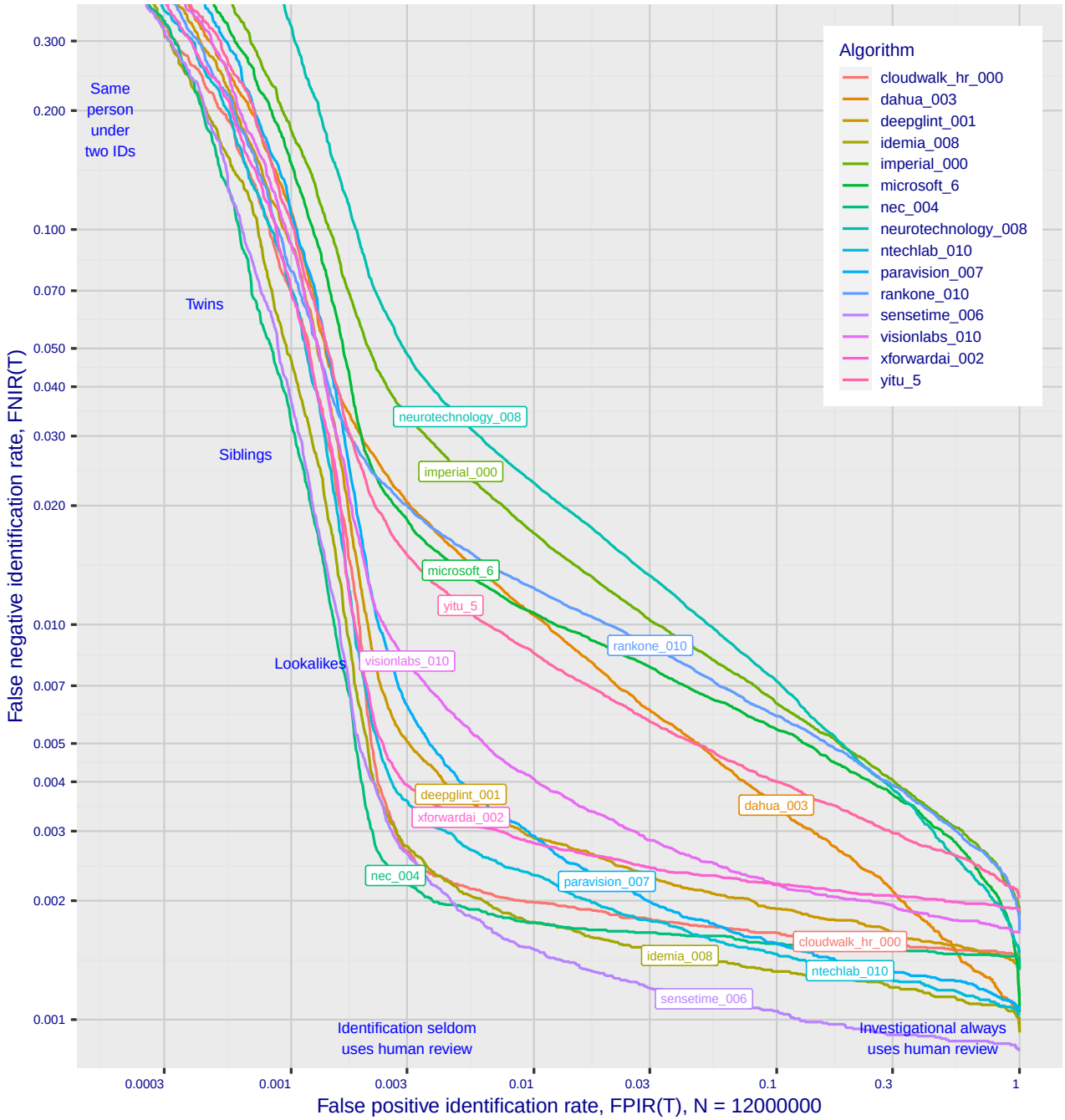

Figure 1: Identification miss rates across the false positive range. N = 12 million individuals are enrolled with one recent image.

generally, on the developer of the algorithm. False negative error rates in a particular scenario range from a few tenths of one percent to beyond fifty percent. This is tabulated exhaustively later: For example Table 9 shows accuracy across datasets. Figure 1 here compares algorithms on mugshot searches in a consolidated gallery of 12 million subjects and 12 million photos. Many algorithms do not achieve the low error rates noted above, and while many of those may still be useful and valuable to end-users, only the most accurate excel on poor quality images and those collected long after the initial enrollment sample.

▷ **Versioning:** While results for up to ten algorithms from each developer are reported here, the intra-provider

accuracy variations are usually smaller than the inter-provider variations. That said different versions give an order of magnitude fewer misses. Some developers demonstrate speed-accuracy tradeoffs[1]. See Figs. 18, 19.

- **Low similarity scores:** In thousands of mugshot cases the correct gallery image is returned at rank 1 but its similarity score is nevertheless low, below some operationally required score threshold. This is not so important when face recognition is used for "lead generation" in investigational applications because human reviewers are specifically required to review potentially long candidate lists and the threshold is effectively 0. In applications where search volumes are higher and labor is not available to review the results from searches, a higher threshold must be applied. This reduces the length of candidate lists and false positive identification rates at the expense of increased false negative miss rates. The tradeoff between the two error rates is reported extensively later.

- **Population size:** As the number of enrolled subjects grows, some mates are displaced from rank one, decreasing accuracy. As tabulated later for N up to 12 million, false negative rates generally rise slowly with population size. This enables use of face recognition in very large populations. However in most positive and negative identification applications[2], a score threshold is set to limit the rate at which non-mate searches produce false positives. This has the consequence that some mated searches will report the mate below threshold, i.e. a miss, even if it is at rank 1. The utility of this is that many non-mated searches will return no candidate identities at all. As the error-tradeoff characteristic shows, investigational miss rates on the right side are very low but then rise steadily (in the center region) as threshold is increased to support "lights-out" applications, and ultimately rise quickly (left side) as discussed below. Thus, if we demand that just one in one thousand non-mate searches produce any false positives, the most accurate algorithms there (Sensetime-004 and NEC-3) would fail on between 3 and 5% of mated searches. Even though the graph shows results for the most accurate algorithms, all but two would fail to find the mate in more than 8% of mated searches. While the two most accurate algorithms produce a relatively flat error tradeoff until the threshold is raised to limit false positives to about 1 in 400 non-mated searches[3]

  Thereafter, as the threshold is raised to further reduce false positives, miss rates rise rapidly. This means that low false positive identification rates are inaccesible with these algorithms, a result that does not apply for ten-finger identification algorithms. The rapid rise occurs because the lower mate scores are mixed with very high non-mate scores, the low scores from poor image quality and ageing, the high non-mates from the presence of lookalikes persons (doppelgangers), twins (discussed next) and, ultimately, the presence of a few unconsolidated subjects i.e. persons present under multiple IDs.

- **False negatives from ageing:** A large source of error in long-run applications where subjects are not re-enrolled on a set schedule is ageing. Changes in facial appearance increase with the time elapsed between photographs. These will depress similarity scores and eventually cause false negatives. All faces age and while this usually proceeds in a graceful and progressive manner, drug use can accelerate this [28]. Elective surgery may be effective in delaying it although this has not been formally quantified with face recognition. As ageing is essentially unavoidable, it can only be mitigated by scheduled re-capture, as in passport re-issuance. To quantify ageing effects, we used the more accurate algorithms to enroll the earliest image of 3.1 million adults and then search

[1] For example, NEC-0 prepares templates much faster than NEC-2 but gives twenty times more misses. Dermalog-5 executes a template search much more quickly than Dermalog-6 but is also much less accurate.

[2] In a positive identification application such as a registered traveler system, a user is making an implicit claim to be enrolled in the system - most users will be. In a negative application, such as with deportees, the implicit claim is that the subejct is not enrolled - most will not be.

[3] The gallery size here is 12 million people, one image per person. Given 331 201 non-mated searches, an exhaustive implementation of one-too-many search would execute almost 4 trillion comparisons. At a false positive identification rate of 0.0025 the number of false positives is, to first order, 828 corresponding to single-comparison false match rate of 828 / 4 trillion = 2.1 10^{-10} i.e. about 1 in 5 billion. Strictly this FMR computation is meaningful only for algorithms that implement 1:N search using N 1:1 comparisons, which is not always the case.

This publication is available free of charge from: https://doi.org/10.6028/NIST.IR.8271

with 10.3 million newer photos taken up to 18 years after the the initial enrollment photo. Figure 2 puts ageing into context by contrasting it with the increase in false negatives that occurs when the number of individuals in an enrollment database becomes larger and the chance of a false positive increases such that higher thresholds may become necessary[4].

The Figure shows, from to bottom, increases in false negative identification rates (FNIR) with the algorithm being tested. This applies to increases due to N on the left side, and increases due to ageing on the right side. The relative spacing of the dots shows that for all algorithms the dependency of FNIR on N (up to 12 million) is considerably less than on ΔT (up to 18 years).

In the inset table, accuracy is seen to degrade progressively with time, as mate scores decline and non-mates displace mates from rank 1 position. More accurate algorithms tend to be less sensitive to ageing. The more accurate algorithms give fewer errors after 18 years of ageing than middle tier algorithms give after four. Note also we do not quantify an ageing rate - more formal methods [2] borrowed from the longitudinal analysis literature have been published for doing so (given suitable repeated measures data). See Figures 60, 81 and 91.

This publication is available free of charge from: https://doi.org/10.6028/NIST.IR.8271

[4]Some algorithms implement stragegies to automatically adjust scores to account for increased population size. This relieves the system owner of having to increase thresholds as N increases.

This publication is available free of charge from: https://doi.org/10.6028/NIST.IR.8271

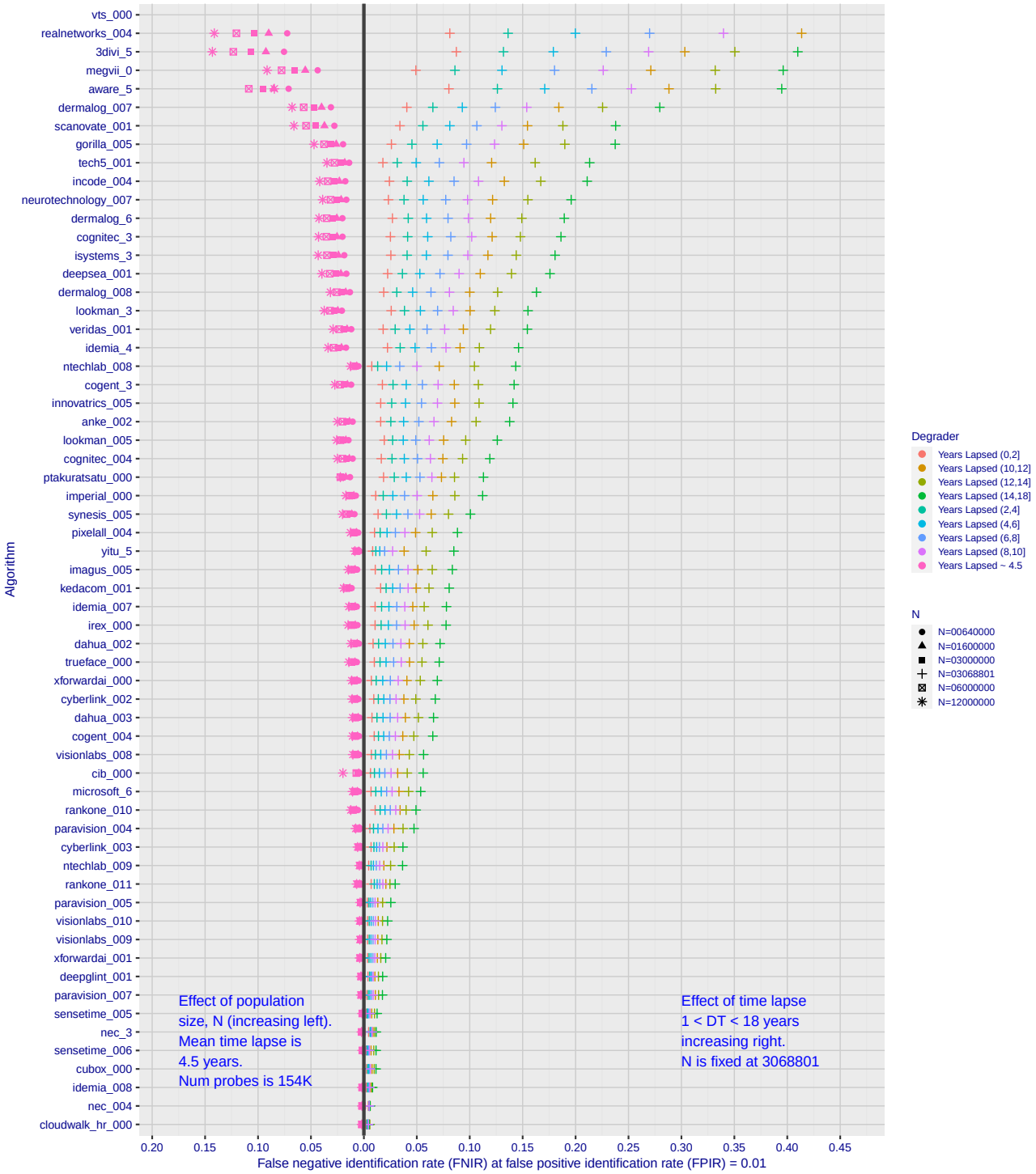

Figure 2: Identification miss rates as a function of enrolled population size, N, and time-lapse, ΔT.

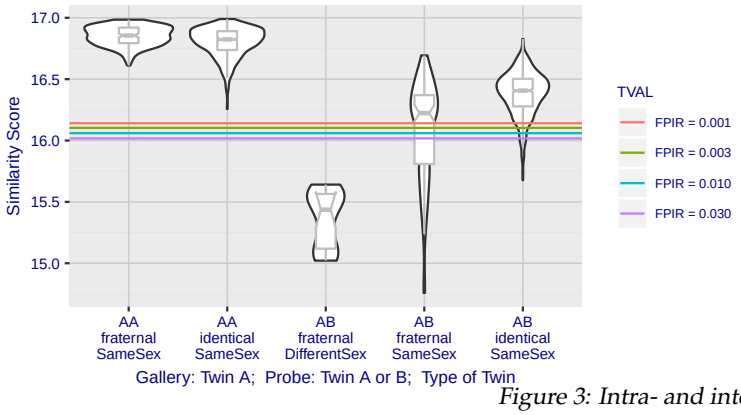

Figure 3: Intra- and inter-twin scores

This publication is available free of charge from: https://doi.org/10.6028/NIST.IR.8271

- **False positives from twins:** By enrolling 640 000 mugshots, adding photos of one twin, and then searching photos of those subjects and their twin the inset figure shows, for one typical algorithm, the similarity is generally greater when searching twins against themselves (A) than when searching twins against their sibling (B) but very often still above even stringent thresholds i.e. those corresponding to one in one thousand searches producing a false positive. Thus twins will very often produce a high-scoring non-match on a candidate list and a false alarm in an online identification system. The plot of Fig. 3 shows that fraternal twins are sometimes correctly rejected at those thresholds - including most different sex twins (at center). Figure **??** shows substantially similar behavior for all algorithms tested. In an investigative search, a twin would typically appear at rank 1, or rank 2 if their sibling happened to also be the gallery. Twins (and triplets etc.) constituted 3.3% of all live births [17] in recent years[5], and because that number is higher today than when the individuals in current adult databases were born, the false positives that arise from twins are now, and will increasingly be, an operational problem. Relative to the United States, twins are born with considerable regional variation. For example they are much less common in East Asia, and much more common in Sub-Saharan Africa [21].

  The presence of twins in the mugshot database is inevitable given its size, around 12.3 million people. As this is not an insignificant sample of the domestic United States population, people with other familial ties will be present also. The data was collected over an extended period and because location information is not available, we are unable to estimate the proportion of the domestic population that is present in the dataset. However, if we assume twins are neither more or less disposed to arrest than the general population, we can estimate that hundreds of thousands of individuals in the dataset are twins. This will affect false positive rates because we randomly set aside 331 201 individuals for nonmate searches, and some proportion of those will be twins with siblings in the gallery.

- **Database integrity:** An operational error rate should be added to all false negative rates in this report reflecting the proportion of images in a real database that are un-matchable. Such anomalies arise from images that: do not contain a face; include multiple persons; cannot be decoded; are rotated by 90° or 180°; depict a face on clothing; and others introduced by a long tail of various clerical errors. While the mugshot trials in this report have been constructed to minimize such effects, they are a real problem in actual operations.

This report is being updated continuously as new algorithms are submitted to FRVT, and run on new datasets. Participation in the one-to-many identification track is independent of participation in the one-to-one verification track of FRVT.

[5]See the CDC's National Vital Statistics Report for 2017: https://www.cdc.gov/nchs/data/nvsr/nvsr67/nvsr67_08-508.pdf

This publication is available free of charge from: https://doi.org/10.6028/NIST.IR.8271

Scope and Context

Audience: This report is intended for developers, integrators, end users, policy makers and others who have some familiarity with biometrics applications. The methods and metrics documented here will be of interest to organizations engaged in tests of face recognition algorithms. Some of these have been incorporated in the ISO/IEC 19795 Part 1 Biometric Testing and Reporting Framework standard, now nearing publication.

Prior benchmarks: Automated face recognition accuracy has improved massively in the two decades since initial commercialization of the various technologies. NIST has tracked that improvement through its conduct of regular independent, free, open, and public evaluations. These have fostered improvements in the state of the art. This report serves as an update to the NIST Interagency Report 8271 on performance of face identification algorithms, published in September 2019.

Demographics: In December 2019, NIST published a first report on demographic dependencies in face recognition, NIST Interagency Report 8280 that documented age, sex and race differentials in one-to-one and one-to-many false positive and false negative rates.

Scope: NIST IR 8271 documented recognition results for four databases containing in excess of 30.2 million still photographs of 14.4 million individuals. That constituted the largest public and independent evaluation of face recognition ever conducted. It includes results for accuracy, speed, investigative vs. identification applications, scalability to large populations, use of multiple images per person, images of cooperative and non-cooperative subjects.

The report also includes results for ageing, recognition of twins, and recognition of profile-view images against frontal galleries. It otherwise does not address causes of recognition failure, neither image-specific problems nor subject-specific factors including demographics. Separate reports on demographic dependencies in face recognition will be published in the future. Additionally out of scope are: performance of live human-in-the-loop transactional systems like automated border control gates; human recognition accuracy as used in forensic applications; and recognition of persons in video sequences (which NIST evaluated separately [9]). Some of those applications share core matching technologies that *are* tested in this report.

Images: Five kinds of images are employed; these are either compared with images of the same kind, or against others from different capture environments as follows. The primary dataset is a set of law enforcement mugshot images (Fig. 5) which are enrolled and then searched with three kinds of images: other mugshots (i.e. within-domain); profile-view photographs (90 degree cross-view); and lower quality webcam images (Fig. 6) collected in similar detention operations (cross-domain). Additionally we compare high quality visa-like photos collected in immigration offices, with: medium quality border crossing images collected in primary immigration lanes; poor quality images collected in ATM-like registered traveller kiosks.

Participation and industry coverage: The report includes performance figures for prototype algorithms from the research laboratories of commercial developers and a few universities. This represents a substantial majority of the face recognition industry, but only a tiny minority of the academic community. Participation was open worldwide. While there is no charge for participation, developers incur some software engineering expense in implementing their algorithms behind the NIST application programming interface (API). The test is a black-box test where the function of the algorithm, and the intellectual property associated with it, is hidden inside pre-compiled libraries.

Recent technology development: Most face recognition research with deep convolutional neural networks (CNNs) has been aimed at achieving invariance to pose, illumination and expression variations that characterize photojournalism and social media images. The initial research [18, 22] employed large numbers of images of relatively few ($\sim 10^4$) individuals to learn invariance. Inevitably much larger populations ($\sim 10^7$) were employed for training [11, 20] but the benchmark, Labeled Faces in the Wild with (essentially) an equal error rate metric [12], represents an easy task,

one-to-one verification at very high false match rates. While a larger scale identification benchmark duly followed, Megaface [15], its primary metric, rank one hit rate, contrasts with the high threshold discrimination task required in most large-population applications of face recognition, namely credential de-duplication, and background checks. There, identification in galleries containing up to 10^8 individuals must be performed using a) very few images per individual and b) stringent thresholds to afford very low false positive identification rates. This track of FRVT was launched to measure the capability of the new technologies, including in these two cases. FRVT has included open-set identification tests since 2002, reporting both false negative and positive identification rates [7].

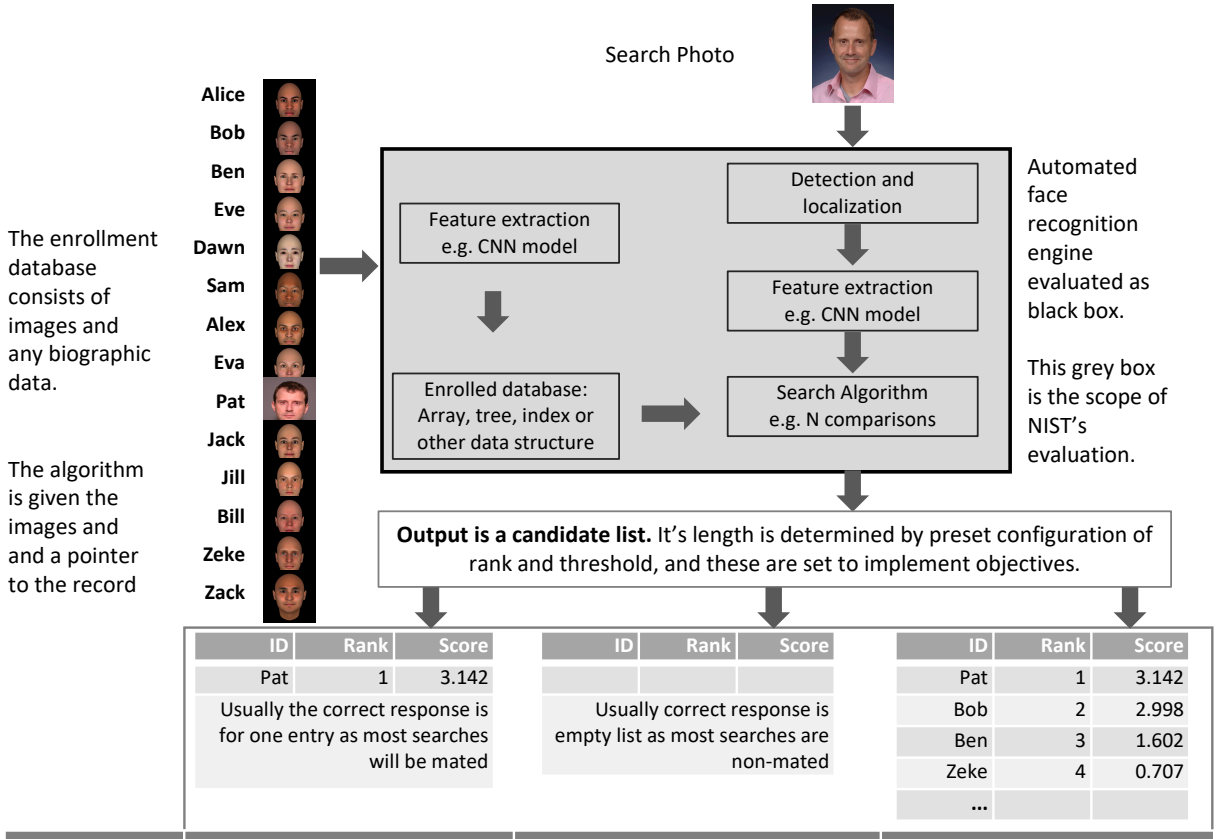

	Positive identification	Negative identification	Post-event investigation
Example	Access to a gym or cruise ship	Watchlist e.g. Detection of deportee or duplicate drivers license applications	Crime scene photos, or of detainee without ID documents.
Claim of identity	Implicit claim to be enrolled	Implicit claim to not be enrolled	No claim: Inquiry
Threshold	High, to implement security objective	High, to limit false positives	Zero
Num. candidates	1	0	L, set by request to algorithm
Human role	Review candidate to assist user in resolution of false negatives, or to detect impostor	Review candidate to determine false positive or correct hit	Review multiple candidates, refer possible hits to examiners see [26]
Intended human involvement frequency	Rare – approx. the false negative identification rate plus prior probability of impostor	Rare – approx. the false positive identification rate plus prior probability of an actual mate	Always
Performance metric of interest	**FNIR at low FPIR. See sec. 3.1, 3.2 and Tables 10, 19**	**FNIR at low FPIR. See sec. 3.1, 3.2 and Tables 10, 19**	**FNIR at ranks 1... 50, say. FPIR = 1. See sec. 3.2 and Table 12, 14, 16**

Performance metrics for applications: This report documents the performance of one-to-many face recognition algorithms. The word "performance" here refers to recognition accuracy and computational resource usage, as measured

This publication is available free of charge from: https://doi.org/10.6028/NIST.IR.8271

by executing those algorithms on massive sequestered datasets.

This report includes extensive tabulation of recognition error rates germane to the main use-cases for face search technology. The Figure below, inspired by the Figure 1 in [23] differentiates different applications of the technolgy. The last row directs readers to the main tables relevant to those applications, respectively threshold-based and rank-based metrics that are special cases of the metrics given in section 3. The terms negative identification and positive identification are taken from the ISO/IEC 2382-37:2017 standardized biometrics vocabulary.

The algorithms are specifically configured for these applications by setting thresholds and candidate list lengths. Both rank-based metrics and threshold-based metrics include tradeoffs. In investigation, overall accuracy will be reduced if labor is only available to review a few candidates from the automated system. Note that when a fixed number of candidates are returned, the false positive identification rate of the automated face recognition engine will be 100%, because a probe image of anyone not enrolled will still return candidates. In identification applications where false positives must be limited to satisfy reviewer labor availability or a security objective, higher false negative rates are implied. This report includes extensive quantification of this threshold-based tradeoff. See Sec. 3

Template diversity: The FRVT is designed to evaluate black-box technologies with the consequence that the templates that hold features extracted from face images are entirely proprietary opaque binary data that embed considerable intellectual property of the developer. Despite migration to CNN-based technologies there is no consensus on the optimal feature vector dimension. This is evidenced by template sizes ranging from below 100 bytes to more than four kilobytes. This diversity of approaches, suggests there is no prospect of a standard template something that would require a common feature set to be extracted from faces. Interoperability in automated face recognition remains solidly based on images and documentary standards for those, in particular the ICAO portrait [27] specification deriving from the ISO/IEC 19794-5 Token frontal [24] standard, which are similar to certain ANSI/NIST Type 10 [26] formats.

Training: The algorithms submitted to NIST have been developed using image datasets that developers do not disclose. The development will often include application of machine learning techniques and will additionally involve iterative training and testing cycles. NIST itself does not perform any training and does not refine or alter the algorithm in any way. Thus the model, data files, and libraries that define an algorithm are fixed for the duration of the tests. This reflects typical operational reality where recognition software, once installed, is fixed and constant until upgraded. This situation persists because on-site training of algorithms on customer data is atypical essentially because training is not a turnkey process.

Automated search and human review: Virtually all applications using automated face search require human review of the outputs at some frequency: Always for investigational applications; rarely in positive identification applications, after rejection (false or otherwise); and rarely in negative identification applications, after an alarm (false or otherwise). The human role is usually to compare a reference image with the query image or the live-subject if present, to render either a definitive decision on "exclusion" (different subjects), or "identification" (same subject), or a declaration that one or both images have "no value" and that no decision can be made. Note that automated face recognition algorithms are not built to do exclusion - low scores from a face comparison arise from different faces *and* poor quality images of the same face.

Human reviewers make recognition errors [5, 19, 25] and are sensitive to image acquisition and quality. Accurate human review is supported by high resolution - as specified in the Type 50, 51 acquisition profiles of the ANSI/NIST Type 10 record [26], and by multiple non-frontal views as specified in the same standard. These often afford views of the ear. Organizations involved in image collection should consider supporting human adjudication by collecting high-resolution frontal and non-frontal views, preparing low resolution versions for automated face recognition [24], and retaining both for any subsequent resolution of candidate matches. Along these lines, the ISO/IEC Joint Technical

This publication is available free of charge from: https://doi.org/10.6028/NIST.IR.8271

Committee 1 subcommittee 37 on biometrics has just initiated projects on image quality assessment and face-aware capture.

This publication is available free of charge from: https://doi.org/10.6028/NIST.IR.8271

Release Notes

FRVT Activities: Since February 2017, NIST has been evaluating one-to-one verification algorithms on an ongoing basis. NIST then restarted FRVT's one-to-many track in February 2018, inviting participants to send up to prototype algorithms. Both tracks allows developers to submit updated algorithms to NIST at any time but no more frequently than four calendar months. This more closely aligns development and evaluation schedules. Results are posted to the web within a few weeks of submission. Details and full report are linked from the Ongoing FRVT site.

FRVT Reports: The results of the FRVT appear in the series NIST Interagency Reports tabulated below. The reports were developed separately and released on different schedules. In prior years NIST has mostly reported FRVT results as a single report; this had the disadvantage that results from completed sub-studies were not published until all other studies were complete.

Date	Link	Title	No.
2014-03-20	PDF	FRVT Performance of Automated Age Estimation Algorithms	7995
2015-04-20	PDF	Face Recognition Vendor Test (FRVT) Performance of Automated Gender Classification Algorithms	8052
2014-05-21	PDF	FRVT Performance of face identification algorithms	8009
2017-03-07	PDF	Face In Video Evaluation (FIVE) Face Recognition of Non-Cooperative Subjects	8173
2017-11-23	PDF	The 2017 IARPA Face Recognition Prize Challenge (FRPC)	8197
2018-11-27	PDF	Face Recognition Vendor Test - Part 2: Identification	8271
2019-09-11	PDF	Face Recognition Vendor Test - Part 2: Identification	8271
2019-12-11	PDF	Face Recognition Vendor Test - Part 3: Demographic Effects	8280
2020-01-03	WWW	Face Recognition Vendor Test (FRVT) - Part 1 Verification	Draft

Details appear on pages linked from `https://www.nist.gov/programs-projects/face-projects`.

Appendices: This report is accompanied by appendices which present exhaustive results on a per-algorithm basis. These are machine-generated and are included because the authors believe that visualization of such data is broadly informative and vital to understanding the context of the report.

Typesetting: Virtually all of the tabulated content in this report was produced automatically. This involved the use of scripting tools to generate directly type-settable LaTeX content. This improves timeliness, flexibility, maintainability, and reduces transcription errors.

Graphics: Many of the Figures in this report were produced using the ggplot2 package running under R, the capabilities of which extend beyond those evident in this document.

This publication is available free of charge from: https://doi.org/10.6028/NIST.IR.8271

Contents

Release Notes 1

Disclaimer 4

Institutional Review Board 4

Acknowledgments 4

Executive Summary 5

Scope and Context 11

Release Notes 15

1 Introduction 17

2 Evaluation datasets 18

3 Performance metrics 24

4 Results 40

Appendices 74

A Accuracy on large-population FRVT 2018 mugshots 74

B Effect of time-lapse: Accuracy after face ageing 119

C Effect of enrolling multiple images 174

D Accuracy with poor quality webcam images 181

E Accuracy for profile-view to frontal recognition 191

F Search duration 195

G Gallery Insertion Timing 202

This publication is available free of charge from: https://doi.org/10.6028/NIST.IR.8271

1 Introduction

One-to-many identification represents the largest market for face recognition technology. Algorithms are used across the world in a diverse range of biometric applications: detection of duplicates in databases, detection of fraudulent applications for credentials such as passports and driving licenses, token-less access control, surveillance, social media tagging, lookalike discovery, criminal investigation, and forensic clustering.

This report contains a breadth of performance measurements relevant to many applications. Performance here refers to accuracy and resource consumption. In most applications, the core accuracy of a facial recognition algorithm is the most important performance variable. Resource consumption will be important also as it drives the amount of hardware, power, and cooling necessary to accommodate high volume workflows. Algorithms consume processing time, they require computer memory, and their static template data requires storage space. This report documents these variables.

1.1 Open-set searches

FRVT tested open-set identification algorithms. Real-world applications are almost always "open-set", meaning that some searches have an enrolled mate, but some do not. For example, some subjects have truly not been issued a visa or drivers license before; some law enforcement searches are from first-time arrestees[6]. In an "open-set" application, algorithms make no prior assumption about whether or not to return a high-scoring result, and for a mated search, the ideal behaviour is that the search produces the correct mate at high score and first rank. For a non-mate search, the ideal behavior is that the search produces zero high-scoring candidates.

Many academic benchmarks execute only closed-set searches. The proportion of mates found in the rank one position is the default accuracy metric. This hit rate metric ignores the score with which a mate is found; weak hits count as much as strong hits. This ignores the real-world imperative that in many applications it is necessary to elevate a threshold to reduce the number of false positives.

[6]Operationally closed-set applications are rare because it is usually not the case that all searches have an enrolled mate. One counter-example, however, is a cruise ship in which all passengers are enrolled and all searches should produce exactly one identity. Another example is forensic identification of dental records from an aircraft crash.

This publication is available free of charge from: https://doi.org/10.6028/NIST.IR.8271

2 Evaluation datasets

This report documents accuracy for four kinds of images - mugshots, webcam, profiles and wild - as described in the following sections.

2.1 Immigration-related images

This report includes benchmark tests sharing a common enrollment of high quality frontal portrait images collected while subject make applications for various immigration benefits. We then search that with two kinds of images, webcam images collected during in-bound immigration and also images collected from registered travelers using a ATM-style kiosk. These are described below and depicted in Figure 4.

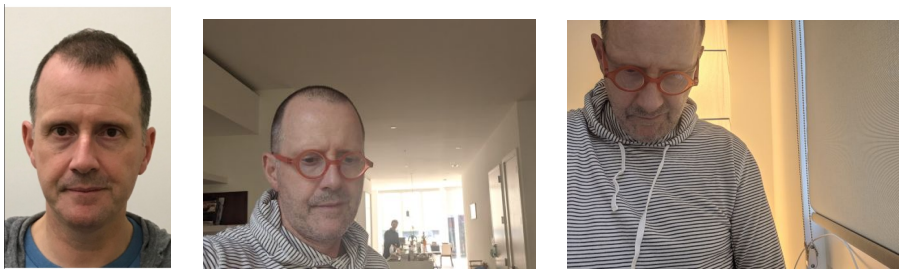

a) Application b) Immigration Lane c) Kiosk

Figure 4: Example photos.

- **Application reference photos**: The images are collected in an attended interview setting using dedicated capture equipment and lighting. The images, at size 300x300 pixels, are smaller than normally indicated by ISO. The images are all high-quality frontal portraits collected in immigration offices and with a white background. As such, potential quality related drivers of high false match rates (such as blur) can be expected to be absent. The images are encoded as ISO/IEC 10918-1 i.e. JPEG. Older images had a compression ration of about 16:1, while newer images, since 2010, are more lightly compressed at 4:1. When these images are provided as input into the algorithm, they are labeled with the type "iso". This report enrols 1 600 000 application images, one per person.

- **Border crossing photos**: Most images are have width 320 and height 240 pixels. They are JPEG compressed at 16:1 i.e. filesize just below 15KB. The images present challenges for face recognition in that subjects often exhibit non-zero yaw and pitch (associated with the rotational degrees of freedom of the camera mount), low contrast (due to varying and intense background lights), and poor spatial resolution (due to inexpensive cameras). There are often subjects standing in the background, usually at very low resolution (see Figure 4b). In such cases, algorithms should detect all faces and determine which is the largest and most centered. When these images are provided as input into the algorithm, they are labeled with the type "wild".

- **Kiosk photos**: These photos were collected from subjects whose attention was focused on interaction with an immigration kiosk. They images were not intended for use with automated face recognition. The camera is situated above a display which the user touches, and is triggered either without directing the subject to look at it, or without waiting for the subject to comply. The images are therefore characterized by pitch-down pose, sometimes exceeding 45 degrees, as in Figure 4c. Yaw-angle variation is mild, with most images close to frontal. The images

This publication is available free of charge from: https://doi.org/10.6028/NIST.IR.8271

have width 320 pixels and height 240 pixels and therefore tall individuals are sometimes cropped. This is often just above the eyes and can occur at the nose or mouth. Conversely, short individuals are sometimes cropped such that only the top part of the face is visible. In a quite small number of cases, there other subjects standing just behind the primary subject such that algoriths should detect all faces and determine which is the largest and most centered. Background ceiling lighting is often visible and this sometimes leads to under-exposure of the face When these images are provided as input into the algorithm, they are labeled with the type "wild".

2.2 Law enforcement images

The main mugshot dataset used is referred to as the FRVT 2018 set. This set was collected over the period 2002 to 2017 in routine United States law enforcement operations. This set yields three subsets

- **Mugshots**: Mugshots comprise about 86% of the database. They have reasonable compliance with the ANSI/NIST ITL1-2011 Type 10 standard's subject acquisition profiles levels 10-20 for frontal images [26]. The most common departure from the standard's requirements is the presence of mild pose variations around frontal - the images of Figure 5 are typical. The images vary in size, with many being 480x600 pixels with JPEG compression applied to produce filesizes of between 18 and 36KB with many images outside this range, implying that about 0.5 bits are being encoded per pixel. When these images are provided as input into the algorithm, they are labeled with the type "mugshot". Example images appear in Fig. 5

  NIST Interagency Report 8238 includes a comparison of this set of mugshots with the smaller and easier sets of mugshots used in tests run in 2010 and 2014.

- **Profile images**: Profile-view images have been collected in law enforcement for more than 100 years, as human capability is improved with orthogonal information. The profile images used in this report were collected during the same session as the frontal mugshot photograph, in the same standardized photographic setup. These would not therefore be used with automated face recognition. A small subset, 200 000 images, were set aside for testing. When these images are provided as input into the algorithm, they are labeled with the type "wild". Example images appear in Fig. 7

- **Webcam images**: The remaining 14% of the images were collected using an inexpensive webcam attached to a flexible operator-directed mount. These images are all of size 240x240 pixels, that are in considerable violation of most quality-related clauses of all face recognition standards. As evident in the figure, the most common defects are non-frontal pose (associated with the rotational degrees of freedom of the camera mount), low contrast (due to varying and intense background lights), and poor spatial resolution (due to inexpensive camera optics) - see examples in Fig 6. The images are overly JPEG compressed, to between 4 and 7KB, implying that only 0.5 to 1 bits are being encoded per color pixel. When these images are provided as input into the algorithm, they are labeled with the type "wild". Example images appear in Fig. 6

These are drawn from NIST Special Database 32 which may be downloaded here.

These images were partitioned in galleries and probesets for the various experiment listed in Table 1.

This publication is available free of charge from: https://doi.org/10.6028/NIST.IR.8271

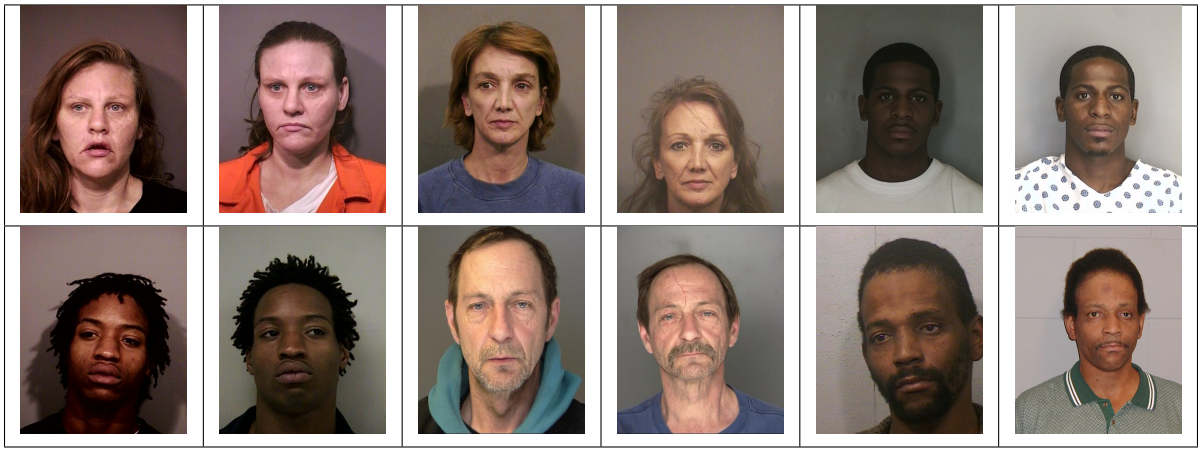

Figure 5: Six mated mugshot pairs representative of the FRVT-2014 (LEO) and FRVT-2018 datasets. The images are collected live, i.e. not scanned from paper. Image source: NIST Special Database 32 the Multiple Encounter Deceased Subjects dataset.

Figure 6: Twelve webcam images representative of probes against the FRVT-2018 mugshot gallery. The first eight images are four mated pairs. Such images present challenges to recognition including pose, non-uniform illumination, low contrast, compression, cropping, and low spatial sampling rate. Image source: NIST Special Database 32 the Multiple Encounter Deceased Subjects dataset.

Figure 7: **[Profile views]** *The three images are a frontal enrollment, subsequent frontal probe, and same-session ninety degree profile view. While collection of both frontal and profile views has been typical in law enforcement for more than a century, the recognition of profile to frontal views has essentially been impossible. However, reasonbly high accuracy results is now possible - see section E.*

This publication is available free of charge from: https://doi.org/10.6028/NIST.IR.8271

Image		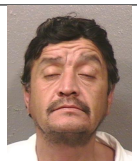		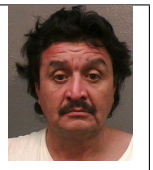
Encounter	1	...	$K_i - 1$	K_i
Capture Time	T_1	...	T_{K_i-1}	T_{K_i}
Role RECENT	Not used	Not used	Enrolled	Search
Role LIFETIME	Enrolled	Enrolled	Enrolled	Search

Figure 8: Depiction of the "recent" and "lifetime" enrollment types. Image source: NIST Special Database 32

2.3 Enrollment strategies

Many operational applications include collection and enrollment of biometric data from subjects on more than one occasion. This might be done on a regular basis, as might occur in credential (re-)issuance, or irregularly, as might happen in a criminal recidivist situation [4]. The number of images per person will depend on the application area. In civil identity credentialing (e.g. passports, driver's licenses), the images will be acquired approximately uniformly over time (e.g. ten years for a passport). While the distribution of dates for such images of a person might be assumed uniform, a number of factors might undermine this assumption[7]. In criminal applications, the number of images would depend on the number of arrests. The distribution of dates for arrest records for a person (i.e. the recidivism distribution) has been modeled using the exponential distribution but is recognized to be more complicated[8].

In any case, the 2010 NIST evaluation of face recognition showed that considerable accuracy benefits accrue with retention and use of *all* historical images [6].

To this end, the FRVT API document provides $K \geq 1$ images of an individual to the enrollment software. The software is tasked with producing a single proprietary undocumented "black-box" template[9] from the K images. This affords the algorithm an ability to generate a *model* of the individual, rather than to simply extract features from each image on a sequential basis.

As depicted in Figure 8, the i-th individual in the FRVT 2018 dataset has K_i images. These are labelled as x_k for $k = 1 \ldots K_i$ in chronological order of capture date. To measure the utility of having multiple enrollment images, this report evaluates three kinds of enrollment:

- ▷ **Recent**: Only the second most recent image, x_{K_i-1} is enrolled. This strategy of enrollment mimics the operational policy of retaining the imagery from the most recent encounter. This might be done operationally to ameliorate the effects of face ageing. Obviously retaining only the most recent image should only be done if the identity of the person is trusted to be correct. For example, in an access control situation retention of the most recent successful *authentication* image would be hazardous if it could be a false positive.

- ▷ **Lifetime-consolidated**: All but the most recent image are enrolled, $x_1 \ldots x_{K_i-1}$. This subject-centric strategy might be adopted if quality variations exist where an older image might be more suitable for matching, despite the ageing effect.

[7] For example, a person might skip applying for a passport for one cycle, letting it expire. In addition, a person might submit identical images (from the same photography session) to consecutive passport applications at five year intervals.
[8] A number of distributions have been considered to model recidivism, see for example [3].
[9] There are no formal face template standards. Template standards only exist for fingerprint minutiae - see ISO/IEC 19794-2:2011.

This publication is available free of charge from: https://doi.org/10.6028/NIST.IR.8271

This publication is available free of charge from: https://doi.org/10.6028/NIST.IR.8271

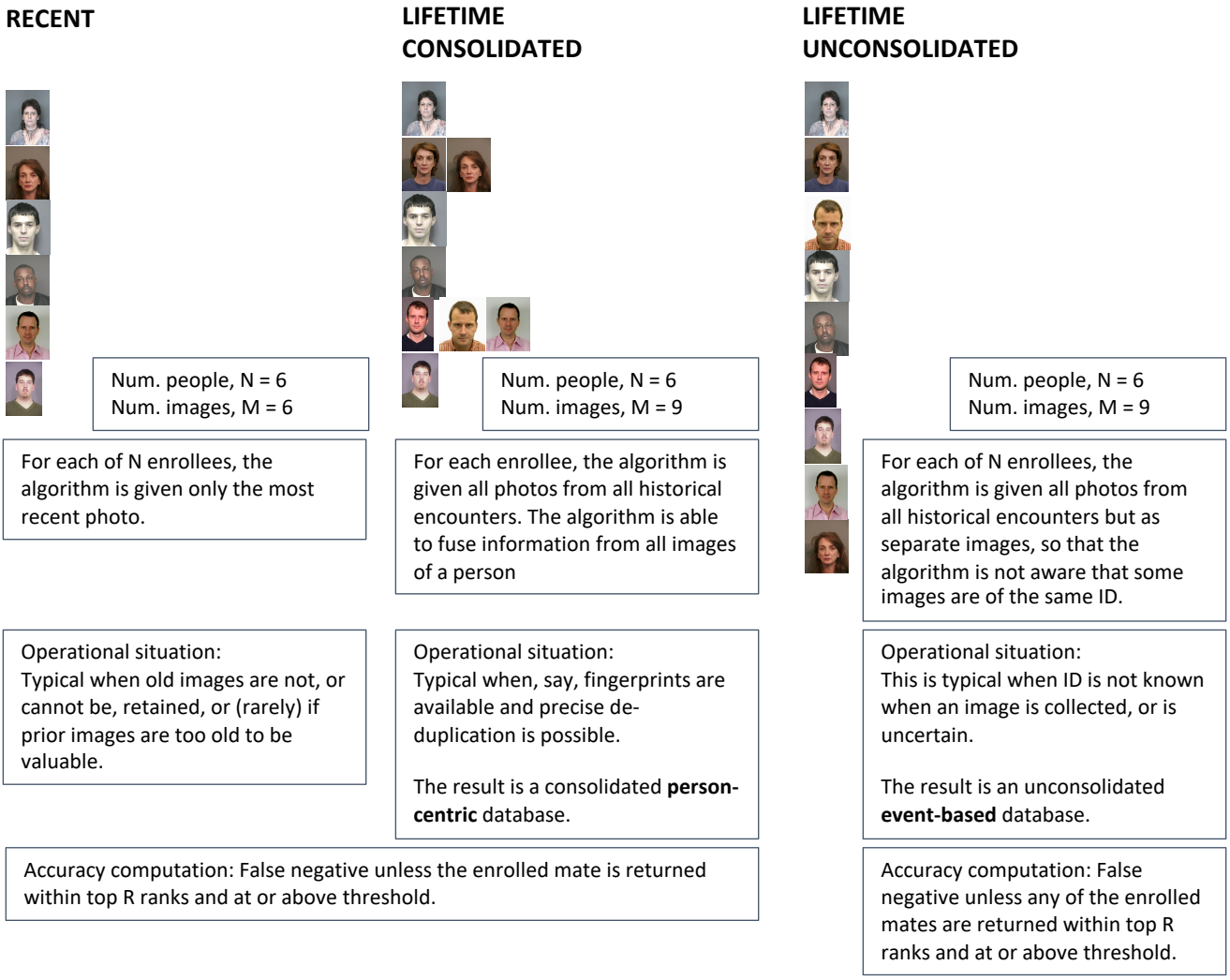

Figure 9: **Enrollment strategies**. *The figure shows the three kinds of enrollment databases examined in this report. Image source: NIST Special Database 32*

	ENROLLMENT				SEARCH			
	TYPE SEE	POPULATION			MATE		NON-MATE	
	SECTION 2.3	FILTER	N-SUBJECTS	N-IMAGES	N-SUBJECTS	N-IMAGES	N-SUBJECTS	N-IMAGES
Mugshot trials from enrollment of single images								
1	RECENT	NATURAL	640 000	640 000	154 549	154 549	331 254	331 254
2	RECENT	NATURAL	1 600 000	1 600 000				
3	RECENT	NATURAL	3 000 000	3 000 000				
4	RECENT	NATURAL	6 000 000	6 000 000				
5	RECENT	NATURAL	12 000 000	12 000 000				
Cross-domain								
13	MUGSHOTS AS ON ROW 2				82 106 WEBCAM	82 106 WEBCAM	331 254 WEBCAM	331 254 WEBCAM
Cross-view								
14	MUGSHOTS AS ON ROW 2				100 000 PROFILE	100 000 PROFILE	100 000 PROFILE	100 000 PROFILE
Mugshot ageing								
17	OLDEST	NATURAL	3 068 801	3 068 801	2 853 221	10 951 064	0	0
Border crossing ageing								
17	OLDEST	NATURAL	1 600 000	1 600 000	903 655	1 922 393	1 393 076	1 680 000
Visa-border								
19	PRIOR	NATURAL	1 600 000 VISA	1 600 000 VISA	80 000 BORDER	80 000 BORDER	80 000 BORDER	80 000 BORDER
20	VISA AS ON ROW 18				21 016 BORDER	21 016 BORDER	21 016 BORDER	21 016 BORDER

Table 1: **Enrollment and search sets**. *Each row summarizes one identification trial. Unless stated otherwise, all entries refer to mugshot images. The term "natural" means that subjects were selected without heed to demographics, i.e. in the distribution native to this dataset. The probe images were collected in a different calendar year to the enrollment image. Missing values in rows 2-12 are the same as in row 1.*

▷ **Lifetime-unconsolidated**: Again all but the most recent image are enrolled $x_1 \ldots x_{K_i-1}$ but now separately, with different identifiers, such that the algorithm is not aware that the images are from the same face. This kind of event- or encounter-centric enrollment is very common when operational constraints preclude reliable consolidation of the historical encounters into a single identity. This aspect also prevents the recognition algorithm from a) building a holistic model of identity (as is common in speaker recognition systems) and b) implementing fusion, for example template-level fusion of feature vectors, or post-search score-level fusion. The result is that searches will typically yield more than one image of a person in the top ranks. This has consequences for appropriate metrics, as detailed in section 3.2.1

NIST first evaluated this kind of enrollment in mid 2018, and the results tables include some comparison of accuracy available from all three enrollment styles.

In all cases, the most recent image, x_{K_i}, is reserved as the search image. For the 1.6 million subject enrollment partition of the FRVT 2018 data, $1 \leq K_i \leq 33$ with $K_i = 1$ in 80.1% of the individuals, $K_i = 2$ in 13.4%, $K_i = 3$ in 3.7%, $K_i = 4$ in 1.4%, $K_i = 5$ in 0.6%, $K_i = 6$ in 0.3%, and $K_i > 6$ is 0.2% for everyone else. This distribution is substantially dependent on United States recidivism rates.

We did not evaluate the case of retaining only the highest quality image, since automated quality assessment is out of scope for this report. We do not anticipate that such strategies will prove beneficial when the quality assessment apparatus is imperfect and unvalidated.

This publication is available free of charge from: https://doi.org/10.6028/NIST.IR.8271

3 Performance metrics

This section gives specific definitions for accuracy and timing metrics. Tests of open-set biometric algorithms must quantify frequency of two error conditions:

- ▷ **False positives**: Type I errors occur when search data from a person who has never been seen before is incorrectly associated with one or more enrollees' data.
- ▷ **Misses**: Type II errors arise when a search of an enrolled person's biometric does not return the correct identity.

Many practitioners prefer to talk about "hit rates" instead of "miss rates" - the first is simply one minus the other as detailed below. Sections 3.1 and 3.2 define metrics for the Type I and Type II performance variables.

Additionally, because recognition algorithms sometimes fail to produce a template from an image, or fail to execute a one-to-many search, the occurrence of such events must be recorded. Further because algorithms might elect to not produce a template from, for example, a poor quality image, these failure rates must be combined with the recognition error rates to support algorithm comparison. This is addressed in section 3.5.

Finally, section 3.7 discusses measurement of computation duration, and section 3.8 addresses the uncertainty associated with various measurements. Template size measurement is included with the results.

3.1 Quantifying false positives

It is typical for a search to be conducted into an enrolled population of N identities, and for the algorithm to be configured to return the closest L candidate identities. These candidates are ranked by their score, in descending order, with all scores required to be greater than or equal to zero. A human analyst might examine either all L candidates, or just the top $R \leq L$ identities, or only those with score greater than threshold, T. The workload associated with such examination is discussed later, in 3.6.

False alarm performance is quantified in two related ways. These express how many searches produces false positives, and then, how many false positives are produced in a search.

False positive identification rate: The first quantity, FPIR, is the proportion of non-mate searches that produce an adverse outcome:

$$\text{FPIR}(N,T) = \frac{\text{Num. non-mate searches where one or more enrolled candidates are returned with score at or above threshold}}{\text{Num. non-mate searches attempted.}} \tag{1}$$

Under this definition, FPIR can be computed from the highest non-mate candidate produced in a search - it is not necessary to consider candidates at rank 2 and above. FPIR is the primary measure of Type I errors in this report.

Selectivity: However, note that in any given search, several non-mate may be returned above threshold. In order to quantify such events, a second quantity, selectivity (SEL), is defined as the *number* of non-mates returned on a candidate list, averaged over all searches.

$$\text{SEL}(N,T) = \frac{\text{Num. non-mate enrolled candidates returned with score at or above threshold}}{\text{Num. non-mate searches attempted.}} \tag{2}$$

where $0 \leq$ SEL(N, T) $\leq$L. Both of these metrics are useful operationally. FPIR is useful for targeting how often an

This publication is available free of charge from: https://doi.org/10.6028/NIST.IR.8271

adverse false positive outcome can occur, while SEL as a number is related to workload associated with adjudicating candidate lists. The relationship between the two quantities is complicated - it depends on whether an algorithm concentrates the false alarms in the results of a few searches or whether it disburses them across many. This was detailed in FRVT 2014, NISTIR 8009. It has not yet been detailed in FRVT 2018.

3.2 Quantifying hits and misses

If L candidates are returned in a search, a shorter candidate list can be prepared by taking the top $R \leq L$ candidates for which the score is above some threshold, $T \geq 0$. This reduction of the candidate list is done because thresholds may be applied, and only short lists might be reviewed (according to policy or labor availability, for example). It is useful then to state accuracy in terms of R and T, so we define a "miss rate" with the general name **false negative identification rate** (FNIR), as follows:

$$\text{FNIR}(N, R, T) = \frac{\text{Num. mate searches with enrolled mate found outside top R ranks or score below threshold}}{\text{Num. mate searches attempted.}} \quad (3)$$

This formulation is simple for evaluation in that it does not distinguish between causes of misses. Thus a mate that is not reported on a candidate list is treated the same as a miss arising from face finding failure, algorithm intolerance of poor quality, or software crashes. Thus if the algorithm fails to produce a candidate list, either because the search failed, or because a search template was not made, the result is regarded as a miss, adding to FNIR.

Hit rates, and true positive identification rates: While FNIR states the "miss rate" as how often the correct candidate is either not above threshold or not at good rank, many communities prefer to talk of "hit rates". This is simply the **true positive identification rate**(TPIR) which is the complement of FNIR giving a positive statement of how often mated searches are successful:

$$\text{TPIR}(N, R, T) = 1 - \text{FNIR}(N, R, T) \quad (4)$$

This report does not report true positive "hit" rates, preferring false negative miss rates for two reasons. First, costs rise linearly with error rates. For example, if we double FNIR in an access control system, then we double user inconvenience and delay. If we express that as decrease of TPIR from, say 98.5% to 97%, then we mentally have to invert the scale to see a doubling in costs. More subtly, readers don't perceive differences in numbers near 100% well, becoming inured to the "high nineties" effect where numbers close to 100 are perceived indifferently.

Reliability is a corresponding term, typically being identical to TPIR, and often cited in automated (fingerprint) identification system (AFIS) evaluations.

An important special case is the **cumulative match characteristic**(CMC) which summarizes accuracy of mated-searches only. It ignores similarity scores by relaxing the threshold requirement, and just reports the fraction of mated searches returning the mate at rank R or better.

$$\text{CMC}(N, R) = 1 - \text{FNIR}(N, R, 0) \quad (5)$$

We primarily cite the complement of this quantity, $\text{FNIR}(N, R, 0)$, the fraction of mates *not* in the top R ranks.

The **rank one hit rate** is the fraction of mated searches yielding the correct candidate at best rank, i.e. CMC(N, 1). While this quantity is the most common summary indicator of an algorithm's efficacy, it is not dependent on similarity scores, so it does not distinguish between strong (high scoring) and weak hits. It also ignores that an adjudicating reviewer is often willing to look at many candidates.

This publication is available free of charge from: https://doi.org/10.6028/NIST.IR.8271

3.2.1 False negative rates for unconsolidated galleries

As detailed in section 2.3 a common type of gallery, here referred to as the lifetime unconsolidate type, is populated with all images of an individual without any association between them. That is, the gallery construction algorithm is not provided with any ID labels that would support processing of a person's images jointly. This constrasts with the lifetime consolidate type where an algorithm may explicitly fuse features from multiple images of a person, or select a best image. In such cases, where the number of enrolled images is a random variable, we define two false negative rates as follows.

The first demands that the algorithm place any of the K_i mates in the top $R \geq 1$ ranks. The proportion of searches for which this does not occur forms a false negative identification rate:

$$\text{FNIR}_{\text{any}}(N, R, T) = 1 - \frac{\text{Num. mate searches where any enrolled mate is found in the top R ranks and at-or-above threshold}}{\text{Num. mate searches attempted.}} \tag{6}$$

The second demands that the algorithm place all K_i mates in the top $R \geq K_i$ ranks. The proportion of searches for which this does not occur forms a false negative identification rate:

$$\text{FNIR}_{\text{all}}(N, R, T) = 1 - \frac{\text{Num. mate searches where all enrolled mates are found in the top R ranks and at-or-above threshold}}{\text{Num. mate searches attempted.}} \tag{7}$$

Placing all mates in the top ranks is a more difficult task than correctly retrieving any image, so it holds that: $\text{FNIR}_{\text{all}} \geq \text{FNIR}_{\text{any}}$. This is evident in the results presented for November 2018 algorithms in Tables starting at **??**.

The information retrieval community might prefer to compute and plot *precision* and *recall*; this is a valid approach, but we advance the two metrics above because they relate to our normal definition of consolidated FNIR, and they cover the two extreme use-cases of wanting any hit vs. all hits.

3.3 DET interpretation

In biometrics, a false negative occurs when an algorithm fails to match two samples of one person – a Type II error. Correspondingly, a false positive occurs when samples from two persons are improperly associated – a Type I error.

Matches are declared by a biometric system when the native comparison score from the recognition algorithm meets some threshold. Comparison scores can be either similarity scores, in which case higher values indicate that the samples are more likely to come from the same person, or dissimilarity scores, in which case higher values indicate different people. Similarity scores are traditionally computed by fingerprint and face recognition algorithms, while dissimilarities are used in iris recognition. In some cases, the dissimilarity score is a distance possessing metric properties. In any case, scores can be either mate scores, coming from a comparison of one person's samples, or nonmate scores, coming from comparison of different persons' samples.

The words "genuine" or "authentic" are synonyms for mate, and the word "impostor" is used as a synonym for nonmate. The words "mate" and "nonmate" are traditionally used in identification applications (such as law enforcement search, or background checks) while genuine and impostor are used in verification applications (such as access control).

An error tradeoff characteristic represents the tradeoff between Type II and Type I classification errors. For identification this plots false negative vs. false positive identification rates i.e. FNIR vs. FPIR parametrically with T. Such plots

This publication is available free of charge from: https://doi.org/10.6028/NIST.IR.8271

are often called detection error tradeoff (DET) characteristics or receiver operating characteristic (ROC). These serve the same function − to show error tradeoff − but differ, for example, in plotting the complement of an error rate (e.g. TPIR = 1 − FNIR) and in transforming the axes, most commonly using logarithms, to show multiple decades of FPIR. More rarely, the function might be the inverse of the Gaussian cumulative distribution function.

The slides of Figures 10 through 15 discuss presentation and interpretation of DETs used in this document for reporting face identification accuracy. Further detail is provided in formal biometrics testing standards, see the various parts of ISO/IEC 19795 Biometrics Testing and Reporting. More terms, including and beyond those to do with accuracy, appear in ISO/IEC 2382-37 Information technology – Vocabulary – Part 37: Harmonized biometric vocabulary.

This publication is available free of charge from: https://doi.org/10.6028/NIST.IR.8271

This publication is available free of charge from: https://doi.org/10.6028/NIST.IR.8271

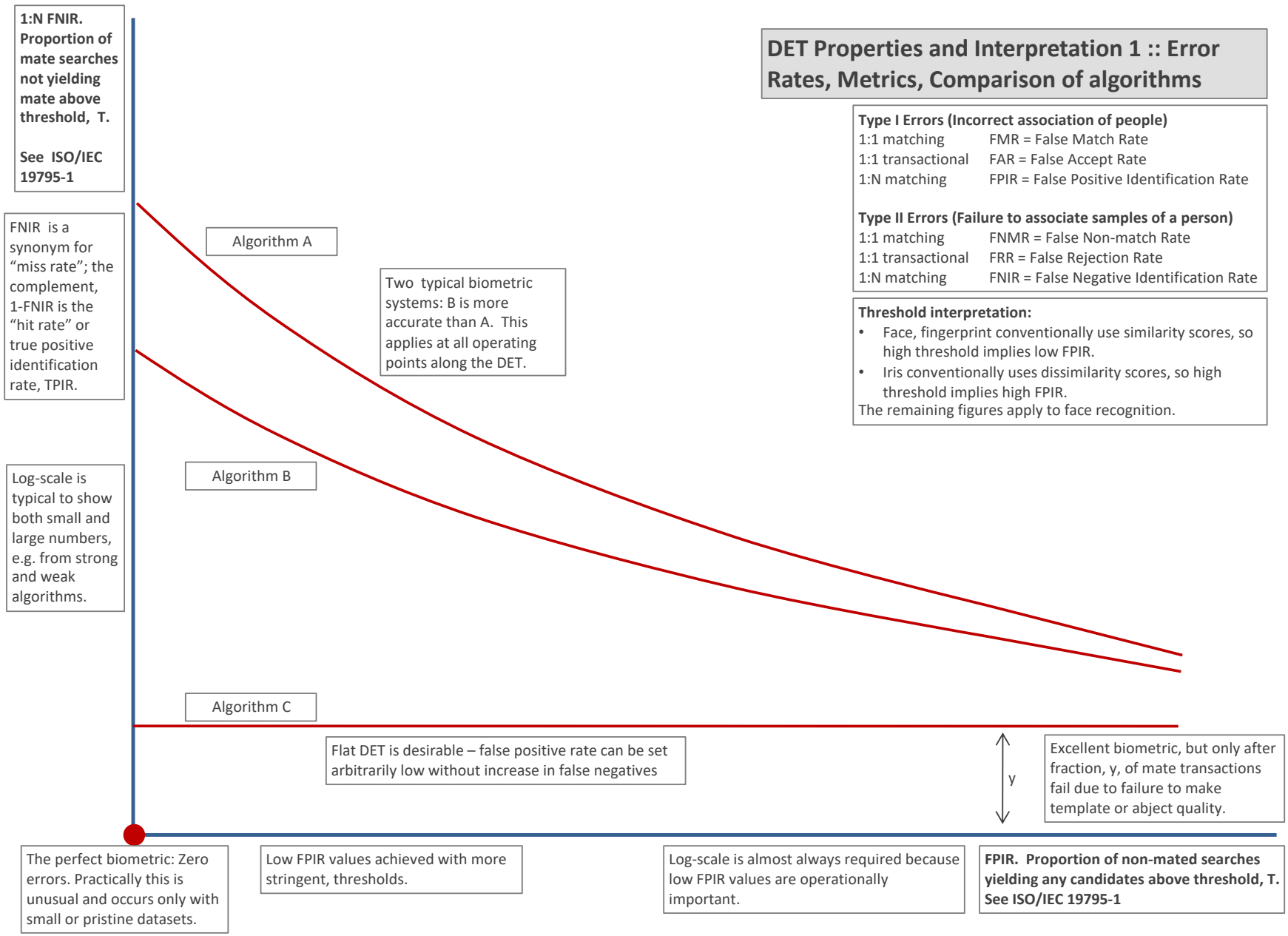

Figure 10: **DET as the primary performance reporting mechanism**.

This publication is available free of charge from: https://doi.org/10.6028/NIST.IR.8271

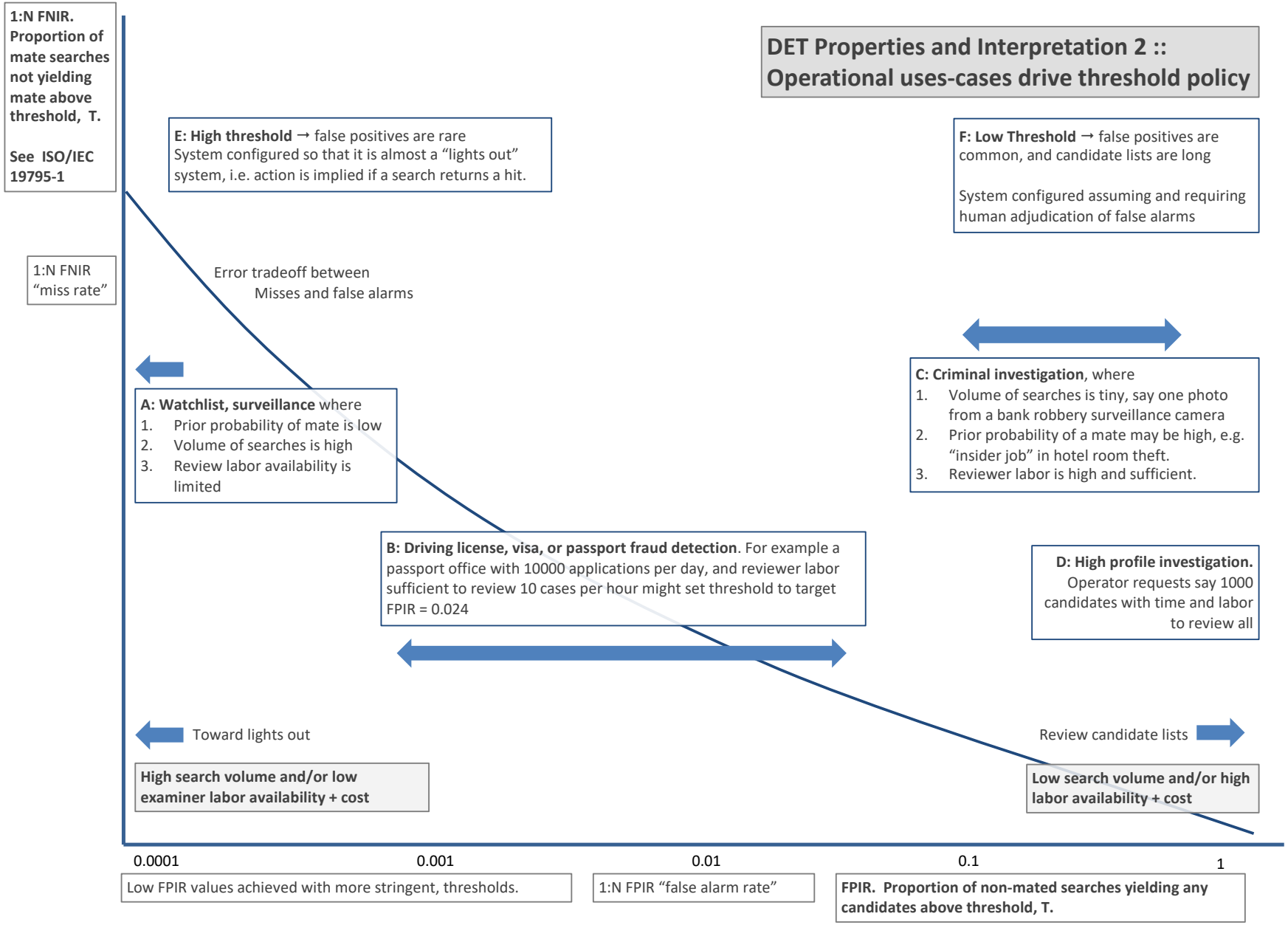

Figure 11: **DET as the primary performance reporting mechanism**.

2021/11/22 08:35:53

FNIR(N, R, T) = False neg. identification rate
FPIR(N, T) = False pos. identification rate
N = Num. enrolled subjects
R = Num. candidates examined
T = Threshold
T = 0 → Investigation
T > 0 → Identification

This publication is available free of charge from: https://doi.org/10.6028/NIST.IR.8271

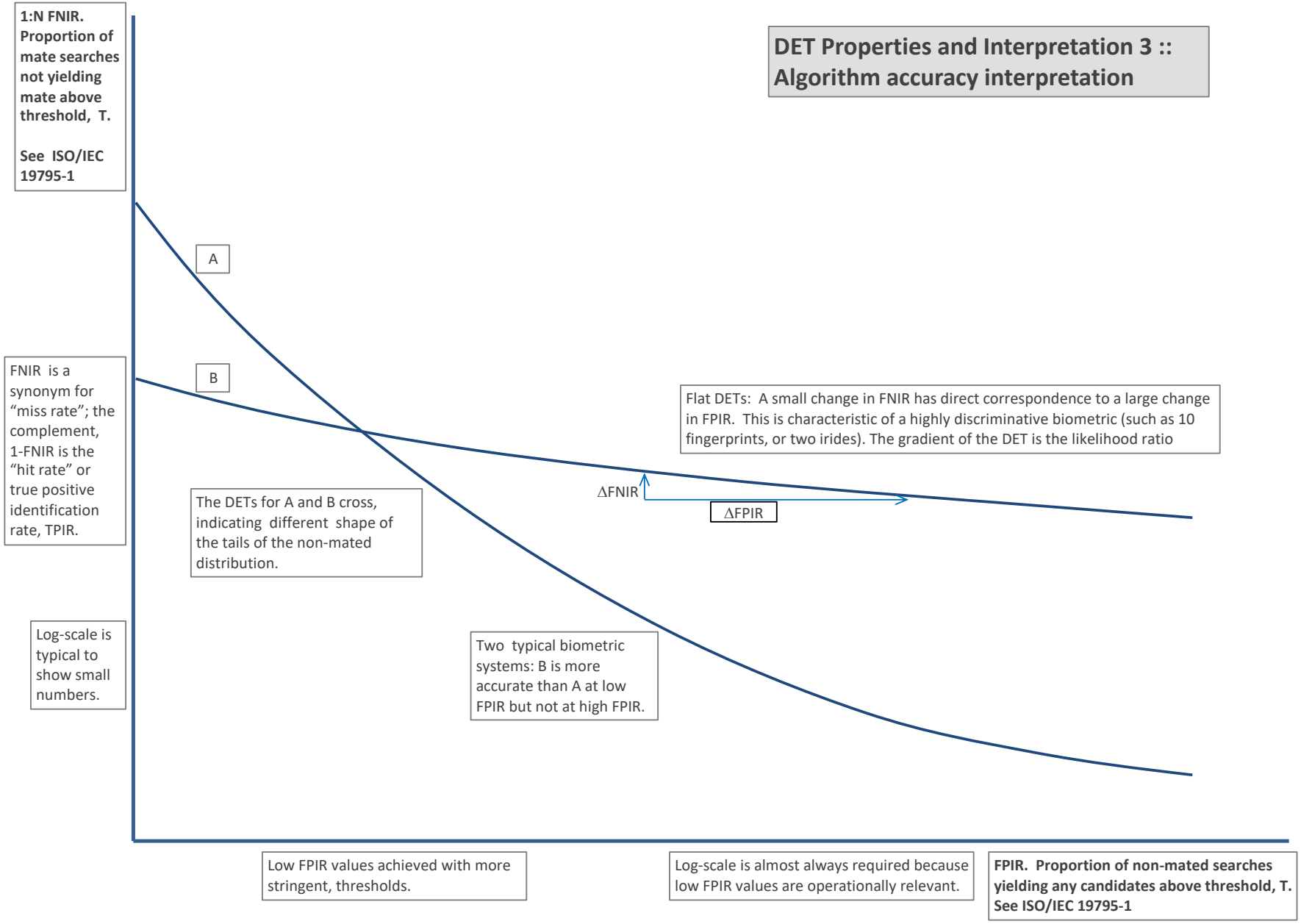

Figure 12: **DET as the primary performance reporting mechanism**.

2021/11/22 08:35:53

FNIR(N, R, T) = False neg. identification rate
FPIR(N, T) = False pos. identification rate
N = Num. enrolled subjects
R = Num. candidates examined
T = Threshold
T = 0 → Investigation
T > 0 → Identification

This publication is available free of charge from: https://doi.org/10.6028/NIST.IR.8271

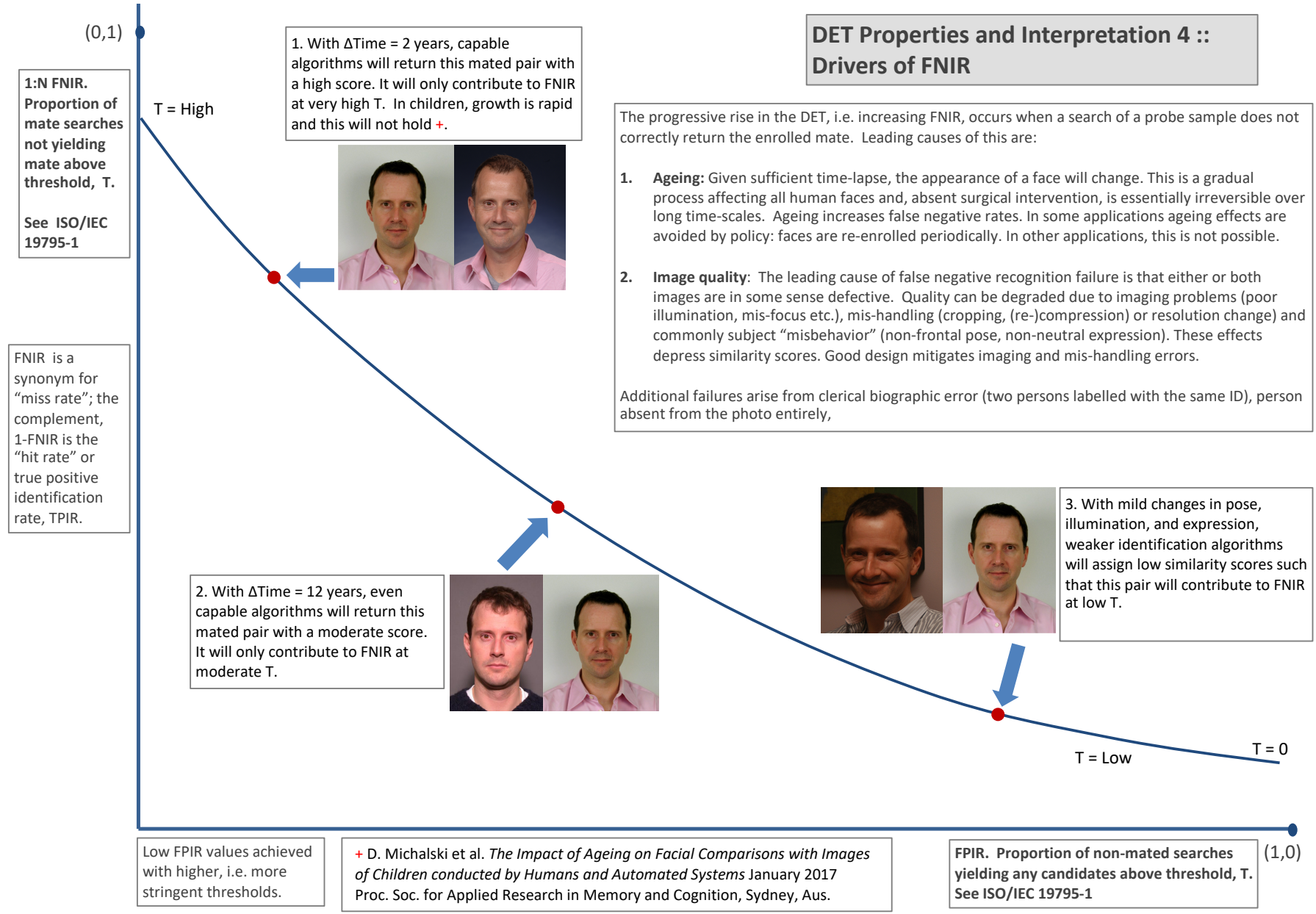

Figure 13: **DET as the primary performance reporting mechanism**.

2021/11/22 08:35:53

FNIR(N, R, T) = False neg. identification rate
FPIR(N, T) = False pos. identification rate
N = Num. enrolled subjects
R = Num. candidates examined
T = Threshold
T = 0 → Investigation
T > 0 → Identification

This publication is available free of charge from: https://doi.org/10.6028/NIST.IR.8271

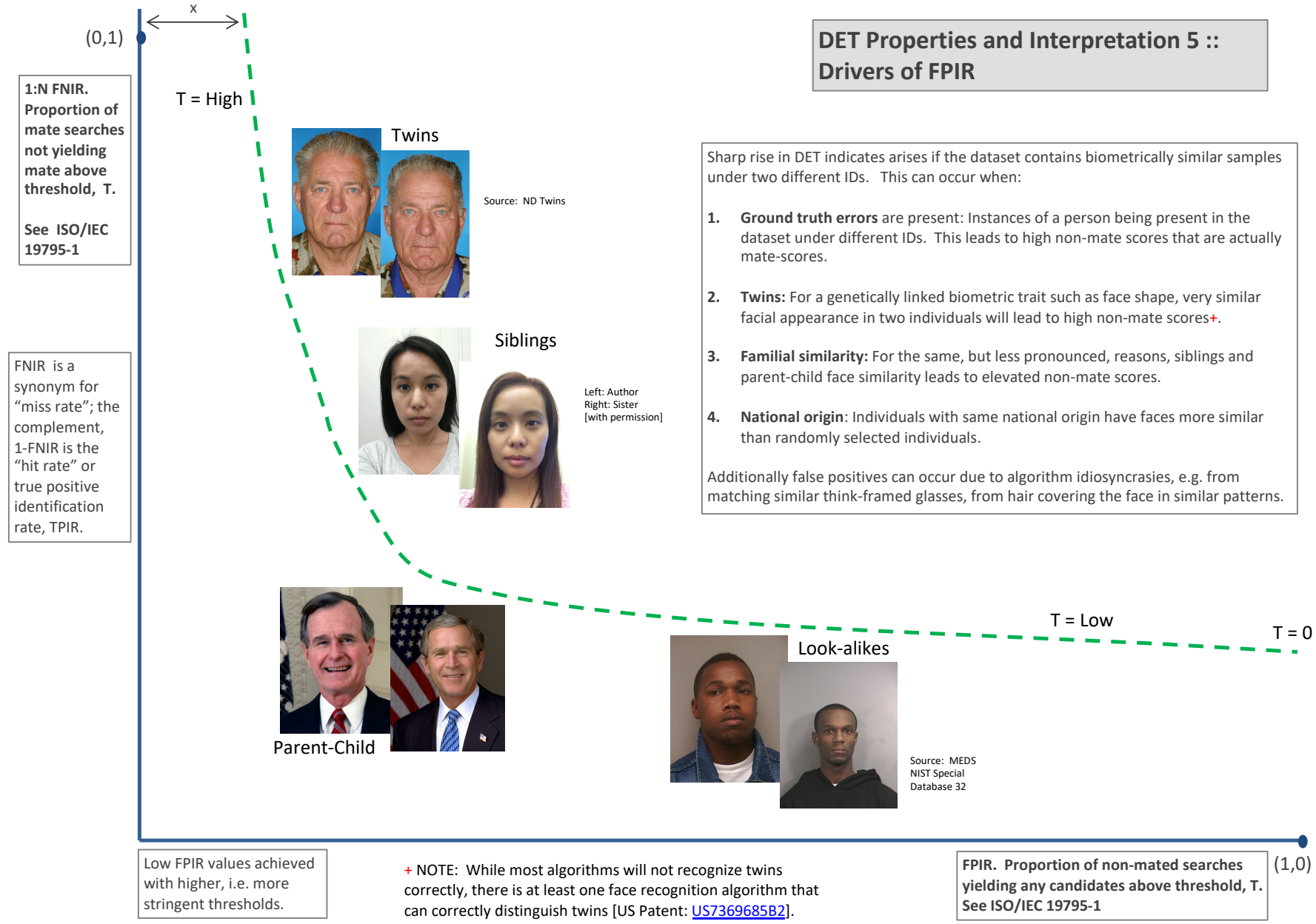

Figure 14: **DET as the primary performance reporting mechanism**.

2021/11/22 08:35:53
FNIR(N, R, T) = False neg. identification rate
FPIR(N, T) = False pos. identification rate
N = Num. enrolled subjects
R = Num. candidates examined
T = Threshold
T = 0 → Investigation
T > 0 → Identification

This publication is available free of charge from: https://doi.org/10.6028/NIST.IR.8271

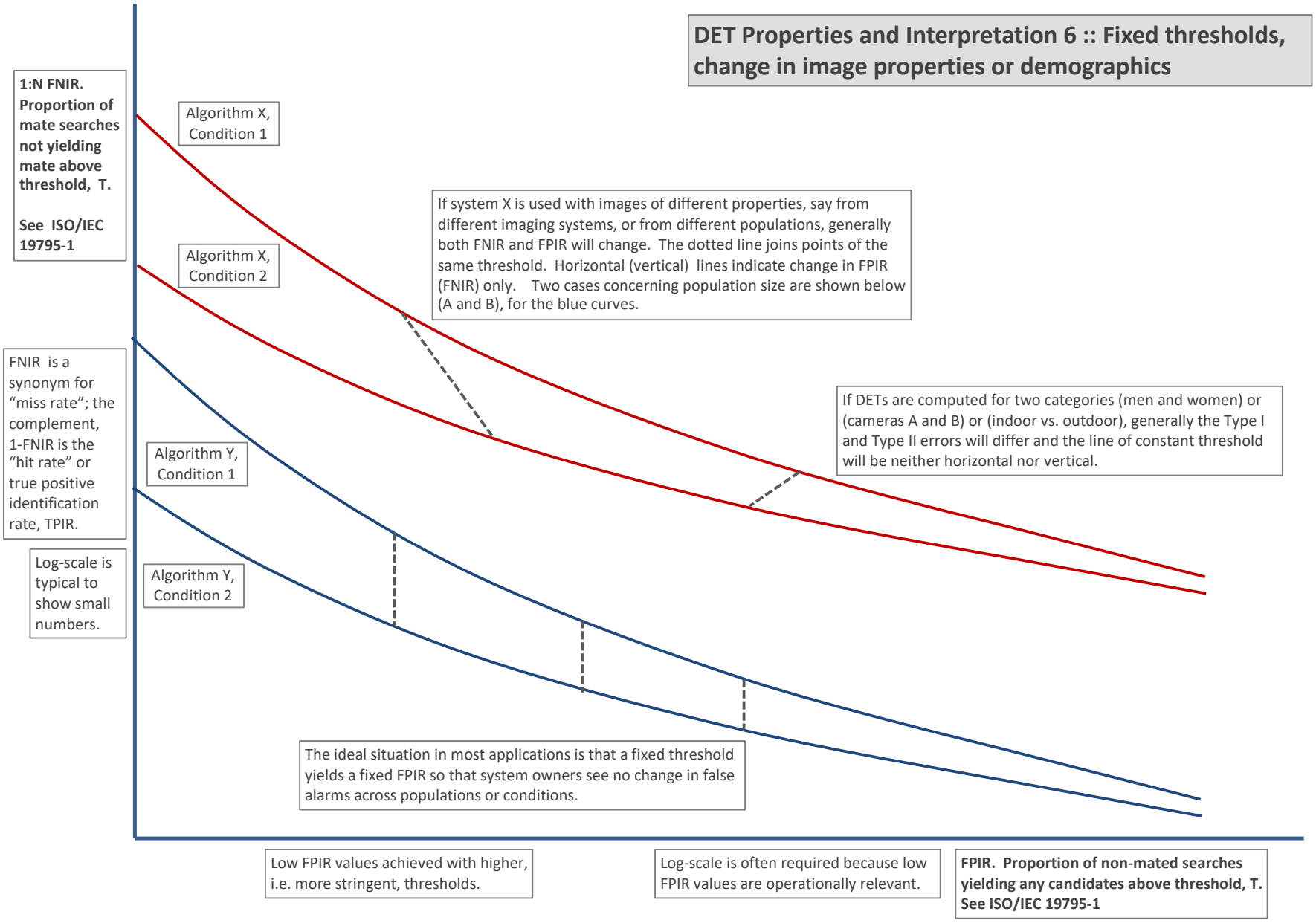

Figure 15: **DET as the primary performance reporting mechanism**.

2021/11/22 08:35:53

FNIR(N, R, T) = False neg. identification rate
FPIR(N, T) = False pos. identification rate
N = Num. enrolled subjects
R = Num. candidates examined
T = Threshold
T = 0 → Investigation
T > 0 → Identification

This publication is available free of charge from: https://doi.org/10.6028/NIST.IR.8271

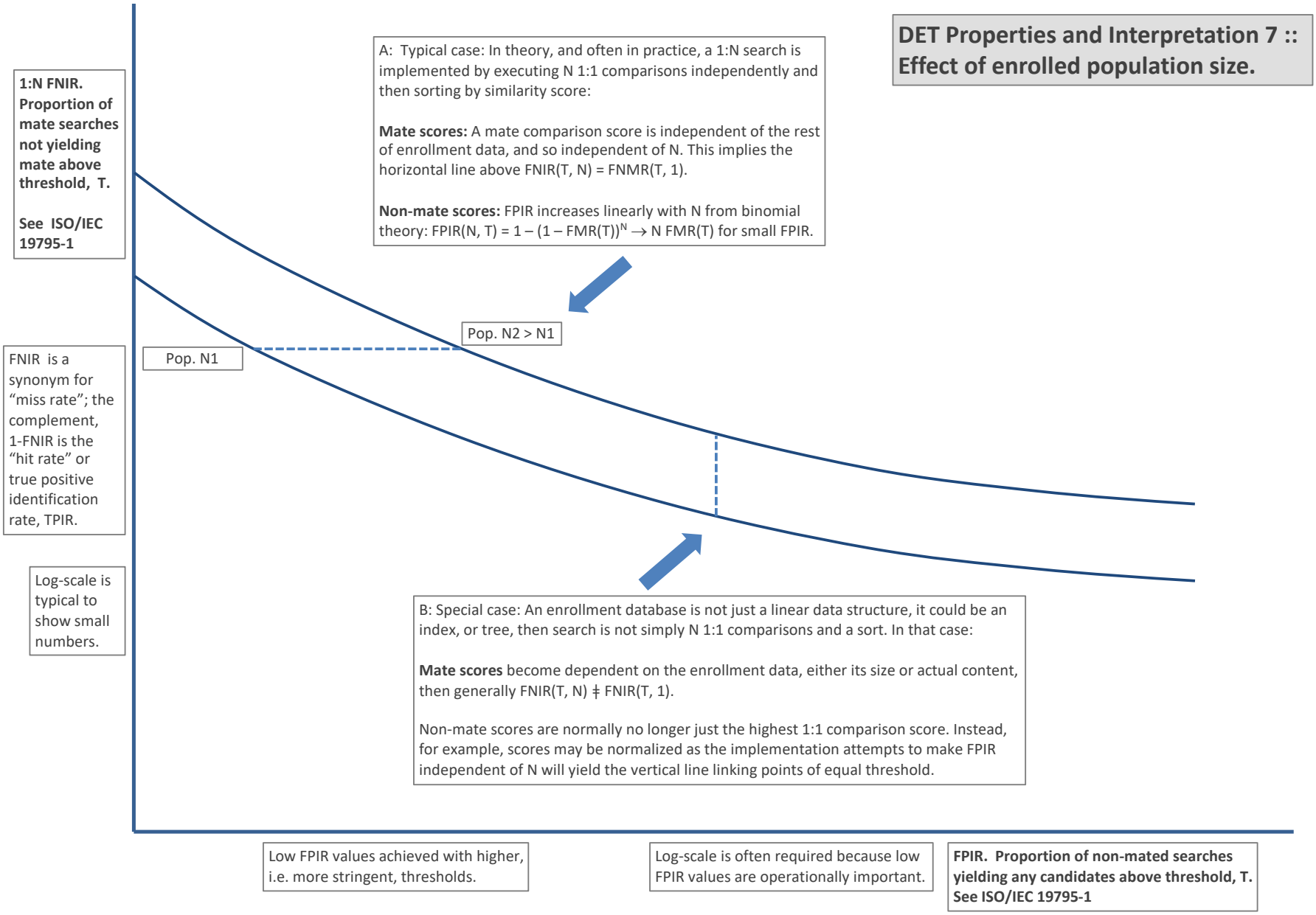

Figure 16: **DET as the primary performance reporting mechanism**.

This publication is available free of charge from: https://doi.org/10.6028/NIST.IR.8271

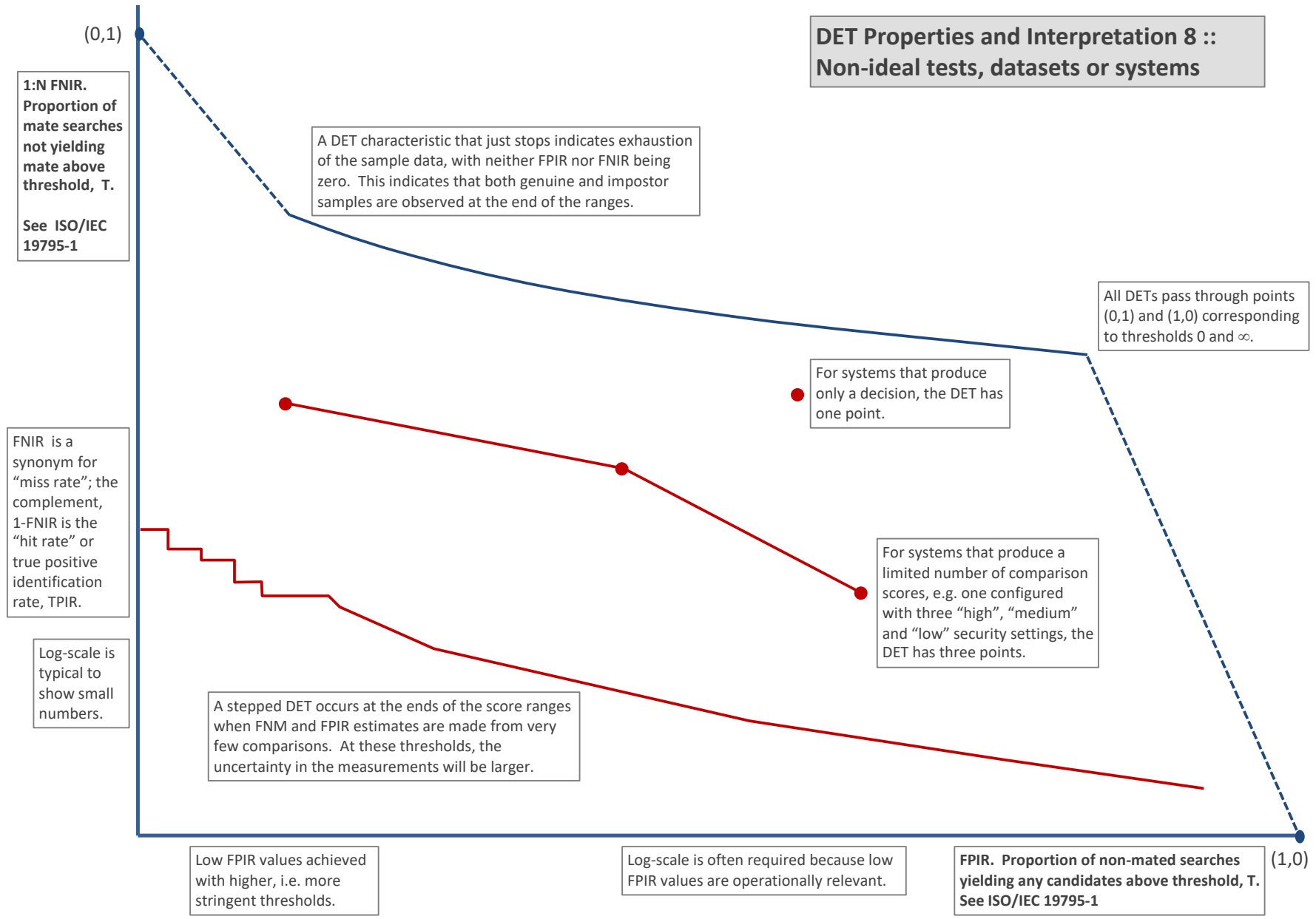

Figure 17: **DET as the primary performance reporting mechanism**.

3.4 Best practice testing requires execution of searches with and without mates

FRVT embeds 1:N searches of two kinds: Those for which there is an enrolled mate, and those for which there is not. The respective numbers for these types of searches appear in Table 1. However, it is common to conduct only mated searches[10]. The cumulative match characteristic is computed from candidate lists produced in mated searches. Even if the CMC is the only metric of interest, the actual trials executed in a test should nevertheless include searches for which no mate exists. As detailed in Table 1 the FRVT reserved disjoint populations of subjects for executing true non-mate searches.

3.5 Failure to extract features

During enrollment some algorithms fail to convert a face image to a template. The proportion of failures is the failure-to-enroll rate, denoted by FTE. Similarly, some search images are not converted to templates. The corresponding proportion is termed failure-to-extract, denoted by FTX.

We do not report FTX because we assume that the same underlying algorithm is used for template generation for enrollment and search.

Failure to extract rates are incorporated into FNIR and FPIR measurements as follows.

- **Enrollment templates**: Any failed enrollment is regarded as producing a zero length template. Algorithms are required by the API [10] to transparently process zero length templates. The effect of template generation failure on search accuracy depends on whether subsequent searches are mated, or non-mated: Mated searches will fail giving elevated FNIR; non-mated searches will not produce false positives so, to first order, FPIR will be reduced by a factor of $1-\text{FTE}$.

- **Search templates and 1:N search**: In cases where the algorithm fails to produce a search template from input imagery, the result is taken to be a candidate list whose entries have no hypothesized identities and zero score. The effect of template generation failure on search accuracy depends on whether searches are mated, or non-mated: Mated searches will fail giving elevated FNIR; Non-mated searches will not produce false positives, so FPIR will be reduced. Thus given a measurement of false negative and positive rates made over only those where failures-to-extract did not occur, those rates - call them $\text{FNIR}^{\dagger}$ and $\text{FPIR}^{\dagger}$ - could be adjusted by an explicit measurement of FTX as follows

$$\text{FNIR} = \text{FTX} + (1 - \text{FTX})\text{FNIR}^{\dagger} \tag{8}$$

$$\text{FPIR} = (1 - \text{FTX})\text{FPIR}^{\dagger} \tag{9}$$

This approach is the correct treatment for positive-identification applications such as access control where cooperative users are enrolled and make attempts at recognition. This approach is not appropriate to negative identification applications, such as visa fraud detection, in which hostile individuals may attempt to evade detection by submitting poor quality samples. In those cases, template generation failures should be investigated as though a false alarm had occurred.

[10]For example, the Megaface benchmark. This is bad practice for several reasons: First, if a developer knows, or can reasonably assume, that a mate always exists, then unrealistic gaming of the test is possible. A second reason is that it does not put FPIR on equal footing with FNIR and that matters because in most applications, not all searches have mates - not everyone has been previously enrolled in a driving license issuance or a criminal justice system - so addressing between-class separation becomes necessary.

This publication is available free of charge from: https://doi.org/10.6028/NIST.IR.8271

This publication is available free of charge from: https://doi.org/10.6028/NIST.IR.8271

3.6 Fixed length candidate lists, threshold independent workload

Suppose an automated face identification algorithm returns L candidates, and a human reviewer is retained to examine up to R candidates, where $R \leq L$ might be set by policy, preference or labor availability. For now, assume also that the reviewer is not provided with, or ignores, similarity scores, and thresholds are not applied. Given the algorithm typically places mates at low (good) ranks, the number of candidates a reviewer can be expected to review can be derived as follows. Note that the reviewer will:

- ▷ Always inspect the first ranked image — Frac. reviewed = 1
- ▷ Then inspect those candidates where mate not confirmed at rank 1 — Frac. reviewed = 1-CMC(1)
- ▷ Then inspect those candidates where mate not confirmed at rank 1 or 2 — Frac. reviewed = 1-CMC(2)

etc. Thus if the reviewer will stop after a maximum of R candidates, the expected number of candidate reviews is

$$M(R) = 1 + (1 - CMC(1)) + (1 - CMC(2)) + \ldots + (1 - CMC(R-1)) \tag{10}$$

$$= R - \sum_{r=1}^{R-1} CMC(r) \tag{11}$$

A recognition algorithm that front-loads the cumulative match characteristic will offer reduced workload for the reviewer. This workload is defined only over the searches for which a mate exists. In the cases where there truly is no mate, the reviewer would review all R candidates. Thus, if the proportion of searches for which a mate does exist is β, which in the law enforcement context would be the recidivism rate [3], the full expression for workload becomes:

$$M(R) = \beta \left(R - \sum_{r=1}^{R-1} CMC(r) \right) \quad + \quad (1 - \beta)R \tag{12}$$

$$= R - \beta \sum_{r=1}^{R-1} CMC(r) \tag{13}$$

3.7 Timing measurement

Algorithms were submitted to NIST as implementations of the application programming interface(API) specified by NIST in the Evaluation Plan [10]. The API includes functions for initialization, template generation, finalization, search, gallery insert, and gallery delete. Two template generation functions are required, one for the preparation of an enrollment template, and one for a search template.

In NIST's test harness, all functions were wrapped by calls to the C++ std::chrono::high resolution clock which on the dedicated timing machine counts 1ns clock ticks. Precision is somewhat worse than that however.

3.8 Uncertainty estimation

3.8.1 Random error

This study leverages operational datasets for measurement of recognition error rates. This affords several advantages. First, large numbers of searches are conducted (see Table 1) giving precision to the measurements. Moreover, for the two mugshot datasets, these do not involve reuse of individuals so binomial statistics can be expected to apply to recognition error counts. In that case, an observed count of a particular recognition outcome (i.e. a false negative or false positive) in M trials will sustain 95% confidence that the actual error rate is no larger than some value.

As an example, the minimum number of mugshot searches conducted in this report is M =154 549, and for an observed FNIR around 0.002, the measurement supports a conclusion that the actual FNIR is no higher than 0.00228 at 99% confidence level. On the false positive side, we tabulate FNIR at FPIR values as low as 0.001. Given estimates based on 331 254 non-mate trials, the actual FPIR values will be below 0.00115 at 99% confidence. In conclusion, large scale evaluation, without reuse of subjects, supports tight uncertainty bounds on the measured error rates.

3.8.2 Systematic error

The FRVT 2018 dataset includes anomalies discovered as a result of inspecting images involved in recognition failures from the most accurate algorithms. Two kinds of failure occur: False negatives (which, for the purpose here, include failures to make templates) and false positives.

False negative errors: We reviewed 600 false negative pairs for which either or both of the leading two algorithms did not put the correct mate in the top 50 candidates. Given 154 549 searches, this number represents 0.39% of the total, resulting in FNIR ~ 0.0039. Of the 600 pairs:

- **A: Poor quality**: About 20% of the pairs included images of very low quality, often greyscale, low resolution, blurred, low contrast, partially cropped, interlaced, or noisy scans of paper images. Additionally, in a few cases, the face is injured or occluded by bandages or heavy cosmetics.
- **B: Ground truth identity label bugs**: About 15% of the pairs are not actually mated. We only assigned this outcome when a pair is clearly not mated.
- **C: Profile views**: About 35% included an image of a profile (side) view of the face, or, more rarely, an image that was rotated 90 degrees in-plane (roll).
- **D: Tattoos**: About 30% included an image of a tattoo that contained a face image. These arise from mis-labelling in the parent dataset metadata.
- **E: Ageing**: There is considerable time-lapse between the two captures.

All these estimates are approximate. Of these, the tattoo and mislabled images can never be matched. These constitute an accuracy floor in the sample implying that FNIR cannot be below 0.0018[11]. The profile-views, low-quality images, and images with considerable ageing can, in principle, be successfully matched - indeed some algorithms do so - so are not part of the accuracy floor.

[11] This value is the sum of two partial false negative rates: FNIR_B = 0.15 * 0.0039 plus FNIR_D = 0.3 * 0.0039

This publication is available free of charge from: https://doi.org/10.6028/NIST.IR.8271

For the microsoft-4 algorithm the lowest miss rate from (recent entry in Table 21) is FNIR(640 000, 50, 0) = 0.0018. This is close to the value estimated from the inspection of misses. It is below the 0.0039 figure because the algorithm does match some profile and poor quality images, that the yitu-2 algorithm does not.

For many tables (e.g. Table 21), the FNIR values obtained for the FRVT-2018 mugshots could be corrected by reducing them by 0.0018. The best values would then be indistinct from zero. The results in this report *were not* adjusted to account for this systematic error.

False positive errors: As shown in Figure 1 and discussed in Figure 14 many of the DET characteristics in this report exhibit a pronounced turn upward at low false positive rates. The shape can be caused by identity labelling errors in the ground truth of a dataset, specifically persons present in the database under two IDs such that some proportion of non-mate pairs are actually mated. To look for such possibilities, we merged the highest 1000 non-mate pairs produced by three different algorithms which resulted in 1839 unique pairs. This constitutes 0.56% of all non-mate searches. We assert that it is *very* difficult for human reviewers to assign the pairs into the following three categories: twins; doppelgangers; or ground-truth errors (instances of the same person under two IDs). Given this difficulty we made no attempt to correct any possible ground truth errors except by removing 57 pairs in the following categories:

- **A: Profile views**: Thirteen pairs included one or two profile-view images. As described in Figure 127, these can cause false positives.
- **B: Same-session photographs**: For twelve pairs, the images were identical or trivially altered (e.g. cropped) versions of the same photo. These were present under a different ID likely due to some clerical or procedural mistake.
- **C: Tattoos of faces**: There were fourteen instances of tattoo photographs that contained faces causing false matches.
- **D: T-shirt faces**: There were six instances of T-shirt photographs (of Bob Marley and Che Guevara) being detected instead of the face and causing false positives.
- **E: Background faces**: There were twelve instances of one subject appearing in the background of two otherwise correct portrait photos.

Note we did not remove any images where there was a chance that the pair was actually a different person.

In any case, the results in this report have not been adjusted for this systematic error.

This publication is available free of charge from: https://doi.org/10.6028/NIST.IR.8271

4 Results

This section gives extensive results for algorithms submitted to FRVT 2018. Three page "report cards" for each algorithm are contained in a separate supplement. Performance metrics were described in section 3. The main results are summarized in tabular form with more exhaustive data included as DET, CMC and related graphs in appendices as follows:

- The three tables 2-4 list algorithms alongside full developer names, acceptance date, size of the provided configuration data, template size and generation time, and search duration data.
  - The **template generation duration** is most important to applications that require fast response. For example, an eGate taking more than two seconds to produce a template might be unacceptable. Note that GPUs may be of utility in expediting this operation for some algorithms, though at additional expense. Two additional factors should be considered[12][13].
  - The **search duration** is the time taken for a search of a search template into a gallery of N enrollment templates. This performance variable, together with the volume of searches, is influential on the amount of hardware needed to sustain an operational deployment. This is measured here with the algorithm running on a single core of a contemporary CPU. Search is most simply implemented as N computations of a distance metric followed by a sort operation to find the closest enrollments. However, considerable optimization of this process is possible, up to and including fast-search algorithms that, by various means, avoid computation of all N distances.
  - The **template size** is the size of the extracted feature vector (or vectors) and any needed header information. Large template sizes may be influential on bus or network bandwidth, storage requirements, and on search duration. While the template itself is an opaque data blob, the feature dimensionality might be estimated by assuming a four-bytes-per-float encoding. There is a wide range of encodings. For the more accurate algorithm, sizes range from 256 bytes to about 2KB bytes, indicating essentially no consensus on face modeling and template design.
  - The **template size multiplier** column shows how, given k input images, the size of the template grows. Most implementations internally extract features from each image and concatenate them, and implement some score-level fusion logic during search. Other implementations, including many of the most accurate algorithms, produce templates whose size does not grow with k. This could be achieved via selection of the best quality image - but this is not optimal in handling ageing where the oldest image could be the best quality. Another mechanism would be feature-level fusion where information is fused from all k inputs. In any case, as a black-box test, the fusion scheme is proprietary and unknown.
  - The size of the **configuration data** is the total size of all files resident in a vendor-provided directory that contains arbitrary read-only files such as parameters, recognition models (e.g caffe). Generally a large value for this quantity may prohibit the use of the algorithm on a resource-constrained device.

[12] The FRVT 2018 API prohibited threading, so some gains from parallelism may be available on multiple-cores or multiple processors, if the feature extraction code could be distributed across them.

[13] Note also that factors of two or more may be realizable by exploiting modern vector processing instructions on CPUs. It is not clear in our measurements whether all developers exploited Intel's AVX2 instructions, for example. Our machine was so equipped, but we insisted that the same compiled library should also run on older machines lacking that instruction. The more sophisticated implementations may have detected AVX2 presence and branched accordingly. The less sophisticated may be defaulted to the reduced instruction set. Readers should see the FRVT 2018 API document for the specific chip details.

This publication is available free of charge from: https://doi.org/10.6028/NIST.IR.8271

This publication is available free of charge from: https://doi.org/10.6028/NIST.IR.8271

▷ Tables 21-22 report core rank-based accuracy for mugshot images. The population size is limited to N = 1.6 million identities because this is the largest gallery size on which all algorithms were executed. Notable observations from these tables are as follows:

- **Accuracy gains since 2018**: NIST Interagency Report 8238 documented massive gains over those reported in the FRVT 2014 report, NIST Interagency Report 8009. Further gains are documented in this report. Comparing the most accurate algorithm in November 2018, NEC-3, the value of FNIR(N, L, T) reduced from 0.0031 to 0.0024 for the Sensetime-004 algorithm with N = 12 million recent images. The tables show broader gains: many developers have made advances since 2018 with between two and five-fold reduction in errors.
- **Wide range in accuracy**: The rank-1 miss rates vary from FNIR(N, 1, 0) = 0.0012 for sensetime-004 up to about 0.5 for the very fast but inaccurate microfocus-x algorithms. Among the developers who are superior to NEC in 2013, the range is from 0.002 to 0.035 for camvi-3. This large accuracy range is consistent with the buyer-beware maxim, and indicates that face recognition software is far from being commoditized.

▷ Tables 25-26 report threshold-based error rates, FNIR(N, L, T), for N = 1.6 million for mugshot-mugshot accuracy on FRVT 2014, FRVT 2018, and also (in pink) mugshot-webcam accuracy using FRVT 2018 enrollments. Notable observations from these tables are as follows:

- **Order of magnitude accuracy gains since 2014**: As with rank-based results, the gains in accuracy are substantial, though somewhat reduced. At FPIR = 0.01, the best improvement over NEC in 2014 is a 27 fold reduction in FNIR using the NEC_2 algorithm. At FPIR = 0.001, the largest gain is a six-fold reduction in FNIR via the NEC_3 algorithm.
- **Broad gains across the industry**: About 19 companies realize accuracy better than the NEC benchmark from 2014. This is somewhat lower than the 28 developers who succeeded on the rank-1 metric. This may be due to the ubiquity of, and emphasis on, the rank-1 metric in many published algorithm development papers.
- **Webcam images**: Searches of webcam images give FNIR(N, T) values around 2 to 3 times higher than mugshot searches. Notably the leading developers with mugshots are approximately the same with poorer quality webcams. But some developers e.g. Camvi, Megvii, TongYi, and Neurotechnology do improve their relative rankings on webcams, perhaps indicating their algorithms were tailored to less constrained images.

▷ Tables 15, 18, 19 and show, respectively, high-threshold, rank 1, and rank 50 FNIR values for all algorithms performing searches into five different gallery sizes, N = 640 000, N = 1 600 000, N = 3 000 000, N = 6 000 000 and 12 000 000. The FPIR = 0.001 table is included to inform high-volume duplicate detection applications. The Rank-1 table is included as a primary accuracy indicator. The Rank-50 table is included to inform agencies who routinely produce 50 candidates for human-review. The notable results are:

- **Slow growth in rank-based miss rates:** FNIR(N, R) generally grows as a power law, aN^b. From the straight lines of many graphs of Figure 20 this is clearly a reasonable model for most, but not all, algorithms. The coefficient a can be interpreted as FNIR in a gallery of size 1. The more important coefficient b indicates scalability, and often, $b \ll 1$, implies very benign growth in FNIR. The coefficients of the models appear in the Tables 18 and 19.
- **Slow growth in threshold-based miss rates:** FNIR(N, T) also generally grows as a power law, aN^b except at the high threshold values corresponding to low FPIR values. This is visible in the plots of Figure 36 which

show straight lines except for FPIR = 0.001, which increase more rapidly with N above 3 000 000. Each trace in those figures shows FNIR(N, T) at fixed FPIR with both N and T varying. Thus at large N, it is usually necessary to elevate T to maintain fixed FPIR. This causes increased FNIR. Why that would no-longer obey a power-law is not known. However, if we expect large galleries to contain individuals with familial relations to the non-mate search images - in the most extreme case, twins - then suppression of false positives becomes more difficult. This is discussed in the Figures starting at Fig. 10

▷ Figure **??** shows false positives from twins against their enrolled siblings, broken out by type of twin: fraternal or identical. The Figure is based on the enrollment of 104 single images on one of a pair of twins, and then the search of 2354 second images. Note that the dataset is heavily skewed towards identical twins which is not representative of the true population. There is also a skew towards same sex fraternal twin pairs compared to different sex fraternal twin pairs again not representative of the true population.

The notable results are:

- For all algorithms tested, the 1087 mated searches (Twin A vs. Twin A) produce scores almost always above typical operational thresholds, with (not shown) matches at rank 1. The images are of good quality, so this is the result expected from the rest of this report.
- For the 1066 identical twin searches (AB), almost all produce the twin at rank 1, with a few producing the mate at further down the candidate lists rank and low score.
- For the 169 fraternal searches (AB) from same sex pairs, most algorithms give a large number of very high scores, implying false positives at all thresholds. However, there there are long tails containing lower scores that are correctly below threshold. In general, scores that are higher in this distribution are all rank 1 whereas the lower scores have much higher ranks.
- (Not shown) Of the 169, there are 24 fraternal searches (AB) involving different sex twins. Here most algorithms correctly report scores well below the lowest threshold, and usually not on the candidate list at all.

This publication is available free of charge from: https://doi.org/10.6028/NIST.IR.8271

This publication is available free of charge from: https://doi.org/10.6028/NIST.IR.8271

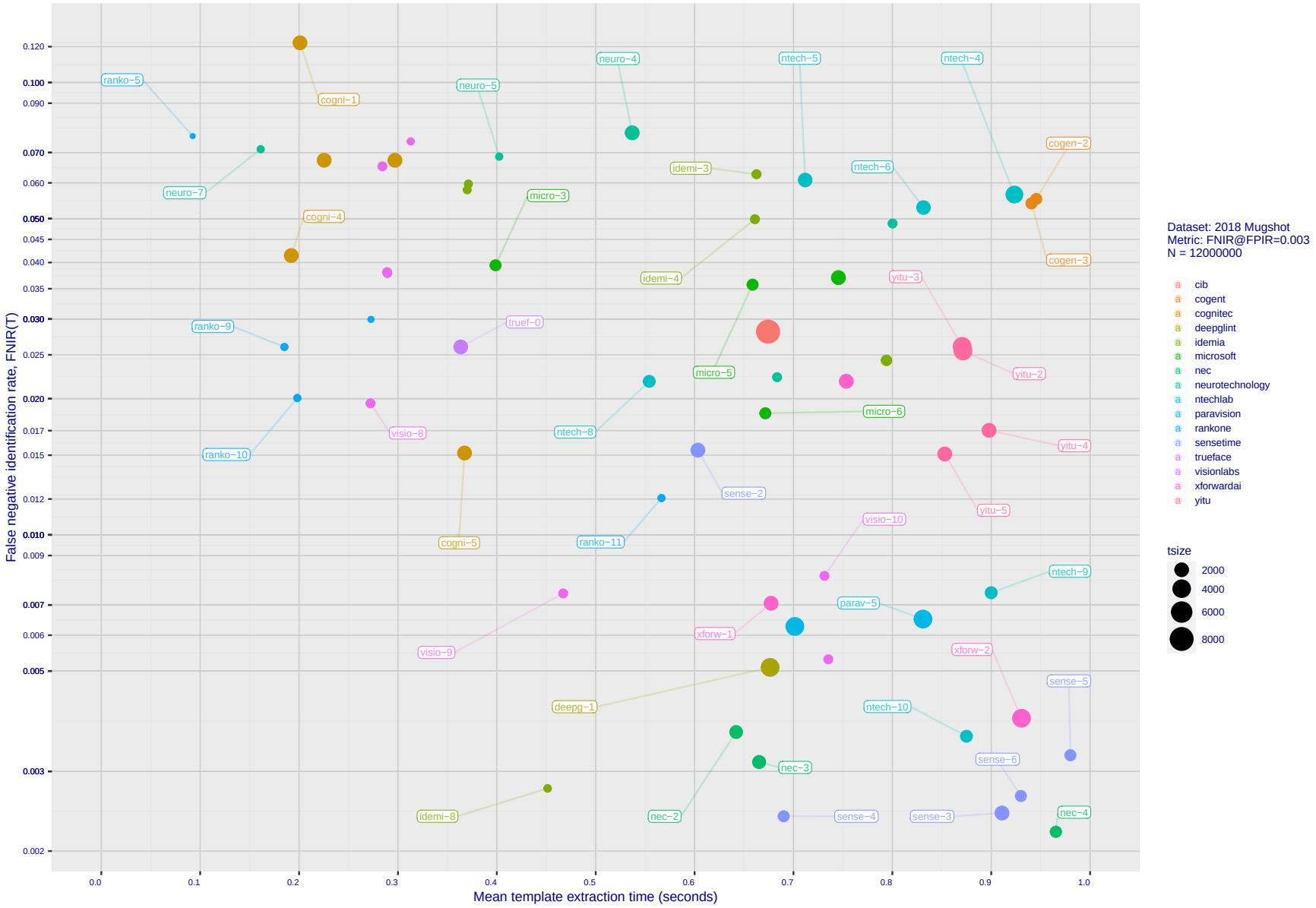

Figure 18: **[Mugshot Dataset] Speed-accuracy tradeoff**. *For developers of the more accurate algorithms the plot shows the tradeoff of high-threshold recognition miss-rates, FNIR(N, N, T) for FPIR(N, T) = 0.003, and template generation time. Developers are coded by color. Template size is encoded by the size of the circle. Some labels are quite distant from the respective point, to avoid superposing text. Without any other influences, the assumption would be that taking time to localize the face, and extract features, would lead to better accuracy. The most notable result, for NEC, is that their slower algorithms are much more accurate than the version that extract features in fewer than 90 milliseconds.*

2021/11/22 08:35:53
FNIR(N, R, T) = False neg. identification rate
FPIR(N, T) = False pos. identification rate
N = Num. enrolled subjects
R = Num. candidates examined
T = Threshold
T = 0 → Investigation
T > 0 → Identification

This publication is available free of charge from: https://doi.org/10.6028/NIST.IR.8271

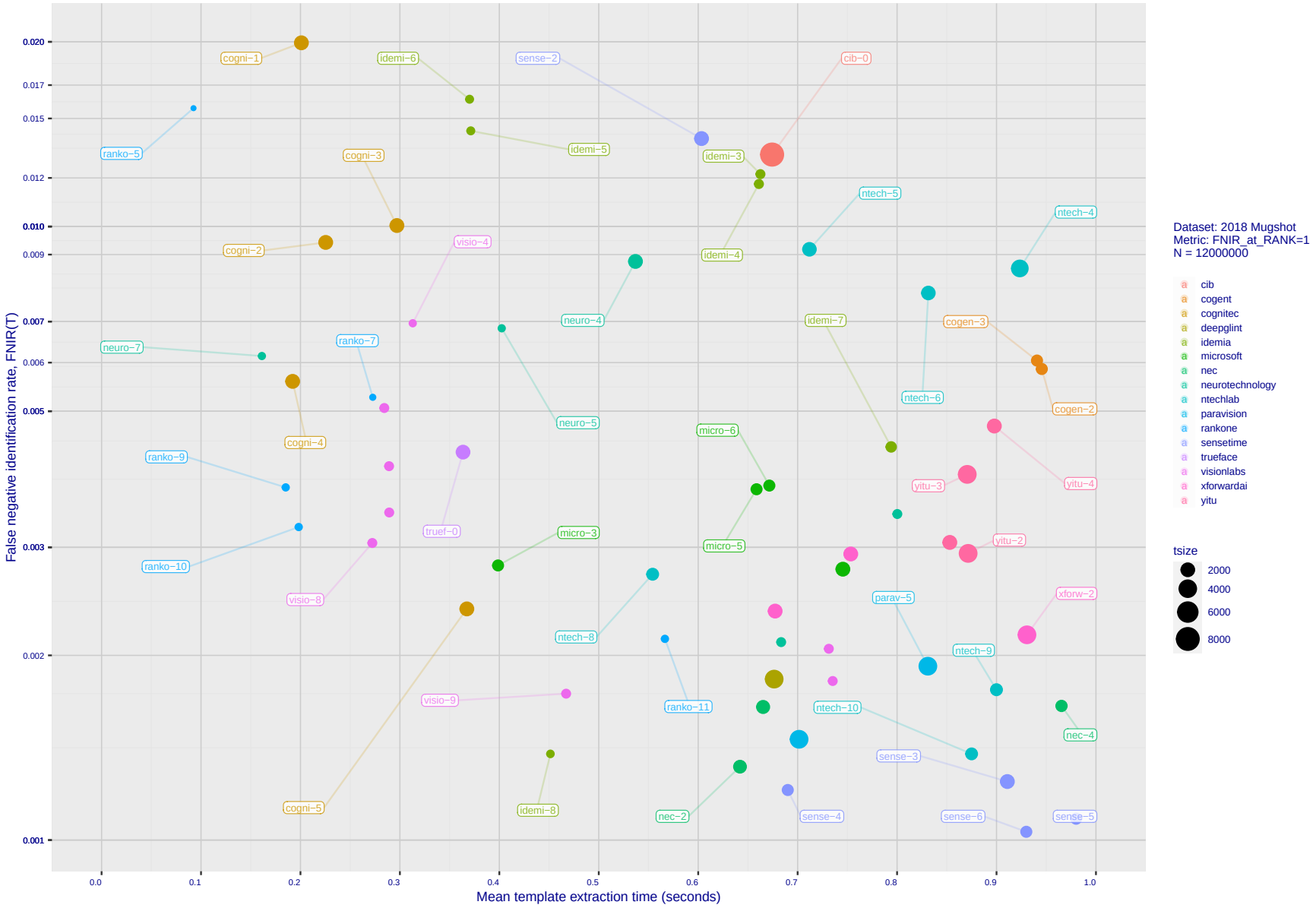

Figure 19: **[Mugshot Dataset] Speed-accuracy tradeoff**. *For developers of the more accurate algorithms the plot shows the tradeoff of rank-one recognition miss-rates, FNIR(N, 1, 0), and template generation time. Developers are coded by color. Template size is encoded by the size of the circle. Some labels are quite distant from the respective point, to avoid superposing text. Without any other influences, the assumption would be that taking time to localize the face, and extract features, would lead to better accuracy. This occurs for NEC with their slower algorithm being much accurate than the version that extract features in fewer than 90 milliseconds.*

2021/11/22 08:35:53
FNIR(N, R, T) = False neg. identification rate
FPIR(N, T) = False pos. identification rate
N = Num. enrolled subjects
R = Num. candidates examined
T = Threshold
T = 0 → Investigation
T > 0 → Identification

This publication is available free of charge from: https://doi.org/10.6028/NIST.IR.8271

	DEVELOPER	SHORT	SEQ.	VALIDATION	CONFIG[1]	LIB[1]	TEMPLATE GENERATION			FINALIZE[2]	SEARCH DURATION[5] MILLISEC					
	FULL NAME	NAME	NUM.	DATE	DATA (MB)	DATA (MB)	SIZE (B)	MULT[3]	TIME (MS)[4]	TIME (S)	L=1	L=50	L=50	L=50	L=50	POWER LAW
											N=1.6M	N=1.6M	N=3M	N=6M	N=12M	(μs)
1	20Face	20face	000	2021-10-01	112	319	[119]2048	-	[20]236	[51]9	[177]6355	[179]6341	-	-	-	
2	3Divi	3divi	5	2018-10-26	186	51	[174]4096	k	[96]638	[144]28	[81]538	[81]537	[76]1377	[73]2614	[69]5530	$^{120}0.07N^{1.1}$
3	3Divi	3divi	6	2018-10-26	187	51	[35]528	k	[97]640	[25]5	[12]33	[13]33	-	-	-	
4	Acer Incorporated	acer	000	2020-08-12	35	67	[27]512	-	[15]198	[15]4	[54]295	[55]295	[46]623	[67]2302	[62]4915	$^{148}0.00N^{1.3}$
5	Acer Incorporated	acer	001	2021-11-08	42	610	[113]2048	-	[11]184	[49]9	[91]619	[88]575	-	-	-	
6	Akurat Satu Indonesia	ptakuratsatu	000	2020-10-23	0	572	[37]538	-	[180]905	[189]28633	[6]15	[6]16	[6]17	[5]17	[4]17	$^{3}6827.74N^{0.1}$
7	Alchera Inc	alchera	2	2018-10-30	7	14	[92]2048	k	[6]114	[171]63	[156]2923	[159]2929	-	-	-	
8	Alchera Inc	alchera	3	2018-10-30	251	14	[104]2048	k	[80]531	[172]63	[157]2955	[160]2956	[136]6546	[137]15013	[137]35262	$^{143}0.10N^{1.2}$
9	Alchera Inc	alchera	004	2021-09-17	476	24	[126]2048	-	[164]853	[156]35	[178]6657	[185]6851	-	-	-	
10	Alivia / Innovation Sys	isystems	3	2018-10-30	350	784	[125]2048	1	[154]825	[116]16	[66]385	[68]389	[61]979	[60]1822	[89]9348	$^{149}0.00N^{1.3}$
11	AllGoVision	allgovision	000	2019-07-30	168	150	[120]2048	k	[50]404	[72]12	[160]3226	[163]3193	[134]6129	[134]12449	[134]25835	$^{68}1.40N^{1.0}$
12	AllGoVision	allgovision	001	2020-07-14	283	126	[131]2048	-	[142]777	[78]13	[159]3174	[162]3183	[133]6073	[132]12284	[133]25701	$^{66}1.42N^{1.0}$
13	Anke Investments	anke	0	2018-10-30	779	27	[157]2072	k	[57]429	[114]16	[93]675	[99]748	[81]1483	[80]2968	[74]6148	$^{90}0.21N^{1.1}$
14	Anke Investments	anke	1	2018-10-30	779	27	[158]2072	k	[58]430	[108]15	[98]707	[102]769	-	-	-	
15	Anke Investments	anke	002	2019-06-27	341	401	[150]2056	k	[92]623	[87]13	[92]624	[94]682	[73]1306	[69]2403	[66]5082	$^{59}0.30N^{1.0}$
16	Aware	aware	5	2018-10-30	368	27	[166]3100	k	[147]792	[154]34	[16]95	[20]98	[19]203	[17]371	[13]252	$^{14}4.13N^{0.7}$
17	Aware	aware	6	2018-10-30	368	27	[2]124	k	[146]789	[2]2	[31]158	[31]162	-	-	-	
18	Ayonix	ayonix	1	2018-10-29	74	2	[54]1036	k	[2]12	[67]11	[50]279	[51]279	-	-	-	
19	Ayonix	ayonix	2	2018-10-30	74	2	[55]1036	1	[1]11	[93]14	[49]279	[50]276	[37]535	[36]1087	[36]2284	$^{75}0.11N^{1.0}$
20	Camvi Technologies	camvitech	4	2018-10-30	233	220	[45]1024	1	[112]686	[152]31	[13]33	[12]32	[11]38	[10]40	[7]48	$^{4}8492.66N^{0.1}$
21	Camvi Technologies	camvitech	5	2018-10-30	257	220	[44]1024	1	[133]751	[150]31	[11]31	[10]30	-	-	-	
22	Canon Inc	cib	000	2020-10-19	426	127	[190]8196	-	[106]674	[176]113	[161]3589	[165]3604	[137]6738	[135]13495	[135]27114	$^{27}2.33N^{1.0}$
23	Canon Inc	canon	001	2021-10-27	1139	91	[172]4096	-	[173]885	[131]21	[180]6804	[183]6789	[151]12741	[147]25650	[145]51922	$^{45}3.82N^{1.0}$
24	Clearview AI Inc	clearviewai	000	2021-11-12	358	316	[178]4096	-	[137]765	[148]30	[103]802	[92]657	[66]1134	[62]1939	[56]3889	$^{19}1.59N^{0.9}$
25	Cloudwalk - Hengrui AI Technology	hr	000	2021-02-10	501	392	[117]2048	-	[181]905	[101]15	[51]282	[49]276	[39]539	[44]1268	[50]3177	$^{124}0.03N^{1.1}$
26	Cognitec Systems GmbH	cognitec	2	2018-10-30	463	26	[134]2052	k	[19]225	[139]27	[141]1733	[143]1763	[122]3660	[120]7279	[118]13895	$^{63}0.83N^{1.0}$
27	Cognitec Systems GmbH	cognitec	3	2018-10-30	465	26	[141]2052	k	[30]297	[112]16	[140]1719	[144]1791	[121]3638	[119]7277	[122]14904	$^{82}0.66N^{1.0}$
28	Cognitec Systems GmbH	cognitec	004	2021-03-08	384	60	[135]2052	-	[14]192	[85]13	[139]1673	[141]1727	[112]2904	[110]5801	[108]11707	$^{24}1.15N^{1.0}$
29	Cognitec Systems GmbH	cognitec	005	2021-07-30	460	61	[147]2052	-	[38]367	[53]9	[132]1556	[133]1551	[114]2916	[118]6561	[119]13958	$^{96}0.38N^{1.1}$
30	Cubox	cubox	000	2021-08-24	529	298	[106]2048	-	[183]917	[60]10	[162]3646	[167]4076	[139]7605	[138]15871	-	$^{89}1.16N^{1.1}$
31	Cyberlink Corp	cyberlink	000	2019-06-12	217	93	[136]2052	1	[100]654	[147]30	[95]696	[96]701	[77]1379	[74]2639	[76]6214	$^{77}0.28N^{1.0}$
32	Cyberlink Corp	cyberlink	001	2019-10-07	459	102	[138]2052	1	[55]423	[145]28	[96]698	[95]700	[75]1350	[108]5524	[111]12031	$^{147}0.00N^{1.3}$
33	Cyberlink Corp	cyberlink	002	2020-07-31	333	109	[185]4140	-	[127]724	[180]6875	[129]1353	[164]3198	[135]6138	[131]12205	[116]13106	$^{17}16.71N^{0.8}$
34	Cyberlink Corp	cyberlink	003	2021-01-05	333	100	[187]6212	-	[115]691	[158]35	[76]488	[97]723	[79]1415	[78]2886	[70]5643	$^{106}0.12N^{1.1}$
35	Cyberlink Corp	cyberlink	004	2021-07-16	371	100	[188]6212	-	[129]728	[135]23	[77]492	[80]504	[60]923	[50]1448	[52]3350	$^{21}0.73N^{0.9}$
36	Dahua Technology Co Ltd	dahua	0	2018-10-29	276	167	[89]2048	k	[43]374	[133]22	-	[47]258	-	-	-	
37	Dahua Technology Co Ltd	dahua	1	2018-10-29	276	167	[83]2048	k	[39]369	[141]28	-	[46]257	[44]602	[42]1202	[48]3007	$^{131}0.02N^{1.2}$
38	Dahua Technology Co Ltd	dahua	002	2019-12-02	607	137	[99]2048	k	[111]685	[127]19	[41]243	[48]269	[69]1189	[79]2950	[79]6732	$^{153}0.00N^{1.5}$
39	Dahua Technology Co Ltd	dahua	003	2020-11-18	889	154	[127]2048	-	[126]723	[120]18	[52]283	[45]249	[34]468	[34]935	[32]1871	$^{29}0.16N^{1.0}$
40	Deepglint	deepglint	001	2019-11-15	448	265	[179]4096	-	[108]676	[155]35	[94]677	[131]1495	[86]1724	[76]2747	[77]6246	$^{15}25.27N^{0.8}$
41	Dermalog	dermalog	5	2018-10-26	0	440	[3]128	1	[79]528	[179]3155	[1]0	[1]0	[1]0	[1]0	[1]0	$^{5}66.21N^{0.2}$
42	Dermalog	dermalog	6	2018-10-26	0	453	[13]256	1	[76]507	[3]2	[28]142	[28]144	[24]269	[23]531	[22]1294	$^{83}0.05N^{1.0}$
43	Dermalog	dermalog	007	2020-02-12	0	424	[4]128	1	[52]410	[1]1	[21]98	[18]96	[21]218	[19]429	[19]1013	$^{113}0.01N^{1.1}$
44	Dermalog	dermalog	008	2021-01-25	0	531	[31]512	-	[41]370	[17]4	[60]335	[41]246	[33]462	[33]924	[31]1849	$^{34}0.15N^{1.0}$
45	Dermalog	dermalog	009	2021-11-09	0	318	[30]512	-	[35]347	[12]3	[45]253	[42]246	[32]461	[32]923	[30]1846	$^{31}0.16N^{1.0}$
46	FarBar Inc	f8	001	2019-10-03	266	19	[87]2048	k	[151]810	[90]14	-	-	-	-	-	
47	Fincore Ltd	fincore	000	2021-08-18	250	224	[111]2048	-	[67]475	[46]9	[86]562	[85]560	-	-	-	
48	Fujitsu Research and Development Center	fujitsulab	000	2021-10-12	497	337	[51]1032	-	[188]945	[27]5	[138]1668	[137]1657	[118]3140	[115]6320	[114]12723	$^{58}0.78N^{1.0}$
49	Gorilla Technology	gorilla	2	2018-10-29	91	1252	[61]1132	k	[34]338	[137]24	[29]145	[29]146	[25]293	[24]612	[26]1509	$^{111}0.02N^{1.1}$
50	Gorilla Technology	gorilla	3	2018-10-26	94	1252	[159]2156	k	[82]559	[184]12020	-	[147]2047	-	-	-	
51	Gorilla Technology	gorilla	004	2020-01-06	182	1244	[160]2192	k	[45]388	[160]41	[53]286	[54]285	[70]1191	[70]2416	[65]5036	$^{146}0.00N^{1.3}$
52	Gorilla Technology	gorilla	005	2021-02-22	306	1420	[189]6288	-	[71]483	[174]78	[102]802	[103]799	[82]1514	[91]4454	[85]8820	$^{133}0.05N^{1.2}$

Notes	
1	Configuration size does not capture static data present in libraries. Libraries are included but the size also includes any ancillary libraries for image processing (e.g. openCV) or numerical computation (e.g. blas).
2	Finalization is the processing of converting N = 1600000 templates into a searchable data structure an operation which can be a simple copy, or the building of an index or tree, for example. The duration of the operation may be data dependent, and may not be linear in the number of input templates.
3	This multiplier expresses the increase in template size when k images are passed to the template generation function.
4	All durations are measured on Intel®Xeon®CPU E5-2630 v4 @ 2.20GHz processors. Estimates are made by wrapping the API function call in calls to std::chrono::high_resolution_clock which on the machine in (3) counts 1ns clock ticks. Precision is somewhat worse than that however.
5	Search durations are measured as in the prior note. The power-law model in the final column mostly fits the empirical results in Figure 128. However in certain cases the model is not correct and should not be used numerically.

Table 2: Summary of algorithms and properties included in this report. The blue superscripts give ranking for the quantity in that column. Missing search durations, denoted by "-", are absent because those runs were not executed, usually because we did not run on the larger galleries. Caution: The power-law model is sometimes an incorrect model. It is included here only to show broad sublinear behavior, which is flagged in green. The models should not be used for prediction.

2021/11/22 08:35:53

FNIR(N, R, T) = False neg. identification rate
FPIR(N, T) = False pos. identification rate

N = Num. enrolled subjects
R = Num. candidates examined

T = Threshold

T = 0 → Investigation
T > 0 → Identification

This publication is available free of charge from: https://doi.org/10.6028/NIST.IR.8271

	DEVELOPER	SHORT	SEQ.	VALIDATION	CONFIG[1]	LIB[1]	TEMPLATE GENERATION			FINALIZE[2]	SEARCH DURATION[5] MILLISEC					
	FULL NAME	NAME	NUM.	DATE	DATA (MB)	DATA (MB)	SIZE (B)	MULT[3]	TIME (MS)[4]	TIME (S)	L=1	L=50	L=50	L=50	L=50	POWER LAW
											N=1.6M	N=1.6M	N=3M	N=6M	N=12M	(μs)
53	Gorilla Technology	gorilla	006	2021-09-30	377	691	[191]8336	-	[138]767	[175]99	[135]1626	[134]1612	[99]2422	[90]4422	[90]9363	[57]$0.59N^{1.0}$
54	Griaule	griaule	000	2021-11-01	0	584	[146]2052	-	[54]417	[36]8	[173]5827	[177]6150	[144]11473	[142]22952	[140]46070	[28]$3.89N^{1.0}$
55	Guangzhou Pixel Solutions Co Ltd	pixelall	002	2019-07-01	0	165	[161]2560	k	[13]190	[105]15	[127]1296	[128]1334	[105]2526	[100]5136	[104]11045	[76]$0.52N^{1.0}$
56	Guangzhou Pixel Solutions Co Ltd	pixelall	003	2019-11-05	0	690	[164]2560	k	[120]703	[134]22	[124]1273	[125]1307	[102]2474	[101]5198	[105]11141	[84]$0.46N^{1.0}$
57	Guangzhou Pixel Solutions Co Ltd	pixelall	004	2020-07-02	0	538	[163]2560	k	[59]449	[119]17	[123]1259	[124]1300	[101]2465	[106]5492	[106]11443	[95]$0.34N^{1.1}$
58	Guangzhou Pixel Solutions Co Ltd	pixelall	005	2021-03-23	0	717	[162]2560	-	[160]840	[66]11	[134]1606	[132]1528	[107]2609	[97]4926	[109]11770	[50]$0.73N^{1.0}$
59	Hikvision Research Institute	hikvision	5	2018-10-29	593	9	[65]1408	1	[89]607	[111]16	[108]883	[109]895	[89]1908	[84]3792	[91]9387	[121]$0.10N^{1.1}$
60	Hikvision Research Institute	hikvision	6	2018-10-29	593	9	[66]1408	1	[87]598	[113]16	[106]871	[108]877	-	-	-	
61	HyperVerge Inc	hyperverge	001	2021-08-11	1791	212	[47]1024	-	[162]845	[23]5	[97]705	[93]681	[74]1346	[75]2681	[71]5680	[65]$0.32N^{1.0}$
62	Idemia	idemia	5	2018-10-29	417	48	[20]352	1	[42]371	[24]5	[25]137	[26]138	[30]437	[29]724	[27]1630	[140]$0.01N^{1.2}$
63	Idemia	idemia	6	2018-10-29	417	48	[21]352	1	[40]370	[21]4	[26]137	[25]138	[31]442	[31]827	[28]1646	[142]$0.01N^{1.2}$
64	Idemia	idemia	007	2020-01-17	738	113	[42]860	1	[148]794	[91]14	[30]151	[30]152	[49]683	[52]1481	[49]3022	[151]$0.00N^{1.4}$
65	Idemia	idemia	008	2021-03-15	378	65	[19]300	-	[61]451	[13]3	[24]132	[24]131	[22]247	[21]501	[20]1013	[47]$0.07N^{1.0}$
66	Imagus Technology Pty Ltd	imagus	005	2021-01-15	222	311	[114]2048	-	[145]786	[89]14	[40]236	[58]313	[47]651	[47]1361	[38]2461	[119]$0.03N^{1.1}$
67	Imagus Technology Pty Ltd	imagus	006	2021-05-27	248	369	[90]2048	-	[179]904	[55]9	[58]317	[40]234	[35]499	[45]1273	[41]2727	[139]$0.01N^{1.2}$
68	Imperial College London	imperial	000	2019-08-28	461	15	[112]2048	1	[84]577	[77]13	[63]360	[67]379	[83]1626	[87]4057	[102]10291	[154]$0.00N^{1.5}$
69	Incode Technologies Inc	incode	2	2018-10-29	71	31	[81]2048	1	[27]289	[110]15	[71]411	[69]404	-	-	-	
70	Incode Technologies Inc	incode	3	2018-10-29	133	31	[132]2048	1	[118]697	[100]15	[70]408	[72]412	[55]847	[53]1608	[60]4486	[115]$0.05N^{1.1}$
71	Incode Technologies Inc	incode	004	2019-06-24	254	50	[108]2048	1	[68]475	[70]12	[64]365	[66]378	[80]1482	[55]1660	[47]2954	[93]$0.12N^{1.1}$
72	Incode Technologies Inc	incode	005	2021-07-29	259	21	[98]2048	-	[73]500	[59]10	[57]316	[76]454	[59]890	[61]1843	[55]3640	[105]$0.07N^{1.1}$
73	Innovatrics	innovatrics	4	2018-10-30	0	400	[59]1076	k	[46]399	[181]10902	[5]8	[4]8	[4]11	[2]9	[3]13	[9]$668.38N^{0.2}$
74	Innovatrics	innovatrics	005	2019-09-30	0	455	[38]538	1	[156]827	[183]11897	[4]8	[5]8	[3]9	[3]9	[2]9	[1]$4055.65N^{0.1}$
75	Innovatrics	innovatrics	007	2021-08-16	175	58	[36]538	-	[141]777	[92]14	[20]97	[21]100	[17]188	[18]378	[17]788	[22]$0.09N^{1.0}$
76	IrexAI	irex	000	2021-02-09	724	46	[165]3080	-	[161]844	[126]19	[90]616	[89]600	[65]1120	[72]2477	[72]5863	[99]$0.13N^{1.1}$
77	Kakao Enterprise	kakao	000	2021-06-23	404	124	[144]2052	-	[159]835	[38]8	[39]213	[38]215	[36]510	[35]971	[33]1955	[101]$0.05N^{1.1}$
78	Kedacom International Pte	kedacom	001	2019-09-16	239	36	[17]292	1	[75]507	[4]2	[100]764	[100]760	[90]1940	[81]2983	[78]6623	[79]$0.31N^{1.0}$
79	Kneron	kneron	000	2020-03-03	366	13	[100]2048	k	[78]523	[82]13	[153]2535	[156]2506	[131]4752	[129]9696	[131]20926	[80]$0.95N^{1.0}$
80	Kneron	kneron	001	2021-06-10	270	69	[82]2048	-	[66]472	[47]9	[154]2690	[158]2642	-	-	-	
81	Line Corporation	line	000	2021-06-02	138	397	[129]2048	-	[70]481	[40]8	[168]5433	[172]5418	[142]10144	-	-	[26]$3.65N^{1.0}$
82	Lomonosov Moscow State University	intsysmsu	000	2019-08-19	375	168	[115]2048	1	[90]614	[83]13	[73]430	[74]431	[58]860	[56]1730	[68]5353	[129]$0.03N^{1.1}$
83	Lookman Electroplast Industries	lookman	3	2018-10-28	203	24	[18]292	1	[33]336	[11]3	[99]739	[98]745	[78]1394	[77]2817	[82]8286	[109]$0.13N^{1.1}$
84	Lookman Electroplast Industries	lookman	4	2018-10-28	184	24	[40]548	1	[31]320	[20]4	[111]981	[112]998	-	-	-	
85	Lookman Electroplast Industries	lookman	005	2019-09-16	239	36	[39]548	1	[74]506	[16]4	[112]1005	[113]1008	[106]2597	[105]5446	[86]8939	[107]$0.19N^{1.1}$
86	Mantra Softech India	mantra	000	2021-10-28	460	61	[145]2052	-	[53]412	[58]10	[110]916	[110]910	[85]1714	[83]3411	[80]6841	[32]$0.57N^{1.0}$
87	Megvii/Face++	megvii	1	2018-10-28	1703	41	[175]4096	1	[94]631	[153]32	[82]552	[86]561	[72]1222	[68]2321	[73]5968	[114]$0.08N^{1.1}$
88	Megvii/Face++	megvii	2	2018-10-28	1735	42	[176]4096	1	[95]635	[151]31	[83]553	[83]558	-	-	-	
89	MicroFocus	microfocus	5	2018-10-29	94	26	[11]256	k	[23]262	[7]2	[36]182	[35]186	[28]354	[28]708	[24]1425	[43]$0.11N^{1.0}$
90	MicroFocus	microfocus	6	2018-10-29	94	26	[12]256	k	[24]262	[9]2	[37]183	[34]186	-	-	-	
91	Microsoft	microsoft	5	2018-10-29	381	155	[46]1024	1	[101]658	[68]11	[133]1606	[138]1673	[117]3076	[114]6302	[117]13160	[56]$0.79N^{1.0}$
92	Microsoft	microsoft	6	2018-10-29	478	155	[43]1024	1	[104]671	[104]15	[136]1642	[136]1618	[123]3710	[116]6401	[115]12892	[72]$0.68N^{1.0}$
93	N-Tech Lab	ntech	5	2018-10-30	1685	113	[77]1940	k	[124]711	[169]55	[43]243	[44]246	[38]538	[37]1100	[44]2867	[125]$0.02N^{1.1}$
94	N-Tech Lab	ntech	6	2018-10-30	1686	117	[78]1940	k	[158]831	[170]63	[42]243	[43]246	[40]546	[38]1104	[45]2873	[127]$0.02N^{1.1}$
95	N-Tech Lab	ntechlab	007	2019-06-25	2450	51	[167]3348	k	[149]795	[173]73	[67]393	[73]427	[53]780	[59]1768	[54]3499	[78]$0.16N^{1.0}$
96	N-Tech Lab	ntechlab	008	2020-01-06	1111	51	[64]1300	k	[81]554	[159]36	[35]179	[32]184	[27]341	[27]683	[23]1395	[41]$0.11N^{1.0}$
97	N-Tech Lab	ntechlab	009	2021-03-01	1208	42	[63]1300	-	[178]899	[157]35	[34]178	[33]184	[26]336	[26]676	[29]1704	[94]$0.05N^{1.1}$
98	N-Tech Lab	ntechlab	010	2021-06-24	351	213	[62]1280	-	[169]874	[28]6	[74]440	[75]435	[54]821	[54]1645	[51]3337	[51]$0.22N^{1.0}$
99	NEC	nec	2	2018-10-30	705	35	[73]1616	k	[98]642	[123]18	[68]405	[71]409	[63]1072	[57]1755	[59]4255	[116]$0.06N^{1.1}$
100	NEC	nec	3	2018-10-30	774	110	[74]1712	k	[102]665	[129]21	[3]7	[3]7	[5]14	[9]40	[10]82	[134]$0.00N^{1.2}$
101	NEC	nec	004	2021-07-19	971	63	[60]1104	-	[191]965	[30]7	[61]349	[62]351	[48]662	[46]1330	[40]2685	[44]$0.20N^{1.0}$
102	Neurotechnology	neurotech	5	2018-10-30	266	53	[8]256	k	[47]402	[8]2	[104]835	[105]839	[84]1690	[82]3219	[87]8955	[100]$0.19N^{1.1}$
103	Neurotechnology	neurotech	6	2018-10-30	564	53	[9]256	k	[128]726	[6]2	[105]839	[106]842	-	-	-	
104	Neurotechnology	neurotech	007	2019-10-03	57	51	[10]256	k	[7]161	[5]2	[116]1118	[117]1110	[94]2143	[89]4397	[88]9045	[55]$0.55N^{1.0}$

Notes	
1	Configuration size does not capture static data present in libraries. Libraries are included but the size also includes any ancillary libraries for image processing (e.g. openCV) or numerical computation (e.g. blas).
2	Finalization is the processing of converting N = 1600000 templates into a searchable data structure an operation which can be a simple copy, or the building of an index or tree, for example. The duration of the operation may be data dependent, and may not be linear in the number of input templates.
3	This multiplier expresses the increase in template size when k images are passed to the template generation function.
4	All durations are measured on Intel®Xeon®CPU E5-2630 v4 @ 2.20GHz processors. Estimates are made by wrapping the API function call in calls to std::chrono::high_resolution_clock which on the machine in (3) counts 1ns clock ticks. Precision is somewhat worse than that however.
5	Search durations are measured as in the prior note. The power-law model in the final column mostly fits the empirical results in Figure 128. However in certain cases the model is not correct and should not be used numerically.

Table 3: Summary of algorithms and properties included in this report. The blue superscripts give ranking for the quantity in that column. Missing search durations, denoted by "-", are absent because those runs were not executed, usually because we did not run on the larger galleries. Caution: The power-law model is sometimes an incorrect model. It is included here only to show broad sublinear behavior, which is flagged in green. The models should not be used for prediction.

2021/11/22 08:35:53

FNIR(N, R, T) = False neg. identification rate
FPIR(N, T) = False pos. identification rate

N = Num. enrolled subjects
R = Num. candidates examined

T = Threshold

T = 0 → Investigation
T > 0 → Identification

This publication is available free of charge from: https://doi.org/10.6028/NIST.IR.8271

	DEVELOPER	SHORT	SEQ.	VALIDATION	CONFIG[1]	LIB[1]	TEMPLATE GENERATION			FINALIZE[2]	SEARCH DURATION[5] MILLISEC					
	FULL NAME	NAME	NUM.	DATE	DATA (MB)	DATA (MB)	SIZE (B)	MULT[3]	TIME (MS)[4]	TIME (S)	L=1	L=50	L=50	L=50	L=50	POWER LAW
											N=1.6M	N=1.6M	N=3M	N=6M	N=12M	(μs)
105	Neutrotechnology	neutrotechnology	008	2021-03-22	355	49	[34]514	-	[150]800	[19]4	[119]1167	[120]1149	[96]2266	[94]4573	[95]9586	[61]$0.55N^{1.0}$
106	Neutrotechnology	neutrotechnology	009	2021-09-01	246	82	[33]513	-	[110]683	[10]3	[114]1035	[115]1049	[92]1977	[88]4270	[83]8756	[88]$0.32N^{1.1}$
107	Newland Computer Co Ltd	newland	2	2018-10-30	96	27	[118]2048	-	[165]855	[106]15	[182]8741	[187]8854	[155]17892	[152]39356	-	[112]$1.32N^{1.1}$
108	Noblis	noblis	1	2018-10-30	114	176	[102]2048	1	[17]206	[102]15	[125]1273	[123]1272	-	-	-	
109	Noblis	noblis	2	2018-10-30	153	176	[186]6144	1	[77]517	[162]43	[152]2513	[157]2522	[132]5649	[133]12432	[139]44262	[144]$0.04N^{1.3}$
110	Paravision (EverAI)	everai	2	2018-10-30	224	304	[105]2048	1	[37]366	[149]30	[48]278	[53]283	-	-	-	
111	Paravision (EverAI)	everai	3	2018-10-30	438	304	[124]2048	1	[125]717	[143]28	[47]278	[52]281	[41]572	[39]1146	[35]2278	[73]$0.12N^{1.0}$
112	Paravision (EverAI)	everai-paravision	004	2019-06-19	527	128	[177]4096	1	[105]672	[165]45	[84]559	[84]559	[108]2611	[117]6445	[120]14519	[152]$0.00N^{1.5}$
113	Paravision (EverAI)	paravision	005	2019-12-11	543	154	[168]4096	1	[157]830	[167]48	[85]561	[87]564	[62]1056	[65]2298	[63]4966	[91]$0.16N^{1.1}$
114	Paravision (EverAI)	paravision	007	2021-02-01	529	235	[170]4096	-	[119]701	[168]48	[87]569	[82]558	[64]1086	[63]2111	[58]4254	[20]$1.11N^{0.9}$
115	Qnap Security	qnap	000	2021-07-28	182	15	[130]2048	-	[62]457	[50]9	[121]1231	[142]1763	-	-	-	
116	Quantasoft	quantasoft	1	2018-10-30	276	452	[93]2048	k	[44]385	[29]6	[183]15422	[188]14858	[153]14717	-	[126]18323	
117	Rank One Computing	rankone	4	2018-10-09	0	101	[1]85	k	[3]36	[31]7	[22]101	[22]101	[18]190	-	-	[25]$0.07N^{1.0}$
118	Rank One Computing	rankone	5	2018-10-24	0	101	[5]133	k	[4]92	[32]7	[27]140	[27]144	[23]266	[22]525	[21]1049	[23]$0.11N^{1.0}$
119	Rank One Computing	rankone	006	2019-06-03	0	133	[6]165	k	[22]245	[37]8	-	-	-	-	-	
120	Rank One Computing	rankone	007	2019-11-12	0	137	[7]165	k	[25]272	[34]7	[23]116	[23]115	[20]215	[20]439	[18]877	[42]$0.07N^{1.0}$
121	Rank One Computing	rankone	009	2020-06-26	0	105	[14]260	k	[12]185	[65]11	[17]95	[19]96	[15]181	[15]362	[16]727	[33]$0.06N^{1.0}$
122	Rank One Computing	rankone	010	2020-11-05	0	135	[16]261	-	[16]198	[61]10	[18]95	[16]95	[14]178	[14]357	[15]714	[30]$0.06N^{1.0}$
123	Rank One Computing	rankone	011	2021-08-27	0	175	[15]261	-	[83]566	[41]8	[19]96	[17]95	[16]183	[16]370	[14]714	[39]$0.06N^{1.0}$
124	Realnetworks Inc	realnetworks	2	2018-10-30	105	104	[184]4104	k	[21]241	[142]28	[143]2008	[148]2048	[125]4194	[124]8642	[123]15035	[49]$1.08N^{1.0}$
125	Realnetworks Inc	realnetworks	003	2019-06-12	93	102	[75]1848	k	[10]173	[76]13	[118]1145	[118]1132	[93]2142	[102]5241	[103]10495	[104]$0.21N^{1.1}$
126	Realnetworks Inc	realnetworks	004	2019-10-17	94	102	[76]1848	1	[9]171	[64]11	[117]1143	[119]1137	[95]2149	[96]4740	[98]9693	[87]$0.36N^{1.0}$
127	Realnetworks Inc	realnetworks	005	2021-06-23	168	209	[149]2056	-	[32]332	[45]9	[137]1654	[135]1616	[116]3030	[112]6068	[112]12134	[36]$1.01N^{1.0}$
128	Remark Holdings	remarkai	0	2018-10-30	187	847	[101]2048	k	[85]593	[95]14	[171]5685	[175]5723	-	-	-	
129	Remark Holdings	remarkai	000	2019-06-12	234	1092	[84]2048	k	[99]650	[75]12	[172]5776	[174]5703	[145]11604	[151]32133	[150]91436	[145]$0.05N^{1.3}$
130	Remark Holdings	remarkai	1	2018-10-30	187	847	[103]2048	k	[56]427	[99]14	[170]5680	[176]5761	[148]12475	[149]28726	[148]59618	[136]$0.37N^{1.2}$
131	Rendip	rendip	000	2021-05-21	0	416	[88]2048	-	[175]890	[52]9	[44]249	[64]368	[51]697	[51]1452	[46]2926	[97]$0.08N^{1.1}$
132	Samsung S1 Corp	s1	000	2021-06-03	257	196	[171]4096	-	[166]865	[128]20	[179]6715	[184]6794	[152]13032	[148]26372	[147]55723	[71]$2.82N^{1.0}$
133	Samsung S1 Corp	s1	001	2021-11-01	240	198	[94]2048	-	[152]813	[42]8	[148]2415	[155]2491	[130]4718	[128]9614	[132]24472	[102]$0.53N^{1.1}$
134	Scanovate Ltd	scanovate	000	2020-01-15	250	446	[110]2048	-	[121]705	[97]14	[131]1419	[130]1412	[115]3008	[130]11616	[110]12012	[137]$0.10N^{1.2}$
135	Scanovate Ltd	scanovate	001	2020-09-10	250	446	[109]2048	-	[107]675	[81]13	[128]1321	[127]1320	[103]2502	[99]5047	[100]10163	[52]$0.65N^{1.0}$
136	Sensetime Group	sensetime	0	2018-10-30	525	6	[182]4104	k	[117]693	[161]41	[78]498	[77]501	[71]1212	[64]2281	[64]5032	[110]$0.09N^{1.1}$
137	Sensetime Group	sensetime	1	2018-10-30	525	6	[181]4104	k	[93]628	[166]48	[80]516	[78]502	[67]1146	[66]2301	[61]4765	[108]$0.09N^{1.1}$
138	Sensetime Group	sensetime	002	2019-06-03	523	6	[152]2056	k	[88]603	[121]18	[62]359	[65]370	[88]1897	[92]4508	[94]9543	[155]$0.00N^{1.5}$
139	Sensetime Group	sensetime	003	2019-12-02	769	76	[151]2056	1	[182]910	[125]19	[166]4885	[171]4989	[147]12325	[144]24712	[142]49445	[118]$0.67N^{1.1}$
140	Sensetime Group	sensetime	004	2020-08-10	456	29	[50]1032	-	[114]690	[74]12	[151]2490	[153]2477	[129]4654	[127]9402	[130]19651	[54]$1.22N^{1.0}$
141	Sensetime Group	sensetime	005	2020-12-17	631	39	[53]1032	-	[192]980	[63]11	[149]2459	[166]3939	[138]7398	[136]14768	[129]19016	[18]$14.03N^{0.9}$
142	Sensetime Group	sensetime	006	2021-07-26	526	54	[52]1032	-	[184]929	[35]7	[147]2414	[152]2422	[127]4527	[125]9128	[127]18640	[46]$1.35N^{1.0}$
143	Shaman Software	shaman	6	2018-10-26	0	200	[128]2048	k	[122]706	[96]14	[89]603	[90]612	-	-	-	
144	Shaman Software	shaman	7	2018-10-26	0	200	[80]2048	k	[123]707	[98]14	[88]602	[91]614	[68]1187	[71]2448	[67]5083	[74]$0.25N^{1.0}$
145	Shanghai Yitu Technology	yitu	4	2018-10-30	2119	136	[153]2070	1	[177]897	[164]45	[126]1288	[122]1203	[100]2440	[103]5241	[97]9671	[70]$0.52N^{1.0}$
146	Shanghai Yitu Technology	yitu	5	2018-10-30	2043	136	[156]2070	1	[163]853	[163]44	[122]1237	[121]1199	[104]2513	[98]5013	[96]9620	[67]$0.55N^{1.0}$
147	Smilart	smilart	4	2018-10-30	65	89	[22]512	k	[8]167	[18]4	[184]16137	[189]15633	-	-	-	
148	Smilart	smilart	5	2018-10-30	562	89	[107]2048	k	[60]450	[94]14	-	-	-	-	-	
149	Staqu Technologies	staqu	000	2021-08-30	1018	690	[169]4096	-	[155]826	[138]24	[167]4950	[170]4933	-	-	-	
150	Synesis	synesis	003	2019-07-04	143	17	[85]2048	k	[18]211	[71]12	[79]507	[79]502	[97]2297	[93]4564	[92]9452	[150]$0.00N^{1.4}$
151	Synesis	synesis	3	2018-10-30	237	150	[173]4096	k	[5]99	[146]29	[101]789	[104]801	[91]1941	[86]3888	[84]8810	[126]$0.07N^{1.1}$
152	Synesis	synesis	005	2020-09-08	494	24	[183]4104	-	[135]756	[136]24	[107]877	[107]865	[119]3182	[95]4658	[99]9750	[138]$0.06N^{1.2}$
153	Tech5 SA	tech5	001	2019-08-19	1394	116	[67]1536	k	[174]887	[57]10	[65]383	[101]766	[110]2767	[113]6149	[75]6178	[117]$0.12N^{1.1}$
154	Tech5 SA	tech5	002	2021-04-07	727	112	[32]513	-	[186]940	[14]4	[165]4682	[182]6689	[149]12541	[145]25145	[144]50239	[35]$4.18N^{1.0}$
155	Tencent Deepsea Lab	deepsea	001	2019-07-29	250	323	[95]2048	1	[132]737	[73]12	[113]1021	[114]1020	[111]2774	[109]5767	[113]12341	[141]$0.06N^{1.2}$
156	Tevian	tevian	5	2018-10-30	773	15	[133]2048	1	[51]405	[103]15	[69]405	[70]408	[56]854	[58]1757	[53]3380	[86]$0.14N^{1.0}$

Notes	
1	Configuration size does not capture static data present in libraries. Libraries are included but the size also includes any ancillary libraries for image processing (e.g. openCV) or numerical computation (e.g. blas).
2	Finalization is the processing of converting N = 1600000 templates into a searchable data structure an operation which can be a simple copy, or the building of an index or tree, for example. The duration of the operation may be data dependent, and may not be linear in the number of input templates.
3	This multiplier expresses the increase in template size when k images are passed to the template generation function.
4	All durations are measured on Intel®Xeon®CPU E5-2630 v4 @ 2.20GHz processors. Estimates are made by wrapping the API function call in calls to std::chrono::high_resolution_clock which on the machine in (3) counts 1ns clock ticks. Precision is somewhat worse than that however.
5	Search durations are measured as in the prior note. The power-law model in the final column mostly fits the empirical results in Figure 128. However in certain cases the model is not correct and should not be used numerically.

Table 4: Summary of algorithms and properties included in this report. The blue superscripts give ranking for the quantity in that column. Missing search durations, denoted by "-", are absent because those runs were not executed, usually because we did not run on the larger galleries. Caution: The power-law model is sometimes an incorrect model. It is included here only to show broad sublinear behavior, which is flagged in green. The models should not be used for prediction.

2021/11/22 08:35:53

FNIR(N, R, T) = False neg. identification rate
FPIR(N, T) = False pos. identification rate

N = Num. enrolled subjects
R = Num. candidates examined

T = Threshold

T = 0 → Investigation
T > 0 → Identification

This publication is available free of charge from: https://doi.org/10.6028/NIST.IR.8271

	DEVELOPER	SHORT	SEQ.	VALIDATION	CONFIG[1]	LIB[1]	TEMPLATE GENERATION			FINALIZE[2]	SEARCH DURATION[5] MILLISEC					
	FULL NAME	NAME	NUM.	DATE	DATA (MB)	DATA (MB)	SIZE (B)	MULT[3]	TIME (MS)[4]	TIME (S)	L=1	L=50	L=50	L=50	L=50	POWER LAW
										N=1.6M	N=1.6M	N=1.6M	N=3M	N=6M	N=12M	(μs)
157	Tevian	tevian	006	2021-04-16	769	19	[49]1032	-	[86]597	[56]10	[55]295	[56]295	[42]578	[41]1187	[43]2741	[98]$0.06N^{1.1}$
158	Tevian	tevian	007	2021-10-12	703	19	[48]1032	-	[140]777	[22]4	[56]297	[57]298	[43]579	[40]1179	[37]2418	[81]$0.11N^{1.0}$
159	Thales	cogent	2	2018-10-30	681	39	[56]1043	k	[189]945	[140]27	[144]2017	[150]2144	[126]4298	[123]8472	[125]16429	[53]$1.08N^{1.0}$
160	Thales	cogent	3	2018-10-30	681	39	[57]1043	k	[187]940	[54]9	[120]1230	[126]1311	[109]2687	[104]5398	[101]10184	[62]$0.62N^{1.0}$
161	Thales	cogent	004	2021-02-10	1376	59	[148]2053	-	[190]947	[88]14	[155]2903	[145]1911	[120]3566	[121]7498	[124]16370	[85]$0.64N^{1.0}$
162	Thales	cogent	005	2021-09-13	1043	56	[58]1062	-	[139]769	[26]5	[109]912	[111]996	[87]1872	[85]3845	[81]7555	[64]$0.44N^{1.0}$
163	TigerIT Americas LLC	tiger	2	2018-10-29	416	518	[143]2052	k	[64]461	[107]15	[142]1816	[146]1921	[124]3833	[122]7526	[121]14820	[69]$0.83N^{1.0}$
164	TigerIT Americas LLC	tiger	3	2018-10-30	416	518	[139]2052	k	[63]461	[191]37431	[38]191	[36]189	-	-	-	
165	Toshiba	toshiba	0	2018-10-30	961	105	[72]1548	k	[171]876	[69]12	[176]6153	[178]6236	[146]12221	[146]25355	[143]49448	[132]$0.36N^{1.2}$
166	Toshiba	toshiba	1	2018-10-30	961	105	[154]2060	k	[170]875	[192]44701	[175]6007	[180]6355	-	-	-	
167	Tripleize	aize	001	2021-08-06	262	150	[96]2048	-	[48]402	[48]9	[158]3087	[161]3080	-	-	-	
168	Trueface.ai	trueface	000	2021-01-27	247	119	[79]2000	-	[36]363	[79]13	[46]271	[61]327	[45]614	[43]1239	[39]2678	[60]$0.15N^{1.0}$
169	Veridas Digital Authentication Solutions S.L.	veridas	001	2021-03-05	347	875	[91]2048	-	[168]872	[80]13	[169]5493	[173]5469	[143]10350	[141]20655	[138]41264	[37]$3.40N^{1.0}$
170	Veridas Digital Authentication Solutions S.L.	veridas	002	2021-07-06	347	870	[121]2048	-	[172]877	[62]10	[59]322	[59]325	[50]685	[48]1365	[42]2730	[92]$0.09N^{1.1}$
171	Veridas Digital Authentication Solutions S.L.	veridas	003	2021-11-09	346	870	[122]2048	-	[167]867	[43]9	[75]440	[60]327	[52]699	[49]1401	[57]3954	[135]$0.02N^{1.2}$
172	Viettel Group	vts	000	2021-03-12	250	257	[123]2048	-	[72]492	[178]2295	[2]4	[2]4	[2]6	[4]11	-	[13]$0.61N^{0.6}$
173	Viettel Group	vts	001	2021-07-16	352	600	[86]2048	-	[176]891	[132]21	[150]2477	[154]2487	[128]4644	[126]9313	[128]18713	[38]$1.53N^{1.0}$
174	Vigilant Solutions	vigilant	5	2018-10-30	335	122	[68]1544	k	[136]762	[124]19	-	[140]1720	-	-	-	
175	Vigilant Solutions	vigilant	6	2018-10-30	337	122	[70]1544	k	[153]816	[130]21	-	[139]1713	-	-	-	
176	Vigilant Solutions	vigilantsolutions	007	2021-01-08	340	51	[69]1544	-	[91]616	[118]16	[130]1354	[129]1352	[113]2911	[111]5966	[107]11466	[103]$0.27N^{1.1}$
177	Vigilant Solutions	vigilantsolutions	008	2021-07-23	340	51	[71]1544	-	[49]403	[84]13	[115]1062	[116]1061	[98]2330	[107]5520	[93]9499	[122]$0.11N^{1.1}$
178	Visidon	visidon	1	2018-10-30	166	42	[137]2052	k	[103]667	[109]15	[163]4370	[169]4472	[140]8454	[139]17262	[136]34288	[48]$2.40N^{1.0}$
179	Visidon	vd	002	2021-05-18	248	42	[140]2052	-	[113]687	[44]9	[145]2089	[151]2336	-	-	-	
180	Visidon	vd	003	2021-10-12	497	43	[142]2052	-	[116]692	[39]8	[146]2095	[149]2082	-	-	-	
181	Visiob-Box	visionbox	000	2021-09-17	252	274	[153]2059	-	[69]481	[117]16	[72]422	[63]359	[57]855	[25]631	[34]2096	[16]$2.46N^{0.8}$
182	VisionLabs	visionlabs	6	2018-10-30	360	17	[24]512	1	[29]289	[188]20290	[14]36	[14]36	[12]39	[11]44	[9]53	[8]$3211.93N^{0.2}$
183	VisionLabs	visionlabs	7	2018-10-30	360	17	[23]512	1	[28]289	[190]34666	[15]63	[15]63	[13]72	[13]80	[11]115	[10]$2076.32N^{0.2}$
184	VisionLabs	visionlabs	008	2019-06-18	348	17	[26]512	1	[26]272	[186]12747	[9]23	[8]24	[7]26	[6]29	[5]33	[6]$2539.61N^{0.2}$
185	VisionLabs	visionlabs	009	2020-08-04	689	20	[29]512	-	[65]467	[187]13245	[10]23	[9]29	[9]34	[12]61	[12]145	[12]$8.88N^{0.6}$
186	VisionLabs	visionlabs	010	2021-02-05	1042	20	[25]512	-	[130]731	[182]11837	[7]21	[11]32	[10]36	[8]39	[6]43	[7]$3183.79N^{0.2}$
187	VisionLabs	visionlabs	011	2021-10-20	1042	20	[28]512	-	[131]735	[185]12255	[8]21	[7]23	[8]26	[7]34	[8]51	[11]$301.26N^{0.3}$
188	Vocord	vocord	5	2018-10-30	1035	185	[41]768	k	[143]780	[33]7	[32]158	[37]204	[29]383	[30]767	[25]1466	[40]$0.12N^{1.0}$
189	Vocord	vocord	6	2018-10-30	1035	185	[192]10240	k	[144]785	[177]243	[33]170	[39]216	-	-	-	
190	Xforward AI Technology	xforwardai	000	2020-07-24	236	171	[97]2048	-	[134]753	[86]13	[164]4603	[186]7647	[154]15723	[143]23900	[146]53729	[123]$0.56N^{1.1}$
191	Xforward AI Technology	xforwardai	001	2021-01-21	332	50	[116]2048	-	[109]677	[115]16	[174]5887	[168]4384	[141]8798	[140]18553	[141]48993	[130]$0.32N^{1.1}$
192	Xforward AI Technology	xforwardai	002	2021-05-24	691	50	[180]4096	-	[185]930	[122]18	[181]6957	[181]6400	[150]12659	[150]31077	[149]65158	[128]$0.52N^{1.1}$

Notes	
1	Configuration size does not capture static data present in libraries. Libraries are included but the size also includes any ancillary libraries for image processing (e.g. openCV) or numerical computation (e.g. blas).
2	Finalization is the processing of converting N = 1600000 templates into a searchable data structure an operation which can be a simple copy, or the building of an index or tree, for example. The duration of the operation may be data dependent, and may not be linear in the number of input templates.
3	This multiplier expresses the increase in template size when k images are passed to the template generation function.
4	All durations are measured on Intel®Xeon®CPU E5-2630 v4 @ 2.20GHz processors. Estimates are made by wrapping the API function call in calls to std::chrono::high_resolution_clock which on the machine in (3) counts 1ns clock ticks. Precision is somewhat worse than that however.
5	Search durations are measured as in the prior note. The power-law model in the final column mostly fits the empirical results in Figure 128. However in certain cases the model is not correct and should not be used numerically.

Table 5: Summary of algorithms and properties included in this report. The blue superscripts give ranking for the quantity in that column. Missing search durations, denoted by "-", are absent because those runs were not executed, usually because we did not run on the larger galleries. Caution: The power-law model is sometimes an incorrect model. It is included here only to show broad sublinear behavior, which is flagged in green. The models should not be used for prediction.

2021/11/22
08:35:53

FNIR(N, R, T) = False neg. identification rate
FPIR(N, T) = False pos. identification rate

N = Num. enrolled subjects
R = Num. candidates examined

T = Threshold

T = 0 → Investigation
T > 0 → Identification

This publication is available free of charge from: https://doi.org/10.6028/NIST.IR.8271

MISS RATES		INVESTIGATION, FNIR(N, R = 1, T = 0)								IDENTIFICATION, FNIR(N, R = L, T $\geq$ 0) FOR FPIR = 0.001							
#	ALGORITHM	(0, 2]	(2, 4]	(4, 6]	(6, 8]	(8, 10]	(10, 12]	(12, 14]	(14, 18]	(0, 2]	(2, 4]	(4, 6]	(6, 8]	(8, 10]	(10, 12]	(12, 14]	(14, 18]
1	3DIVI-005	[92]0.0207	[96]0.0304	[96]0.0415	[96]0.0533	[96]0.0646	[96]0.0735	[96]0.0884	[97]0.1148	[100]0.1580	[97]0.2316	[92]0.3033	[97]0.3740	[97]0.4285	[97]0.4742	[98]0.5329	[96]0.5975
2	ANKE-000	[94]0.0162	[94]0.0245	[94]0.0333	[94]0.0428	[94]0.0515	[94]0.0615	[94]0.0780	[93]0.1028	[95]0.1132	[95]0.1761	[95]0.2402	[95]0.3057	[94]0.3640	[94]0.4200	[94]0.4928	[94]0.5680
3	ANKE-002	[48]0.0055	[49]0.0074	[49]0.0090	[48]0.0103	[47]0.0116	[48]0.0135	[47]0.0162	[46]0.0202	[53]0.0329	[53]0.0560	[55]0.0843	[56]0.1169	[56]0.1481	[56]0.1820	[56]0.2280	[55]0.2831
4	AWARE-005	[105]0.0328	[105]0.0519	[105]0.0712	[103]0.0910	[103]0.1078	[103]0.1235	[103]0.1457	[103]0.1831	[105]0.3605	[106]0.4949	[106]0.5948	[106]0.6783	[107]0.7393	[107]0.7905	[107]0.8408	[108]0.8831
5	AWARE-006	[109]0.0702	[109]0.1110	[109]0.1502	[109]0.1899	[109]0.2253	[110]0.2614	[109]0.3045	[109]0.3659								
6	AYONIX-002	[112]0.3360	[113]0.4389	[113]0.5144	[113]0.5814	[113]0.6340	[113]0.6818	[113]0.7297	[114]0.7774	[109]0.8288	[110]0.9013	[110]0.9375	[110]0.9603	[110]0.9744	[111]0.9837	[111]0.9893	[111]0.9927
7	CAMVI-004	[108]0.0623	[108]0.0944	[108]0.1243	[108]0.1548	[107]0.1812	[107]0.2056	[107]0.2344	[105]0.2672	[90]0.0810	[90]0.1267	[82]0.1721	[87]0.2203	[87]0.2619	[85]0.3040	[84]0.3543	[80]0.4124
8	CAMVI-005	[110]0.0849	[110]0.1255	[110]0.1631	[110]0.1989	[110]0.2298	[109]0.2585	[108]0.2915	[108]0.3246								
9	CIB-000	[13]0.0022	[13]0.0030	[14]0.0037	[14]0.0044	[16]0.0049	[16]0.0057	[16]0.0069	[16]0.0062	[24]0.0139	[25]0.0240	[26]0.0373	[27]0.0525	[27]0.0689	[25]0.0859	[25]0.1109	[25]0.1454
10	CLOUDWALK-HR-000	[7]0.0019	[6]0.0024	[7]0.0029	[6]0.0032	[5]0.0032	[4]0.0036	[2]0.0041	[1]0.0020	[1]0.0029	[1]0.0041	[1]0.0054	[1]0.0064	[2]0.0073	[2]0.0085	[2]0.0102	[2]0.0112
11	COGENT-000	[89]0.0128	[90]0.0184	[92]0.0250	[92]0.0327	[91]0.0407	[90]0.0488	[89]0.0611	[89]0.0794	[77]0.0559	[77]0.0923	[75]0.1342	[76]0.1812	[74]0.2243	[73]0.2675	[72]0.3240	[76]0.3992
12	COGENT-001	[90]0.0128	[89]0.0184	[91]0.0250	[91]0.0327	[92]0.0407	[91]0.0488	[90]0.0611	[88]0.0794	[76]0.0559	[78]0.0923	[76]0.1342	[75]0.1812	[75]0.2243	[74]0.2675	[73]0.3240	[77]0.3992
13	COGENT-002	[68]0.0081	[65]0.0105	[62]0.0123	[63]0.0137	[61]0.0157	[61]0.0175	[59]0.0215	[59]0.0280	[68]0.0499	[67]0.0827	[66]0.1207	[66]0.1639	[66]0.2037	[65]0.2432	[66]0.2972	[67]0.3638
14	COGENT-003	[70]0.0082	[66]0.0108	[64]0.0128	[66]0.0145	[65]0.0168	[62]0.0191	[68]0.0239	[65]0.0312	[79]0.0582	[79]0.0971	[79]0.1417	[79]0.1918	[79]0.2380	[80]0.2836	[82]0.3440	[83]0.4207
15	COGENT-004	[58]0.0066	[52]0.0080	[44]0.0085	[38]0.0080	[30]0.0083	[30]0.0092	[31]0.0106	[34]0.0130	[62]0.0410	[64]0.0720	[64]0.1099	[64]0.1539	[63]0.1974	[66]0.2443	[69]0.3043	[69]0.3757
16	COGNITEC-000	[104]0.0265	[102]0.0423	[102]0.0588	[102]0.0757	[101]0.0894	[101]0.1014	[101]0.1169	[100]0.1381	[99]0.1522	[98]0.2330	[98]0.3051	[98]0.3751	[98]0.4300	[98]0.4779	[97]0.5307	[95]0.5913
17	COGNITEC-001	[92]0.0149	[93]0.0228	[93]0.0312	[93]0.0399	[93]0.0479	[93]0.0546	[92]0.0656	[90]0.0806	[92]0.0963	[92]0.1562	[92]0.2157	[92]0.2771	[92]0.3287	[92]0.3771	[91]0.4343	[90]0.4959
18	COGNITEC-002	[76]0.0101	[79]0.0138	[80]0.0170	[80]0.0201	[80]0.0237	[79]0.0264	[77]0.0309	[76]0.0389	[71]0.0517	[70]0.0879	[71]0.1269	[72]0.1707	[70]0.2098	[67]0.2463	[65]0.2919	[65]0.3535
19	COGNITEC-003	[77]0.0104	[80]0.0140	[81]0.0174	[81]0.0205	[81]0.0238	[80]0.0266	[78]0.0311	[78]0.0401	[70]0.0504	[69]0.0855	[68]0.1235	[68]0.1662	[67]0.2045	[64]0.2403	[64]0.2854	[63]0.3451
20	COGNITEC-004	[63]0.0073	[62]0.0099	[61]0.0118	[58]0.0130	[58]0.0147	[60]0.0163	[56]0.0189	[55]0.0239	[52]0.0325	[52]0.0548	[51]0.0798	[50]0.1074	[49]0.1325	[50]0.1591	[47]0.1952	[46]0.2414
21	CUBOX-000	[6]0.0019	[4]0.0024	[4]0.0028	[4]0.0031	[4]0.0032	[5]0.0037	[5]0.0044	[4]0.0027	[6]0.0039	[6]0.0059	[7]0.0083	[8]0.0111	[8]0.0141	[9]0.0185	[9]0.0252	[9]0.0339
22	CYBERLINK-002	[49]0.0055	[44]0.0068	[40]0.0075	[34]0.0078	[31]0.0084	[31]0.0094	[32]0.0107	[30]0.0114	[31]0.0180	[32]0.0302	[32]0.0460	[31]0.0643	[32]0.0837	[32]0.1058	[31]0.1370	[31]0.1787
23	CYBERLINK-003	[34]0.0041	[33]0.0052	[26]0.0057	[24]0.0058	[24]0.0061	[24]0.0068	[20]0.0078	[23]0.0078	[18]0.0109	[18]0.0175	[19]0.0259	[20]0.0356	[20]0.0468	[20]0.0594	[20]0.0787	[21]0.1072
24	DAHUA-002	[29]0.0035	[27]0.0047	[27]0.0058	[26]0.0067	[27]0.0074	[26]0.0082	[28]0.0100	[28]0.0108	[29]0.0169	[31]0.0294	[30]0.0449	[29]0.0635	[29]0.0817	[30]0.1013	[28]0.1291	[27]0.1638
25	DAHUA-003	[18]0.0026	[18]0.0036	[18]0.0043	[19]0.0050	[19]0.0055	[18]0.0062	[22]0.0080	[19]0.0073	[28]0.0160	[29]0.0280	[28]0.0432	[28]0.0615	[28]0.0794	[28]0.0987	[27]0.1270	[26]0.1587
26	DEEPGLINT-001	[16]0.0024	[15]0.0032	[15]0.0037	[12]0.0040	[12]0.0043	[14]0.0049	[14]0.0060	[14]0.0052	[12]0.0058	[10]0.0087	[11]0.0119	[11]0.0155	[11]0.0199	[12]0.0249	[11]0.0338	[11]0.0463
27	DEEPSEA-001	[69]0.0081	[69]0.0116	[72]0.0149	[73]0.0182	[73]0.0216	[78]0.0260	[80]0.0332	[80]0.0432	[65]0.0458	[65]0.0752	[63]0.1086	[62]0.1460	[62]0.1812	[62]0.2186	[62]0.2663	[61]0.3213
28	DERMALOG-006	[81]0.0113	[81]0.0142	[77]0.0163	[76]0.0183	[73]0.0200	[72]0.0218	[70]0.0251	[68]0.0329	[74]0.0545	[72]0.0889	[72]0.1271	[71]0.1697	[69]0.2090	[69]0.2498	[68]0.3028	[68]0.3670
29	DERMALOG-007	[87]0.0125	[87]0.0170	[87]0.0214	[87]0.0264	[86]0.0309	[85]0.0356	[86]0.0432	[86]0.0579	[91]0.0910	[91]0.1453	[91]0.2009	[91]0.2602	[91]0.3134	[91]0.3649	[90]0.4289	[91]0.5007
30	DERMALOG-008	[51]0.0057	[51]0.0077	[53]0.0095	[53]0.0110	[52]0.0128	[54]0.0148	[53]0.0180	[54]0.0223	[69]0.0501	[68]0.0850	[69]0.1247	[70]0.1692	[71]0.2105	[70]0.2541	[70]0.3102	[70]0.3762
31	GORILLA-002	[99]0.0213	[99]0.0359	[100]0.0528	[101]0.0716	[102]0.0895	[102]0.1088	[102]0.1367	[102]0.1765	[102]0.1828	[103]0.2787	[103]0.3654	[103]0.4485	[103]0.5168	[101]0.5823	[101]0.6508	[101]0.7180
32	GORILLA-005	[37]0.0044	[46]0.0070	[57]0.0102	[61]0.0136	[66]0.0170	[70]0.0204	[73]0.0272	[75]0.0373	[78]0.0566	[80]0.0973	[81]0.1432	[80]0.1937	[80]0.2398	[82]0.2862	[81]0.3437	[81]0.4150
33	IDEMIA-003	[80]0.0110	[85]0.0151	[85]0.0196	[84]0.0238	[83]0.0281	[83]0.0313	[83]0.0368	[82]0.0504	[86]0.0717	[85]0.1147	[85]0.1614	[85]0.2113	[84]0.2553	[84]0.2976	[83]0.3537	[84]0.4334
34	IDEMIA-004	[79]0.0107	[83]0.0148	[84]0.0192	[83]0.0233	[82]0.0277	[82]0.0312	[82]0.0367	[83]0.0512	[57]0.0373	[54]0.0587	[53]0.0833	[52]0.1100	[51]0.1340	[49]0.1580	[46]0.1911	[47]0.2482
35	IDEMIA-005	[83]0.0118	[86]0.0167	[89]0.0218	[88]0.0270	[87]0.0317	[86]0.0357	[85]0.0425	[85]0.0579	[64]0.0440	[63]0.0689	[59]0.0964	[58]0.1254	[57]0.1513	[55]0.1762	[50]0.2113	[51]0.2698
36	IDEMIA-006	[86]0.0124	[88]0.0171	[88]0.0218	[86]0.0263	[85]0.0302	[84]0.0321	[81]0.0356	[81]0.0471	[61]0.0409	[58]0.0620	[56]0.0850	[51]0.1097	[48]0.1309	[43]0.1486	[41]0.1738	[40]0.2200
37	IDEMIA-007	[46]0.0050	[47]0.0071	[47]0.0089	[49]0.0106	[50]0.0124	[50]0.0142	[50]0.0171	[52]0.0220	[35]0.0202	[35]0.0335	[33]0.0491	[32]0.0663	[30]0.0825	[29]0.0999	[26]0.1240	[28]0.1645
38	IDEMIA-008	[4]0.0018	[5]0.0024	[5]0.0029	[5]0.0032	[7]0.0035	[6]0.0039	[6]0.0046	[8]0.0033	[3]0.0034	[3]0.0051	[5]0.0069	[5]0.0087	[5]0.0102	[4]0.0123	[3]0.0146	[3]0.0186
39	IMAGUS-005	[32]0.0039	[32]0.0052	[30]0.0061	[28]0.0067	[29]0.0077	[29]0.0088	[29]0.0103	[29]0.0109	[38]0.0212	[38]0.0357	[39]0.0539	[39]0.0755	[37]0.0967	[37]0.1183	[36]0.1485	[34]0.1893
40	IMPERIAL-000	[33]0.0040	[34]0.0054	[35]0.0067	[39]0.0079	[39]0.0093	[40]0.0112	[39]0.0139	[41]0.0178	[48]0.0286	[50]0.0503	[50]0.0779	[53]0.1116	[55]0.1455	[57]0.1844	[59]0.2341	[58]0.2951
41	INCODE-003	[93]0.0155	[95]0.0247	[95]0.0348	[95]0.0463	[95]0.0571	[95]0.0674	[95]0.0856	[96]0.1114	[101]0.1627	[101]0.2507	[101]0.3322	[99]0.4122	[99]0.4772	[100]0.5368	[100]0.6059	[100]0.6766
42	INCODE-004	[55]0.0061	[58]0.0087	[58]0.0110	[60]0.0136	[63]0.0161	[63]0.0185	[66]0.0236	[64]0.0309	[72]0.0532	[73]0.0908	[74]0.1334	[74]0.1809	[76]0.2245	[75]0.2675	[74]0.3249	[73]0.3932
43	INNOVATRICS-004	[113]0.3594	[112]0.3629	[112]0.3688	[111]0.3754	[111]0.3813	[111]0.3870	[111]0.3960	[111]0.4135	[106]0.4234	[105]0.4642	[105]0.5073	[105]0.5522	[104]0.5902	[104]0.6274	[102]0.6736	[102]0.7253
44	INNOVATRICS-005	[40]0.0046	[40]0.0063	[41]0.0078	[44]0.0092	[44]0.0106	[42]0.0124	[42]0.0149	[42]0.0178	[54]0.0343	[55]0.0590	[57]0.0886	[57]0.1222	[58]0.1544	[59]0.1881	[58]0.2321	[56]0.2874

Table 6: **Accuracy for the FRVT 2018 mugshot sets under ageing**. *The second row shows the time lapse between gallery and subsequent probe images, in years. The first two columns identify the algorithm The next 8 values give rank-based FNIR with R = 1, T = 0 and FPIR = 1. All these are relevant to investigational uses where candidates from all searches would need human review. The second 8 values give threshold-based FNIR with T $\geq$ 0, FPIR = 0.001 and no rank criterion. The shaded cells indictate indicate the three most accurate algorithms for that elapsed time. The gallery size is 3068801. The total number of searches is 10951064.*

2021/11/22 08:35:53

FNIR(N, R, T) = FPIR(N, T) = False neg. identification rate False pos. identification rate

N = Num. enrolled subjects R = Num. candidates examined

T = Threshold

T = 0 → Investigation T > 0 → Identification

This publication is available free of charge from: https://doi.org/10.6028/NIST.IR.8271

MISS RATES		INVESTIGATION, FNIR(N, R = 1, T = 0)								IDENTIFICATION, FNIR(N, R = L, T $\geq$ 0) FOR FPIR = 0.001							
#	ALGORITHM	(0, 2]	(2, 4]	(4, 6]	(6, 8]	(8, 10]	(10, 12]	(12, 14]	(14, 18]	(0, 2]	(2, 4]	(4, 6]	(6, 8]	(8, 10]	(10, 12]	(12, 14]	(14, 18]
45	IREX-000	[23]0.0031	[23]0.0042	[24]0.0051	[25]0.0060	[25]0.0068	[25]0.0080	[26]0.0095	[27]0.0107	[51]0.0313	[51]0.0539	[52]0.0815	[55]0.1137	[54]0.1442	[54]0.1755	[55]0.2181	[52]0.2718
46	ISYSTEMS-002	[75]0.0101	[78]0.0135	[79]0.0169	[78]0.0197	[79]0.0228	[76]0.0256	[76]0.0304	[77]0.0398	[89]0.0779	[89]0.1258	[90]0.1759	[89]0.2299	[89]0.2758	[88]0.3204	[88]0.3763	[86]0.4401
47	ISYSTEMS-003	[74]0.0089	[68]0.0115	[68]0.0139	[68]0.0158	[69]0.0177	[69]0.0198	[65]0.0234	[62]0.0303	[83]0.0647	[83]0.1056	[83]0.1502	[83]0.1986	[82]0.2402	[78]0.2819	[77]0.3351	[75]0.3976
48	KEDACOM-001	[82]0.0116	[74]0.0130	[66]0.0135	[59]0.0133	[56]0.0135	[49]0.0141	[43]0.0151	[40]0.0176	[40]0.0241	[40]0.0360	[38]0.0513	[33]0.0689	[33]0.0866	[33]0.1060	[29]0.1327	[29]0.1694
49	LOOKMAN-003	[85]0.0123	[82]0.0144	[76]0.0158	[69]0.0168	[70]0.0178	[65]0.0188	[58]0.0212	[58]0.0260	[63]0.0438	[61]0.0687	[60]0.0978	[60]0.1296	[59]0.1581	[58]0.1879	[57]0.2294	[54]0.2756
50	LOOKMAN-005	[84]0.0118	[76]0.0134	[69]0.0142	[65]0.0144	[60]0.0150	[59]0.0160	[51]0.0176	[49]0.0213	[50]0.0310	[48]0.0480	[45]0.0698	[45]0.0954	[45]0.1216	[45]0.1491	[45]0.1890	[45]0.2381
51	MICROFOCUS-005	[114]0.4269	[114]0.5527	[114]0.6355	[115]0.7024	[115]0.7503	[115]0.7876	[115]0.8234	[116]0.8601	[110]0.8338	[111]0.9113	[111]0.9468	[111]0.9667	[111]0.9771	[110]0.9836	[110]0.9880	[110]0.9924
52	MICROSOFT-003	[27]0.0034	[31]0.0050	[32]0.0064	[35]0.0078	[37]0.0092	[37]0.0107	[38]0.0135	[39]0.0166	[49]0.0288	[49]0.0503	[49]0.0763	[49]0.1067	[53]0.1359	[52]0.1680	[51]0.2116	[49]0.2644
53	MICROSOFT-004	[24]0.0032	[26]0.0047	[28]0.0060	[31]0.0075	[34]0.0087	[34]0.0103	[37]0.0131	[37]0.0159	[46]0.0268	[47]0.0470	[48]0.0716	[47]0.1007	[47]0.1291	[51]0.1610	[49]0.2052	[48]0.2590
54	MICROSOFT-005	[21]0.0031	[28]0.0047	[34]0.0066	[42]0.0084	[42]0.0103	[46]0.0131	[48]0.0164	[44]0.0185	[42]0.0243	[43]0.0432	[43]0.0658	[43]0.0913	[44]0.1172	[42]0.1476	[44]0.1874	[42]0.2272
55	MICROSOFT-006	[25]0.0032	[30]0.0049	[33]0.0065	[41]0.0081	[41]0.0096	[41]0.0117	[40]0.0144	[38]0.0160	[23]0.0134	[23]0.0233	[24]0.0346	[22]0.0462	[21]0.0578	[22]0.0713	[22]0.0903	[22]0.1156
56	NEC-000	[96]0.0195	[98]0.0316	[98]0.0445	[98]0.0581	[97]0.0699	[98]0.0817	[98]0.0998	[98]0.1237	[88]0.0759	[88]0.1245	[88]0.1729	[88]0.2240	[88]0.2671	[87]0.3117	[85]0.3639	[85]0.4348
57	NEC-001	[103]0.0246	[101]0.0382	[99]0.0524	[99]0.0672	[100]0.0793	[100]0.0904	[99]0.1076	[99]0.1317	[93]0.1019	[93]0.1623	[93]0.2214	[93]0.2834	[93]0.3341	[93]0.3844	[93]0.4440	[92]0.5183
58	NEC-002	[26]0.0033	[21]0.0041	[17]0.0043	[15]0.0044	[14]0.0045	[13]0.0049	[13]0.0056	[10]0.0041	[15]0.0066	[11]0.0090	[10]0.0111	[10]0.0131	[9]0.0149	[7]0.0171	[8]0.0207	[8]0.0267
59	NEC-003	[30]0.0036	[25]0.0046	[23]0.0051	[23]0.0055	[23]0.0059	[19]0.0067	[19]0.0077	[21]0.0073	[9]0.0056	[9]0.0076	[9]0.0091	[7]0.0105	[6]0.0119	[6]0.0137	[5]0.0162	[5]0.0209
60	NEC-004	[31]0.0039	[24]0.0045	[21]0.0047	[17]0.0046	[13]0.0044	[12]0.0046	[12]0.0052	[9]0.0036	[7]0.0046	[5]0.0057	[2]0.0063	[2]0.0066	[1]0.0069	[1]0.0076	[1]0.0090	[1]0.0105
61	NEUROTECHNOLOGY-003	[100]0.0234	[100]0.0379	[101]0.0549	[100]0.0682	[99]0.0720	[97]0.0747	[97]0.0886	[95]0.1066	[108]0.6802	[108]0.8187	[109]0.8920	[109]0.9355	[109]0.9594	[109]0.9738	[109]0.9828	[109]0.9885
62	NEUROTECHNOLOGY-004	[78]0.0104	[77]0.0134	[75]0.0156	[72]0.0173	[71]0.0195	[71]0.0212	[69]0.0245	[66]0.0320	[82]0.0642	[81]0.1015	[80]0.1426	[78]0.1881	[77]0.2299	[76]0.2722	[75]0.3269	[74]0.3943
63	NEUROTECHNOLOGY-005	[73]0.0089	[70]0.0116	[67]0.0136	[67]0.0152	[68]0.0173	[68]0.0196	[64]0.0233	[63]0.0306	[75]0.0556	[75]0.0913	[73]0.1315	[73]0.1766	[73]0.2192	[72]0.2617	[71]0.3174	[71]0.3843
64	NEUROTECHNOLOGY-007	[65]0.0078	[64]0.0103	[63]0.0124	[64]0.0140	[62]0.0161	[62]0.0185	[61]0.0225	[60]0.0290	[81]0.0641	[84]0.1069	[84]0.1546	[84]0.2075	[85]0.2572	[86]0.3081	[87]0.3713	[87]0.4421
65	NOBLIS-002	[111]0.1520	[111]0.2419	[111]0.3296	[112]0.4114	[112]0.4856	[112]0.5528	[112]0.6061	[112]0.6532	[112]0.9984	[112]0.9996	[112]0.9998	[112]0.9999	[112]0.9999	[112]1.0000	[114]1.0000	[116]1.0000
66	NTECHLAB-003	[64]0.0078	[75]0.0131	[86]0.0202	[89]0.0295	[90]0.0405	[92]0.0543	[93]0.0761	[94]0.1035	[67]0.0491	[71]0.0881	[78]0.1384	[82]0.1985	[86]0.2594	[89]0.3270	[89]0.4065	[89]0.4891
67	NTECHLAB-004	[61]0.0068	[67]0.0110	[78]0.0167	[85]0.0239	[88]0.0330	[89]0.0447	[91]0.0641	[92]0.0891	[59]0.0379	[62]0.0688	[65]0.1108	[65]0.1629	[72]0.2192	[81]0.2846	[86]0.3657	[88]0.4524
68	NTECHLAB-006	[50]0.0056	[61]0.0095	[71]0.0148	[82]0.0218	[84]0.0301	[87]0.0413	[88]0.0591	[91]0.0814	[55]0.0349	[59]0.0636	[62]0.1023	[63]0.1506	[65]0.2024	[71]0.2617	[78]0.3374	[82]0.4185
69	NTECHLAB-007	[36]0.0044	[42]0.0066	[48]0.0089	[56]0.0118	[59]0.0150	[66]0.0189	[71]0.0255	[71]0.0342	[44]0.0256	[45]0.0450	[47]0.0705	[48]0.1012	[50]0.1334	[53]0.1692	[52]0.2170	[53]0.2752
70	NTECHLAB-008	[17]0.0025	[20]0.0038	[25]0.0052	[30]0.0074	[43]0.0104	[51]0.0146	[67]0.0236	[72]0.0348	[25]0.0143	[27]0.0267	[31]0.0459	[36]0.0733	[39]0.1062	[41]0.1469	[48]0.2044	[50]0.2698
71	NTECHLAB-009	[12]0.0022	[14]0.0031	[15]0.0038	[16]0.0045	[18]0.0055	[21]0.0067	[24]0.0088	[26]0.0100	[17]0.0073	[17]0.0117	[17]0.0170	[17]0.0238	[18]0.0319	[18]0.0419	[18]0.0577	[19]0.0833
72	PARAVISION-002	[52]0.0058	[57]0.0083	[59]0.0111	[62]0.0137	[64]0.0162	[64]0.0187	[63]0.0229	[61]0.0295								
73	PARAVISION-003	[43]0.0048	[43]0.0067	[50]0.0090	[51]0.0109	[53]0.0128	[52]0.0148	[52]0.0178	[50]0.0219	[56]0.0354	[57]0.0618	[58]0.0931	[59]0.1290	[60]0.1625	[60]0.1964	[60]0.2408	[52]0.2924
74	PARAVISION-004	[15]0.0024	[16]0.0032	[16]0.0040	[18]0.0047	[17]0.0053	[17]0.0061	[17]0.0073	[18]0.0072	[19]0.0118	[22]0.0209	[23]0.0327	[23]0.0465	[23]0.0613	[23]0.0779	[23]0.1008	[23]0.1285
75	PARAVISION-005	[11]0.0021	[12]0.0028	[12]0.0035	[13]0.0041	[15]0.0046	[15]0.0054	[15]0.0067	[17]0.0070	[11]0.0057	[12]0.0093	[12]0.0144	[14]0.0207	[15]0.0278	[15]0.0368	[16]0.0508	[16]0.0715
76	PARAVISION-007	[5]0.0019	[7]0.0025	[6]0.0029	[8]0.0033	[8]0.0036	[8]0.0042	[8]0.0049	[6]0.0030	[10]0.0057	[13]0.0094	[14]0.0144	[13]0.0206	[14]0.0275	[14]0.0357	[14]0.0485	[14]0.0652
77	PIXELALL-002	[71]0.0085	[72]0.0119	[70]0.0147	[71]0.0172	[72]0.0198	[73]0.0225	[72]0.0270	[73]0.0349	[96]0.1193	[96]0.1900	[96]0.2601	[96]0.3332	[96]0.3955	[96]0.4565	[96]0.5268	[97]0.6030
78	PIXELALL-003	[45]0.0050	[41]0.0063	[38]0.0072	[33]0.0077	[32]0.0085	[32]0.0095	[33]0.0113	[31]0.0119	[43]0.0248	[42]0.0418	[42]0.0622	[42]0.0861	[42]0.1104	[39]0.1364	[39]0.1723	[38]0.2167
79	PIXELALL-004	[44]0.0049	[39]0.0063	[39]0.0072	[36]0.0079	[35]0.0089	[36]0.0103	[36]0.0127	[35]0.0146	[37]0.0211	[39]0.0360	[41]0.0553	[41]0.0792	[38]0.1045	[38]0.1317	[38]0.1700	[41]0.2246
80	PTAKURATSATU-000	[53]0.0061	[54]0.0082	[54]0.0097	[52]0.0109	[48]0.0120	[45]0.0131	[41]0.0146	[43]0.0180	[58]0.0375	[56]0.0596	[54]0.0842	[54]0.1116	[52]0.1357	[48]0.1553	[42]0.1820	[44]0.2326
81	RANKONE-002	[98]0.0212	[97]0.0313	[97]0.0431	[97]0.0562	[98]0.0712	[99]0.0881	[100]0.1130	[101]0.1543	[94]0.1111	[94]0.1707	[94]0.2305	[94]0.2968	[95]0.3646	[95]0.4345	[95]0.5172	[98]0.6110
82	RANKONE-004	[107]0.0424	[106]0.0643	[106]0.0875	[106]0.1127	[106]0.1364	[104]0.1579	[104]0.1914	[104]0.2378	[103]0.1855	[102]0.2681	[102]0.3431	[100]0.4155	[100]0.4785	[99]0.5350	[99]0.5980	[99]0.6722
83	RANKONE-005	[91]0.0136	[92]0.0192	[90]0.0246	[90]0.0303	[89]0.0362	[88]0.0422	[87]0.0521	[87]0.0694	[80]0.0582	[74]0.0910	[70]0.1260	[67]0.1645	[64]0.2005	[63]0.2353	[63]0.2816	[64]0.3522
84	RANKONE-007	[66]0.0078	[63]0.0099	[60]0.0113	[57]0.0123	[57]0.0139	[58]0.0156	[57]0.0191	[56]0.0242	[41]0.0242	[41]0.0376	[40]0.0542	[37]0.0737	[36]0.0935	[35]0.1130	[33]0.1416	[33]0.1811
85	RANKONE-009	[47]0.0054	[48]0.0072	[45]0.0085	[46]0.0098	[46]0.0113	[44]0.0130	[49]0.0169	[53]0.0220	[36]0.0208	[37]0.0345	[36]0.0504	[35]0.0706	[35]0.0930	[36]0.1174	[37]0.1504	[36]0.2002
86	RANKONE-010	[41]0.0047	[37]0.0061	[37]0.0070	[32]0.0076	[33]0.0087	[33]0.0098	[34]0.0113	[32]0.0120	[30]0.0177	[28]0.0269	[25]0.0368	[25]0.0479	[22]0.0590	[21]0.0688	[21]0.0803	[20]0.0991
87	RANKONE-011	[22]0.0031	[22]0.0041	[22]0.0047	[22]0.0053	[21]0.0058	[22]0.0067	[18]0.0077	[20]0.0073	[22]0.0127	[19]0.0194	[20]0.0265	[19]0.0345	[19]0.0422	[19]0.0499	[19]0.0611	[18]0.0756
88	REALNETWORKS-002	[106]0.0381	[107]0.0687	[107]0.1062	[107]0.1495	[108]0.1963	[108]0.2513	[110]0.3206	[110]0.3927	[104]0.2153	[104]0.3323	[104]0.4444	[104]0.5485	[105]0.6355	[105]0.7132	[106]0.7855	[106]0.8437

Table 7: **Accuracy for the FRVT 2018 mugshot sets under ageing**. *The second row shows the time lapse between gallery and subsequent probe images, in years. The first two columns identify the algorithm The next 8 values give rank-based FNIR with R = 1, T = 0 and FPIR = 1. All these are relevant to investigational uses where candidates from all searches would need human review. The second 8 values give threshold-based FNIR with T $\geq$ 0, FPIR = 0.001 and no rank criterion. The shaded cells indictate indicate the three most accurate algorithms for that elapsed time. The gallery size is 3068801. The total number of searches is 10951064.*

This publication is available free of charge from: https://doi.org/10.6028/NIST.IR.8271

MISS RATES		INVESTIGATION, FNIR(N, R = 1, T = 0)								IDENTIFICATION, FNIR(N, R = L, T $\geq$ 0) FOR FPIR = 0.001							
#	ALGORITHM	(0, 2]	(2, 4]	(4, 6]	(6, 8]	(8, 10]	(10, 12]	(12, 14]	(14, 18]	(0, 2]	(2, 4]	(4, 6]	(6, 8]	(8, 10]	(10, 12]	(12, 14]	(14, 18]
89	REALNETWORKS-003	102 0.0245	104 0.0437	104 0.0686	105 0.0975	105 0.1312	106 0.1719	106 0.2294	107 0.2907	97 0.1468	99 0.2370	100 0.3313	102 0.4269	102 0.5142	103 0.5979	104 0.6815	104 0.7567
90	REALNETWORKS-004	101 0.0244	103 0.0428	103 0.0663	104 0.0939	104 0.1251	105 0.1634	105 0.2170	106 0.2785	98 0.1484	100 0.2377	99 0.3303	101 0.4249	101 0.5106	102 0.5924	103 0.6758	103 0.7534
91	SCANOVATE-001	67 0.0079	71 0.0117	74 0.0151	77 0.0185	77 0.0221	77 0.0259	79 0.0321	79 0.0427	87 0.0727	87 0.1169	86 0.1650	86 0.2115	83 0.2528	83 0.2925	80 0.3437	79 0.4084
92	SENSETIME-002	95 0.0186	91 0.0191	83 0.0183	74 0.0179	67 0.0173	47 0.0133	25 0.0089	15 0.0059	39 0.0220	24 0.0236	18 0.0237	18 0.0240	12 0.0245	10 0.0219	7 0.0195	6 0.0222
93	SENSETIME-003	10 0.0021	11 0.0028	10 0.0031	7 0.0033	6 0.0035	7 0.0040	7 0.0047	7 0.0033	8 0.0046	8 0.0064	6 0.0076	4 0.0086	4 0.0101	3 0.0122	4 0.0155	4 0.0196
94	SENSETIME-004	3 0.0016	3 0.0022	3 0.0025	3 0.0028	3 0.0030	3 0.0035	4 0.0043	3 0.0025	4 0.0036	4 0.0052	3 0.0066	3 0.0081	3 0.0099	5 0.0126	6 0.0169	7 0.0230
95	SENSETIME-005	2 0.0015	2 0.0020	2 0.0024	2 0.0026	2 0.0029	2 0.0035	3 0.0043	5 0.0028	5 0.0036	7 0.0059	8 0.0089	9 0.0128	10 0.0177	11 0.0240	12 0.0345	12 0.0493
96	SENSETIME-006	1 0.0015	1 0.0019	1 0.0022	1 0.0025	1 0.0027	1 0.0033	1 0.0040	2 0.0021	2 0.0031	2 0.0049	4 0.0068	6 0.0097	7 0.0132	8 0.0184	10 0.0262	10 0.0359
97	SIAT-002	116 0.8309	116 0.8310	116 0.8311	116 0.8306	116 0.8296	116 0.8302	116 0.8300	115 0.8301	111 0.8340	109 0.8368	108 0.8404	108 0.8445	108 0.8480	108 0.8532	108 0.8595	107 0.8691
98	SYNESIS-003	88 0.0125	84 0.0151	82 0.0174	79 0.0199	78 0.0223	74 0.0240	74 0.0279	69 0.0331	84 0.0658	82 0.1052	82 0.1483	81 0.1968	81 0.2399	79 0.2834	79 0.3405	78 0.4046
99	SYNESIS-005	39 0.0044	36 0.0058	36 0.0070	39 0.0080	36 0.0091	35 0.0103	35 0.0125	36 0.0152	45 0.0262	44 0.0444	44 0.0666	44 0.0923	43 0.1156	40 0.1399	40 0.1736	39 0.2185
100	TECH5-001	56 0.0061	60 0.0093	65 0.0128	70 0.0171	76 0.0221	81 0.0289	84 0.0412	84 0.0560	85 0.0660	86 0.1156	89 0.1733	90 0.2385	90 0.2998	90 0.3629	92 0.4424	93 0.5284
101	TOSHIBA-001	72 0.0086	73 0.0119	73 0.0150	73 0.0178	74 0.0209	75 0.0241	75 0.0292	74 0.0365								
102	TRUEFACE-000	35 0.0043	35 0.0057	29 0.0061	27 0.0067	26 0.0073	27 0.0084	27 0.0097	25 0.0099	34 0.0200	36 0.0338	37 0.0504	34 0.0705	34 0.0904	34 0.1112	32 0.1401	32 0.1792
103	VERIDAS-001	57 0.0063	55 0.0083	55 0.0099	55 0.0113	55 0.0132	53 0.0148	54 0.0184	51 0.0219	60 0.0403	60 0.0684	61 0.1012	61 0.1386	61 0.1741	61 0.2113	61 0.2611	62 0.3233
104	VISIONLABS-004	42 0.0048	45 0.0069	51 0.0091	54 0.0111	54 0.0130	56 0.0152	55 0.0187	57 0.0242	73 0.0540	76 0.0916	77 0.1358	77 0.1855	78 0.2303	77 0.2745	76 0.3312	72 0.3913
105	VISIONLABS-005	38 0.0044	38 0.0063	42 0.0081	45 0.0095	45 0.0109	43 0.0125	44 0.0151	45 0.0187	66 0.0479	66 0.0812	67 0.1212	69 0.1664	68 0.2078	68 0.2473	67 0.2999	66 0.3577
106	VISIONLABS-006	28 0.0035	29 0.0048	31 0.0061	29 0.0069	28 0.0077	28 0.0087	30 0.0105	33 0.0120	47 0.0273	46 0.0465	46 0.0702	46 0.0970	46 0.1228	44 0.1486	43 0.1847	43 0.2295
107	VISIONLABS-008	20 0.0028	19 0.0037	20 0.0047	21 0.0053	22 0.0058	20 0.0067	23 0.0081	24 0.0085	26 0.0143	26 0.0241	27 0.0373	26 0.0519	26 0.0677	24 0.0850	24 0.1104	24 0.1444
108	VISIONLABS-009	9 0.0020	9 0.0026	9 0.0030	9 0.0034	10 0.0038	10 0.0044	11 0.0052	12 0.0046	14 0.0065	15 0.0105	15 0.0156	15 0.0217	16 0.0289	16 0.0368	15 0.0499	15 0.0681
109	VISIONLABS-010	8 0.0020	8 0.0025	8 0.0030	10 0.0034	9 0.0036	9 0.0043	9 0.0051	13 0.0047	16 0.0069	16 0.0113	16 0.0170	16 0.0238	17 0.0316	17 0.0411	17 0.0557	17 0.0740
110	VTS-000	115 0.5878	115 0.6312	115 0.6602	114 0.6863	114 0.7073	114 0.7246	114 0.7458	113 0.7747	107 0.5929	107 0.6397	107 0.6729	107 0.7034	106 0.7279	106 0.7493	105 0.7739	105 0.8076
111	XFORWARDAI-000	19 0.0027	17 0.0034	19 0.0044	20 0.0052	20 0.0058	23 0.0067	21 0.0079	22 0.0076	27 0.0157	30 0.0281	29 0.0443	30 0.0635	31 0.0834	31 0.1050	30 0.1330	30 0.1714
112	XFORWARDAI-001	14 0.0023	10 0.0028	11 0.0034	11 0.0037	11 0.0039	11 0.0045	10 0.0052	11 0.0043	13 0.0060	14 0.0096	13 0.0144	12 0.0200	13 0.0260	13 0.0334	13 0.0435	13 0.0586
113	YITU-002	59 0.0066	56 0.0083	52 0.0094	47 0.0101	49 0.0121	55 0.0150	60 0.0223	67 0.0328	32 0.0189	33 0.0317	34 0.0494	38 0.0750	40 0.1066	46 0.1494	53 0.2171	59 0.2958
114	YITU-003	62 0.0072	59 0.0089	56 0.0100	50 0.0107	51 0.0125	57 0.0153	62 0.0226	70 0.0334	33 0.0194	34 0.0321	35 0.0500	40 0.0756	41 0.1071	47 0.1500	54 0.2177	60 0.2964
115	YITU-004	54 0.0061	50 0.0075	43 0.0081	40 0.0081	38 0.0092	38 0.0107	46 0.0154	48 0.0207	21 0.0125	21 0.0204	22 0.0314	24 0.0469	25 0.0671	27 0.0955	35 0.1421	37 0.2006
116	YITU-005	60 0.0067	53 0.0080	46 0.0087	43 0.0085	40 0.0094	39 0.0108	45 0.0151	47 0.0204	20 0.0124	20 0.0198	21 0.0308	21 0.0462	24 0.0667	26 0.0953	34 0.1418	35 0.1930

Table 8: **Accuracy for the FRVT 2018 mugshot sets under ageing**. *The second row shows the time lapse between gallery and subsequent probe images, in years. The first two columns identify the algorithm The next 8 values give rank-based FNIR with R = 1, T = 0 and FPIR = 1. All these are relevant to investigational uses where candidates from all searches would need human review. The second 8 values give threshold-based FNIR with T $\geq$ 0, FPIR = 0.001 and no rank criterion. The shaded cells indictate indicate the three most accurate algorithms for that elapsed time. The gallery size is 3068801. The total number of searches is 10951064.*

This publication is available free of charge from: https://doi.org/10.6028/NIST.IR.8271

#	ALGORITHM	INVESTIGATION MODE						IDENTIFICATION MODE						FAILURE TO EXTRACT					
		RANK ONE MISS RATE, FNIR(N, 0, 1)						HIGH T ⟶ FPIR = 0.001, FNIR(N, T, L)						FEATURES					
		N=1.6M						N=1.6M											
	GALLERY	MUGSHOT	MUGSHOT	MUGSHOT	VISA	BORDER	VISA	MUGSHOT	MUGSHOT	MUGSHOT	VISA	BORDER	VISA	MUGSHOT	MUGSHOT	MUGSHOT	VISA	BORDER	KIOSK
	PROBE	MUGSHOT	WEBCAM	PROFILE	BORDER	BOR¿10YR	KIOSK	MUGSHOT	WEBCAM	PROFILE	BORDER	BOR¿10YR	KIOSK	MUGSHOT	WEBCAM	PROFILE	BORDER	BOR¿10YR	KIOSK
1	20FACE-000	[219] 0.055	[209] 0.085	[120] 0.736	[144] 0.056	[70] 0.239	[139] 0.243	[215] 0.348	[211] 0.450	[177] 1.000	[147] 0.424	[68] 0.772	[142] 0.938	0.000	0.000	0.000		0.000	
2	3DIVI-003	[228] 0.083	[224] 0.206		[156] 0.141		[162] 0.474	[224] 0.400	[224] 0.626		[158] 0.605		[129] 0.821	0.002	0.005				
3	3DIVI-004	[188] 0.018	[197] 0.062		[138] 0.035		[143] 0.279	[196] 0.169	[202] 0.343		[138] 0.277		[109] 0.607	0.002	0.005				
4	3DIVI-005	[189] 0.018	[196] 0.062	[166] 0.930	[174] 0.821		[144] 0.279	[193] 0.166	[200] 0.339	[119] 0.996	[163] 0.864		[108] 0.597	0.002	0.005	0.442			
5	3DIVI-006	[199] 0.024	[204] 0.074		[140] 0.047		[152] 0.312	[195] 0.168	[201] 0.342		[139] 0.283		[112] 0.615	0.002	0.005				
6	ACER-000	[166] 0.011	[160] 0.036	[147] 0.827	[125] 0.025		[127] 0.209	[186] 0.146	[180] 0.246	[73] 0.981	[133] 0.201		[96] 0.490	0.000	0.000	0.042			
7	ACER-001	[121] 0.005	[113] 0.020	[70] 0.422	[92] 0.008	[59] 0.050	[46] 0.098	[129] 0.056	[113] 0.109	[151] 0.999	[97] 0.068	[63] 0.406	[95] 0.479	0.001	0.001	0.041		0.000	
8	AIZE-001	[127] 0.006	[125] 0.022	[111] 0.683	[114] 0.016	[61] 0.050	[111] 0.165	[149] 0.077	[139] 0.143	[99] 0.994	[109] 0.101	[58] 0.364	[80] 0.387	0.001	0.001	0.047		0.000	
9	ALCHERA-000	[184] 0.016	[184] 0.047	[154] 0.870	[139] 0.046		[149] 0.292	[183] 0.138	[166] 0.216	[135] 0.999	[128] 0.176		[125] 0.803	0.006	0.014	0.328			
10	ALCHERA-001	[254] 0.987	[250] 1.000		[176] 1.000		[233] 1.000	[251] 0.999	[252] 1.000		[190] 1.000		[202] 1.000	0.006	0.013	0.324			
11	ALCHERA-002	[229] 0.095	[221] 0.166	[179] 0.954	[171] 0.668		[160] 0.446	[231] 0.486	[221] 0.591	[157] 1.000	[162] 0.827		[126] 0.811	0.001	0.002	0.106			
12	ALCHERA-003	[163] 0.010	[158] 0.035	[121] 0.741	[115] 0.016		[125] 0.206	[187] 0.155	[177] 0.239	[145] 0.999	[127] 0.172		[92] 0.464	0.001	0.002	0.106			
13	ALCHERA-004	[168] 0.011	[163] 0.038	[62] 0.345	[116] 0.017	[67] 0.088	[100] 0.144	[223] 0.394	[217] 0.529	[95] 0.991	[148] 0.424	[66] 0.708	[105] 0.546	0.001	0.001	0.046		0.000	
14	ALLGOVISION-000	[171] 0.011	[154] 0.033	[157] 0.894	[121] 0.021		[146] 0.282	[161] 0.088	[155] 0.166	[92] 0.990	[112] 0.117		[102] 0.526	0.002	0.003	0.122			
15	ALLGOVISION-001	[154] 0.009	[169] 0.038	[107] 0.661	[120] 0.021		[137] 0.241	[166] 0.102	[170] 0.221	[82] 0.986	[122] 0.150		[97] 0.491	0.001	0.001	0.042			
16	ANKE-000	[179] 0.013	[164] 0.038	[169] 0.931	[180] 1.000		[178] 1.000	[171] 0.117	[169] 0.220	[100] 0.994	[214] 1.000		[240] 1.000	0.000	0.001	0.080			
17	ANKE-001	[180] 0.013	[165] 0.038	[174] 0.946	[196] 1.000		[193] 1.000	[175] 0.119	[168] 0.220	[105] 0.994	[228] 1.000		[248] 1.000	0.000	0.001	0.080			
18	ANKE-002	[86] 0.003	[89] 0.016	[86] 0.522	[61] 0.005		[78] 0.119	[91] 0.032	[79] 0.079	[51] 0.948	[64] 0.034		[52] 0.245	0.001	0.001	0.049			
19	AWARE-003	[206] 0.031	[210] 0.090	[191] 0.966	[162] 0.316		[148] 0.290	[179] 0.128	[194] 0.298	[79] 0.984	[149] 0.428		[103] 0.530	0.004	0.003	0.874			
20	AWARE-004	[223] 0.068	[223] 0.176	[198] 0.976	[154] 0.122		[158] 0.414	[209] 0.269	[216] 0.509	[162] 1.000	[144] 0.397		[127] 0.816	0.003	0.003	0.776			
21	AWARE-005	[207] 0.031	[198] 0.067	[199] 0.978	[142] 0.048		[151] 0.308	[218] 0.364	[181] 0.253	[163] 1.000	[137] 0.255		[138] 0.916	0.001	0.002	0.189			
22	AWARE-006	[225] 0.070	[217] 0.128	[201] 0.983	[153] 0.111		[159] 0.421	[210] 0.276	[205] 0.398	[155] 0.999	[142] 0.368		[119] 0.749	0.001	0.002	0.189			
23	AYONIX-000	[248] 0.450	[245] 0.685	[210] 0.996	[170] 0.607		[173] 0.867	[240] 0.811	[239] 0.939	[126] 0.998	[167] 0.954		[150] 0.982	0.010	0.031	0.939			
24	AYONIX-001	[243] 0.341	[238] 0.527	[205] 0.993	[175] 0.994		[171] 0.778	[242] 0.824	[234] 0.920	[152] 0.999	[171] 0.999		[146] 0.969	0.010	0.031	0.939			
25	AYONIX-002	[244] 0.341	[239] 0.527	[206] 0.993	[166] 0.464		[170] 0.778	[241] 0.824	[235] 0.920	[153] 0.999	[164] 0.915		[147] 0.969	0.010	0.031	0.939			
26	CAMVI-003	[218] 0.052	[211] 0.090	[159] 0.911	[150] 0.093		[155] 0.360	[144] 0.071	[132] 0.132	[59] 0.970	[111] 0.114		[83] 0.402	0.006	0.013	0.675			
27	CAMVI-004	[216] 0.047	[205] 0.077	[123] 0.744	[148] 0.072		[150] 0.296	[145] 0.072	[134] 0.136	[149] 0.999	[108] 0.100		[123] 0.787	0.000	0.000	0.000			
28	CAMVI-005	[222] 0.065	[215] 0.103	[125] 0.746	[151] 0.098		[154] 0.341	[165] 0.099	[162] 0.179	[159] 1.000	[123] 0.156		[158] 0.999	0.000	0.000	0.000			
29	CANON-001	[7] 0.001	[3] 0.006	[16] 0.088	[6] 0.001	[7] 0.007	[6] 0.062	[23] 0.005	[17] 0.023	[9] 0.365	[13] 0.008	[16] 0.068	[19] 0.139	0.001	0.000	0.042		0.000	
30	CIB-000	[29] 0.002	[12] 0.008	[20] 0.100	[14] 0.002	[20] 0.011	[10] 0.069	[39] 0.012	[38] 0.045	[170] 1.000	[34] 0.017	[28] 0.141	[135] 0.894	0.000	0.000	0.000		0.000	
31	CLEARVIEWAI-000	[8] 0.001	[8] 0.007	[5] 0.062	[5] 0.001	[4] 0.006	[2] 0.056	[24] 0.006	[20] 0.025	[64] 0.974	[14] 0.008	[12] 0.057	[61] 0.268	0.000	0.000	0.037		0.000	
32	CLOUDWALK-HR-000	[24] 0.001	[25] 0.010	[6] 0.064	[11] 0.002	[6] 0.006	[3] 0.057	[6] 0.002	[6] 0.013	[1] 0.133	[6] 0.005	[3] 0.033	[6] 0.099	0.001	0.000	0.042		0.000	
33	COGENT-000	[164] 0.010	[182] 0.046	[189] 0.965				[121] 0.053	[138] 0.140	[112] 0.995				0.000	0.000	0.000			
34	COGENT-001	[165] 0.010	[181] 0.046	[190] 0.965				[120] 0.053	[136] 0.140	[111] 0.995				0.000	0.000	0.000			
35	COGENT-002	[101] 0.004	[115] 0.020	[164] 0.925				[107] 0.044	[104] 0.098	[124] 0.998				0.000	0.000	0.000			
36	COGENT-003	[103] 0.004	[119] 0.021	[173] 0.939				[112] 0.046	[98] 0.095	[127] 0.998				0.000	0.000	0.000			
37	COGENT-004	[56] 0.002	[60] 0.013	[163] 0.922	[53] 0.004	[37] 0.019	[73] 0.113	[92] 0.033	[44] 0.051	[122] 0.997	[43] 0.022	[25] 0.126	[90] 0.456	0.000	0.000	0.000		0.000	
38	COGENT-005	[37] 0.002	[33] 0.010	[25] 0.126	[15] 0.002	[18] 0.010	[79] 0.120	[28] 0.009	[32] 0.037	[88] 0.989	[24] 0.011	[18] 0.082	[136] 0.905	0.000	0.000	0.000		0.000	
39	COGNITEC-000	[201] 0.025	[192] 0.059	[187] 0.964				[191] 0.161	[195] 0.303	[96] 0.992				0.003	0.002	0.924			
40	COGNITEC-001	[172] 0.012	[156] 0.034	[182] 0.958				[167] 0.102	[174] 0.230	[229] 1.000				0.003	0.002	0.924			
41	COGNITEC-002	[128] 0.006	[141] 0.025	[176] 0.949				[123] 0.053	[161] 0.178	[169] 1.000				0.003	0.002	0.924			
42	COGNITEC-003	[132] 0.006	[140] 0.025	[168] 0.930				[119] 0.053	[153] 0.162	[174] 1.000				0.004	0.002	0.878			
43	COGNITEC-004	[94] 0.003	[88] 0.016	[144] 0.813	[107] 0.013	[64] 0.057	[99] 0.143	[90] 0.031	[102] 0.097	[89] 0.990	[96] 0.068	[57] 0.316	[62] 0.288	0.002	0.001	0.635		0.006	
44	COGNITEC-005	[34] 0.002	[31] 0.010	[117] 0.713	[122] 0.021	[58] 0.037	[75] 0.115	[30] 0.010	[36] 0.041	[251] 1.000	[71] 0.041	[35] 0.157	[35] 0.179	0.002	0.001	0.614		0.017	
45	CUBOX-000	[19] 0.001	[28] 0.010	[2] 0.058	[9] 0.002	[2] 0.004	[1] 0.049	[11] 0.003	[12] 0.019	[2] 0.168	[2] 0.004	[2] 0.028	[1] 0.073	0.001	0.000	0.042		0.000	
46	CYBERLINK-000	[105] 0.004	[112] 0.020	[118] 0.717	[87] 0.007		[92] 0.134	[130] 0.056	[117] 0.116	[114] 0.995	[94] 0.063		[75] 0.339	0.001	0.001	0.063			

Table 9: **Miss rates by dataset:** *At left, rank 1 miss rates relevant to investigations; at right, with threshold set to target FPIR = 0.01 for higher volume, low prior, uses. Yellow indicates most accurate algorithm. Throughout blue superscripts indicate the rank of the algorithm for that column.*

2021/11/22 08:35:53

FNIR(N, R, T) = False neg. identification rate
FPIR(N, T) = False pos. identification rate

N = Num. enrolled subjects
R = Num. candidates examined

T = Threshold

T = 0 → Investigation
T > 0 → Identification

This publication is available free of charge from: https://doi.org/10.6028/NIST.IR.8271

#	ALGORITHM	INVESTIGATION MODE						IDENTIFICATION MODE						FAILURE TO EXTRACT					
		RANK ONE MISS RATE, FNIR(N, 0, 1)						HIGH T ⟶ FPIR = 0.001, FNIR(N, T, L)						FEATURES					
		N=1.6M						N=1.6M											
	GALLERY	MUGSHOT	MUGSHOT	MUGSHOT	VISA	BORDER	VISA	MUGSHOT	MUGSHOT	MUGSHOT	VISA	BORDER	VISA	MUGSHOT	MUGSHOT	MUGSHOT	VISA	BORDER	KIOSK
	PROBE	MUGSHOT	WEBCAM	PROFILE	BORDER	BOR¿10YR	KIOSK	MUGSHOT	WEBCAM	PROFILE	BORDER	BOR¿10YR	KIOSK	MUGSHOT	WEBCAM	PROFILE	BORDER	BOR¿10YR	KIOSK
47	CYBERLINK-001	[99]0.004	[101]0.018	[119]0.731	[81]0.007		[91]0.133	[124]0.054	[114]0.109	[109]0.995	[91]0.062		[113]0.652	0.000	0.000	0.040			
48	CYBERLINK-002	[79]0.003	[50]0.012	[99]0.577	[49]0.004		[64]0.107	[47]0.015	[51]0.053	[87]0.988	[46]0.024		[63]0.288	0.001	0.000	0.042			
49	CYBERLINK-003	[31]0.002	[19]0.009	[78]0.474	[32]0.003	[21]0.012	[31]0.082	[26]0.008	[29]0.035	[62]0.972	[25]0.012	[21]0.100	[77]0.368	0.000	0.000	0.039		0.000	
50	CYBERLINK-004	[36]0.002	[47]0.011	[71]0.423	[30]0.003	[19]0.011	[56]0.104	[25]0.007	[30]0.036	[181]1.000	[27]0.013	[22]0.109	[145]0.954	0.000	0.000	0.011		0.000	
51	DAHUA-000	[158]0.009	[143]0.026					[157]0.086	[133]0.135					0.004	0.003				
52	DAHUA-001	[136]0.007	[135]0.024	[115]0.703				[147]0.073	[125]0.122	[73]0.980				0.002	0.002	0.346			
53	DAHUA-002	[48]0.002	[49]0.012	[53]0.304	[28]0.003		[33]0.084	[48]0.015	[40]0.046	[26]0.638	[31]0.017		[27]0.159	0.001	0.000	0.099			
54	DAHUA-003	[13]0.001	[9]0.007	[37]0.206	[12]0.002	[15]0.009	[14]0.073	[44]0.014	[35]0.041	[22]0.579	[26]0.013	[17]0.081	[18]0.134	0.000	0.000	0.000		0.000	
55	DEEPGLINT-001	[22]0.001	[7]0.007	[36]0.200	[23]0.002		[15]0.073	[14]0.003	[7]0.014	[156]1.000	[9]0.006		[26]0.159	0.000	0.000	0.038			
56	DEEPSEA-001	[110]0.004	[86]0.016	[145]0.814	[95]0.010		[98]0.140	[111]0.046	[106]0.101	[80]0.985	[101]0.077		[73]0.326	0.000	0.001	0.047			
57	DERMALOG-003	[233]0.126	[228]0.217		[161]0.296		[165]0.560	[230]0.482	[226]0.655		[161]0.677		[133]0.870	0.002	0.002	0.103			
58	DERMALOG-004	[232]0.125	[225]0.215	[167]0.930	[155]0.135		[161]0.467	[229]0.480	[227]0.657	[115]0.995	[157]0.603		[132]0.856	0.001	0.002	0.107			
59	DERMALOG-005	[183]0.015	[162]0.037	[114]0.701	[160]0.242		[152]0.384	[160]0.088	[146]0.154	[90]0.990	[140]0.300		[111]0.614	0.001	0.002	0.102			
60	DERMALOG-006	[149]0.008	[139]0.024	[105]0.619	[96]0.010		[107]0.155	[118]0.052	[109]0.105	[74]0.981	[89]0.059		[72]0.318	0.003	0.006	0.181			
61	DERMALOG-007	[157]0.009	[144]0.027	[109]0.675	[111]0.014		[113]0.170	[158]0.086	[144]0.152	[91]0.990	[107]0.099		[107]0.557	0.001	0.002	0.102			
62	DERMALOG-008	[87]0.003	[79]0.015	[84]0.516	[78]0.007	[54]0.029	[97]0.139	[109]0.045	[95]0.094	[186]1.000	[86]0.057	[61]0.382	[143]0.940	0.000	0.000	0.002		0.000	
63	DERMALOG-009	[85]0.003	[75]0.014	[33]0.167	[85]0.007	[72]0.999	[59]0.106	[66]0.021	[66]0.066	[171]1.000	[55]0.031	[70]0.999	[131]0.840	0.001	0.001	0.018		0.003	
64	EYEDEA-003	[227]0.080	[219]0.148	[185]0.960	[152]0.101		[156]0.379	[220]0.388	[219]0.543	[106]0.994	[155]0.570		[124]0.792	0.001	0.003	0.161			
65	F8-001	[176]0.012		[108]0.669	[191]1.000		[191]1.000	[192]0.166		[134]0.998				0.004	1.000	0.158			
66	FINCORE-000	[167]0.011	[157]0.034	[131]0.767	[132]0.032	[68]0.117	[122]0.191	[182]0.134	[167]0.217	[166]1.000	[129]0.187	[65]0.598	[91]0.458	0.000	0.001	0.043		0.000	
67	FUJITSULAB-000	[63]0.002	[68]0.014	[74]0.440	[52]0.004	[40]0.023	[47]0.098	[67]0.021	[56]0.056		[45]0.024	[40]0.177	[51]0.240	0.000	0.001	0.016		0.000	
68	GLORY-000	[237]0.178	[232]0.320	[209]0.994	[159]0.228		[167]0.678	[219]0.367	[220]0.547	[108]0.995	[151]0.453		[130]0.839	0.011	0.013	0.985			
69	GLORY-001	[234]0.127	[229]0.267	[204]0.992	[158]0.178		[166]0.594	[211]0.305	[218]0.537	[97]0.993	[146]0.408		[128]0.819	0.011	0.013	0.988			
70	GORILLA-001	[220]0.060	[212]0.095	[171]0.936	[147]0.069		[153]0.329	[225]0.406	[212]0.453	[192]1.000	[152]0.468		[243]1.000	0.001	0.001	0.069			
71	GORILLA-002	[195]0.020	[178]0.044	[127]0.753	[126]0.027		[132]0.214	[199]0.188	[188]0.268	[185]1.000	[136]0.250		[162]1.000	0.001	0.001	0.069			
72	GORILLA-003	[208]0.036	[200]0.070	[146]0.821	[141]0.048		[141]0.265	[213]0.318	[209]0.434	[254]1.000	[145]0.407		[243]1.000	0.001	0.001	0.069			
73	GORILLA-004	[133]0.006	[136]0.024	[113]0.697	[100]0.012		[110]0.162	[163]0.089	[152]0.160	[53]0.959	[117]0.135		[87]0.438	0.000	0.001	0.042			
74	GORILLA-005	[93]0.003	[102]0.018	[38]0.209	[72]0.006		[81]0.124	[134]0.058	[138]0.142	[29]0.700	[105]0.088		[70]0.315	0.000	0.000	0.040			
75	GORILLA-006	[41]0.002	[52]0.012	[23]0.122	[38]0.003	[33]0.018	[58]0.105	[82]0.027	[90]0.089	[21]0.531	[49]0.028	[39]0.166	[45]0.218	0.000	0.000	0.041		0.000	
76	GRIAULE-000	[77]0.002	[62]0.014	[57]0.327	[99]0.011	[56]0.031	[82]0.126	[64]0.020	[63]0.063	[110]0.995	[61]0.033	[44]0.185	[41]0.198	0.000	0.002	0.090		0.001	
77	HIK-003	[173]0.012	[147]0.027	[112]0.689	[103]0.012		[104]0.151	[168]0.103	[148]0.158	[57]0.969	[120]0.142		[89]0.445	0.000	0.000	0.048			
78	HIK-004	[170]0.011	[145]0.027	[122]0.743	[101]0.012		[106]0.152	[164]0.099	[145]0.153	[65]0.976	[118]0.137		[86]0.434	0.000	0.000	0.048			
79	HIK-005	[115]0.005	[91]0.017	[90]0.535	[83]0.007		[69]0.111	[104]0.044	[78]0.077	[154]0.999	[95]0.068		[104]0.541	0.000	0.000	0.000			
80	HIK-006	[114]0.005	[90]0.017	[91]0.535				[113]0.047	[86]0.086	[178]1.000				0.000	0.000	0.000			
81	HYPERVERGE-001	[17]0.001	[40]0.011	[9]0.067	[8]0.002	[8]0.007	[5]0.061	[17]0.004	[26]0.031	[5]0.220	[12]0.007	[10]0.053	[8]0.101	0.001	0.000	0.041		0.000	
82	IDEMIA-003	[139]0.007	[155]0.034	[180]0.958	[117]0.018		[128]0.210	[114]0.047	[154]0.165		[114]0.123		[125]0.766	0.000	0.000	0.041			
83	IDEMIA-004	[135]0.007	[153]0.032	[175]0.947	[118]0.018		[129]0.210	[100]0.037	[121]0.118	[63]0.973	[113]0.123		[121]0.766	0.000	0.000	0.041			
84	IDEMIA-005	[148]0.008	[170]0.039	[178]0.954	[123]0.021		[133]0.217	[106]0.044	[143]0.150	[68]0.978	[115]0.130		[134]0.879	0.000	0.000	0.041			
85	IDEMIA-006	[161]0.010	[202]0.072	[193]0.969	[128]0.030		[140]0.253	[103]0.043	[172]0.226	[76]0.982	[121]0.144		[117]0.733	0.000	0.000	0.041			
86	IDEMIA-007	[78]0.003	[83]0.015	[249]1.000	[73]0.006	[57]0.036	[88]0.131	[58]0.018	[53]0.055	[230]1.000	[82]0.052	[42]0.182	[227]1.000	0.000	0.000	0.040		0.000	
87	IDEMIA-008	[6]0.001	[4]0.007	[14]0.079	[7]0.001	[10]0.007	[18]0.075	[5]0.002	[5]0.013	[4]0.204	[5]0.005	[6]0.036	[10]0.106	0.000	0.000	0.040		0.000	
88	IMAGUS-002	[240]0.220	[230]0.301	[203]0.988				[238]0.749	[231]0.816	[187]1.000				0.004	0.008	0.550			
89	IMAGUS-003	[245]0.356	[236]0.513	[207]0.993				[239]0.807	[233]0.909	[172]1.000				0.004	0.008	0.550			
90	IMAGUS-005	[53]0.002	[51]0.012	[55]0.319	[71]0.006	[39]0.022	[90]0.132	[61]0.018	[65]0.066	[40]0.838	[51]0.029	[38]0.161	[48]0.231	0.000	0.000	0.000		0.000	
91	IMAGUS-006	[57]0.002	[65]0.014	[51]0.293	[54]0.004	[38]0.019	[72]0.112	[63]0.019	[69]0.069	[47]0.897	[50]0.028	[37]0.161	[56]0.260	0.000	0.000	0.000		0.000	
92	IMPERIAL-000	[76]0.002	[80]0.015	[50]0.280	[58]0.004		[45]0.097	[77]0.026	[68]0.068	[138]0.999	[72]0.042		[53]0.245	0.000	0.000	0.000			

Table 10: **Miss rates by dataset:** *At left, rank 1 miss rates relevant to investigations; at right, with threshold set to target FPIR = 0.01 for higher volume, low prior, uses. Yellow indicates most accurate algorithm. Throughout blue superscripts indicate the rank of the algorithm for that column.*

2021/11/22 08:35:53

FNIR(N, R, T) = False neg. identification rate
FPIR(N, T) = False pos. identification rate
N = Num. enrolled subjects
R = Num. candidates examined
T = Threshold
T = 0 → Investigation
T > 0 → Identification

This publication is available free of charge from: https://doi.org/10.6028/NIST.IR.8271

#	ALGORITHM	INVESTIGATION MODE						IDENTIFICATION MODE						FAILURE TO EXTRACT					
		RANK ONE MISS RATE, FNIR(N, 0, 1)						HIGH T → FPIR = 0.001, FNIR(N, T, L)						FEATURES					
		N=1.6M						N=1.6M											
	GALLERY	MUGSHOT	MUGSHOT	MUGSHOT	VISA	BORDER	VISA	MUGSHOT	MUGSHOT	MUGSHOT	VISA	BORDER	VISA	MUGSHOT	MUGSHOT	MUGSHOT	VISA	BORDER	KIOSK
	PROBE	MUGSHOT	WEBCAM	PROFILE	BORDER	BOR¿10YR	KIOSK	MUGSHOT	WEBCAM	PROFILE	BORDER	BOR¿10YR	KIOSK	MUGSHOT	WEBCAM	PROFILE	BORDER	BOR¿10YR	KIOSK
93	INCODE-000	[217]0.049	[214]0.100	[177]0.951				[212]0.310	[207]0.420	[130]0.998				0.001	0.004	0.173			
94	INCODE-001	[186]0.017	[183]0.046	[128]0.762				[202]0.212	[191]0.296	[179]1.000				0.001	0.004	0.173			
95	INCODE-002	[190]0.018	[185]0.048	[149]0.843				[198]0.184	[189]0.269	[98]0.993				0.000	0.001	0.066			
96	INCODE-003	[178]0.013	[172]0.040	[129]0.764				[194]0.167	[185]0.264	[150]0.999				0.000	0.001	0.066			
97	INCODE-004	[100]0.004	[99]0.017	[79]0.475	[93]0.008		[94]0.135	[126]0.054	[124]0.120	[107]0.995	[93]0.063		[68]0.313	0.000	0.001	0.066			
98	INCODE-005	[35]0.002	[45]0.011	[29]0.147	[22]0.002	[25]0.013	[26]0.079	[35]0.011	[37]0.043	[19]0.528	[33]0.017	[30]0.145	[24]0.155	0.000	0.000	0.042		0.000	
99	INNOVATRICS-002	[215]0.045	[203]0.074	[152]0.853				[207]0.234	[196]0.310	[184]1.000				0.000	0.001	0.046			
100	INNOVATRICS-003	[202]0.026	[188]0.055	[151]0.845				[203]0.221	[192]0.297	[161]1.000				0.000	0.001	0.046			
101	INNOVATRICS-004	[177]0.012	[174]0.040	[181]0.958				[181]0.132	[171]0.222	[72]0.980				0.000	0.001	0.046			
102	INNOVATRICS-005	[75]0.002	[74]0.014	[69]0.407	[60]0.005		[66]0.109	[93]0.034	[89]0.089	[41]0.846	[78]0.047		[54]0.251	0.000	0.001	0.041			
103	INNOVATRICS-007	[38]0.002	[44]0.011	[46]0.248	[25]0.002	[27]0.013	[20]0.077	[40]0.013	[45]0.051	[30]0.743	[32]0.017	[20]0.093	[23]0.154	0.000	0.001	0.041		0.000	
104	INTSYSMSU-000	[235]0.146	[134]0.023	[98]0.562	[149]0.072		[89]0.132	[249]0.998	[244]1.000	[160]1.000	[170]0.999		[159]0.999	0.000	0.000	0.050			
105	IREX-000	[111]0.004	[21]0.010	[110]0.681	[21]0.002	[22]0.012	[29]0.082	[86]0.028	[60]0.060	[52]0.957	[75]0.044	[56]0.302	[32]0.170	0.000	0.000	0.042		0.000	
106	ISYSTEMS-002	[134]0.006	[142]0.026	[150]0.844				[151]0.078	[128]0.126	[123]0.998				0.002	0.002	0.142			
107	ISYSTEMS-003	[122]0.005	[131]0.023	[134]0.791				[135]0.059	[112]0.107	[164]1.000				0.002	0.002	0.142			
108	KAKAO-000	[23]0.001	[35]0.011	[22]0.119	[24]0.002	[24]0.013	[23]0.078	[50]0.015	[55]0.056	[15]0.468	[37]0.019	[27]0.141	[25]0.158	0.000	0.000	0.041		0.000	
109	KEDACOM-001	[144]0.008	[159]0.036	[195]0.972	[134]0.034		[134]0.237	[73]0.023	[73]0.072	[84]0.986	[85]0.055		[66]0.305	0.000	0.000	0.000			
110	KNERON-000	[129]0.006	[146]0.027	[96]0.552	[127]0.028		[123]0.195							0.000	0.000	0.000			
111	KNERON-001	[205]0.030	[244]0.621	[45]0.237	[157]0.144	[69]0.207	[145]0.280							0.000	0.000	0.000		0.000	
112	LINE-000	[64]0.002	[66]0.014	[43]0.223	[64]0.005	[52]0.029	[61]0.107	[89]0.031	[99]0.095		[76]0.046	[54]0.278	[217]1.000	0.000	0.000	0.000		0.000	
113	LOOKMAN-003	[153]0.009	[168]0.038		[137]0.035		[136]0.239	[105]0.044	[116]0.112		[104]0.084		[76]0.355	0.000	0.000				
114	LOOKMAN-004	[155]0.009	[171]0.039	[197]0.973				[108]0.045	[111]0.105	[66]0.977				0.000	0.000	0.000			
115	LOOKMAN-005	[147]0.008	[161]0.036	[196]0.972	[136]0.035		[135]0.237	[88]0.030	[85]0.086	[69]0.978	[92]0.062		[67]0.308	0.000	0.000	0.000			
116	MANTRA-000	[40]0.002	[29]0.010	[116]0.709	[80]0.007	[44]0.024	[70]0.112	[32]0.010	[34]0.041	[212]1.000	[52]0.029	[33]0.152	[161]1.000	0.002	0.001	0.591		0.003	
117	MEGVII-001	[174]0.012	[98]0.017		[226]1.000			[146]0.072	[103]0.097					0.002	0.000				
118	MEGVII-002	[175]0.012	[100]0.017	[75]0.450	[177]1.000			[150]0.077	[101]0.096	[133]0.998				0.002	0.000	0.033			
119	MICROFOCUS-003	[252]0.594	[248]0.781		[173]0.708		[175]0.907	[245]0.931	[243]0.979		[169]0.982		[154]0.991	0.001	0.005				
120	MICROFOCUS-004	[250]0.576	[247]0.758		[172]0.701		[174]0.904	[250]0.999	[241]0.975		[168]0.974		[152]0.989	0.001	0.005				
121	MICROFOCUS-005	[246]0.424	[242]0.601		[168]0.494		[169]0.777	[243]0.835	[237]0.928		[166]0.935		[151]0.985	0.001	0.005				
122	MICROFOCUS-006	[247]0.427	[241]0.583		[167]0.490		[172]0.782	[247]0.978	[236]0.923		[165]0.923		[148]0.971	0.001	0.005				
123	MICROSOFT-003	[32]0.002	[55]0.012		[48]0.004		[67]0.109	[84]0.028	[93]0.091		[66]0.036		[50]0.233	0.000	0.001				
124	MICROSOFT-004	[25]0.001	[54]0.012		[41]0.004		[68]0.109	[78]0.026	[87]0.087		[62]0.033		[46]0.222	0.000	0.001				
125	MICROSOFT-005	[50]0.002	[39]0.011	[28]0.144	[35]0.003		[48]0.099	[76]0.026	[71]0.070	[23]0.587	[47]0.027		[36]0.180	0.000	0.001	0.049			
126	MICROSOFT-006	[55]0.002	[48]0.011	[31]0.150	[45]0.004		[50]0.100	[36]0.012	[31]0.037	[10]0.386	[58]0.032		[33]0.178	0.000	0.001	0.049			
127	NEC-000	[187]0.017	[176]0.041	[184]0.959	[124]0.025		[138]0.243	[153]0.079	[137]0.140	[70]0.979			[94]0.474	0.001	0.002	0.890			
128	NEC-001	[196]0.021	[189]0.056	[192]0.967	[133]0.033		[142]0.277	[170]0.106	[164]0.197	[83]0.986	[116]0.133		[93]0.468	0.005	0.003	0.934			
129	NEC-002	[5]0.001	[18]0.009	[65]0.363	[40]0.003		[76]0.117	[10]0.003	[14]0.020	[148]0.999	[16]0.008		[115]0.676	0.000	0.001	0.041			
130	NEC-003	[16]0.001	[26]0.010	[64]0.352	[44]0.004	[23]0.013	[80]0.120	[8]0.002	[11]0.017	[37]0.824	[19]0.008	[7]0.036	[114]0.668	0.000	0.001	0.041		0.001	
131	NEC-004	[20]0.001	[16]0.009	[92]0.538	[34]0.003	[12]0.007	[17]0.075	[3]0.002	[4]0.013	[25]0.622	[3]0.004	[1]0.019	[7]0.100	0.000	0.001	0.041		0.001	
132	NEUROTECHNOLOGY-003	[197]0.022	[177]0.042	[186]0.961				[236]0.636	[187]0.266	[232]1.000				0.000	0.001	0.131			
133	NEUROTECHNOLOGY-004	[124]0.006	[111]0.020	[194]0.970				[140]0.063	[118]0.117	[103]0.994				0.000	0.001	0.131			
134	NEUROTECHNOLOGY-005	[109]0.004	[138]0.024	[156]0.893				[127]0.054	[130]0.130	[125]0.998				0.000	0.000	0.030			
135	NEUROTECHNOLOGY-006	[191]0.018	[180]0.045	[103]0.606				[208]0.249	[206]0.418					0.000	0.000				
136	NEUROTECHNOLOGY-007	[104]0.004	[118]0.021	[137]0.796	[94]0.009		[119]0.180	[139]0.062	[158]0.173	[167]1.000	[141]0.339		[189]1.000	0.001	0.001	0.041			
137	NEUROTECHNOLOGY-008	[62]0.002	[73]0.014	[76]0.457	[51]0.004	[42]0.023	[52]0.101	[122]0.053	[81]0.080	[175]1.000	[65]0.035	[55]0.293	[42]0.203	0.000	0.001	0.052		0.001	
138	NEUROTECHNOLOGY-009	[21]0.001	[37]0.011	[35]0.179	[17]0.002	[26]0.013	[25]0.079	[51]0.015	[49]0.052	[24]0.588	[39]0.020	[34]0.153	[29]0.165	0.001	0.000	0.046		0.000	

Table 11: **Miss rates by dataset:** *At left, rank 1 miss rates relevant to investigations; at right, with threshold set to target FPIR = 0.01 for higher volume, low prior, uses. Yellow indicates most accurate algorithm. Throughout blue superscripts indicate the rank of the algorithm for that column.*

FNIR(N, R, T) = False neg. identification rate
FPIR(N, T) = False pos. identification rate
N = Num. enrolled subjects
R = Num. candidates examined
T = Threshold
T = 0 → Investigation
T > 0 → Identification

This publication is available free of charge from: https://doi.org/10.6028/NIST.IR.8271

#	ALGORITHM	INVESTIGATION MODE						IDENTIFICATION MODE						FAILURE TO EXTRACT					
		RANK ONE MISS RATE, FNIR(N, 0, 1)						HIGH T → FPIR = 0.001, FNIR(N, T, L)						FEATURES					
		N=1.6M						N=1.6M											
	GALLERY	MUGSHOT	MUGSHOT	MUGSHOT	VISA	BORDER	VISA	MUGSHOT	MUGSHOT	MUGSHOT	VISA	BORDER	VISA	MUGSHOT	MUGSHOT	MUGSHOT	VISA	BORDER	KIOSK
	PROBE	MUGSHOT	WEBCAM	PROFILE	BORDER	BOR¿10YR	KIOSK	MUGSHOT	WEBCAM	PROFILE	BORDER	BOR¿10YR	KIOSK	MUGSHOT	WEBCAM	PROFILE	BORDER	BOR¿10YR	KIOSK
139	NEWLAND-002	[226]0.079	[216]0.117	[170]0.936				[227]0.438	[213]0.466	[142]0.999				0.007	0.012	0.200			
140	NOBLIS-001	[242]0.249	[237]0.522	[208]0.993				[252]1.000	[246]1.000	[189]1.000				0.000	0.000	0.000			
141	NOBLIS-002	[238]0.179	[234]0.392	[200]0.982				[248]0.997	[255]1.000	[176]1.000				0.000	0.000	0.000			
142	NTECHLAB-003	[130]0.006	[128]0.023	[80]0.504				[125]0.054	[119]0.118	[39]0.837				0.000	0.000	0.040			
143	NTECHLAB-004	[118]0.005	[107]0.019	[81]0.506	[89]0.008		[85]0.129	[101]0.041	[110]0.105	[38]0.833	[84]0.053		[58]0.263	0.000	0.000	0.040			
144	NTECHLAB-005	[116]0.005	[103]0.018	[66]0.367	[91]0.008		[77]0.118	[102]0.042	[108]0.102	[33]0.771	[99]0.073		[64]0.294	0.000	0.000	0.040			
145	NTECHLAB-006	[108]0.004	[95]0.017	[63]0.347	[86]0.007		[74]0.113	[96]0.037	[96]0.094	[32]0.754	[87]0.057		[57]0.260	0.000	0.000	0.040			
146	NTECHLAB-007	[80]0.003	[56]0.012	[56]0.326	[57]0.004		[62]0.107	[75]0.026	[67]0.067	[31]0.750	[59]0.032		[47]0.223	0.000	0.000	0.042			
147	NTECHLAB-008	[39]0.002	[22]0.010	[32]0.157	[39]0.003		[34]0.084	[45]0.014	[39]0.045	[20]0.529	[63]0.033		[37]0.183	0.000	0.000	0.044			
148	NTECHLAB-009	[15]0.001	[10]0.008	[26]0.138	[16]0.002	[28]0.013	[16]0.074	[20]0.005	[16]0.022	[12]0.430	[28]0.015	[23]0.109	[20]0.142	0.000	0.000	0.041		0.001	
149	NTECHLAB-010	[9]0.001	[13]0.008	[15]0.085	[10]0.002	[13]0.008	[4]0.057	[9]0.003	[9]0.015	[7]0.252	[10]0.007	[13]0.059	[4]0.098	0.001	0.001	0.043		0.000	
150	PARAVISION-000	[192]0.019	[162]0.038	[89]0.534	[165]0.423		[164]0.529	[162]0.089	[156]0.170	[144]0.999	[153]0.470		[141]0.926	0.000	0.000	0.000			
151	PARAVISION-001	[102]0.004	[116]0.020	[58]0.329	[164]0.414		[163]0.484	[115]0.049	[129]0.128	[137]0.999	[150]0.444		[118]0.739	0.000	0.000	0.000			
152	PARAVISION-002	[107]0.004	[122]0.022	[60]0.335	[112]0.015		[115]0.175	[116]0.050	[122]0.119	[77]0.983	[102]0.080		[98]0.497	0.000	0.000	0.032			
153	PARAVISION-003	[92]0.003	[108]0.019	[47]0.252	[113]0.015		[112]0.167	[94]0.035	[100]0.096	[104]0.994	[88]0.058		[65]0.296	0.000	0.000	0.032			
154	PARAVISION-004	[33]0.002	[32]0.010	[21]0.104	[69]0.006		[71]0.112	[34]0.010	[33]0.038	[190]1.000	[35]0.018		[137]0.908	0.000	0.000	0.032			
155	PARAVISION-005	[27]0.002	[23]0.010	[13]0.079	[82]0.007		[60]0.106	[16]0.004	[18]0.024	[71]0.980	[23]0.011		[16]0.132	0.000	0.000	0.038			
156	PARAVISION-007	[11]0.001	[11]0.008	[8]0.066	[63]0.005	[17]0.010	[51]0.101	[15]0.004	[19]0.025	[182]1.000	[21]0.009	[24]0.113	[208]1.000	0.000	0.000	0.000		0.000	
157	PIXELALL-002	[113]0.005	[124]0.022	[142]0.810	[98]0.011		[120]0.187	[169]0.105	[204]0.388	[183]1.000	[156]0.602		[209]1.000	0.000	0.000	0.000			
158	PIXELALL-003	[61]0.002	[72]0.014	[83]0.515	[77]0.006		[103]0.151	[70]0.022	[74]0.073	[158]1.000	[69]0.037		[106]0.554	0.000	0.000	0.000			
159	PIXELALL-004	[59]0.002	[77]0.015	[87]0.523	[66]0.005		[105]0.152	[60]0.018	[80]0.079	[173]1.000	[80]0.051		[155]0.994	0.000	0.000	0.000			
160	PIXELALL-005	[51]0.002	[38]0.011	[49]0.264	[102]0.012	[49]0.028	[101]0.146	[38]0.012	[43]0.050	[180]1.000	[48]0.027	[46]0.203	[160]1.000	0.000	0.000	0.000		0.000	
161	PTAKURATSATU-000	[90]0.003	[94]0.017	[102]0.605	[65]0.005	[47]0.027	[57]0.105	[95]0.037	[129]0.124	[49]0.924	[77]0.046	[48]0.206	[49]0.232	0.000	0.001	0.039		0.000	
162	QNAP-000	[145]0.008	[149]0.027	[85]0.522	[109]0.013	[62]0.054	[108]0.158	[180]0.129	[176]0.238	[193]1.000	[130]0.191	[64]0.539	[157]0.998	0.001	0.000	0.054		0.000	
163	QUANTASOFT-001	[239]0.218	[246]0.727					[237]0.639						0.000	0.000				
164	RANKONE-002	[194]0.019	[201]0.071					[173]0.118	[183]0.261					0.000	0.000				
165	RANKONE-003	[193]0.019	[199]0.068					[174]0.118	[182]0.255					0.000	0.000				
166	RANKONE-004	[214]0.041	[218]0.141					[200]0.193	[208]0.426					0.000	0.000				
167	RANKONE-005	[159]0.009	[175]0.041	[202]0.986				[136]0.059	[159]0.173	[128]0.998				0.000	0.000	0.489			
168	RANKONE-006	[120]0.005		[139]0.797				[97]0.037		[67]0.977				0.002		0.167			
169	RANKONE-007	[96]0.003	[105]0.019	[136]0.796				[72]0.022	[97]0.095	[56]0.967				0.001	0.001	0.102			
170	RANKONE-009	[71]0.002	[58]0.013	[93]0.549	[68]0.006		[93]0.134	[56]0.018	[76]0.076	[58]0.969	[90]0.062		[74]0.328	0.000	0.000	0.000			
171	RANKONE-010	[65]0.002	[24]0.010	[67]0.374	[62]0.005	[46]0.027	[83]0.126	[43]0.014	[58]0.058	[35]0.802	[83]0.052	[49]0.208	[55]0.259	0.000	0.000	0.000		0.000	
172	RANKONE-011	[26]0.002	[46]0.011	[42]0.223	[43]0.004	[36]0.019	[32]0.082	[27]0.009	[41]0.048		[68]0.037	[41]0.182	[149]0.977	0.000	0.000	0.000		0.000	
173	REALNETWORKS-000	[212]0.040	[208]0.078					[206]0.234	[198]0.319					0.001	0.000				
174	REALNETWORKS-001	[213]0.040	[207]0.078					[205]0.234	[199]0.319					0.001	0.000				
175	REALNETWORKS-002	[209]0.039	[206]0.078					[204]0.231	[197]0.315					0.001	0.000				
176	REALNETWORKS-003	[200]0.024	[195]0.062	[132]0.771	[131]0.031		[126]0.209	[190]0.159	[186]0.266	[132]0.998	[125]0.164		[99]0.500	0.001	0.000	0.009			
177	REALNETWORKS-004	[198]0.024	[193]0.059	[138]0.797	[130]0.031		[131]0.213	[189]0.158	[184]0.263	[146]0.999	[126]0.170		[110]0.613	0.001	0.000	0.009			
178	REALNETWORKS-005	[67]0.002	[61]0.013	[73]0.433	[55]0.004	[41]0.023	[54]0.102	[83]0.028	[75]0.074	[60]0.971	[67]0.037	[50]0.223	[44]0.215	0.000	0.000	0.006		0.000	
179	REMARKAI-000	[98]0.003	[104]0.018	[106]0.660	[88]0.008		[102]0.148	[128]0.055	[123]0.120	[143]0.999	[98]0.069		[116]0.717	0.000	0.000	0.000			
180	REMARKAI-000	[152]0.009	[152]0.030					[178]0.128	[165]0.203					0.000	0.001				
181	REMARKAI-002	[150]0.008	[151]0.029	[140]0.802				[177]0.124	[163]0.196	[94]0.991				0.000	0.001	0.017			
182	RENDIP-000	[30]0.002	[78]0.015	[72]0.424	[74]0.006	[48]0.028	[35]0.084	[37]0.012	[59]0.059	[46]0.894	[41]0.022	[43]0.185	[30]0.167	0.000	0.000	0.041		0.000	
183	S1-000	[73]0.002	[93]0.017	[48]0.258	[67]0.005	[45]0.025	[38]0.090	[85]0.028	[84]0.085	[194]1.000	[79]0.047	[79]1.000	[195]1.000	0.000	0.000	0.040		0.000	
184	S1-001	[91]0.003	[69]0.014	[41]0.215	[29]0.003	[34]0.018	[19]0.077	[52]0.016	[48]0.052	[81]0.985	[36]0.019	[26]0.136	[21]0.148	0.001	0.000	0.035		0.000	

Table 12: **Miss rates by dataset:** *At left, rank 1 miss rates relevant to investigations; at right, with threshold set to target FPIR = 0.01 for higher volume, low prior, uses. Yellow indicates most accurate algorithm. Throughout blue superscripts indicate the rank of the algorithm for that column.*

This publication is available free of charge from: https://doi.org/10.6028/NIST.IR.8271

#	ALGORITHM	INVESTIGATION MODE						IDENTIFICATION MODE						FAILURE TO EXTRACT					
		RANK ONE MISS RATE, FNIR(N, 0, 1)						HIGH T → FPIR = 0.001, FNIR(N, T, L)						FEATURES					
		N=1.6M						N=1.6M											
	GALLERY	MUGSHOT	MUGSHOT	MUGSHOT	VISA	BORDER	VISA	MUGSHOT	MUGSHOT	MUGSHOT	VISA	BORDER	VISA	MUGSHOT	MUGSHOT	MUGSHOT	VISA	BORDER	KIOSK
	PROBE	MUGSHOT	WEBCAM	PROFILE	BORDER	BOR¿10YR	KIOSK	MUGSHOT	WEBCAM	PROFILE	BORDER	BOR¿10YR	KIOSK	MUGSHOT	WEBCAM	PROFILE	BORDER	BOR¿10YR	KIOSK
185	SCANOVATE-000	[119]0.005	[179]0.045	[97]0.560	[135]0.035		[130]0.211	[143]0.067	[179]0.240	[45]0.893	[134]0.215		[82]0.400	0.000	0.001	0.057			
186	SCANOVATE-001	[123]0.005	[173]0.040	[101]0.585	[129]0.031		[118]0.178	[154]0.081	[173]0.227	[48]0.911	[131]0.192		[85]0.404	0.000	0.001	0.044			
187	SENSETIME-000	[69]0.002	[85]0.016	[88]0.528				[68]0.021	[62]0.063	[215]1.000				0.004	0.000	0.042			
188	SENSETIME-001	[70]0.002	[84]0.016					[71]0.022	[64]0.064					0.004	0.000				
189	SENSETIME-002	[181]0.014	[109]0.020	[68]0.384	[97]0.011		[55]0.104	[46]0.015	[24]0.028	[102]0.994	[57]0.032		[101]0.523	0.009	0.000	0.040			
190	SENSETIME-003	[4]0.001	[5]0.007	[30]0.150	[27]0.003		[39]0.091	[4]0.002	[1]0.012	[16]0.477	[17]0.008		[17]0.133	0.000	0.000	0.041			
191	SENSETIME-004	[3]0.001	[6]0.007	[12]0.072	[20]0.002		[36]0.084	[1]0.002	[3]0.013	[6]0.229	[8]0.006		[13]0.113	0.000	0.000	0.041			
192	SENSETIME-005	[2]0.001	[2]0.006	[4]0.059	[19]0.002	[11]0.007	[28]0.082	[7]0.002	[8]0.014	[3]0.173	[11]0.007	[9]0.051	[9]0.104	0.000	0.000	0.041		0.000	
193	SENSETIME-006	[1]0.001	[1]0.006	[1]0.055	[1]0.001	[1]0.004	[6]0.064	[2]0.002	[2]0.012	[131]0.998	[1]0.004	[4]0.034	[3]0.093	0.000	0.000	0.025		0.000	
194	SHAMAN-003	[230]0.124	[222]0.172					[228]0.451	[222]0.597					0.020	0.011				
195	SHAMAN-004	[241]0.222	[231]0.319					[235]0.615	[229]0.754					0.020	0.011				
196	SHAMAN-006	[211]0.040	[191]0.058	[172]0.938				[184]0.141	[175]0.237	[61]0.972				0.020	0.011	0.869			
197	SHAMAN-007	[210]0.040	[190]0.057					[185]0.141	[178]0.240					0.020	0.010				
198	SIAT-001	[44]0.002	[233]0.333		[56]0.004		[49]0.099	[54]0.018	[203]0.365		[54]0.031			0.000	0.000				
199	SIAT-002	[46]0.002	[235]0.446		[163]0.348		[53]0.102	[69]0.022	[214]0.478		[143]0.372		[140]0.923	0.000	0.000				
200	SMILART-004	[253]0.965	[249]0.974					[246]0.968	[242]0.976					0.011	0.013				
201	SMILART-005													0.011	0.013				
202	STAQU-000	[141]0.007	[114]0.020	[104]0.613	[119]0.020	[63]0.055	[109]0.159	[137]0.062	[210]0.443	[165]1.000	[154]0.535	[69]0.961	[166]1.000	0.000	0.000	0.000		0.000	
203	SYNESIS-003	[185]0.016	[132]0.023	[148]0.827	[105]0.013		[95]0.136	[141]0.065	[126]0.123	[54]0.960	[100]0.075		[69]0.314	0.000	0.001	0.063			
204	SYNESIS-003	[236]0.170	[227]0.235					[233]0.582	[225]0.646					0.006	0.015				
205	SYNESIS-005	[151]0.009	[59]0.013	[124]0.744	[37]0.003		[40]0.092	[74]0.025	[72]0.072	[78]0.984	[60]0.032		[43]0.214	0.001	0.000	0.135			
206	TECH5-001	[106]0.004	[92]0.017	[100]0.584	[79]0.007		[63]0.107	[131]0.057	[238]0.935	[195]1.000	[135]0.244		[156]0.994	0.000	0.000	0.006			
207	TECH5-002	[81]0.003	[36]0.011	[54]0.312	[36]0.003	[53]0.029	[37]0.089	[81]0.027	[70]0.070	[36]0.805	[70]0.039	[47]0.205	[88]0.440	0.001	0.000	0.041		0.000	
208	TEVIAN-003	[182]0.015	[186]0.052					[197]0.177	[193]0.298					0.001	0.002				
209	TEVIAN-004	[169]0.011	[166]0.038					[172]0.117	[160]0.176					0.001	0.002				
210	TEVIAN-005	[142]0.007	[150]0.028	[77]0.467				[159]0.087	[140]0.144	[55]0.962				0.001	0.002	0.116			
211	TEVIAN-006	[74]0.002	[42]0.011	[24]0.123	[31]0.003	[29]0.013	[13]0.071	[31]0.010	[27]0.032	[11]0.425	[29]0.016	[19]0.093	[144]0.951	0.001	0.000	0.062		0.000	
212	TEVIAN-007	[43]0.002	[20]0.009	[19]0.093	[13]0.002	[16]0.009	[9]0.067	[22]0.005	[15]0.022	[8]0.301	[22]0.009	[15]0.065	[14]0.122	0.000	0.000	0.062		0.000	
213	TIGER-000	[221]0.062	[213]0.095					[222]0.390	[215]0.500					0.000	0.000				
214	TIGER-002	[125]0.006	[129]0.023	[82]0.514				[155]0.086	[150]0.158	[140]0.999				0.000	0.000	0.056			
215	TIGER-003	[126]0.006	[130]0.023					[156]0.086	[149]0.158					0.000	0.000				
216	TONGYITRANS-000	[137]0.007	[129]0.022					[148]0.074	[115]0.112					0.003	0.001				
217	TONGYITRANS-001	[138]0.007	[126]0.022					[142]0.066	[107]0.101					0.003	0.001				
218	TOSHIBA-000	[112]0.004	[120]0.022	[130]0.766				[138]0.062	[120]0.118	[113]0.995				0.000	0.000	0.070			
219	TOSHIBA-001	[117]0.005	[123]0.022					[133]0.058	[94]0.092					0.000	0.000				
220	TRUEFACE-000	[95]0.003	[63]0.014	[44]0.230	[84]0.007	[43]0.024	[41]0.092	[59]0.018	[61]0.062	[42]0.882	[53]0.030	[45]0.194	[39]0.188	0.001	0.001	0.047		0.003	
221	VD-000	[249]0.474	[240]0.551					[244]0.917	[240]0.946					0.011	0.013				
222	VD-001	[204]0.028	[187]0.053					[201]0.201	[190]0.281					0.005	0.001				
223	VD-002	[160]0.010	[148]0.027	[155]0.893	[108]0.013	[60]0.050	[116]0.176	[152]0.079	[142]0.148	[116]0.996	[106]0.095	[59]0.367	[78]0.372	0.004	0.003	0.156		0.002	
224	VD-003	[143]0.008	[121]0.022	[133]0.773	[90]0.008	[55]0.030	[96]0.137	[110]0.046	[105]0.100	[141]0.999	[81]0.051	[51]0.244	[71]0.315	0.003	0.003	0.144		0.002	
225	VERIDAS-001	[84]0.003	[71]0.014	[95]0.550	[75]0.006	[51]0.028	[86]0.131	[99]0.037	[82]0.082	[86]0.987	[74]0.044	[52]0.266	[60]0.264	0.000	0.002	0.093		0.001	
226	VERIDAS-002	[83]0.003	[70]0.014	[94]0.550	[76]0.006	[50]0.028	[87]0.131	[98]0.037	[83]0.082	[85]0.987	[73]0.044	[53]0.266	[59]0.264	0.000	0.002	0.093		0.001	
227	VERIDAS-003	[45]0.002	[41]0.011	[52]0.297	[50]0.004	[31]0.016	[65]0.108	[53]0.017	[54]0.055	[120]0.997	[38]0.020	[32]0.150	[34]0.178	0.000	0.002	0.093		0.001	
228	VIGILANTSOLUTIONS-003	[224]0.069	[220]0.151	[183]0.958				[226]0.408	[228]0.660	[136]0.999				0.000	0.001	0.127			
229	VIGILANTSOLUTIONS-004	[231]0.125	[228]0.244	[188]0.965				[232]0.549	[232]0.817	[118]0.996				0.000	0.001	0.127			
230	VIGILANTSOLUTIONS-005	[156]0.009		[161]0.920				[221]0.388		[188]1.000				0.000	0.001	0.127			

Table 13: **Miss rates by dataset:** *At left, rank 1 miss rates relevant to investigations; at right, with threshold set to target FPIR = 0.01 for higher volume, low prior, uses. Yellow indicates most accurate algorithm. Throughout blue superscripts indicate the rank of the algorithm for that column.*

This publication is available free of charge from: https://doi.org/10.6028/NIST.IR.8271

#	ALGORITHM	INVESTIGATION MODE						IDENTIFICATION MODE						FAILURE TO EXTRACT					
		RANK ONE MISS RATE, FNIR(N, 0, 1)						HIGH T → FPIR = 0.001, FNIR(N, T, L)						FEATURES					
		N=1.6M						N=1.6M											
	GALLERY	MUGSHOT	MUGSHOT	MUGSHOT	VISA	BORDER	VISA	MUGSHOT	MUGSHOT	MUGSHOT	VISA	BORDER	VISA	MUGSHOT	MUGSHOT	MUGSHOT	VISA	BORDER	KIOSK
	PROBE	MUGSHOT	WEBCAM	PROFILE	BORDER	BOR¿10YR	KIOSK	MUGSHOT	WEBCAM	PROFILE	BORDER	BOR¿10YR	KIOSK	MUGSHOT	WEBCAM	PROFILE	BORDER	BOR¿10YR	KIOSK
231	VIGILANTSOLUTIONS-006	[162]0.010		[162]0.921				[216]0.353		[191]1.000				0.000	0.001	0.127			
232	VIGILANTSOLUTIONS-007	[97]0.003	[96]0.017	[165]0.925	[106]0.013	[65]0.068	[114]0.175	[87]0.028	[88]0.088	[117]0.996	[103]0.081	[60]0.371	[81]0.391	0.000	0.001	0.127		0.001	
233	VIGILANTSOLUTIONS-008	[89]0.003	[97]0.017	[160]0.913	[110]0.014	[66]0.072	[117]0.178	[65]0.021	[77]0.077	[139]0.999	[110]0.104	[62]0.398	[100]0.511	0.000	0.001	0.127		0.001	
234	VISIONBOX-000	[52]0.002	[43]0.011	[126]0.752	[59]0.005	[32]0.017	[24]0.078	[57]0.018	[57]0.057	[93]0.990	[44]0.023	[31]0.146	[28]0.162	0.000	0.001	0.043		0.001	
235	VISIONLABS-004	[82]0.003	[110]0.020	[61]0.343				[132]0.058	[151]0.159	[44]0.890				0.001	0.001	0.046			
236	VISIONLABS-005	[72]0.002	[106]0.019	[59]0.334				[117]0.050	[141]0.147	[43]0.888				0.001	0.001	0.046			
237	VISIONLABS-006	[49]0.002	[82]0.015	[40]0.211	[46]0.004		[44]0.096	[80]0.027	[92]0.090	[27]0.672				0.001	0.001	0.051			
238	VISIONLABS-007	[42]0.002	[81]0.015	[39]0.211	[42]0.004		[43]0.095	[79]0.027	[91]0.090	[28]0.672	[56]0.031		[38]0.185	0.001	0.001	0.051			
239	VISIONLABS-008	[58]0.002	[64]0.014	[27]0.141	[18]0.002		[27]0.081	[41]0.013	[47]0.051	[17]0.481	[30]0.017		[22]0.151	0.001	0.000	0.075			
240	VISIONLABS-009	[10]0.001	[15]0.008	[18]0.091	[4]0.001		[12]0.071	[18]0.005	[21]0.025	[34]0.799	[20]0.008		[12]0.113	0.000	0.000	0.060			
241	VISIONLABS-010	[18]0.001	[34]0.010	[11]0.069	[3]0.001	[5]0.006	[11]0.069	[21]0.005	[23]0.027		[15]0.008	[11]0.055	[11]0.109	0.000	0.000	0.040		0.000	
242	VISIONLABS-011	[12]0.001	[17]0.009	[7]0.064	[2]0.001	[3]0.004	[7]0.063	[13]0.003	[13]0.020		[4]0.004	[5]0.034	[2]0.090	0.000	0.000	0.032		0.000	
243	VOCORD-003	[131]0.006	[139]0.024	[141]0.804	[146]0.061		[121]0.188	[176]0.122	[147]0.155	[129]0.998	[124]0.157		[84]0.404	0.001	0.011	0.425			
244	VOCORD-004	[146]0.008	[117]0.021	[135]0.792	[104]0.012		[84]0.127	[217]0.355	[157]0.173	[168]1.000	[132]0.193		[153]0.991	0.000	0.000	0.000			
245	VOCORD-005	[140]0.007	[133]0.023	[143]0.812	[143]0.055		[124]0.206	[188]0.158	[131]0.130	[121]0.997	[119]0.138		[79]0.381	0.001	0.009	0.554			
246	VOCORD-006	[255]1.000	[252]1.000	[212]1.000	[231]1.000		[232]1.000	[254]1.000	[251]1.000	[218]1.000	[191]1.000		[203]1.000	0.001	0.009	0.554			
247	VTS-000	[251]0.594	[243]0.608	[158]0.909	[169]0.607	[71]0.724	[168]0.739	[234]0.598	[223]0.619	[147]0.999	[159]0.613	[67]0.760	[120]0.761	0.000	0.001	0.047		0.000	
248	VTS-001	[28]0.002	[27]0.010	[34]0.167	[70]0.006	[35]0.018	[22]0.077	[42]0.013	[46]0.051	[101]0.994	[42]0.022	[29]0.141	[40]0.192	0.000	0.000	0.040		0.000	
249	XFORWARDAI-000	[66]0.002	[67]0.014	[17]0.089	[47]0.004	[30]0.015	[42]0.094	[49]0.015	[52]0.053	[13]0.440	[40]0.021	[36]0.159	[31]0.169	0.000	0.000	0.000		0.000	
250	XFORWARDAI-001	[60]0.002	[57]0.013	[10]0.067	[33]0.003	[14]0.009	[30]0.082	[19]0.005	[25]0.028	[14]0.448	[18]0.008	[14]0.062	[15]0.123	0.000	0.000	0.000		0.000	
251	XFORWARDAI-002	[54]0.002	[53]0.012	[3]0.059	[26]0.002	[9]0.007	[21]0.077	[12]0.003	[10]0.016	[18]0.525	[7]0.005	[8]0.041	[5]0.099	0.000	0.000	0.000		0.000	
252	YISHENG-001	[203]0.027	[194]0.060		[145]0.058		[147]0.287	[214]0.346	[230]0.808		[160]0.666		[139]0.919	0.002	0.005				
253	YITU-002	[47]0.002	[30]0.010					[55]0.018	[42]0.049					0.000	0.000				
254	YITU-003	[88]0.003	[87]0.016					[62]0.019	[50]0.052					0.003	0.001				
255	YITU-004	[14]0.001	[14]0.008	[153]0.866				[29]0.010	[22]0.027	[50]0.936				0.000	0.000	0.000			
256	YITU-005	[68]0.002	[76]0.014					[33]0.010	[28]0.032					0.003	0.001				

Table 14: **Miss rates by dataset:** *At left, rank 1 miss rates relevant to investigations; at right, with threshold set to target FPIR = 0.01 for higher volume, low prior, uses. Yellow indicates most accurate algorithm. Throughout blue superscripts indicate the rank of the algorithm for that column.*

This publication is available free of charge from: https://doi.org/10.6028/NIST.IR.8271

MISSES BELOW THRESHOLD, T FNIR(N, T> 0, R >L)		ENROL MOST RECENT DATASET: FRVT 2018 MUGSHOTS				
#	ALGORITHM	N=0.64M	N=1.6M	N=3.0M	N=6.0M	N=12.0M
1	3DIVI-005	[193]0.1358	[193]0.1664	[166]0.1915	[157]0.2370	[151]0.3054
2	ACER-000	[187]0.1185	[186]0.1455	[161]0.1714	[151]0.2074	[144]0.2537
3	ALCHERA-003	[185]0.1176	[182]0.1553	[162]0.1853	[158]0.2409	[159]0.3553
4	ALLGOVISION-000	[160]0.0688	[161]0.0881	[144]0.1084	[136]0.1389	[124]0.2129
5	ALLGOVISION-001	[166]0.0785	[166]0.1017	[151]0.1218	[143]0.1584	[131]0.2273
6	ANKE-000	[172]0.0942	[171]0.1169	[156]0.1404	[148]0.1776	[145]0.2559
7	ANKE-002	[91]0.0229	[91]0.0318	[92]0.0406	[87]0.0605	[77]0.1466
8	AWARE-003	[182]0.1098	[179]0.1283	[157]0.1447	[146]0.1768	[136]0.2364
9	AWARE-005	[220]0.3389	[218]0.3643	[173]0.3993	[166]0.4526	[143]0.2531
10	AYONIX-002	[241]0.7862	[241]0.8242	[179]0.8508	[171]0.8704	[167]0.8939
11	CAMVI-004	[117]0.0367	[145]0.0716	[139]0.0983	[160]0.2508	[148]0.2701
12	CANON-001	[23]0.0039	[23]0.0054	[23]0.0074	[21]0.0158	[25]0.0924
13	CIB-000	[37]0.0086	[39]0.0125	[39]0.0160	[44]0.0303	[60]0.1251
14	CLEARVIEWAI-000	[24]0.0040	[24]0.0058	[24]0.0078	[22]0.0159	[28]0.0971
15	CLOUDWALK-HR-000	[7]0.0019	[6]0.0020	[4]0.0023	[8]0.0072	[11]0.0701
16	COGENT-000	[135]0.0430	[121]0.0527	[120]0.0695	[122]0.1133	[113]0.1960
17	COGENT-001	[134]0.0430	[120]0.0527	[121]0.0695	[121]0.1133	[114]0.1960
18	COGENT-002	[103]0.0322	[107]0.0444	[107]0.0610	[119]0.1116	[126]0.2180
19	COGENT-003	[104]0.0328	[112]0.0463	[118]0.0683	[129]0.1294	[138]0.2445
20	COGENT-004	[88]0.0210	[92]0.0331	[102]0.0527	[124]0.1138	[123]0.2119
21	COGENT-005	[29]0.0064	[28]0.0091	[28]0.0123	[45]0.0303	[56]0.1233
22	COGNITEC-000	[195]0.1377	[191]0.1606	[165]0.1870	[153]0.2176	[150]0.2831
23	COGNITEC-001	[168]0.0807	[167]0.1017	[150]0.1214	[139]0.1513	[129]0.2238
24	COGNITEC-002	[127]0.0406	[125]0.0531	[114]0.0666	[107]0.0935	[109]0.1874
25	COGNITEC-003	[125]0.0400	[119]0.0526	[110]0.0650	[103]0.0895	[102]0.1772
26	COGNITEC-004	[90]0.0222	[90]0.0313	[88]0.0388	[82]0.0540	[42]0.1103
27	COGNITEC-005	[28]0.0063	[30]0.0096	[33]0.0144	[39]0.0287	[27]0.0967
28	CYBERLINK-000	[129]0.0414	[130]0.0565	[125]0.0707	[115]0.1031	[120]0.2050
29	CYBERLINK-001	[121]0.0392	[124]0.0536	[119]0.0695	[112]0.0973	[103]0.1794
30	CYBERLINK-002	[44]0.0105	[47]0.0148	[52]0.0202	[63]0.0399	[61]0.1255
31	CYBERLINK-003	[26]0.0056	[26]0.0077	[25]0.0100	[28]0.0235	[57]0.1237
32	CYBERLINK-004	[25]0.0051	[25]0.0071	[26]0.0102	[24]0.0199	[64]0.1269
33	DAHUA-001	[149]0.0569	[147]0.0727	[133]0.0878	[125]0.1148	[108]0.1867
34	DAHUA-002	[49]0.0108	[48]0.0151	[47]0.0191	[41]0.0291	[51]0.1153
35	DAHUA-003	[42]0.0100	[44]0.0139	[45]0.0180	[42]0.0296	[45]0.1130
36	DEEPGLINT-001	[14]0.0027	[14]0.0033	[13]0.0043	[15]0.0121	[24]0.0922
37	DEEPSEA-001	[113]0.0347	[111]0.0462	[106]0.0586	[101]0.0802	[99]0.1708
38	DERMALOG-005	[164]0.0700	[160]0.0880	[146]0.1144	[142]0.1578	[139]0.2451
39	DERMALOG-006	[122]0.0395	[118]0.0517	[111]0.0659	[111]0.0973	[101]0.1745
40	DERMALOG-007	[161]0.0691	[158]0.0863	[145]0.1107	[138]0.1504	[134]0.2299
41	DERMALOG-008	[109]0.0338	[109]0.0455	[109]0.0626	[116]0.1060	[132]0.2276
42	DERMALOG-009	[66]0.0148	[66]0.0206	[67]0.0268	[66]0.0416	[71]0.1374
43	FUJITSULAB-000	[67]0.0148	[67]0.0206	[71]0.0277	[84]0.0541	[100]0.1739
44	GORILLA-002	[199]0.1539	[199]0.1880	[169]0.2184	[161]0.2596	[158]0.3398
45	GORILLA-004	[163]0.0699	[163]0.0892	[142]0.1048	[134]0.1370	[117]0.1969
46	GORILLA-005	[139]0.0453	[134]0.0583	[124]0.0704	[113]0.0974	[78]0.1474
47	GORILLA-006	[83]0.0196	[82]0.0275	[77]0.0331	[76]0.0516	[44]0.1113
48	GRIAULE-000	[63]0.0145	[64]0.0201	[64]0.0253	[65]0.0407	[76]0.1440
49	HIK-003	[169]0.0828	[168]0.1028	[149]0.1202	[141]0.1525	[141]0.2480
50	HIK-004	[167]0.0796	[164]0.0988	[147]0.1147	[137]0.1474	[142]0.2483
51	HIK-005	[101]0.0312	[104]0.0436	[105]0.0560	[105]0.0911	[125]0.2129
52	HYPERVERGE-001	[17]0.0033	[17]0.0045	[17]0.0059	[12]0.0117	[19]0.0872
53	IDEMIA-003	[111]0.0346	[114]0.0471	[134]0.0892	[163]0.2789	[162]0.4311
54	IDEMIA-004	[100]0.0300	[100]0.0373	[94]0.0447	[88]0.0617	[97]0.1635
55	IDEMIA-005	[116]0.0360	[106]0.0440	[103]0.0537	[100]0.0764	[110]0.1915
56	IDEMIA-006	[114]0.0351	[103]0.0433	[101]0.0525	[97]0.0734	[127]0.2201
57	IDEMIA-007	[59]0.0136	[58]0.0181	[54]0.0228	[55]0.0357	[74]0.1402
58	IDEMIA-008	[5]0.0016	[5]0.0019	[6]0.0024	[4]0.0053	[6]0.0470
59	IMAGUS-005	[60]0.0137	[61]0.0185	[59]0.0237	[56]0.0368	[38]0.1067
60	IMAGUS-006	[61]0.0137	[63]0.0190	[62]0.0244	[61]0.0396	[52]0.1159
61	IMPERIAL-000	[77]0.0187	[77]0.0259	[85]0.0358	[96]0.0733	[104]0.1794
62	INCODE-003	[192]0.1324	[194]0.1672	[167]0.1961	[156]0.2345	[153]0.3123
63	INCODE-004	[126]0.0403	[126]0.0538	[113]0.0662	[106]0.0917	[94]0.1619
64	INCODE-005	[35]0.0083	[35]0.0113	[34]0.0145	[29]0.0247	[21]0.0912
65	INNOVATRICS-007	[40]0.0093	[40]0.0125	[38]0.0159	[32]0.0259	[39]0.1092
66	INTSYSMSU-000	[251]0.9982	[249]0.9984	[183]0.9985	[174]0.9987	[170]0.9988
67	IREX-000	[81]0.0190	[86]0.0280	[89]0.0391	[92]0.0677	[81]0.1479
68	ISYSTEMS-002	[151]0.0584	[151]0.0783	[138]0.0973	[135]0.1373	[133]0.2295
69	ISYSTEMS-003	[137]0.0438	[135]0.0590	[131]0.0807	[127]0.1259	[135]0.2357
70	KAKAO-000	[50]0.0109	[50]0.0151	[49]0.0196	[50]0.0324	[30]0.1010
71	KEDACOM-001	[74]0.0181	[73]0.0227	[65]0.0265	[68]0.0422	[70]0.1340
72	LOOKMAN-003	[112]0.0346	[105]0.0437	[99]0.0514	[95]0.0724	[95]0.1620

Table 15: **Identification-mode: Effect of N on FNIR at high threshold.** *Values are threshold-based miss rates i.e.* FNIR *at* FPIR = *0.001 for five enrollment population sizes, N. The right six columns apply for enrollment of one image. Missing entries usually apply because another algorithm from the same developer was run instead. Some developers are missing because less accurate algorithms were not run on galleries with $N \geq 3\,000\,000$. Throughout blue superscripts indicate the rank of the algorithm for that column.*

This publication is available free of charge from: https://doi.org/10.6028/NIST.IR.8271

MISSES BELOW THRESHOLD, T		ENROL MOST RECENT				
FNIR(N, T> 0, R >L)		DATASET: FRVT 2018 MUGSHOTS				
#	ALGORITHM	N=0.64M	N=1.6M	N=3.0M	N=6.0M	N=12.0M
73	LOOKMAN-005	[92]0.0240	[88]0.0301	[84]0.0356	[75]0.0512	[69]0.1334
74	MANTRA-000	[30]0.0065	[32]0.0101	[35]0.0151	[46]0.0308	[32]0.1035
75	MEGVII-001	[147]0.0562	[146]0.0722	[132]0.0872	[131]0.1309	[149]0.2713
76	MICROFOCUS-005	[248]0.9732	[243]0.8354	[180]0.8555	[172]0.8755	[168]0.8954
77	MICROSOFT-003	[84]0.0198	[84]0.0278	[83]0.0356	[81]0.0538	[87]0.1539
78	MICROSOFT-004	[76]0.0185	[78]0.0259	[78]0.0333	[77]0.0517	[85]0.1510
79	MICROSOFT-005	[75]0.0181	[76]0.0256	[76]0.0320	[74]0.0512	[83]0.1491
80	MICROSOFT-006	[39]0.0091	[36]0.0120	[40]0.0162	[43]0.0301	[82]0.1482
81	NEC-000	[155]0.0637	[153]0.0789	[137]0.0933	[126]0.1163	[112]0.1941
82	NEC-001	[170]0.0863	[170]0.1055	[152]0.1249	[140]0.1519	[130]0.2253
83	NEC-002	[9]0.0020	[10]0.0026	[10]0.0033	[17]0.0135	[9]0.0653
84	NEC-003	[10]0.0021	[5]0.0024	[7]0.0028	[6]0.0059	[8]0.0540
85	NEC-004	[6]0.0017	[3]0.0018	[1]0.0020	[1]0.0037	[1]0.0329
86	NEUROTECHNOLOGY-003	[235]0.5698	[236]0.6362	[178]0.7035	[170]0.7602	[166]0.8224
87	NEUROTECHNOLOGY-004	[141]0.0466	[140]0.0629	[126]0.0779	[123]0.1135	[122]0.2102
88	NEUROTECHNOLOGY-005	[123]0.0396	[127]0.0538	[116]0.0675	[110]0.0950	[116]0.1966
89	NEUROTECHNOLOGY-007	[136]0.0436	[139]0.0623	[128]0.0802	[132]0.1320	[137]0.2393
90	NEUROTECHNOLOGY-008	[110]0.0339	[122]0.0530	[135]0.0893	[147]0.1769	[156]0.3288
91	NEUROTECHNOLOGY-009	[48]0.0108	[51]0.0152	[50]0.0196	[48]0.0324	[41]0.1102
92	NTECHLAB-003	[131]0.0421	[125]0.0537	[115]0.0674	[104]0.0907	[92]0.1582
93	NTECHLAB-004	[102]0.0312	[101]0.0405	[100]0.0519	[94]0.0722	[84]0.1503
94	NTECHLAB-005	[106]0.0334	[102]0.0424	[104]0.0537	[99]0.0760	[90]0.1543
95	NTECHLAB-006	[98]0.0288	[96]0.0367	[97]0.0471	[91]0.0670	[86]0.1523
96	NTECHLAB-007	[78]0.0188	[75]0.0256	[74]0.0317	[73]0.0495	[68]0.1306
97	NTECHLAB-008	[47]0.0107	[45]0.0145	[46]0.0187	[38]0.0286	[29]0.0995
98	NTECHLAB-009	[20]0.0037	[20]0.0049	[20]0.0062	[16]0.0125	[14]0.0735
99	NTECHLAB-010	[8]0.0020	[9]0.0025	[8]0.0030	[9]0.0077	[13]0.0710
100	PARAVISION-003	[94]0.0260	[94]0.0351	[95]0.0447	[90]0.0657	[96]0.1630
101	PARAVISION-004	[32]0.0074	[34]0.0101	[32]0.0136	[35]0.0267	[62]0.1256
102	PARAVISION-005	[16]0.0032	[16]0.0041	[16]0.0057	[23]0.0174	[33]0.1037
103	PARAVISION-007	[15]0.0030	[15]0.0040	[15]0.0055	[25]0.0211	[40]0.1097
104	PIXELALL-002	[165]0.0716	[169]0.1052	[159]0.1475	[159]0.2489	[161]0.3904
105	PIXELALL-003	[70]0.0158	[70]0.0218	[73]0.0288	[70]0.0474	[49]0.1138
106	PIXELALL-004	[55]0.0129	[60]0.0183	[63]0.0245	[57]0.0378	[72]0.1375
107	PIXELALL-005	[38]0.0087	[38]0.0121	[42]0.0171	[30]0.0250	[35]0.1052
108	PTAKURATSATU-000	[95]0.0275	[95]0.0366	[96]0.0458	[79]0.0523	[7]0.0523
109	QUANTASOFT-001	[237]0.6387	[237]0.6387	[177]0.6387		[164]0.6387
110	RANKONE-002	[178]0.0973	[173]0.1175	[154]0.1359	[144]0.1718	[147]0.2613
111	RANKONE-003	[177]0.0973	[174]0.1175	[153]0.1359	[145]0.1718	[146]0.2613
112	RANKONE-005	[142]0.0473	[136]0.0592	[122]0.0700	[108]0.0944	[118]0.1998
113	RANKONE-007	[72]0.0168	[72]0.0222	[66]0.0266	[59]0.0381	[46]0.1132
114	RANKONE-009	[56]0.0132	[56]0.0177	[56]0.0230	[52]0.0344	[23]0.0921
115	RANKONE-010	[45]0.0106	[43]0.0136	[43]0.0174	[34]0.0265	[16]0.0785
116	RANKONE-011	[27]0.0063	[27]0.0087	[27]0.0115	[36]0.0269	[48]0.1135
117	REALNETWORKS-002	[205]0.1943	[204]0.2314	[172]0.2656	[165]0.3134	[155]0.3208
118	REALNETWORKS-003	[191]0.1300	[190]0.1594	[164]0.1858	[154]0.2246	[152]0.3076
119	REALNETWORKS-004	[190]0.1279	[189]0.1581	[163]0.1857	[155]0.2329	[154]0.3179
120	REALNETWORKS-005	[85]0.0202	[83]0.0277	[82]0.0355	[86]0.0560	[75]0.1431
121	REMARKAI-000	[128]0.0406	[128]0.0552	[117]0.0676	[114]0.1028	[119]0.2003
122	RENDIP-000	[36]0.0085	[37]0.0121	[37]0.0156	[37]0.0277	[54]0.1182
123	S1-000	[87]0.0204	[85]0.0279	[87]0.0382	[89]0.0630	[98]0.1707
124	S1-001	[51]0.0115	[52]0.0156	[51]0.0199	[60]0.0392	[63]0.1256
125	SCANOVATE-000	[143]0.0498	[143]0.0667	[129]0.0804	[118]0.1097	[43]0.1109
126	SCANOVATE-001	[154]0.0630	[154]0.0815	[140]0.0993	[128]0.1292	[115]0.1960
127	SENSETIME-000	[69]0.0158	[68]0.0208	[69]0.0270	[62]0.0398	[55]0.1232
128	SENSETIME-001	[71]0.0161	[71]0.0219	[72]0.0277	[67]0.0420	[66]0.1304
129	SENSETIME-002	[64]0.0146	[46]0.0148	[36]0.0153	[27]0.0234	[10]0.0657
130	SENSETIME-003	[3]0.0016	[4]0.0018	[3]0.0021	[5]0.0054	[4]0.0451
131	SENSETIME-004	[2]0.0015	[1]0.0018	[2]0.0021	[2]0.0040	[2]0.0354
132	SENSETIME-005	[4]0.0016	[7]0.0022	[9]0.0031	[11]0.0089	[5]0.0454
133	SENSETIME-006	[1]0.0014	[2]0.0018	[5]0.0023	[3]0.0047	[3]0.0372
134	SHAMAN-007	[189]0.1212	[185]0.1413	[160]0.1587	[149]0.1879	[140]0.2460
135	SIAT-001	[58]0.0136	[54]0.0176	[57]0.0230	[51]0.0344	[31]0.1035
136	SIAT-002	[68]0.0154	[69]0.0216	[70]0.0273	[64]0.0404	[65]0.1283
137	SYNESIS-003	[144]0.0499	[141]0.0652	[130]0.0804	[117]0.1095	[111]0.1916
138	SYNESIS-003	[233]0.5341	[233]0.5821	[176]0.6113	[169]0.6479	[165]0.6822
139	SYNESIS-005	[73]0.0181	[74]0.0248	[75]0.0319	[78]0.0518	[91]0.1580
140	TECH5-001	[130]0.0420	[131]0.0574	[136]0.0911	[152]0.2106	[160]0.3725
141	TECH5-002	[82]0.0194	[81]0.0269	[81]0.0346	[80]0.0537	[93]0.1607
142	TEVIAN-005	[162]0.0692	[159]0.0873	[143]0.1066	[130]0.1301	[106]0.1840
143	TEVIAN-006	[34]0.0078	[31]0.0098	[30]0.0130	[33]0.0261	[67]0.1305
144	TEVIAN-007	[22]0.0038	[22]0.0052	[21]0.0065	[20]0.0154	[26]0.0957

Table 16: **Identification-mode: Effect of N on FNIR at high threshold.** *Values are threshold-based miss rates i.e.* FNIR *at* FPIR = *0.001 for five enrollment population sizes, N. The right six columns apply for enrollment of one image. Missing entries usually apply because another algorithm from the same developer was run instead. Some developers are missing because less accurate algorithms were not run on galleries with $N \geq 3\,000\,000$. Throughout blue superscripts indicate the rank of the algorithm for that column.*

This publication is available free of charge from: https://doi.org/10.6028/NIST.IR.8271

MISSES BELOW THRESHOLD, T FNIR(N, T> 0, R >L)		ENROL MOST RECENT DATASET: FRVT 2018 MUGSHOTS				
#	ALGORITHM	N=0.64M	N=1.6M	N=3.0M	N=6.0M	N=12.0M
145	TIGER-002	[157] 0.0647	[155] 0.0861	[141] 0.1036	[133] 0.1332	[128] 0.2231
146	TOSHIBA-000	[140] 0.0460	[138] 0.0620	[127] 0.0780	[120] 0.1117	[121] 0.2082
147	TRUEFACE-000	[57] 0.0134	[59] 0.0182	[60] 0.0238	[58] 0.0380	[73] 0.1385
148	VD-001	[201] 0.1642	[201] 0.2015	[171] 0.2351	[162] 0.2736	[157] 0.3293
149	VERIDAS-001	[96] 0.0278	[99] 0.0373	[98] 0.0491	[98] 0.0753	[88] 0.1541
150	VERIDAS-002	[97] 0.0278	[98] 0.0373	[86] 0.0373	[72] 0.0491	[15] 0.0753
151	VERIDAS-003	[52] 0.0117	[53] 0.0166	[53] 0.0219	[69] 0.0446	[89] 0.1543
152	VIGILANTSOLUTIONS-008	[65] 0.0146	[65] 0.0205	[68] 0.0269	[71] 0.0489	[53] 0.1164
153	VISIONBOX-000	[53] 0.0122	[57] 0.0177	[61] 0.0239		[169] 0.9538
154	VISIONLABS-004	[133] 0.0427	[132] 0.0578	[123] 0.0703	[109] 0.0949	[107] 0.1853
155	VISIONLABS-005	[119] 0.0369	[117] 0.0502	[108] 0.0626	[102] 0.0847	[105] 0.1815
156	VISIONLABS-006	[79] 0.0188	[80] 0.0267	[80] 0.0336	[85] 0.0542	[79] 0.1478
157	VISIONLABS-007	[80] 0.0188	[79] 0.0266	[79] 0.0335	[83] 0.0540	[80] 0.1479
158	VISIONLABS-008	[41] 0.0096	[41] 0.0131	[41] 0.0166	[40] 0.0291	[59] 0.1247
159	VISIONLABS-009	[18] 0.0034	[18] 0.0046	[18] 0.0060	[18] 0.0140	[20] 0.0881
160	VISIONLABS-010	[21] 0.0038	[21] 0.0051	[22] 0.0070	[19] 0.0149	[22] 0.0920
161	VISIONLABS-011	[12] 0.0025	[13] 0.0033	[14] 0.0044	[14] 0.0120	[18] 0.0825
162	VOCORD-005	[186] 0.1179	[188] 0.1577	[168] 0.2183	[164] 0.3122	[163] 0.4490
163	VTS-001	[43] 0.0102	[42] 0.0133	[44] 0.0175	[47] 0.0322	[58] 0.1243
164	XFORWARDAI-000	[46] 0.0107	[49] 0.0151	[48] 0.0195	[49] 0.0324	[36] 0.1057
165	XFORWARDAI-001	[19] 0.0037	[19] 0.0049	[19] 0.0060	[13] 0.0120	[17] 0.0800
166	XFORWARDAI-002	[13] 0.0026	[12] 0.0030	[12] 0.0035	[10] 0.0078	[12] 0.0706
167	YITU-002	[54] 0.0129	[55] 0.0177	[55] 0.0228	[53] 0.0345	[47] 0.1133
168	YITU-003	[62] 0.0138	[62] 0.0185	[58] 0.0236	[54] 0.0353	[50] 0.1148
169	YITU-004	[31] 0.0067	[29] 0.0096	[29] 0.0129	[26] 0.0232	[34] 0.1046
170	YITU-005	[33] 0.0074	[33] 0.0101	[31] 0.0135	[31] 0.0255	[37] 0.1057

Table 17: **Identification-mode: Effect of N on FNIR at high threshold.** *Values are threshold-based miss rates i.e.* FNIR *at* FPIR = *0.001 for five enrollment population sizes, N. The right six columns apply for enrollment of one image. Missing entries usually apply because another algorithm from the same developer was run instead. Some developers are missing because less accurate algorithms were not run on galleries with* $N \geq 3\,000\,000$. *Throughout blue superscripts indicate the rank of the algorithm for that column.*

This publication is available free of charge from: https://doi.org/10.6028/NIST.IR.8271

MISSES AT GIVEN RANK FNIR(N, T= 0, R)		ENROL MOST RECENT											
		RANK 1						RANK 50					
#	ALGORITHM	N=0.64M	N=1.6M	N=3.0M	N=6.0M	N=12.0M	aN^b	N=0.64M	N=1.6M	N=3.0M	N=6.0M	N=12.0M	aN^b
1	3DIVI-005	[191] 0.0137	[189] 0.0176	[159] 0.0210	[153] 0.0253	[150] 0.0302	[122] 0.0004 N^0.271 [132]	[173] 0.0040	[172] 0.0049	[149] 0.0057	[145] 0.0068	[142] 0.0081	[47] 0.0002 N^0.240 [137]
2	ACER-000	[160] 0.0081	[166] 0.0106	[147] 0.0128	[145] 0.0157	[143] 0.0195	[55] 0.0001 N^0.299 [156]	[122] 0.0020	[138] 0.0026	[128] 0.0031	[128] 0.0037	[124] 0.0045	[18] 0.0000 N^0.284 [150]
3	ALCHERA-003	[156] 0.0079	[163] 0.0104	[145] 0.0123	[144] 0.0147	[141] 0.0180	[80] 0.0002 N^0.278 [143]	[150] 0.0027	[153] 0.0032	[134] 0.0035	[131] 0.0042	[125] 0.0048	[51] 0.0002 N^0.199 [127]
4	ALLGOVISION-000	[174] 0.0101	[171] 0.0114	[146] 0.0127	[143] 0.0145	[140] 0.0166	[149] 0.0010 N^0.171 [75]	[192] 0.0063	[188] 0.0067	[154] 0.0071	[148] 0.0075	[141] 0.0081	[154] 0.0020 N^0.086 [85]
5	ALLGOVISION-001	[148] 0.0069	[154] 0.0090	[140] 0.0107	[138] 0.0128	[137] 0.0157	[69] 0.0002 N^0.277 [141]	[142] 0.0023	[143] 0.0027	[129] 0.0031	[124] 0.0036	[121] 0.0043	[40] 0.0001 N^0.211 [132]
6	ANKE-000	[127] 0.0102	[129] 0.0132	[155] 0.0155	[150] 0.0188	[146] 0.0225	[106] 0.0003 N^0.270 [131]	[164] 0.0032	[165] 0.0040	[145] 0.0046	[139] 0.0056	[133] 0.0066	[39] 0.0001 N^0.247 [139]
7	ANKE-002	[85] 0.0024	[86] 0.0028	[86] 0.0032	[83] 0.0037	[78] 0.0043	[63] 0.0002 N^0.203 [87]	[97] 0.0016	[97] 0.0017	[90] 0.0017	[80] 0.0018	[75] 0.0019	[97] 0.0006 N^0.067 [76]
8	AWARE-003	[208] 0.0238	[206] 0.0306	[170] 0.0361	[164] 0.0431	[163] 0.0506	[146] 0.0008 N^0.258 [126]	[186] 0.0055	[194] 0.0075	[164] 0.0092	[159] 0.0113	[160] 0.0143	[29] 0.0001 N^0.323 [160]
9	AWARE-005	[209] 0.0245	[207] 0.0311	[171] 0.0366	[165] 0.0434	[154] 0.0312	[163] 0.0056 N^0.118 [40]	[190] 0.0062	[200] 0.0082	[166] 0.0101	[162] 0.0128	[144] 0.0089	[116] 0.0007 N^0.169 [122]
10	AYONIX-002	[243] 0.2935	[244] 0.3414	[181] 0.3736	[173] 0.4101	[169] 0.4465	[168] 0.0440 N^0.143 [52]	[242] 0.0950	[244] 0.1274	[181] 0.1524	[172] 0.1828	[168] 0.2150	[156] 0.0023 N^0.279 [148]
11	CAMVI-004	[184] 0.0124	[216] 0.0468	[175] 0.0719	[172] 0.2363	[168] 0.2367	[2] 0.0000 N^1.055 [170]	[215] 0.0117	[230] 0.0464	[177] 0.0715	[173] 0.2361	[169] 0.2364	[2] 0.0000 N^1.071 [170]
12	CANON-001	[9] 0.0011	[7] 0.0011	[9] 0.0012	[9] 0.0013	[8] 0.0014	[92] 0.0002 N^0.113 [36]	[14] 0.0009	[13] 0.0009	[13] 0.0009	[12] 0.0009	[12] 0.0010	[96] 0.0006 N^0.026 [34]
13	CIB-000	[30] 0.0014	[29] 0.0015	[27] 0.0017	[30] 0.0019	[131] 0.0131	[3] 0.0000 N^0.635 [169]	[41] 0.0012	[34] 0.0012	[32] 0.0012	[32] 0.0012	[156] 0.0122	[3] 0.0000 N^0.647 [169]
14	CLEARVIEWAI-000	[7] 0.0010	[8] 0.0011	[8] 0.0012	[10] 0.0013	[10] 0.0015	[73] 0.0002 N^0.129 [46]	[15] 0.0009	[12] 0.0009	[12] 0.0009	[13] 0.0009	[11] 0.0010	[107] 0.0007 N^0.019 [26]
15	CLOUDWALK-HR-000	[34] 0.0015	[24] 0.0015	[22] 0.0015	[17] 0.0016	[14] 0.0017	[142] 0.0007 N^0.054 [9]	[85] 0.0014	[70] 0.0014	[61] 0.0014	[57] 0.0014	[42] 0.0014	[141] 0.0012 N^0.012 [12]
16	COGENT-000	[176] 0.0101	[164] 0.0105	[142] 0.0109	[133] 0.0115	[128] 0.0125	[161] 0.0038 N^0.071 [14]	[131] 0.0021	[132] 0.0024	[123] 0.0028	[127] 0.0036	[147] 0.0095	[7] 0.0000 N^0.466 [166]
17	COGENT-001	[175] 0.0101	[165] 0.0105	[141] 0.0109	[134] 0.0115	[129] 0.0125	[160] 0.0038 N^0.071 [13]	[132] 0.0021	[131] 0.0024	[124] 0.0028	[126] 0.0036	[148] 0.0095	[8] 0.0000 N^0.466 [165]
18	COGENT-002	[97] 0.0029	[101] 0.0036	[99] 0.0041	[97] 0.0049	[93] 0.0059	[40] 0.0001 N^0.244 [118]	[81] 0.0014	[88] 0.0015	[84] 0.0017	[86] 0.0019	[86] 0.0021	[52] 0.0002 N^0.144 [116]
19	COGENT-003	[103] 0.0031	[103] 0.0038	[103] 0.0043	[100] 0.0051	[96] 0.0060	[52] 0.0001 N^0.230 [108]	[91] 0.0015	[98] 0.0017	[101] 0.0018	[97] 0.0020	[92] 0.0022	[57] 0.0002 N^0.143 [115]
20	COGENT-004	[56] 0.0018	[56] 0.0020	[55] 0.0022	[54] 0.0025	[47] 0.0028	[86] 0.0002 N^0.159 [65]	[74] 0.0013	[69] 0.0014	[66] 0.0014	[60] 0.0015	[51] 0.0015	[102] 0.0007 N^0.050 [59]
21	COGENT-005	[42] 0.0016	[37] 0.0017	[35] 0.0018	[33] 0.0020	[28] 0.0021	[121] 0.0004 N^0.108 [31]	[75] 0.0013	[60] 0.0013	[55] 0.0014	[48] 0.0014	[41] 0.0014	[139] 0.0011 N^0.017 [20]
22	COGNITEC-000	[202] 0.0195	[201] 0.0252	[167] 0.0297	[162] 0.0352	[158] 0.0417	[139] 0.0006 N^0.259 [127]	[182] 0.0050	[186] 0.0065	[161] 0.0077	[158] 0.0097	[155] 0.0122	[36] 0.0001 N^0.305 [154]
23	COGNITEC-001	[170] 0.0090	[172] 0.0117	[152] 0.0139	[148] 0.0166	[144] 0.0199	[98] 0.0002 N^0.271 [134]	[160] 0.0030	[159] 0.0034	[142] 0.0040	[138] 0.0046	[129] 0.0054	[50] 0.0002 N^0.207 [131]
24	COGNITEC-002	[130] 0.0048	[128] 0.0057	[120] 0.0067	[115] 0.0079	[115] 0.0094	[87] 0.0002 N^0.232 [110]	[144] 0.0024	[140] 0.0026	[126] 0.0028	[119] 0.0030	[111] 0.0034	[83] 0.0005 N^0.117 [102]
25	COGNITEC-003	[133] 0.0053	[132] 0.0062	[123] 0.0072	[120] 0.0085	[118] 0.0100	[104] 0.0003 N^0.222 [99]	[157] 0.0028	[151] 0.0030	[131] 0.0032	[122] 0.0035	[115] 0.0037	[121] 0.0008 N^0.097 [93]
26	COGNITEC-004	[93] 0.0027	[94] 0.0032	[94] 0.0037	[92] 0.0045	[90] 0.0056	[31] 0.0001 N^0.253 [124]	[72] 0.0013	[72] 0.0014	[72] 0.0015	[73] 0.0017	[69] 0.0019	[61] 0.0002 N^0.123 [107]
27	COGNITEC-005	[31] 0.0014	[34] 0.0016	[37] 0.0018	[36] 0.0021	[36] 0.0024	[56] 0.0001 N^0.169 [72]	[30] 0.0011	[30] 0.0011	[28] 0.0012	[28] 0.0012	[22] 0.0012	[101] 0.0007 N^0.037 [41]
28	CYBERLINK-000	[109] 0.0034	[105] 0.0040	[106] 0.0046	[102] 0.0054	[98] 0.0063	[82] 0.0002 N^0.209 [93]	[129] 0.0021	[123] 0.0022	[116] 0.0023	[113] 0.0025	[105] 0.0027	[93] 0.0006 N^0.092 [90]
29	CYBERLINK-001	[100] 0.0030	[99] 0.0035	[101] 0.0042	[99] 0.0050	[95] 0.0060	[41] 0.0001 N^0.243 [117]	[101] 0.0016	[103] 0.0017	[94] 0.0018	[92] 0.0020	[89] 0.0022	[73] 0.0004 N^0.109 [97]
30	CYBERLINK-002	[86] 0.0024	[79] 0.0026	[77] 0.0028	[72] 0.0031	[62] 0.0035	[133] 0.0005 N^0.121 [41]	[124] 0.0020	[118] 0.0021	[111] 0.0021	[105] 0.0022	[91] 0.0022	[144] 0.0012 N^0.036 [40]
31	CYBERLINK-003	[32] 0.0015	[31] 0.0016	[28] 0.0017	[24] 0.0018	[21] 0.0020	[116] 0.0003 N^0.110 [33]	[34] 0.0011	[32] 0.0012	[30] 0.0012	[31] 0.0012	[27] 0.0013	[90] 0.0006 N^0.047 [55]
32	CYBERLINK-004	[45] 0.0016	[36] 0.0017	[34] 0.0018	[27] 0.0019	[23] 0.0021	[134] 0.0005 N^0.085 [23]	[82] 0.0014	[73] 0.0014	[63] 0.0014	[58] 0.0014	[47] 0.0015	[138] 0.0010 N^0.022 [29]
33	DAHUA-001	[135] 0.0053	[136] 0.0067	[127] 0.0079	[125] 0.0093	[122] 0.0112	[71] 0.0002 N^0.256 [125]	[154] 0.0027	[146] 0.0029	[130] 0.0031	[121] 0.0034	[117] 0.0038	[87] 0.0005 N^0.121 [105]
34	DAHUA-002	[50] 0.0017	[48] 0.0018	[49] 0.0021	[45] 0.0023	[41] 0.0027	[81] 0.0002 N^0.156 [59]	[66] 0.0013	[61] 0.0013	[58] 0.0014	[53] 0.0014	[45] 0.0015	[112] 0.0007 N^0.043 [52]
35	DAHUA-003	[8] 0.0010	[13] 0.0012	[14] 0.0014	[19] 0.0016	[19] 0.0018	[22] 0.0001 N^0.199 [86]	[12] 0.0009	[10] 0.0009	[10] 0.0009	[10] 0.0009	[9] 0.0009	[91] 0.0006 N^0.027 [35]
36	DEEPGLINT-001	[27] 0.0014	[22] 0.0014	[20] 0.0015	[20] 0.0016	[18] 0.0018	[126] 0.0004 N^0.089 [24]	[64] 0.0013	[52] 0.0013	[49] 0.0013	[40] 0.0013	[35] 0.0013	[136] 0.0010 N^0.017 [19]
37	DEEPSEA-001	[108] 0.0033	[110] 0.0043	[111] 0.0052	[109] 0.0065	[107] 0.0081	[17] 0.0001 N^0.311 [159]	[55] 0.0012	[67] 0.0014	[76] 0.0015	[75] 0.0017	[79] 0.0020	[43] 0.0001 N^0.157 [120]
38	DERMALOG-005	[183] 0.0114	[183] 0.0149	[157] 0.0201	[158] 0.0289	[161] 0.0447	[7] 0.0000 N^0.470 [168]	[209] 0.0094	[210] 0.0122	[172] 0.0171	[166] 0.0254	[164] 0.0406	[9] 0.0000 N^0.505 [167]
39	DERMALOG-006	[151] 0.0075	[149] 0.0081	[135] 0.0086	[126] 0.0093	[119] 0.0104	[155] 0.0017 N^0.109 [32]	[191] 0.0062	[185] 0.0063	[151] 0.0064	[144] 0.0065	[134] 0.0068	[161] 0.0043 N^0.028 [36]
40	DERMALOG-007	[158] 0.0080	[157] 0.0092	[139] 0.0102	[136] 0.0118	[133] 0.0140	[137] 0.0006 N^0.190 [83]	[184] 0.0051	[179] 0.0054	[148] 0.0056	[140] 0.0058	[132] 0.0063	[155] 0.0020 N^0.068 [77]
41	DERMALOG-008	[84] 0.0024	[87] 0.0029	[88] 0.0034	[87] 0.0040	[86] 0.0048	[35] 0.0001 N^0.239 [115]	[90] 0.0015	[85] 0.0015	[82] 0.0016	[76] 0.0017	[70] 0.0019	[77] 0.0004 N^0.088 [86]
42	DERMALOG-009	[90] 0.0026	[85] 0.0028	[81] 0.0030	[76] 0.0033	[65] 0.0037	[135] 0.0005 N^0.121 [42]	[133] 0.0022	[125] 0.0022	[114] 0.0022	[107] 0.0023	[95] 0.0024	[142] 0.0015 N^0.028 [37]
43	FUJITSULAB-000	[62] 0.0019	[63] 0.0022	[68] 0.0025	[66] 0.0029	[59] 0.0033	[57] 0.0001 N^0.190 [82]	[73] 0.0013	[65] 0.0014	[64] 0.0014	[59] 0.0015	[55] 0.0016	[89] 0.0006 N^0.059 [68]
44	GORILLA-002	[193] 0.0147	[195] 0.0197	[163] 0.0238	[157] 0.0288	[155] 0.0351	[109] 0.0003 N^0.295 [152]	[163] 0.0032	[162] 0.0041	[147] 0.0049	[143] 0.0062	[140] 0.0080	[19] 0.0000 N^0.315 [157]
45	GORILLA-004	[131] 0.0048	[133] 0.0063	[125] 0.0075	[124] 0.0091	[124] 0.0114	[36] 0.0001 N^0.292 [150]	[95] 0.0015	[105] 0.0018	[112] 0.0021	[111] 0.0025	[109] 0.0029	[31] 0.0001 N^0.222 [134]
46	GORILLA-005	[89] 0.0026	[93] 0.0032	[96] 0.0038	[94] 0.0046	[91] 0.0056	[19] 0.0001 N^0.271 [136]	[52] 0.0012	[51] 0.0013	[60] 0.0014	[68] 0.0016	[65] 0.0018	[59] 0.0002 N^0.127 [109]
47	GORILLA-006	[35] 0.0015	[41] 0.0017	[48] 0.0020	[49] 0.0024	[49] 0.0029	[20] 0.0001 N^0.226 [105]	[27] 0.0010	[27] 0.0011	[27] 0.0011	[24] 0.0012	[24] 0.0012	[84] 0.0005 N^0.056 [65]
48	GRIAULE-000	[80] 0.0022	[77] 0.0025	[75] 0.0028	[70] 0.0030	[63] 0.0035	[108] 0.0003 N^0.152 [57]	[99] 0.0016	[96] 0.0017	[96] 0.0018	[82] 0.0018	[71] 0.0019	[105] 0.0007 N^0.062 [71]
49	HIK-003	[171] 0.0091	[173] 0.0117	[153] 0.0140	[149] 0.0169	[145] 0.0203	[94] 0.0002 N^0.274 [139]	[143] 0.0024	[150] 0.0030	[138] 0.0036	[135] 0.0044	[128] 0.0053	[24] 0.0001 N^0.278 [147]
50	HIK-004	[169] 0.0088	[170] 0.0113	[150] 0.0134	[146] 0.0163	[142] 0.0195	[96] 0.0002 N^0.271 [137]	[146] 0.0024	[147] 0.0030	[135] 0.0035	[132] 0.0042	[127] 0.0052	[30] 0.0001 N^0.259 [144]
51	HIK-005	[113] 0.0036	[115] 0.0046	[113] 0.0053	[108] 0.0065	[106] 0.0081	[33] 0.0001 N^0.274 [138]	[47] 0.0012	[81] 0.0015	[81] 0.0016	[85] 0.0019	[88] 0.0022	[34] 0.0001 N^0.202 [129]
52	HYPERVERGE-001	[21] 0.0013	[17] 0.0014	[15] 0.0014	[14] 0.0015	[13] 0.0017	[127] 0.0004 N^0.084 [20]	[63] 0.0013	[54] 0.0013	[46] 0.0013	[36] 0.0013	[28] 0.0013	[143] 0.0012 N^0.004 [8]
53	IDEMIA-003	[136] 0.0054	[139] 0.0069	[132] 0.0084	[131] 0.0101	[127] 0.0122	[48] 0.0001 N^0.281 [145]	[138] 0.0023	[144] 0.0027	[127] 0.0031	[125] 0.0036	[119] 0.0041	[44] 0.0002 N^0.201 [128]
54	IDEMIA-004	[139] 0.0054	[135] 0.0066	[129] 0.0079	[130] 0.0097	[126] 0.0117	[53] 0.0001 N^0.270 [130]	[115] 0.0018	[119] 0.0021	[120] 0.0025	[118] 0.0030	[114] 0.0036	[28] 0.0001 N^0.241 [138]
55	IDEMIA-005	[144] 0.0064	[148] 0.0081	[137] 0.0097	[135] 0.0118	[134] 0.0143	[60] 0.0002 N^0.277 [142]	[137] 0.0022	[149] 0.0030	[137] 0.0036	[136] 0.0044	[130] 0.0055	[16] 0.0000 N^0.300 [153]
56	IDEMIA-006	[153] 0.0076	[161] 0.0096	[144] 0.0113	[140] 0.0135	[139] 0.0161	[97] 0.0002 N^0.259 [128]	[156] 0.0028	[162] 0.0037	[144] 0.0046	[141] 0.0059	[138] 0.0076	[14] 0.0000 N^0.341 [162]
57	IDEMIA-007	[71] 0.0021	[78] 0.0026	[80] 0.0030	[78] 0.0036	[79] 0.0044	[23] 0.0001 N^0.250 [122]	[31] 0.0011	[36] 0.0012	[38] 0.0012	[50] 0.0014	[50] 0.0015	[62] 0.0002 N^0.110 [99]
58	IDEMIA-008	[5] 0.0010	[6] 0.0011	[6] 0.0011	[6] 0.0013	[6] 0.0014	[78] 0.0002 N^0.121 [43]	[13] 0.0009	[11] 0.0009	[11] 0.0009	[11] 0.0009	[8] 0.0009	[111] 0.0007 N^0.016 [17]
59	IMAGUS-005	[55] 0.0018	[53] 0.0019	[53] 0.0022	[53] 0.0025	[45] 0.0028	[85] 0.0002 N^0.158 [64]	[59] 0.0013	[63] 0.0013	[56] 0.0014	[56] 0.0014	[53] 0.0016	[86] 0.0005 N^0.066 [75]
60	IMAGUS-006	[57] 0.0018	[57] 0.0020	[54] 0.0022	[52] 0.0025	[48] 0.0029	[89] 0.0002 N^0.156 [58]	[79] 0.0014	[75] 0.0014	[71] 0.0015	[62] 0.0015	[57] 0.0016	[110] 0.0007 N^0.049 [58]
61	IMPERIAL-000	[78] 0.0022	[76] 0.0024	[73] 0.0027	[71] 0.0030	[64] 0.0035	[103] 0.0003 N^0.157 [60]	[104] 0.0016	[100] 0.0017	[92] 0.0017	[79] 0.0018	[68] 0.0018	[130] 0.0009 N^0.041 [48]
62	INCODE-003	[173] 0.0098	[178] 0.0129	[154] 0.0154	[151] 0.0191	[147] 0.0233	[77] 0.0002 N^0.296 [153]	[145] 0.0024	[152] 0.0031	[140] 0.0036	[137] 0.0046	[131] 0.0056	[22] 0.0001 N^0.285 [151]
63	INCODE-004	[98] 0.0029	[100] 0.0035	[100] 0.0041	[98] 0.0049	[94] 0.0060	[39] 0.0001 N^0.244 [119]	[113] 0.0018	[108] 0.0019	[107] 0.0020	[101] 0.0021	[90] 0.0022	[95] 0.0006 N^0.027 [81]
64	INCODE-005	[37] 0.0015	[35] 0.0017	[33] 0.0018	[34] 0.0020	[32] 0.0023	[93] 0.0002 N^0.140 [50]	[51] 0.0012	[44] 0.0013	[43] 0.0013	[43] 0.0013	[39] 0.0014	[109] 0.0007 N^0.041 [45]
65	INNOVATRICS-007	[43] 0.0016	[38] 0.0017	[39] 0.0019	[37] 0.0021	[37] 0.0024	[91] 0.0002 N^0.143 [54]	[49] 0.0012	[45] 0.0012	[41] 0.0013	[37] 0.0013	[33] 0.0013	[114] 0.0007 N^0.037 [42]
66	INTSYSMSU-000	[235] 0.1395	[235] 0.1457	[177] 0.1498	[169] 0.1544	[165] 0.1591	[170] 0.0768 N^0.045 [6]	[244] 0.1098	[242] 0.1163	[180] 0.1206	[171] 0.1252	[167] 0.1296	[170] 0.0519 N^0.056 [66]
67	IREX-000	[122] 0.0043	[111] 0.0044	[104] 0.0044	[93] 0.0046	[85] 0.0048	[157] 0.0028 N^0.032 [4]	[177] 0.0043	[168] 0.0043	[143] 0.0043	[134] 0.0043	[120] 0.0043	[160] 0.0042 N^0.002 [4]
68	ISYSTEMS-002	[134] 0.0053	[134] 0.0064	[124] 0.0072	[119] 0.0083	[116] 0.0096	[119] 0.0003 N^0.204 [89]	[166] 0.0033	[160] 0.0034	[136] 0.0036	[129] 0.0038	[118] 0.0041	[145] 0.0013 N^0.071 [78]
69	ISYSTEMS-003	[126] 0.0046	[122] 0.0052	[114] 0.0057	[110] 0.0066	[104] 0.0076	[128] 0.0004 N^0.174 [77]	[162] 0.0031	[156] 0.0033	[132] 0.0034	[123] 0.0035	[116] 0.0037	[146] 0.0013 N^0.063 [73]
70	KAKAO-000	[18] 0.0013	[23] 0.0015	[25] 0.0016	[29] 0.0019	[31] 0.0022	[34] 0.0001 N^0.192 [85]	[18] 0.0009	[17] 0.0010	[16] 0.0010	[18] 0.0010	[17] 0.0011	[80] 0.0005 N^0.050 [60]
71	KEDACOM-001	[154] 0.0076	[144] 0.0077	[128] 0.0079	[118] 0.0083	[109] 0.0087	[162] 0.0040 N^0.047 [7]	[196] 0.0071	[190] 0.0072	[158] 0.0072	[146] 0.0073	[135] 0.0073	[165] 0.0063 N^0.009 [10]
72	KNERON-000	[129] 0.0048	[129] 0.0059	[121] 0.0067	[116] 0.0079	[114] 0.0093	[95] 0.0002 N^0.226 [104]	[179] 0.0048	[181] 0.0059	[153] 0.0067	[151] 0.0079	[146] 0.0093	[60] 0.0002 N^0.226 [135]

Table 18: **Investigation-mode: Effect of N on FNIR on recent images** *For five enrollment population sizes, N, with T = 0 and FPIR = 1. The left five columns are rank 1 miss rates The right five columns are rank 50 miss rates Missing entries usually apply because another algorithm from the same developer was run instead. Some developers are missing because less accurate algorithms were not run on galleries with $N > 1\,600\,000$. Throughout blue superscripts indicate the rank of the algorithm for that column, and yellow highlighting indicates the most accurate value. Caution: The Power-low models are mostly intended to draw attention to the kind of behavior, not as a model to be used for prediction.*

This publication is available free of charge from: https://doi.org/10.6028/NIST.IR.8271

MISSES AT GIVEN RANK FNIR(N, T= 0, R)		ENROL MOST RECENT											
		RANK 1						RANK 50					
#	ALGORITHM	N=0.64M	N=1.6M	N=3.0M	N=6.0M	N=12.0M	aN^b	N=0.64M	N=1.6M	N=3.0M	N=6.0M	N=12.0M	aN^b
73	LOOKMAN-003	163 0.0083	153 0.0088	136 0.0091	128 0.0096	120 0.0104	158 0.0030 $N^{0.076}$ 16	200 0.0072	193 0.0074	160 0.0075	149 0.0076	139 0.0077	163 0.0054 $N^{0.022}$ 28
74	LOOKMAN-005	155 0.0078	147 0.0080	131 0.0083	121 0.0086	112 0.0092	159 0.0038 $N^{0.053}$ 8	198 0.0072	191 0.0072	159 0.0073	147 0.0073	136 0.0074	164 0.0060 $N^{0.013}$ 15
75	MANTRA-000	38 0.0015	40 0.0017	40 0.0019	41 0.0022	38 0.0025	59 0.0002 $N^{0.171}$ 74	45 0.0012	38 0.0012	36 0.0012	34 0.0013	29 0.0013	100 0.0007 $N^{0.042}$ 49
76	MEGVII-001	179 0.0105	174 0.0118	148 0.0128	142 0.0142	138 0.0161	153 0.0015 $N^{0.143}$ 53	202 0.0077	199 0.0080	162 0.0082	156 0.0086	145 0.0089	159 0.0040 $N^{0.048}$ 57
77	MICROFOCUS-005	246 0.3700	246 0.4242	182 0.4610	174 0.5000	170 0.5391	169 0.0674 $N^{0.128}$ 45	247 0.1300	249 0.1724	182 0.2046	174 0.2425	170 0.2810	158 0.0040 $N^{0.263}$ 145
78	MICROSOFT-003	17 0.0013	32 0.0016	38 0.0018	41 0.0022	46 0.0028	13 0.0000 $N^{0.271}$ 135	2 0.0006	2 0.0006	4 0.0007	5 0.0008	7 0.0009	27 0.0001 $N^{0.158}$ 121
79	MICROSOFT-004	16 0.0012	25 0.0015	32 0.0018	40 0.0021	44 0.0028	12 0.0000 $N^{0.281}$ 144	1 0.0006	1 0.0006	1 0.0007	1 0.0007	4 0.0009	37 0.0001 $N^{0.139}$ 113
80	MICROSOFT-005	36 0.0015	50 0.0019	59 0.0023	68 0.0030	68 0.0037	8 0.0000 $N^{0.320}$ 161	3 0.0006	3 0.0006	2 0.0007	2 0.0008	5 0.0009	38 0.0001 $N^{0.136}$ 112
81	MICROSOFT-006	40 0.0016	55 0.0020	65 0.0025	69 0.0030	72 0.0038	11 0.0000 $N^{0.305}$ 157	4 0.0006	4 0.0007	3 0.0007	8 0.0009	14 0.0010	21 0.0000 $N^{0.184}$ 124
82	NEC-000	187 0.0131	187 0.0170	158 0.0203	152 0.0244	149 0.0294	115 0.0003 $N^{0.276}$ 140	159 0.0029	164 0.0038	146 0.0048	142 0.0059	137 0.0074	15 0.0000 $N^{0.319}$ 158
83	NEC-001	199 0.0180	196 0.0209	162 0.0233	156 0.0266	151 0.0304	154 0.0016 $N^{0.179}$ 79	213 0.0109	206 0.0113	167 0.0116	160 0.0121	157 0.0129	162 0.0051 $N^{0.056}$ 64
84	NEC-002	3 0.0009	5 0.0010	5 0.0011	5 0.0012	5 0.0013	84 0.0002 $N^{0.113}$ 38	5 0.0008	5 0.0008	5 0.0008	4 0.0008	3 0.0008	79 0.0005 $N^{0.038}$ 43
85	NEC-003	19 0.0013	16 0.0014	16 0.0015	16 0.0016	11 0.0016	129 0.0005 $N^{0.079}$ 17	43 0.0012	35 0.0012	33 0.0012	30 0.0012	25 0.0012	128 0.0009 $N^{0.019}$ 25
86	NEC-004	26 0.0014	20 0.0014	18 0.0015	15 0.0016	12 0.0017	138 0.0006 $N^{0.059}$ 11	61 0.0013	50 0.0013	47 0.0013	45 0.0013	31 0.0013	137 0.0010 $N^{0.016}$ 18
87	NEUROTECHNOLOGY-003	198 0.0179	197 0.0225	164 0.0263	159 0.0306	156 0.0361	145 0.0007 $N^{0.239}$ 116	176 0.0042	180 0.0057	157 0.0072	157 0.0090	154 0.0112	20 0.0000 $N^{0.334}$ 161
88	NEUROTECHNOLOGY-004	127 0.0046	124 0.0056	119 0.0064	114 0.0074	110 0.0088	99 0.0002 $N^{0.220}$ 98	135 0.0022	133 0.0025	125 0.0028	120 0.0031	112 0.0034	64 0.0003 $N^{0.154}$ 118
89	NEUROTECHNOLOGY-005	112 0.0035	109 0.0043	108 0.0049	104 0.0057	99 0.0068	74 0.0002 $N^{0.223}$ 101	130 0.0021	128 0.0023	118 0.0024	114 0.0025	106 0.0028	94 0.0006 $N^{0.092}$ 91
90	NEUROTECHNOLOGY-007	106 0.0032	104 0.0039	105 0.0044	101 0.0052	97 0.0062	65 0.0002 $N^{0.222}$ 100	125 0.0020	121 0.0022	115 0.0023	108 0.0024	100 0.0026	115 0.0007 $N^{0.076}$ 80
91	NEUROTECHNOLOGY-008	59 0.0019	62 0.0022	62 0.0025	64 0.0029	60 0.0034	42 0.0001 $N^{0.205}$ 91	70 0.0013	58 0.0013	54 0.0013	51 0.0014	46 0.0015	113 0.0007 $N^{0.043}$ 50
92	NEUROTECHNOLOGY-009	20 0.0013	21 0.0014	23 0.0016	25 0.0018	24 0.0021	54 0.0001 $N^{0.162}$ 67	29 0.0011	29 0.0011	26 0.0011	23 0.0012	20 0.0012	118 0.0007 $N^{0.029}$ 38
93	NTECHLAB-003	128 0.0046	130 0.0062	126 0.0076	127 0.0094	123 0.0114	24 0.0001 $N^{0.310}$ 158	68 0.0013	91 0.0016	100 0.0018	104 0.0022	101 0.0026	23 0.0001 $N^{0.237}$ 136
94	NTECHLAB-004	115 0.0037	118 0.0048	115 0.0058	111 0.0071	108 0.0085	26 0.0001 $N^{0.291}$ 149	35 0.0011	64 0.0013	75 0.0015	74 0.0017	84 0.0021	33 0.0001 $N^{0.198}$ 126
95	NTECHLAB-005	110 0.0035	116 0.0047	116 0.0058	112 0.0073	113 0.0092	15 0.0000 $N^{0.334}$ 164	9 0.0008	25 0.0011	35 0.0012	65 0.0015	73 0.0019	10 0.0000 $N^{0.283}$ 149
96	NTECHLAB-006	99 0.0030	108 0.0041	109 0.0050	106 0.0062	105 0.0078	14 0.0000 $N^{0.326}$ 163	6 0.0008	14 0.0009	24 0.0011	35 0.0013	58 0.0016	12 0.0000 $N^{0.253}$ 140
97	NTECHLAB-007	76 0.0022	80 0.0027	82 0.0031	82 0.0037	80 0.0044	28 0.0001 $N^{0.245}$ 120	33 0.0011	39 0.0012	42 0.0013	52 0.0014	52 0.0015	63 0.0003 $N^{0.109}$ 98
98	NTECHLAB-008	29 0.0014	39 0.0017	42 0.0020	50 0.0024	42 0.0027	21 0.0001 $N^{0.224}$ 103	23 0.0010	24 0.0010	22 0.0011	22 0.0011	21 0.0012	75 0.0004 $N^{0.065}$ 74
99	NTECHLAB-009	15 0.0012	15 0.0013	13 0.0014	13 0.0015	16 0.0018	72 0.0002 $N^{0.140}$ 49	19 0.0009	16 0.0009	15 0.0010	16 0.0010	15 0.0010	88 0.0005 $N^{0.041}$ 46
100	NTECHLAB-010	10 0.0011	9 0.0011	7 0.0012	7 0.0013	7 0.0014	111 0.0003 $N^{0.091}$ 26	25 0.0010	22 0.0010	17 0.0010	15 0.0010	13 0.0010	131 0.0009 $N^{0.005}$ 9
101	PARAVISION-003	92 0.0026	92 0.0031	91 0.0035	89 0.0042	87 0.0048	61 0.0002 $N^{0.210}$ 94	103 0.0016	102 0.0017	99 0.0018	94 0.0020	85 0.0021	81 0.0005 $N^{0.089}$ 87
102	PARAVISION-004	39 0.0015	33 0.0016	31 0.0017	28 0.0019	25 0.0021	117 0.0003 $N^{0.111}$ 34	65 0.0013	56 0.0013	48 0.0013	41 0.0013	37 0.0014	135 0.0010 $N^{0.020}$ 27
103	PARAVISION-005	33 0.0015	27 0.0015	24 0.0016	23 0.0018	20 0.0019	125 0.0004 $N^{0.094}$ 28	69 0.0013	59 0.0013	52 0.0013	44 0.0013	36 0.0014	140 0.0011 $N^{0.015}$ 16
104	PARAVISION-007	13 0.0011	11 0.0012	11 0.0012	8 0.0013	9 0.0015	113 0.0003 $N^{0.091}$ 25	24 0.0010	20 0.0010	18 0.0010	17 0.0010	16 0.0011	123 0.0008 $N^{0.018}$ 23
105	PIXELALL-002	117 0.0037	113 0.0045	110 0.0052	107 0.0062	103 0.0075	58 0.0002 $N^{0.238}$ 114	108 0.0017	114 0.0019	110 0.0021	109 0.0024	102 0.0027	56 0.0002 $N^{0.154}$ 119
106	PIXELALL-003	61 0.0019	61 0.0021	61 0.0024	59 0.0028	57 0.0032	66 0.0002 $N^{0.182}$ 81	80 0.0014	74 0.0014	65 0.0014	61 0.0015	54 0.0016	120 0.0007 $N^{0.045}$ 53
107	PIXELALL-004	51 0.0017	59 0.0020	58 0.0023	56 0.0026	52 0.0030	50 0.0001 $N^{0.192}$ 84	67 0.0013	62 0.0013	59 0.0014	55 0.0014	48 0.0015	104 0.0007 $N^{0.046}$ 54
108	PIXELALL-005	54 0.0018	51 0.0019	43 0.0020	39 0.0021	35 0.0024	131 0.0005 $N^{0.098}$ 29	94 0.0015	90 0.0016	80 0.0016	69 0.0016	60 0.0016	142 0.0012 $N^{0.018}$ 21
109	PTAKURATSATU-000	88 0.0025	90 0.0030	93 0.0036	86 0.0040	74 0.0040	107 0.0003 $N^{0.167}$ 70	93 0.0015	92 0.0016	102 0.0018	91 0.0020	77 0.0020	76 0.0004 $N^{0.096}$ 92
110	QUANTASOFT-001	242 0.2177	239 0.2177	180 0.2177		166 0.2177	171 0.2177 $N^{0.000}$ 1	245 0.1116	241 0.1116	179 0.1116		166 0.1116	171 0.1116 $N^{0.000}$ 1
111	RANKONE-002	194 0.0155	194 0.0194	161 0.0224	154 0.0262	152 0.0304	143 0.0007 $N^{0.230}$ 106	180 0.0048	184 0.0060	156 0.0071	154 0.0085	151 0.0102	46 0.0002 $N^{0.254}$ 143
112	RANKONE-003	195 0.0155	193 0.0194	160 0.0224	155 0.0262	153 0.0304	144 0.0007 $N^{0.230}$ 107	181 0.0048	183 0.0060	155 0.0071	155 0.0085	152 0.0102	45 0.0002 $N^{0.254}$ 142
113	RANKONE-005	152 0.0075	159 0.0094	143 0.0110	139 0.0132	136 0.0156	101 0.0003 $N^{0.251}$ 123	153 0.0026	154 0.0032	139 0.0036	133 0.0043	126 0.0050	41 0.0001 $N^{0.221}$ 133
114	RANKONE-007	96 0.0028	96 0.0034	95 0.0038	91 0.0045	89 0.0053	68 0.0002 $N^{0.211}$ 95	92 0.0015	94 0.0017	92 0.0018	89 0.0019	87 0.0021	66 0.0003 $N^{0.123}$ 106
115	RANKONE-009	66 0.0020	71 0.0024	72 0.0027	74 0.0032	71 0.0038	38 0.0001 $N^{0.219}$ 97	76 0.0013	71 0.0014	69 0.0015	63 0.0015	56 0.0016	92 0.0006 $N^{0.059}$ 69
116	RANKONE-010	69 0.0020	65 0.0022	64 0.0025	63 0.0029	58 0.0032	90 0.0002 $N^{0.164}$ 69	87 0.0014	78 0.0015	74 0.0015	67 0.0016	62 0.0017	98 0.0006 $N^{0.058}$ 67
117	RANKONE-011	24 0.0014	26 0.0015	26 0.0017	26 0.0018	27 0.0021	75 0.0002 $N^{0.150}$ 56	36 0.0011	31 0.0012	31 0.0012	27 0.0012	23 0.0012	126 0.0008 $N^{0.023}$ 30
118	REALNETWORKS-002	213 0.0299	209 0.0393	173 0.0470	167 0.0562	164 0.0580	151 0.0013 $N^{0.236}$ 113	185 0.0054	195 0.0076	165 0.0097	161 0.0126	158 0.0132	32 0.0001 $N^{0.320}$ 159
119	REALNETWORKS-003	200 0.0183	200 0.0242	166 0.0291	161 0.0352	160 0.0423	124 0.0004 $N^{0.287}$ 148	175 0.0041	176 0.0054	152 0.0064	152 0.0080	150 0.0101	26 0.0001 $N^{0.307}$ 155
120	REALNETWORKS-004	197 0.0175	198 0.0236	165 0.0284	160 0.0347	157 0.0416	118 0.0003 $N^{0.295}$ 151	172 0.0040	173 0.0050	150 0.0061	150 0.0078	149 0.0099	25 0.0001 $N^{0.315}$ 156
121	REALNETWORKS-005	65 0.0020	67 0.0023	70 0.0026	67 0.0030	66 0.0037	46 0.0001 $N^{0.207}$ 92	38 0.0012	42 0.0012	45 0.0013	49 0.0014	44 0.0015	74 0.0004 $N^{0.081}$ 82
122	REMARKAI-000	95 0.0027	98 0.0034	98 0.0040	96 0.0048	92 0.0058	30 0.0001 $N^{0.260}$ 129	88 0.0014	87 0.0015	83 0.0016	78 0.0018	78 0.0020	68 0.0003 $N^{0.108}$ 95
123	RENDIP-000	28 0.0014	30 0.0015	30 0.0017	31 0.0019	30 0.0022	67 0.0002 $N^{0.158}$ 62	39 0.0012	37 0.0012	34 0.0012	29 0.0012	26 0.0013	125 0.0008 $N^{0.025}$ 32
124	S1-000	70 0.0021	73 0.0024	76 0.0028	75 0.0032	70 0.0037	51 0.0001 $N^{0.203}$ 88	89 0.0014	84 0.0015	77 0.0015	71 0.0016	64 0.0017	103 0.0007 $N^{0.055}$ 63
125	S1-001	104 0.0031	91 0.0031	89 0.0034	79 0.0036	75 0.0040	147 0.0009 $N^{0.092}$ 27	139 0.0023	130 0.0023	117 0.0024	110 0.0024	99 0.0025	151 0.0017 $N^{0.023}$ 31
126	SCANOVATE-000	118 0.0038	119 0.0050	117 0.0059	113 0.0073	102 0.0073	70 0.0002 $N^{0.235}$ 112	83 0.0014	89 0.0015	89 0.0017	99 0.0020	82 0.0020	54 0.0002 $N^{0.142}$ 114
127	SCANOVATE-001	120 0.0041	123 0.0053	118 0.0064	117 0.0079	117 0.0098	25 0.0001 $N^{0.299}$ 154	78 0.0013	86 0.0015	88 0.0017	100 0.0021	98 0.0024	35 0.0001 $N^{0.207}$ 130
128	SENSETIME-000	75 0.0022	69 0.0023	69 0.0026	62 0.0028	56 0.0032	120 0.0003 $N^{0.135}$ 47	105 0.0016	104 0.0017	95 0.0018	83 0.0018	80 0.0020	117 0.0007 $N^{0.060}$ 70
129	SENSETIME-001	74 0.0022	70 0.0023	66 0.0025	65 0.0029	67 0.0037	79 0.0002 $N^{0.177}$ 78	102 0.0016	93 0.0016	82 0.0017	81 0.0018	96 0.0024	65 0.0003 $N^{0.125}$ 108
130	SENSETIME-002	190 0.0136	181 0.0137	151 0.0137	141 0.0138	132 0.0139	166 0.0124 $N^{0.007}$ 2	219 0.0136	212 0.0136	169 0.0136	163 0.0136	159 0.0136	167 0.0135 $N^{0.001}$ 3
131	SENSETIME-003	6 0.0010	4 0.0010	4 0.0010	4 0.0011	4 0.0012	110 0.0003 $N^{0.085}$ 22	17 0.0009	15 0.0009	14 0.0009	14 0.0010	10 0.0010	122 0.0008 $N^{0.013}$ 14
132	SENSETIME-004	4 0.0010	3 0.0010	3 0.0010	3 0.0011	3 0.0012	112 0.0003 $N^{0.081}$ 18	10 0.0008	8 0.0009	8 0.0009	7 0.0009	6 0.0009	99 0.0007 $N^{0.018}$ 24
133	SENSETIME-005	1 0.0008	2 0.0009	2 0.0009	2 0.0010	2 0.0011	102 0.0003 $N^{0.085}$ 21	7 0.0008	6 0.0008	6 0.0008	3 0.0008	1 0.0008	124 0.0008 $N^{0.002}$ 5
134	SENSETIME-006	2 0.0008	1 0.0009	1 0.0009	1 0.0010	1 0.0010	114 0.0003 $N^{0.069}$ 12	8 0.0008	7 0.0008	7 0.0008	6 0.0008	2 0.0008	108 0.0007 $N^{0.011}$ 11
135	SHAMAN-007	217 0.0371	210 0.0396	172 0.0416	166 0.0443	162 0.0473	165 0.0122 $N^{0.083}$ 19	232 0.0308	226 0.0314	175 0.0319	167 0.0326	163 0.0337	168 0.0207 $N^{0.029}$ 39
136	SIAT-001	48 0.0017	44 0.0018	45 0.0020	46 0.0023	43 0.0027	62 0.0002 $N^{0.173}$ 76	28 0.0010	28 0.0011	29 0.0012	33 0.0013	32 0.0013	69 0.0003 $N^{0.085}$ 84
137	SIAT-002	47 0.0016	46 0.0018	47 0.0020	47 0.0023	40 0.0027	64 0.0002 $N^{0.171}$ 73	37 0.0011	40 0.0012	40 0.0013	39 0.0013	38 0.0014	85 0.0005 $N^{0.062}$ 72
138	SYNESIS-003	196 0.0161	185 0.0162	156 0.0163	147 0.0165	148 0.0254	156 0.0027 $N^{0.127}$ 44	222 0.0160	217 0.0160	171 0.0160	165 0.0160	162 0.0245	132 0.0009 $N^{0.192}$ 125
139	SYNESIS-003	236 0.1456	236 0.1700	178 0.1876	170 0.2088	167 0.2317	167 0.0177 $N^{0.158}$ 63	238 0.0828	238 0.0869	178 0.0920	170 0.0998	165 0.1104	169 0.0218 $N^{0.098}$ 94
140	SYNESIS-005	165 0.0085	151 0.0085	134 0.0085	122 0.0086	111 0.0088	164 0.0072 $N^{0.012}$ 3	206 0.0085	201 0.0085	163 0.0085	153 0.0085	143 0.0085	166 0.0085 $N^{0.000}$ 2
141	TECH5-001	105 0.0032	106 0.0040	107 0.0047	103 0.0057	101 0.0071	29 0.0001 $N^{0.271}$ 133	96 0.0016	99 0.0017	98 0.0018	93 0.0020	93 0.0023	67 0.0003 $N^{0.119}$ 103
142	TECH5-002	67 0.0020	81 0.0027	84 0.0031	81 0.0037	83 0.0047	16 0.0000 $N^{0.285}$ 147	16 0.0009	19 0.0010	23 0.0011	25 0.0012	30 0.0013	48 0.0002 $N^{0.127}$ 110
143	TEVIAN-005	140 0.0056	142 0.0073	133 0.0084	132 0.0105	130 0.0130	49 0.0001 $N^{0.283}$ 146	121 0.0020	127 0.0023	121 0.0025	116 0.0028	110 0.0034	49 0.0002 $N^{0.178}$ 123
144	TEVIAN-006	82 0.0023	74 0.0024	71 0.0026	60 0.0028	55 0.0031	136 0.0005 $N^{0.106}$ 30	98 0.0016	95 0.0017	86 0.0017	77 0.0017	67 0.0018	129 0.0009 $N^{0.041}$ 47

Table 19: **Investigation-mode: Effect of N on FNIR on recent images** *For five enrollment population sizes, N, with T = 0 and FPIR = 1. The left five columns are rank 1 miss rates The right five columns are rank 50 miss rates Missing entries usually apply because another algorithm from the same developer was run instead. Some developers are missing because less accurate algorithms were not run on galleries with N > 1 600 000. Throughout blue superscripts indicate the rank of the algorithm for that column, and yellow highlighting indicates the most accurate value. Caution: The Power-low models are mostly intended to draw attention to the kind of behavior, not as a model to be used for prediction.*

This publication is available free of charge from: https://doi.org/10.6028/NIST.IR.8271

MISSES AT GIVEN RANK FNIR(N, T= 0, R)		ENROL MOST RECENT											
		RANK 1						RANK 50					
#	ALGORITHM	N=0.64M	N=1.6M	N=3.0M	N=6.0M	N=12.0M	aN^b	N=0.64M	N=1.6M	N=3.0M	N=6.0M	N=12.0M	aN^b
145	TEVIAN-007	52 0.0017	43 0.0018	36 0.0018	35 0.0020	26 0.0021	140 0.0006 N^0.073 15	56 0.0013	47 0.0013	44 0.0013	42 0.0013	34 0.0013	127 0.0009 N^0.026 33
146	TIGER-002	123 0.0044	125 0.0056	122 0.0068	123 0.0086	121 0.0105	27 0.0001 N^0.299 155	60 0.0013	83 0.0015	93 0.0018	102 0.0021	103 0.0027	17 0.0000 N^0.253 141
147	TOSHIBA-000	111 0.0035	112 0.0045	112 0.0052	105 0.0061	135 0.0154	5 0.0000 N^0.449 167	100 0.0016	107 0.0018	106 0.0019	103 0.0021	153 0.0105	4 0.0000 N^0.539 168
148	TRUEFACE-000	102 0.0031	95 0.0033	92 0.0035	85 0.0039	77 0.0043	141 0.0006 N^0.115 39	150 0.0025	136 0.0026	122 0.0026	115 0.0027	109 0.0028	149 0.0015 N^0.038 44
149	VD-001	207 0.0230	204 0.0276	168 0.0315	163 0.0363	159 0.0418	152 0.0015 N^0.204 90	216 0.0120	211 0.0130	170 0.0140	164 0.0154	161 0.0170	157 0.0024 N^0.120 104
150	VERIDAS-001	83 0.0023	84 0.0028	85 0.0032	84 0.0037	81 0.0045	37 0.0001 N^0.231 109	86 0.0014	79 0.0015	73 0.0015	72 0.0016	66 0.0018	78 0.0005 N^0.083 83
151	VERIDAS-002	81 0.0023	83 0.0028	74 0.0028	73 0.0032	69 0.0037	105 0.0003 N^0.158 61	84 0.0014	77 0.0015	68 0.0015	64 0.0015	59 0.0016	119 0.0007 N^0.047 56
152	VERIDAS-003	49 0.0017	45 0.0018	41 0.0020	43 0.0022	39 0.0026	88 0.0002 N^0.150 55	58 0.0013	55 0.0013	50 0.0013	46 0.0014	43 0.0014	106 0.0007 N^0.043 51
153	VIGILANTSOLUTIONS-008	87 0.0025	89 0.0029	90 0.0034	88 0.0040	82 0.0047	47 0.0001 N^0.224 102	40 0.0012	49 0.0013	62 0.0014	66 0.0015	63 0.0017	53 0.0002 N^0.130 111
154	VISIONBOX-000	53 0.0017	52 0.0019	56 0.0022	219 1.0000	171 0.9526	1 0.0000 N^2.570 171	54 0.0012	46 0.0013	51 0.0013	176 1.0000	171 0.9525	1 0.0000 N^2.719 171
155	VISIONLABS-004	77 0.0022	82 0.0027	87 0.0032	90 0.0044	100 0.0070	6 0.0000 N^0.387 165	53 0.0012	68 0.0014	85 0.0017	112 0.0025	123 0.0045	5 0.0000 N^0.435 164
156	VISIONLABS-005	64 0.0020	72 0.0024	79 0.0029	80 0.0037	88 0.0051	10 0.0000 N^0.322 162	50 0.0012	53 0.0013	78 0.0016	90 0.0019	108 0.0029	11 0.0000 N^0.298 152
157	VISIONLABS-006	46 0.0016	49 0.0018	57 0.0022	61 0.0028	76 0.0041	9 0.0000 N^0.314 160	46 0.0012	48 0.0013	70 0.0015	84 0.0019	104 0.0027	13 0.0000 N^0.275 146
158	VISIONLABS-007	44 0.0016	42 0.0018	44 0.0020	48 0.0023	61 0.0034	18 0.0001 N^0.248 121	42 0.0012	41 0.0012	39 0.0013	38 0.0013	76 0.0020	42 0.0001 N^0.152 117
159	VISIONLABS-008	58 0.0019	58 0.0020	52 0.0021	55 0.0025	53 0.0030	76 0.0002 N^0.169 71	106 0.0016	101 0.0017	91 0.0017	95 0.0020	94 0.0023	70 0.0003 N^0.114 100
160	VISIONLABS-009	11 0.0011	10 0.0011	10 0.0012	11 0.0014	15 0.0017	44 0.0001 N^0.160 66	21 0.0010	18 0.0010	19 0.0010	21 0.0011	40 0.0014	58 0.0002 N^0.109 96
161	VISIONLABS-010	23 0.0014	18 0.0014	21 0.0015	21 0.0017	22 0.0021	83 0.0002 N^0.137 48	57 0.0013	45 0.0013	53 0.0013	54 0.0014	61 0.0017	72 0.0004 N^0.090 89
162	VISIONLABS-011	12 0.0011	12 0.0012	12 0.0013	12 0.0014	17 0.0018	43 0.0001 N^0.162 68	26 0.0010	26 0.0011	25 0.0011	26 0.0012	49 0.0015	55 0.0002 N^0.114 101
163	VOCORD-005	141 0.0060	140 0.0070	130 0.0082	129 0.0097	125 0.0117	100 0.0003 N^0.232 111	167 0.0033	161 0.0035	141 0.0037	130 0.0040	122 0.0043	133 0.0010 N^0.090 88
164	VTS-001	22 0.0014	28 0.0015	29 0.0017	32 0.0019	33 0.0023	45 0.0001 N^0.179 80	22 0.0010	21 0.0010	20 0.0010	19 0.0011	18 0.0011	82 0.0005 N^0.051 61
165	XFORWARDAI-000	73 0.0021	66 0.0023	60 0.0024	57 0.0027	50 0.0029	130 0.0005 N^0.111 35	119 0.0019	113 0.0019	105 0.0019	96 0.0020	81 0.0020	148 0.0015 N^0.018 22
166	XFORWARDAI-001	68 0.0020	60 0.0020	50 0.0021	42 0.0022	34 0.0024	148 0.0009 N^0.055 10	118 0.0019	112 0.0019	104 0.0019	88 0.0019	74 0.0019	153 0.0018 N^0.004 7
167	XFORWARDAI-002	63 0.0019	54 0.0020	46 0.0020	38 0.0021	29 0.0022	150 0.0011 N^0.038 5	117 0.0019	111 0.0019	103 0.0019	87 0.0019	72 0.0019	152 0.0018 N^0.003 6
168	YITU-002	41 0.0016	47 0.0018	51 0.0021	51 0.0024	51 0.0029	32 0.0001 N^0.213 96	20 0.0009	23 0.0010	21 0.0010	20 0.0011	19 0.0012	71 0.0004 N^0.073 79
169	YITU-003	91 0.0026	88 0.0029	83 0.0031	77 0.0035	73 0.0039	123 0.0004 N^0.141 51	126 0.0020	120 0.0021	113 0.0022	106 0.0023	97 0.0024	134 0.0010 N^0.054 62
170	YITU-004	14 0.0011	14 0.0013	19 0.0015	22 0.0017	84 0.0047	4 0.0000 N^0.438 166	11 0.0008	9 0.0009	9 0.0009	9 0.0009	113 0.0036	6 0.0000 N^0.395 163
171	YITU-005	79 0.0022	68 0.0023	63 0.0025	58 0.0027	54 0.0031	132 0.0005 N^0.113 37	120 0.0020	115 0.0020	109 0.0020	98 0.0020	83 0.0020	150 0.0017 N^0.012 13

Table 20: **Investigation-mode: Effect of N on FNIR on recent images** *For five enrollment population sizes, N, with T = 0 and FPIR = 1. The left five columns are rank 1 miss rates The right five columns are rank 50 miss rates Missing entries usually apply because another algorithm from the same developer was run instead. Some developers are missing because less accurate algorithms were not run on galleries with $N > 1\,600\,000$. Throughout blue superscripts indicate the rank of the algorithm for that column, and yellow highlighting indicates the most accurate value. Caution: The Power-low models are mostly intended to draw attention to the kind of behavior, not as a model to be used for prediction.*

This publication is available free of charge from: https://doi.org/10.6028/NIST.IR.8271

MISSES OUTSIDE RANK R		RESOURCE USAGE		ENROL MOST RECENT, N = 1.6M					
FNIR(N, T=0, R)		TEMPLATE		FRVT 2018 MUGSHOTS					
#	ALGORITHM	BYTES	MSEC	R=1	R=5	R=10	R=20	R=50	WORK-10
1	20FACE-000	123 2048	40 247	219 0.0552	213 0.0269	212 0.0198	209 0.0146	203 0.0099	214 1.275
2	3DIVI-003	35 512	132 625	228 0.0833	223 0.0444	223 0.0349	219 0.0270	219 0.0191	224 1.447
3	3DIVI-004	236 4096	133 628	188 0.0175	181 0.0091	179 0.0075	176 0.0061	171 0.0049	185 1.092
4	3DIVI-005	227 4096	140 653	189 0.0176	182 0.0091	177 0.0074	175 0.0061	172 0.0049	186 1.092
5	3DIVI-006	51 528	139 653	199 0.0240	205 0.0171	208 0.0160	210 0.0154	215 0.0148	204 1.162
6	ACER-000	32 512	30 201	166 0.0106	150 0.0051	147 0.0041	146 0.0034	138 0.0026	151 1.053
7	ACER-001	131 2048	21 184	121 0.0051	125 0.0032	124 0.0028	124 0.0025	124 0.0022	124 1.031
8	AIZE-001	134 2048	78 403	127 0.0056	129 0.0037	134 0.0033	135 0.0030	142 0.0027	129 1.035
9	ALCHERA-000	132 2048	44 263	184 0.0161	193 0.0124	198 0.0117	203 0.0111	205 0.0105	192 1.116
10	ALCHERA-001	119 2048	6 66	254 0.9869	254 0.9782	254 0.9735	254 0.9679	253 0.9590	254 9.811
11	ALCHERA-002	161 2048	14 115	229 0.0949	228 0.0555	226 0.0443	226 0.0354	221 0.0254	228 1.544
12	ALCHERA-003	151 2048	120 548	163 0.0104	153 0.0054	153 0.0045	153 0.0038	153 0.0032	155 1.055
13	ALCHERA-004	169 2048	220 854	168 0.0110	149 0.0049	142 0.0038	138 0.0032	135 0.0025	149 1.051
14	ALLGOVISION-000	148 2048	88 425	171 0.0114	176 0.0084	182 0.0078	183 0.0073	188 0.0067	176 1.079
15	ALLGOVISION-001	154 2048	199 792	154 0.0090	147 0.0048	146 0.0040	145 0.0033	143 0.0027	147 1.048
16	ANKE-000	209 2072	90 431	179 0.0132	167 0.0073	166 0.0060	165 0.0050	165 0.0040	172 1.072
17	ANKE-001	210 2072	92 433	180 0.0132	168 0.0073	168 0.0061	166 0.0050	166 0.0040	173 1.073
18	ANKE-002	202 2056	135 641	86 0.0028	86 0.0020	85 0.0018	92 0.0018	97 0.0017	87 1.019
19	AWARE-003	211 2076	178 716	206 0.0306	203 0.0162	200 0.0127	197 0.0100	194 0.0075	205 1.163
20	AWARE-004	2 92	171 712	223 0.0679	220 0.0348	217 0.0274	217 0.0208	214 0.0145	220 1.354
21	AWARE-005	222 3100	206 827	207 0.0311	204 0.0167	202 0.0134	199 0.0107	200 0.0082	206 1.167
22	AWARE-006	3 124	205 818	225 0.0697	222 0.0369	218 0.0288	218 0.0223	216 0.0158	222 1.371
23	AYONIX-000	79 1036	1 10	248 0.4505	249 0.3540	249 0.3176	249 0.2834	249 0.2381	249 4.288
24	AYONIX-001	80 1036	3 12	243 0.3414	243 0.2338	243 0.1977	244 0.1652	243 0.1274	243 3.226
25	AYONIX-002	81 1036	2 11	244 0.3414	244 0.2338	244 0.1977	243 0.1652	244 0.1274	244 3.226
26	CAMVI-003	69 1024	168 707	218 0.0520	227 0.0517	228 0.0517	231 0.0517	231 0.0517	226 1.466
27	CAMVI-004	70 1024	177 718	216 0.0468	225 0.0465	227 0.0465	228 0.0464	230 0.0464	223 1.419
28	CAMVI-005	68 1024	190 769	222 0.0652	229 0.0648	232 0.0648	233 0.0648	235 0.0647	229 1.584
29	CANON-001	233 4096	233 893	7 0.0011	13 0.0010	11 0.0010	13 0.0009	13 0.0009	10 1.009
30	CIB-000	254 8196	147 674	29 0.0015	30 0.0013	31 0.0012	32 0.0012	34 0.0012	32 1.012
31	CLEARVIEWAI-000	231 4096	187 765	8 0.0011	12 0.0010	14 0.0010	12 0.0009	12 0.0009	8 1.009
32	CLOUDWALK-HR-000	159 2048	239 908	24 0.0015	48 0.0014	53 0.0014	61 0.0014	70 0.0014	44 1.013
33	COGENT-000	48 525	121 551	164 0.0105	186 0.0096	192 0.0095	140 0.0032	132 0.0024	182 1.088
34	COGENT-001	49 525	122 552	165 0.0105	187 0.0096	191 0.0095	139 0.0032	131 0.0024	183 1.088
35	COGENT-002	83 1043	254 987	101 0.0036	95 0.0022	94 0.0020	90 0.0018	88 0.0015	96 1.021
36	COGENT-003	84 1043	252 960	103 0.0038	106 0.0024	102 0.0021	105 0.0019	98 0.0017	104 1.023
37	COGENT-004	198 2053	250 952	56 0.0020	58 0.0016	60 0.0015	67 0.0015	69 0.0014	57 1.015
38	COGENT-005	85 1062	193 774	37 0.0017	47 0.0014	47 0.0014	55 0.0014	60 0.0013	47 1.013
39	COGNITEC-000	195 2052	19 176	201 0.0252	199 0.0136	197 0.0107	196 0.0085	186 0.0065	200 1.136
40	COGNITEC-001	197 2052	31 202	172 0.0117	160 0.0062	159 0.0051	161 0.0042	159 0.0034	160 1.062
41	COGNITEC-002	184 2052	36 227	128 0.0057	128 0.0037	129 0.0032	131 0.0029	140 0.0026	128 1.035
42	COGNITEC-003	191 2052	54 297	132 0.0062	136 0.0040	138 0.0036	144 0.0033	151 0.0030	135 1.039
43	COGNITEC-004	187 2052	27 192	94 0.0032	89 0.0020	80 0.0018	73 0.0015	72 0.0014	90 1.020
44	COGNITEC-005	188 2052	67 367	34 0.0016	28 0.0013	28 0.0012	27 0.0012	30 0.0011	27 1.012
45	CUBOX-000	126 2048	242 918	19 0.0014	40 0.0014	48 0.0014	56 0.0014	66 0.0014	36 1.012
46	CYBERLINK-000	193 2052	162 699	105 0.0040	116 0.0028	120 0.0026	122 0.0024	123 0.0022	115 1.027
47	CYBERLINK-001	186 2052	91 433	99 0.0035	101 0.0023	100 0.0021	95 0.0018	103 0.0017	99 1.022
48	CYBERLINK-002	249 4140	184 738	79 0.0026	97 0.0023	108 0.0022	114 0.0021	118 0.0021	94 1.021
49	CYBERLINK-003	251 6212	161 696	31 0.0016	31 0.0013	32 0.0013	31 0.0012	32 0.0012	33 1.012
50	CYBERLINK-004	252 6212	185 738	36 0.0017	52 0.0015	59 0.0015	63 0.0014	73 0.0014	50 1.014
51	DAHUA-000	118 2048	73 378	158 0.0093	163 0.0066	167 0.0061	173 0.0057	177 0.0054	161 1.062
52	DAHUA-001	171 2048	69 371	136 0.0067	137 0.0040	135 0.0036	142 0.0033	146 0.0029	137 1.040
53	DAHUA-002	167 2048	163 699	48 0.0018	50 0.0015	56 0.0014	60 0.0014	61 0.0013	51 1.014
54	DAHUA-003	133 2048	180 725	13 0.0012	9 0.0010	9 0.0009	10 0.0009	10 0.0009	7 1.009
55	DEEPGLINT-001	237 4096	152 687	22 0.0014	37 0.0014	38 0.0013	45 0.0013	52 0.0013	35 1.012
56	DEEPSEA-001	121 2048	196 780	110 0.0043	96 0.0022	83 0.0018	79 0.0016	67 0.0014	100 1.022
57	DERMALOG-003	4 128	34 211	233 0.1259	232 0.0744	231 0.0603	230 0.0480	229 0.0347	232 1.731
58	DERMALOG-004	6 128	32 208	232 0.1251	231 0.0739	230 0.0598	229 0.0475	228 0.0343	231 1.727
59	DERMALOG-005	5 128	114 532	183 0.0149	196 0.0129	199 0.0125	205 0.0123	210 0.0122	193 1.118
60	DERMALOG-006	16 256	111 514	149 0.0081	166 0.0069	169 0.0066	177 0.0065	185 0.0063	164 1.063
61	DERMALOG-007	7 128	85 413	157 0.0092	164 0.0066	165 0.0060	172 0.0057	179 0.0054	162 1.062
62	DERMALOG-008	37 512	68 370	87 0.0029	85 0.0020	82 0.0018	82 0.0017	83 0.0015	86 1.019
63	DERMALOG-009	42 512	63 347	85 0.0028	104 0.0024	113 0.0023	117 0.0023	125 0.0022	98 1.022
64	EYEDEA-003	82 1036	74 385	227 0.0800	224 0.0451	224 0.0362	220 0.0289	220 0.0211	225 1.448
65	F8-001	152 2048	219 851	176 0.0120	188 0.0105	195 0.0102	198 0.0100	202 0.0099	188 1.096
66	FINCORE-000	116 2048	102 477	167 0.0108	152 0.0052	149 0.0042	148 0.0034	141 0.0026	153 1.054
67	FUJITSULAB-000	77 1032	249 950	63 0.0022	63 0.0016	64 0.0015	65 0.0015	65 0.0014	63 1.015
68	GLORY-000	30 418	15 160	237 0.1781	239 0.1391	239 0.1266	239 0.1154	239 0.1007	238 2.298
69	GLORY-001	106 1726	80 405	234 0.1268	234 0.0967	234 0.0869	235 0.0778	236 0.0673	234 1.903
70	GORILLA-001	212 2156	17 169	220 0.0603	215 0.0304	214 0.0230	214 0.0174	209 0.0117	215 1.309
71	GORILLA-002	88 1132	63 341	195 0.0197	183 0.0092	173 0.0070	168 0.0054	167 0.0041	187 1.096
72	GORILLA-003	213 2156	124 563	208 0.0361	201 0.0146	196 0.0106	190 0.0078	178 0.0054	203 1.158

Table 21: **Rank-based accuracy for the FRVT 2018 mugshot sets**. *In columns 3 and 4 are template size and template generation duration. Thereafter values are rank-based FNIR with T = 0 and FPIR = 1. This is appropriate to investigational uses but not those with higher volumes where candidates from all searches would need review. The next column is a workload statistic, a small value shows an algorithm front-loads mates into the first 10 candidates. Throughout, blue superscripts indicate the rank of the algorithm for that column, and the best value is highlighted in yellow.*

This publication is available free of charge from: https://doi.org/10.6028/NIST.IR.8271

MISSES OUTSIDE RANK R		RESOURCE USAGE		ENROL MOST RECENT, N = 1.6M					
FNIR(N, T=0, R)		TEMPLATE		FRVT 2018 MUGSHOTS					
#	ALGORITHM	BYTES	MSEC	R=1	R=5	R=10	R=20	R=50	WORK-10
73	GORILLA-004	[214]2192	[76]395	[133]0.0063	[124]0.0032	[121]0.0026	[118]0.0023	[105]0.0018	[125]1.033
74	GORILLA-005	[253]6288	[105]483	[93]0.0032	[75]0.0019	[75]0.0017	[68]0.0015	[51]0.0013	[84]1.018
75	GORILLA-006	[255]8336	[189]768	[41]0.0017	[27]0.0013	[25]0.0012	[26]0.0012	[27]0.0011	[30]1.012
76	GRIAULE-000	[180]2052	[87]419	[77]0.0025	[83]0.0020	[87]0.0019	[93]0.0018	[96]0.0017	[81]1.018
77	HIK-003	[95]1408	[134]633	[173]0.0117	[158]0.0060	[157]0.0048	[158]0.0039	[150]0.0030	[159]1.061
78	HIK-004	[89]1152	[110]510	[170]0.0113	[156]0.0059	[156]0.0047	[151]0.0037	[147]0.0030	[158]1.060
79	HIK-005	[93]1408	[131]619	[115]0.0046	[108]0.0025	[97]0.0020	[84]0.0017	[81]0.0015	[109]1.025
80	HIK-006	[94]1408	[128]610	[114]0.0046	[109]0.0025	[96]0.0020	[86]0.0017	[80]0.0015	[110]1.025
81	HYPERVERGE-001	[64]1024	[218]846	[17]0.0014	[29]0.0013	[34]0.0013	[41]0.0013	[54]0.0013	[26]1.012
82	IDEMIA-003	[52]528	[153]689	[139]0.0069	[143]0.0045	[144]0.0039	[147]0.0034	[144]0.0027	[140]1.043
83	IDEMIA-004	[50]528	[145]669	[135]0.0066	[133]0.0038	[130]0.0032	[129]0.0027	[119]0.0021	[131]1.038
84	IDEMIA-005	[29]352	[71]374	[148]0.0081	[140]0.0044	[139]0.0036	[141]0.0032	[149]0.0030	[143]1.044
85	IDEMIA-006	[28]352	[70]373	[161]0.0096	[151]0.0052	[150]0.0042	[156]0.0039	[162]0.0037	[150]1.052
86	IDEMIA-007	[61]860	[201]807	[78]0.0026	[59]0.0016	[52]0.0014	[40]0.0013	[36]0.0012	[64]1.015
87	IDEMIA-008	[27]300	[95]451	[6]0.0011	[6]0.0009	[10]0.0009	[11]0.0009	[11]0.0009	[5]1.009
88	IMAGUS-002	[36]512	[7]76	[240]0.2203	[238]0.1342	[237]0.1090	[236]0.0871	[234]0.0632	[239]2.308
89	IMAGUS-003	[40]512	[5]57	[245]0.3559	[245]0.2491	[245]0.2132	[245]0.1791	[245]0.1397	[245]3.363
90	IMAGUS-005	[160]2048	[198]788	[53]0.0019	[60]0.0016	[61]0.0015	[59]0.0014	[63]0.0013	[58]1.015
91	IMAGUS-006	[147]2048	[237]905	[57]0.0020	[64]0.0016	[66]0.0015	[69]0.0015	[75]0.0014	[60]1.015
92	IMPERIAL-000	[140]2048	[142]654	[76]0.0024	[77]0.0019	[84]0.0018	[91]0.0018	[100]0.0017	[76]1.018
93	INCODE-000	[65]1024	[25]190	[217]0.0489	[212]0.0261	[213]0.0204	[211]0.0160	[208]0.0117	[212]1.262
94	INCODE-001	[117]2048	[156]690	[186]0.0166	[177]0.0084	[171]0.0067	[170]0.0055	[169]0.0043	[178]1.086
95	INCODE-002	[156]2048	[51]291	[190]0.0178	[180]0.0090	[174]0.0070	[171]0.0056	[170]0.0043	[184]1.092
96	INCODE-003	[136]2048	[165]704	[178]0.0129	[162]0.0064	[160]0.0051	[159]0.0040	[152]0.0031	[166]1.066
97	INCODE-004	[138]2048	[109]508	[100]0.0035	[102]0.0024	[104]0.0021	[108]0.0020	[108]0.0019	[101]1.023
98	INCODE-005	[149]2048	[108]500	[35]0.0017	[38]0.0014	[45]0.0014	[43]0.0013	[44]0.0013	[40]1.013
99	INNOVATRICS-002	[54]530	[41]255	[215]0.0451	[218]0.0342	[220]0.0322	[222]0.0308	[224]0.0297	[219]1.321
100	INNOVATRICS-003	[53]530	[42]255	[202]0.0263	[194]0.0126	[190]0.0095	[185]0.0074	[175]0.0053	[192]1.129
101	INNOVATRICS-004	[86]1076	[82]406	[177]0.0123	[161]0.0063	[158]0.0050	[160]0.0040	[155]0.0032	[165]1.064
102	INNOVATRICS-005	[55]538	[216]842	[75]0.0024	[71]0.0018	[74]0.0017	[77]0.0016	[76]0.0014	[71]1.017
103	INNOVATRICS-007	[56]538	[197]785	[38]0.0017	[44]0.0014	[39]0.0013	[38]0.0013	[43]0.0012	[42]1.013
104	INTSYSMSU-000	[125]2048	[149]675	[235]0.1457	[237]0.1320	[240]0.1272	[240]0.1225	[242]0.1163	[237]2.203
105	IREX-000	[221]3080	[256]2379	[111]0.0044	[138]0.0043	[152]0.0043	[162]0.0043	[168]0.0043	[136]1.039
106	ISYSTEMS-002	[176]2048	[59]316	[134]0.0064	[139]0.0043	[145]0.0039	[150]0.0037	[160]0.0034	[139]1.041
107	ISYSTEMS-003	[165]2048	[221]856	[122]0.0052	[134]0.0039	[140]0.0036	[149]0.0034	[156]0.0033	[130]1.037
108	KAKAO-000	[189]2052	[213]840	[23]0.0015	[19]0.0011	[19]0.0011	[16]0.0010	[17]0.0010	[19]1.010
109	KEDACOM-001	[26]292	[116]537	[144]0.0077	[169]0.0074	[175]0.0073	[182]0.0072	[190]0.0072	[167]1.067
110	KNERON-000	[139]2048	[113]530	[129]0.0059	[157]0.0059	[164]0.0059	[174]0.0059	[181]0.0059	[152]1.053
111	KNERON-001	[157]2048	[101]468	[205]0.0295	[214]0.0295	[219]0.0295	[221]0.0295	[223]0.0295	[213]1.266
112	LINE-000	[155]2048	[103]482	[64]0.0022	[56]0.0015	[49]0.0014	[36]0.0013	[33]0.0012	[56]1.015
113	LOOKMAN-003	[25]292	[64]342	[153]0.0088	[173]0.0078	[181]0.0076	[187]0.0075	[193]0.0074	[170]1.071
114	LOOKMAN-004	[58]548	[60]325	[155]0.0091	[174]0.0079	[180]0.0076	[186]0.0075	[192]0.0073	[171]1.072
115	LOOKMAN-005	[59]548	[112]514	[147]0.0080	[171]0.0075	[178]0.0074	[184]0.0073	[191]0.0072	[168]1.068
116	MANTRA-000	[181]2052	[83]412	[40]0.0017	[34]0.0013	[35]0.0013	[35]0.0012	[38]0.0012	[38]1.013
117	MEGVII-001	[228]4096	[138]652	[174]0.0118	[184]0.0093	[184]0.0087	[194]0.0084	[199]0.0080	[179]1.086
118	MEGVII-002	[238]4096	[143]656	[175]0.0118	[185]0.0093	[186]0.0088	[193]0.0084	[198]0.0080	[180]1.087
119	MICROFOCUS-003	[21]256	[47]269	[252]0.5942	[251]0.4692	[251]0.4204	[251]0.3724	[251]0.3095	[251]5.361
120	MICROFOCUS-004	[14]256	[48]270	[250]0.5763	[250]0.4519	[250]0.4026	[250]0.3560	[250]0.2957	[250]5.199
121	MICROFOCUS-005	[20]256	[46]266	[246]0.4242	[246]0.3028	[246]0.2606	[246]0.2209	[247]0.1724	[246]3.861
122	MICROFOCUS-006	[18]256	[45]265	[247]0.4268	[247]0.3049	[247]0.2623	[248]0.2233	[248]0.1746	[247]3.880
123	MICROSOFT-003	[66]1024	[79]404	[32]0.0016	[11]0.0010	[6]0.0009	[3]0.0008	[2]0.0006	[13]1.009
124	MICROSOFT-004	[142]2048	[192]773	[25]0.0015	[5]0.0009	[1]0.0008	[1]0.0007	[1]0.0006	[11]1.009
125	MICROSOFT-005	[71]1024	[146]673	[50]0.0019	[8]0.0010	[5]0.0008	[2]0.0008	[3]0.0006	[16]1.010
126	MICROSOFT-006	[67]1024	[159]695	[55]0.0020	[20]0.0011	[12]0.0010	[4]0.0008	[4]0.0007	[21]1.011
127	NEC-000	[219]2592	[8]82	[187]0.0170	[179]0.0086	[170]0.0066	[167]0.0052	[164]0.0038	[181]1.087
128	NEC-001	[220]2592	[9]88	[196]0.0209	[200]0.0141	[201]0.0128	[204]0.0119	[206]0.0113	[199]1.135
129	NEC-002	[104]1616	[141]653	[5]0.0010	[4]0.0009	[4]0.0008	[5]0.0008	[5]0.0008	[3]1.008
130	NEC-003	[105]1712	[155]690	[16]0.0014	[26]0.0012	[27]0.0012	[34]0.0012	[35]0.0012	[23]1.011
131	NEC-004	[87]1104	[253]967	[20]0.0014	[35]0.0013	[43]0.0013	[44]0.0013	[50]0.0013	[34]1.012
132	NEUROTECHNOLOGY-003	[174]2048	[119]547	[197]0.0225	[195]0.0126	[193]0.0100	[191]0.0078	[180]0.0057	[196]1.125
133	NEUROTECHNOLOGY-004	[175]2048	[118]543	[124]0.0056	[127]0.0036	[133]0.0032	[134]0.0029	[133]0.0025	[127]1.035
134	NEUROTECHNOLOGY-005	[15]256	[84]412	[109]0.0043	[118]0.0029	[122]0.0027	[123]0.0024	[128]0.0023	[118]1.028
135	NEUROTECHNOLOGY-006	[19]256	[186]746	[191]0.0180	[175]0.0079	[163]0.0059	[163]0.0046	[157]0.0033	[173]1.083
136	NEUROTECHNOLOGY-007	[13]256	[18]169	[104]0.0039	[113]0.0027	[118]0.0025	[119]0.0023	[121]0.0022	[111]1.026
137	NEUROTECHNOLOGY-008	[47]514	[200]804	[62]0.0022	[53]0.0015	[55]0.0014	[57]0.0014	[58]0.0013	[55]1.015
138	NEUROTECHNOLOGY-009	[45]513	[151]686	[21]0.0014	[23]0.0012	[24]0.0012	[25]0.0011	[29]0.0011	[22]1.011
139	NEWLAND-002	[143]2048	[225]868	[226]0.0786	[226]0.0480	[225]0.0397	[225]0.0332	[222]0.0263	[227]1.468
140	NOBLIS-001	[146]2048	[33]211	[242]0.2492	[242]0.1772	[242]0.1542	[242]0.1339	[240]0.1112	[242]2.679
141	NOBLIS-002	[250]6144	[115]535	[238]0.1794	[235]0.1108	[235]0.0903	[234]0.0722	[233]0.0535	[235]2.077
142	NTECHLAB-003	[225]3484	[209]831	[130]0.0062	[120]0.0029	[114]0.0023	[106]0.0019	[91]0.0016	[123]1.030
143	NTECHLAB-004	[224]3484	[243]929	[118]0.0048	[99]0.0023	[88]0.0019	[81]0.0016	[64]0.0013	[107]1.024
144	NTECHLAB-005	[109]1940	[176]717	[116]0.0047	[94]0.0022	[78]0.0017	[48]0.0013	[25]0.0011	[102]1.023

Table 22: **Rank-based accuracy for the FRVT 2018 mugshot sets**. *In columns 3 and 4 are template size and template generation duration. Thereafter values are rank-based FNIR with T = 0 and FPIR = 1. This is appropriate to investigational uses but not those with higher volumes where candidates from all searches would need review. The next column is a workload statistic, a small value shows an algorithm front-loads mates into the first 10 candidates. Throughout, blue superscripts indicate the rank of the algorithm for that column, and the best value is highlighted in yellow.*

This publication is available free of charge from: https://doi.org/10.6028/NIST.IR.8271

MISSES OUTSIDE RANK R		RESOURCE USAGE		ENROL MOST RECENT, N = 1.6M					
FNIR(N, T=0, R)		TEMPLATE		FRVT 2018 MUGSHOTS					
#	ALGORITHM	BYTES	MSEC	R=1	R=5	R=10	R=20	R=50	WORK-10
145	NTECHLAB-006	[110]1940	[214]841	[108]0.0041	[76]0.0019	[62]0.0015	[30]0.0012	[14]0.0009	[89]1.019
146	NTECHLAB-007	[223]3348	[212]834	[80]0.0027	[65]0.0017	[54]0.0014	[51]0.0013	[39]0.0012	[67]1.016
147	NTECHLAB-008	[91]1300	[123]562	[39]0.0017	[22]0.0012	[23]0.0012	[23]0.0011	[24]0.0010	[25]1.012
148	NTECHLAB-009	[92]1300	[236]900	[15]0.0013	[16]0.0011	[16]0.0010	[15]0.0010	[16]0.0009	[17]1.010
149	NTECHLAB-010	[90]1280	[228]875	[9]0.0011	[14]0.0010	[15]0.0010	[17]0.0010	[22]0.0010	[12]1.009
150	PARAVISION-000	[120]2048	[94]438	[192]0.0188	[206]0.0171	[210]0.0167	[213]0.0165	[218]0.0164	[202]1.156
151	PARAVISION-001	[158]2048	[126]590	[102]0.0038	[105]0.0024	[105]0.0022	[111]0.0020	[109]0.0019	[105]1.023
152	PARAVISION-002	[150]2048	[72]377	[102]0.0040	[110]0.0025	[111]0.0022	[113]0.0021	[110]0.0019	[108]1.025
153	PARAVISION-003	[164]2048	[182]735	[92]0.0031	[93]0.0022	[99]0.0020	[101]0.0019	[102]0.0017	[93]1.021
154	PARAVISION-004	[239]4096	[179]720	[33]0.0016	[41]0.0014	[44]0.0013	[49]0.0013	[56]0.0013	[41]1.013
155	PARAVISION-005	[229]4096	[222]858	[27]0.0015	[39]0.0014	[41]0.0013	[50]0.0013	[59]0.0013	[37]1.013
156	PARAVISION-007	[240]4096	[166]706	[11]0.0012	[17]0.0011	[18]0.0010	[19]0.0010	[20]0.0010	[15]1.010
157	PIXELALL-002	[215]2560	[28]198	[113]0.0045	[119]0.0029	[119]0.0025	[116]0.0022	[114]0.0019	[119]1.028
158	PIXELALL-003	[216]2560	[178]719	[61]0.0021	[61]0.0016	[65]0.0015	[64]0.0014	[74]0.0014	[62]1.015
159	PIXELALL-004	[217]2560	[96]453	[59]0.0020	[55]0.0015	[58]0.0015	[62]0.0014	[62]0.0013	[54]1.014
160	PIXELALL-005	[218]2560	[217]845	[51]0.0019	[67]0.0017	[68]0.0016	[80]0.0016	[90]0.0016	[61]1.015
161	PTAKURATSATU-000	[57]538	[241]910	[90]0.0030	[92]0.0021	[93]0.0019	[88]0.0018	[92]0.0016	[91]1.020
162	QNAP-000	[130]2048	[97]457	[145]0.0078	[141]0.0044	[141]0.0037	[143]0.0033	[145]0.0028	[141]1.043
163	QUANTASOFT-001	[114]2048	[77]396	[239]0.2177	[241]0.1643	[241]0.1468	[241]0.1312	[241]0.1116	[241]2.539
164	RANKONE-002	[8]133	[12]113	[194]0.0194	[189]0.0112	[189]0.0093	[188]0.0077	[184]0.0060	[189]1.111
165	RANKONE-003	[9]133	[13]114	[193]0.0194	[190]0.0112	[188]0.0093	[189]0.0077	[183]0.0060	[190]1.111
166	RANKONE-004	[1]85	[4]36	[214]0.0415	[211]0.0226	[211]0.0177	[207]0.0141	[204]0.0102	[211]1.225
167	RANKONE-005	[10]133	[10]94	[159]0.0094	[154]0.0054	[154]0.0046	[157]0.0039	[154]0.0032	[154]1.054
168	RANKONE-006	[11]165	[43]261	[120]0.0050	[123]0.0030	[123]0.0027	[121]0.0024	[116]0.0021	[122]1.030
169	RANKONE-007	[12]165	[50]278	[96]0.0034	[100]0.0023	[101]0.0021	[98]0.0018	[94]0.0017	[92]1.022
170	RANKONE-009	[22]260	[26]191	[71]0.0024	[62]0.0016	[67]0.0015	[70]0.0015	[71]0.0014	[65]1.015
171	RANKONE-010	[23]261	[29]200	[65]0.0022	[69]0.0018	[71]0.0016	[76]0.0015	[78]0.0015	[68]1.016
172	RANKONE-011	[24]261	[125]567	[26]0.0015	[25]0.0012	[26]0.0012	[28]0.0012	[31]0.0012	[24]1.011
173	REALNETWORKS-000	[241]4100	[38]244	[212]0.0402	[209]0.0195	[206]0.0149	[202]0.0111	[197]0.0077	[209]1.201
174	REALNETWORKS-001	[244]4104	[37]243	[213]0.0402	[210]0.0195	[205]0.0149	[201]0.0111	[196]0.0077	[210]1.201
175	REALNETWORKS-002	[245]4104	[39]245	[209]0.0393	[208]0.0189	[204]0.0142	[200]0.0108	[195]0.0076	[208]1.195
176	REALNETWORKS-003	[107]1848	[20]178	[200]0.0242	[192]0.0117	[187]0.0090	[181]0.0070	[176]0.0054	[194]1.120
177	REALNETWORKS-004	[108]1848	[22]185	[198]0.0236	[191]0.0112	[185]0.0087	[179]0.0068	[173]0.0050	[191]1.116
178	REALNETWORKS-005	[199]2056	[62]337	[67]0.0023	[57]0.0016	[50]0.0014	[53]0.0013	[42]0.0012	[59]1.015
179	REMARKAI-000	[178]2048	[157]691	[98]0.0034	[91]0.0021	[86]0.0019	[83]0.0017	[87]0.0015	[92]1.020
180	REMARKAI-000	[163]2048	[129]615	[152]0.0086	[142]0.0044	[136]0.0036	[137]0.0031	[134]0.0025	[144]1.045
181	REMARKAI-002	[112]2048	[93]434	[150]0.0081	[135]0.0040	[128]0.0031	[125]0.0026	[117]0.0021	[138]1.041
182	RENDIP-000	[124]2048	[234]894	[30]0.0015	[33]0.0013	[29]0.0012	[33]0.0012	[37]0.0012	[31]1.012
183	S1-000	[232]4096	[224]865	[73]0.0024	[68]0.0018	[72]0.0017	[78]0.0016	[84]0.0015	[70]1.017
184	S1-001	[141]2048	[202]814	[91]0.0031	[107]0.0025	[117]0.0024	[120]0.0024	[130]0.0023	[103]1.023
185	SCANOVATE-000	[120]2048	[172]712	[119]0.0050	[112]0.0026	[107]0.0022	[96]0.0018	[89]0.0015	[114]1.026
186	SCANOVATE-001	[177]2048	[148]675	[123]0.0053	[114]0.0027	[110]0.0022	[97]0.0018	[86]0.0015	[117]1.028
187	SENSETIME-000	[243]4104	[174]715	[69]0.0023	[87]0.0020	[91]0.0019	[94]0.0018	[104]0.0017	[82]1.018
188	SENSETIME-001	[242]4104	[144]656	[70]0.0023	[84]0.0020	[89]0.0019	[87]0.0017	[93]0.0016	[79]1.018
189	SENSETIME-002	[201]2056	[137]650	[181]0.0137	[198]0.0136	[203]0.0136	[206]0.0136	[212]0.0136	[195]1.122
190	SENSETIME-003	[200]2056	[247]940	[4]0.0010	[10]0.0010	[13]0.0010	[14]0.0009	[15]0.0009	[6]1.009
191	SENSETIME-004	[75]1032	[170]710	[3]0.0010	[3]0.0009	[7]0.0009	[8]0.0009	[8]0.0009	[4]1.008
192	SENSETIME-005	[74]1032	[253]1007	[2]0.0009	[1]0.0008	[2]0.0008	[6]0.0008	[6]0.0008	[1]1.008
193	SENSETIME-006	[76]1032	[251]956	[1]0.0009	[2]0.0008	[3]0.0008	[7]0.0008	[7]0.0008	[2]1.008
194	SHAMAN-003	[168]2048	[164]704	[230]0.1243	[233]0.0823	[233]0.0708	[232]0.0616	[232]0.0518	[233]1.789
195	SHAMAN-004	[129]2048	[136]642	[241]0.2221	[240]0.1473	[238]0.1241	[238]0.1049	[237]0.0825	[240]2.411
196	SHAMAN-006	[115]2048	[167]706	[211]0.0398	[219]0.0344	[222]0.0332	[224]0.0323	[227]0.0315	[218]1.316
197	SHAMAN-007	[145]2048	[169]709	[210]0.0396	[217]0.0342	[221]0.0331	[223]0.0322	[226]0.0314	[216]1.315
198	SIAT-001	[185]2052	[215]842	[44]0.0018	[43]0.0014	[33]0.0013	[29]0.0012	[28]0.0011	[43]1.013
199	SIAT-002	[190]2052	[238]906	[46]0.0018	[42]0.0014	[42]0.0013	[42]0.0013	[40]0.0012	[46]1.013
200	SMILART-004	[41]512	[16]167	[253]0.9648	[253]0.9641	[253]0.9640	[253]0.9639	[254]0.9638	[253]9.678
201	SMILART-005	[173]2048	[99]464						[256]10.000
202	STAQU-000	[235]4096	[207]827	[141]0.0071	[159]0.0060	[161]0.0057	[169]0.0055	[174]0.0053	[156]1.056
203	SYNESIS-003	[135]2048	[35]215	[185]0.0162	[202]0.0160	[207]0.0160	[212]0.0160	[217]0.0160	[201]1.144
204	SYNESIS-003	[234]4096	[11]103	[236]0.1700	[236]0.1172	[236]0.1047	[237]0.0953	[238]0.0869	[236]2.120
205	SYNESIS-005	[246]4104	[191]772	[151]0.0085	[178]0.0085	[183]0.0085	[195]0.0085	[201]0.0085	[175]1.076
206	TECH5-001	[96]1536	[235]898	[106]0.0040	[103]0.0024	[103]0.0021	[99]0.0018	[99]0.0017	[106]1.024
207	TECH5-002	[46]513	[248]941	[81]0.0027	[46]0.0014	[30]0.0012	[24]0.0011	[19]0.0010	[53]1.014
208	TEVIAN-003	[166]2048	[56]300	[182]0.0147	[170]0.0074	[162]0.0059	[164]0.0047	[163]0.0037	[174]1.075
209	TEVIAN-004	[137]2048	[55]299	[169]0.0113	[155]0.0057	[155]0.0047	[152]0.0037	[148]0.0030	[157]1.058
210	TEVIAN-005	[113]2048	[86]416	[142]0.0073	[132]0.0038	[127]0.0031	[128]0.0027	[127]0.0023	[134]1.038
211	TEVIAN-006	[73]1032	[127]599	[74]0.0024	[72]0.0018	[79]0.0018	[85]0.0017	[95]0.0017	[72]1.017
212	TEVIAN-007	[78]1032	[195]779	[43]0.0018	[36]0.0014	[40]0.0013	[47]0.0013	[47]0.0013	[39]1.013
213	TIGER-000	[196]2052	[89]428	[221]0.0616	[216]0.0310	[215]0.0236	[215]0.0178	[209]0.0120	[217]1.315
214	TIGER-002	[183]2052	[100]464	[125]0.0056	[121]0.0029	[116]0.0024	[102]0.0019	[83]0.0015	[120]1.030
215	TIGER-003	[194]2052	[98]464	[126]0.0056	[122]0.0029	[115]0.0024	[100]0.0019	[82]0.0015	[121]1.030
216	TONGYITRANS-000	[205]2070	[24]190	[137]0.0069	[130]0.0038	[132]0.0032	[133]0.0029	[139]0.0026	[132]1.038

Table 23: **Rank-based accuracy for the FRVT 2018 mugshot sets**. *In columns 3 and 4 are template size and template generation duration. Thereafter values are rank-based FNIR with T = 0 and FPIR = 1. This is appropriate to investigational uses but not those with higher volumes where candidates from all searches would need review. The next column is a workload statistic, a small value shows an algorithm front-loads mates into the first 10 candidates. Throughout, blue superscripts indicate the rank of the algorithm for that column, and the best value is highlighted in yellow.*

This publication is available free of charge from: https://doi.org/10.6028/NIST.IR.8271

MISSES OUTSIDE RANK R		RESOURCE USAGE		ENROL MOST RECENT, N = 1.6M					
FNIR(N, T=0, R)		TEMPLATE		FRVT 2018 MUGSHOTS					
#	ALGORITHM	BYTES	MSEC	R=1	R=5	R=10	R=20	R=50	WORK-10
217	TONGYITRANS-001	[206]2070	[23]189	[138]0.0069	[131]0.0038	[131]0.0032	[132]0.0029	[137]0.0026	[133]1.038
218	TOSHIBA-000	[103]1548	[244]930	[112]0.0045	[111]0.0026	[109]0.0022	[110]0.0020	[107]0.0018	[112]1.026
219	TOSHIBA-001	[204]2060	[245]931	[117]0.0048	[115]0.0027	[112]0.0023	[112]0.0020	[106]0.0018	[116]1.027
220	TRUEFACE-000	[111]2000	[66]365	[93]0.0033	[117]0.0028	[125]0.0028	[127]0.0026	[136]0.0026	[113]1.026
221	VD-000	[72]1028	[61]337	[249]0.4737	[248]0.3204	[248]0.2695	[247]0.2215	[246]0.1678	[248]4.058
222	VD-001	[179]2052	[160]695	[204]0.0276	[207]0.0181	[205]0.0162	[208]0.0146	[211]0.0130	[207]1.174
223	VD-002	[192]2052	[154]689	[160]0.0095	[172]0.0077	[176]0.0073	[180]0.0070	[189]0.0068	[169]1.071
224	VD-003	[182]2052	[158]693	[143]0.0076	[165]0.0069	[172]0.0067	[178]0.0066	[187]0.0066	[163]1.063
225	VERIDAS-001	[162]2048	[230]885	[84]0.0028	[80]0.0019	[72]0.0017	[75]0.0015	[79]0.0015	[80]1.018
226	VERIDAS-002	[122]2048	[231]888	[83]0.0028	[79]0.0019	[73]0.0017	[74]0.0015	[77]0.0015	[78]1.018
227	VERIDAS-003	[122]2048	[229]877	[45]0.0018	[51]0.0015	[51]0.0014	[52]0.0013	[55]0.0013	[49]1.014
228	VIGILANTSOLUTIONS-003	[97]1544	[210]832	[224]0.0694	[221]0.0349	[216]0.0262	[216]0.0201	[213]0.0140	[221]1.355
229	VIGILANTSOLUTIONS-004	[98]1544	[208]830	[231]0.1249	[230]0.0706	[229]0.0557	[227]0.0434	[225]0.0305	[230]1.699
230	VIGILANTSOLUTIONS-005	[100]1544	[194]778	[156]0.0092	[144]0.0045	[132]0.0036	[130]0.0029	[122]0.0022	[145]1.046
231	VIGILANTSOLUTIONS-006	[99]1544	[211]834	[162]0.0099	[146]0.0048	[143]0.0038	[136]0.0030	[126]0.0022	[148]1.049
232	VIGILANTSOLUTIONS-007	[102]1544	[130]618	[97]0.0034	[82]0.0020	[76]0.0017	[72]0.0015	[57]0.0013	[88]1.019
233	VIGILANTSOLUTIONS-008	[101]1544	[81]405	[89]0.0029	[74]0.0018	[69]0.0016	[66]0.0015	[49]0.0013	[77]1.018
234	VISIONBOX-000	[203]2059	[104]482	[52]0.0019	[54]0.0015	[57]0.0014	[54]0.0013	[46]0.0013	[52]1.014
235	VISIONLABS-004	[17]256	[58]315	[82]0.0027	[70]0.0018	[70]0.0016	[71]0.0015	[68]0.0014	[74]1.017
236	VISIONLABS-005	[43]512	[57]300	[72]0.0024	[66]0.0017	[63]0.0015	[58]0.0014	[53]0.0013	[66]1.016
237	VISIONLABS-006	[39]512	[52]292	[49]0.0018	[49]0.0015	[46]0.0014	[46]0.0013	[48]0.0013	[48]1.014
238	VISIONLABS-007	[38]512	[53]293	[42]0.0018	[45]0.0014	[37]0.0013	[37]0.0013	[41]0.0012	[45]1.013
239	VISIONLABS-008	[44]512	[49]277	[58]0.0020	[73]0.0018	[81]0.0018	[89]0.0018	[101]0.0017	[69]1.017
240	VISIONLABS-009	[34]512	[107]494	[10]0.0011	[15]0.0011	[17]0.0010	[18]0.0010	[18]0.0010	[14]1.010
241	VISIONLABS-010	[31]512	[181]732	[18]0.0014	[32]0.0013	[36]0.0013	[39]0.0013	[45]0.0013	[29]1.012
242	VISIONLABS-011	[33]512	[183]736	[12]0.0012	[18]0.0011	[21]0.0011	[21]0.0011	[26]0.0011	[18]1.010
243	VOCORD-003	[63]896	[173]714	[131]0.0062	[126]0.0035	[126]0.0030	[126]0.0026	[129]0.0023	[126]1.035
244	VOCORD-004	[62]896	[117]538	[146]0.0079	[148]0.0049	[151]0.0043	[155]0.0038	[158]0.0034	[146]1.048
245	VOCORD-005	[60]768	[204]822	[140]0.0070	[145]0.0046	[148]0.0041	[154]0.0038	[161]0.0035	[142]1.044
246	VOCORD-006	[256]10240	[205]825	[255]1.0000	[256]1.0000	[255]1.0000	[255]1.0000	[255]1.0000	[255]10.000
247	VTS-000	[128]2048	[106]492	[251]0.5937	[252]0.5936	[252]0.5936	[252]0.5936	[252]0.5936	[252]6.343
248	VTS-001	[153]2048	[232]891	[28]0.0015	[21]0.0012	[20]0.0011	[20]0.0011	[21]0.0010	[20]1.011
249	XFORWARDAI-000	[172]2048	[188]768	[66]0.0023	[88]0.0020	[95]0.0020	[107]0.0019	[113]0.0019	[83]1.018
250	XFORWARDAI-001	[141]2048	[150]681	[60]0.0020	[81]0.0019	[92]0.0019	[104]0.0019	[112]0.0019	[75]1.018
251	XFORWARDAI-002	[230]4096	[246]935	[54]0.0020	[78]0.0019	[90]0.0019	[103]0.0019	[111]0.0019	[73]1.017
252	YISHENG-001	[226]3704	[75]387	[203]0.0265	[197]0.0130	[194]0.0102	[192]0.0080	[182]0.0059	[198]1.134
253	YITU-002	[247]4138	[226]870	[47]0.0018	[24]0.0012	[22]0.0011	[22]0.0011	[23]0.0010	[28]1.012
254	YITU-003	[248]4138	[227]871	[88]0.0029	[98]0.0023	[106]0.0022	[115]0.0021	[120]0.0021	[95]1.021
255	YITU-004	[208]2070	[240]910	[14]0.0013	[7]0.0009	[8]0.0009	[9]0.0009	[9]0.0009	[9]1.009
256	YITU-005	[207]2070	[223]861	[68]0.0023	[90]0.0021	[98]0.0020	[109]0.0020	[115]0.0020	[85]1.019

Table 24: **Rank-based accuracy for the FRVT 2018 mugshot sets**. *In columns 3 and 4 are template size and template generation duration. Thereafter values are rank-based FNIR with T = 0 and FPIR = 1. This is appropriate to investigational uses but not those with higher volumes where candidates from all searches would need review. The next column is a workload statistic, a small value shows an algorithm front-loads mates into the first 10 candidates. Throughout, blue superscripts indicate the rank of the algorithm for that column, and the best value is highlighted in yellow.*

This publication is available free of charge from: https://doi.org/10.6028/NIST.IR.8271

MISSES BELOW THRESHOLD, T		ENROL RECENT MUGSHOT, N = 1.6M									ENROL APPLICATION PORTRAIT, N = 1.6M					
		ENROL: MUGSHOT			ENROL: MUGSHOT			ENROL: MUGSHOT			ENROL: VISA		ENROL: BORDER		ENROL: VISA	
		PROBE: MUGSHOT			PROBE: WEBCAM			PROBE: PROFILE			PROBE: BORDER		PROBE: BORDER 10+YR		PROBE: KIOSK	
#	ALGORITHM	FPIR=0.0003	FPIR=0.001	FPIR=0.01	FPIR=0.0003	FPIR=0.001	FPIR=0.01	FPIR=0.0003	FPIR=0.001	FPIR=0.01	FPIR=0.001	FPIR=0.01	FPIR=0.001	FPIR=0.01	FPIR=0.001	FPIR=0.01
1	20FACE-000	[208] 0.462	[215] 0.348	[222] 0.230	[217] 0.763	[211] 0.450	[211] 0.301	[185] 1.000	[177] 1.000	[191] 1.000	[147] 0.424	[146] 0.255	[68] 0.772	[69] 0.599	[142] 0.938	[154] 0.836
2	3DIVI-003	[210] 0.482	[224] 0.400	[228] 0.282	[212] 0.685	[224] 0.626	[226] 0.497				[158] 0.605	[158] 0.445			[129] 0.821	[144] 0.717
3	3DIVI-004	[183] 0.256	[196] 0.169	[200] 0.093	[184] 0.400	[202] 0.343	[206] 0.237				[138] 0.277	[141] 0.172			[109] 0.607	[126] 0.485
4	3DIVI-005	[181] 0.255	[193] 0.166	[199] 0.093	[183] 0.395	[200] 0.339	[205] 0.234	[117] 0.998	[119] 0.996	[128] 0.990	[163] 0.864	[165] 0.846			[108] 0.597	[125] 0.484
5	3DIVI-006	[180] 0.253	[195] 0.168	[202] 0.096	[187] 0.403	[201] 0.342	[207] 0.238				[139] 0.283	[142] 0.174			[112] 0.615	[127] 0.490
6	ACER-000	[168] 0.208	[186] 0.146	[189] 0.074	[169] 0.300	[180] 0.246	[181] 0.157	[69] 0.987	[25] 0.981	[93] 0.955	[133] 0.201	[137] 0.114			[96] 0.490	[111] 0.363
7	ACER-001	[115] 0.109	[129] 0.056	[133] 0.026	[108] 0.136	[113] 0.109	[116] 0.069	[145] 1.000	[151] 0.999	[172] 0.998	[97] 0.068	[97] 0.036	[63] 0.406	[64] 0.250	[95] 0.479	[70] 0.206
8	AIZE-001	[126] 0.127	[149] 0.077	[147] 0.034	[135] 0.187	[139] 0.143	[138] 0.087	[91] 0.995	[99] 0.994	[118] 0.983	[109] 0.101	[111] 0.052	[58] 0.364	[61] 0.216	[80] 0.387	[95] 0.289
9	ALCHERA-000	[173] 0.231	[183] 0.138	[184] 0.070	[158] 0.259	[166] 0.216	[175] 0.146	[128] 0.999	[135] 0.999	[156] 0.996	[128] 0.176	[135] 0.111			[125] 0.803	[121] 0.456
10	ALCHERA-001	[251] 1.000	[251] 0.999	[253] 0.999	[252] 1.000	[252] 1.000	[252] 1.000				[190] 1.000	[243] 1.000			[202] 1.000	[256] 1.000
11	ALCHERA-002	[230] 0.807	[231] 0.486	[231] 0.302	[211] 0.685	[221] 0.591	[221] 0.442	[159] 1.000	[157] 1.000	[176] 0.999	[162] 0.827	[162] 0.770			[126] 0.811	[141] 0.705
12	ALCHERA-003	[204] 0.450	[187] 0.155	[185] 0.070	[170] 0.304	[177] 0.239	[180] 0.152	[152] 1.000	[145] 0.999	[161] 0.997	[127] 0.172	[128] 0.097			[92] 0.464	[110] 0.362
13	ALCHERA-004	[214] 0.520	[223] 0.394	[221] 0.211	[208] 0.642	[217] 0.529	[215] 0.327	[92] 0.995	[95] 0.991	[64] 0.813	[148] 0.424	[144] 0.232	[66] 0.708	[68] 0.515	[105] 0.546	[119] 0.398
14	ALLGOVISION-000	[134] 0.138	[161] 0.088	[166] 0.045	[146] 0.202	[155] 0.166	[162] 0.106	[78] 0.993	[92] 0.990	[117] 0.982	[112] 0.117	[117] 0.066			[102] 0.526	[118] 0.396
15	ALLGOVISION-001	[143] 0.155	[166] 0.102	[172] 0.053	[163] 0.275	[170] 0.221	[174] 0.141	[82] 0.993	[82] 0.986	[80] 0.933	[122] 0.150	[124] 0.081			[97] 0.491	[117] 0.389
16	ANKE-000	[154] 0.184	[171] 0.117	[181] 0.063	[156] 0.256	[169] 0.220	[178] 0.151	[88] 0.995	[100] 0.994	[126] 0.990	[214] 1.000	[207] 1.000			[240] 1.000	[197] 1.000
17	ANKE-001	[152] 0.183	[175] 0.119	[182] 0.063	[157] 0.256	[168] 0.220	[179] 0.151	[93] 0.995	[105] 0.994	[137] 0.992	[228] 1.000	[201] 1.000			[248] 1.000	[210] 1.000
18	ANKE-002	[81] 0.062	[91] 0.032	[90] 0.014	[75] 0.103	[79] 0.079	[81] 0.050	[49] 0.975	[51] 0.948	[60] 0.795	[64] 0.034	[66] 0.018			[52] 0.245	[64] 0.190
19	AWARE-003	[151] 0.174	[179] 0.128	[192] 0.082	[179] 0.351	[194] 0.298	[199] 0.204	[66] 0.987	[29] 0.984	[112] 0.977	[149] 0.428	[152] 0.378			[103] 0.530	[120] 0.443
20	AWARE-004	[196] 0.355	[209] 0.269	[217] 0.175	[204] 0.619	[216] 0.509	[219] 0.375	[156] 1.000	[162] 1.000	[180] 0.999	[144] 0.397	[148] 0.279			[127] 0.816	[136] 0.631
21	AWARE-005	[220] 0.608	[218] 0.364	[194] 0.085	[174] 0.342	[181] 0.253	[183] 0.163	[154] 1.000	[163] 1.000	[179] 0.999	[137] 0.255	[139] 0.122			[138] 0.916	[143] 0.714
22	AWARE-006	[209] 0.475	[210] 0.276	[218] 0.175	[195] 0.466	[205] 0.398	[210] 0.283	[141] 1.000	[155] 0.999	[173] 0.999	[142] 0.368	[145] 0.254			[119] 0.749	[133] 0.623
23	AYONIX-000	[233] 0.846	[240] 0.811	[245] 0.724	[230] 0.956	[239] 0.939	[241] 0.892	[118] 0.998	[126] 0.998	[154] 0.995	[167] 0.954	[167] 0.891			[150] 0.982	[159] 0.959
24	AYONIX-001	[234] 0.875	[242] 0.824	[243] 0.701	[225] 0.946	[234] 0.920	[237] 0.845	[151] 1.000	[152] 0.999	[157] 0.996	[171] 0.999	[171] 0.998			[146] 0.969	[156] 0.926
25	AYONIX-002	[235] 0.876	[241] 0.824	[244] 0.702	[226] 0.946	[235] 0.920	[236] 0.845	[150] 1.000	[153] 0.999	[158] 0.996	[164] 0.915	[163] 0.821			[147] 0.969	[155] 0.926
26	CAMVI-003	[104] 0.094	[144] 0.071	[177] 0.058	[117] 0.152	[132] 0.132	[163] 0.108	[55] 0.979	[59] 0.970	[86] 0.940	[111] 0.114	[129] 0.100			[83] 0.402	[114] 0.377
27	CAMVI-004	[113] 0.107	[145] 0.072	[175] 0.054	[153] 0.240	[134] 0.136	[152] 0.100	[143] 1.000	[149] 0.999	[164] 0.998	[108] 0.100	[123] 0.081			[123] 0.787	[128] 0.507
28	CAMVI-005	[135] 0.139	[165] 0.099	[191] 0.076	[193] 0.451	[162] 0.179	[169] 0.132	[147] 1.000	[159] 1.000	[170] 0.998	[123] 0.156	[136] 0.112			[158] 0.999	[165] 0.983
29	CANON-001	[18] 0.012	[23] 0.005	[21] 0.002	[17] 0.031	[17] 0.023	[17] 0.015	[18] 0.633	[9] 0.365	[16] 0.217	[13] 0.008	[14] 0.004	[16] 0.068	[17] 0.034	[19] 0.139	[12] 0.092
30	CIB-000	[56] 0.044	[39] 0.012	[35] 0.005	[53] 0.077	[38] 0.045	[37] 0.025	[163] 1.000	[170] 1.000	[187] 1.000	[34] 0.017	[27] 0.008	[28] 0.141	[26] 0.068	[135] 0.894	[129] 0.521
31	CLEARVIEWAI-000	[20] 0.013	[24] 0.006	[20] 0.002	[23] 0.036	[20] 0.025	[19] 0.016	[130] 0.999	[64] 0.974	[8] 0.149	[14] 0.008	[9] 0.004	[12] 0.057	[12] 0.027	[61] 0.268	[6] 0.080
32	CLOUDWALK-HR-000	[5] 0.004	[6] 0.002	[9] 0.002	[4] 0.015	[6] 0.013	[9] 0.012	[1] 0.188	[1] 0.133	[2] 0.095	[6] 0.005	[5] 0.003	[3] 0.033	[5] 0.018	[6] 0.099	[2] 0.075
33	COGENT-000	[130] 0.143	[121] 0.053	[139] 0.029	[127] 0.175	[135] 0.140	[154] 0.100	[97] 0.996	[112] 0.995	[134] 0.991						
34	COGENT-001	[138] 0.143	[120] 0.053	[138] 0.029	[128] 0.175	[136] 0.140	[156] 0.100	[98] 0.996	[111] 0.995	[133] 0.991						
35	COGENT-002	[149] 0.159	[107] 0.044	[101] 0.017	[94] 0.124	[104] 0.098	[108] 0.063	[122] 0.998	[124] 0.998	[143] 0.994						
36	COGENT-003	[166] 0.203	[112] 0.046	[95] 0.016	[92] 0.121	[98] 0.095	[105] 0.061	[123] 0.999	[127] 0.998	[152] 0.995						
37	COGENT-004	[169] 0.209	[92] 0.033	[43] 0.006	[43] 0.067	[44] 0.051	[45] 0.031	[116] 0.998	[122] 0.997	[153] 0.995	[43] 0.022	[42] 0.012	[25] 0.126	[28] 0.072	[90] 0.456	[58] 0.178
38	COGENT-005	[69] 0.050	[28] 0.009	[29] 0.004	[30] 0.050	[32] 0.037	[33] 0.023	[96] 0.996	[88] 0.989	[23] 0.323	[24] 0.011	[22] 0.006	[18] 0.082	[19] 0.043	[136] 0.905	[66] 0.202
39	COGNITEC-000	[172] 0.226	[191] 0.161	[201] 0.095	[191] 0.439	[195] 0.303	[197] 0.200	[95] 0.996	[96] 0.992	[101] 0.971						
40	COGNITEC-001	[164] 0.192	[167] 0.102	[173] 0.053	[240] 0.997	[174] 0.230	[171] 0.135	[209] 1.000	[229] 1.000	[97] 0.965						
41	COGNITEC-002	[122] 0.122	[123] 0.053	[128] 0.025	[237] 0.990	[161] 0.178	[159] 0.101	[251] 1.000	[169] 1.000	[94] 0.956						
42	COGNITEC-003	[108] 0.099	[119] 0.053	[130] 0.025	[150] 0.222	[153] 0.162	[153] 0.100	[191] 1.000	[174] 1.000	[87] 0.946						
43	COGNITEC-004	[75] 0.055	[90] 0.031	[91] 0.014	[97] 0.127	[102] 0.097	[97] 0.058	[90] 0.995	[89] 0.990	[75] 0.919	[96] 0.068	[98] 0.038	[57] 0.316	[60] 0.196	[62] 0.288	[75] 0.218
44	COGNITEC-005	[76] 0.055	[30] 0.010	[27] 0.004	[34] 0.058	[36] 0.041	[30] 0.022	[200] 1.000	[251] 1.000	[70] 0.878	[71] 0.041	[84] 0.028	[35] 0.157	[39] 0.092	[35] 0.179	[41] 0.145
45	CUBOX-000	[8] 0.005	[11] 0.003	[13] 0.002	[12] 0.022	[12] 0.019	[14] 0.014	[4] 0.276	[2] 0.168	[4] 0.104	[2] 0.004	[3] 0.003	[2] 0.028	[2] 0.014	[1] 0.073	[1] 0.062
46	CYBERLINK-000	[133] 0.137	[130] 0.056	[121] 0.023	[122] 0.162	[117] 0.116	[119] 0.070	[109] 0.997	[114] 0.995	[116] 0.981	[94] 0.063	[92] 0.032			[75] 0.339	[82] 0.232

Table 25: **Threshold-based accuracy**. *Values are FNIR(N, T, L) with N = 1.6 million with thresholds set to produce FPIR = 0.0003, 0.001, and 0.01 in non-mate searches. Throughout blue superscripts indicate the rank of the algorithm for that column. Caution: The Power-low models are mostly intended to draw attention to the kind of behavior, not as a model to be used for prediction.*

2021/11/22 08:35:53

FNIR(N, R, T) = FPIR(N, T) = False neg. identification rate / False pos. identification rate

N = Num. enrolled subjects
R = Num. candidates examined

T = Threshold

T = 0 → Investigation
T > 0 → Identification

This publication is available free of charge from: https://doi.org/10.6028/NIST.IR.8271

MISSES BELOW THRESHOLD, T		ENROL RECENT MUGSHOT, N = 1.6M									ENROL APPLICATION PORTRAIT, N = 1.6M					
		ENROL: MUGSHOT			ENROL: MUGSHOT			ENROL: MUGSHOT			ENROL: VISA		ENROL: BORDER		ENROL: VISA	
		PROBE: MUGSHOT			PROBE: WEBCAM			PROBE: PROFILE			PROBE: BORDER		PROBE: BORDER 10+YR		PROBE: KIOSK	
#	ALGORITHM	FPIR=0.0003	FPIR=0.001	FPIR=0.01	FPIR=0.0003	FPIR=0.001	FPIR=0.01	FPIR=0.0003	FPIR=0.001	FPIR=0.01	FPIR=0.001	FPIR=0.01	FPIR=0.001	FPIR=0.01	FPIR=0.001	FPIR=0.01
47	CYBERLINK-001	[105]0.096	[124]0.054	[119]0.022	[110]0.138	[114]0.109	[113]0.067	[108]0.997	[109]0.995	[119]0.984	[91]0.062	[88]0.031			[113]0.652	[84]0.239
48	CYBERLINK-002	[50]0.038	[47]0.015	[48]0.006	[46]0.068	[51]0.053	[50]0.032	[84]0.994	[87]0.988	[95]0.957	[46]0.024	[45]0.013			[63]0.288	[48]0.157
49	CYBERLINK-003	[59]0.045	[26]0.008	[26]0.004	[27]0.045	[29]0.035	[26]0.021	[85]0.995	[62]0.972	[66]0.845	[25]0.012	[26]0.007	[21]0.100	[22]0.051	[77]0.368	[27]0.120
50	CYBERLINK-004	[162]0.188	[25]0.007	[25]0.003	[38]0.063	[30]0.036	[29]0.022	[186]1.000	[181]1.000	[181]0.999	[27]0.013	[25]0.007	[22]0.109	[20]0.050	[145]0.954	[98]0.291
51	DAHUA-000	[128]0.128	[157]0.086	[163]0.045	[130]0.179	[133]0.135	[137]0.083									
52	DAHUA-001	[112]0.106	[147]0.073	[151]0.037	[116]0.151	[125]0.122	[128]0.075	[68]0.987	[73]0.980	[81]0.933						
53	DAHUA-002	[35]0.026	[48]0.015	[46]0.006	[35]0.060	[40]0.046	[41]0.029	[22]0.681	[26]0.638	[36]0.522	[31]0.017	[31]0.008			[27]0.159	[30]0.125
54	DAHUA-003	[34]0.025	[44]0.014	[39]0.005	[31]0.054	[35]0.041	[35]0.024	[19]0.647	[22]0.579	[30]0.447	[26]0.013	[24]0.006	[17]0.081	[18]0.043	[18]0.134	[19]0.109
55	DEEPGLINT-001	[13]0.010	[14]0.003	[14]0.002	[7]0.018	[7]0.014	[5]0.010	[183]1.000	[156]1.000	[32]0.503	[9]0.006	[15]0.004			[26]0.159	[15]0.097
56	DEEPSEA-001	[93]0.073	[111]0.046	[117]0.022	[100]0.129	[106]0.101	[100]0.059	[72]0.988	[80]0.985	[106]0.973	[101]0.077	[103]0.041			[73]0.326	[85]0.251
57	DERMALOG-003	[216]0.550	[230]0.482	[234]0.360	[215]0.715	[226]0.655	[230]0.526				[161]0.677	[160]0.554			[133]0.870	[151]0.791
58	DERMALOG-004	[218]0.554	[229]0.480	[233]0.358	[214]0.711	[227]0.657	[228]0.526	[102]0.997	[115]0.995	[136]0.991	[157]0.603	[159]0.458			[132]0.856	[147]0.751
59	DERMALOG-005	[163]0.189	[160]0.088	[159]0.043	[142]0.201	[146]0.154	[149]0.096	[100]0.996	[90]0.990	[90]0.950	[140]0.300	[147]0.267			[111]0.614	[122]0.459
60	DERMALOG-006	[107]0.098	[118]0.052	[132]0.026	[109]0.137	[109]0.105	[112]0.067	[23]0.989	[74]0.981	[82]0.933	[89]0.059	[90]0.031			[72]0.318	[80]0.230
61	DERMALOG-007	[160]0.188	[158]0.086	[157]0.040	[141]0.200	[144]0.152	[146]0.093	[99]0.996	[91]0.990	[89]0.950	[107]0.099	[110]0.052			[107]0.557	[102]0.299
62	DERMALOG-008	[185]0.268	[109]0.045	[100]0.017	[151]0.231	[95]0.094	[92]0.054	[164]1.000	[186]1.000	[188]1.000	[86]0.057	[81]0.025	[61]0.382	[58]0.158	[143]0.940	[139]0.678
63	DERMALOG-009	[54]0.041	[66]0.021	[68]0.009	[61]0.086	[66]0.066	[66]0.040	[160]1.000	[171]1.000	[185]1.000	[55]0.031	[57]0.016	[70]0.999	[71]0.999	[131]0.840	[76]0.222
64	EYEDEA-003	[213]0.509	[220]0.388	[226]0.265	[206]0.625	[219]0.543	[220]0.404	[103]0.997	[106]0.994	[125]0.990	[155]0.570	[154]0.392			[124]0.792	[138]0.658
65	F8-001	[206]0.458	[192]0.166	[148]0.036				[129]0.999	[134]0.998	[155]0.995						
66	FINCORE-000	[159]0.187	[182]0.134	[188]0.071	[162]0.267	[167]0.217	[172]0.140	[153]1.000	[166]1.000	[148]0.995	[129]0.187	[134]0.108	[65]0.598	[67]0.418	[91]0.458	[107]0.349
67	FUJITSULAB-000	[177]0.246	[67]0.021	[65]0.008	[48]0.070	[56]0.056	[58]0.035				[45]0.024	[49]0.013	[40]0.177	[43]0.093	[51]0.240	[47]0.156
68	GLORY-000	[203]0.441	[219]0.367	[230]0.295	[202]0.586	[220]0.547	[224]0.470	[87]0.995	[108]0.995	[140]0.993	[151]0.453	[153]0.381			[130]0.839	[152]0.795
69	GLORY-001	[195]0.355	[211]0.305	[223]0.236	[201]0.582	[218]0.537	[222]0.448	[83]0.994	[97]0.993	[130]0.991	[146]0.408	[150]0.336			[128]0.819	[148]0.753
70	GORILLA-001	[228]0.747	[225]0.406	[224]0.246	[203]0.590	[212]0.453	[213]0.314	[171]1.000	[192]1.000	[203]1.000	[152]0.468	[149]0.299			[245]1.000	[142]0.710
71	GORILLA-002	[184]0.266	[199]0.188	[206]0.106	[176]0.342	[188]0.268	[189]0.170	[176]1.000	[185]1.000	[141]0.993	[136]0.250	[140]0.137			[162]1.000	[124]0.466
72	GORILLA-003	[226]0.694	[213]0.318	[216]0.157	[210]0.684	[209]0.434	[208]0.247	[204]1.000	[254]1.000	[194]1.000	[145]0.407	[143]0.213			[243]1.000	[131]0.562
73	GORILLA-004	[131]0.135	[163]0.089	[160]0.043	[143]0.202	[152]0.160	[157]0.101	[47]0.972	[53]0.959	[72]0.903	[117]0.135	[120]0.072			[87]0.438	[104]0.309
74	GORILLA-005	[102]0.086	[134]0.058	[134]0.026	[129]0.179	[138]0.142	[140]0.088	[26]0.770	[29]0.700	[37]0.553	[105]0.088	[102]0.040			[70]0.315	[77]0.223
75	GORILLA-006	[62]0.046	[82]0.027	[78]0.011	[87]0.118	[90]0.089	[88]0.053	[15]0.602	[21]0.531	[26]0.369	[49]0.028	[47]0.013	[39]0.166	[42]0.093	[45]0.218	[46]0.154
76	GRIAULE-000	[55]0.044	[64]0.020	[67]0.009	[59]0.082	[63]0.063	[62]0.038	[112]0.997	[110]0.995	[91]0.952	[61]0.033	[73]0.020	[44]0.185	[45]0.107	[41]0.198	[52]0.166
77	HIK-003	[148]0.159	[168]0.103	[176]0.057	[138]0.190	[148]0.158	[161]0.105	[57]0.980	[57]0.969	[77]0.925	[120]0.142	[122]0.080			[89]0.445	[109]0.359
78	HIK-004	[143]0.156	[164]0.099	[174]0.054	[133]0.182	[145]0.153	[158]0.101	[62]0.983	[65]0.976	[88]0.947	[118]0.137	[121]0.077			[86]0.434	[108]0.353
79	HIK-005	[110]0.102	[104]0.044	[105]0.019	[71]0.098	[78]0.077	[80]0.048	[148]1.000	[154]0.999	[166]0.998	[95]0.068	[95]0.036			[104]0.541	[87]0.258
80	HIK-006	[137]0.142	[113]0.047	[108]0.020	[80]0.111	[86]0.086	[86]0.052	[178]1.000	[178]1.000	[182]0.999						
81	HYPERVERGE-001	[11]0.009	[17]0.004	[18]0.002	[24]0.039	[26]0.031	[25]0.020	[3]0.275	[5]0.220	[7]0.146	[12]0.007	[13]0.004	[10]0.053	[13]0.027	[8]0.101	[7]0.083
82	IDEMIA-003	[217]0.552	[114]0.047	[112]0.021	[244]1.000	[154]0.165	[132]0.079			[256]1.000	[114]0.123	[113]0.061			[122]0.766	[134]0.630
83	IDEMIA-004	[74]0.055	[100]0.037	[111]0.021	[112]0.144	[121]0.118	[131]0.079	[52]0.976	[63]0.973	[98]0.968	[113]0.123	[114]0.061			[121]0.766	[135]0.630
84	IDEMIA-005	[88]0.066	[106]0.044	[131]0.026	[132]0.181	[143]0.150	[160]0.102	[56]0.979	[68]0.978	[104]0.973	[115]0.130	[119]0.070			[134]0.879	[145]0.743
85	IDEMIA-006	[86]0.065	[103]0.043	[129]0.025	[161]0.266	[172]0.226	[182]0.161	[65]0.984	[76]0.982	[115]0.980	[121]0.144	[126]0.090			[117]0.733	[130]0.531
86	IDEMIA-007	[46]0.035	[58]0.018	[60]0.008	[52]0.073	[53]0.055	[51]0.033	[211]1.000	[230]1.000	[233]1.000	[82]0.052	[78]0.022	[42]0.182	[46]0.109	[227]1.000	[163]0.982
87	IDEMIA-008	[5]0.004	[5]0.002	[5]0.001	[6]0.016	[5]0.013	[3]0.009	[5]0.276	[4]0.204	[5]0.136	[5]0.005	[4]0.003	[6]0.036	[7]0.019	[10]0.106	[11]0.092
88	IMAGUS-002	[238]0.908	[238]0.749	[240]0.564	[224]0.944	[231]0.816	[233]0.645	[167]1.000	[187]1.000	[193]1.000						
89	IMAGUS-003	[237]0.898	[239]0.807	[242]0.669	[229]0.954	[233]0.909	[235]0.809	[173]1.000	[172]1.000	[189]1.000						
90	IMAGUS-005	[44]0.034	[61]0.018	[61]0.008	[62]0.088	[65]0.066	[64]0.040	[38]0.926	[40]0.838	[46]0.647	[51]0.029	[58]0.016	[38]0.161	[44]0.094	[48]0.231	[63]0.189
91	IMAGUS-006	[51]0.039	[63]0.019	[62]0.008	[66]0.093	[69]0.069	[72]0.042	[59]0.980	[47]0.897	[41]0.621	[50]0.028	[53]0.015	[37]0.161	[40]0.092	[56]0.260	[60]0.181
92	IMPERIAL-000	[142]0.154	[77]0.026	[71]0.009	[64]0.089	[68]0.068	[69]0.041	[182]1.000	[138]0.999	[147]0.995	[72]0.042	[74]0.020			[53]0.245	[53]0.168

Table 26: **Threshold-based accuracy**. *Values are FNIR(N, T, L) with N = 1.6 million with thresholds set to produce FPIR = 0.0003, 0.001, and 0.01 in non-mate searches. Throughout blue superscripts indicate the rank of the algorithm for that column. Caution: The Power-low models are mostly intended to draw attention to the kind of behavior, not as a model to be used for prediction.*

2021/11/22 08:35:53

FNIR(N, R, T) = False neg. identification rate
FPIR(N, T) = False pos. identification rate
N = Num. enrolled subjects
R = Num. candidates examined
T = Threshold
T = 0 → Investigation
T > 0 → Identification

This publication is available free of charge from: https://doi.org/10.6028/NIST.IR.8271

MISSES BELOW THRESHOLD, T		ENROL RECENT MUGSHOT, N = 1.6M									ENROL APPLICATION PORTRAIT, N = 1.6M					
		ENROL: MUGSHOT			ENROL: MUGSHOT			ENROL: MUGSHOT			ENROL: VISA		ENROL: BORDER		ENROL: VISA	
		PROBE: MUGSHOT			PROBE: WEBCAM			PROBE: PROFILE			PROBE: BORDER		PROBE: BORDER 10+YR		PROBE: KIOSK	
#	ALGORITHM	FPIR=0.0003	FPIR=0.001	FPIR=0.01	FPIR=0.0003	FPIR=0.001	FPIR=0.01	FPIR=0.0003	FPIR=0.001	FPIR=0.01	FPIR=0.001	FPIR=0.01	FPIR=0.001	FPIR=0.01	FPIR=0.001	FPIR=0.01
93	INCODE-000	202 0.423	212 0.310	219 0.199	197 0.486	207 0.420	212 0.304	149 1.000	130 0.998	144 0.994						
94	INCODE-001	192 0.319	202 0.212	207 0.112	178 0.348	191 0.296	195 0.198	179 1.000	179 1.000	186 1.000						
95	INCODE-002	189 0.285	198 0.184	205 0.100	173 0.333	189 0.269	191 0.176	113 0.998	98 0.993	111 0.976						
96	INCODE-003	190 0.286	194 0.167	193 0.084	182 0.372	185 0.264	185 0.164	157 1.000	150 0.999	159 0.996						
97	INCODE-004	109 0.099	126 0.054	123 0.023	124 0.167	124 0.120	120 0.070	110 0.997	107 0.995	79 0.929	93 0.063	89 0.031			68 0.313	78 0.226
98	INCODE-005	25 0.021	35 0.011	33 0.005	32 0.055	37 0.043	38 0.026	17 0.614	19 0.528	27 0.372	33 0.017	33 0.009	30 0.145	29 0.073	24 0.155	22 0.116
99	INNOVATRICS-002	200 0.379	207 0.234	215 0.139	186 0.403	196 0.310	201 0.209	178 1.000	184 1.000	184 0.999						
100	INNOVATRICS-003	191 0.297	203 0.221	211 0.132	180 0.351	192 0.297	198 0.203	158 1.000	161 1.000	169 0.998						
101	INNOVATRICS-004	157 0.184	181 0.132	190 0.074	159 0.262	171 0.222	176 0.149	64 0.984	72 0.980	103 0.973						
102	INNOVATRICS-005	78 0.057	93 0.034	92 0.014	83 0.114	89 0.089	87 0.052	35 0.890	41 0.846	51 0.723	78 0.047	77 0.022			54 0.251	61 0.182
103	INNOVATRICS-007	29 0.024	40 0.013	40 0.005	39 0.065	45 0.051	46 0.032	29 0.806	30 0.743	38 0.567	32 0.017	34 0.009	20 0.093	23 0.053	23 0.154	29 0.120
104	INTSYSMSU-000	247 0.999	249 0.998	251 0.990	242 1.000	244 1.000	245 0.998	155 1.000	160 1.000	165 0.998	170 0.999	170 0.989			159 0.999	167 0.988
105	IREX-000	90 0.068	86 0.028	59 0.008	72 0.099	60 0.060	48 0.032	71 0.988	52 0.957	50 0.680	75 0.044	41 0.011	56 0.302	25 0.062	32 0.170	37 0.135
106	ISYSTEMS-002	144 0.155	151 0.078	144 0.032	120 0.161	128 0.126	134 0.080	120 0.998	123 0.998	139 0.993						
107	ISYSTEMS-003	167 0.204	135 0.059	126 0.024	107 0.135	112 0.107	115 0.068	161 1.000	164 1.000	163 0.997						
108	KAKAO-000	38 0.028	50 0.015	49 0.006	51 0.071	55 0.056	56 0.034	11 0.539	15 0.468	24 0.327	37 0.019	35 0.010	27 0.141	30 0.075	25 0.158	28 0.120
109	KEDACOM-001	53 0.041	73 0.023	89 0.013	69 0.096	73 0.072	91 0.054	74 0.989	84 0.986	107 0.973	85 0.055	104 0.043			66 0.305	89 0.264
110	KNERON-000			146 0.033			151 0.099									
111	KNERON-001			170 0.052												
112	LINE-000	82 0.062	89 0.031	88 0.012	104 0.132	99 0.095	93 0.054			199 1.000	76 0.046	75 0.021	54 0.278	57 0.151	217 1.000	90 0.268
113	LOOKMAN-003	87 0.066	105 0.044	127 0.025	103 0.131	116 0.112	135 0.082				104 0.084	115 0.061			76 0.355	103 0.304
114	LOOKMAN-004	94 0.074	108 0.045	124 0.024	93 0.123	111 0.105	126 0.075	54 0.979	66 0.977	109 0.974						
115	LOOKMAN-005	68 0.050	88 0.030	98 0.017	73 0.102	85 0.086	109 0.063	58 0.980	69 0.978	105 0.973	92 0.062	106 0.047			62 0.308	92 0.273
116	MANTRA-000	89 0.066	32 0.010	28 0.004	36 0.063	34 0.041	28 0.022	226 1.000	212 1.000	178 0.999	52 0.029	50 0.014	33 0.152	35 0.081	161 1.000	44 0.151
117	MEGVII-001	170 0.210	146 0.072	150 0.037	89 0.119	103 0.097	102 0.061									
118	MEGVII-002	183 0.258	150 0.077	152 0.037	90 0.120	101 0.096	99 0.059	127 0.999	133 0.998	69 0.872						
119	MICROFOCUS-003	241 0.958	245 0.931	248 0.866	236 0.988	243 0.979	243 0.948				169 0.982	169 0.945			154 0.991	162 0.977
120	MICROFOCUS-004	249 0.999	250 0.999	254 0.999	235 0.984	241 0.975	242 0.940				168 0.974	168 0.935			152 0.989	161 0.976
121	MICROFOCUS-005	236 0.883	243 0.835	246 0.736	228 0.951	237 0.928	239 0.865				166 0.935	166 0.848			151 0.985	160 0.965
122	MICROFOCUS-006	245 0.983	247 0.978	249 0.963	227 0.950	236 0.923	238 0.858				165 0.923	164 0.843			148 0.971	157 0.939
123	MICROSOFT-003	66 0.049	84 0.028	83 0.012	84 0.117	93 0.091	96 0.056				66 0.036	71 0.019			50 0.233	57 0.176
124	MICROSOFT-004	61 0.046	78 0.026	77 0.011	81 0.111	87 0.087	90 0.053				62 0.033	67 0.018			46 0.222	55 0.170
125	MICROSOFT-005	63 0.047	76 0.026	76 0.010	65 0.090	71 0.070	70 0.041	136 0.999	23 0.587	25 0.354	47 0.027	48 0.013			36 0.180	36 0.134
126	MICROSOFT-006	33 0.025	36 0.012	45 0.006	28 0.048	31 0.037	36 0.024	8 0.452	10 0.386	18 0.281	58 0.032	54 0.015			33 0.178	38 0.138
127	NEC-000	118 0.113	153 0.079	167 0.047	125 0.171	137 0.140	144 0.093	61 0.983	70 0.979	100 0.969					94 0.474	115 0.377
128	NEC-001	141 0.148	170 0.106	180 0.060	152 0.238	164 0.197	170 0.133	75 0.991	83 0.986	102 0.972	116 0.133	125 0.082			93 0.468	116 0.378
129	NEC-002	23 0.018	10 0.003	8 0.002	16 0.029	14 0.020	11 0.013	144 1.000	148 0.999	149 0.995	16 0.008	20 0.005			115 0.676	99 0.292
130	NEC-003	7 0.005	8 0.002	11 0.002	11 0.021	11 0.017	10 0.013	36 0.902	37 0.824	43 0.628	19 0.008	21 0.006	7 0.036	8 0.023	114 0.668	88 0.261
131	NEC-004	1 0.003	3 0.002	7 0.002	3 0.015	4 0.013	7 0.010	20 0.654	25 0.622	39 0.575	3 0.004	7 0.004	1 0.019	1 0.012	7 0.100	8 0.088
132	NEUROTECHNOLOGY-003	248 0.999	236 0.636	204 0.099	218 0.773	187 0.266	184 0.164	214 1.000	232 1.000	235 1.000						
133	NEUROTECHNOLOGY-004	120 0.120	140 0.063	136 0.028	113 0.146	118 0.117	122 0.073	101 0.996	103 0.994	127 0.990						
134	NEUROTECHNOLOGY-005	119 0.117	127 0.054	118 0.022	155 0.252	130 0.130	125 0.074	126 0.999	125 0.998	124 0.989						
135	NEUROTECHNOLOGY-006	246 0.987	208 0.249	209 0.121	246 1.000	206 0.418	200 0.206									
136	NEUROTECHNOLOGY-007	179 0.252	139 0.062	115 0.021	239 0.996	158 0.173	114 0.068	180 1.000	167 1.000	162 0.997	141 0.339	96 0.036			189 1.000	168 0.989
137	NEUROTECHNOLOGY-008	229 0.797	122 0.053	87 0.012	79 0.110	81 0.080	78 0.047	181 1.000	175 1.000	195 1.000	65 0.035	63 0.017	55 0.293	56 0.149	42 0.203	45 0.152
138	NEUROTECHNOLOGY-009	36 0.027	51 0.015	44 0.006	41 0.066	49 0.052	47 0.032	21 0.661	24 0.588	29 0.436	30 0.020	37 0.010	34 0.153	37 0.082	29 0.165	33 0.129

Table 27: **Threshold-based accuracy**. *Values are FNIR(N, T, L) with N = 1.6 million with thresholds set to produce FPIR = 0.0003, 0.001, and 0.01 in non-mate searches. Throughout blue superscripts indicate the rank of the algorithm for that column. Caution: The Power-low models are mostly intended to draw attention to the kind of behavior, not as a model to be used for prediction.*

2021/11/22 08:35:53

FNIR(N, R, T) = False neg. identification rate
FPIR(N, T) = False pos. identification rate

N = Num. enrolled subjects
R = Num. candidates examined

T = Threshold

T = 0 → Investigation
T > 0 → Identification

This publication is available free of charge from: https://doi.org/10.6028/NIST.IR.8271

MISSES BELOW THRESHOLD, T		ENROL RECENT MUGSHOT, N = 1.6M									ENROL APPLICATION PORTRAIT, N = 1.6M					
		ENROL: MUGSHOT			ENROL: MUGSHOT			ENROL: MUGSHOT			ENROL: VISA		ENROL: BORDER		ENROL: VISA	
		PROBE: MUGSHOT			PROBE: WEBCAM			PROBE: PROFILE			PROBE: BORDER		PROBE: BORDER 10+YR		PROBE: KIOSK	
#	ALGORITHM	FPIR=0.0003	FPIR=0.001	FPIR=0.01	FPIR=0.0003	FPIR=0.001	FPIR=0.01	FPIR=0.0003	FPIR=0.001	FPIR=0.01	FPIR=0.001	FPIR=0.01	FPIR=0.001	FPIR=0.01	FPIR=0.001	FPIR=0.01
139	NEWLAND-002	215 0.523	227 0.438	229 0.294	198 0.535	213 0.466	216 0.335	133 0.999	142 0.999	168 0.998						
140	NOBLIS-001	252 1.000	252 1.000	252 0.991	248 1.000	246 1.000	248 1.000	165 1.000	189 1.000	201 1.000						
141	NOBLIS-002	250 1.000	248 0.997	238 0.488	254 1.000	255 1.000	256 1.000	184 1.000	176 1.000	197 1.000						
142	NTECHLAB-003	97 0.080	125 0.054	137 0.028	114 0.148	119 0.118	127 0.075	33 0.873	39 0.837	58 0.752						
143	NTECHLAB-004	84 0.063	101 0.041	113 0.021	102 0.131	110 0.105	111 0.065	32 0.868	38 0.833	56 0.746	84 0.053	87 0.030			58 0.263	74 0.214
144	NTECHLAB-005	83 0.062	102 0.042	114 0.021	101 0.130	108 0.102	110 0.063	30 0.816	33 0.771	48 0.661	99 0.073	100 0.039			64 0.294	79 0.227
145	NTECHLAB-006	77 0.056	96 0.037	103 0.018	91 0.121	96 0.094	98 0.059	28 0.802	32 0.754	44 0.635	87 0.057	91 0.032			57 0.260	72 0.207
146	NTECHLAB-007	52 0.040	75 0.026	84 0.012	60 0.085	67 0.067	68 0.041	27 0.796	31 0.750	45 0.642	59 0.032	64 0.017			47 0.223	56 0.176
147	NTECHLAB-008	31 0.024	45 0.014	51 0.007	33 0.057	39 0.045	42 0.029	14 0.601	20 0.529	28 0.391	63 0.033	68 0.018			37 0.183	39 0.140
148	NTECHLAB-009	12 0.010	20 0.005	22 0.003	15 0.028	16 0.022	15 0.014	10 0.522	12 0.430	20 0.311	28 0.015	29 0.008	23 0.109	24 0.061	20 0.142	20 0.114
149	NTECHLAB-010	9 0.005	9 0.003	6 0.002	8 0.018	9 0.015	8 0.011	7 0.334	7 0.252	11 0.169	10 0.007	12 0.004	13 0.059	15 0.031	4 0.098	3 0.077
150	PARAVISION-000	188 0.278	162 0.089	165 0.045	192 0.447	156 0.170	155 0.100	172 1.000	144 0.999	160 0.997	153 0.470	157 0.443			141 0.926	150 0.779
151	PARAVISION-001	136 0.140	115 0.049	110 0.020	147 0.207	129 0.128	124 0.074	177 1.000	137 0.999	145 0.994	150 0.444	156 0.428			118 0.739	132 0.573
152	PARAVISION-002	101 0.085	116 0.050	120 0.022	118 0.152	122 0.119	129 0.076	77 0.992	77 0.983	57 0.748	102 0.080	105 0.043			98 0.497	91 0.268
153	PARAVISION-003	85 0.063	94 0.035	94 0.016	96 0.124	100 0.096	101 0.060	107 0.997	104 0.994	52 0.733	88 0.058	94 0.034			65 0.296	81 0.232
154	PARAVISION-004	32 0.025	34 0.010	32 0.004	29 0.049	33 0.038	34 0.024	168 1.000	190 1.000	62 0.797	35 0.018	40 0.011			137 0.908	73 0.211
155	PARAVISION-005	22 0.014	16 0.004	17 0.002	18 0.031	18 0.024	20 0.016	105 0.997	71 0.980	12 0.181	23 0.011	30 0.008			16 0.132	26 0.120
156	PARAVISION-007	64 0.048	15 0.004	12 0.002	199 0.560	19 0.025	18 0.015	174 1.000	182 1.000	198 1.000	21 0.009	23 0.006	24 0.113	10 0.024	208 1.000	176 1.000
157	PIXELALL-002	223 0.664	169 0.105	140 0.030	232 0.974	204 0.388	136 0.083		183 1.000	192 1.000	156 0.602	108 0.047			209 1.000	170 1.000
158	PIXELALL-003	65 0.049	70 0.022	69 0.009	74 0.102	74 0.073	73 0.043		158 1.000	167 0.998	69 0.037	72 0.020			106 0.554	86 0.255
159	PIXELALL-004	121 0.120	60 0.018	55 0.007	219 0.783	80 0.079	61 0.037		173 1.000	175 0.999	80 0.051	55 0.015			155 0.994	158 0.942
160	PIXELALL-005	96 0.079	38 0.012	34 0.005	194 0.456	43 0.050	39 0.027		180 1.000	183 0.999	48 0.027	60 0.017	46 0.203	27 0.071	160 1.000	164 0.983
161	PTAKURATSATU-000	70 0.057	95 0.037	99 0.017	123 0.165	127 0.124	121 0.071	45 0.947	49 0.924	68 0.868	77 0.046	76 0.022	45 0.206	50 0.120	49 0.232	59 0.179
162	QNAP-000	244 0.972	180 0.129	171 0.052	241 0.998	176 0.238	165 0.117	188 1.000	193 1.000	196 1.000	130 0.191	118 0.068	64 0.539	66 0.263	157 0.998	166 0.985
163	QUANTASOFT-001	227 0.713	237 0.639	239 0.493												
164	RANKONE-002	155 0.184	173 0.118	187 0.071	171 0.308	183 0.261	194 0.190									
165	RANKONE-003	156 0.184	174 0.118	186 0.071	168 0.300	182 0.255	192 0.187									
166	RANKONE-004	178 0.250	200 0.193	210 0.124	196 0.482	208 0.426	214 0.324									
167	RANKONE-005	100 0.096	136 0.059	145 0.033	148 0.212	159 0.173	166 0.119	135 0.999	128 0.998	146 0.994						
168	RANKONE-006	80 0.061	97 0.037	106 0.020				67 0.987	67 0.977	83 0.937						
169	RANKONE-007	43 0.034	72 0.022	80 0.011	88 0.118	97 0.095	103 0.061	51 0.975	56 0.967	76 0.924						
170	RANKONE-009	40 0.031	56 0.018	64 0.008	70 0.098	76 0.076	75 0.045	60 0.983	58 0.969	67 0.859	90 0.062	86 0.029			74 0.328	71 0.206
171	RANKONE-010	27 0.023	43 0.014	56 0.007	54 0.077	58 0.058	60 0.036	37 0.905	35 0.802	47 0.652	83 0.052	83 0.027	49 0.208	49 0.119	55 0.259	65 0.194
172	RANKONE-011	116 0.109	27 0.009	30 0.004	57 0.079	41 0.048	43 0.029				68 0.037	65 0.017	41 0.182	41 0.092	149 0.977	123 0.465
173	REALNETWORKS-000	199 0.374	206 0.234	214 0.138	189 0.433	198 0.319	202 0.209									
174	REALNETWORKS-001	198 0.374	205 0.234	213 0.138	190 0.433	199 0.319	203 0.209									
175	REALNETWORKS-002	197 0.370	204 0.231	212 0.137	188 0.416	197 0.315	204 0.209									
176	REALNETWORKS-003	180 0.273	190 0.159	196 0.090	175 0.342	186 0.266	190 0.172	132 0.999	132 0.998	121 0.987	125 0.164	130 0.103			99 0.500	112 0.364
177	REALNETWORKS-004	176 0.242	189 0.158	195 0.090	181 0.353	184 0.263	187 0.169	146 1.000	146 0.999	138 0.992	126 0.170	131 0.103			110 0.613	113 0.370
178	REALNETWORKS-005	71 0.052	83 0.028	86 0.012	68 0.094	75 0.074	77 0.047	63 0.984	60 0.971	71 0.896	67 0.037	61 0.017	50 0.223	52 0.123	44 0.215	51 0.165
179	REMARKAI-000	125 0.125	128 0.055	122 0.023	126 0.173	123 0.120	118 0.070	139 0.999	143 0.999	150 0.995	98 0.069	93 0.033			116 0.717	105 0.315
180	REMARKAI-000	165 0.197	178 0.128	179 0.059	160 0.263	165 0.203	168 0.123									
181	REMARKAI-002	161 0.188	177 0.124	178 0.059	154 0.248	163 0.196	167 0.122	81 0.993	94 0.991	114 0.980						
182	RENDIP-000	28 0.023	37 0.012	38 0.005	137 0.189	59 0.059	55 0.034	44 0.945	46 0.894	55 0.744	41 0.022	46 0.013	43 0.185	38 0.089	30 0.167	34 0.130
183	S1-000	132 0.137	85 0.028	79 0.011	99 0.129	84 0.085	79 0.048	187 1.000	194 1.000	40 0.596	79 0.047	69 0.018	79 1.000	51 0.123	195 1.000	137 0.632
184	S1-001	73 0.054	52 0.016	53 0.007	40 0.066	48 0.052	54 0.033	76 0.992	81 0.985	92 0.952	36 0.019	36 0.010	26 0.136	31 0.075	21 0.148	24 0.119

Table 28: **Threshold-based accuracy**. *Values are FNIR(N, T, L) with N = 1.6 million with thresholds set to produce FPIR = 0.0003, 0.001, and 0.01 in non-mate searches. Throughout blue superscripts indicate the rank of the algorithm for that column. Caution: The Power-low models are mostly intended to draw attention to the kind of behavior, not as a model to be used for prediction.*

FNIR(N, R, T) = False neg. identification rate
FPIR(N, T) = False pos. identification rate
N = Num. enrolled subjects
R = Num. candidates examined
T = Threshold
T = 0 → Investigation
T > 0 → Identification

This publication is available free of charge from: https://doi.org/10.6028/NIST.IR.8271

MISSES BELOW THRESHOLD, T		ENROL RECENT MUGSHOT, N = 1.6M									ENROL APPLICATION PORTRAIT, N = 1.6M					
		ENROL: MUGSHOT			ENROL: MUGSHOT			ENROL: MUGSHOT			ENROL: VISA		ENROL: BORDER		ENROL: VISA	
		PROBE: MUGSHOT			PROBE: WEBCAM			PROBE: PROFILE			PROBE: BORDER		PROBE: BORDER 10+YR		PROBE: KIOSK	
#	ALGORITHM	FPIR=0.0003	FPIR=0.001	FPIR=0.01	FPIR=0.0003	FPIR=0.001	FPIR=0.01	FPIR=0.0003	FPIR=0.001	FPIR=0.01	FPIR=0.001	FPIR=0.01	FPIR=0.001	FPIR=0.01	FPIR=0.001	FPIR=0.01
185	SCANOVATE-000	[111]0.103	[143]0.067	[141]0.030	[167]0.296	[179]0.240	[177]0.150	[40]0.931	[45]0.893	[63]0.803	[134]0.215	[138]0.118			[82]0.400	[101]0.299
186	SCANOVATE-001	[127]0.128	[154]0.081	[153]0.037	[166]0.281	[173]0.227	[173]0.140	[41]0.935	[48]0.911	[65]0.834	[131]0.192	[132]0.103			[85]0.404	[97]0.290
187	SENSETIME-000	[47]0.036	[68]0.021	[70]0.009	[55]0.078	[62]0.063	[65]0.040	[229]1.000	[215]1.000	[122]0.988						
188	SENSETIME-001	[48]0.036	[71]0.022	[73]0.010	[58]0.080	[64]0.064	[71]0.041									
189	SENSETIME-002	[49]0.037	[46]0.015	[93]0.014	[95]0.124	[24]0.028	[32]0.023	[104]0.997	[102]0.994	[113]0.979	[57]0.032	[62]0.017			[101]0.523	[50]0.160
190	SENSETIME-003	[4]0.004	[4]0.002	[4]0.001	[1]0.014	[1]0.012	[2]0.009	[16]0.607	[16]0.477	[21]0.311	[17]0.008	[19]0.005			[17]0.133	[21]0.115
191	SENSETIME-004	[2]0.003	[1]0.002	[3]0.001	[2]0.015	[3]0.013	[6]0.010	[6]0.301	[6]0.229	[9]0.149	[8]0.006	[8]0.004			[13]0.113	[16]0.100
192	SENSETIME-005	[15]0.011	[7]0.002	[2]0.001	[9]0.018	[8]0.014	[4]0.010	[2]0.259	[3]0.173	[3]0.103	[11]0.007	[11]0.004	[9]0.051	[9]0.023	[9]0.104	[13]0.093
193	SENSETIME-006	[6]0.005	[2]0.002	[1]0.001	[5]0.016	[2]0.012	[1]0.009	[124]0.999	[131]0.998	[49]0.680	[1]0.004	[1]0.002	[4]0.034	[3]0.016	[3]0.093	[5]0.079
194	SHAMAN-003	[212]0.506	[228]0.451	[232]0.347	[209]0.650	[222]0.597	[225]0.472									
195	SHAMAN-004	[224]0.679	[235]0.615	[237]0.488	[220]0.812	[229]0.754	[232]0.639									
196	SHAMAN-006	[158]0.185	[184]0.141	[198]0.092	[164]0.278	[175]0.237	[186]0.168	[53]0.978	[61]0.972	[96]0.960						
197	SHAMAN-007	[153]0.183	[185]0.141	[197]0.092	[165]0.280	[178]0.240	[188]0.169									
198	SIAT-001	[130]0.132	[54]0.018	[32]0.007	[207]0.641	[203]0.365	[217]0.348				[54]0.031	[51]0.014				
199	SIAT-002	[201]0.417	[69]0.022	[57]0.007	[223]0.942	[214]0.478	[223]0.460				[143]0.372	[151]0.356			[140]0.923	[54]0.169
200	SMILART-004	[243]0.970	[246]0.968	[250]0.965	[233]0.977	[242]0.976	[244]0.973									
201	SMILART-005															
202	STAQU-000	[193]0.334	[137]0.062	[116]0.022	[221]0.848	[210]0.443	[104]0.061	[162]1.000	[165]1.000	[127]0.999	[154]0.535	[101]0.039	[69]0.961	[59]0.183	[166]1.000	[169]0.999
203	SYNESIS-003	[117]0.111	[141]0.065	[142]0.032	[119]0.155	[126]0.123	[130]0.078	[48]0.973	[54]0.960	[73]0.911	[100]0.075	[99]0.039			[69]0.314	[83]0.235
204	SYNESIS-003	[222]0.648	[233]0.582	[236]0.443	[213]0.708	[225]0.646	[227]0.524									
205	SYNESIS-005	[67]0.050	[74]0.025	[82]0.011	[63]0.088	[72]0.072	[74]0.043	[89]0.995	[78]0.984	[59]0.795	[60]0.032	[56]0.016			[43]0.214	[49]0.158
206	TECH5-001	[231]0.807	[131]0.057	[102]0.018	[238]0.994	[238]0.935	[95]0.055	[195]1.000	[195]1.000	[190]1.000	[135]0.244	[85]0.028			[156]0.994	[153]0.817
207	TECH5-002	[72]0.053	[81]0.027	[85]0.012	[67]0.094	[70]0.070	[67]0.040	[34]0.874	[36]0.805	[42]0.627	[70]0.039	[70]0.019	[47]0.205	[47]0.111	[88]0.440	[62]0.182
208	TEVIAN-003	[175]0.239	[197]0.177	[203]0.096	[177]0.346	[193]0.298	[196]0.198									
209	TEVIAN-004	[150]0.170	[172]0.117	[183]0.063	[149]0.216	[160]0.176	[164]0.115									
210	TEVIAN-005	[129]0.129	[159]0.087	[164]0.045	[131]0.180	[140]0.144	[141]0.089	[70]0.988	[55]0.962	[61]0.796						
211	TEVIAN-006	[30]0.024	[31]0.010	[37]0.005	[26]0.041	[27]0.032	[27]0.021	[12]0.562	[11]0.425	[19]0.291	[29]0.016	[32]0.009	[19]0.093	[21]0.050	[144]0.951	[23]0.117
212	TEVIAN-007	[16]0.011	[22]0.005	[23]0.003	[14]0.028	[15]0.022	[16]0.015	[9]0.504	[8]0.301	[13]0.183	[22]0.009	[17]0.005	[15]0.065	[16]0.033	[14]0.122	[18]0.102
213	TIGER-000	[207]0.462	[222]0.390	[225]0.261	[200]0.565	[215]0.500	[218]0.366									
214	TIGER-002	[146]0.158	[155]0.086	[156]0.039	[145]0.202	[150]0.158	[148]0.095	[140]0.999	[140]0.999	[110]0.975						
215	TIGER-003	[147]0.158	[156]0.086	[155]0.039	[144]0.202	[149]0.158	[147]0.095									
216	TONGYITRANS-000	[114]0.107	[148]0.074	[154]0.038	[111]0.141	[115]0.112	[117]0.069									
217	TONGYITRANS-001	[124]0.124	[142]0.066	[143]0.032	[98]0.128	[107]0.101	[107]0.062									
218	TOSHIBA-000	[123]0.123	[138]0.062	[135]0.027	[115]0.150	[120]0.118	[123]0.074	[106]0.997	[113]0.995	[123]0.988						
219	TOSHIBA-001	[171]0.225	[133]0.058	[104]0.019	[106]0.133	[94]0.092	[94]0.054									
220	TRUEFACE-000	[60]0.046	[59]0.018	[63]0.008	[56]0.079	[61]0.062	[63]0.039	[94]0.995	[42]0.882	[31]0.499	[53]0.030	[59]0.016	[45]0.194	[48]0.111	[39]0.188	[42]0.145
221	VD-000	[240]0.950	[244]0.917	[247]0.827	[231]0.968	[240]0.946	[240]0.871									
222	VD-001	[187]0.278	[201]0.201	[208]0.116	[172]0.331	[190]0.281	[193]0.188									
223	VD-002	[140]0.144	[152]0.079	[149]0.036	[136]0.188	[142]0.148	[142]0.092	[115]0.998	[116]0.996	[120]0.987	[106]0.095	[109]0.048	[59]0.367	[62]0.220	[78]0.372	[93]0.280
224	VD-003	[174]0.234	[110]0.046	[107]0.020	[105]0.133	[105]0.100	[106]0.061	[137]0.999	[141]0.999	[142]0.994	[81]0.051	[82]0.027	[51]0.244	[53]0.133	[71]0.315	[67]0.203
225	VERIDAS-001	[98]0.080	[99]0.037	[97]0.016	[77]0.106	[82]0.082	[82]0.051	[79]0.993	[86]0.987	[84]0.938	[74]0.044	[79]0.023	[52]0.266	[54]0.146	[60]0.264	[68]0.204
226	VERIDAS-002	[99]0.080	[98]0.037	[96]0.016	[78]0.106	[83]0.082	[83]0.051	[80]0.993	[85]0.987	[85]0.938	[73]0.044	[80]0.023	[53]0.266	[55]0.146	[59]0.264	[69]0.204
227	VERIDAS-003	[91]0.072	[53]0.017	[47]0.006	[49]0.071	[54]0.055	[52]0.033	[121]0.998	[120]0.997	[78]0.927	[38]0.020	[39]0.011	[32]0.150	[32]0.078	[34]0.178	[40]0.142
228	VIGILANTSOLUTIONS-003	[211]0.482	[226]0.408	[227]0.282	[216]0.730	[228]0.660	[229]0.526	[134]0.999	[136]0.999	[151]0.995						
229	VIGILANTSOLUTIONS-004	[221]0.624	[232]0.549	[235]0.422	[222]0.858	[232]0.817	[234]0.709	[119]0.998	[118]0.996	[132]0.991						
230	VIGILANTSOLUTIONS-005	[239]0.936	[221]0.388	[158]0.043				[166]1.000	[188]1.000	[200]1.000						

Table 29: **Threshold-based accuracy**. *Values are FNIR(N, T, L) with N = 1.6 million with thresholds set to produce FPIR = 0.0003, 0.001, and 0.01 in non-mate searches. Throughout blue superscripts indicate the rank of the algorithm for that column. Caution: The Power-low models are mostly intended to draw attention to the kind of behavior, not as a model to be used for prediction.*

This publication is available free of charge from: https://doi.org/10.6028/NIST.IR.8271

MISSES BELOW THRESHOLD, T		ENROL RECENT MUGSHOT, N = 1.6M									ENROL APPLICATION PORTRAIT, N = 1.6M					
		ENROL: MUGSHOT			ENROL: MUGSHOT			ENROL: MUGSHOT			ENROL: VISA		ENROL: BORDER		ENROL: VISA	
		PROBE: MUGSHOT			PROBE: WEBCAM			PROBE: PROFILE			PROBE: BORDER		PROBE: BORDER 10+YR		PROBE: KIOSK	
#	ALGORITHM	FPIR=0.0003	FPIR=0.001	FPIR=0.01	FPIR=0.0003	FPIR=0.001	FPIR=0.01	FPIR=0.0003	FPIR=0.001	FPIR=0.01	FPIR=0.001	FPIR=0.01	FPIR=0.001	FPIR=0.01	FPIR=0.001	FPIR=0.01
231	VIGILANTSOLUTIONS-006	[242]0.959	[216]0.353	[161]0.043				[169]1.000	[191]1.000	[202]1.000						
232	VIGILANTSOLUTIONS-007	[95]0.076	[87]0.028	[81]0.011	[82]0.113	[88]0.088	[89]0.053	[111]0.997	[117]0.996	[135]0.991	[103]0.081	[107]0.047	[60]0.371	[63]0.242	[81]0.391	[100]0.295
233	VIGILANTSOLUTIONS-008	[70]0.051	[65]0.021	[72]0.010	[76]0.105	[77]0.077	[76]0.046	[142]1.000	[139]0.999	[131]0.991	[110]0.104	[112]0.054	[62]0.398	[65]0.259	[100]0.511	[106]0.316
234	VISIONBOX-000	[92]0.073	[57]0.018	[54]0.007	[50]0.071	[57]0.057	[59]0.035	[86]0.995	[93]0.990	[108]0.974	[44]0.023	[43]0.012	[31]0.146	[34]0.081	[28]0.162	[31]0.126
235	VISIONLABS-004	[103]0.091	[132]0.058	[125]0.024	[140]0.199	[151]0.159	[150]0.097	[42]0.944	[44]0.890	[54]0.742						
236	VISIONLABS-005	[100]0.080	[117]0.050	[109]0.020	[134]0.183	[141]0.147	[139]0.087	[43]0.945	[43]0.888	[53]0.736						
237	VISIONLABS-006	[58]0.044	[80]0.027	[75]0.010	[86]0.117	[92]0.090	[85]0.051	[25]0.764	[27]0.672	[35]0.511						
238	VISIONLABS-007	[57]0.044	[79]0.027	[74]0.010	[85]0.117	[91]0.090	[84]0.051	[24]0.764	[28]0.672	[34]0.511	[56]0.031	[52]0.014			[38]0.185	[43]0.145
239	VISIONLABS-008	[37]0.028	[41]0.013	[41]0.006	[45]0.068	[47]0.051	[49]0.032	[13]0.574	[17]0.481	[22]0.317	[30]0.017	[28]0.008			[22]0.151	[25]0.119
240	VISIONLABS-009	[19]0.012	[18]0.005	[15]0.002	[19]0.032	[21]0.025	[21]0.017	[39]0.930	[34]0.799	[15]0.196	[20]0.008	[16]0.004			[12]0.113	[14]0.093
241	VISIONLABS-010	[21]0.014	[21]0.005	[19]0.002	[20]0.034	[23]0.027	[23]0.019			[10]0.169	[15]0.008	[10]0.004	[11]0.055	[11]0.027	[11]0.109	[10]0.089
242	VISIONLABS-011	[17]0.011	[13]0.003	[10]0.002	[13]0.024	[13]0.020	[13]0.014			[14]0.194	[4]0.004	[2]0.002	[5]0.034	[4]0.017	[2]0.090	[4]0.079
243	VOCORD-003	[194]0.354	[176]0.122	[168]0.048	[139]0.195	[147]0.155	[145]0.093	[125]0.999	[129]0.998	[129]0.991	[124]0.157	[133]0.105			[84]0.404	[96]0.289
244	VOCORD-004	[232]0.826	[217]0.355	[169]0.051	[185]0.401	[157]0.173	[143]0.093	[170]1.000	[168]1.000	[174]0.999	[132]0.193	[116]0.065			[153]0.991	[149]0.776
245	VOCORD-005	[225]0.689	[188]0.158	[162]0.044	[121]0.161	[131]0.130	[133]0.080	[131]0.999	[121]0.997	[99]0.968	[119]0.138	[127]0.090			[79]0.381	[94]0.287
246	VOCORD-006	[254]1.000	[254]1.000	[255]1.000	[253]1.000	[251]1.000	[253]1.000	[232]1.000	[218]1.000	[222]1.000	[191]1.000	[242]1.000			[203]1.000	[255]1.000
247	VTS-000	[219]0.605	[234]0.598	[241]0.595	[205]0.624	[223]0.619	[231]0.613	[138]0.999	[147]0.999	[171]0.998	[159]0.613	[161]0.609	[67]0.760	[70]0.739	[120]0.761	[146]0.749
248	VTS-001	[45]0.035	[42]0.013	[42]0.006	[44]0.067	[46]0.051	[44]0.031	[114]0.998	[101]0.994	[33]0.510	[42]0.022	[44]0.012	[29]0.141	[33]0.079	[40]0.192	[32]0.126
249	XFORWARDAI-000	[39]0.029	[49]0.015	[50]0.006	[47]0.070	[52]0.053	[57]0.034	[23]0.698	[13]0.440	[17]0.250	[40]0.021	[38]0.011	[36]0.159	[36]0.082	[31]0.169	[35]0.134
250	XFORWARDAI-001	[14]0.010	[19]0.005	[24]0.003	[22]0.036	[25]0.028	[24]0.020	[31]0.838	[14]0.448	[6]0.143	[18]0.008	[18]0.005	[14]0.062	[14]0.030	[15]0.123	[17]0.102
251	XFORWARDAI-002	[10]0.007	[12]0.003	[16]0.002	[10]0.018	[10]0.016	[12]0.014	[50]0.975	[18]0.525	[1]0.095	[7]0.005	[6]0.003	[8]0.041	[6]0.018	[5]0.099	[9]0.089
252	YISHENG-001	[205]0.452	[214]0.346	[220]0.206	[234]0.983	[230]0.808	[209]0.269				[160]0.666	[155]0.396			[139]0.919	[140]0.695
253	YITU-002	[41]0.031	[55]0.018	[58]0.008	[37]0.063	[42]0.049	[40]0.028									
254	YITU-003	[42]0.032	[62]0.019	[66]0.009	[42]0.067	[50]0.052	[53]0.033									
255	YITU-004	[24]0.019	[29]0.010	[31]0.004	[21]0.035	[22]0.027	[22]0.017	[46]0.948	[50]0.936	[74]0.913						
256	YITU-005	[26]0.022	[33]0.010	[36]0.005	[25]0.039	[28]0.032	[31]0.023									

Table 30: **Threshold-based accuracy**. *Values are FNIR(N, T, L) with N = 1.6 million with thresholds set to produce FPIR = 0.0003, 0.001, and 0.01 in non-mate searches. Throughout blue superscripts indicate the rank of the algorithm for that column. Caution: The Power-low models are mostly intended to draw attention to the kind of behavior, not as a model to be used for prediction.*

Appendices

Appendix A Accuracy on large-population FRVT 2018 mugshots

This publication is available free of charge from: https://doi.org/10.6028/NIST.IR.8271

2021/11/22	FNIR(N, R, T) =	False neg. identification rate	N = Num. enrolled subjects	T = Threshold	$T = 0 \rightarrow$ Investigation
08:35:53	FPIR(N, T) =	False pos. identification rate	R = Num. candidates examined		$T > 0 \rightarrow$ Identification

This publication is available free of charge from: https://doi.org/10.6028/NIST.IR.8271

This publication is available free of charge from: https://doi.org/10.6028/NIST.IR.8271

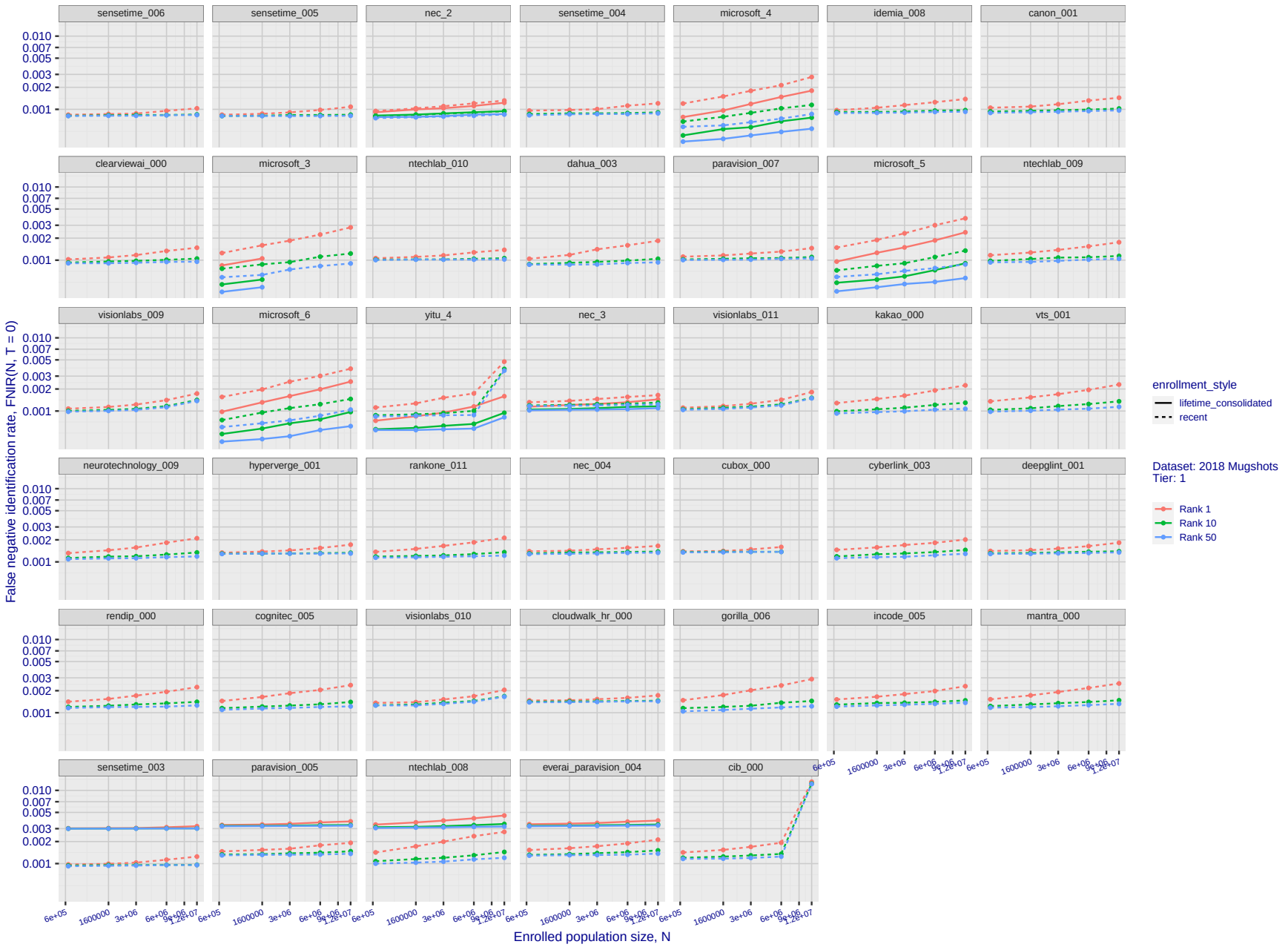

Figure 20: **[FRVT-2018 Mugshot Dataset] Rank-based identification miss rates vs. number of enrolled subjects**. *The figure shows false negative identification rates, FNIR(N, R), across various gallery sizes and ranks 1, 10 and 50. The threshold is set to zero, so this metric rewards even weak scoring rank 1 mates. This also means FPIR = 1, so any search without an enrolled mate will return non-mated candidates. For clarity, results are sorted and reported into tiers spanning multiple pages, the tiering criteria being rank 1 hit rate on a gallery size of 640 000.*

2021/11/22 08:35:53

FNIR(N, R, T) = False neg. identification rate
FPIR(N, T) = False pos. identification rate

N = Num. enrolled subjects
R = Num. candidates examined

T = Threshold

T = 0 → Investigation
T > 0 → Identification

This publication is available free of charge from: https://doi.org/10.6028/NIST.IR.8271

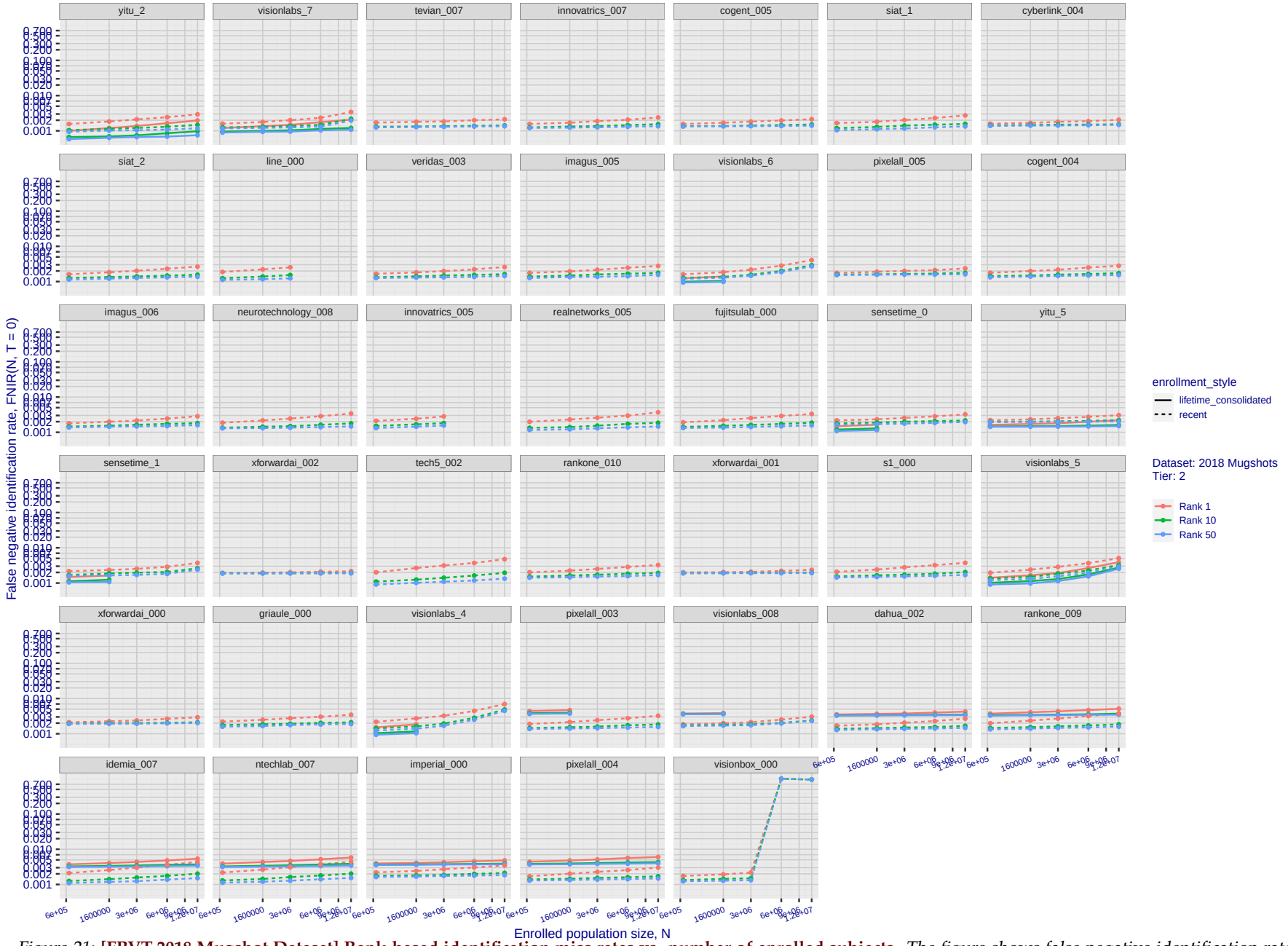

Figure 21: **[FRVT-2018 Mugshot Dataset] Rank-based identification miss rates vs. number of enrolled subjects**. *The figure shows false negative identification rates, FNIR(N, R), across various gallery sizes and ranks 1, 10 and 50. The threshold is set to zero, so this metric rewards even weak scoring rank 1 mates. This also means FPIR = 1, so any search without an enrolled mate will return non-mated candidates. For clarity, results are sorted and reported into tiers spanning multiple pages, the tiering criteria being rank 1 hit rate on a gallery size of 640 000.*

2021/11/22 08:35:53

FNIR(N, R, T) = False neg. identification rate
FPIR(N, T) = False pos. identification rate
N = Num. enrolled subjects
R = Num. candidates examined
T = Threshold
T = 0 → Investigation
T > 0 → Identification

This publication is available free of charge from: https://doi.org/10.6028/NIST.IR.8271

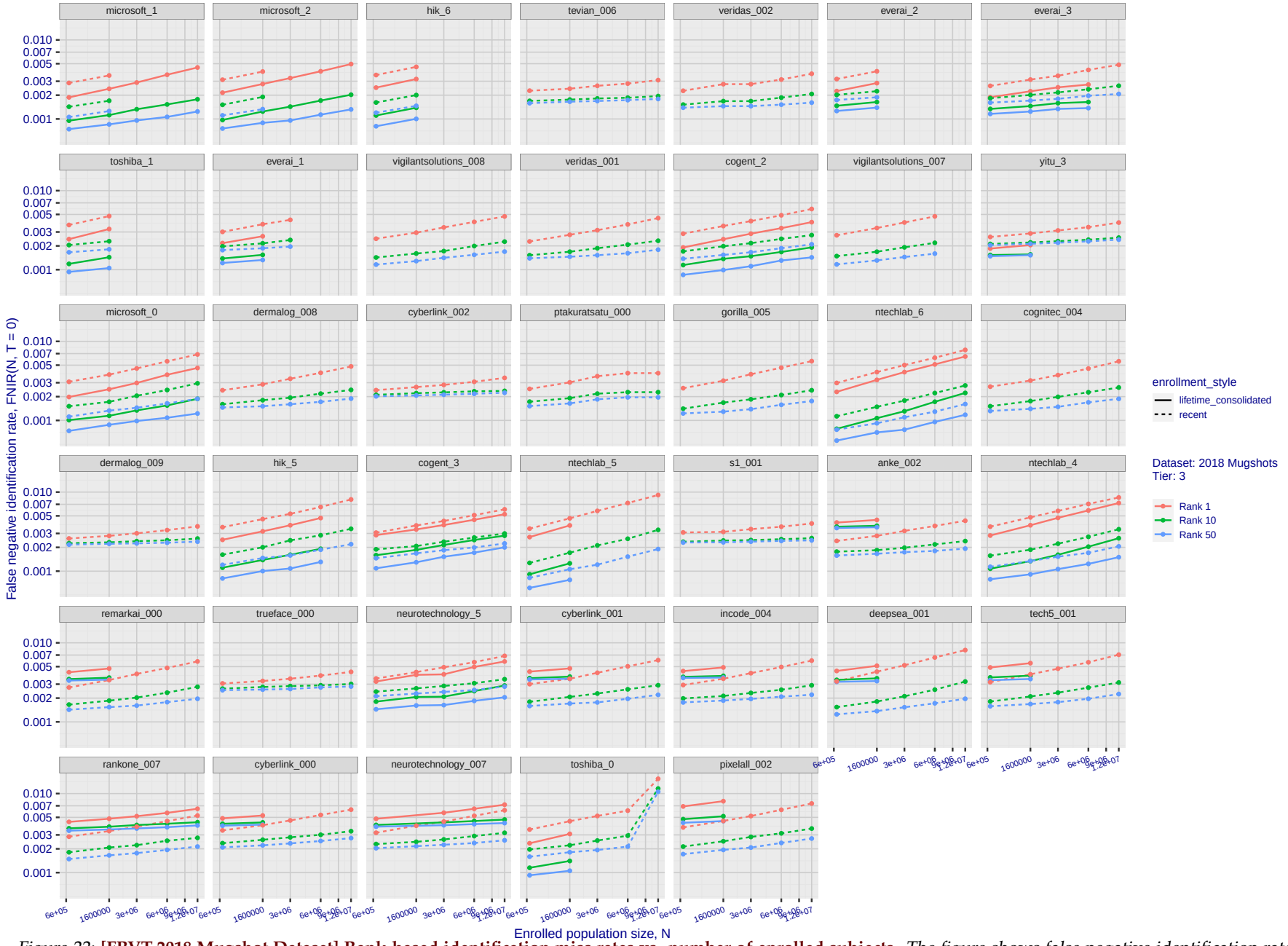

Figure 22: **[FRVT-2018 Mugshot Dataset] Rank-based identification miss rates vs. number of enrolled subjects**. *The figure shows false negative identification rates, FNIR(N, R), across various gallery sizes and ranks 1, 10 and 50. The threshold is set to zero, so this metric rewards even weak scoring rank 1 mates. This also means FPIR = 1, so any search without an enrolled mate will return non-mated candidates. For clarity, results are sorted and reported into tiers spanning multiple pages, the tiering criteria being rank 1 hit rate on a gallery size of 640 000.*

2021/11/22
08:35:53

FNIR(N, R, T) = False neg. identification rate
FPIR(N, T) = False pos. identification rate

N = Num. enrolled subjects
R = Num. candidates examined

T = Threshold

T = 0 → Investigation
T > 0 → Identification

This publication is available free of charge from: https://doi.org/10.6028/NIST.IR.8271

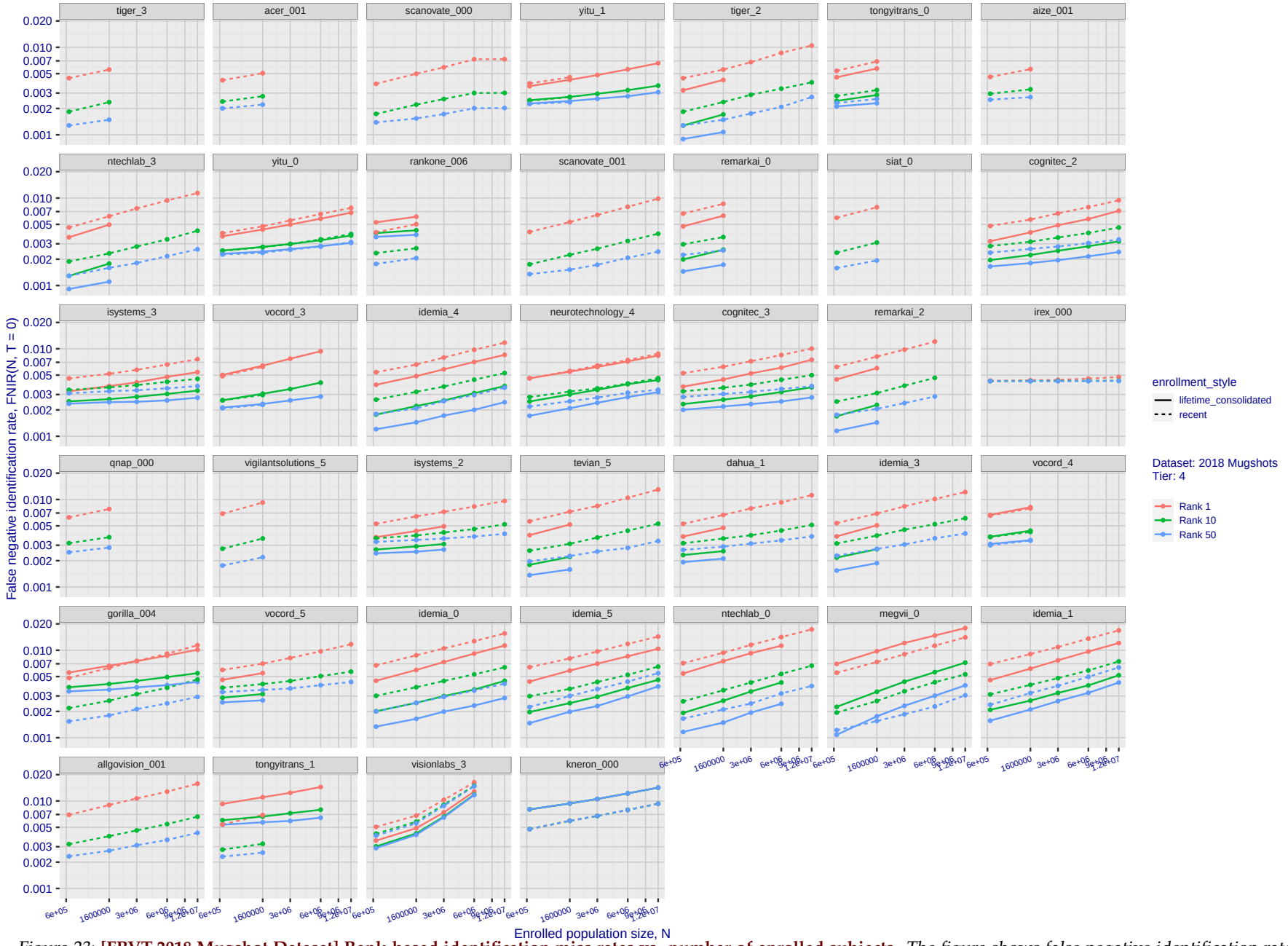

Figure 23: **[FRVT-2018 Mugshot Dataset] Rank-based identification miss rates vs. number of enrolled subjects**. *The figure shows false negative identification rates, FNIR(N, R), across various gallery sizes and ranks 1, 10 and 50. The threshold is set to zero, so this metric rewards even weak scoring rank 1 mates. This also means FPIR = 1, so any search without an enrolled mate will return non-mated candidates. For clarity, results are sorted and reported into tiers spanning multiple pages, the tiering criteria being rank 1 hit rate on a gallery size of 640 000.*

2021/11/22
08:35:53
FNIR(N, R, T) = False neg. identification rate
FPIR(N, T) = False pos. identification rate
N = Num. enrolled subjects
R = Num. candidates examined
T = Threshold
T = 0 → Investigation
T > 0 → Identification

This publication is available free of charge from: https://doi.org/10.6028/NIST.IR.8271

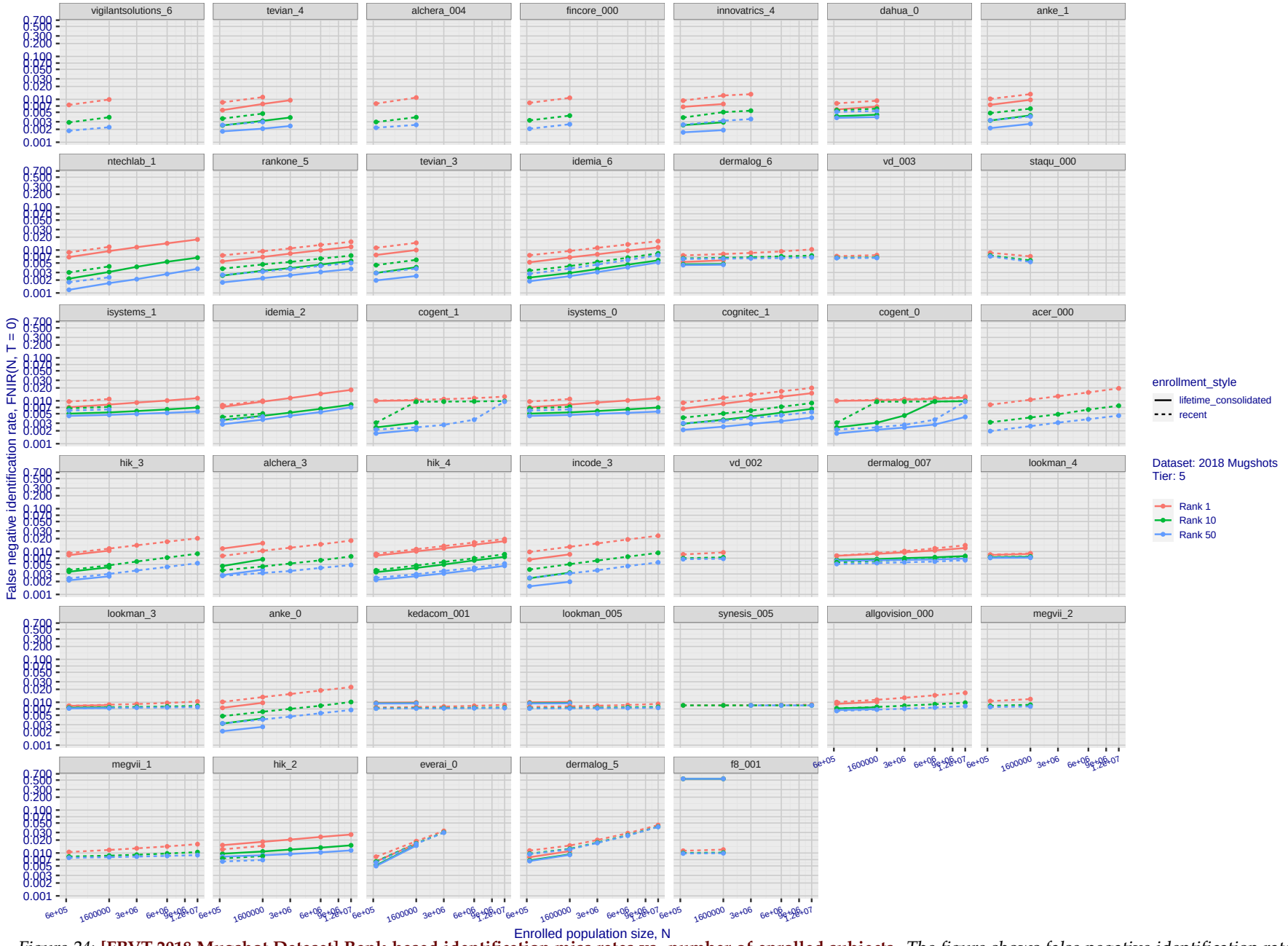

Figure 24: **[FRVT-2018 Mugshot Dataset] Rank-based identification miss rates vs. number of enrolled subjects**. *The figure shows false negative identification rates, FNIR(N, R), across various gallery sizes and ranks 1, 10 and 50. The threshold is set to zero, so this metric rewards even weak scoring rank 1 mates. This also means FPIR = 1, so any search without an enrolled mate will return non-mated candidates. For clarity, results are sorted and reported into tiers spanning multiple pages, the tiering criteria being rank 1 hit rate on a gallery size of 640 000.*

2021/11/22
08:35:53

FNIR(N, R, T) = False neg. identification rate
FPIR(N, T) = False pos. identification rate

N = Num. enrolled subjects
R = Num. candidates examined

T = Threshold

T = 0 → Investigation
T > 0 → Identification

This publication is available free of charge from: https://doi.org/10.6028/NIST.IR.8271

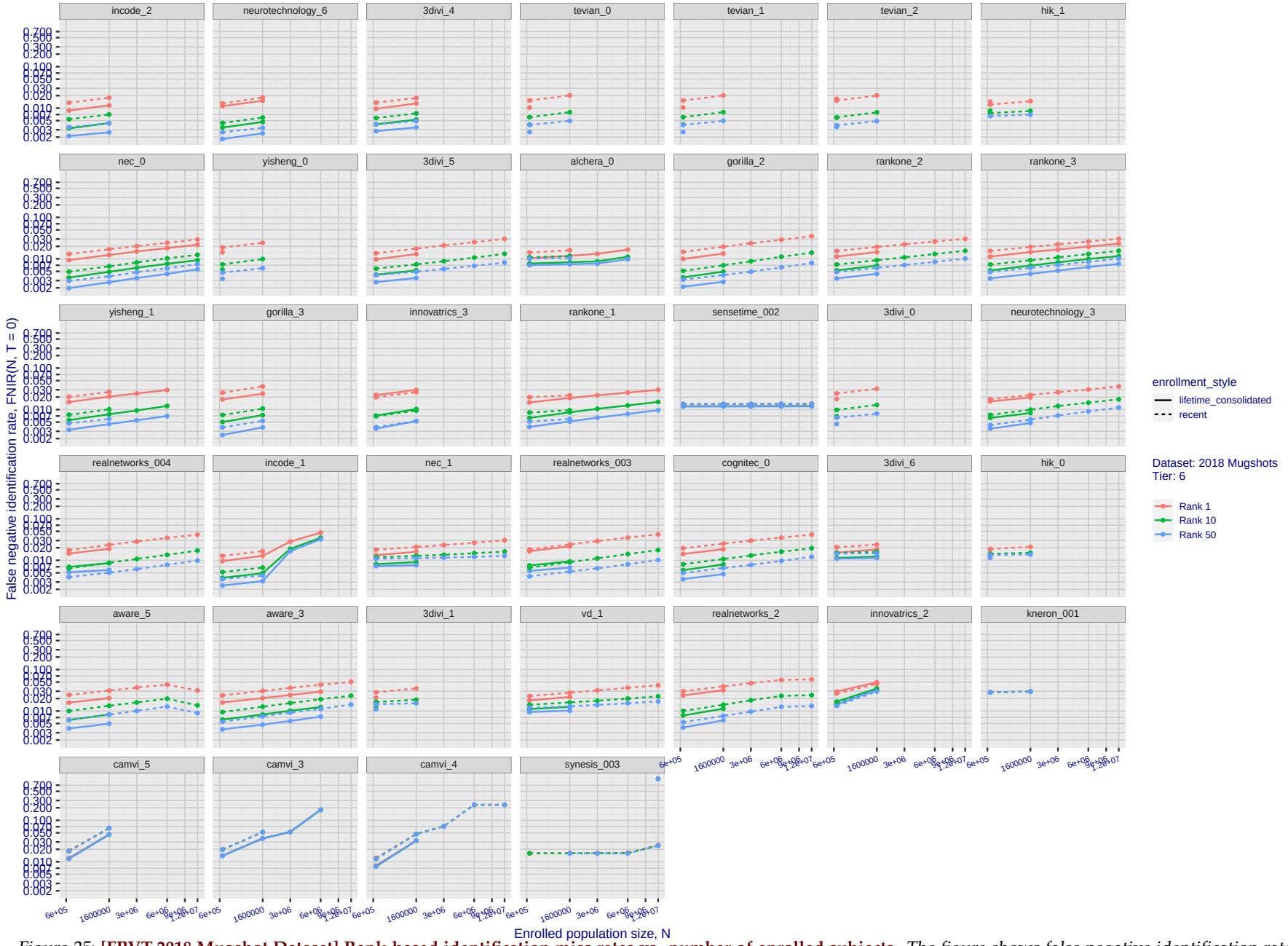

Figure 25: **[FRVT-2018 Mugshot Dataset] Rank-based identification miss rates vs. number of enrolled subjects**. *The figure shows false negative identification rates, FNIR(N, R), across various gallery sizes and ranks 1, 10 and 50. The threshold is set to zero, so this metric rewards even weak scoring rank 1 mates. This also means FPIR = 1, so any search without an enrolled mate will return non-mated candidates. For clarity, results are sorted and reported into tiers spanning multiple pages, the tiering criteria being rank 1 hit rate on a gallery size of 640 000.*

2021/11/22
08:35:53
FNIR(N, R, T) = False neg. identification rate
FPIR(N, T) = False pos. identification rate
N = Num. enrolled subjects
R = Num. candidates examined
T = Threshold
T = 0 → Investigation
T > 0 → Identification

This publication is available free of charge from: https://doi.org/10.6028/NIST.IR.8271

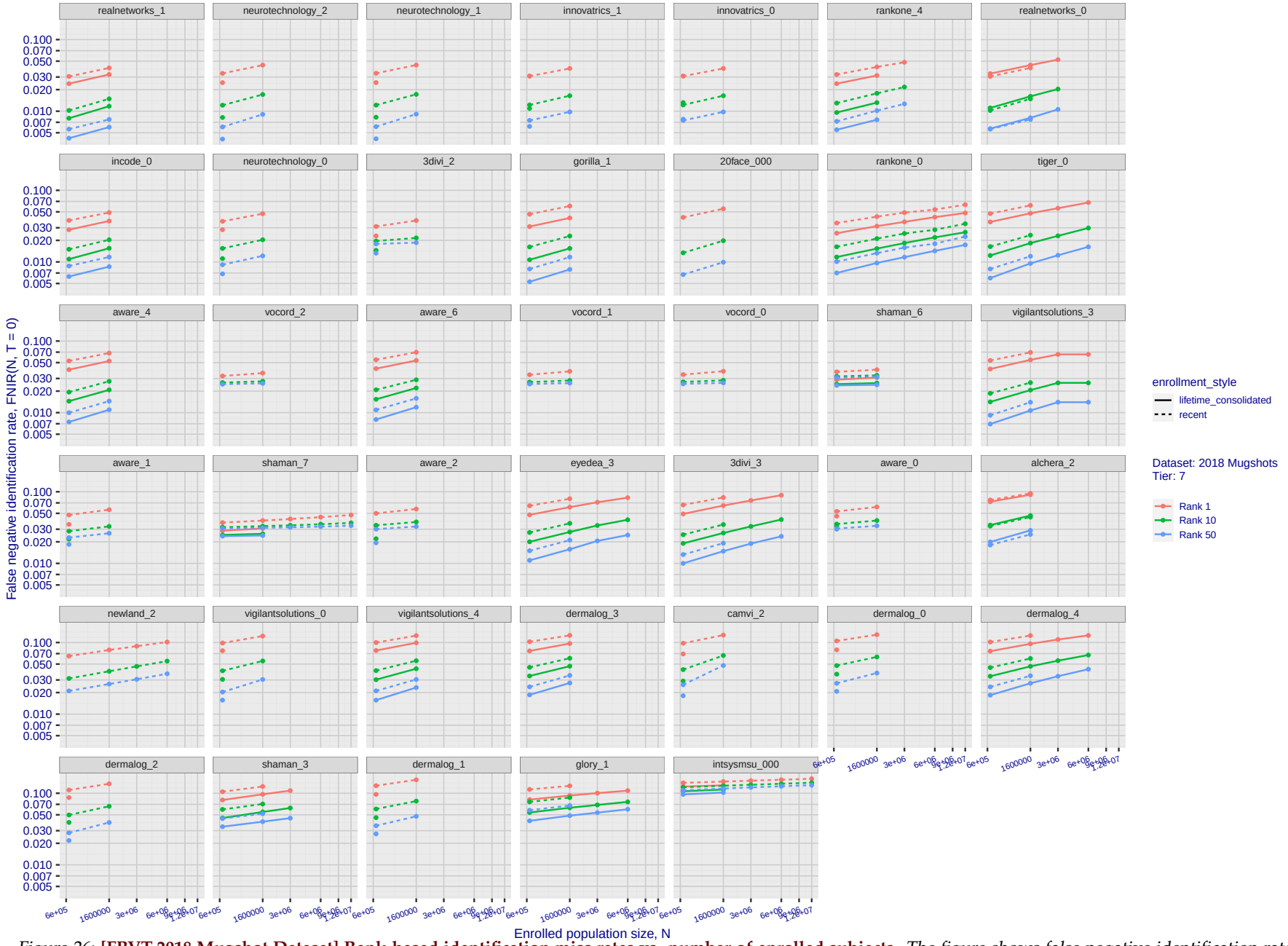

Figure 26: **[FRVT-2018 Mugshot Dataset] Rank-based identification miss rates vs. number of enrolled subjects**. *The figure shows false negative identification rates, FNIR(N, R), across various gallery sizes and ranks 1, 10 and 50. The threshold is set to zero, so this metric rewards even weak scoring rank 1 mates. This also means FPIR = 1, so any search without an enrolled mate will return non-mated candidates. For clarity, results are sorted and reported into tiers spanning multiple pages, the tiering criteria being rank 1 hit rate on a gallery size of 640 000.*

2021/11/22
08:35:53

FNIR(N, R, T) = False neg. identification rate
FPIR(N, T) = False pos. identification rate
N = Num. enrolled subjects
R = Num. candidates examined
T = Threshold
T = 0 → Investigation
T > 0 → Identification

This publication is available free of charge from: https://doi.org/10.6028/NIST.IR.8271

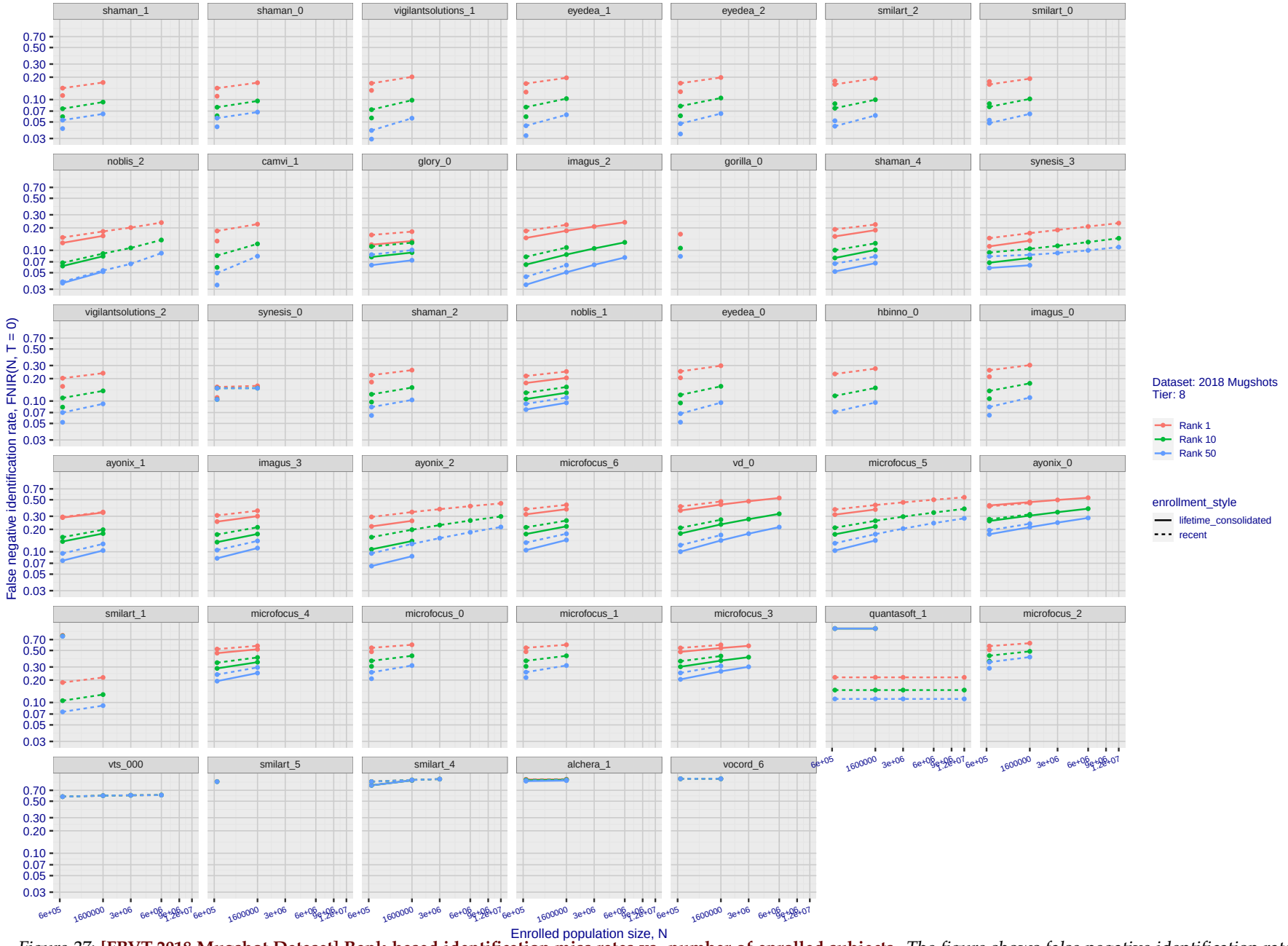

Figure 27: **[FRVT-2018 Mugshot Dataset] Rank-based identification miss rates vs. number of enrolled subjects**. *The figure shows false negative identification rates, FNIR(N, R), across various gallery sizes and ranks 1, 10 and 50. The threshold is set to zero, so this metric rewards even weak scoring rank 1 mates. This also means FPIR = 1, so any search without an enrolled mate will return non-mated candidates. For clarity, results are sorted and reported into tiers spanning multiple pages, the tiering criteria being rank 1 hit rate on a gallery size of 640 000.*

2021/11/22
08:35:53

FNIR(N, R, T) = False neg. identification rate
FPIR(N, T) = False pos. identification rate

N = Num. enrolled subjects
R = Num. candidates examined

T = Threshold

T = 0 → Investigation
T > 0 → Identification

2021/11/22	FNIR(N, R, T) =	False neg. identification rate	N = Num. enrolled subjects	T = Threshold	$T = 0 \rightarrow$ Investigation
08:35:53	FPIR(N, T) =	False pos. identification rate	R = Num. candidates examined		$T > 0 \rightarrow$ Identification

This publication is available free of charge from: https://doi.org/10.6028/NIST.IR.8271

This publication is available free of charge from: https://doi.org/10.6028/NIST.IR.8271

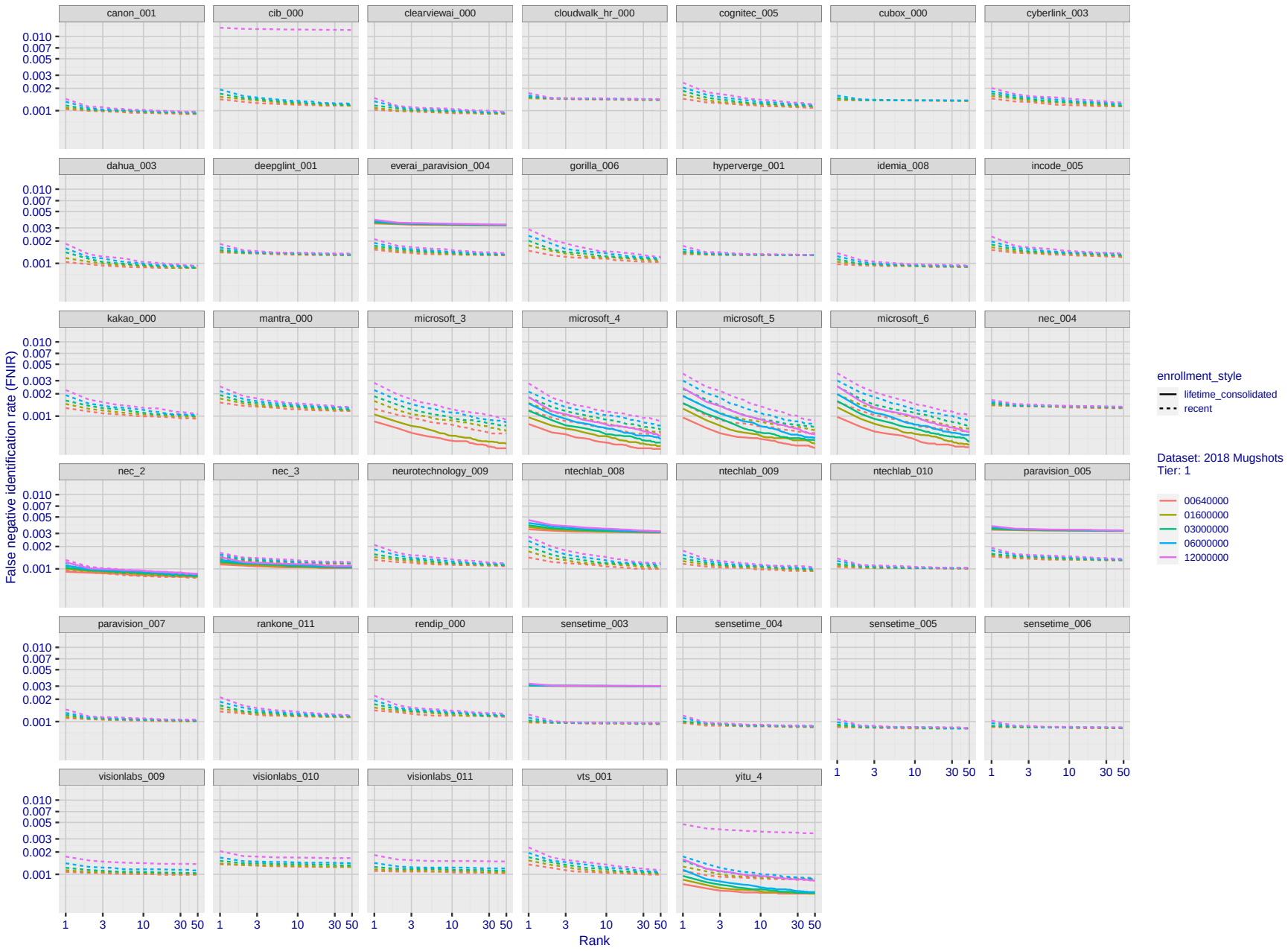

Figure 28: **[FRVT-2018 Mugshot Dataset] Rank-based identification miss rates vs. rank**. *The figure shows false negative identification rates (FNIR) for ranks up to 50. This metric is appropriate to investigational applications where human reviewers will adjudicate sorted candidate lists. Note that with threshold set to zero, FPIR = 1, i.e. any search without an enrolled mate will return non-mated candidates. Results are sorted and reported into tiers for clarity, with the tiering criteria being rank 1 hit rate on a gallery size of N = 640 000 subjects.*

2021/11/22 08:35:53
FNIR(N, R, T) = False neg. identification rate
FPIR(N, T) = False pos. identification rate
N = Num. enrolled subjects
R = Num. candidates examined
T = Threshold
T = 0 → Investigation
T > 0 → Identification

This publication is available free of charge from: https://doi.org/10.6028/NIST.IR.8271

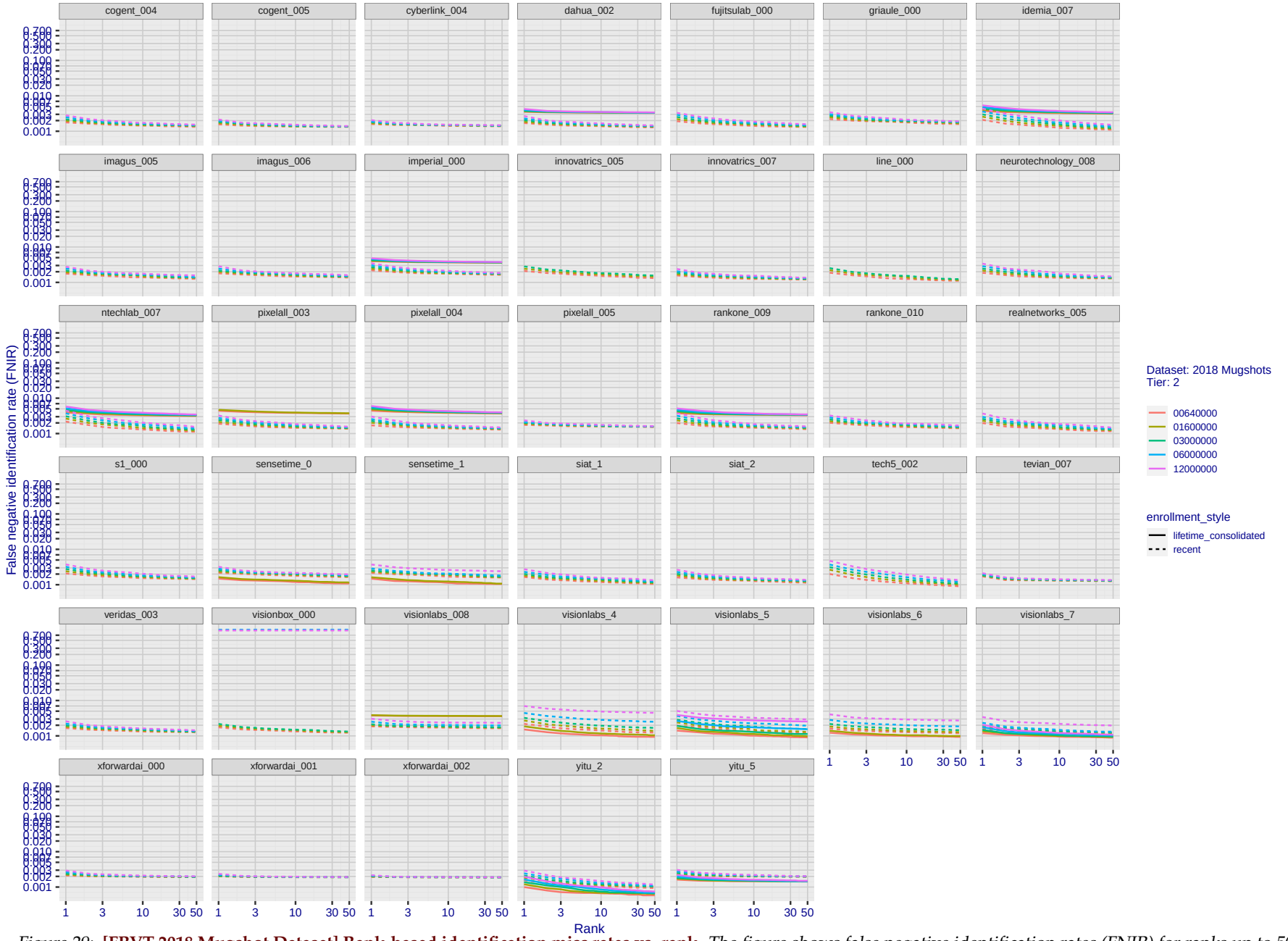

Figure 29: **[FRVT-2018 Mugshot Dataset] Rank-based identification miss rates vs. rank**. *The figure shows false negative identification rates (FNIR) for ranks up to 50. This metric is appropriate to investigational applications where human reviewers will adjudicate sorted candidate lists. Note that with threshold set to zero, FPIR = 1, i.e. any search without an enrolled mate will return non-mated candidates. Results are sorted and reported into tiers for clarity, with the tiering criteria being rank 1 hit rate on a gallery size of N = 640 000 subjects.*

This publication is available free of charge from: https://doi.org/10.6028/NIST.IR.8271

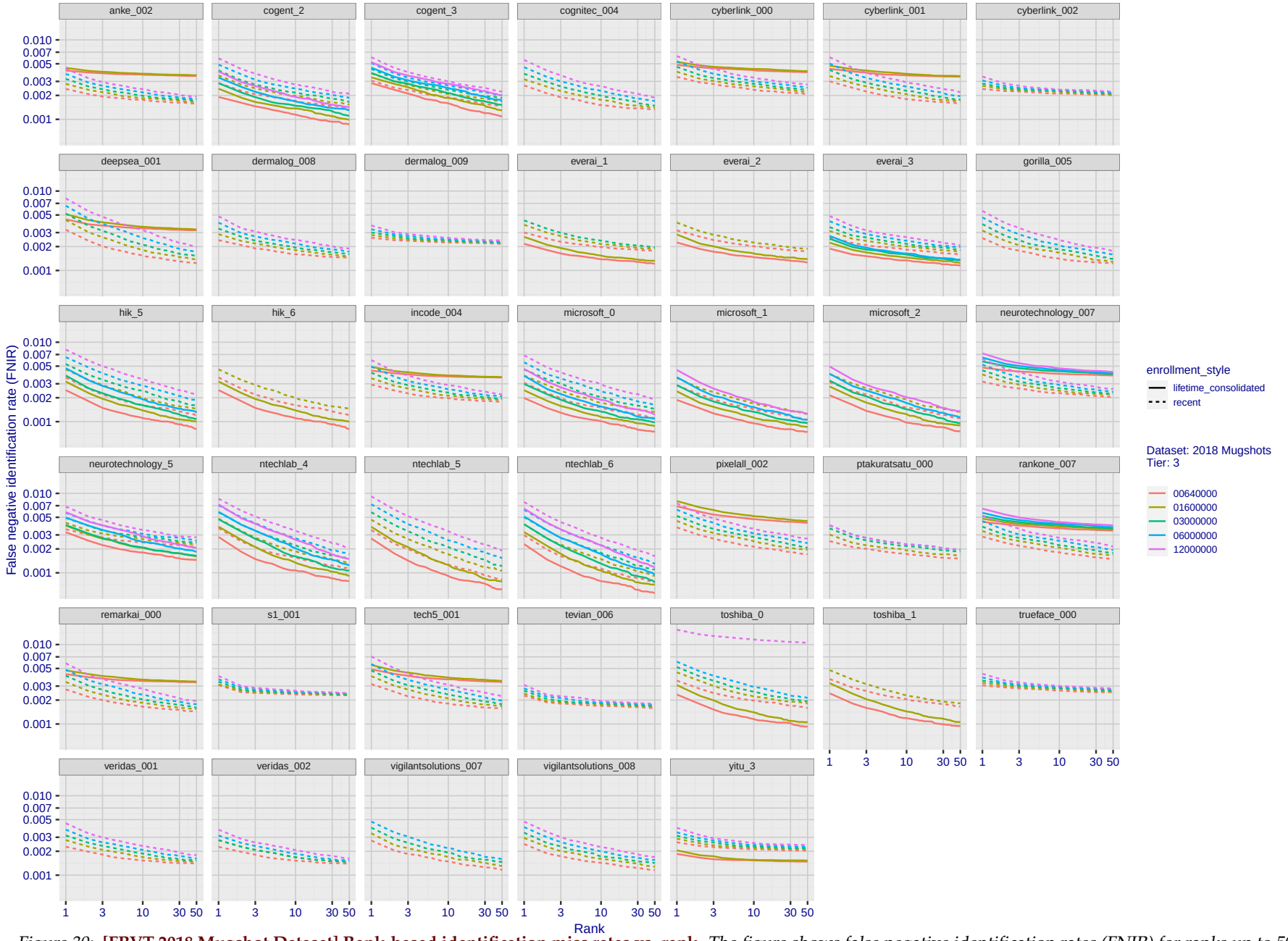

Figure 30: **[FRVT-2018 Mugshot Dataset] Rank-based identification miss rates vs. rank**. *The figure shows false negative identification rates (FNIR) for ranks up to 50. This metric is appropriate to investigational applications where human reviewers will adjudicate sorted candidate lists. Note that with threshold set to zero, FPIR = 1, i.e. any search without an enrolled mate will return non-mated candidates. Results are sorted and reported into tiers for clarity, with the tiering criteria being rank 1 hit rate on a gallery size of N = 640 000 subjects.*

FNIR(N, R, T) =
FPIR(N, T) =

False neg. identification rate
False pos. identification rate

N = Num. enrolled subjects
R = Num. candidates examined

T = Threshold

T = 0 → Investigation
T > 0 → Identification

This publication is available free of charge from: https://doi.org/10.6028/NIST.IR.8271

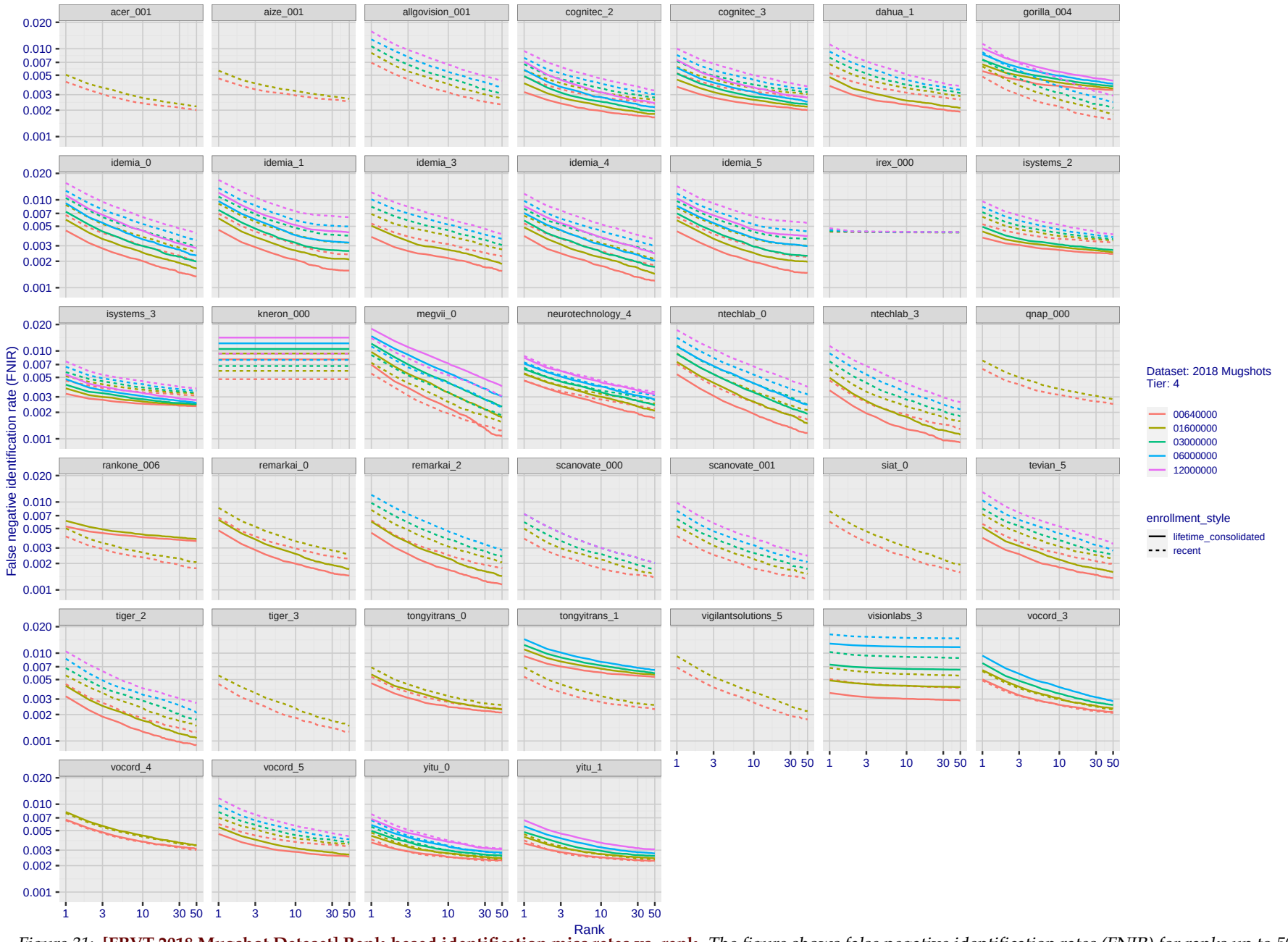

Figure 31: **[FRVT-2018 Mugshot Dataset] Rank-based identification miss rates vs. rank**. *The figure shows false negative identification rates (FNIR) for ranks up to 50. This metric is appropriate to investigational applications where human reviewers will adjudicate sorted candidate lists. Note that with threshold set to zero, FPIR = 1, i.e. any search without an enrolled mate will return non-mated candidates. Results are sorted and reported into tiers for clarity, with the tiering criteria being rank 1 hit rate on a gallery size of N = 640 000 subjects.*

2021/11/22
08:35:53
FNIR(N, R, T) = False neg. identification rate
FPIR(N, T) = False pos. identification rate
N = Num. enrolled subjects
R = Num. candidates examined
T = Threshold
T = 0 → Investigation
T > 0 → Identification

This publication is available free of charge from: https://doi.org/10.6028/NIST.IR.8271

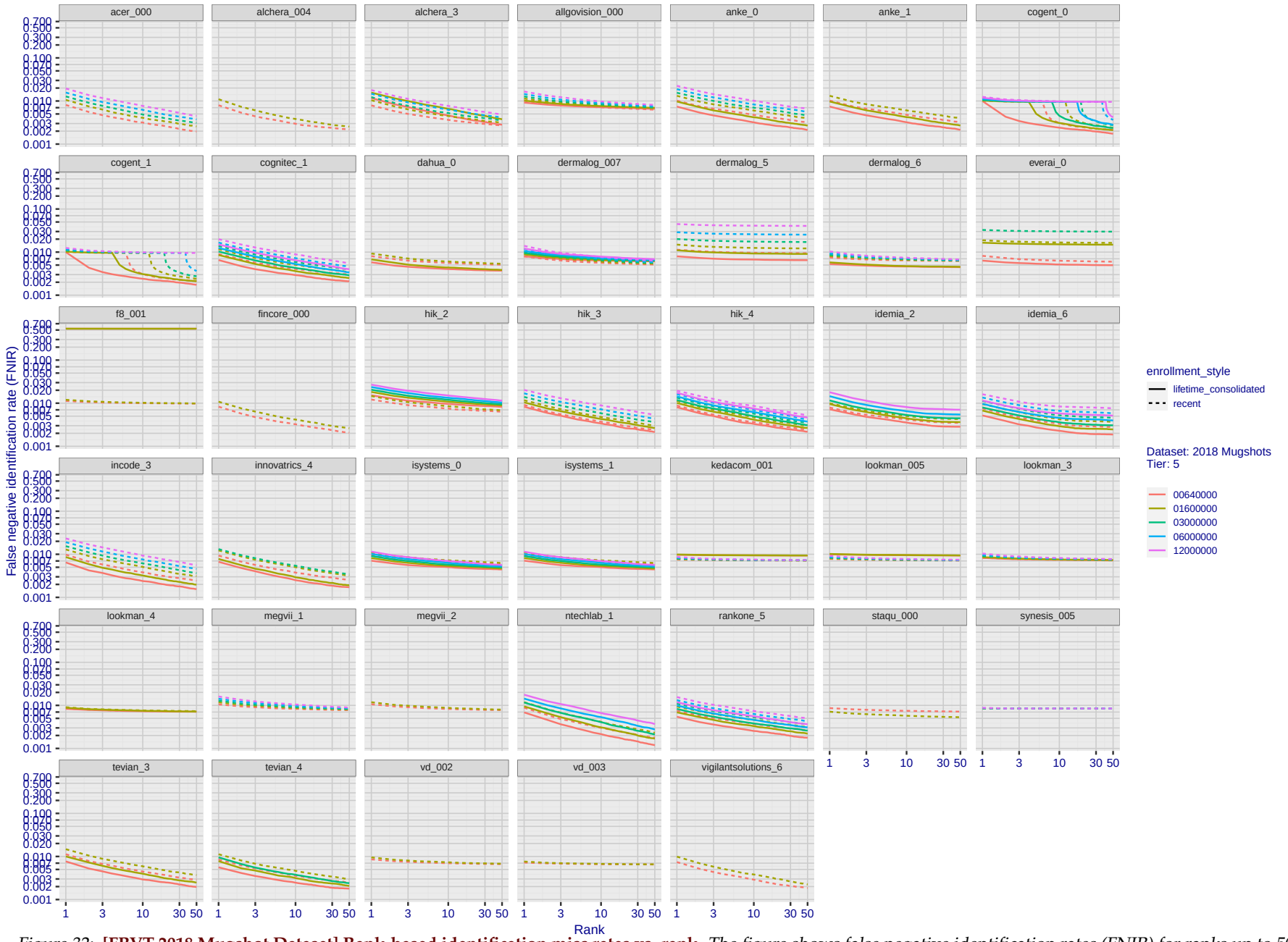

Figure 32: **[FRVT-2018 Mugshot Dataset] Rank-based identification miss rates vs. rank**. *The figure shows false negative identification rates (FNIR) for ranks up to 50. This metric is appropriate to investigational applications where human reviewers will adjudicate sorted candidate lists. Note that with threshold set to zero, FPIR = 1, i.e. any search without an enrolled mate will return non-mated candidates. Results are sorted and reported into tiers for clarity, with the tiering criteria being rank 1 hit rate on a gallery size of N = 640 000 subjects.*

2021/11/22 08:35:53

FNIR(N, R, T) = False neg. identification rate
FPIR(N, T) = False pos. identification rate

N = Num. enrolled subjects
R = Num. candidates examined

T = Threshold

T = 0 → Investigation
T > 0 → Identification

This publication is available free of charge from: https://doi.org/10.6028/NIST.IR.8271

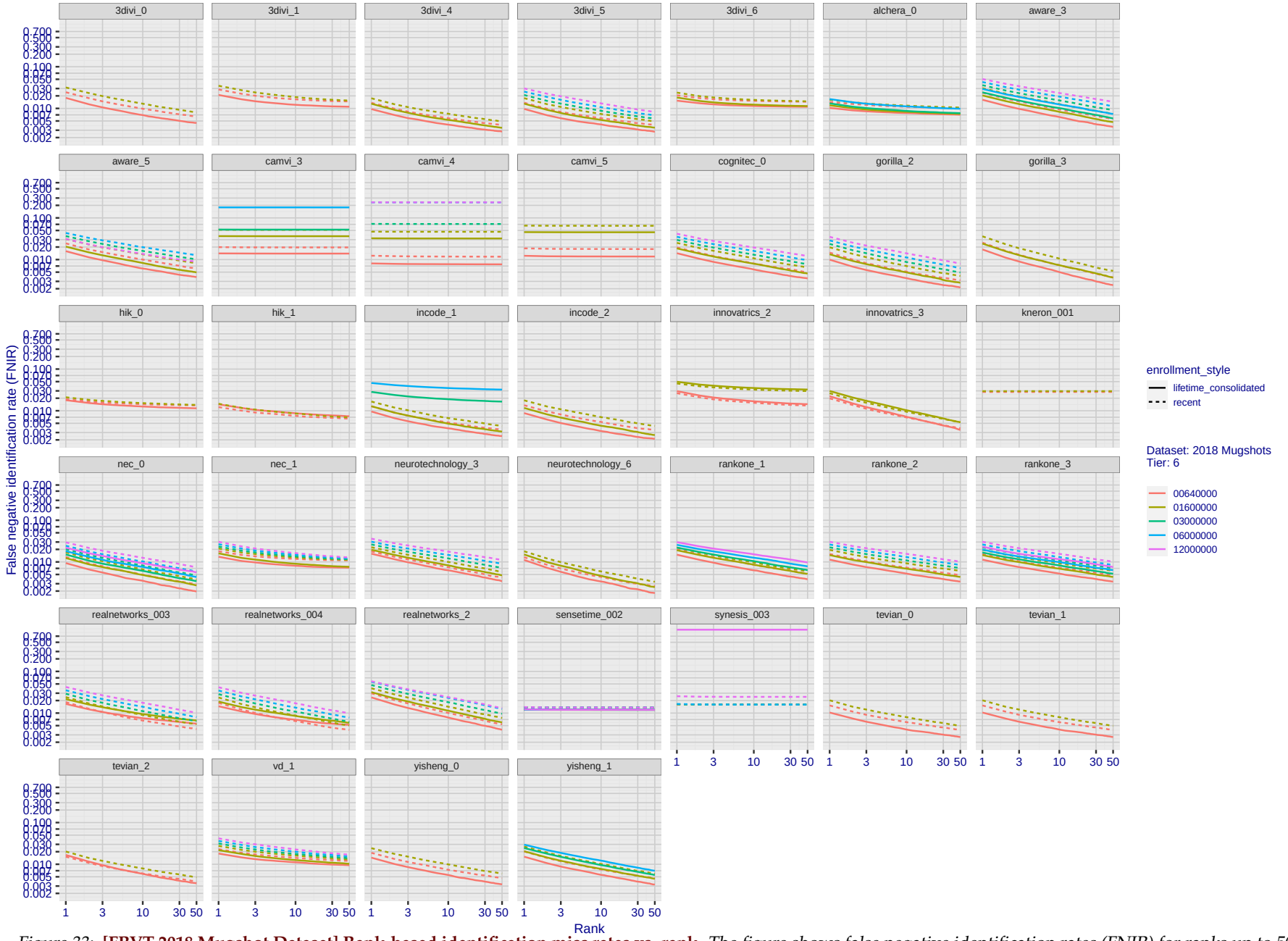

Figure 33: **[FRVT-2018 Mugshot Dataset] Rank-based identification miss rates vs. rank**. *The figure shows false negative identification rates (FNIR) for ranks up to 50. This metric is appropriate to investigational applications where human reviewers will adjudicate sorted candidate lists. Note that with threshold set to zero, FPIR = 1, i.e. any search without an enrolled mate will return non-mated candidates. Results are sorted and reported into tiers for clarity, with the tiering criteria being rank 1 hit rate on a gallery size of N = 640 000 subjects.*

2021/11/22
08:35:53
FNIR(N, R, T) = False neg. identification rate
FPIR(N, T) = False pos. identification rate
N = Num. enrolled subjects
R = Num. candidates examined
T = Threshold
T = 0 → Investigation
T > 0 → Identification

This publication is available free of charge from: https://doi.org/10.6028/NIST.IR.8271

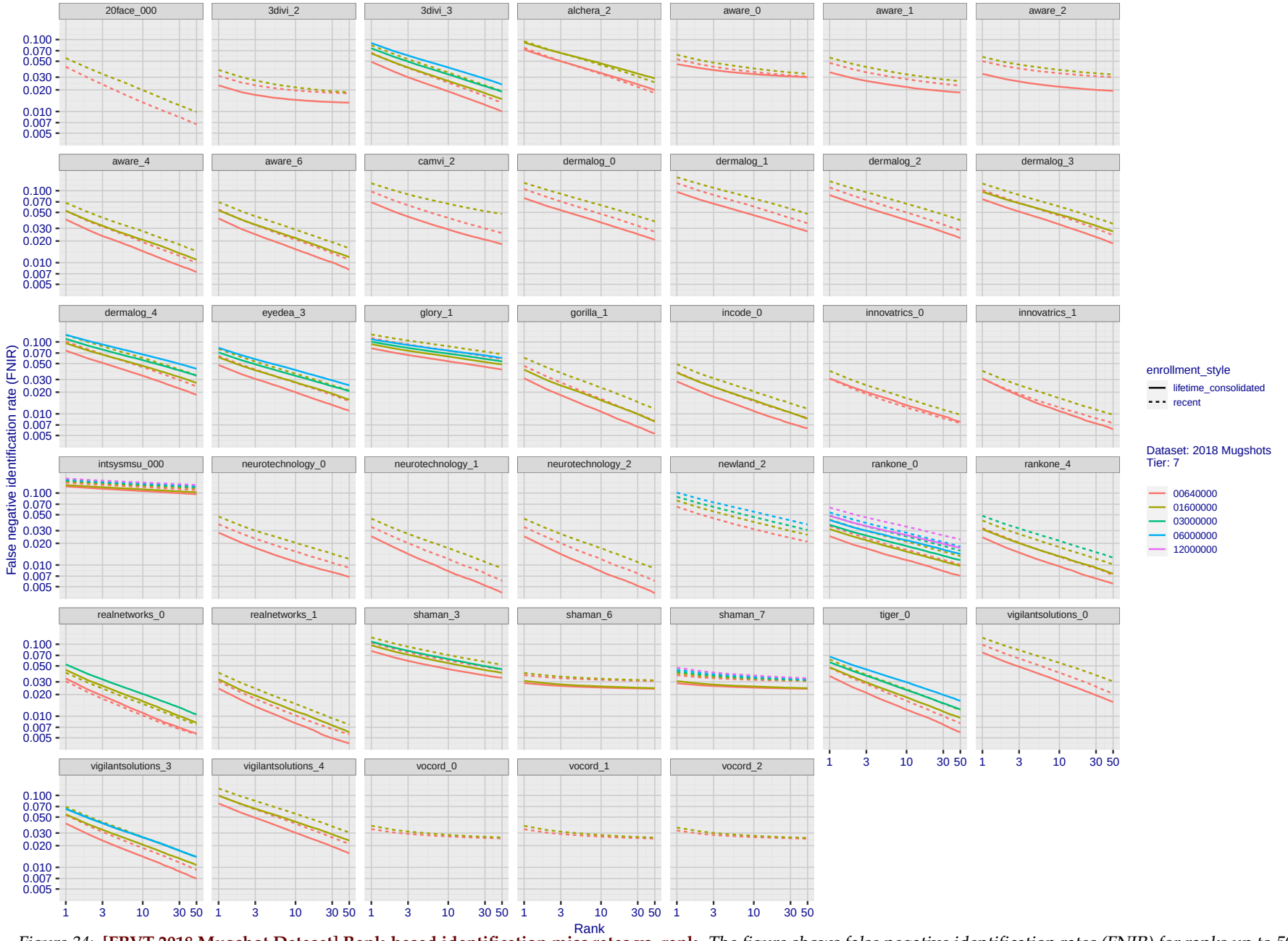

Figure 34: **[FRVT-2018 Mugshot Dataset] Rank-based identification miss rates vs. rank**. *The figure shows false negative identification rates (FNIR) for ranks up to 50. This metric is appropriate to investigational applications where human reviewers will adjudicate sorted candidate lists. Note that with threshold set to zero, FPIR = 1, i.e. any search without an enrolled mate will return non-mated candidates. Results are sorted and reported into tiers for clarity, with the tiering criteria being rank 1 hit rate on a gallery size of N = 640 000 subjects.*

This publication is available free of charge from: https://doi.org/10.6028/NIST.IR.8271

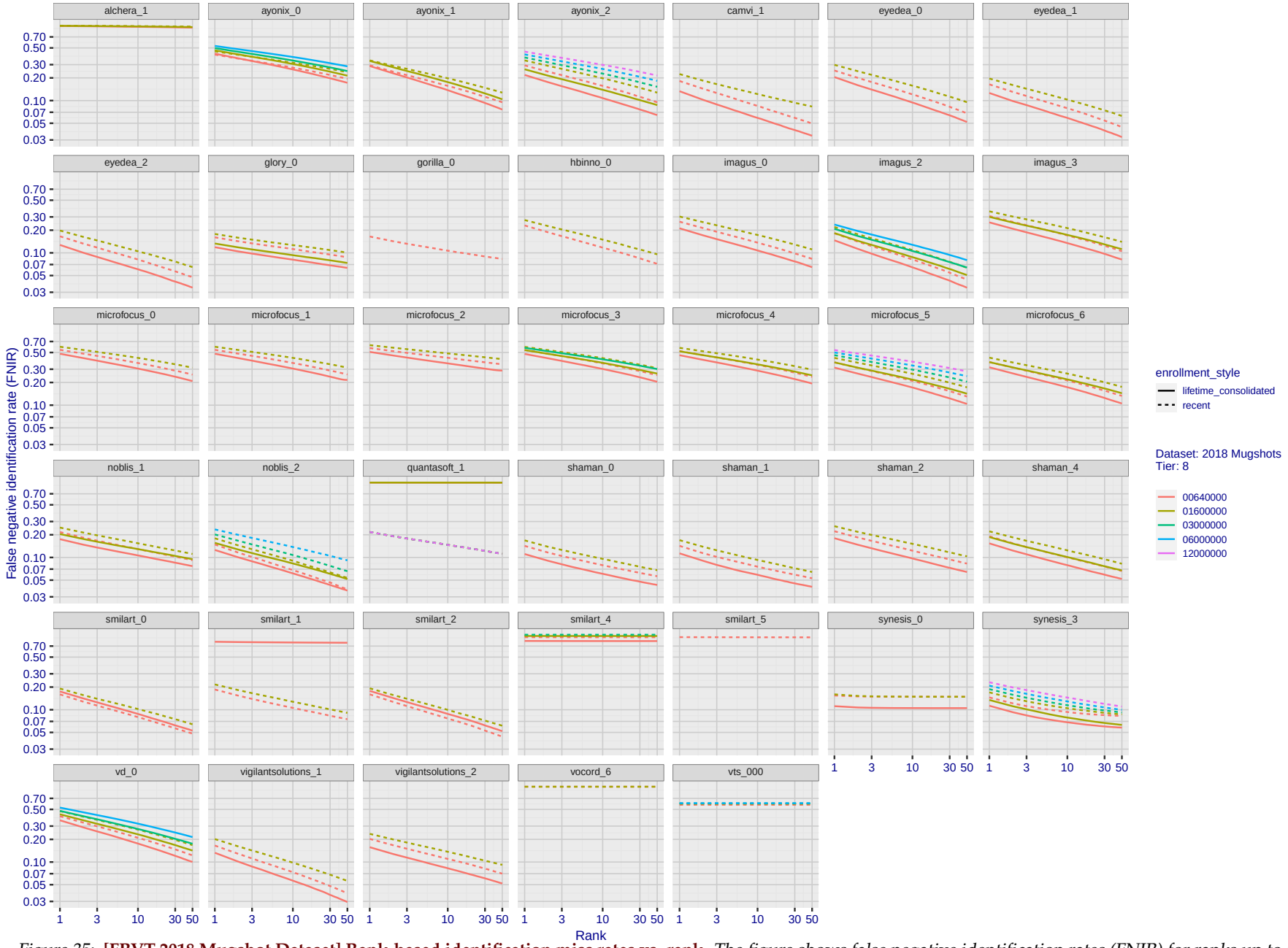

Figure 35: **[FRVT-2018 Mugshot Dataset] Rank-based identification miss rates vs. rank**. *The figure shows false negative identification rates (FNIR) for ranks up to 50. This metric is appropriate to investigational applications where human reviewers will adjudicate sorted candidate lists. Note that with threshold set to zero, FPIR = 1, i.e. any search without an enrolled mate will return non-mated candidates. Results are sorted and reported into tiers for clarity, with the tiering criteria being rank 1 hit rate on a gallery size of N = 640 000 subjects.*

2021/11/22 08:35:53
FNIR(N, R, T) = False neg. identification rate
FPIR(N, T) = False pos. identification rate
N = Num. enrolled subjects
R = Num. candidates examined
T = Threshold
T = 0 → Investigation
T > 0 → Identification

2021/11/22	FNIR(N, R, T) =	False neg. identification rate	N = Num. enrolled subjects	T = Threshold	$T = 0 \rightarrow$ Investigation
08:35:53	FPIR(N, T) =	False pos. identification rate	R = Num. candidates examined		$T > 0 \rightarrow$ Identification

This publication is available free of charge from: https://doi.org/10.6028/NIST.IR.8271

This publication is available free of charge from: https://doi.org/10.6028/NIST.IR.8271

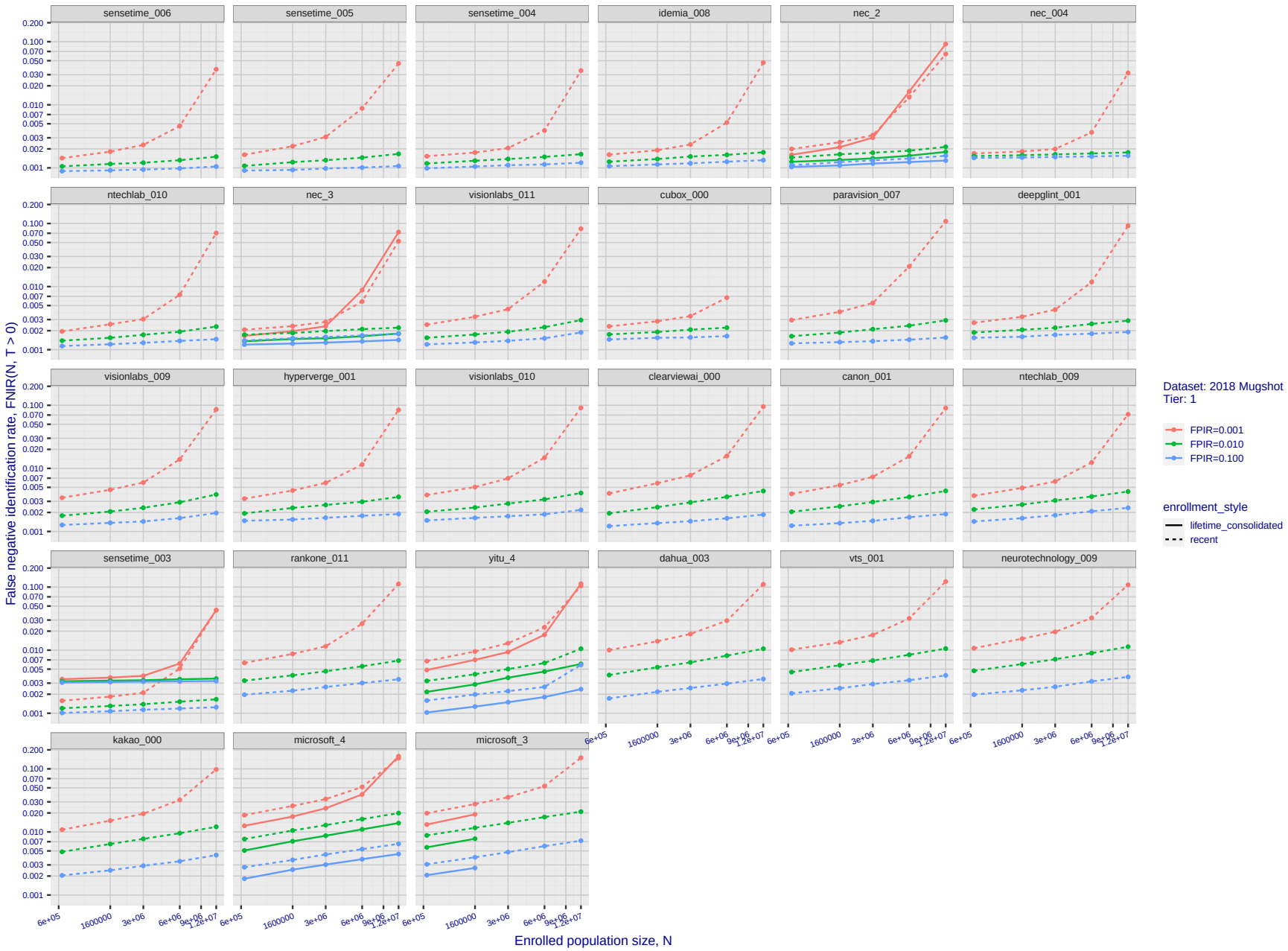

Figure 36: **[FRVT-2018 Mugshot Dataset] Threshold-based identification miss rates vs. number of enrolled subjects**. *The figure shows FNIR(N, T) across various gallery sizes when the threshold is set to achieve the given FPIRs. The rank criterion is irrelevant at high thresholds as mates are always at rank 1. The results are computed from the trials listed in rows 1-10 of Table 1. Less accurate algorithms were not run on large N, so results are missing. For clarity, results are sorted and reported into tiers spanning multiple pages. The tiering criteria is complicated: First paging by FNIR(N_b, 1, 0), then sorting by median FNIR(N_b, T), N_b = 640 000.*

2021/11/22
08:35:53
FNIR(N, R, T) = False neg. identification rate
FPIR(N, T) = False pos. identification rate
N = Num. enrolled subjects
R = Num. candidates examined
T = Threshold
T = 0 → Investigation
T > 0 → Identification

This publication is available free of charge from: https://doi.org/10.6028/NIST.IR.8271

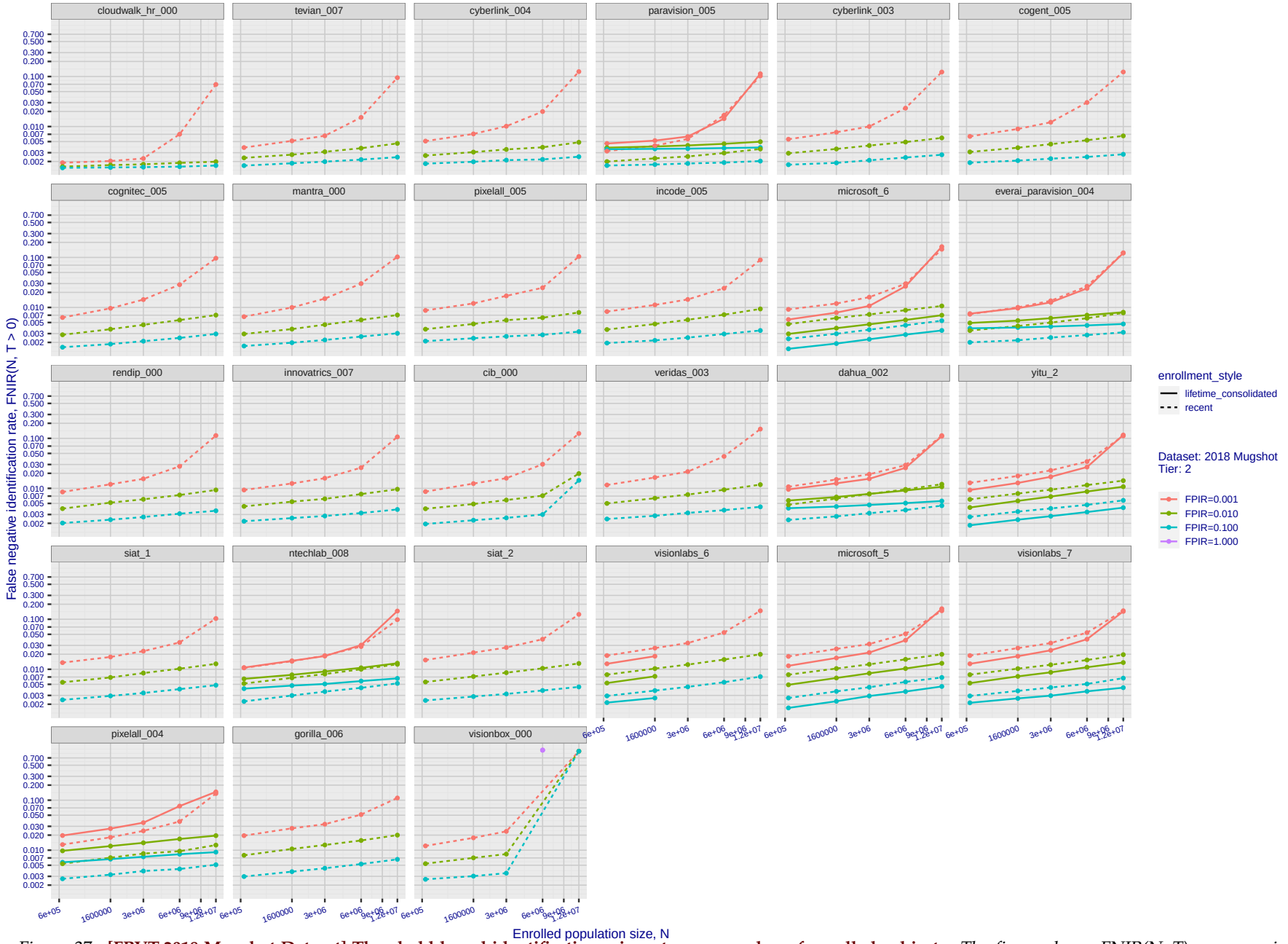

Figure 37: **[FRVT-2018 Mugshot Dataset] Threshold-based identification miss rates vs. number of enrolled subjects**. *The figure shows FNIR(N, T) across various gallery sizes when the threshold is set to achieve the given FPIRs. The rank criterion is irrelevant at high thresholds as mates are always at rank 1. The results are computed from the trials listed in rows 1-10 of Table 1. Less accurate algorithms were not run on large N, so results are missing. For clarity, results are sorted and reported into tiers spanning multiple pages. The tiering criteria is complicated: First paging by FNIR(N_b, 1, 0), then sorting by median FNIR(N_b, T), N_b = 640 000.*

2021/11/22
08:35:53

FNIR(N, R, T) = False neg. identification rate
FPIR(N, T) = False pos. identification rate

N = Num. enrolled subjects
R = Num. candidates examined

T = Threshold

T = 0 → Investigation
T > 0 → Identification

This publication is available free of charge from: https://doi.org/10.6028/NIST.IR.8271

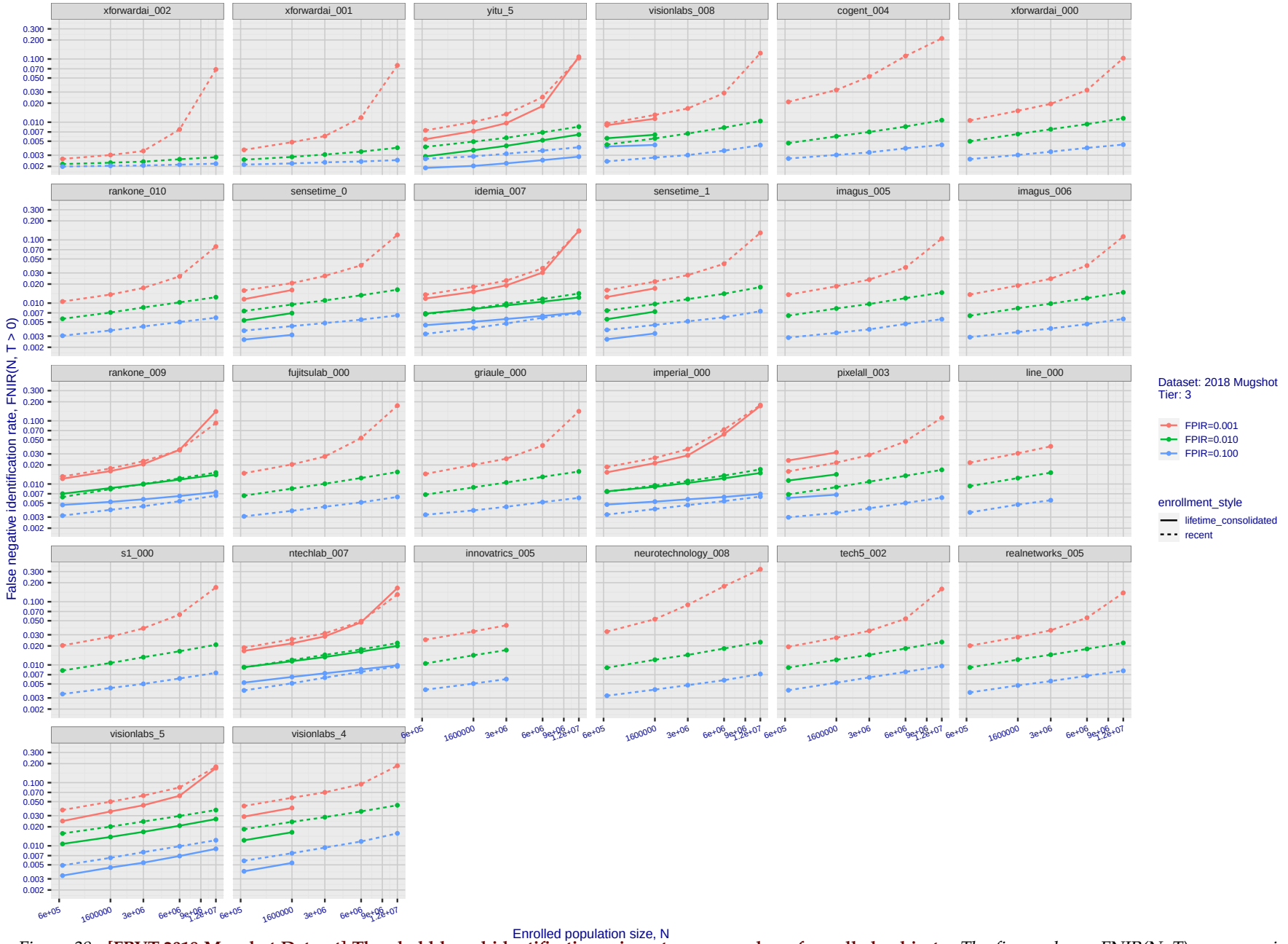

Figure 38: **[FRVT-2018 Mugshot Dataset] Threshold-based identification miss rates vs. number of enrolled subjects**. *The figure shows FNIR(N, T) across various gallery sizes when the threshold is set to achieve the given FPIRs. The rank criterion is irrelevant at high thresholds as mates are always at rank 1. The results are computed from the trials listed in rows 1-10 of Table 1. Less accurate algorithms were not run on large N, so results are missing. For clarity, results are sorted and reported into tiers spanning multiple pages. The tiering criteria is complicated: First paging by FNIR(N_b, 1, 0), then sorting by median FNIR(N_b, T), N_b = 640 000.*

2021/11/22 08:35:53
FNIR(N, R, T) = False neg. identification rate
FPIR(N, T) = False pos. identification rate
N = Num. enrolled subjects
R = Num. candidates examined
T = Threshold
T = 0 → Investigation
T > 0 → Identification

This publication is available free of charge from: https://doi.org/10.6028/NIST.IR.8271

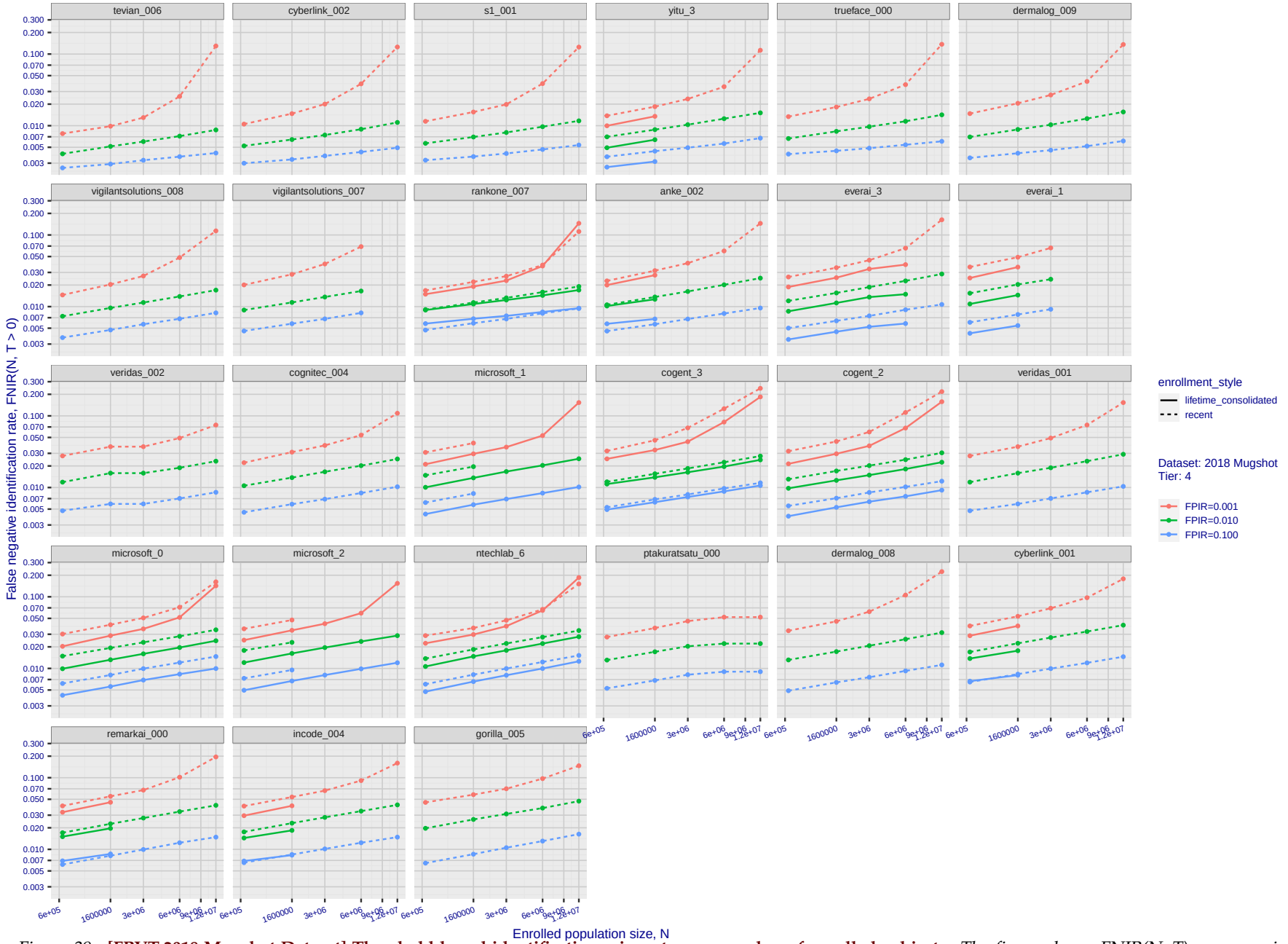

Figure 39: **[FRVT-2018 Mugshot Dataset] Threshold-based identification miss rates vs. number of enrolled subjects**. *The figure shows FNIR(N, T) across various gallery sizes when the threshold is set to achieve the given FPIRs. The rank criterion is irrelevant at high thresholds as mates are always at rank 1. The results are computed from the trials listed in rows 1-10 of Table 1. Less accurate algorithms were not run on large N, so results are missing. For clarity, results are sorted and reported into tiers spanning multiple pages. The tiering criteria is complicated: First paging by FNIR(N_b, 1, 0), then sorting by median FNIR(N_b, T), N_b = 640 000.*

2021/11/22
08:35:53

FNIR(N, R, T) = False neg. identification rate
FPIR(N, T) = False pos. identification rate

N = Num. enrolled subjects
R = Num. candidates examined

T = Threshold

T = 0 → Investigation
T > 0 → Identification

This publication is available free of charge from: https://doi.org/10.6028/NIST.IR.8271

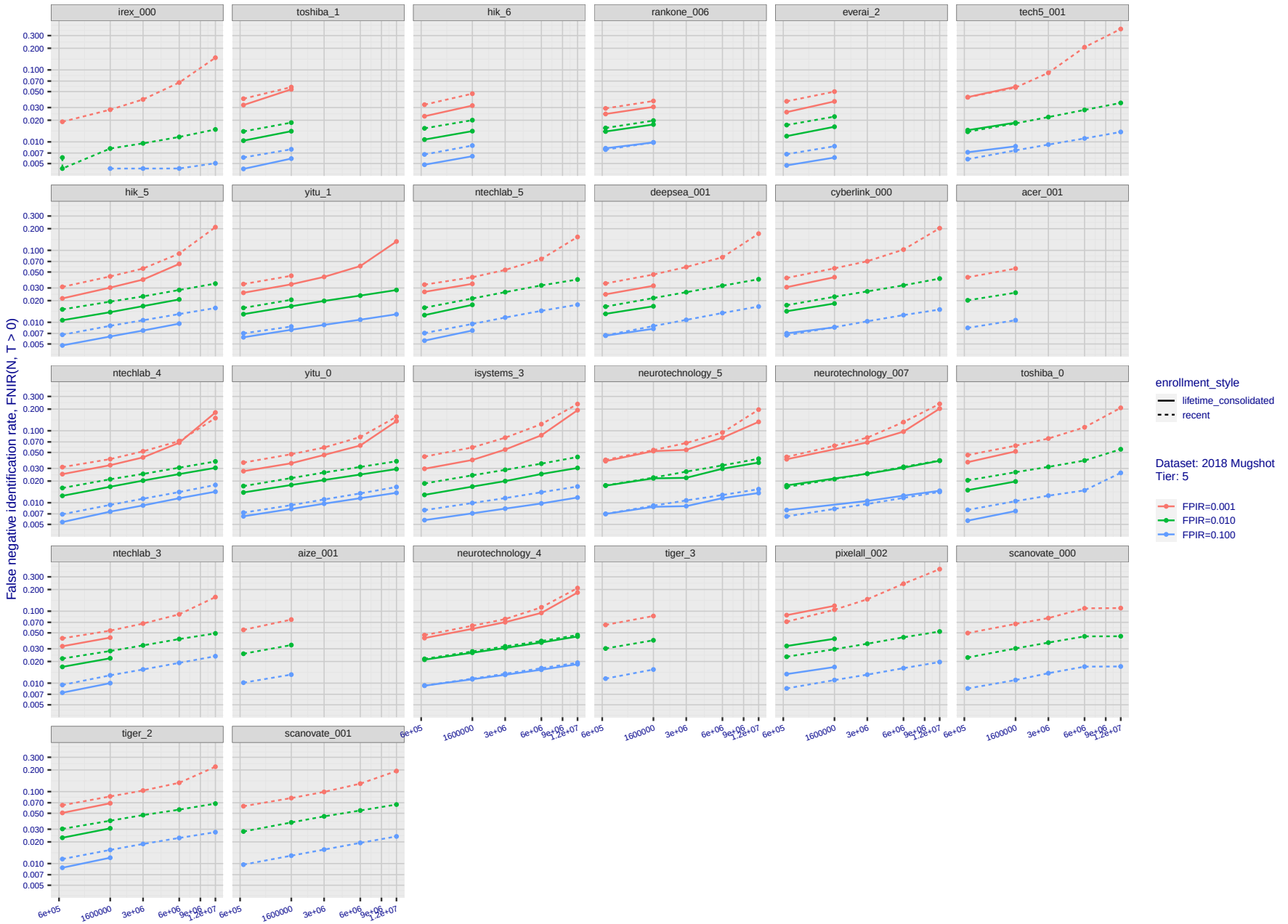

Figure 40: **[FRVT-2018 Mugshot Dataset] Threshold-based identification miss rates vs. number of enrolled subjects**. *The figure shows FNIR(N, T) across various gallery sizes when the threshold is set to achieve the given FPIRs. The rank criterion is irrelevant at high thresholds as mates are always at rank 1. The results are computed from the trials listed in rows 1-10 of Table 1. Less accurate algorithms were not run on large N, so results are missing. For clarity, results are sorted and reported into tiers spanning multiple pages. The tiering criteria is complicated: First paging by FNIR(N_b, 1, 0), then sorting by median FNIR(N_b, T), N_b = 640 000.*

2021/11/22 08:35:53
FNIR(N, R, T) = False neg. identification rate
FPIR(N, T) = False pos. identification rate
N = Num. enrolled subjects
R = Num. candidates examined
T = Threshold
T = 0 → Investigation
T > 0 → Identification

This publication is available free of charge from: https://doi.org/10.6028/NIST.IR.8271

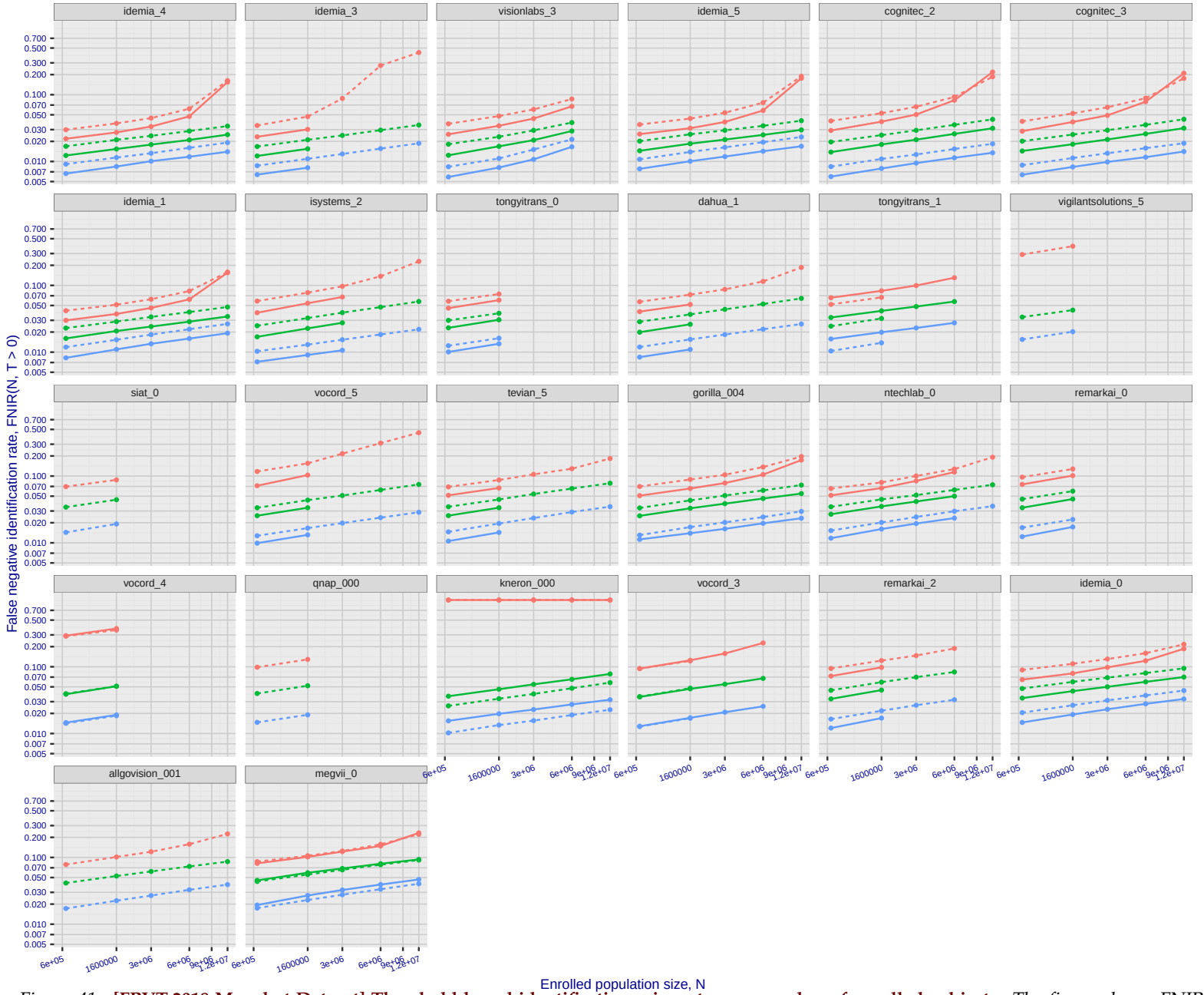

Figure 41: **[FRVT-2018 Mugshot Dataset] Threshold-based identification miss rates vs. number of enrolled subjects**. *The figure shows FNIR(N, T) across various gallery sizes when the threshold is set to achieve the given FPIRs. The rank criterion is irrelevant at high thresholds as mates are always at rank 1. The results are computed from the trials listed in rows 1-10 of Table 1. Less accurate algorithms were not run on large N, so results are missing. For clarity, results are sorted and reported into tiers spanning multiple pages. The tiering criteria is complicated: First paging by FNIR(N_b, 1, 0), then sorting by median FNIR(N_b, T), N_b = 640 000.*

FNIR(N, R, T) = False neg. identification rate
FPIR(N, T) = False pos. identification rate
N = Num. enrolled subjects
R = Num. candidates examined
T = Threshold
T = 0 → Investigation
T > 0 → Identification

This publication is available free of charge from: https://doi.org/10.6028/NIST.IR.8271

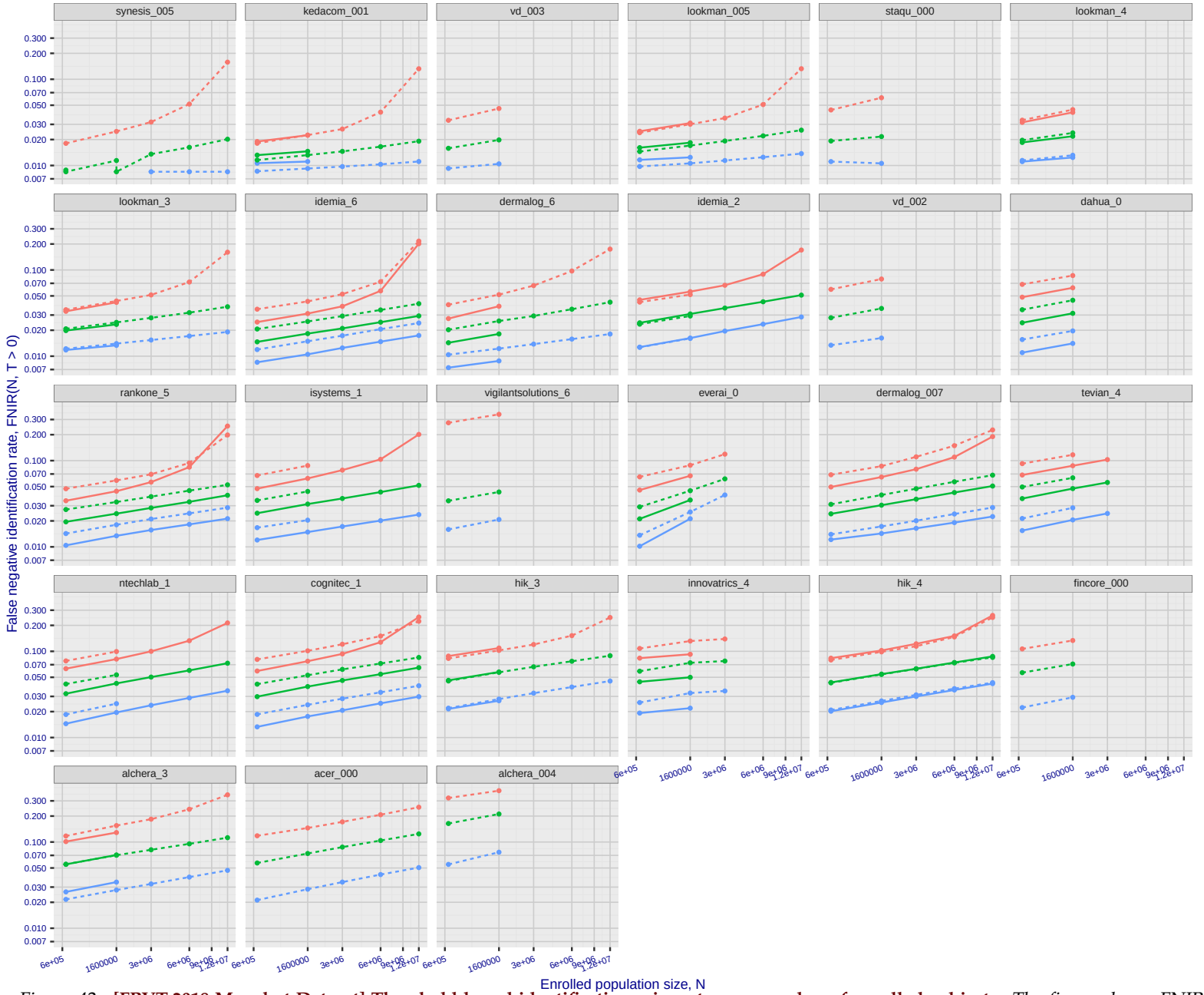

Figure 42: **[FRVT-2018 Mugshot Dataset] Threshold-based identification miss rates vs. number of enrolled subjects**. *The figure shows FNIR(N, T) across various gallery sizes when the threshold is set to achieve the given FPIRs. The rank criterion is irrelevant at high thresholds as mates are always at rank 1. The results are computed from the trials listed in rows 1-10 of Table 1. Less accurate algorithms were not run on large N, so results are missing. For clarity, results are sorted and reported into tiers spanning multiple pages. The tiering criteria is complicated: First paging by FNIR(N_b, 1, 0), then sorting by median FNIR(N_b, T), N_b = 640 000.*

FNIR(N, R, T) = False neg. identification rate
FPIR(N, T) = False pos. identification rate

N = Num. enrolled subjects
R = Num. candidates examined

T = Threshold

T = 0 → Investigation
T > 0 → Identification

This publication is available free of charge from: https://doi.org/10.6028/NIST.IR.8271

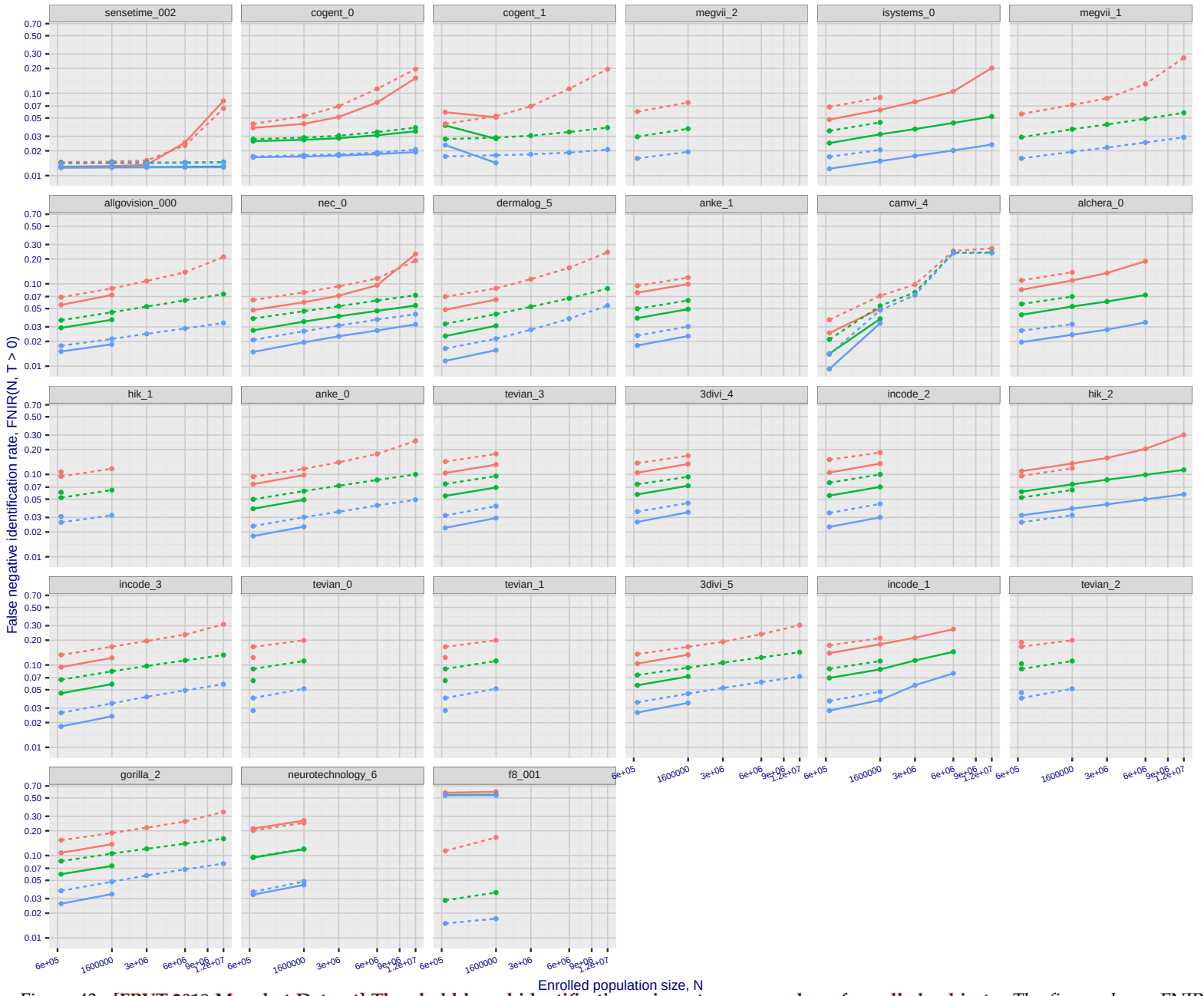

Figure 43: **[FRVT-2018 Mugshot Dataset] Threshold-based identification miss rates vs. number of enrolled subjects**. *The figure shows FNIR(N, T) across various gallery sizes when the threshold is set to achieve the given FPIRs. The rank criterion is irrelevant at high thresholds as mates are always at rank 1. The results are computed from the trials listed in rows 1-10 of Table 1. Less accurate algorithms were not run on large N, so results are missing. For clarity, results are sorted and reported into tiers spanning multiple pages. The tiering criteria is complicated: First paging by FNIR(N_b, 1, 0), then sorting by median FNIR(N_b, T), N_b = 640 000.*

2021/11/22 08:35:53
FNIR(N, R, T) = False neg. identification rate
FPIR(N, T) = False pos. identification rate
N = Num. enrolled subjects
R = Num. candidates examined
T = Threshold
T = 0 → Investigation
T > 0 → Identification

This publication is available free of charge from: https://doi.org/10.6028/NIST.IR.8271

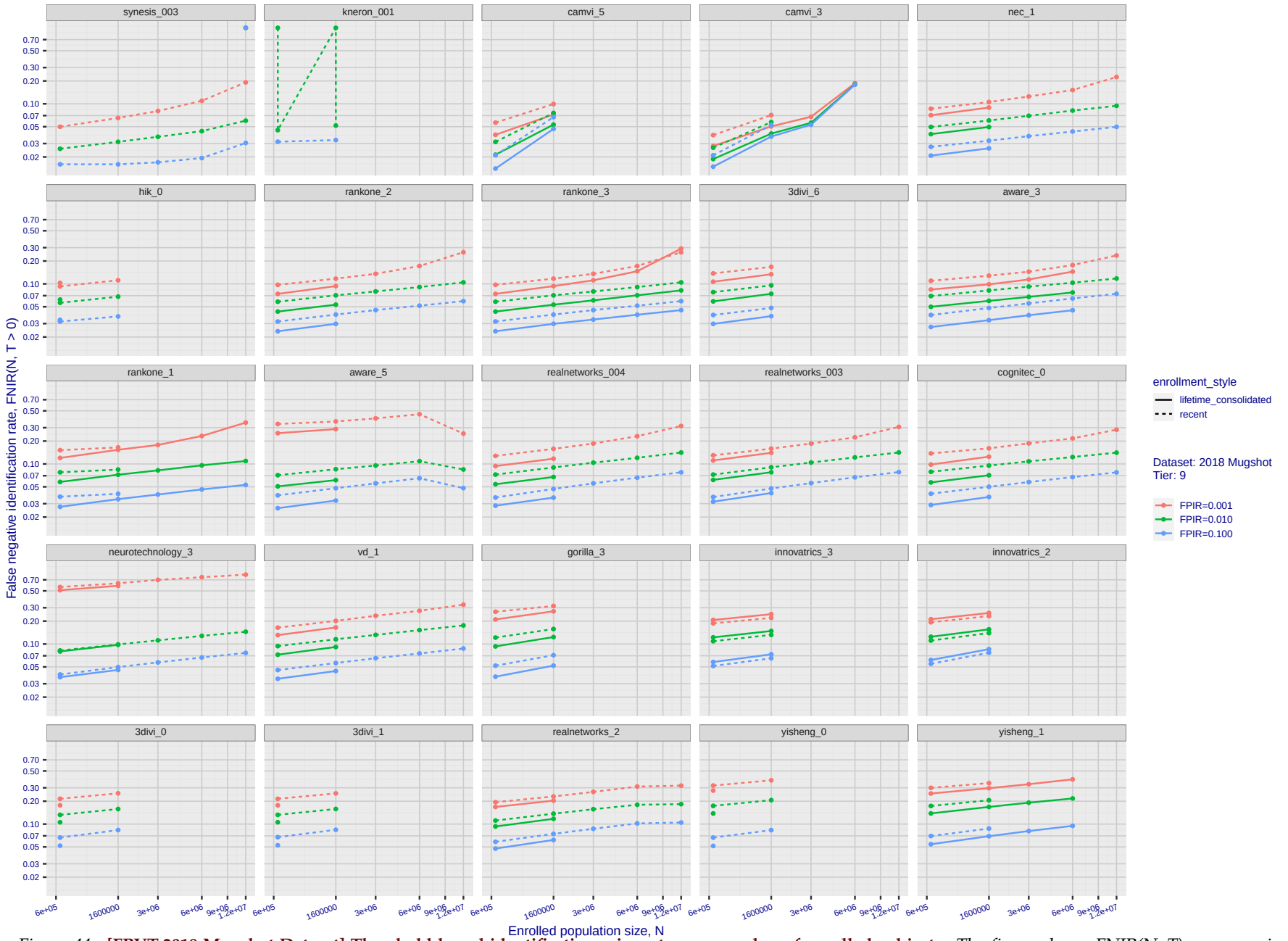

Figure 44: **[FRVT-2018 Mugshot Dataset] Threshold-based identification miss rates vs. number of enrolled subjects**. *The figure shows FNIR(N, T) across various gallery sizes when the threshold is set to achieve the given FPIRs. The rank criterion is irrelevant at high thresholds as mates are always at rank 1. The results are computed from the trials listed in rows 1-10 of Table 1. Less accurate algorithms were not run on large N, so results are missing. For clarity, results are sorted and reported into tiers spanning multiple pages. The tiering criteria is complicated: First paging by FNIR(N_b, 1, 0), then sorting by median FNIR(N_b, T), N_b = 640 000.*

2021/11/22 08:35:53

FNIR(N, R, T) = False neg. identification rate
FPIR(N, T) = False pos. identification rate

N = Num. enrolled subjects
R = Num. candidates examined

T = Threshold

T = 0 → Investigation
T > 0 → Identification

This publication is available free of charge from: https://doi.org/10.6028/NIST.IR.8271

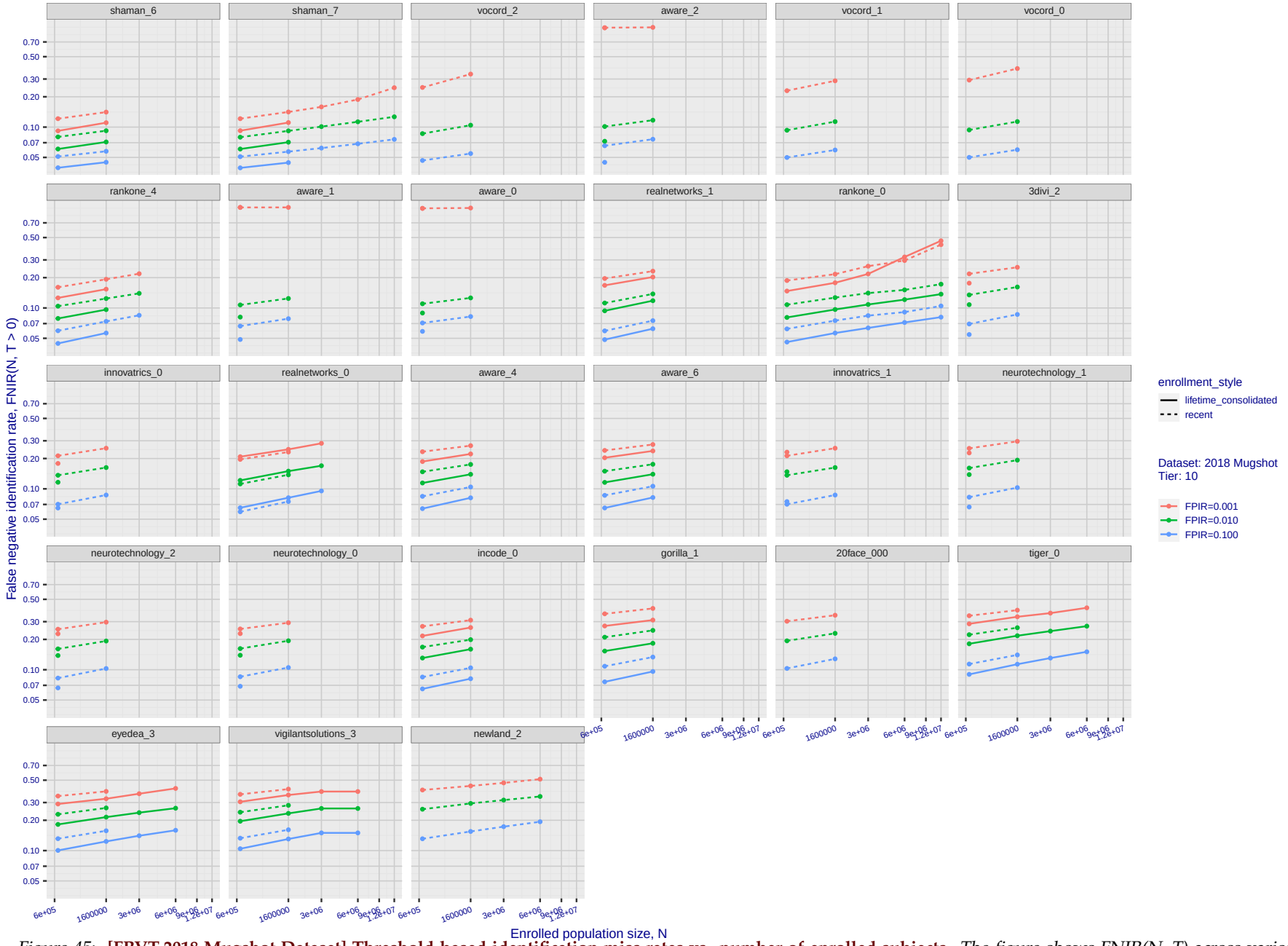

Figure 45: **[FRVT-2018 Mugshot Dataset] Threshold-based identification miss rates vs. number of enrolled subjects**. *The figure shows FNIR(N, T) across various gallery sizes when the threshold is set to achieve the given FPIRs. The rank criterion is irrelevant at high thresholds as mates are always at rank 1. The results are computed from the trials listed in rows 1-10 of Table 1. Less accurate algorithms were not run on large N, so results are missing. For clarity, results are sorted and reported into tiers spanning multiple pages. The tiering criteria is complicated: First paging by FNIR(N_b, 1, 0), then sorting by median FNIR(N_b, T), N_b = 640 000.*

This publication is available free of charge from: https://doi.org/10.6028/NIST.IR.8271

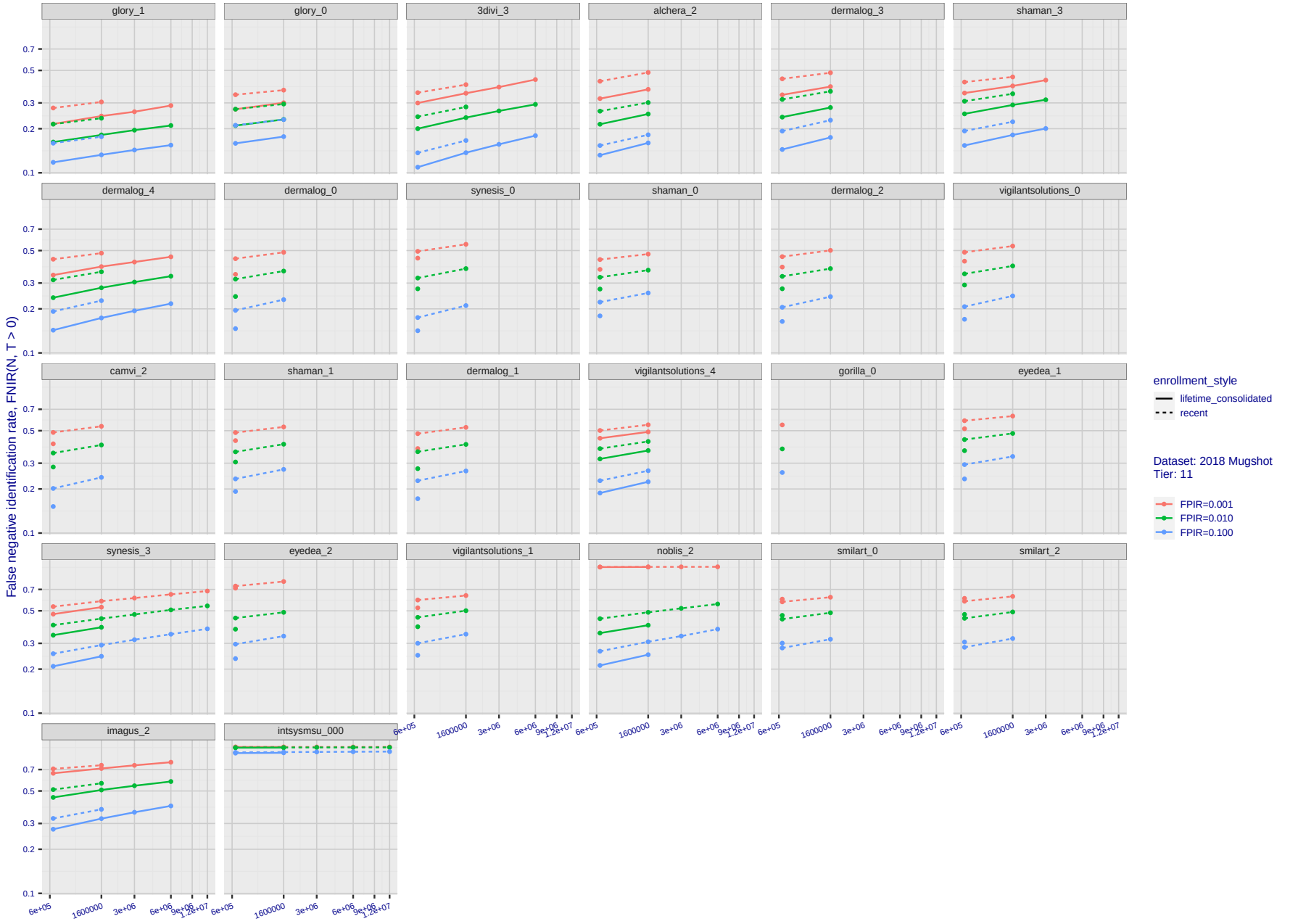

Figure 46: **[FRVT-2018 Mugshot Dataset] Threshold-based identification miss rates vs. number of enrolled subjects**. *The figure shows FNIR(N, T) across various gallery sizes when the threshold is set to achieve the given FPIRs. The rank criterion is irrelevant at high thresholds as mates are always at rank 1. The results are computed from the trials listed in rows 1-10 of Table 1. Less accurate algorithms were not run on large N, so results are missing. For clarity, results are sorted and reported into tiers spanning multiple pages. The tiering criteria is complicated: First paging by FNIR(N_b, 1, 0), then sorting by median FNIR(N_b, T), N_b = 640 000.*

This publication is available free of charge from: https://doi.org/10.6028/NIST.IR.8271

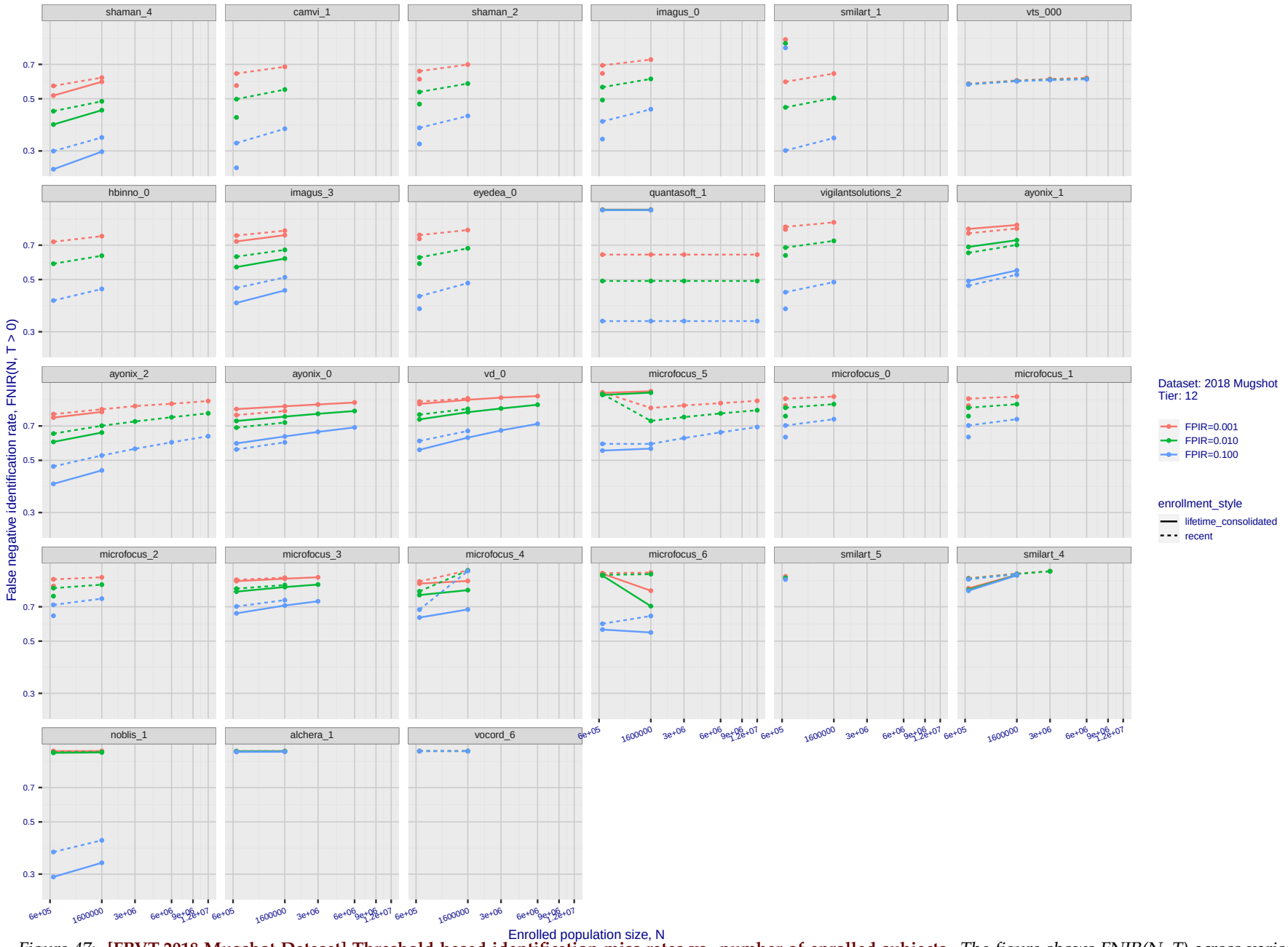

Figure 47: **[FRVT-2018 Mugshot Dataset] Threshold-based identification miss rates vs. number of enrolled subjects**. *The figure shows FNIR(N, T) across various gallery sizes when the threshold is set to achieve the given FPIRs. The rank criterion is irrelevant at high thresholds as mates are always at rank 1. The results are computed from the trials listed in rows 1-10 of Table 1. Less accurate algorithms were not run on large N, so results are missing. For clarity, results are sorted and reported into tiers spanning multiple pages. The tiering criteria is complicated: First paging by FNIR(N_b, 1, 0), then sorting by median FNIR(N_b, T), N_b = 640 000.*

2021/11/22
08:35:53

FNIR(N, R, T) = False neg. identification rate
FPIR(N, T) = False pos. identification rate
N = Num. enrolled subjects
R = Num. candidates examined
T = Threshold
T = 0 → Investigation
T > 0 → Identification

2021/11/22	FNIR(N, R, T) =	False neg. identification rate	N = Num. enrolled subjects	T = Threshold	$T = 0 \rightarrow$ Investigation
08:35:53	FPIR(N, T) =	False pos. identification rate	R = Num. candidates examined		$T > 0 \rightarrow$ Identification

This publication is available free of charge from: https://doi.org/10.6028/NIST.IR.8271

This publication is available free of charge from: https://doi.org/10.6028/NIST.IR.8271

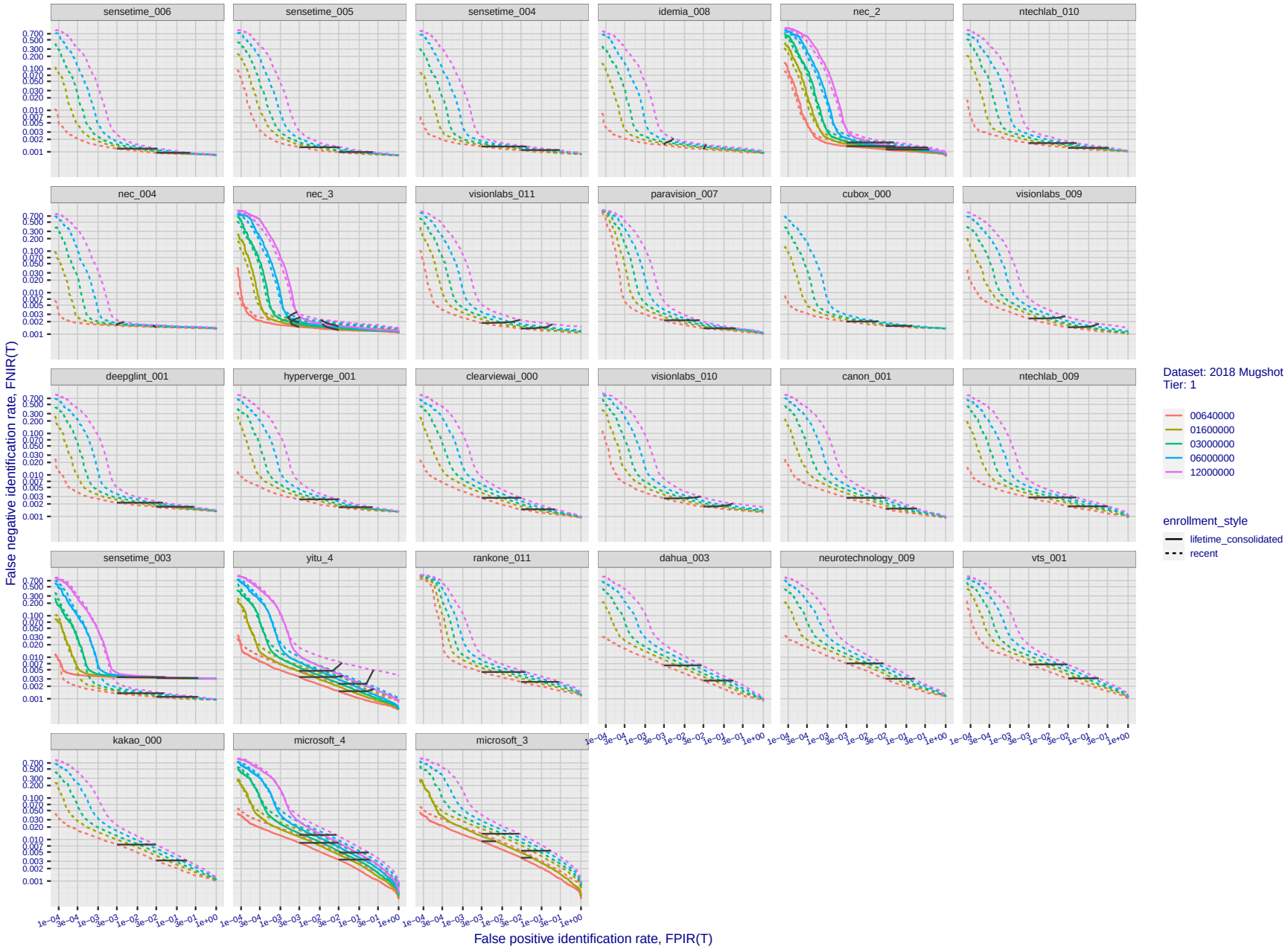

2021/11/22 08:35:53

FNIR(N, R, T) = False neg. identification rate
FPIR(N, T) = False pos. identification rate

N = Num. enrolled subjects
R = Num. candidates examined

T = Threshold

T = 0 → Investigation
T > 0 → Identification

Figure 48: **[FRVT-2018 Mugshot Dataset] Identification miss rates vs. false positive rates**. *The figure shows miss rates FNIR(N, L, T) as a function of FPIR(N, T), with N ranging from 640 000 to 12 000 000 as noted in rows 1-10 of Table 1. These error tradeoff characteristics are useful for applications where a threshold must be elevated to limit false positives, such as when human reviewer labor is not matched to the volume of searches. Dark lines join points of equal threshold: If horizontal, FPIR(T) rises with N, and mate scores are independent of N. Other algorithms adjust scores in an attempt to make FPIR independent of N.*

This publication is available free of charge from: https://doi.org/10.6028/NIST.IR.8271

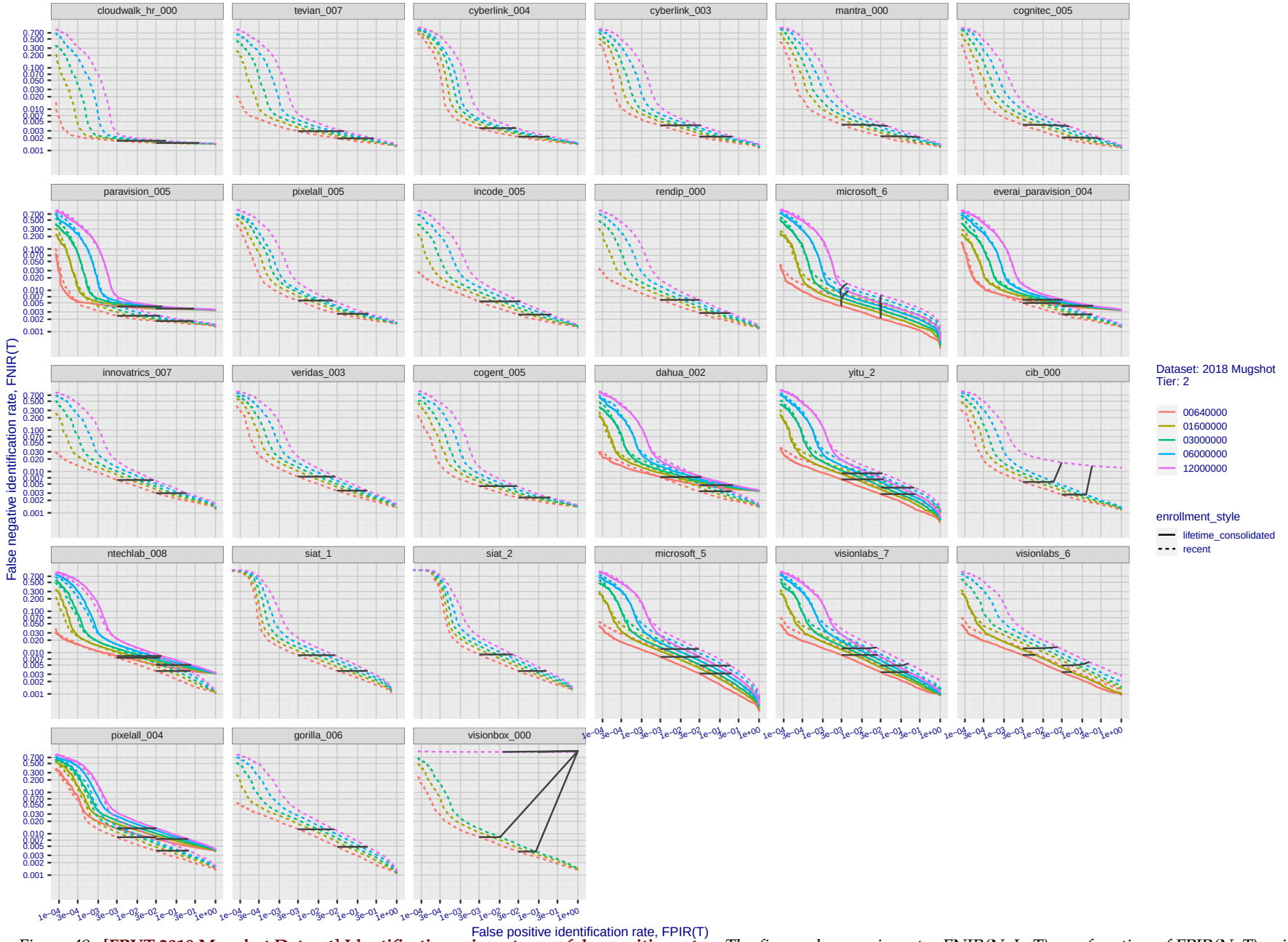

Figure 49: **[FRVT-2018 Mugshot Dataset] Identification miss rates vs. false positive rates**. *The figure shows miss rates FNIR(N, L, T) as a function of FPIR(N, T), with N ranging from 640 000 to 12 000 000 as noted in rows 1-10 of Table 1. These error tradeoff characteristics are useful for applications where a threshold must be elevated to limit false positives, such as when human reviewer labor is not matched to the volume of searches. Dark lines join points of equal threshold: If horizontal, FPIR(T) rises with N, and mate scores are independent of N. Other algorithms adjust scores in an attempt to make FPIR independent of N.*

This publication is available free of charge from: https://doi.org/10.6028/NIST.IR.8271

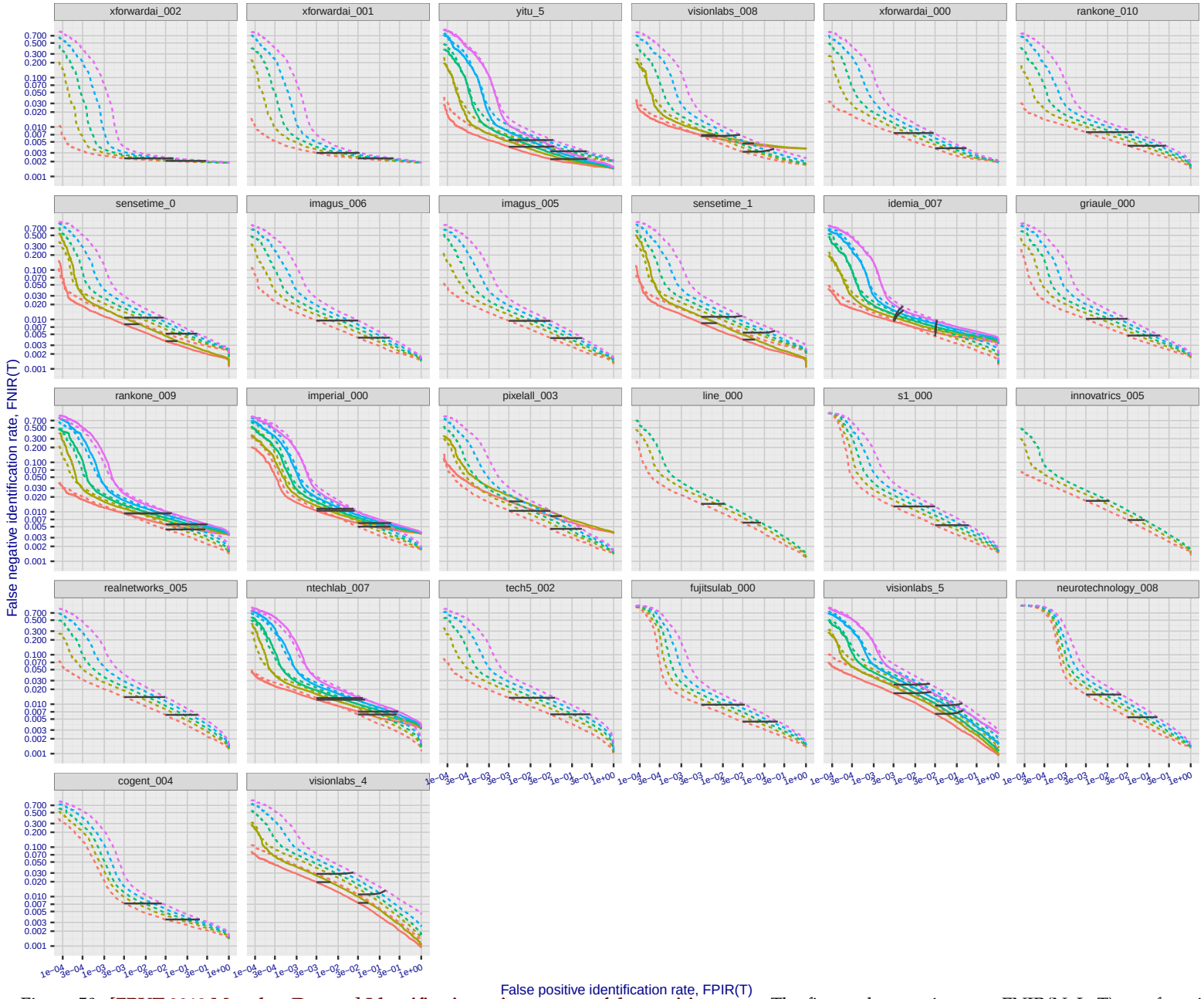

Figure 50: **[FRVT-2018 Mugshot Dataset] Identification miss rates vs. false positive rates**. *The figure shows miss rates FNIR(N, L, T) as a function of FPIR(N, T), with N ranging from 640 000 to 12 000 000 as noted in rows 1-10 of Table 1. These error tradeoff characteristics are useful for applications where a threshold must be elevated to limit false positives, such as when human reviewer labor is not matched to the volume of searches. Dark lines join points of equal threshold: If horizontal, FPIR(T) rises with N, and mate scores are independent of N. Other algorithms adjust scores in an attempt to make FPIR independent of N.*

2021/11/22
08:35:53
FNIR(N, R, T) = False neg. identification rate
FPIR(N, T) = False pos. identification rate
N = Num. enrolled subjects
R = Num. candidates examined
T = Threshold
T = 0 → Investigation
T > 0 → Identification

This publication is available free of charge from: https://doi.org/10.6028/NIST.IR.8271

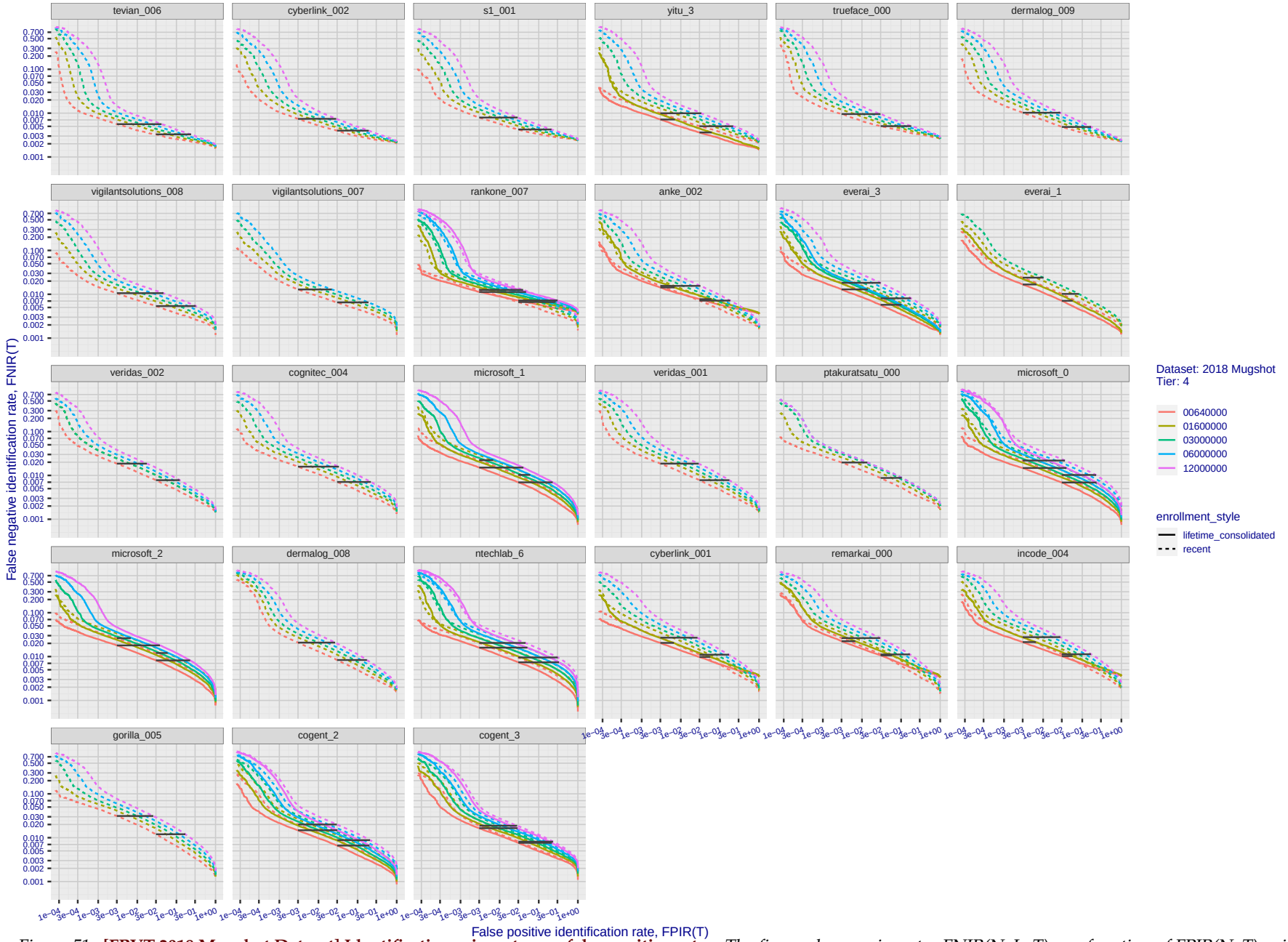

Figure 51: **[FRVT-2018 Mugshot Dataset] Identification miss rates vs. false positive rates**. *The figure shows miss rates FNIR(N, L, T) as a function of FPIR(N, T), with N ranging from 640 000 to 12 000 000 as noted in rows 1-10 of Table 1. These error tradeoff characteristics are useful for applications where a threshold must be elevated to limit false positives, such as when human reviewer labor is not matched to the volume of searches. Dark lines join points of equal threshold: If horizontal, FPIR(T) rises with N, and mate scores are independent of N. Other algorithms adjust scores in an attempt to make FPIR independent of N.*

This publication is available free of charge from: https://doi.org/10.6028/NIST.IR.8271

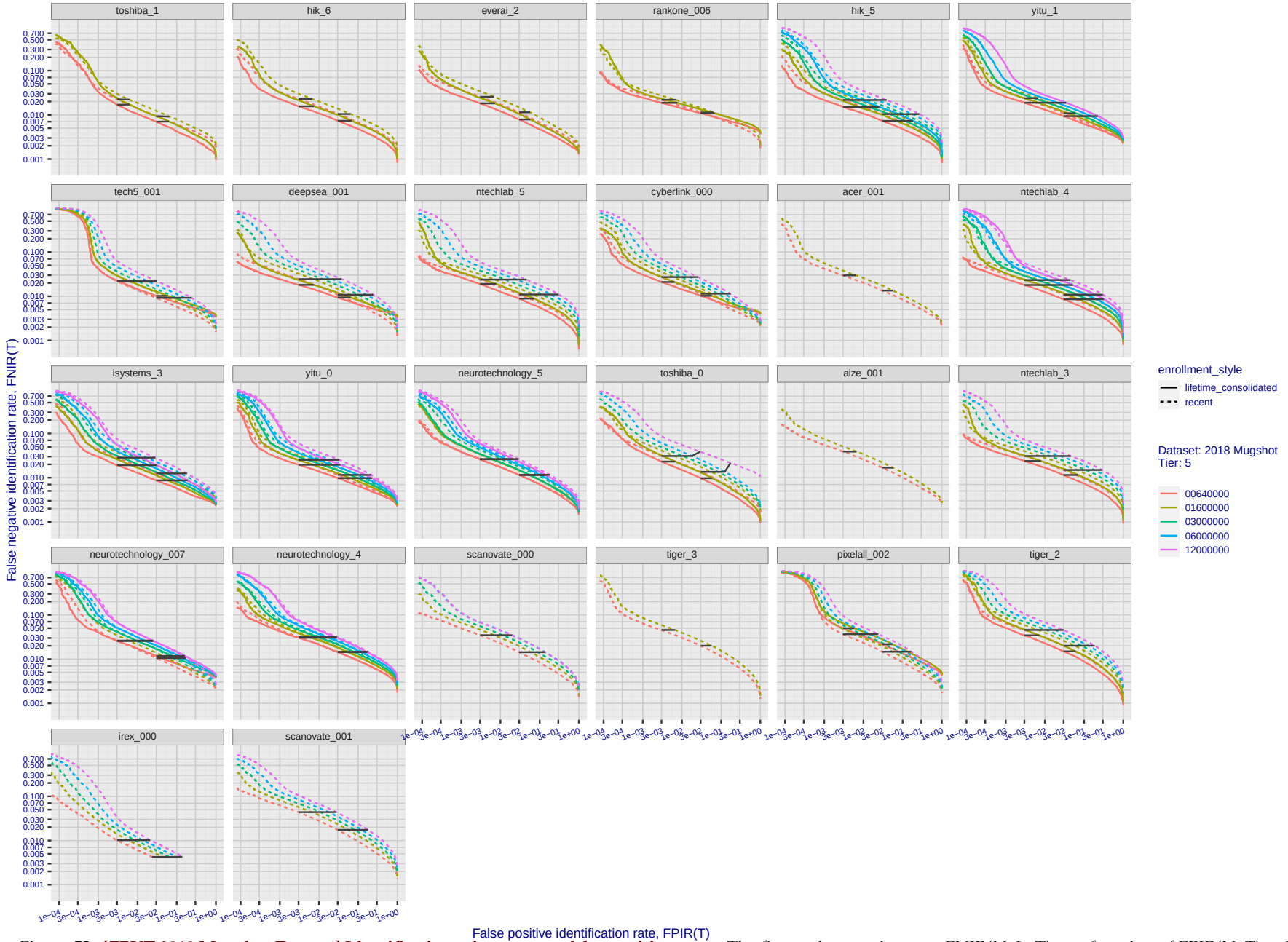

Figure 52: **[FRVT-2018 Mugshot Dataset] Identification miss rates vs. false positive rates**. *The figure shows miss rates FNIR(N, L, T) as a function of FPIR(N, T), with N ranging from 640 000 to 12 000 000 as noted in rows 1-10 of Table 1. These error tradeoff characteristics are useful for applications where a threshold must be elevated to limit false positives, such as when human reviewer labor is not matched to the volume of searches. Dark lines join points of equal threshold: If horizontal, FPIR(T) rises with N, and mate scores are independent of N. Other algorithms adjust scores in an attempt to make FPIR independent of N.*

2021/11/22
08:35:53

FNIR(N, R, T) = False neg. identification rate
FPIR(N, T) = False pos. identification rate

N = Num. enrolled subjects
R = Num. candidates examined

T = Threshold

T = 0 → Investigation
T > 0 → Identification

This publication is available free of charge from: https://doi.org/10.6028/NIST.IR.8271

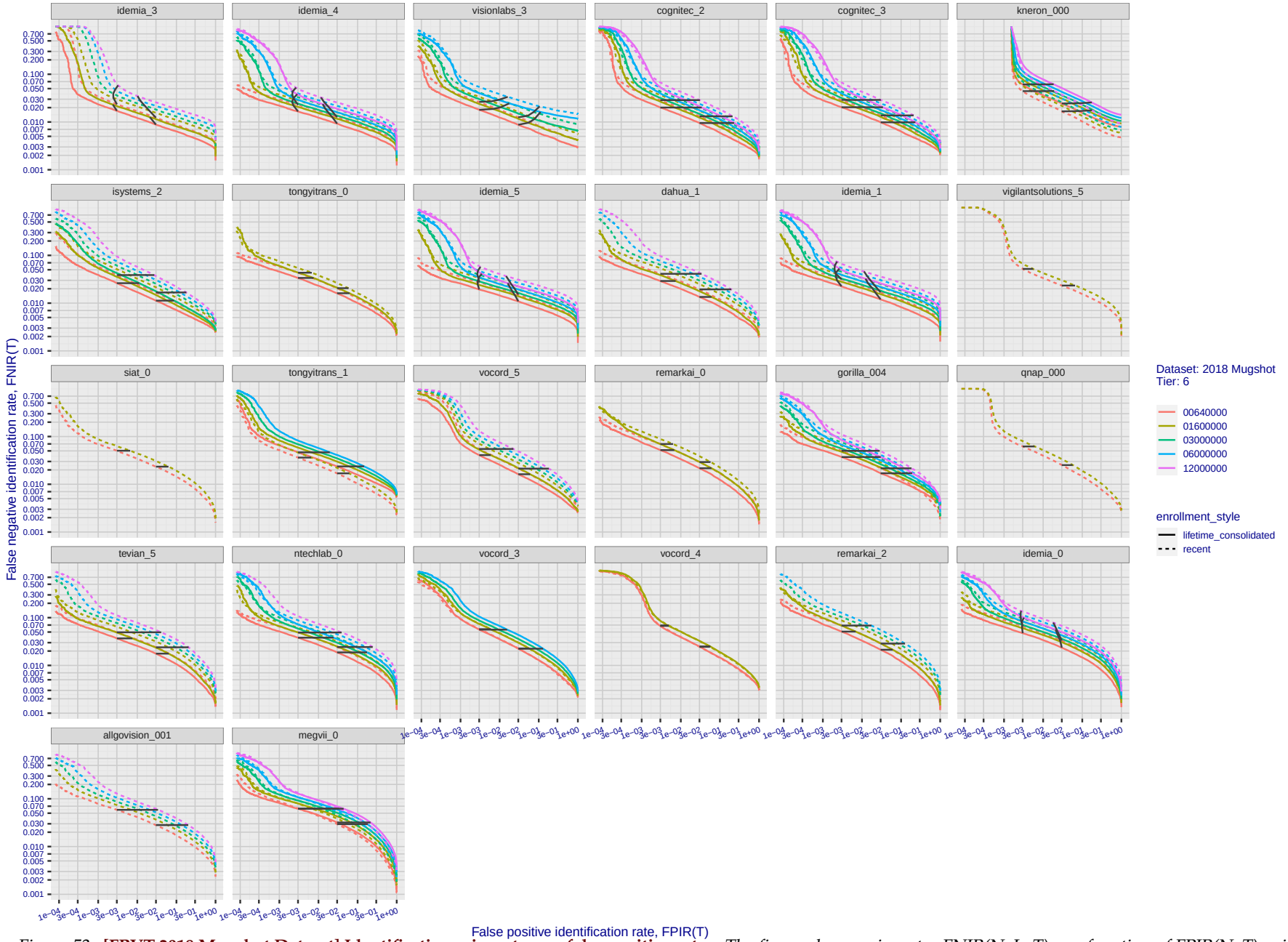

Figure 53: **[FRVT-2018 Mugshot Dataset] Identification miss rates vs. false positive rates**. *The figure shows miss rates FNIR(N, L, T) as a function of FPIR(N, T), with N ranging from 640 000 to 12 000 000 as noted in rows 1-10 of Table 1. These error tradeoff characteristics are useful for applications where a threshold must be elevated to limit false positives, such as when human reviewer labor is not matched to the volume of searches. Dark lines join points of equal threshold: If horizontal, FPIR(T) rises with N, and mate scores are independent of N. Other algorithms adjust scores in an attempt to make FPIR independent of N.*

2021/11/22
08:35:53

FNIR(N, R, T) = False neg. identification rate
FPIR(N, T) = False pos. identification rate

N = Num. enrolled subjects
R = Num. candidates examined

T = Threshold

T = 0 → Investigation
T > 0 → Identification

This publication is available free of charge from: https://doi.org/10.6028/NIST.IR.8271

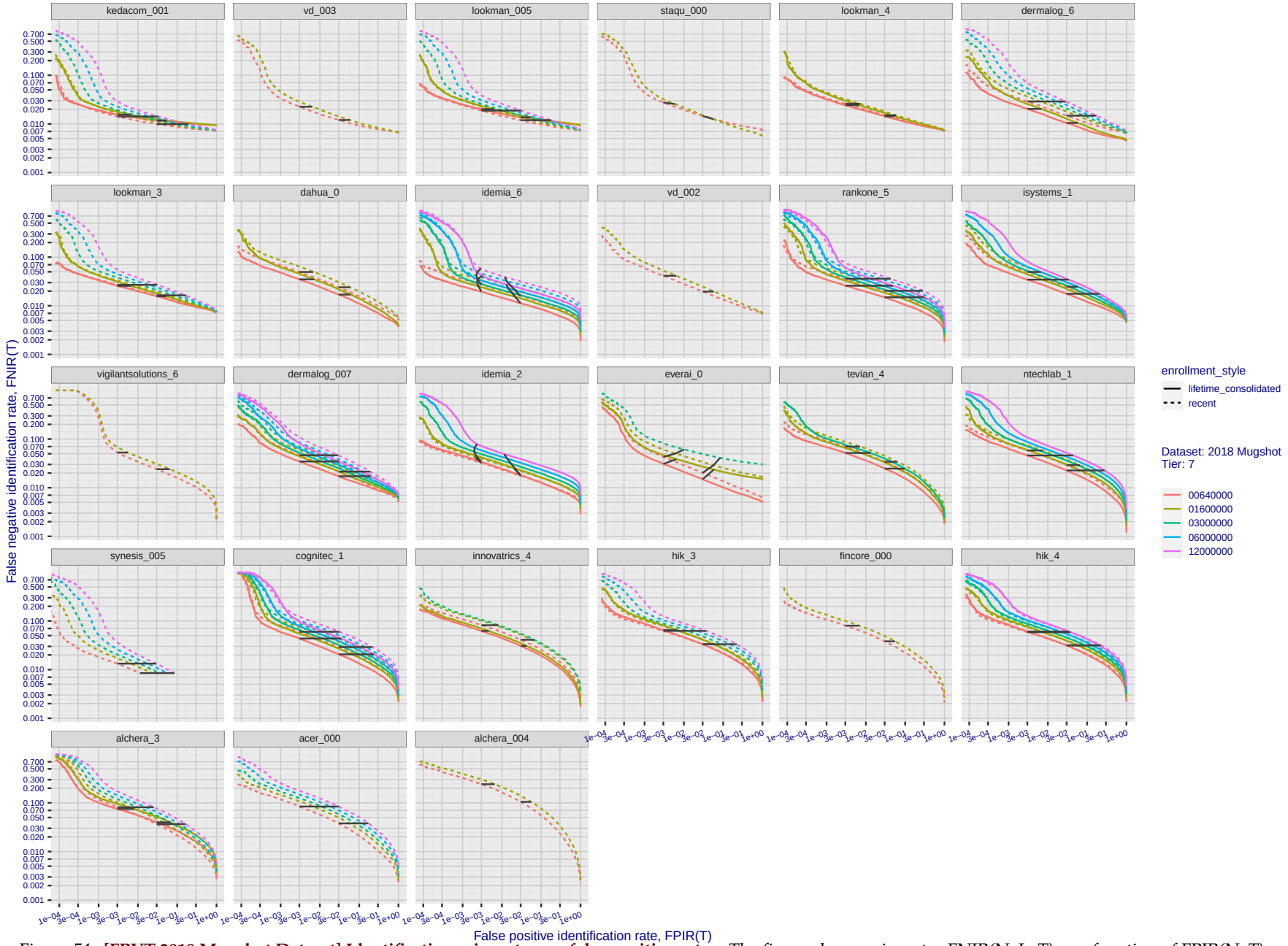

Figure 54: **[FRVT-2018 Mugshot Dataset] Identification miss rates vs. false positive rates**. *The figure shows miss rates FNIR(N, L, T) as a function of FPIR(N, T), with N ranging from 640 000 to 12 000 000 as noted in rows 1-10 of Table 1. These error tradeoff characteristics are useful for applications where a threshold must be elevated to limit false positives, such as when human reviewer labor is not matched to the volume of searches. Dark lines join points of equal threshold: If horizontal, FPIR(T) rises with N, and mate scores are independent of N. Other algorithms adjust scores in an attempt to make FPIR independent of N.*

This publication is available free of charge from: https://doi.org/10.6028/NIST.IR.8271

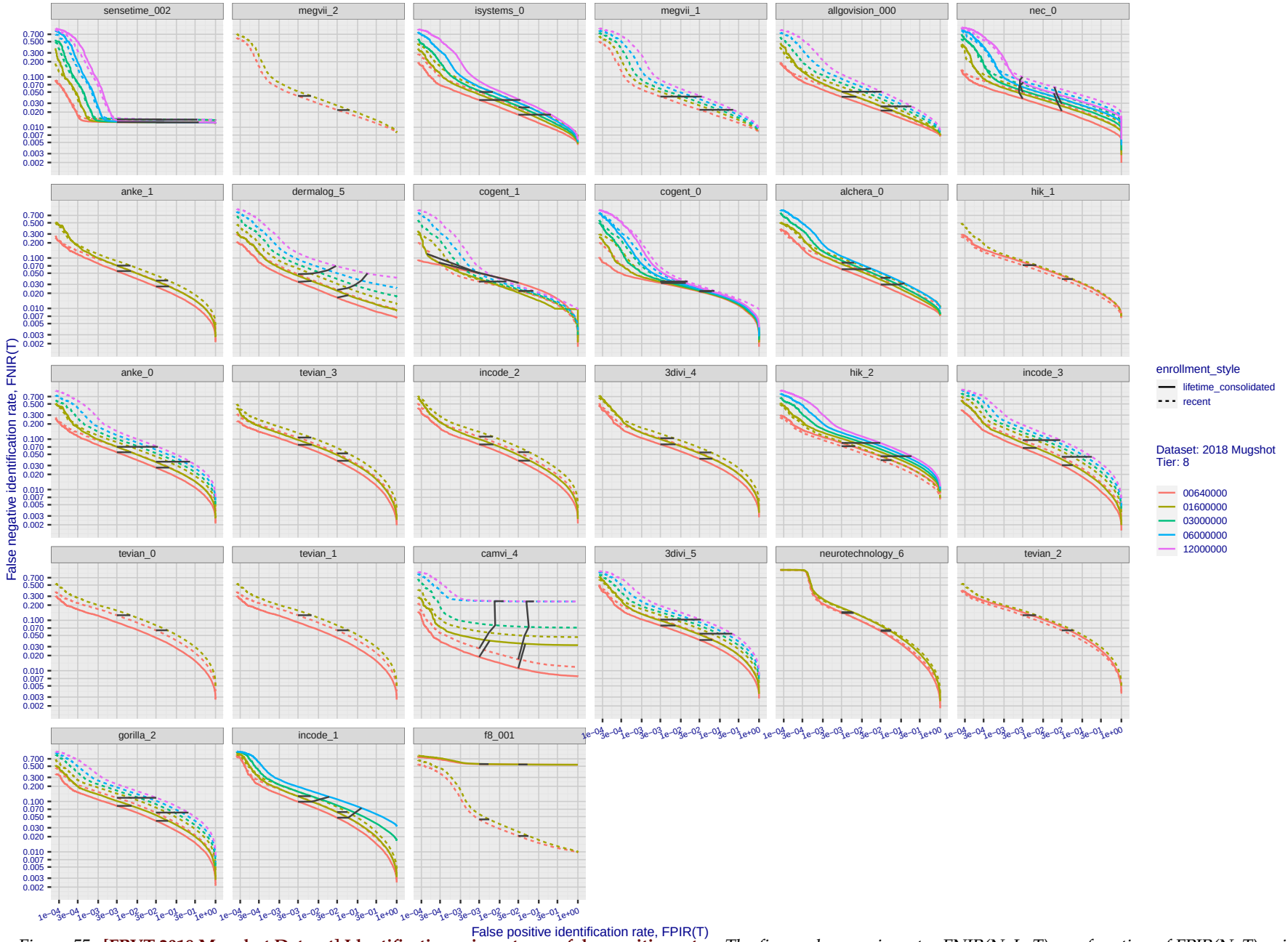

Figure 55: **[FRVT-2018 Mugshot Dataset] Identification miss rates vs. false positive rates**. *The figure shows miss rates FNIR(N, L, T) as a function of FPIR(N, T), with N ranging from 640 000 to 12 000 000 as noted in rows 1-10 of Table 1. These error tradeoff characteristics are useful for applications where a threshold must be elevated to limit false positives, such as when human reviewer labor is not matched to the volume of searches. Dark lines join points of equal threshold: If horizontal, FPIR(T) rises with N, and mate scores are independent of N. Other algorithms adjust scores in an attempt to make FPIR independent of N.*

2021/11/22
08:35:53

FNIR(N, R, T) = False neg. identification rate
FPIR(N, T) = False pos. identification rate

N = Num. enrolled subjects
R = Num. candidates examined

T = Threshold

T = 0 → Investigation
T > 0 → Identification

This publication is available free of charge from: https://doi.org/10.6028/NIST.IR.8271

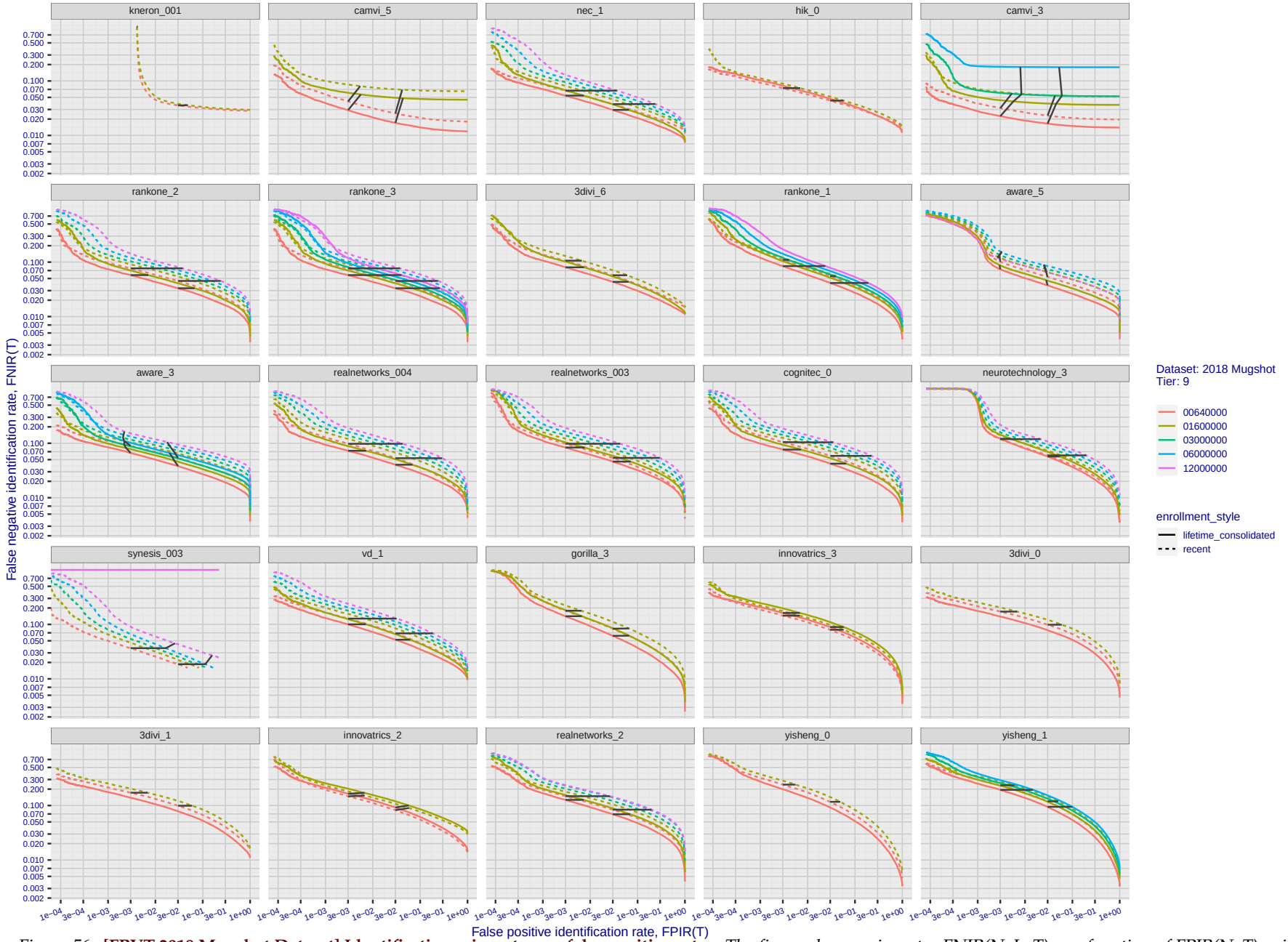

Figure 56: **[FRVT-2018 Mugshot Dataset] Identification miss rates vs. false positive rates**. *The figure shows miss rates FNIR(N, L, T) as a function of FPIR(N, T), with N ranging from 640 000 to 12 000 000 as noted in rows 1-10 of Table 1. These error tradeoff characteristics are useful for applications where a threshold must be elevated to limit false positives, such as when human reviewer labor is not matched to the volume of searches. Dark lines join points of equal threshold: If horizontal, FPIR(T) rises with N, and mate scores are independent of N. Other algorithms adjust scores in an attempt to make FPIR independent of N.*

2021/11/22
08:35:53

FNIR(N, R, T) = False neg. identification rate
FPIR(N, T) = False pos. identification rate

N = Num. enrolled subjects
R = Num. candidates examined

T = Threshold

T = 0 → Investigation
T > 0 → Identification

This publication is available free of charge from: https://doi.org/10.6028/NIST.IR.8271

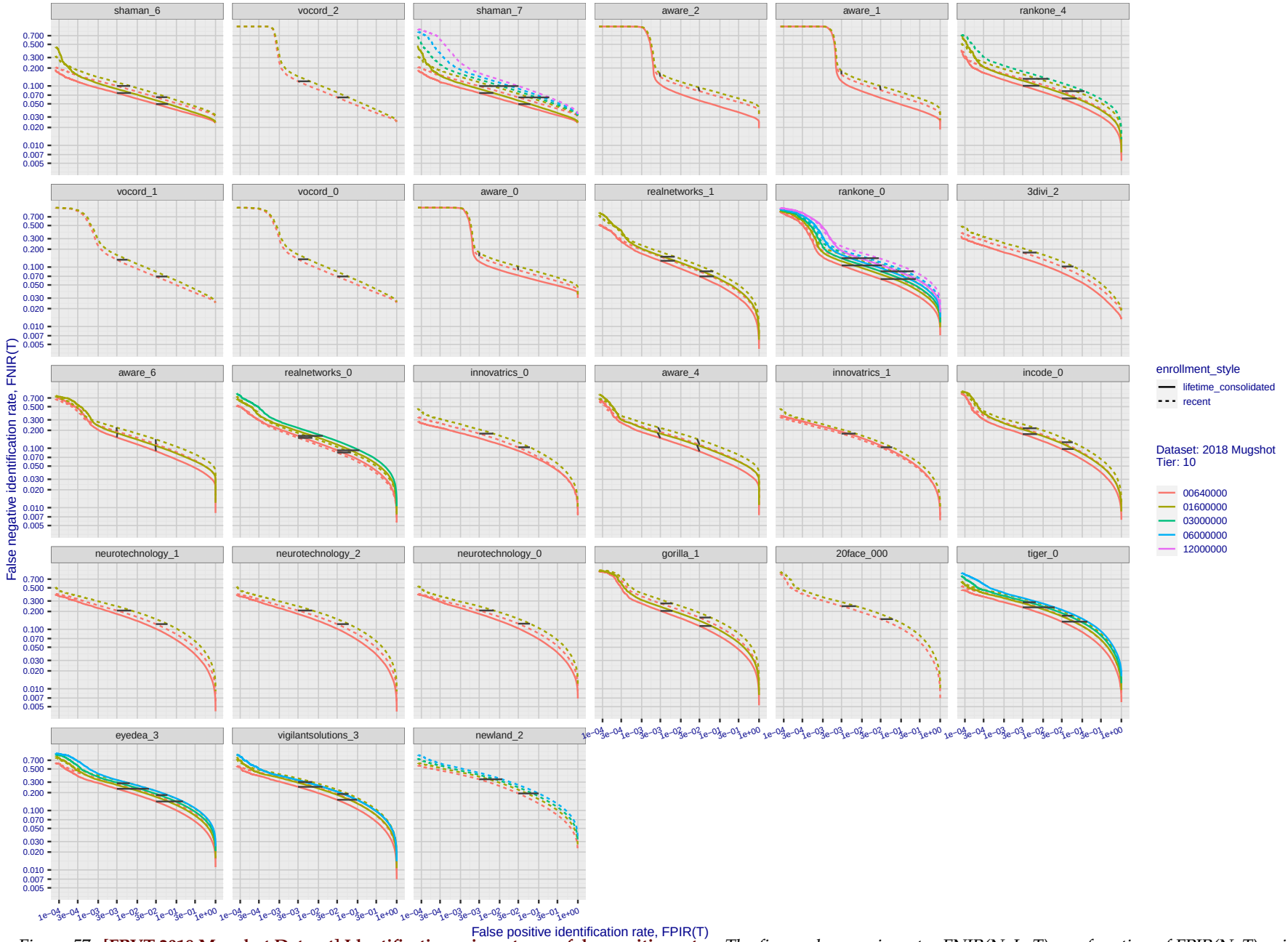

Figure 57: **[FRVT-2018 Mugshot Dataset] Identification miss rates vs. false positive rates**. *The figure shows miss rates FNIR(N, L, T) as a function of FPIR(N, T), with N ranging from 640 000 to 12 000 000 as noted in rows 1-10 of Table 1. These error tradeoff characteristics are useful for applications where a threshold must be elevated to limit false positives, such as when human reviewer labor is not matched to the volume of searches. Dark lines join points of equal threshold: If horizontal, FPIR(T) rises with N, and mate scores are independent of N. Other algorithms adjust scores in an attempt to make FPIR independent of N.*

2021/11/22
08:35:53

FNIR(N, R, T) = False neg. identification rate
FPIR(N, T) = False pos. identification rate

N = Num. enrolled subjects
R = Num. candidates examined

T = Threshold

T = 0 → Investigation
T > 0 → Identification

This publication is available free of charge from: https://doi.org/10.6028/NIST.IR.8271

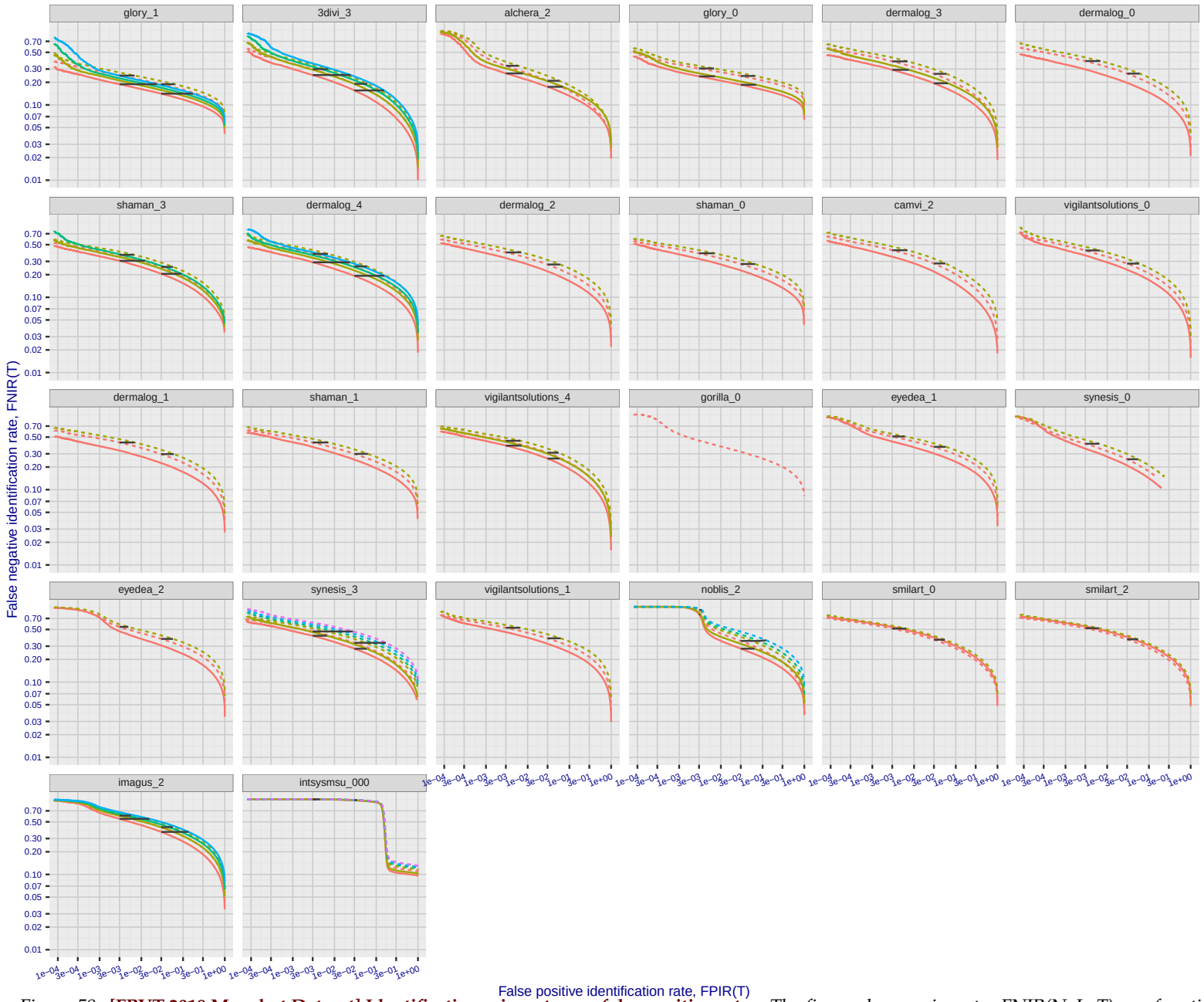

Figure 58: **[FRVT-2018 Mugshot Dataset] Identification miss rates vs. false positive rates**. *The figure shows miss rates FNIR(N, L, T) as a function of FPIR(N, T), with N ranging from 640 000 to 12 000 000 as noted in rows 1-10 of Table 1. These error tradeoff characteristics are useful for applications where a threshold must be elevated to limit false positives, such as when human reviewer labor is not matched to the volume of searches. Dark lines join points of equal threshold: If horizontal, FPIR(T) rises with N, and mate scores are independent of N. Other algorithms adjust scores in an attempt to make FPIR independent of N.*

2021/11/22
08:35:53

FNIR(N, R, T) = False neg. identification rate
FPIR(N, T) = False pos. identification rate

N = Num. enrolled subjects
R = Num. candidates examined

T = Threshold

T = 0 → Investigation
T > 0 → Identification

This publication is available free of charge from: https://doi.org/10.6028/NIST.IR.8271

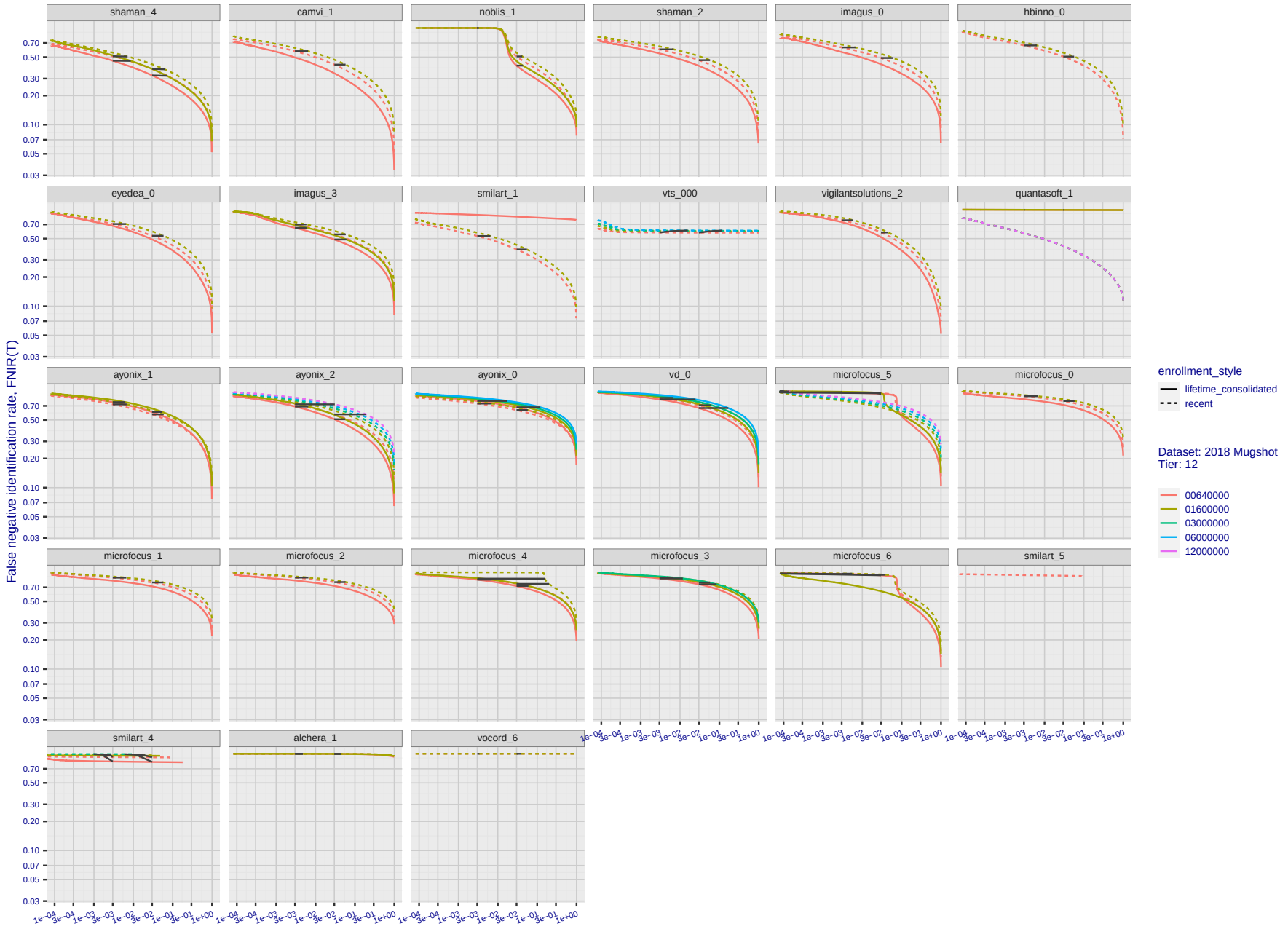

Figure 59: **[FRVT-2018 Mugshot Dataset] Identification miss rates vs. false positive rates**. *The figure shows miss rates FNIR(N, L, T) as a function of FPIR(N, T), with N ranging from 640 000 to 12 000 000 as noted in rows 1-10 of Table 1. These error tradeoff characteristics are useful for applications where a threshold must be elevated to limit false positives, such as when human reviewer labor is not matched to the volume of searches. Dark lines join points of equal threshold: If horizontal, FPIR(T) rises with N, and mate scores are independent of N. Other algorithms adjust scores in an attempt to make FPIR independent of N.*

2021/11/22
08:35:53

FNIR(N, R, T) = False neg. identification rate
FPIR(N, T) = False pos. identification rate

N = Num. enrolled subjects
R = Num. candidates examined

T = Threshold

T = 0 → Investigation
T > 0 → Identification

Appendix B Effect of time-lapse: Accuracy after face ageing

This publication is available free of charge from: https://doi.org/10.6028/NIST.IR.8271

This publication is available free of charge from: https://doi.org/10.6028/NIST.IR.8271

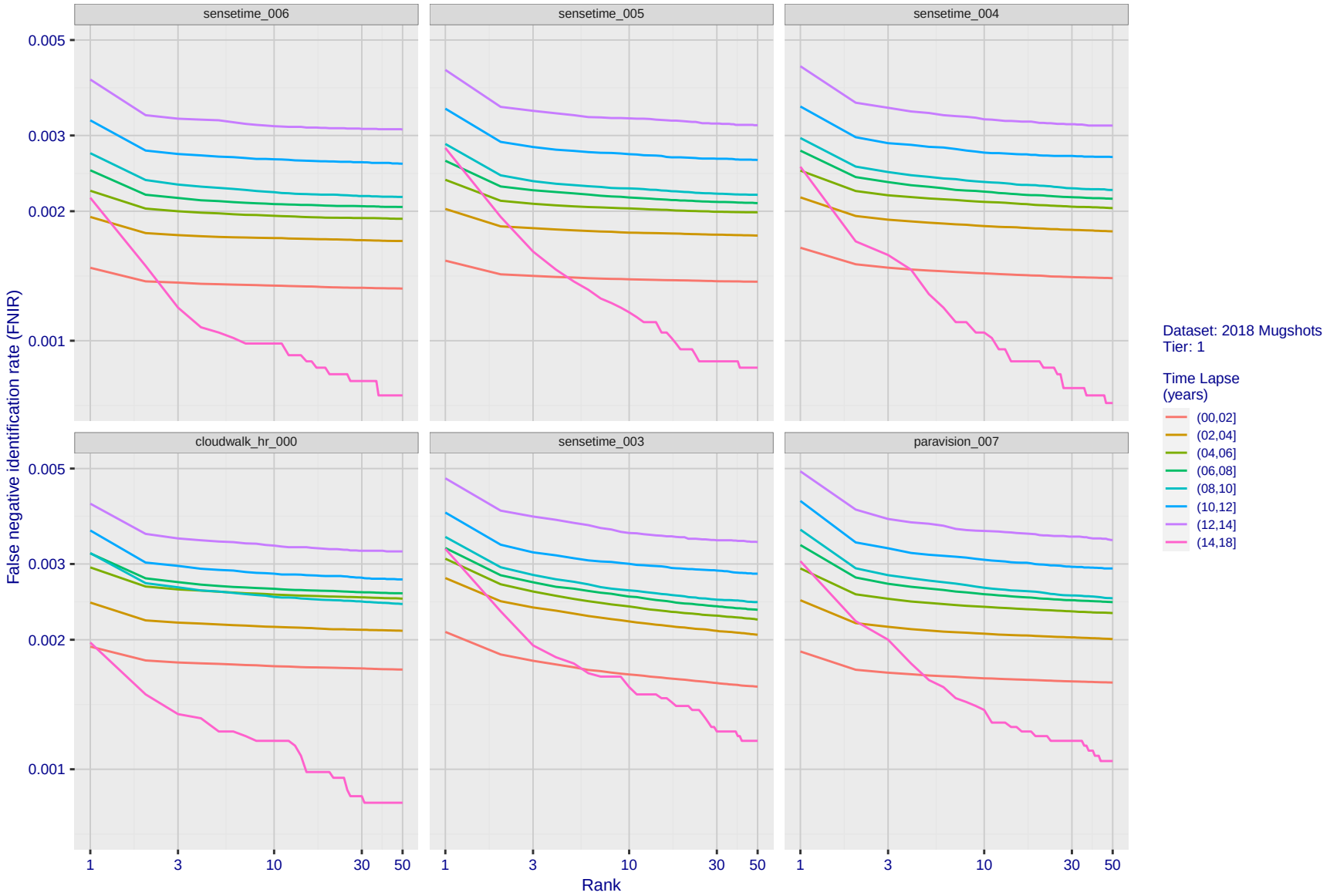

Figure 60: **[FRVT-2018 Mugshot Ageing Dataset] Identification miss rates vs. rank by time-elapsed**. *The oldest image of each individual is enrolled. Thereafter, all more recent images are searched. Miss rates are computed over all searches noted in row 17 of Table 1 and binned by number of years between search and initial enrollment.*

2021/11/22 08:35:53

FNIR(N, R, T) = False neg. identification rate
FPIR(N, T) = False pos. identification rate

N = Num. enrolled subjects
R = Num. candidates examined

T = Threshold

T = 0 → Investigation
T > 0 → Identification

This publication is available free of charge from: https://doi.org/10.6028/NIST.IR.8271

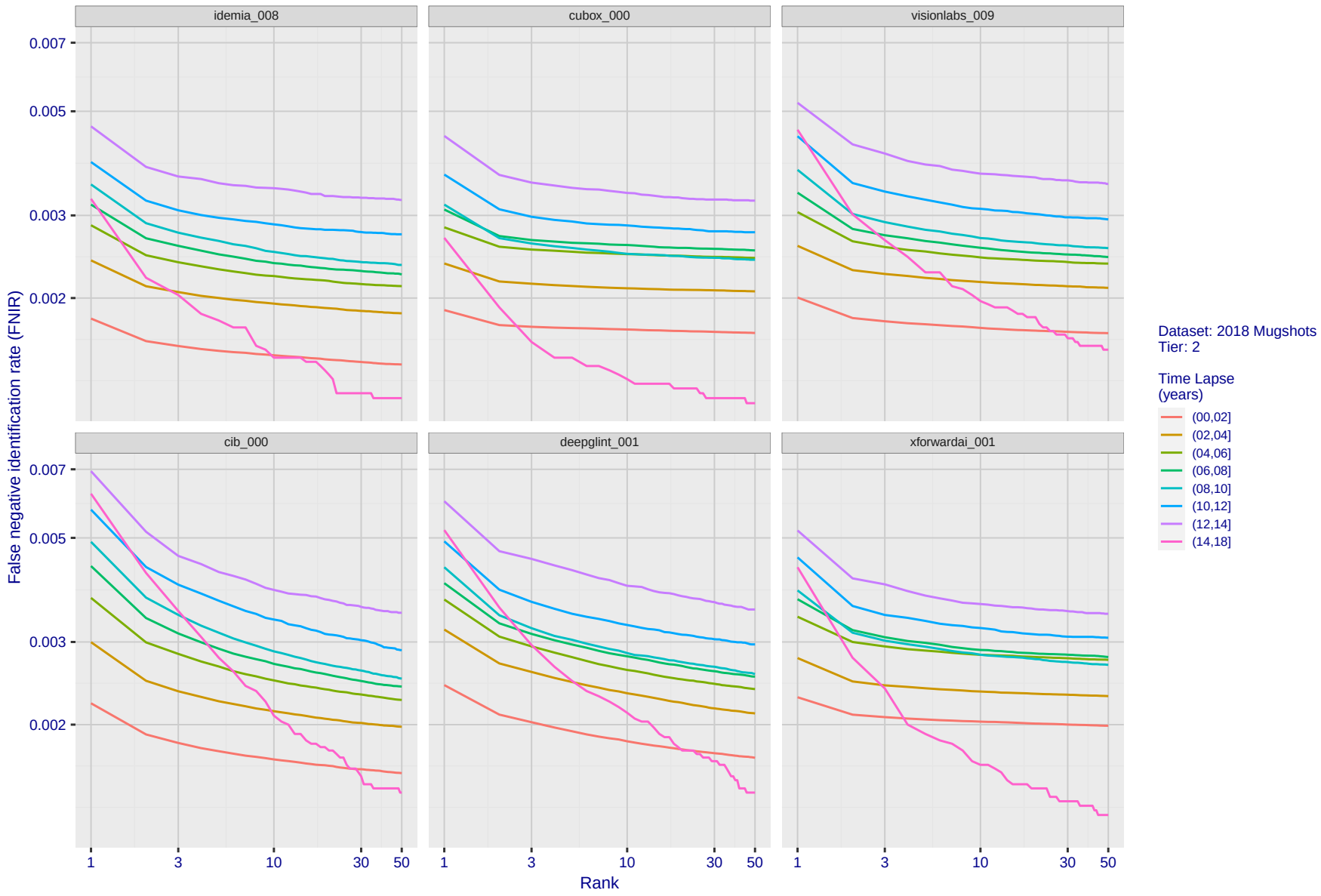

Figure 61: **[FRVT-2018 Mugshot Ageing Dataset] Identification miss rates vs. rank by time-elapsed**. *The oldest image of each individual is enrolled. Thereafter, all more recent images are searched. Miss rates are computed over all searches noted in row 17 of Table 1 and binned by number of years between search and initial enrollment.*

2021/11/22
08:35:53

FNIR(N, R, T) = False neg. identification rate
FPIR(N, T) = False pos. identification rate

N = Num. enrolled subjects
R = Num. candidates examined

T = Threshold

T = 0 → Investigation
T > 0 → Identification

This publication is available free of charge from: https://doi.org/10.6028/NIST.IR.8271

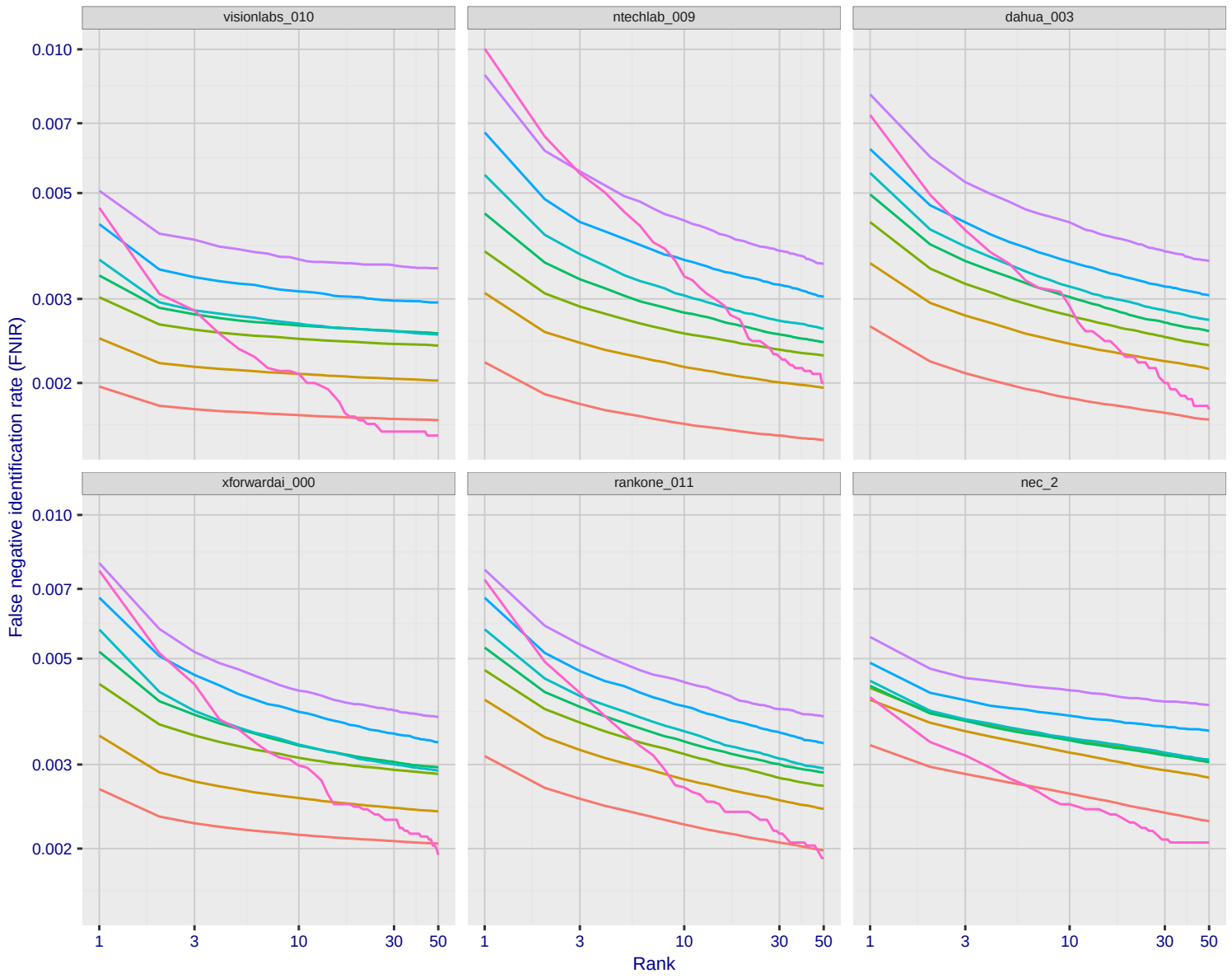

Figure 62: **[FRVT-2018 Mugshot Ageing Dataset] Identification miss rates vs. rank by time-elapsed**. *The oldest image of each individual is enrolled. Thereafter, all more recent images are searched. Miss rates are computed over all searches noted in row 17 of Table 1 and binned by number of years between search and initial enrollment.*

2021/11/22
08:35:53
FNIR(N, R, T) = False neg. identification rate
FPIR(N, T) = False pos. identification rate
N = Num. enrolled subjects
R = Num. candidates examined
T = Threshold
T = 0 → Investigation
T > 0 → Identification

This publication is available free of charge from: https://doi.org/10.6028/NIST.IR.8271

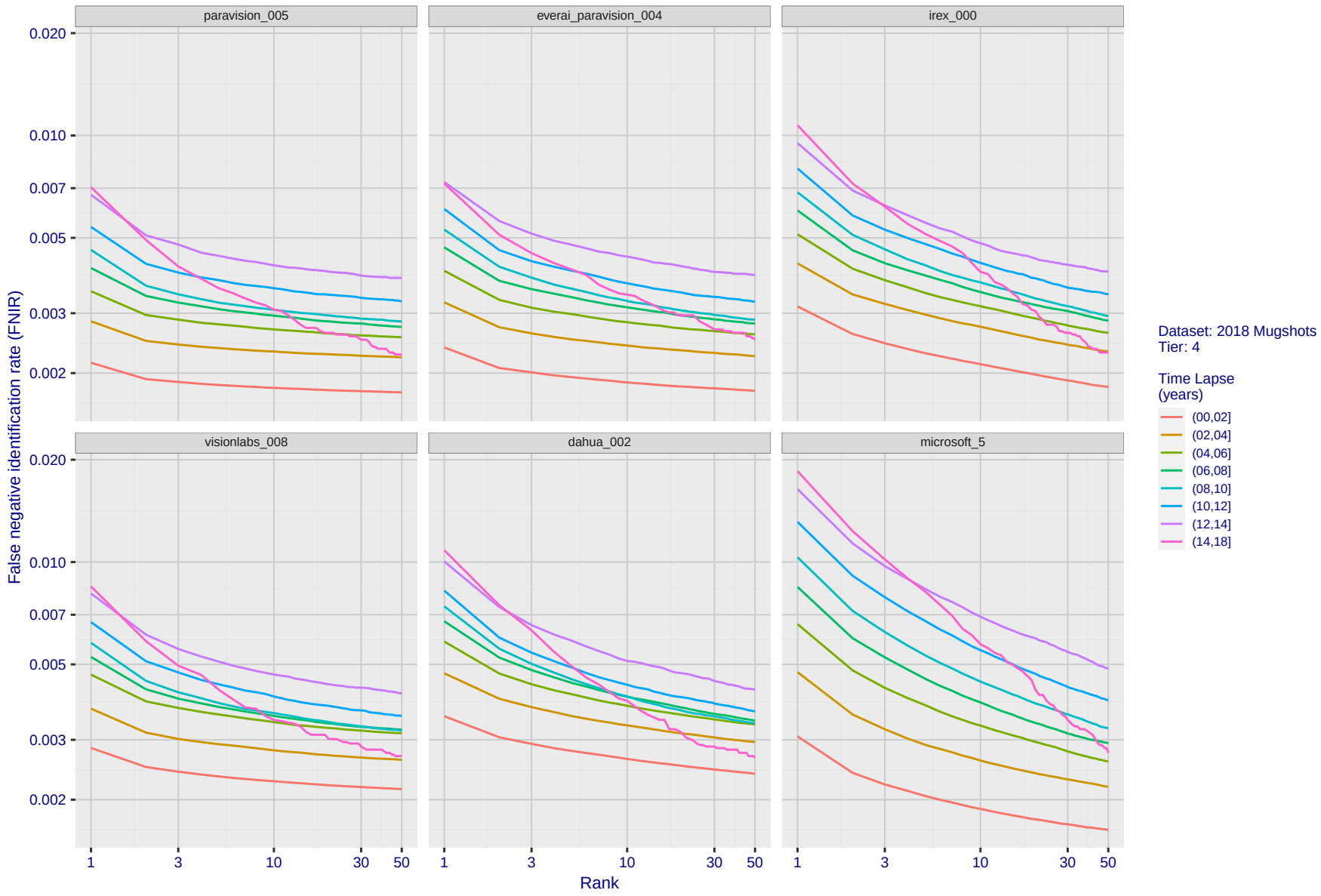

Figure 63: **[FRVT-2018 Mugshot Ageing Dataset] Identification miss rates vs. rank by time-elapsed**. *The oldest image of each individual is enrolled. Thereafter, all more recent images are searched. Miss rates are computed over all searches noted in row 17 of Table 1 and binned by number of years between search and initial enrollment.*

2021/11/22
08:35:53
FNIR(N, R, T) = False neg. identification rate
FPIR(N, T) = False pos. identification rate
N = Num. enrolled subjects
R = Num. candidates examined
T = Threshold
T = 0 → Investigation
T > 0 → Identification

This publication is available free of charge from: https://doi.org/10.6028/NIST.IR.8271

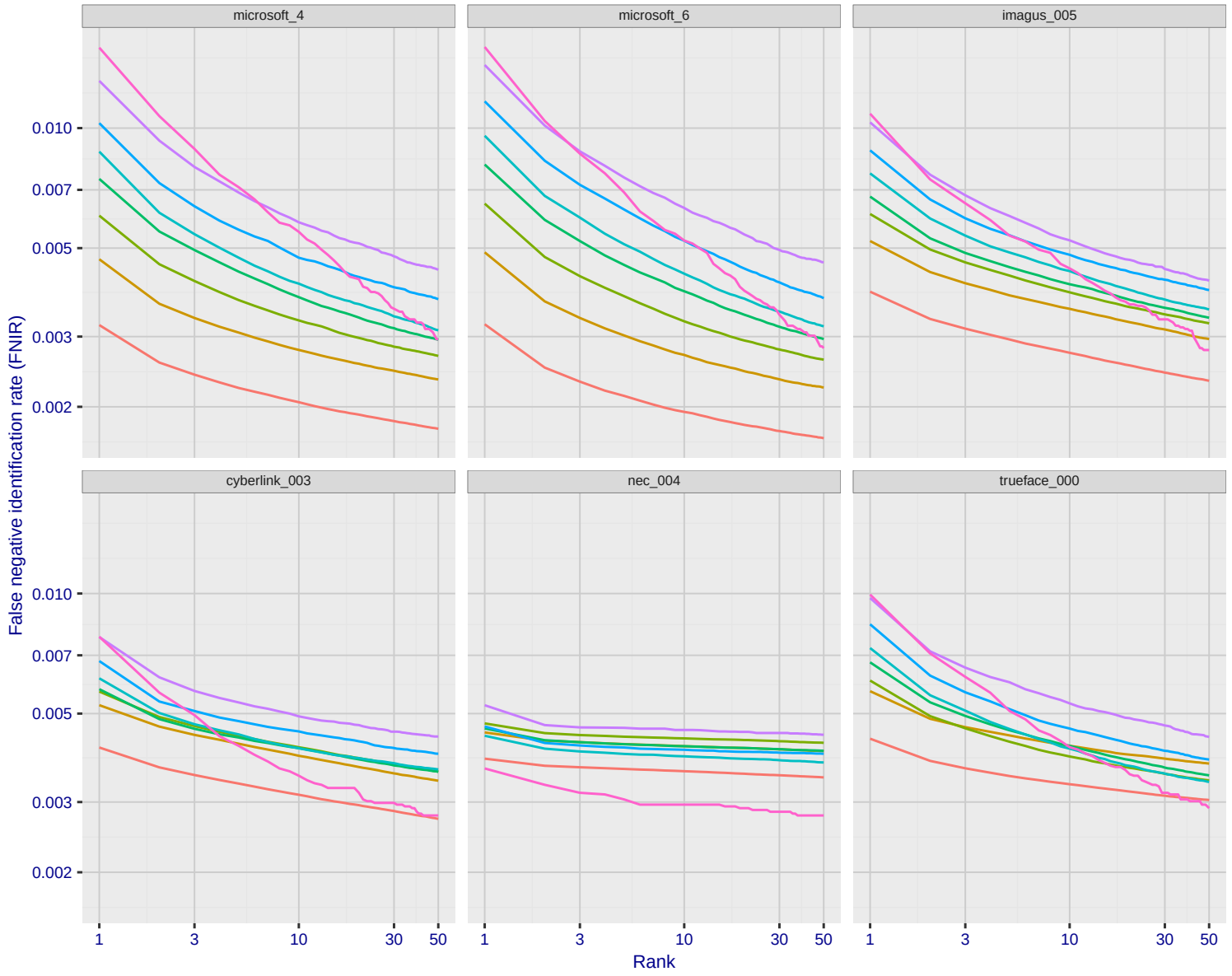

Figure 64: **[FRVT-2018 Mugshot Ageing Dataset] Identification miss rates vs. rank by time-elapsed**. *The oldest image of each individual is enrolled. Thereafter, all more recent images are searched. Miss rates are computed over all searches noted in row 17 of Table 1 and binned by number of years between search and initial enrollment.*

2021/11/22
08:35:53

FNIR(N, R, T) = False neg. identification rate
FPIR(N, T) = False pos. identification rate

N = Num. enrolled subjects
R = Num. candidates examined

T = Threshold

T = 0 → Investigation
T > 0 → Identification

This publication is available free of charge from: https://doi.org/10.6028/NIST.IR.8271

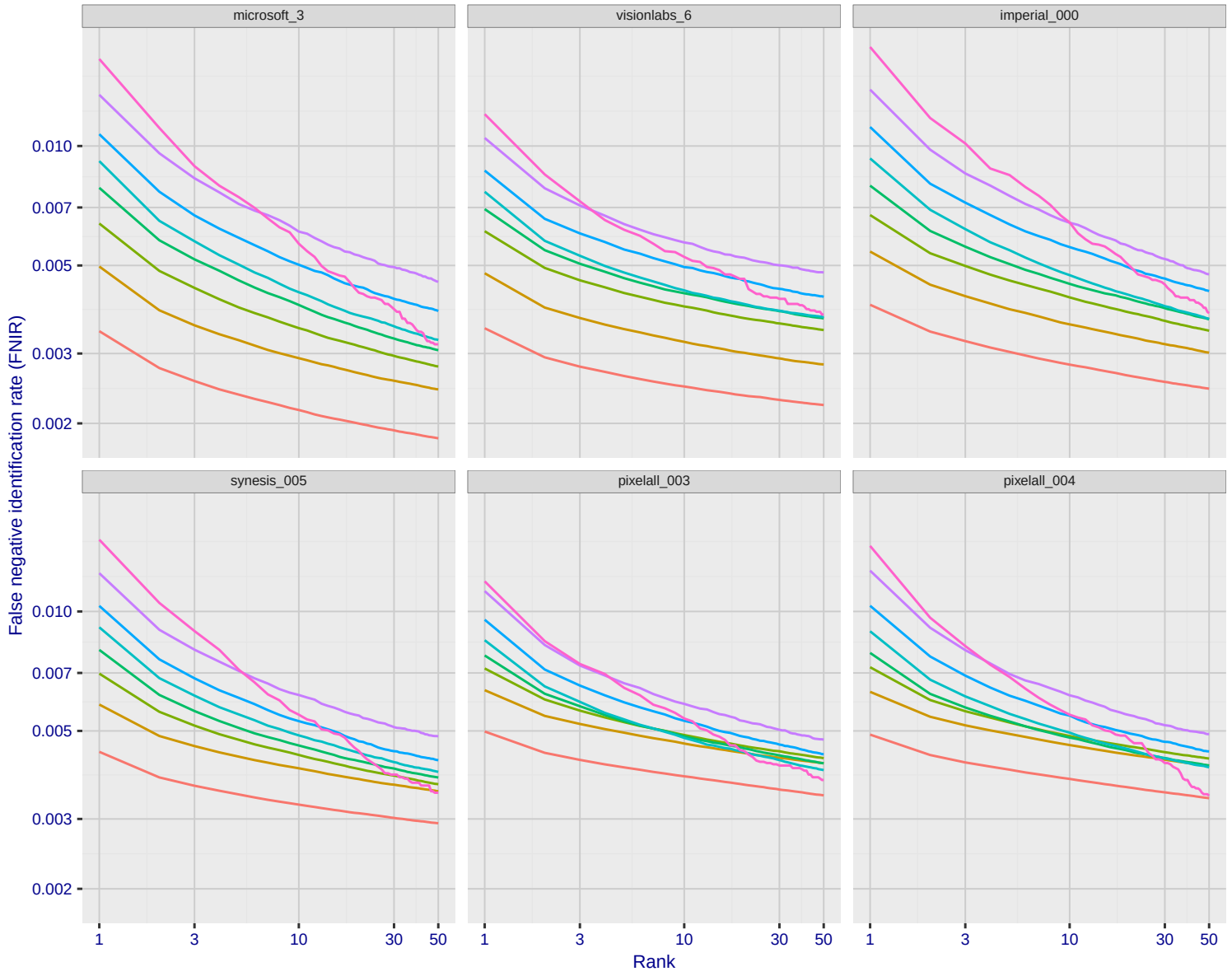

Figure 65: **[FRVT-2018 Mugshot Ageing Dataset] Identification miss rates vs. rank by time-elapsed**. *The oldest image of each individual is enrolled. Thereafter, all more recent images are searched. Miss rates are computed over all searches noted in row 17 of Table 1 and binned by number of years between search and initial enrollment.*

2021/11/22 08:35:53
FNIR(N, R, T) = False neg. identification rate
FPIR(N, T) = False pos. identification rate
N = Num. enrolled subjects
R = Num. candidates examined
T = Threshold
T = 0 → Investigation
T > 0 → Identification

This publication is available free of charge from: https://doi.org/10.6028/NIST.IR.8271

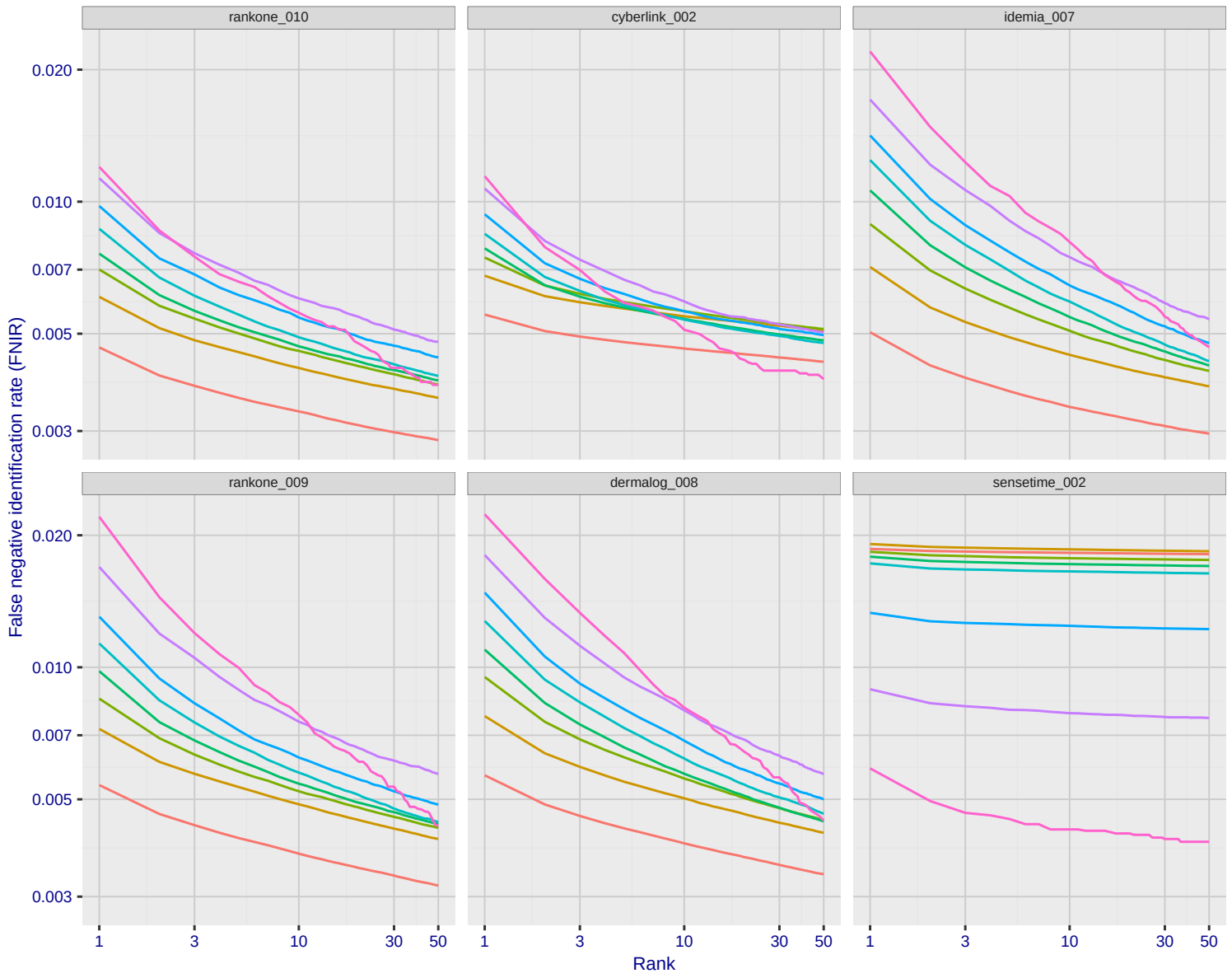

Figure 66: **[FRVT-2018 Mugshot Ageing Dataset] Identification miss rates vs. rank by time-elapsed**. *The oldest image of each individual is enrolled. Thereafter, all more recent images are searched. Miss rates are computed over all searches noted in row 17 of Table 1 and binned by number of years between search and initial enrollment.*

2021/11/22
08:35:53
FNIR(N, R, T) = False neg. identification rate
FPIR(N, T) = False pos. identification rate
N = Num. enrolled subjects
R = Num. candidates examined
T = Threshold
T = 0 → Investigation
T > 0 → Identification

This publication is available free of charge from: https://doi.org/10.6028/NIST.IR.8271

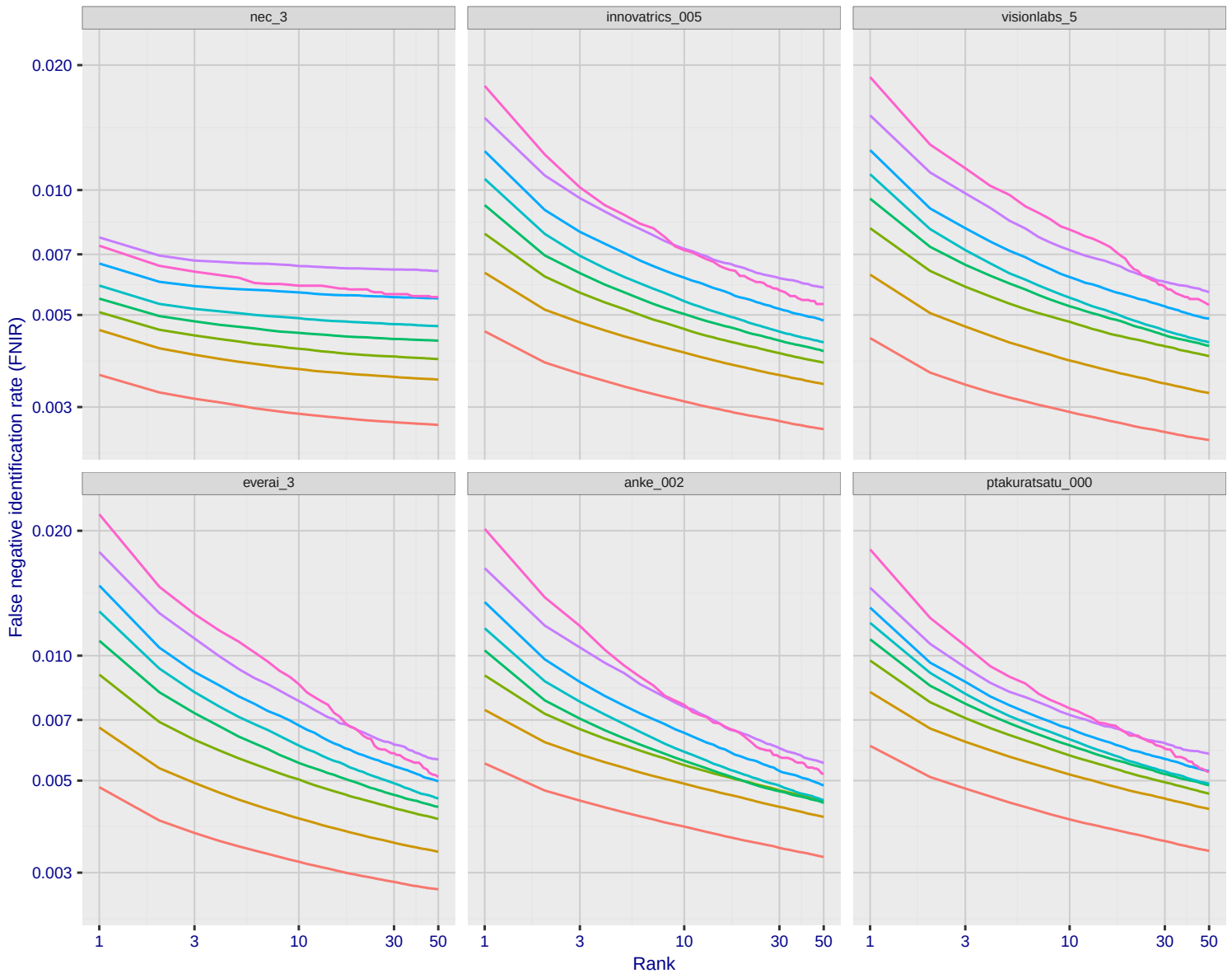

Figure 67: **[FRVT-2018 Mugshot Ageing Dataset] Identification miss rates vs. rank by time-elapsed**. *The oldest image of each individual is enrolled. Thereafter, all more recent images are searched. Miss rates are computed over all searches noted in row 17 of Table 1 and binned by number of years between search and initial enrollment.*

2021/11/22
08:35:53
FNIR(N, R, T) = False neg. identification rate
FPIR(N, T) = False pos. identification rate
N = Num. enrolled subjects
R = Num. candidates examined
T = Threshold
T = 0 → Investigation
T > 0 → Identification

This publication is available free of charge from: https://doi.org/10.6028/NIST.IR.8271

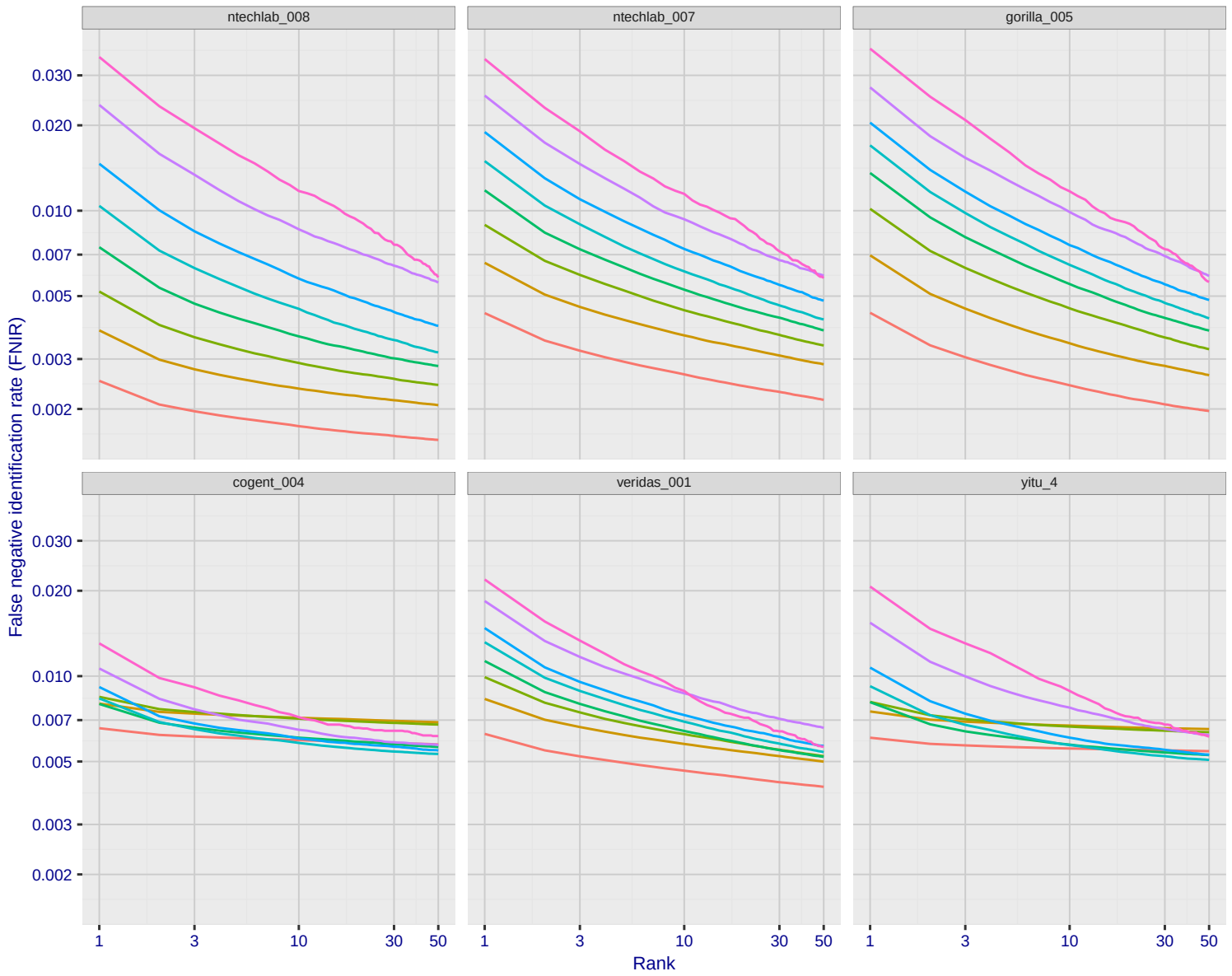

Figure 68: **[FRVT-2018 Mugshot Ageing Dataset] Identification miss rates vs. rank by time-elapsed**. *The oldest image of each individual is enrolled. Thereafter, all more recent images are searched. Miss rates are computed over all searches noted in row 17 of Table 1 and binned by number of years between search and initial enrollment.*

2021/11/22
08:35:53
FNIR(N, R, T) = False neg. identification rate
FPIR(N, T) = False pos. identification rate
N = Num. enrolled subjects
R = Num. candidates examined
T = Threshold
T = 0 → Investigation
T > 0 → Identification

This publication is available free of charge from: https://doi.org/10.6028/NIST.IR.8271

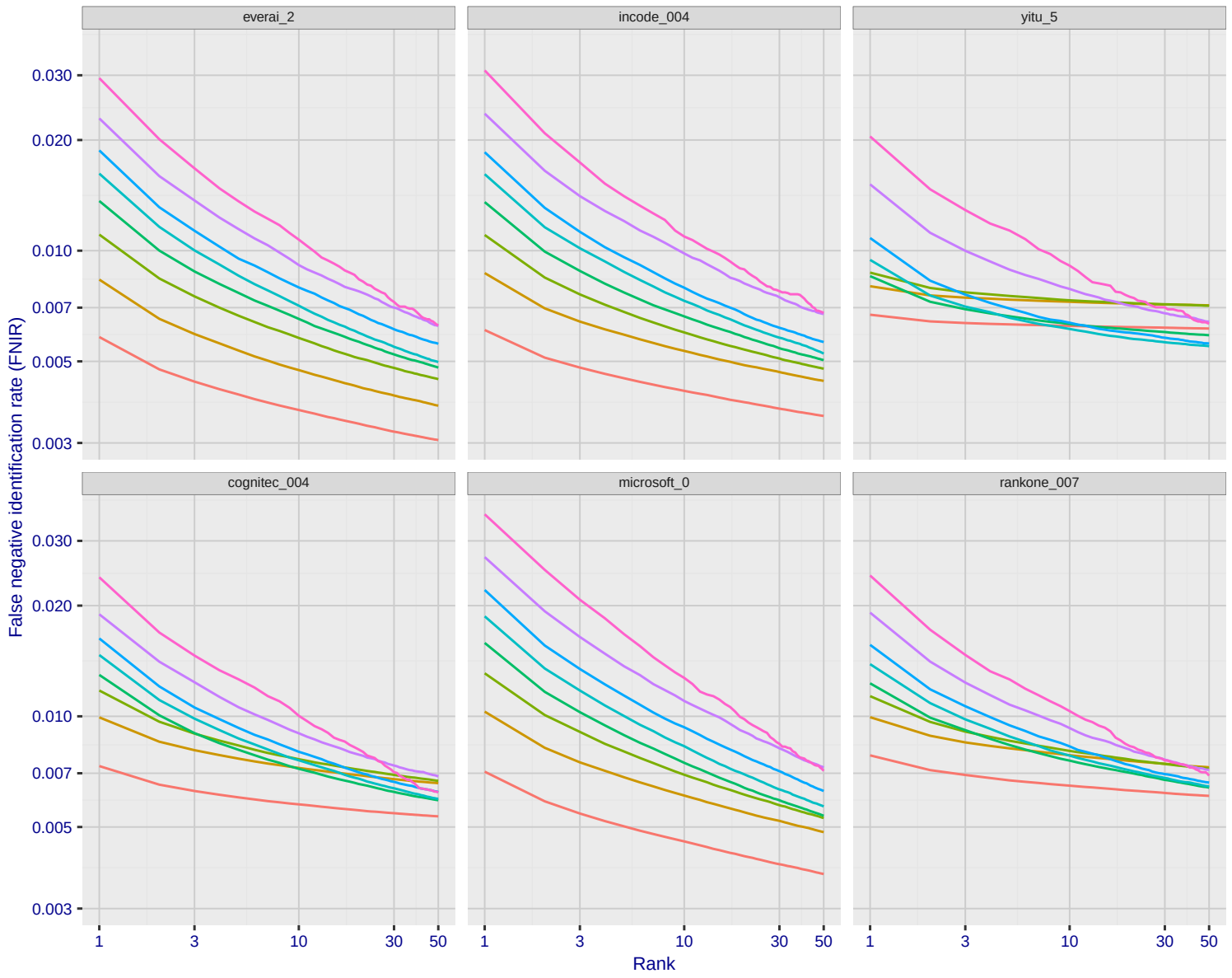

Figure 69: **[FRVT-2018 Mugshot Ageing Dataset] Identification miss rates vs. rank by time-elapsed**. *The oldest image of each individual is enrolled. Thereafter, all more recent images are searched. Miss rates are computed over all searches noted in row 17 of Table 1 and binned by number of years between search and initial enrollment.*

2021/11/22
08:35:53

FNIR(N, R, T) = False neg. identification rate
FPIR(N, T) = False pos. identification rate

N = Num. enrolled subjects
R = Num. candidates examined

T = Threshold

T = 0 → Investigation
T > 0 → Identification

This publication is available free of charge from: https://doi.org/10.6028/NIST.IR.8271

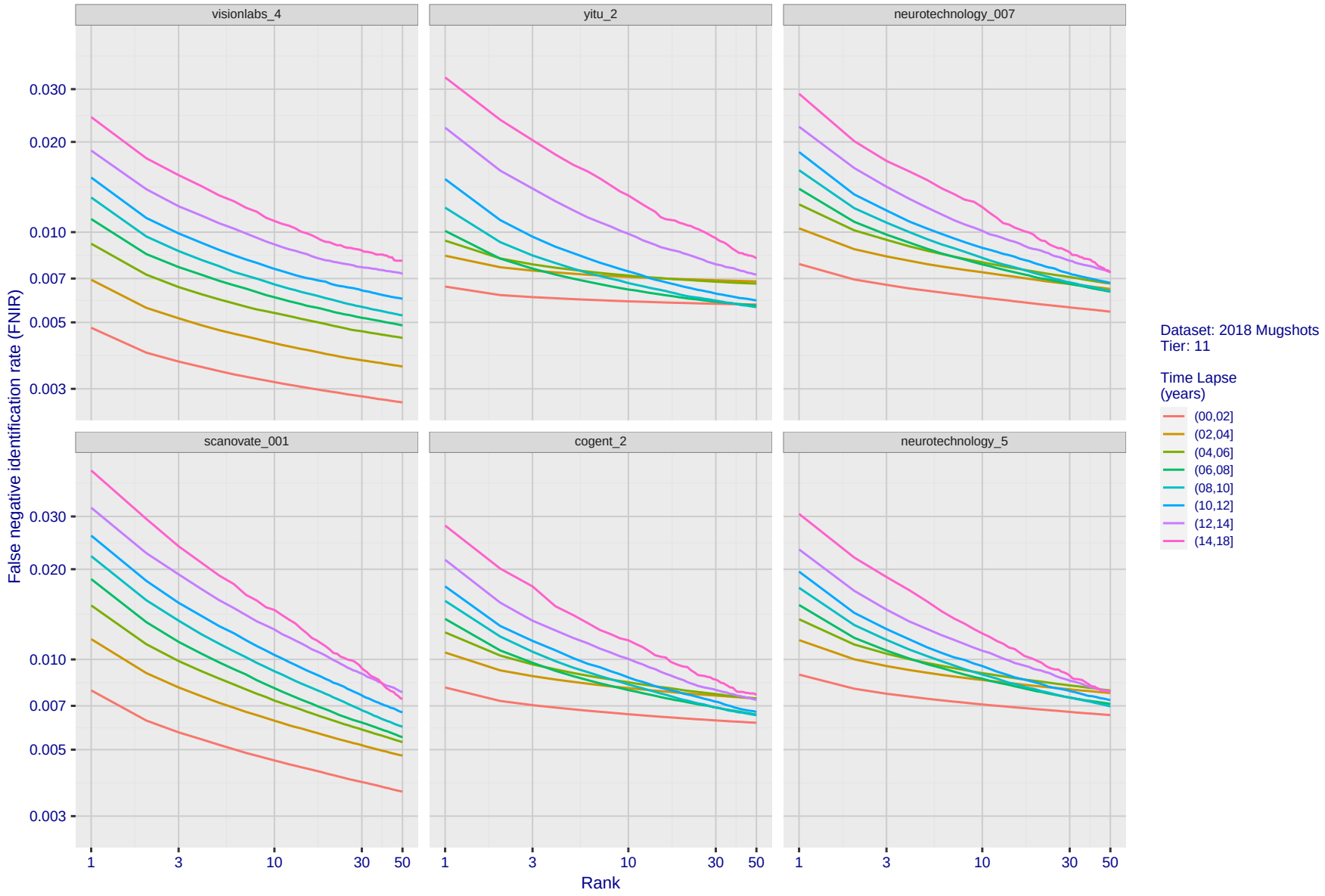

Figure 70: **[FRVT-2018 Mugshot Ageing Dataset] Identification miss rates vs. rank by time-elapsed**. *The oldest image of each individual is enrolled. Thereafter, all more recent images are searched. Miss rates are computed over all searches noted in row 17 of Table 1 and binned by number of years between search and initial enrollment.*

2021/11/22 08:35:53
FNIR(N, R, T) = False neg. identification rate
FPIR(N, T) = False pos. identification rate
N = Num. enrolled subjects
R = Num. candidates examined
T = Threshold
T = 0 → Investigation
T > 0 → Identification

This publication is available free of charge from: https://doi.org/10.6028/NIST.IR.8271

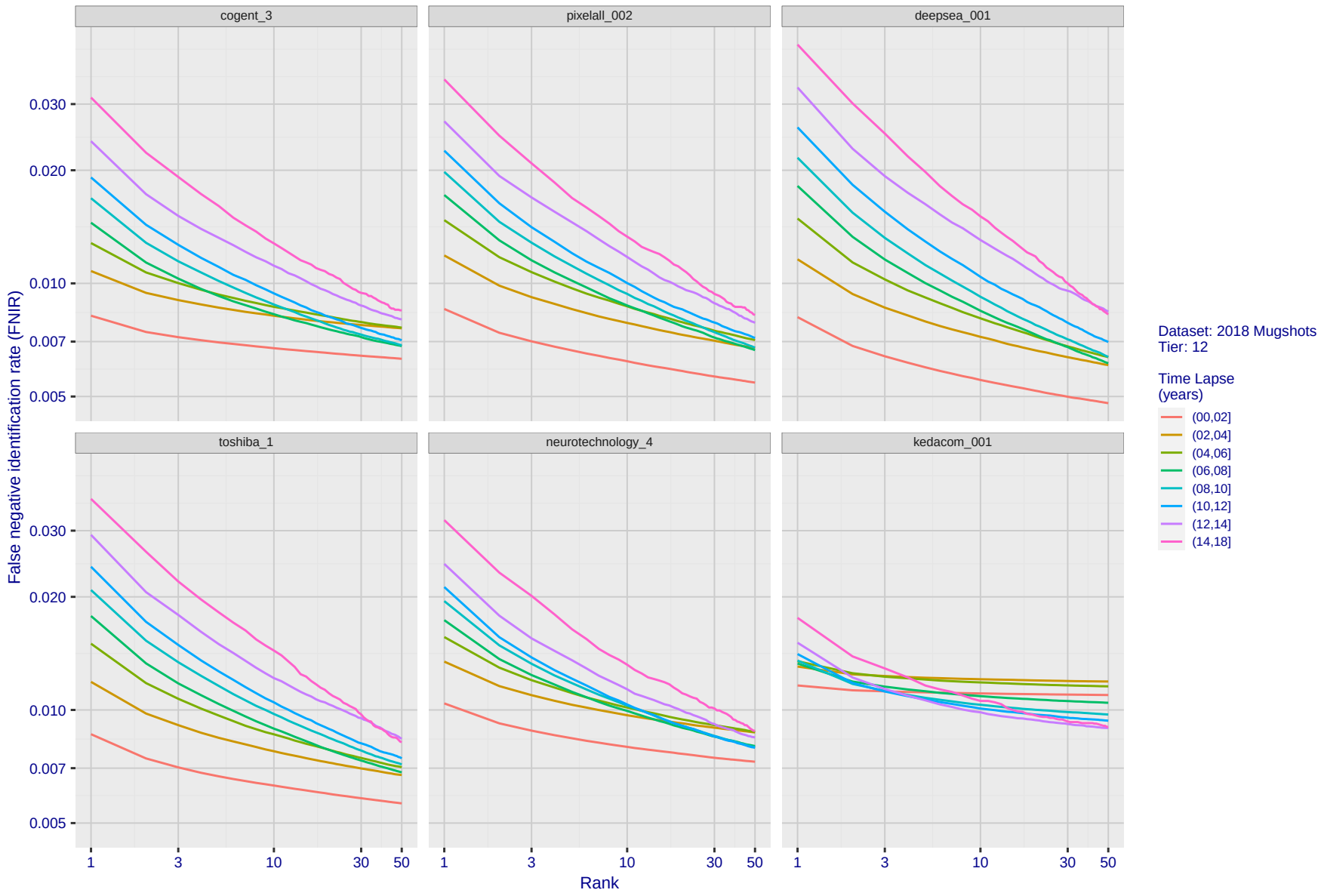

Figure 71: **[FRVT-2018 Mugshot Ageing Dataset] Identification miss rates vs. rank by time-elapsed**. *The oldest image of each individual is enrolled. Thereafter, all more recent images are searched. Miss rates are computed over all searches noted in row 17 of Table 1 and binned by number of years between search and initial enrollment.*

2021/11/22
08:35:53

FNIR(N, R, T) = False neg. identification rate
FPIR(N, T) = False pos. identification rate

N = Num. enrolled subjects
R = Num. candidates examined

T = Threshold

T = 0 → Investigation
T > 0 → Identification

This publication is available free of charge from: https://doi.org/10.6028/NIST.IR.8271

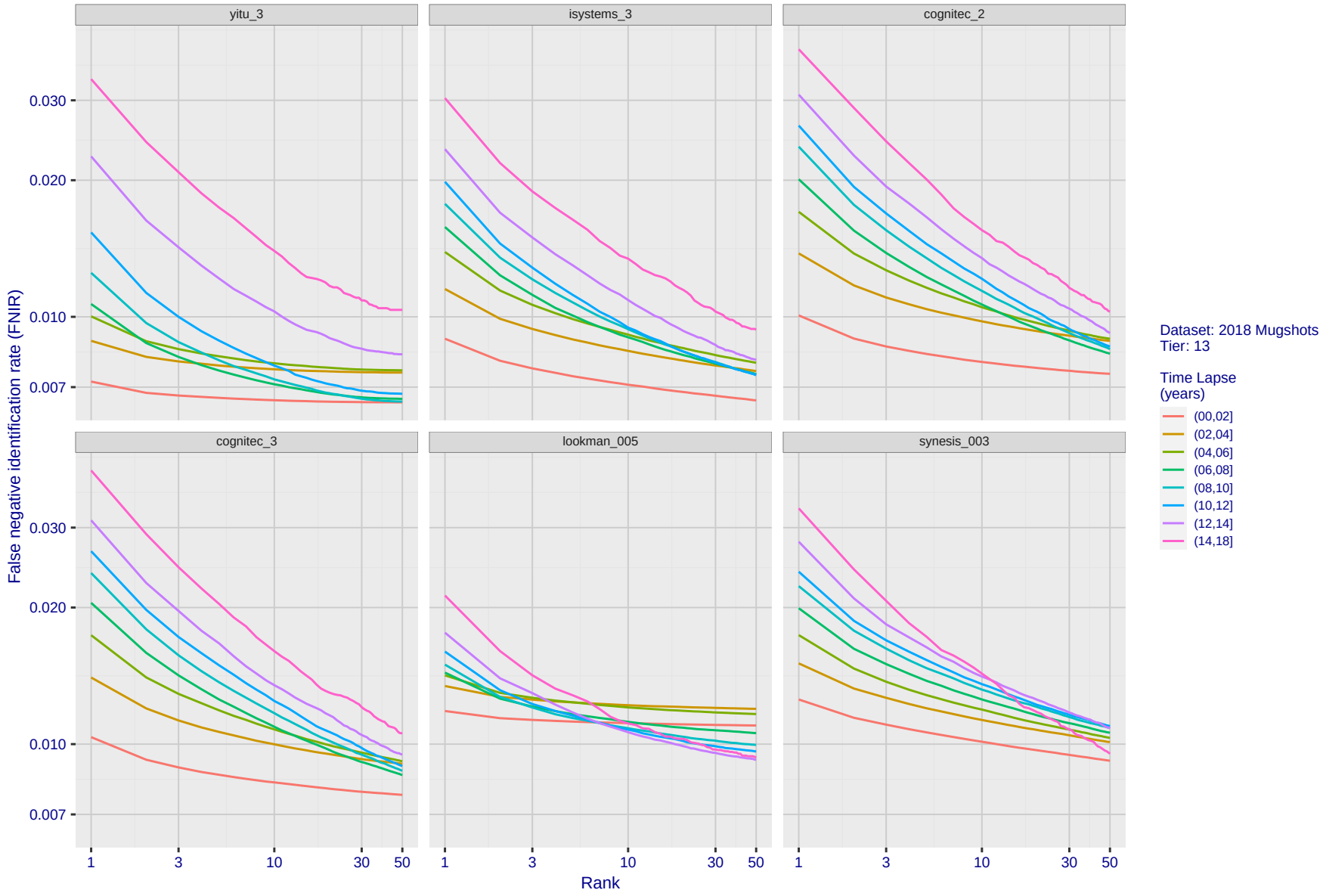

Figure 72: **[FRVT-2018 Mugshot Ageing Dataset] Identification miss rates vs. rank by time-elapsed**. *The oldest image of each individual is enrolled. Thereafter, all more recent images are searched. Miss rates are computed over all searches noted in row 17 of Table 1 and binned by number of years between search and initial enrollment.*

2021/11/22
08:35:53

FNIR(N, R, T) = False neg. identification rate
FPIR(N, T) = False pos. identification rate

N = Num. enrolled subjects
R = Num. candidates examined

T = Threshold

T = 0 → Investigation
T > 0 → Identification

This publication is available free of charge from: https://doi.org/10.6028/NIST.IR.8271

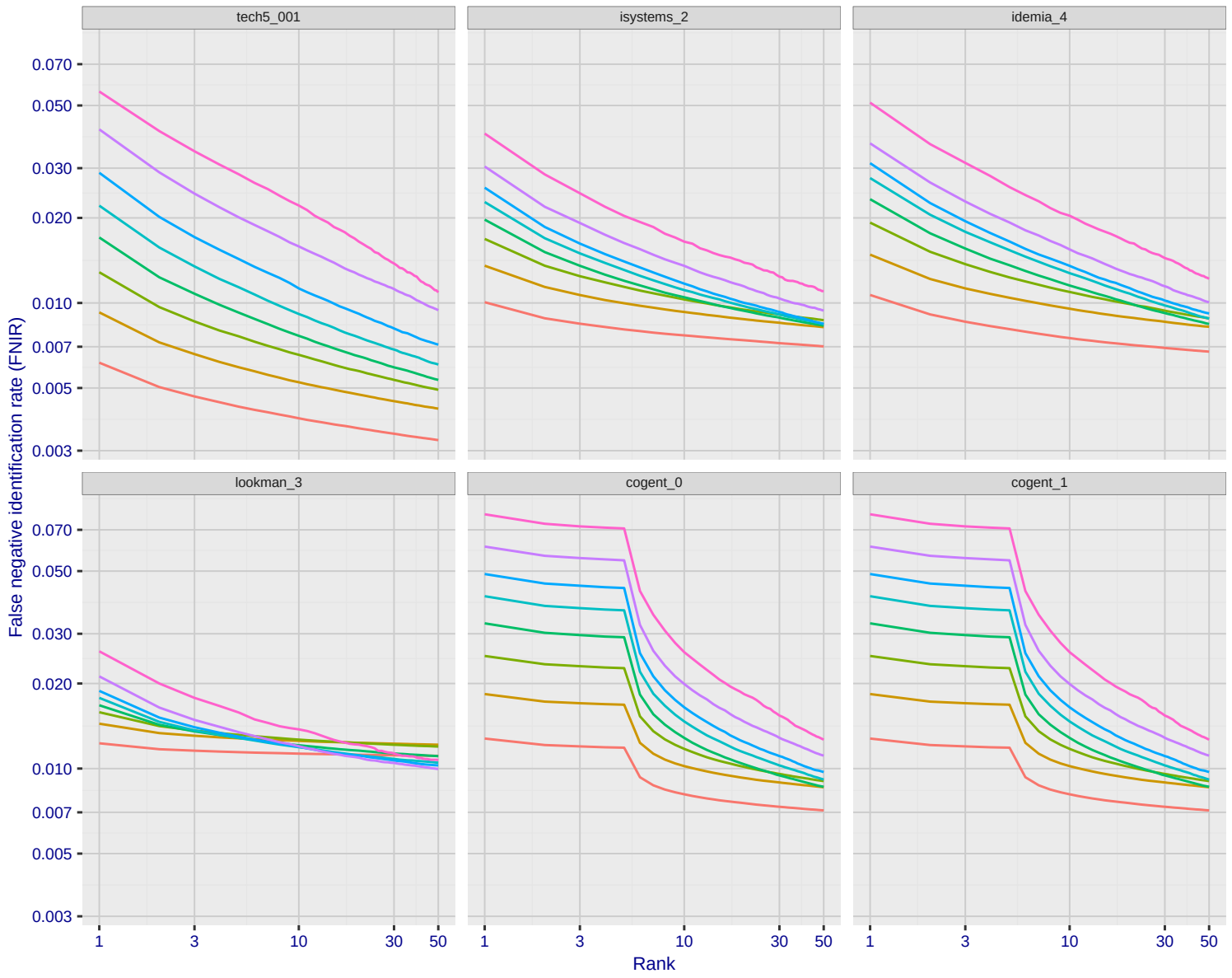

Figure 73: **[FRVT-2018 Mugshot Ageing Dataset] Identification miss rates vs. rank by time-elapsed**. *The oldest image of each individual is enrolled. Thereafter, all more recent images are searched. Miss rates are computed over all searches noted in row 17 of Table 1 and binned by number of years between search and initial enrollment.*

2021/11/22 08:35:53
FNIR(N, R, T) = False neg. identification rate
FPIR(N, T) = False pos. identification rate
N = Num. enrolled subjects
R = Num. candidates examined
T = Threshold
T = 0 → Investigation
T > 0 → Identification

This publication is available free of charge from: https://doi.org/10.6028/NIST.IR.8271

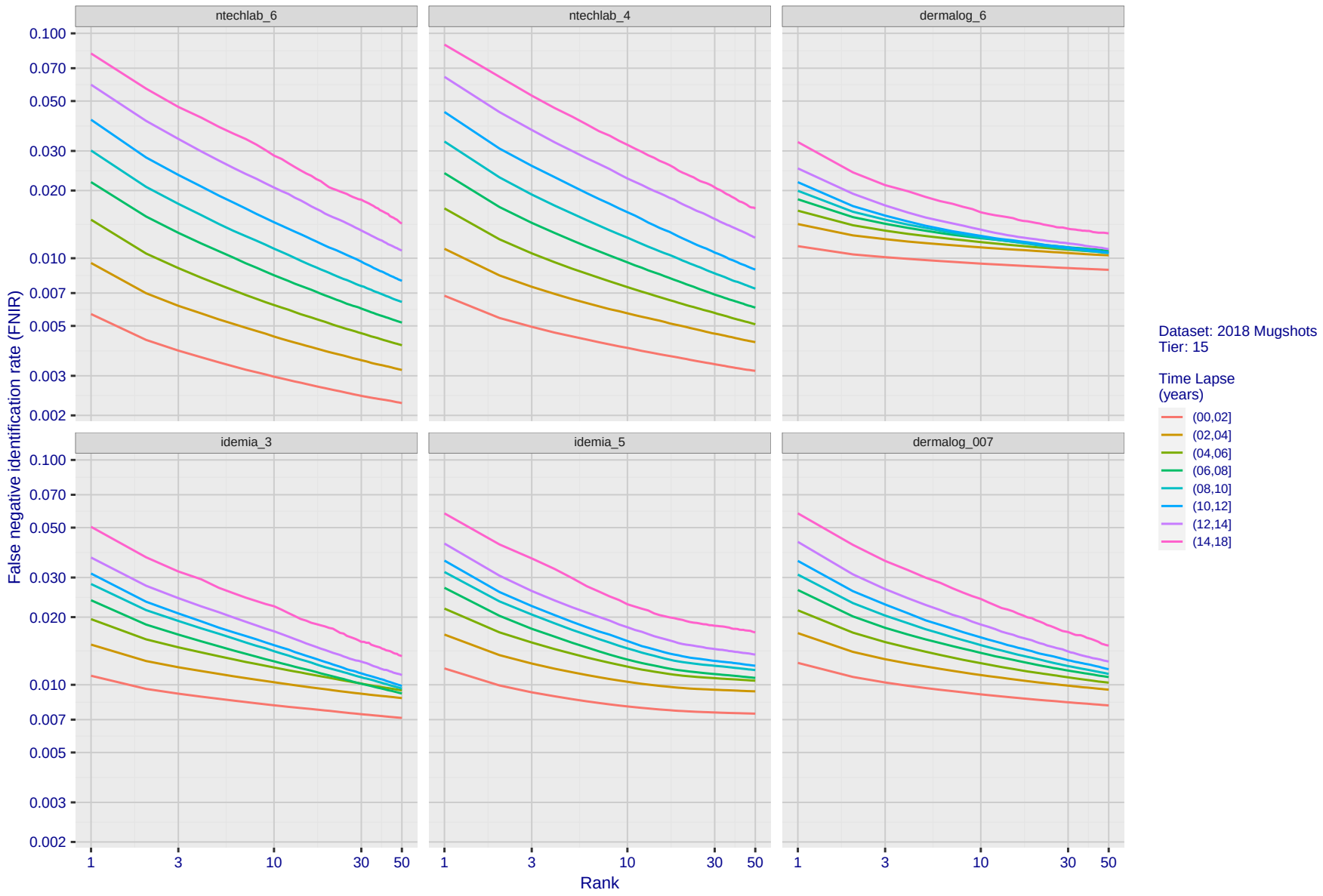

Figure 74: **[FRVT-2018 Mugshot Ageing Dataset] Identification miss rates vs. rank by time-elapsed**. *The oldest image of each individual is enrolled. Thereafter, all more recent images are searched. Miss rates are computed over all searches noted in row 17 of Table 1 and binned by number of years between search and initial enrollment.*

2021/11/22
08:35:53
FNIR(N, R, T) = False neg. identification rate
FPIR(N, T) = False pos. identification rate
N = Num. enrolled subjects
R = Num. candidates examined
T = Threshold
T = 0 → Investigation
T > 0 → Identification

This publication is available free of charge from: https://doi.org/10.6028/NIST.IR.8271

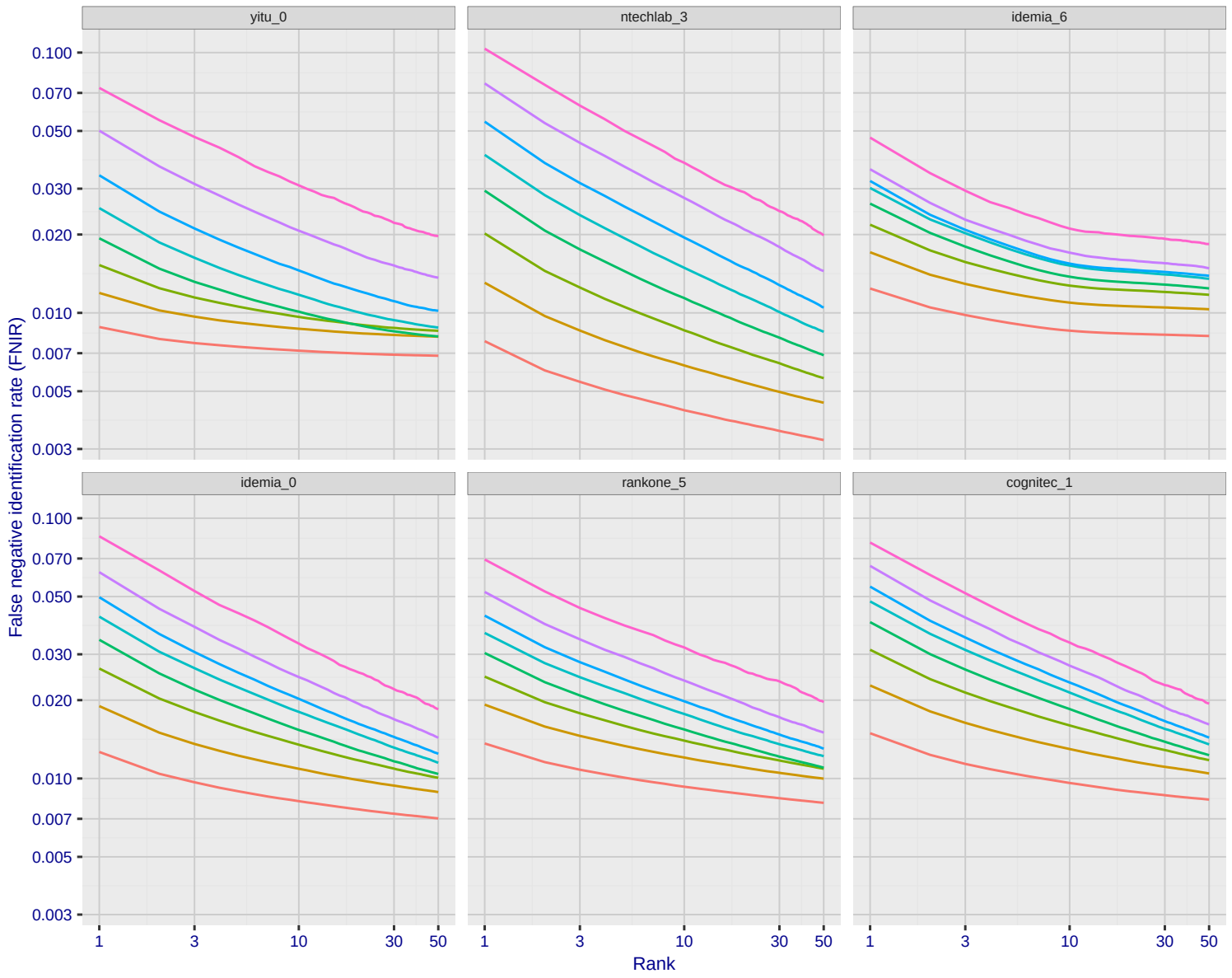

Figure 75: **[FRVT-2018 Mugshot Ageing Dataset] Identification miss rates vs. rank by time-elapsed**. *The oldest image of each individual is enrolled. Thereafter, all more recent images are searched. Miss rates are computed over all searches noted in row 17 of Table 1 and binned by number of years between search and initial enrollment.*

2021/11/22
08:35:53
FNIR(N, R, T) = False neg. identification rate
FPIR(N, T) = False pos. identification rate
N = Num. enrolled subjects
R = Num. candidates examined
T = Threshold
T = 0 → Investigation
T > 0 → Identification

This publication is available free of charge from: https://doi.org/10.6028/NIST.IR.8271

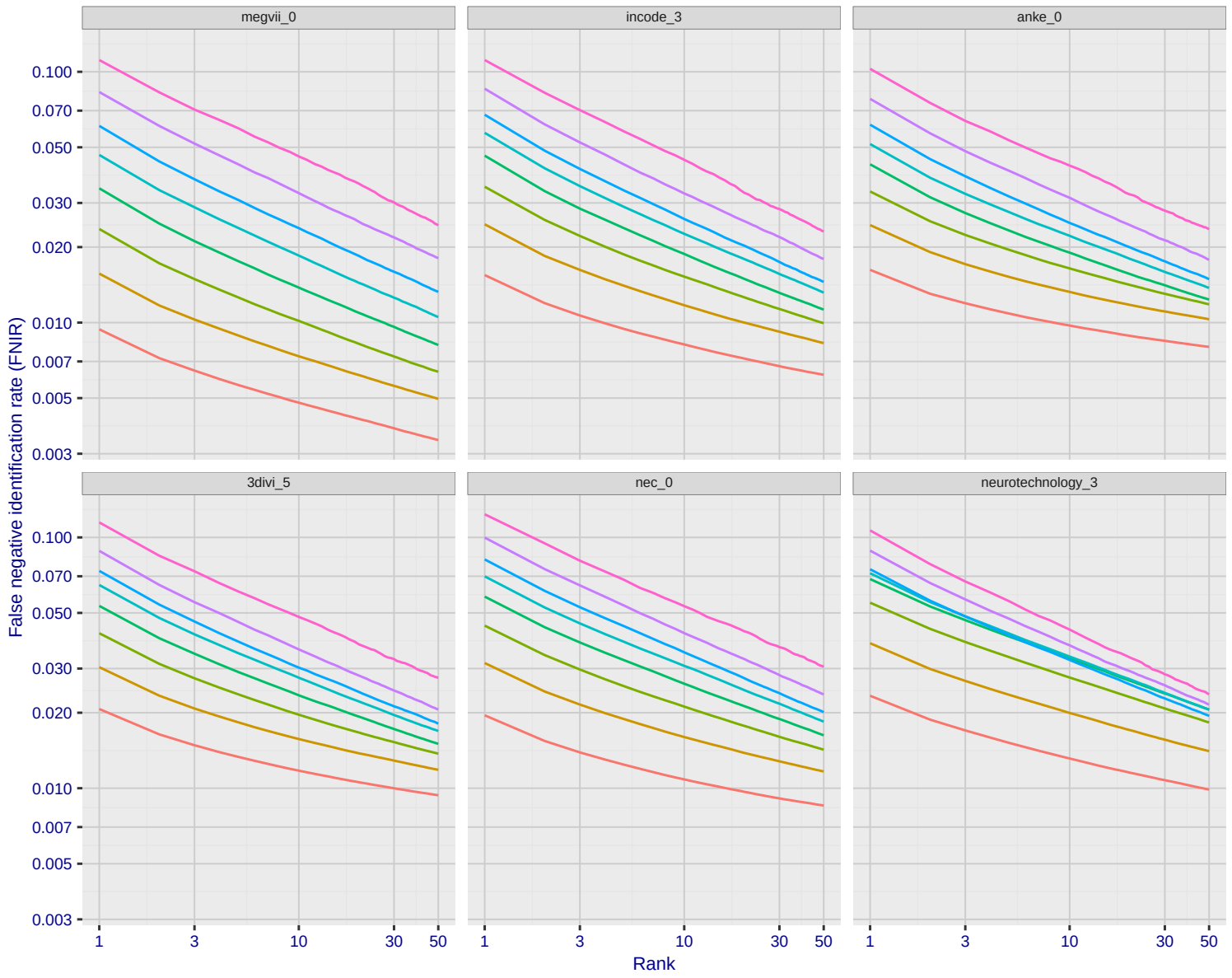

Figure 76: **[FRVT-2018 Mugshot Ageing Dataset] Identification miss rates vs. rank by time-elapsed**. *The oldest image of each individual is enrolled. Thereafter, all more recent images are searched. Miss rates are computed over all searches noted in row 17 of Table 1 and binned by number of years between search and initial enrollment.*

2021/11/22 08:35:53

FNIR(N, R, T) = False neg. identification rate
FPIR(N, T) = False pos. identification rate

N = Num. enrolled subjects
R = Num. candidates examined

T = Threshold

T = 0 → Investigation
T > 0 → Identification

This publication is available free of charge from: https://doi.org/10.6028/NIST.IR.8271

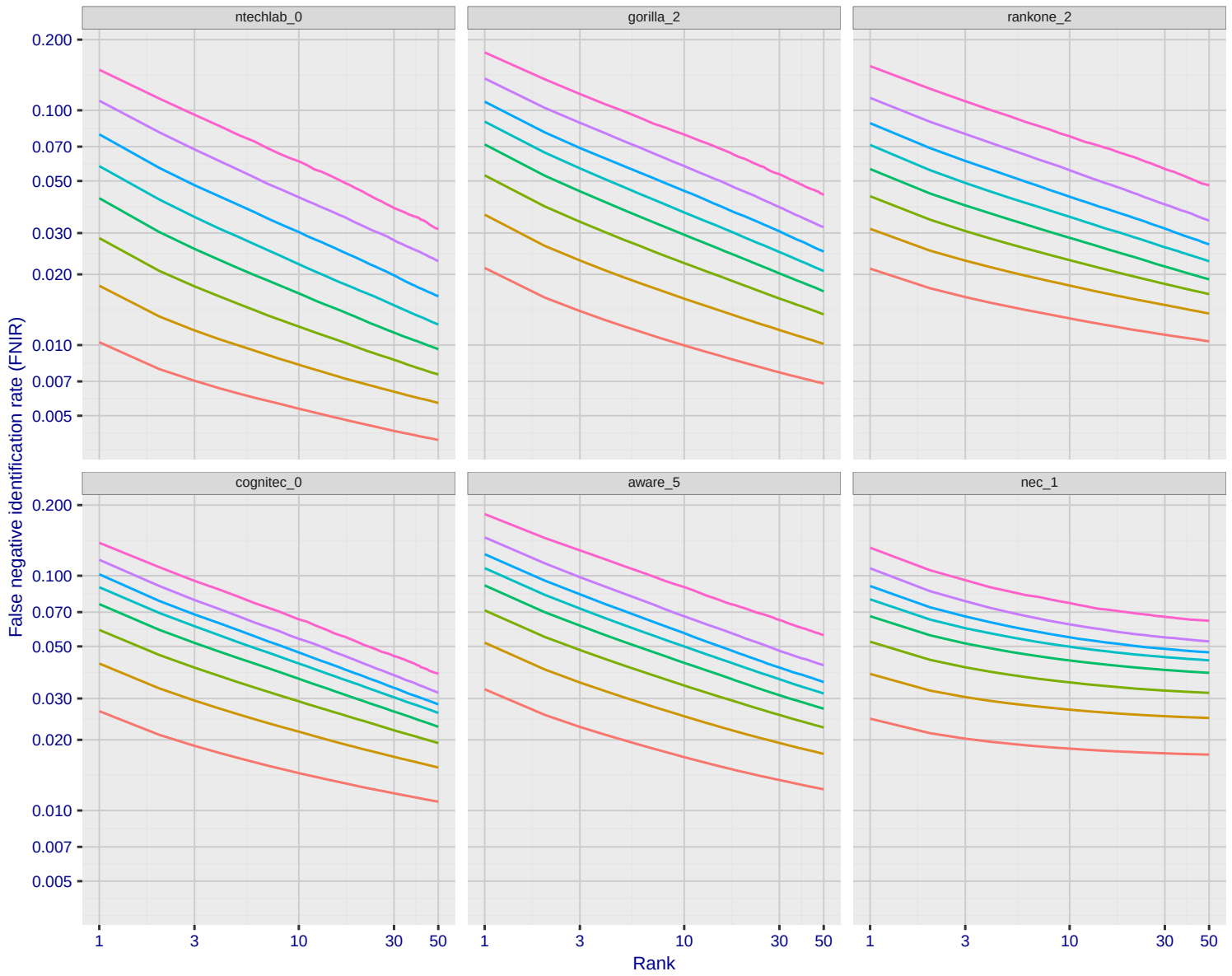

Figure 77: **[FRVT-2018 Mugshot Ageing Dataset] Identification miss rates vs. rank by time-elapsed**. *The oldest image of each individual is enrolled. Thereafter, all more recent images are searched. Miss rates are computed over all searches noted in row 17 of Table 1 and binned by number of years between search and initial enrollment.*

2021/11/22 08:35:53
FNIR(N, R, T) = False neg. identification rate
FPIR(N, T) = False pos. identification rate
N = Num. enrolled subjects
R = Num. candidates examined
T = Threshold
T = 0 → Investigation
T > 0 → Identification

This publication is available free of charge from: https://doi.org/10.6028/NIST.IR.8271

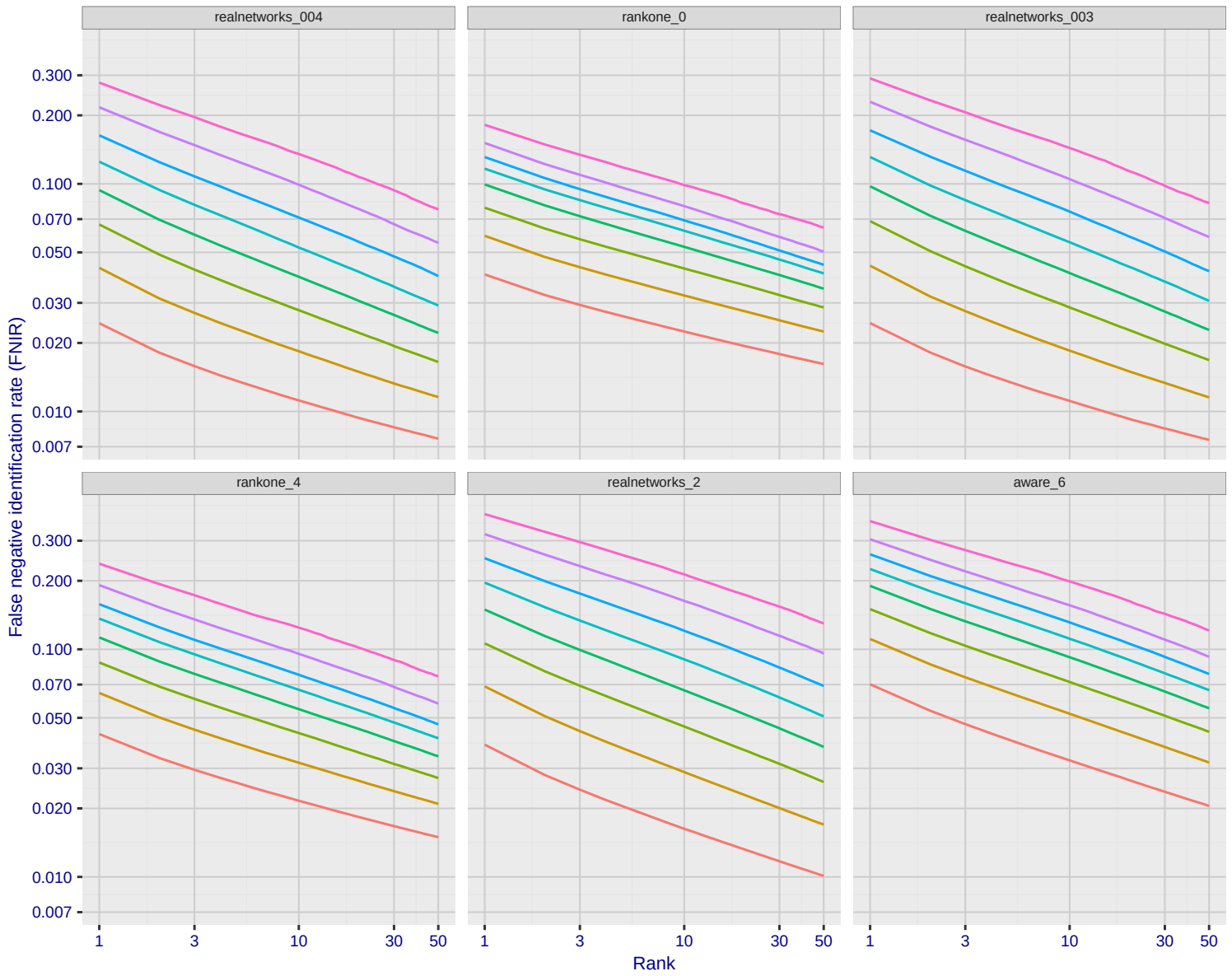

Figure 78: **[FRVT-2018 Mugshot Ageing Dataset] Identification miss rates vs. rank by time-elapsed**. *The oldest image of each individual is enrolled. Thereafter, all more recent images are searched. Miss rates are computed over all searches noted in row 17 of Table 1 and binned by number of years between search and initial enrollment.*

2021/11/22
08:35:53
FNIR(N, R, T) = False neg. identification rate
FPIR(N, T) = False pos. identification rate
N = Num. enrolled subjects
R = Num. candidates examined
T = Threshold
T = 0 → Investigation
T > 0 → Identification

This publication is available free of charge from: https://doi.org/10.6028/NIST.IR.8271

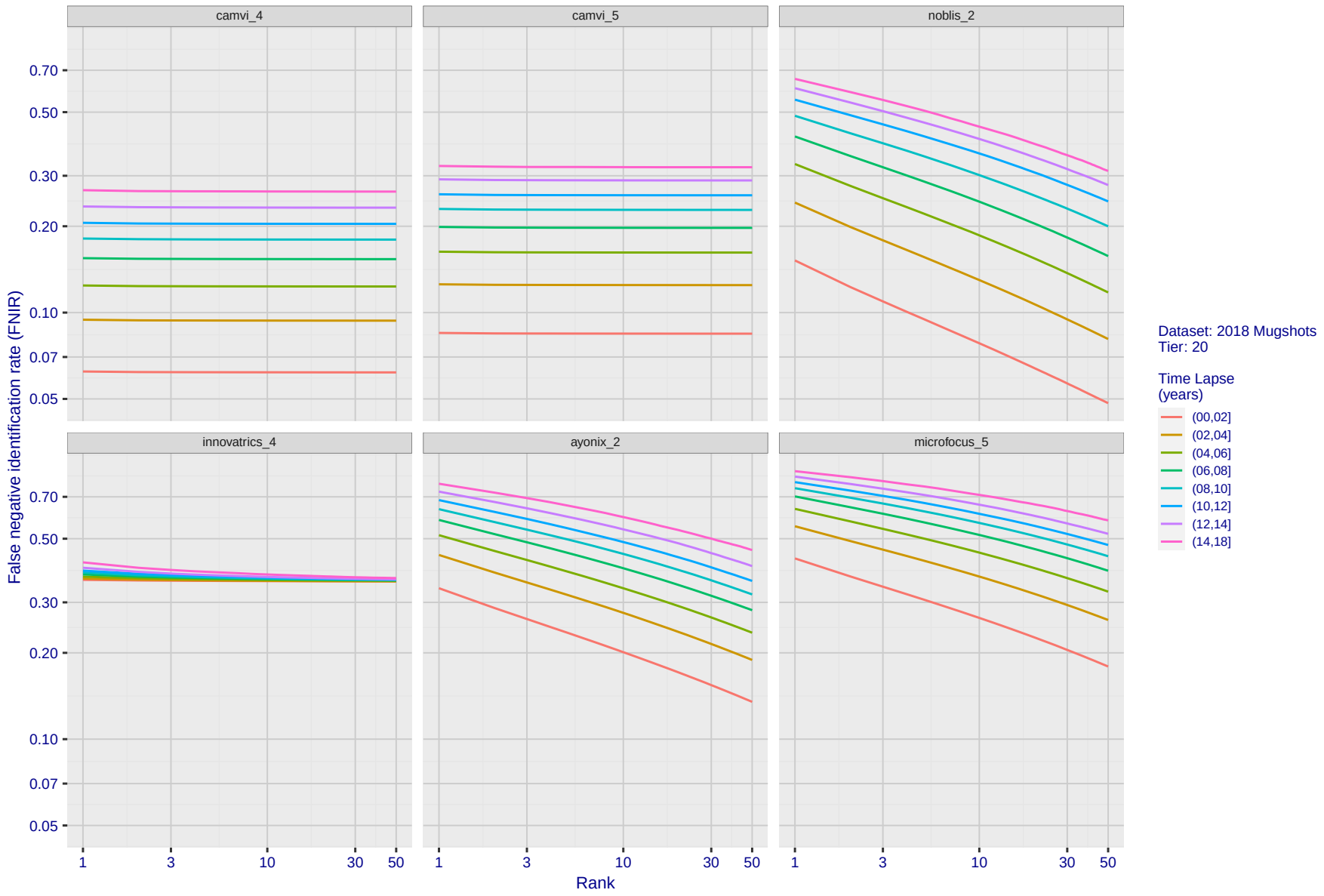

Figure 79: **[FRVT-2018 Mugshot Ageing Dataset] Identification miss rates vs. rank by time-elapsed**. *The oldest image of each individual is enrolled. Thereafter, all more recent images are searched. Miss rates are computed over all searches noted in row 17 of Table 1 and binned by number of years between search and initial enrollment.*

2021/11/22
08:35:53
FNIR(N, R, T) = False neg. identification rate
FPIR(N, T) = False pos. identification rate
N = Num. enrolled subjects
R = Num. candidates examined
T = Threshold
T = 0 → Investigation
T > 0 → Identification

This publication is available free of charge from: https://doi.org/10.6028/NIST.IR.8271

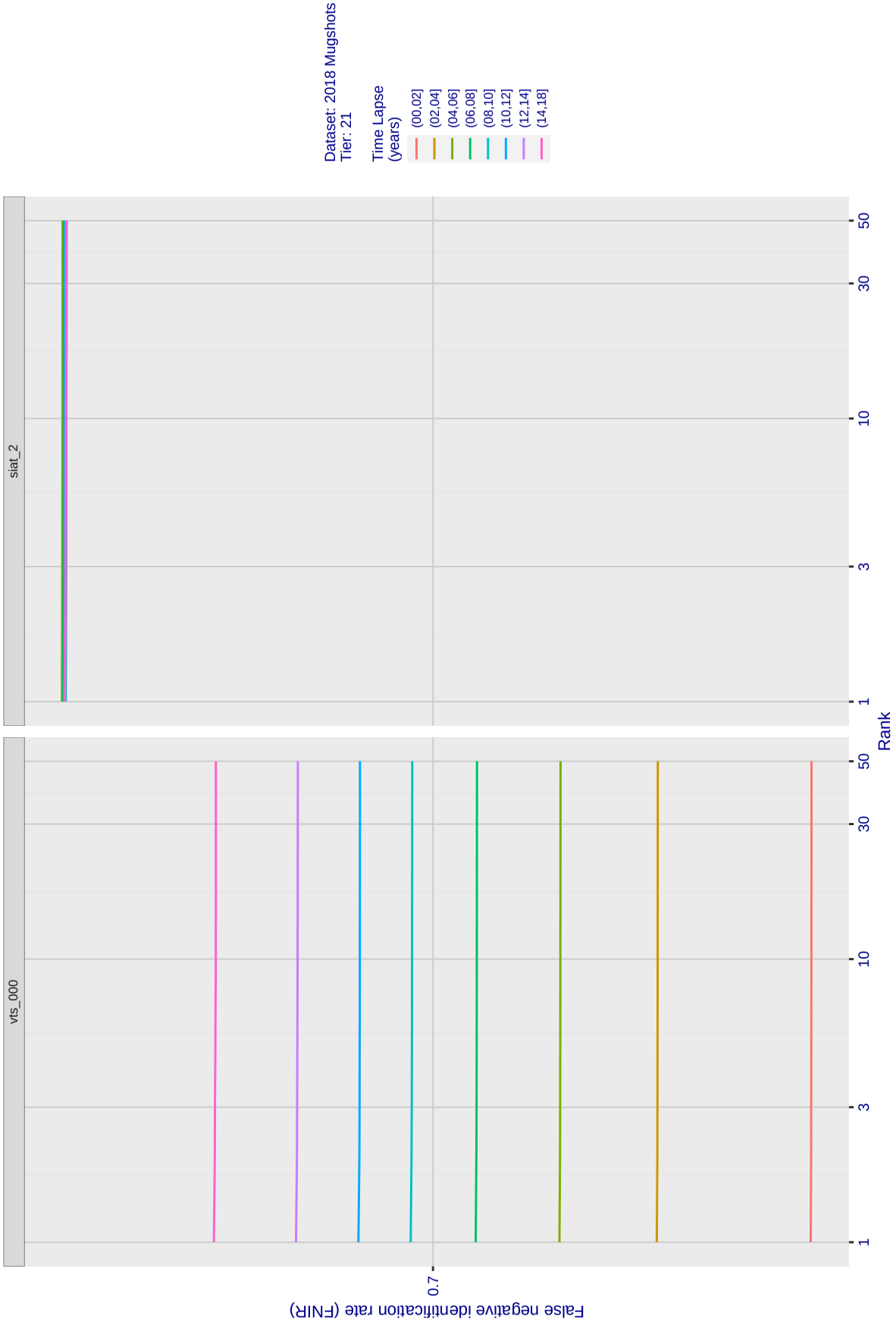

Figure 80: **[FRVT-2018 Mugshot Ageing Dataset] Identification miss rates vs. rank by time-elapsed.** *The oldest image of each individual is enrolled. Thereafter, all more recent images are searched. Miss rates are computed over all searches noted in row 17 of Table 1 and binned by number of years between search and initial enrollment.*

2021/11/22	FNIR(N, R, T) =	False neg. identification rate	N = Num. enrolled subjects	T = Threshold	$T = 0 \rightarrow$ Investigation
08:35:53	FPIR(N, T) =	False pos. identification rate	R = Num. candidates examined		$T > 0 \rightarrow$ Identification

This publication is available free of charge from: https://doi.org/10.6028/NIST.IR.8271

This publication is available free of charge from: https://doi.org/10.6028/NIST.IR.8271

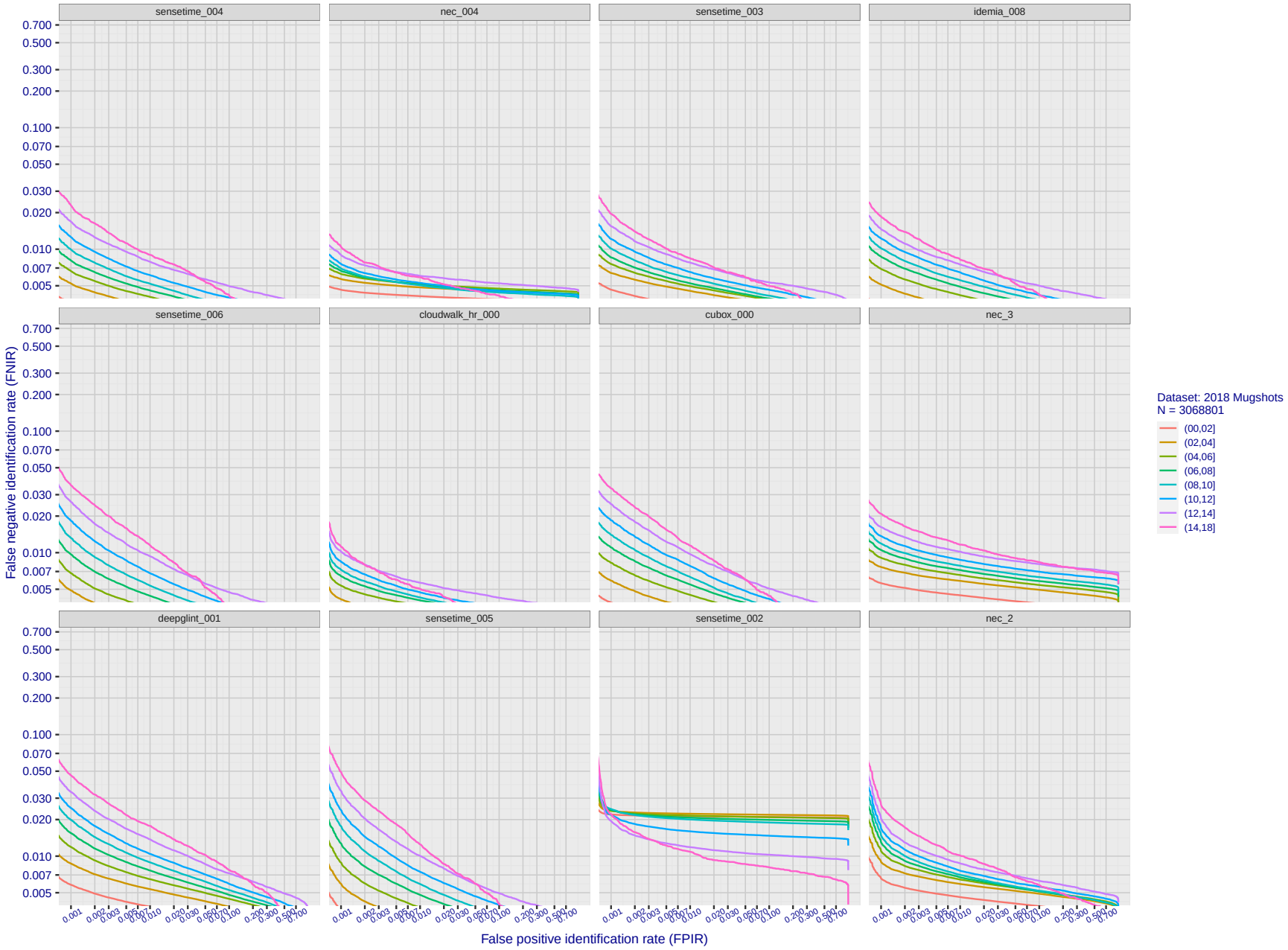

Figure 81: **[FRVT-2018 Mugshot Ageing Dataset] Identification miss rates vs. FPIR by time-elapsed**. *The oldest image of each individual is enrolled. Thereafter, all more recent images are searched. Miss rates are computed over all searches noted in row 17 of Table 1 and binned by number of years between search and initial enrollment. FPIR is computed from the same FRVT 2018 non-mates noted in row 3 of Table 1 with N = 3 000 000.*

2021/11/22 08:35:53 FNIR(N, R, T) = FPIR(N, T) = False neg. identification rate False pos. identification rate N = Num. enrolled subjects R = Num. candidates examined T = Threshold T = 0 → Investigation T > 0 → Identification

This publication is available free of charge from: https://doi.org/10.6028/NIST.IR.8271

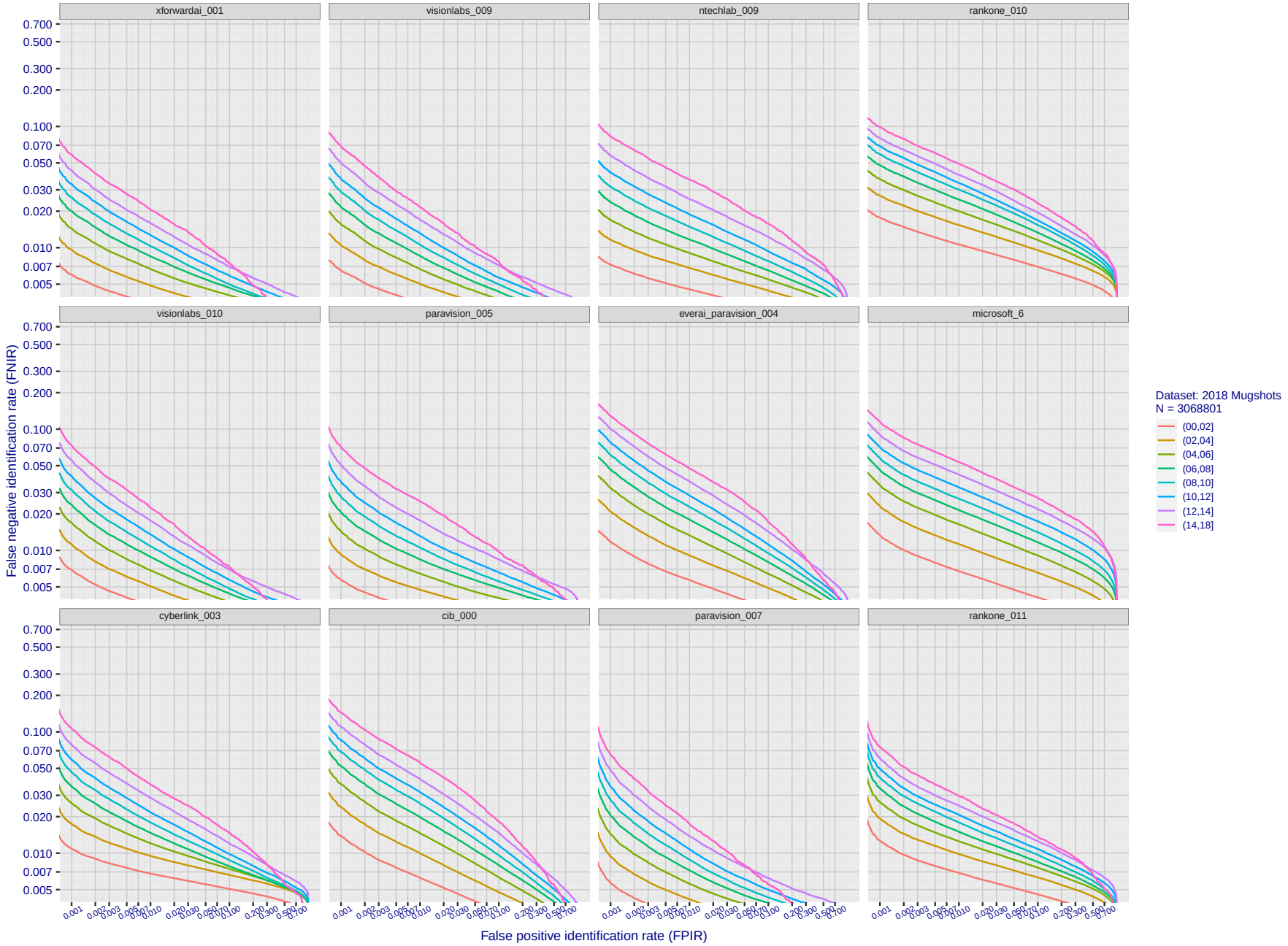

Figure 82: **[FRVT-2018 Mugshot Ageing Dataset] Identification miss rates vs. FPIR by time-elapsed**. *The oldest image of each individual is enrolled. Thereafter, all more recent images are searched. Miss rates are computed over all searches noted in row 17 of Table 1 and binned by number of years between search and initial enrollment. FPIR is computed from the same FRVT 2018 non-mates noted in row 3 of Table 1 with N = 3 000 000.*

2021/11/22
08:35:53
FNIR(N, R, T) = False neg. identification rate
FPIR(N, T) = False pos. identification rate
N = Num. enrolled subjects
R = Num. candidates examined
T = Threshold
T = 0 → Investigation
T > 0 → Identification

This publication is available free of charge from: https://doi.org/10.6028/NIST.IR.8271

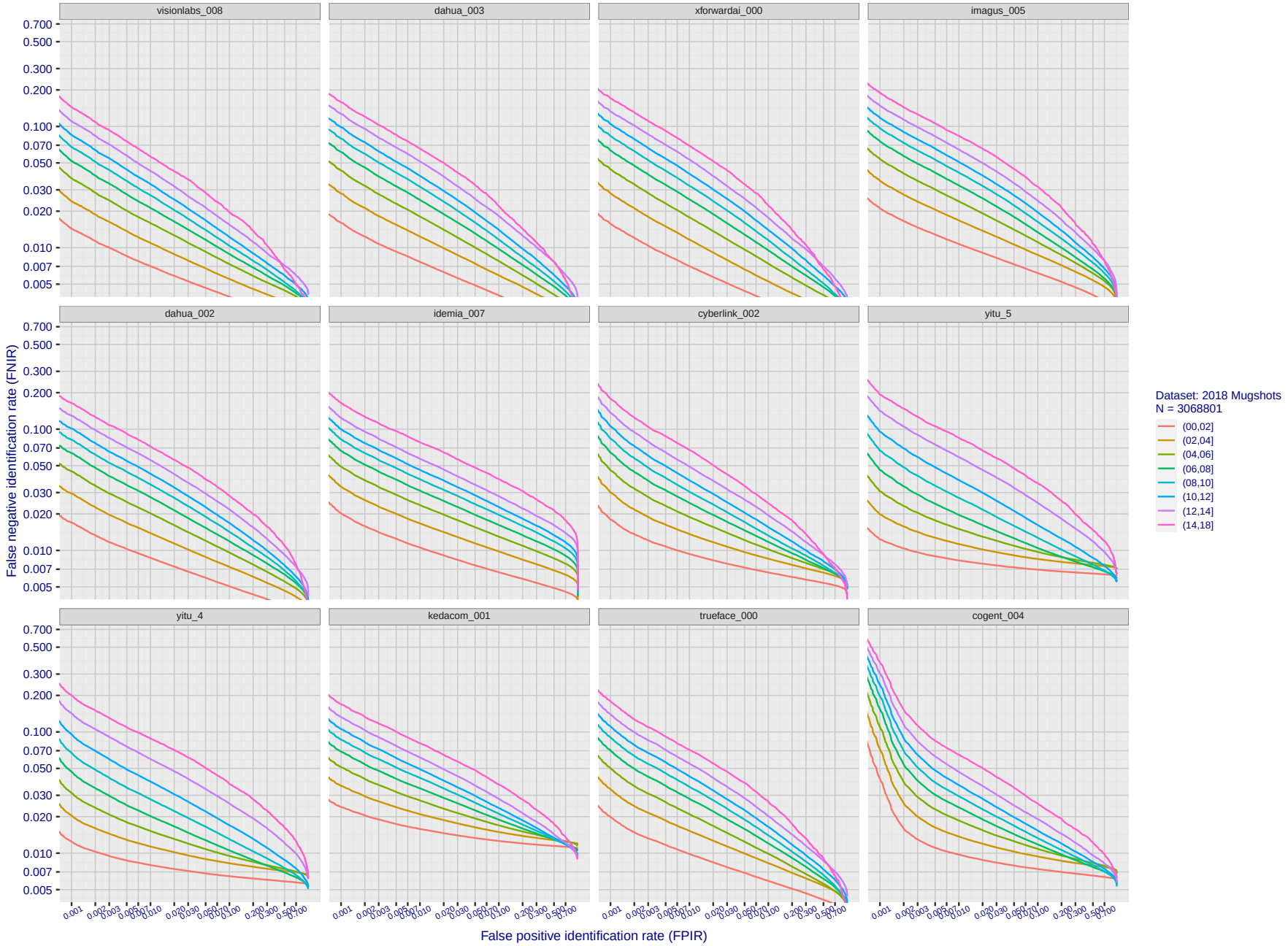

Figure 83: **[FRVT-2018 Mugshot Ageing Dataset] Identification miss rates vs. FPIR by time-elapsed**. *The oldest image of each individual is enrolled. Thereafter, all more recent images are searched. Miss rates are computed over all searches noted in row 17 of Table 1 and binned by number of years between search and initial enrollment. FPIR is computed from the same FRVT 2018 non-mates noted in row 3 of Table 1 with N = 3 000 000.*

2021/11/22 08:35:53

FNIR(N, R, T) = False neg. identification rate
FPIR(N, T) = False pos. identification rate

N = Num. enrolled subjects
R = Num. candidates examined

T = Threshold

T = 0 → Investigation
T > 0 → Identification

This publication is available free of charge from: https://doi.org/10.6028/NIST.IR.8271

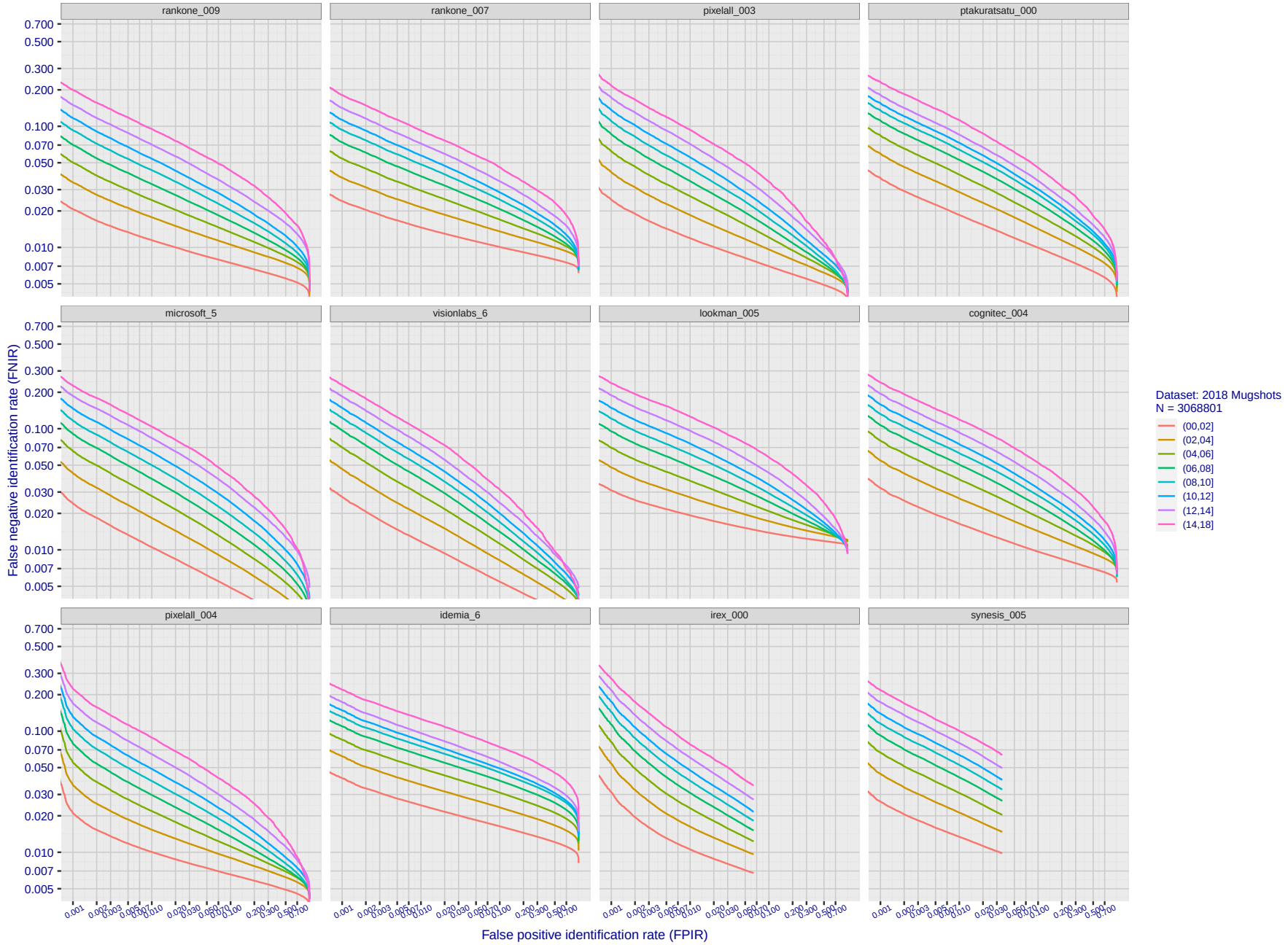

Figure 84: **[FRVT-2018 Mugshot Ageing Dataset] Identification miss rates vs. FPIR by time-elapsed**. *The oldest image of each individual is enrolled. Thereafter, all more recent images are searched. Miss rates are computed over all searches noted in row 17 of Table 1 and binned by number of years between search and initial enrollment. FPIR is computed from the same FRVT 2018 non-mates noted in row 3 of Table 1 with N = 3 000 000.*

This publication is available free of charge from: https://doi.org/10.6028/NIST.IR.8271

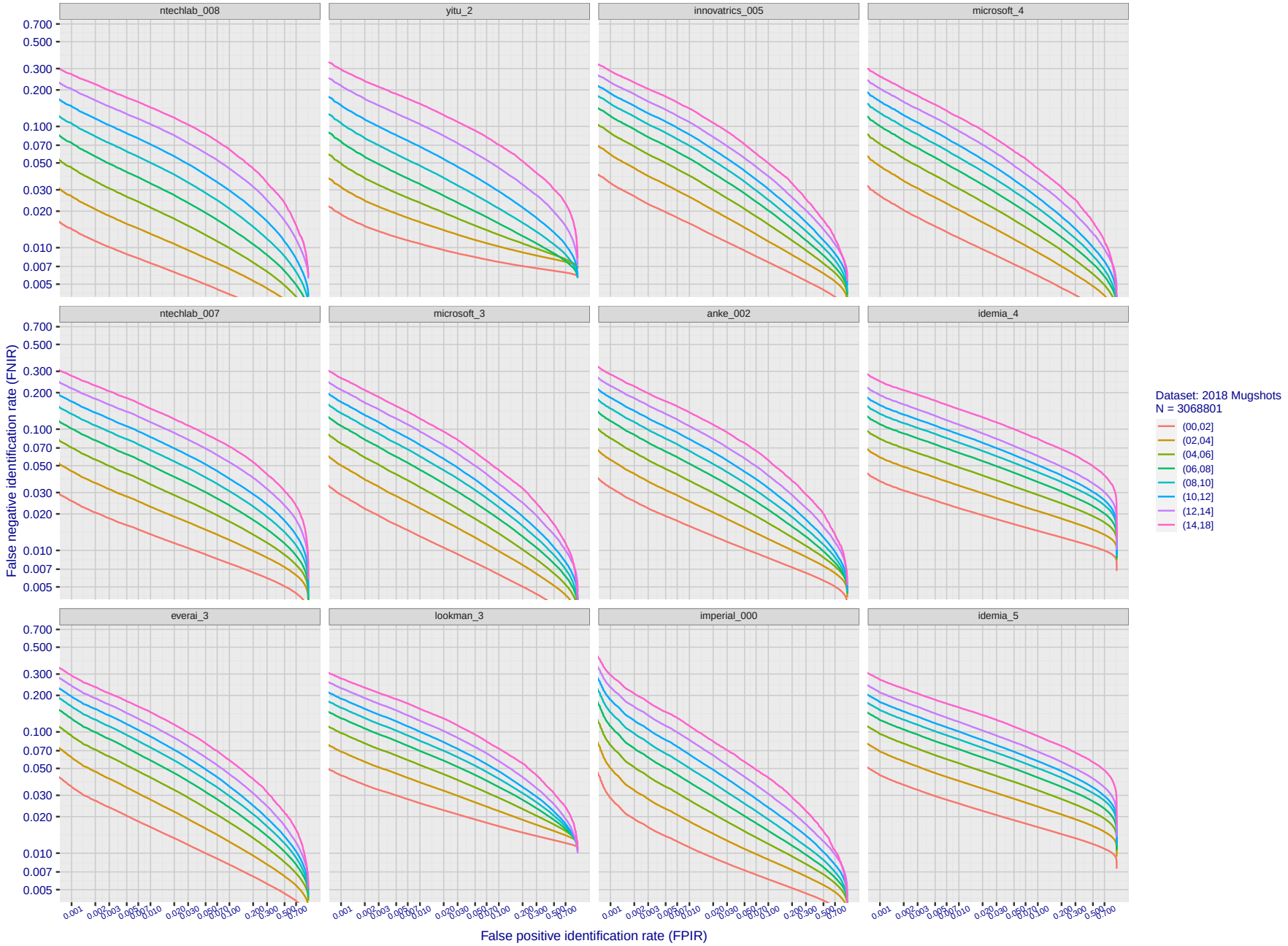

Figure 85: **[FRVT-2018 Mugshot Ageing Dataset] Identification miss rates vs. FPIR by time-elapsed**. *The oldest image of each individual is enrolled. Thereafter, all more recent images are searched. Miss rates are computed over all searches noted in row 17 of Table 1 and binned by number of years between search and initial enrollment. FPIR is computed from the same FRVT 2018 non-mates noted in row 3 of Table 1 with N = 3 000 000.*

2021/11/22 08:35:53
FNIR(N, R, T) = False neg. identification rate
FPIR(N, T) = False pos. identification rate
N = Num. enrolled subjects
R = Num. candidates examined
T = Threshold
T = 0 → Investigation
T > 0 → Identification

This publication is available free of charge from: https://doi.org/10.6028/NIST.IR.8271

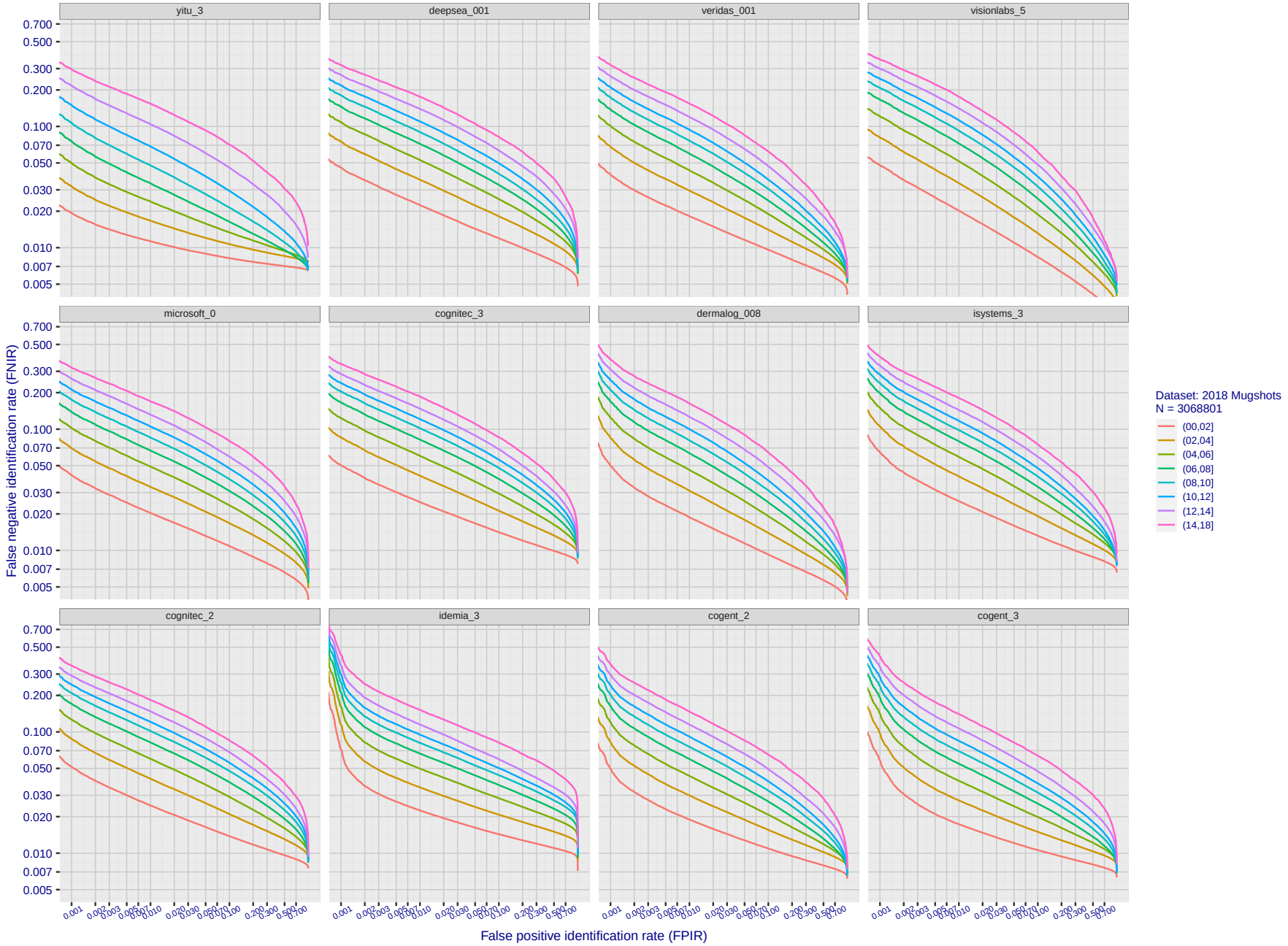

Figure 86: **[FRVT-2018 Mugshot Ageing Dataset] Identification miss rates vs. FPIR by time-elapsed**. *The oldest image of each individual is enrolled. Thereafter, all more recent images are searched. Miss rates are computed over all searches noted in row 17 of Table 1 and binned by number of years between search and initial enrollment. FPIR is computed from the same FRVT 2018 non-mates noted in row 3 of Table 1 with N = 3 000 000.*

2021/11/22
08:35:53
FNIR(N, R, T) = False neg. identification rate
FPIR(N, T) = False pos. identification rate
N = Num. enrolled subjects
R = Num. candidates examined
T = Threshold
T = 0 → Investigation
T > 0 → Identification

This publication is available free of charge from: https://doi.org/10.6028/NIST.IR.8271

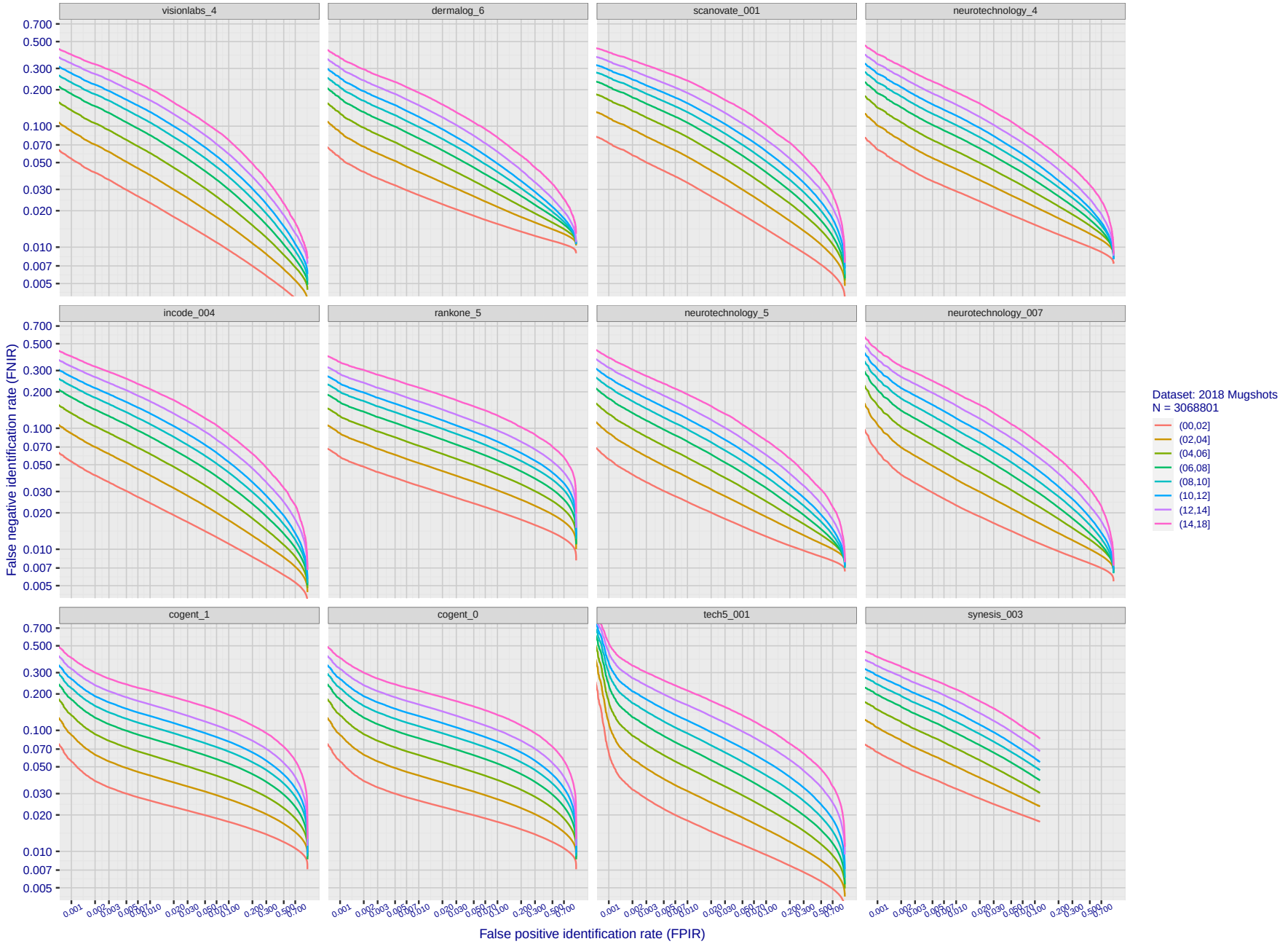

Figure 87: **[FRVT-2018 Mugshot Ageing Dataset] Identification miss rates vs. FPIR by time-elapsed**. *The oldest image of each individual is enrolled. Thereafter, all more recent images are searched. Miss rates are computed over all searches noted in row 17 of Table 1 and binned by number of years between search and initial enrollment. FPIR is computed from the same FRVT 2018 non-mates noted in row 3 of Table 1 with N = 3 000 000.*

2021/11/22
08:35:53

FNIR(N, R, T) = False neg. identification rate
FPIR(N, T) = False pos. identification rate

N = Num. enrolled subjects
R = Num. candidates examined

T = Threshold

T = 0 → Investigation
T > 0 → Identification

This publication is available free of charge from: https://doi.org/10.6028/NIST.IR.8271

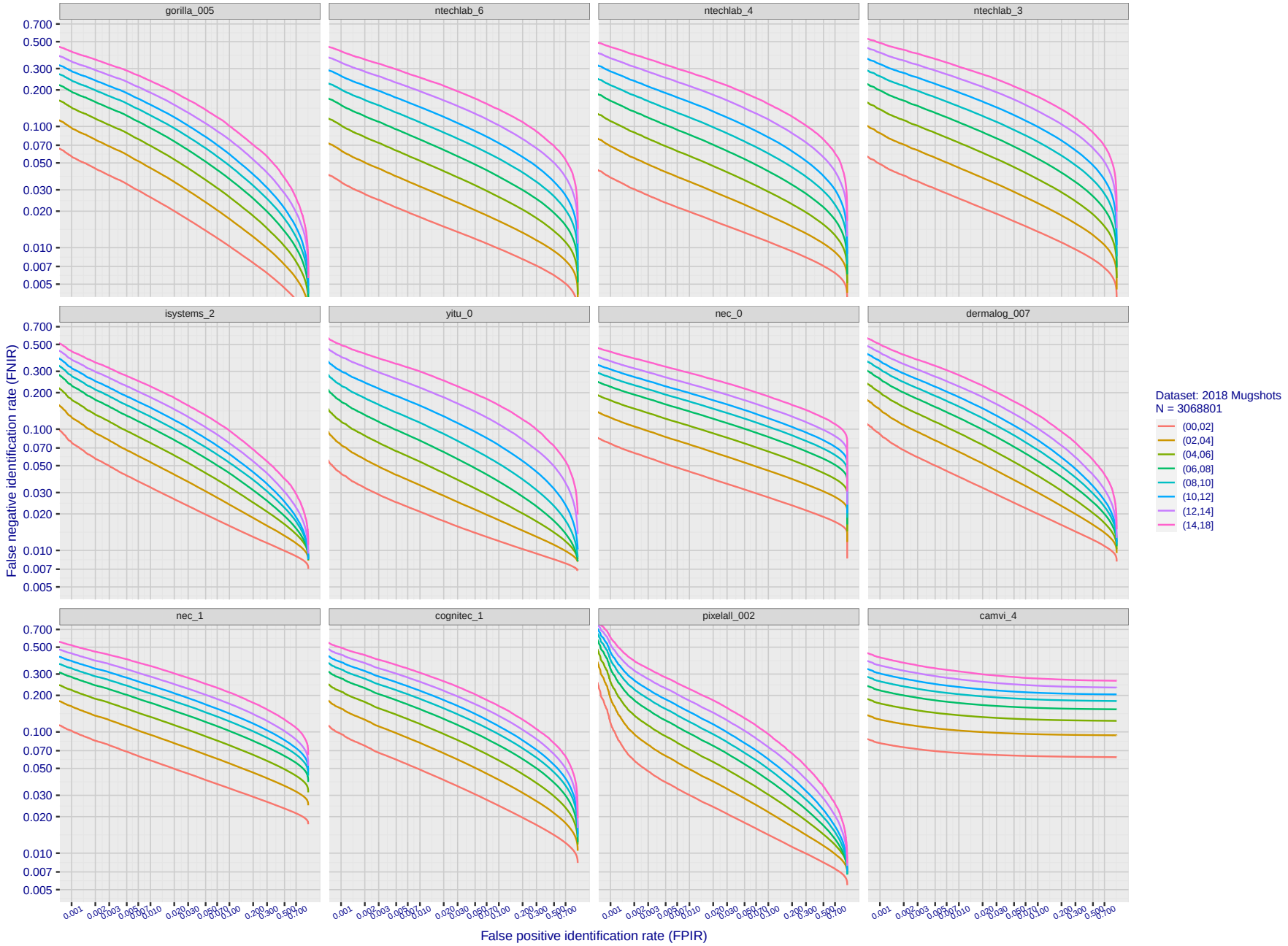

Figure 88: **[FRVT-2018 Mugshot Ageing Dataset] Identification miss rates vs. FPIR by time-elapsed**. *The oldest image of each individual is enrolled. Thereafter, all more recent images are searched. Miss rates are computed over all searches noted in row 17 of Table 1 and binned by number of years between search and initial enrollment. FPIR is computed from the same FRVT 2018 non-mates noted in row 3 of Table 1 with N = 3 000 000.*

2021/11/22
08:35:53
FNIR(N, R, T) = False neg. identification rate
FPIR(N, T) = False pos. identification rate
N = Num. enrolled subjects
R = Num. candidates examined
T = Threshold
T = 0 → Investigation
T > 0 → Identification

This publication is available free of charge from: https://doi.org/10.6028/NIST.IR.8271

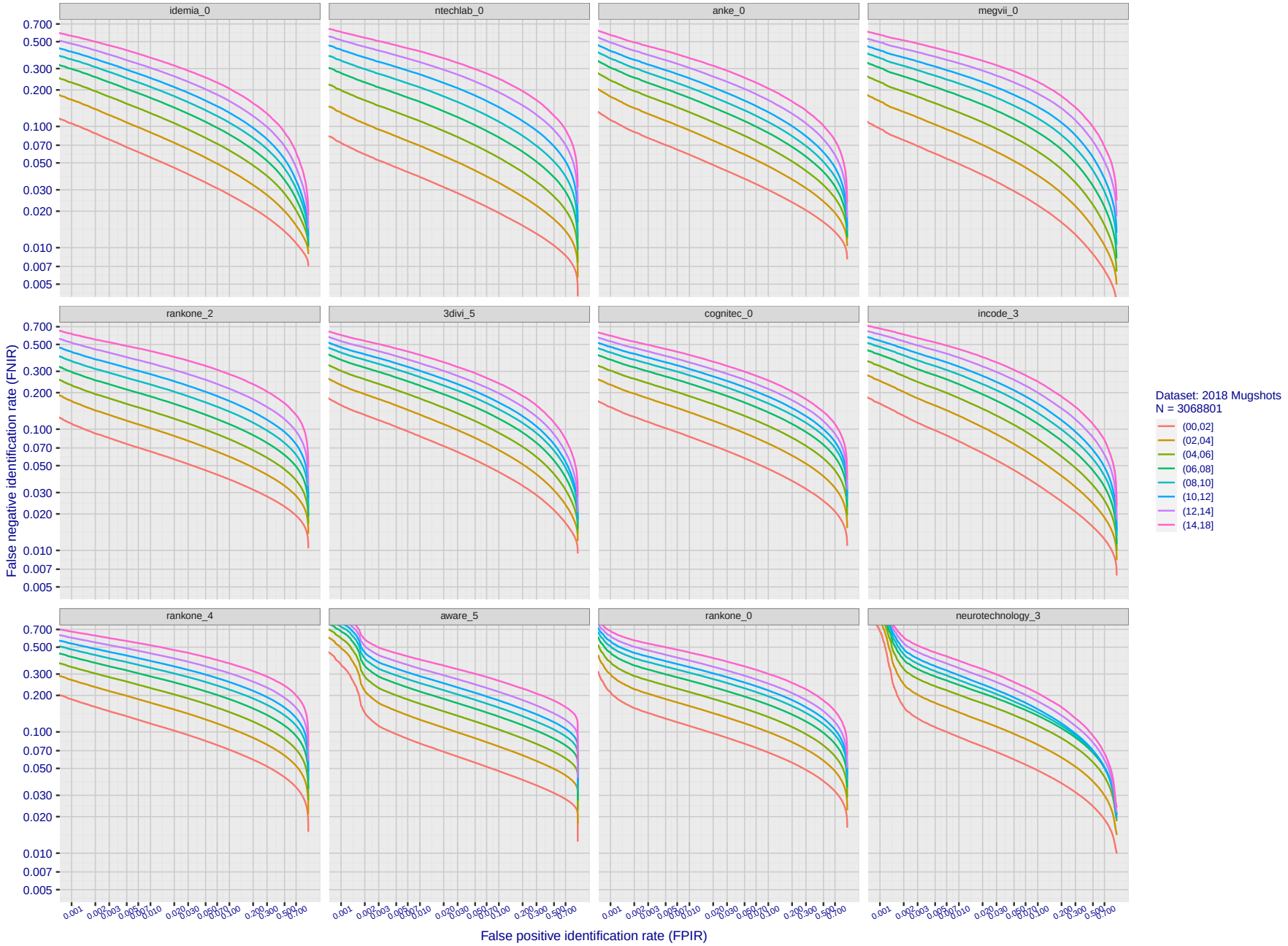

Figure 89: **[FRVT-2018 Mugshot Ageing Dataset] Identification miss rates vs. FPIR by time-elapsed**. *The oldest image of each individual is enrolled. Thereafter, all more recent images are searched. Miss rates are computed over all searches noted in row 17 of Table 1 and binned by number of years between search and initial enrollment. FPIR is computed from the same FRVT 2018 non-mates noted in row 3 of Table 1 with N = 3 000 000.*

2021/11/22 08:35:53

FNIR(N, R, T) = False neg. identification rate
FPIR(N, T) = False pos. identification rate

N = Num. enrolled subjects
R = Num. candidates examined

T = Threshold

T = 0 → Investigation
T > 0 → Identification

This publication is available free of charge from: https://doi.org/10.6028/NIST.IR.8271

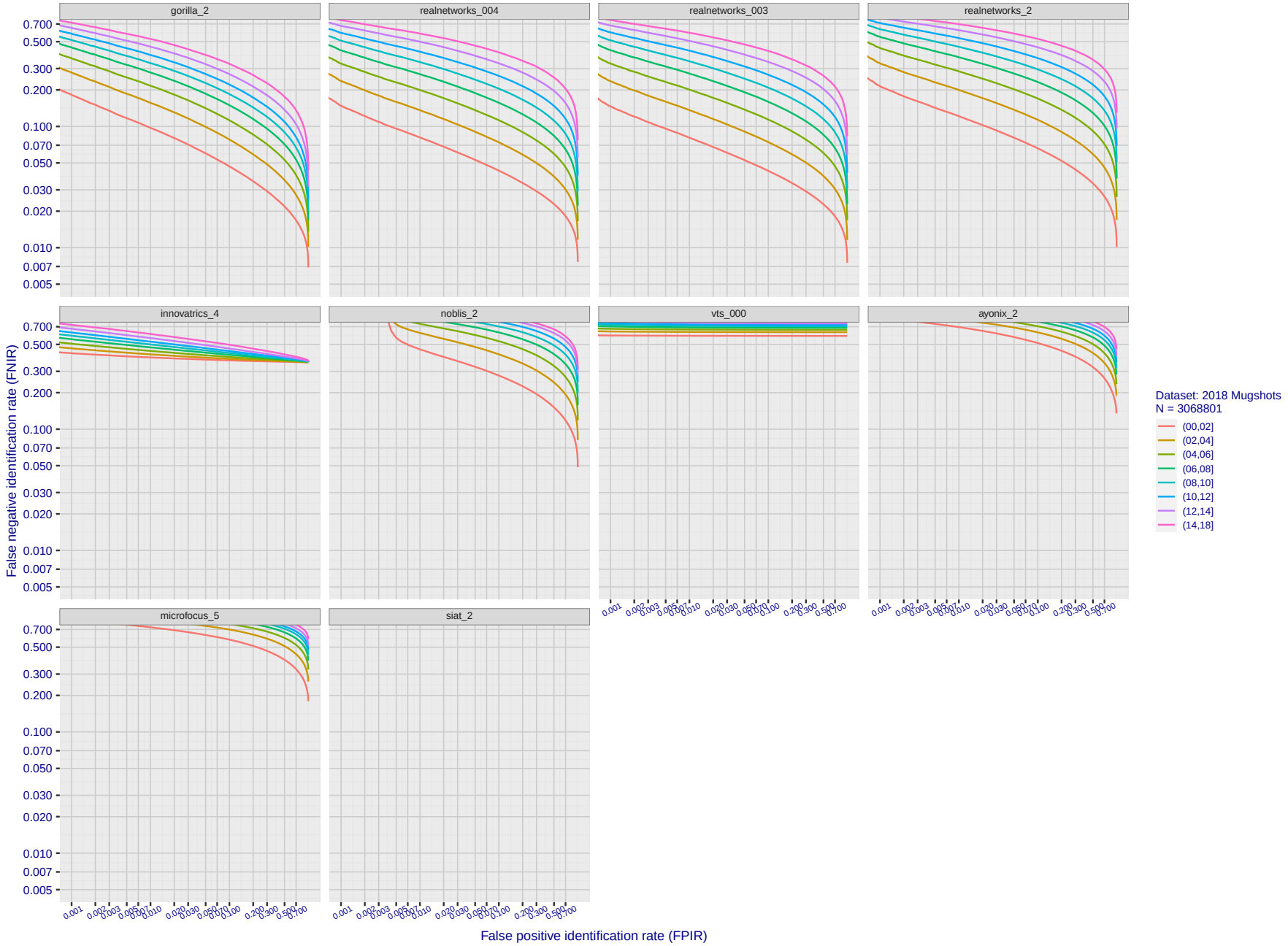

Figure 90: **[FRVT-2018 Mugshot Ageing Dataset] Identification miss rates vs. FPIR by time-elapsed**. *The oldest image of each individual is enrolled. Thereafter, all more recent images are searched. Miss rates are computed over all searches noted in row 17 of Table 1 and binned by number of years between search and initial enrollment. FPIR is computed from the same FRVT 2018 non-mates noted in row 3 of Table 1 with N = 3 000 000.*

2021/11/22 08:35:53

FNIR(N, R, T) = False neg. identification rate
FPIR(N, T) = False pos. identification rate

N = Num. enrolled subjects
R = Num. candidates examined

T = Threshold

T = 0 → Investigation
T > 0 → Identification

2021/11/22	FNIR(N, R, T) =	False neg. identification rate	N = Num. enrolled subjects	T = Threshold	$T = 0 \rightarrow$ Investigation
08:35:53	FPIR(N, T) =	False pos. identification rate	R = Num. candidates examined		$T > 0 \rightarrow$ Identification

This publication is available free of charge from: https://doi.org/10.6028/NIST.IR.8271

This publication is available free of charge from: https://doi.org/10.6028/NIST.IR.8271

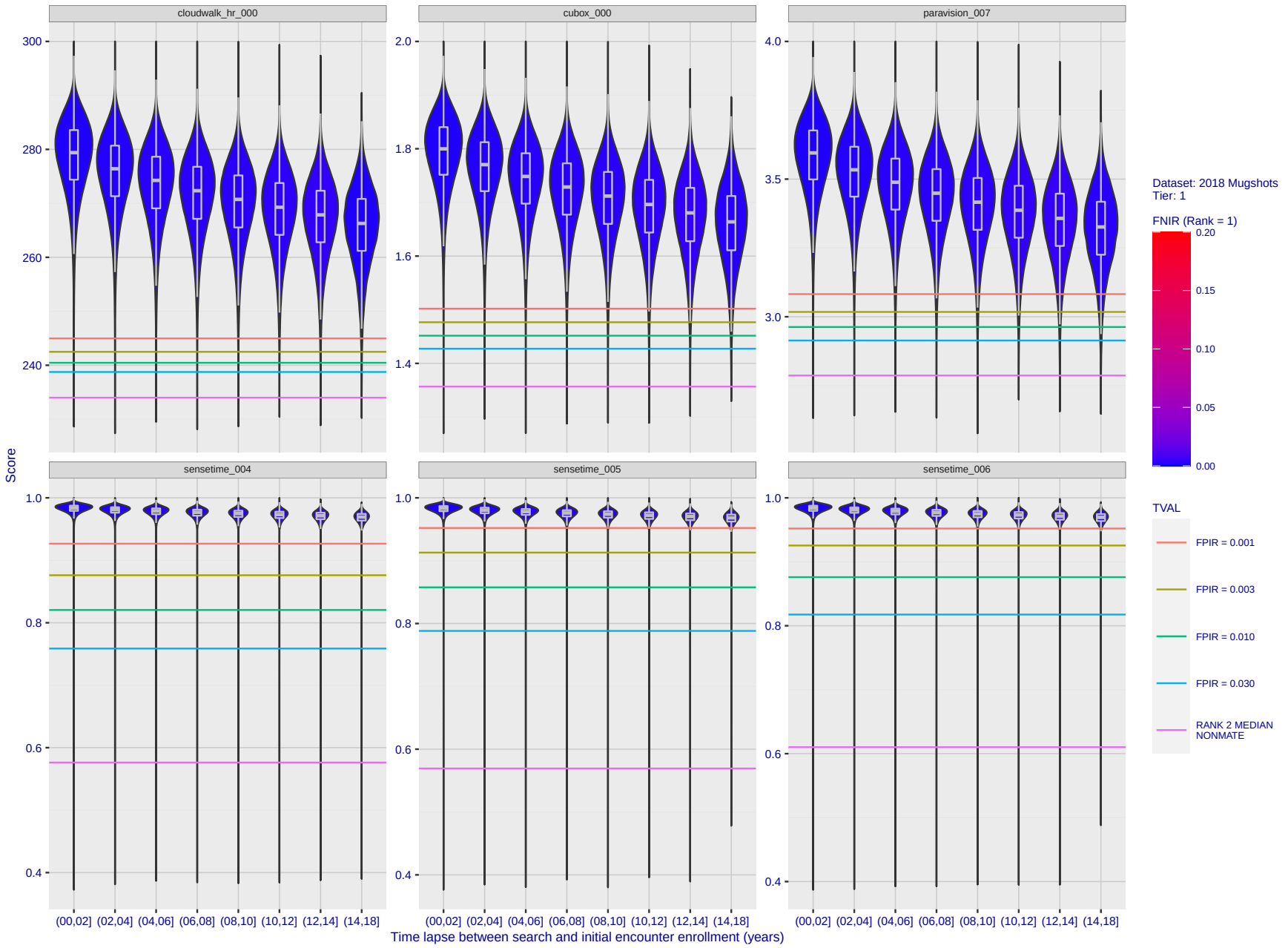

Figure 91: **[FRVT-2018 Mugshot Ageing Dataset] Native mate scores vs. time-elapsed**. *The oldest image of each individual is enrolled. Thereafter, all more recent images are searched. Mated score distributions are computed over all searches noted in row 17 of Table 1 binned by number of years between search and initial enrollment.*

2021/11/22 08:35:53
FNIR(N, R, T) = False neg. identification rate
FPIR(N, T) = False pos. identification rate
N = Num. enrolled subjects
R = Num. candidates examined
T = Threshold
T = 0 → Investigation
T > 0 → Identification

This publication is available free of charge from: https://doi.org/10.6028/NIST.IR.8271

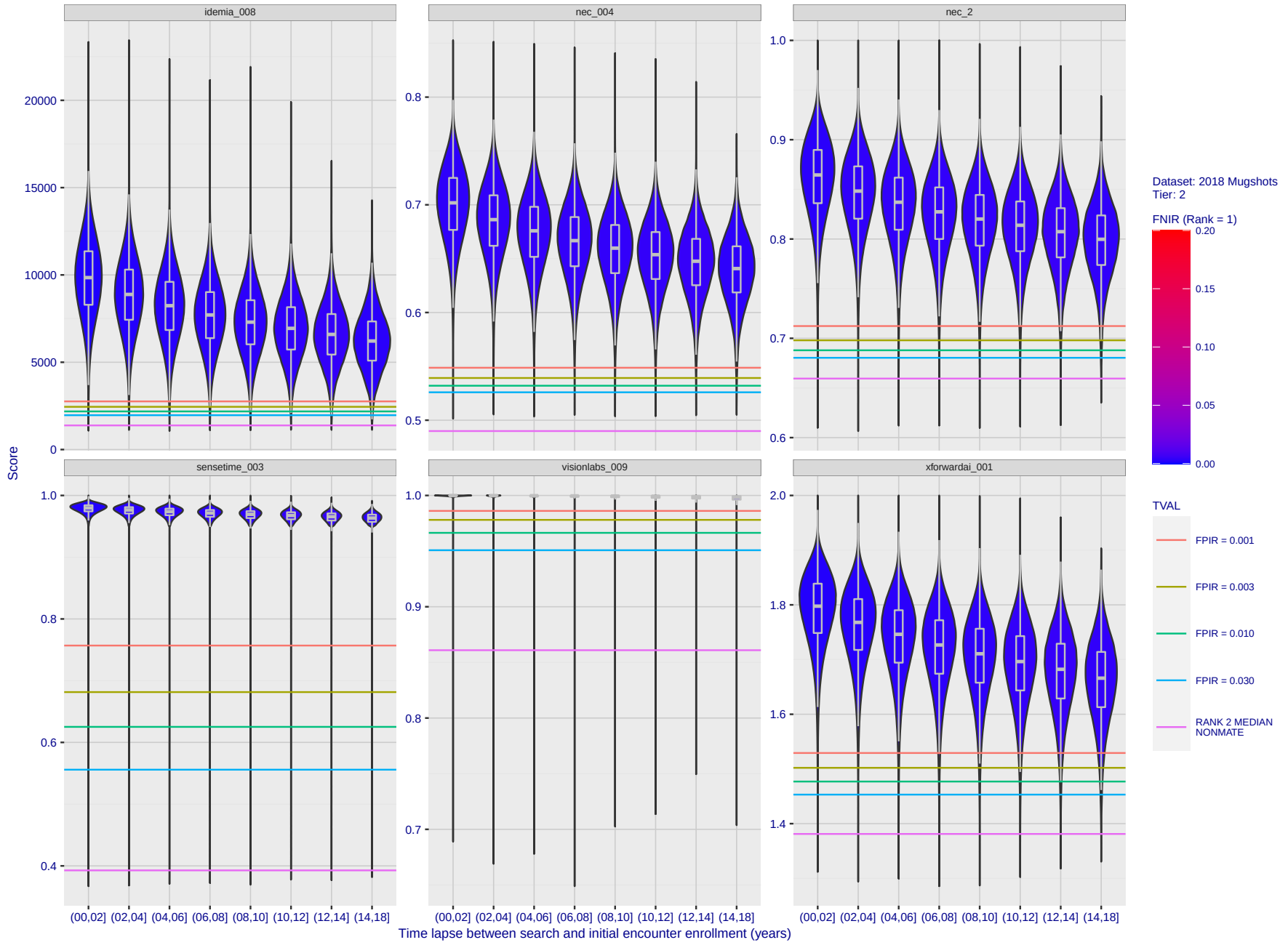

Figure 92: **[FRVT-2018 Mugshot Ageing Dataset] Native mate scores vs. time-elapsed**. *The oldest image of each individual is enrolled. Thereafter, all more recent images are searched. Mated score distributions are computed over all searches noted in row 17 of Table 1 binned by number of years between search and initial enrollment.*

2021/11/22 08:35:53

FNIR(N, R, T) = FPIR(N, T) =

False neg. identification rate
False pos. identification rate

N = Num. enrolled subjects
R = Num. candidates examined

T = Threshold

T = 0 → Investigation
T > 0 → Identification

This publication is available free of charge from: https://doi.org/10.6028/NIST.IR.8271

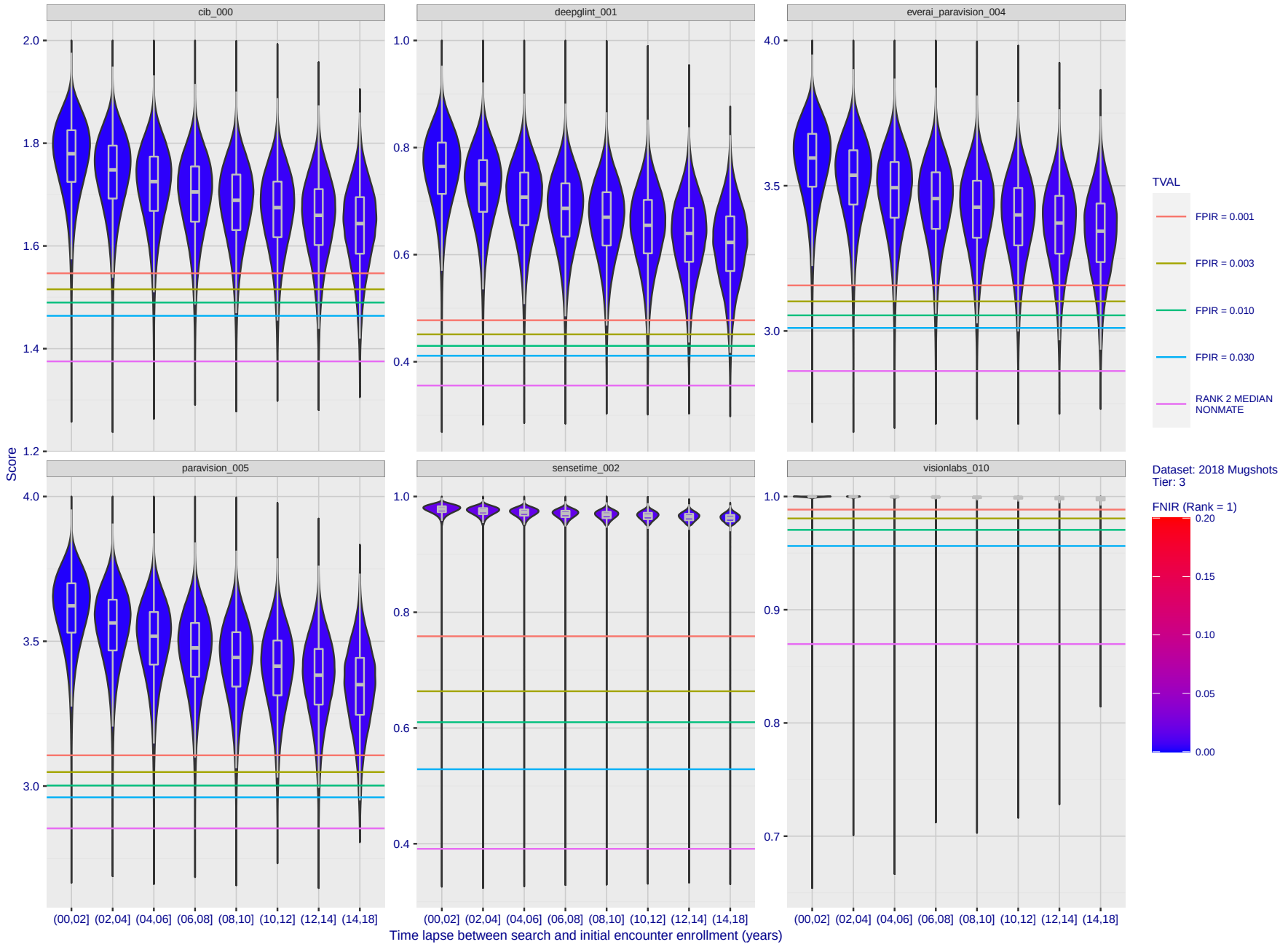

Figure 93: **[FRVT-2018 Mugshot Ageing Dataset] Native mate scores vs. time-elapsed**. *The oldest image of each individual is enrolled. Thereafter, all more recent images are searched. Mated score distributions are computed over all searches noted in row 17 of Table 1 binned by number of years between search and initial enrollment.*

2021/11/22 08:35:53
FNIR(N, R, T) = False neg. identification rate
FPIR(N, T) = False pos. identification rate
N = Num. enrolled subjects
R = Num. candidates examined
T = Threshold
T = 0 → Investigation
T > 0 → Identification

This publication is available free of charge from: https://doi.org/10.6028/NIST.IR.8271

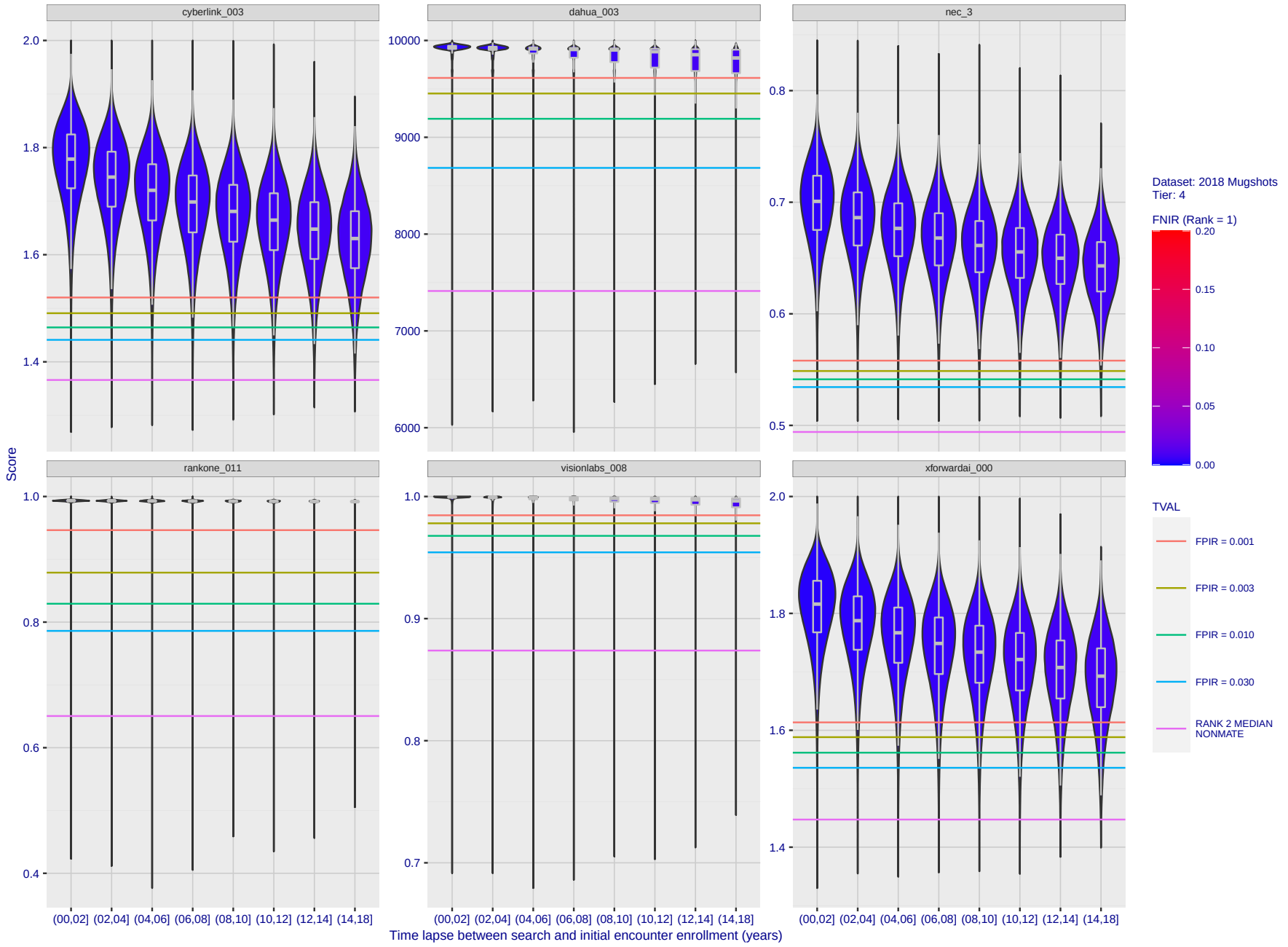

Figure 94: **[FRVT-2018 Mugshot Ageing Dataset] Native mate scores vs. time-elapsed**. *The oldest image of each individual is enrolled. Thereafter, all more recent images are searched. Mated score distributions are computed over all searches noted in row 17 of Table 1 binned by number of years between search and initial enrollment.*

2021/11/22 08:35:53

FNIR(N, R, T) = False neg. identification rate
FPIR(N, T) = False pos. identification rate

N = Num. enrolled subjects
R = Num. candidates examined

T = Threshold

T = 0 → Investigation
T > 0 → Identification

This publication is available free of charge from: https://doi.org/10.6028/NIST.IR.8271

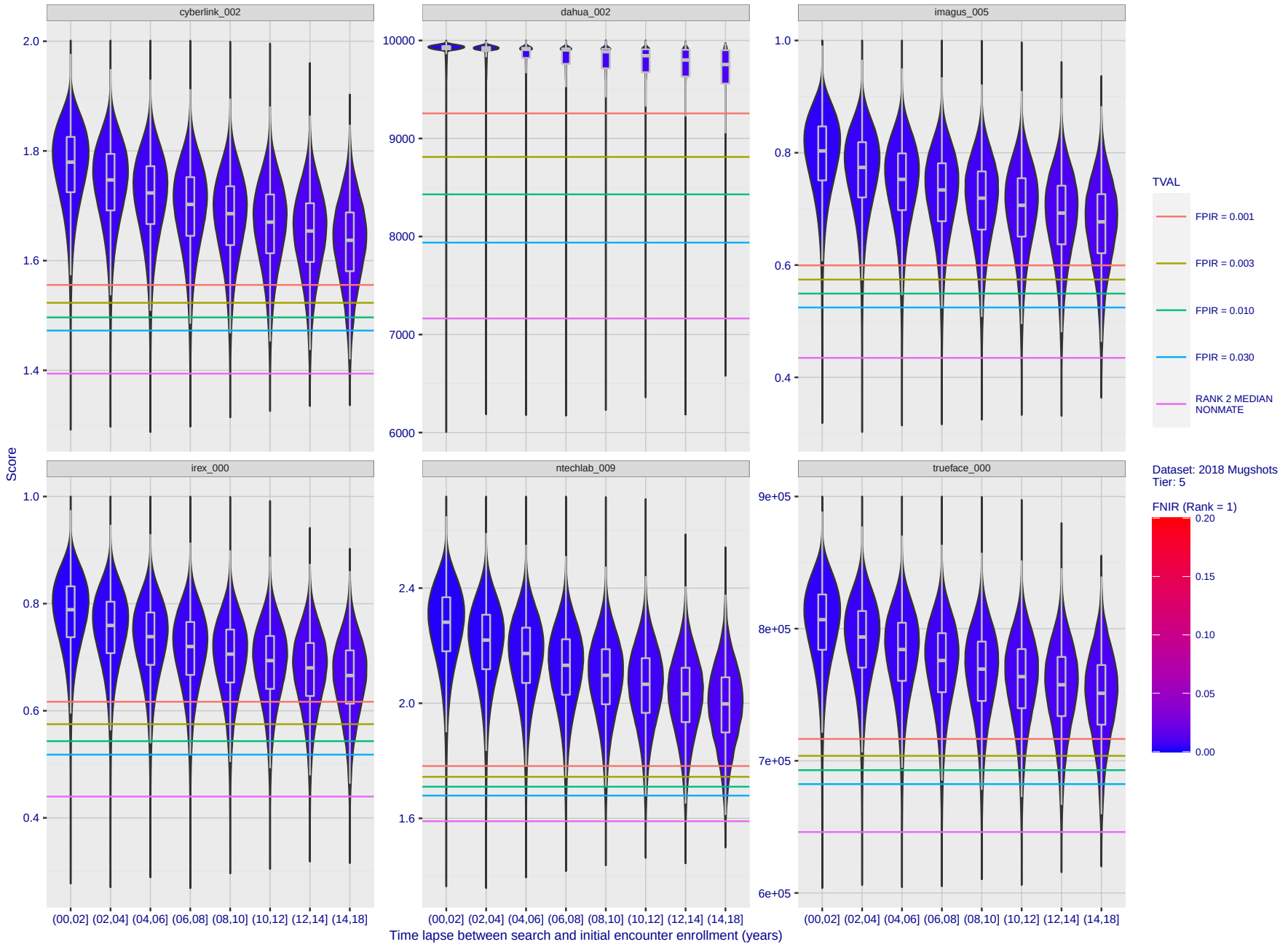

Figure 95: **[FRVT-2018 Mugshot Ageing Dataset] Native mate scores vs. time-elapsed**. *The oldest image of each individual is enrolled. Thereafter, all more recent images are searched. Mated score distributions are computed over all searches noted in row 17 of Table 1 binned by number of years between search and initial enrollment.*

2021/11/22 08:35:53
FNIR(N, R, T) = False neg. identification rate
FPIR(N, T) = False pos. identification rate
N = Num. enrolled subjects
R = Num. candidates examined
T = Threshold
T = 0 → Investigation
T > 0 → Identification

This publication is available free of charge from: https://doi.org/10.6028/NIST.IR.8271

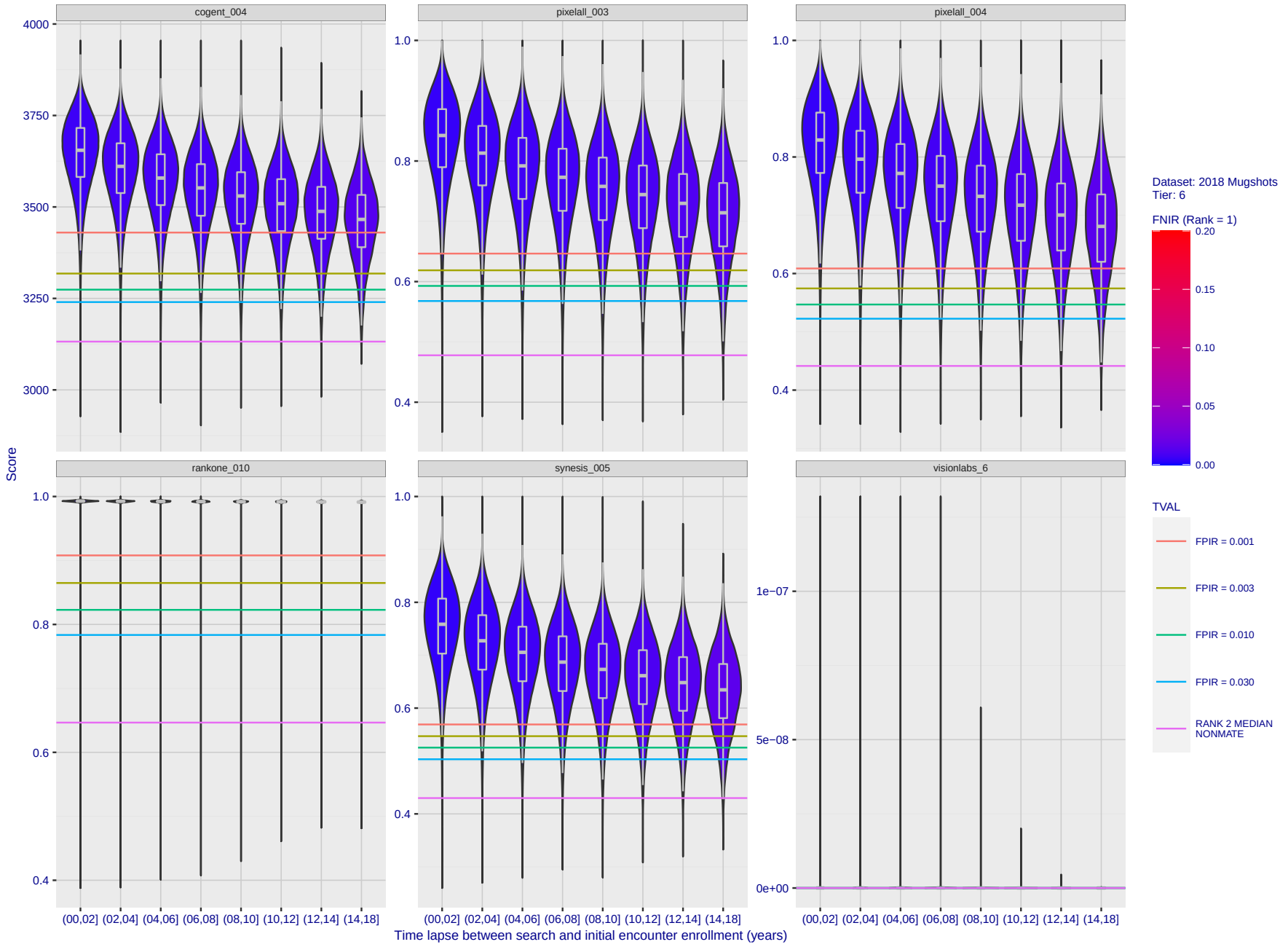

Figure 96: **[FRVT-2018 Mugshot Ageing Dataset] Native mate scores vs. time-elapsed**. *The oldest image of each individual is enrolled. Thereafter, all more recent images are searched. Mated score distributions are computed over all searches noted in row 17 of Table 1 binned by number of years between search and initial enrollment.*

2021/11/22 08:35:53
FNIR(N, R, T) = False neg. identification rate
FPIR(N, T) = False pos. identification rate
N = Num. enrolled subjects
R = Num. candidates examined
T = Threshold
T = 0 → Investigation
T > 0 → Identification

This publication is available free of charge from: https://doi.org/10.6028/NIST.IR.8271

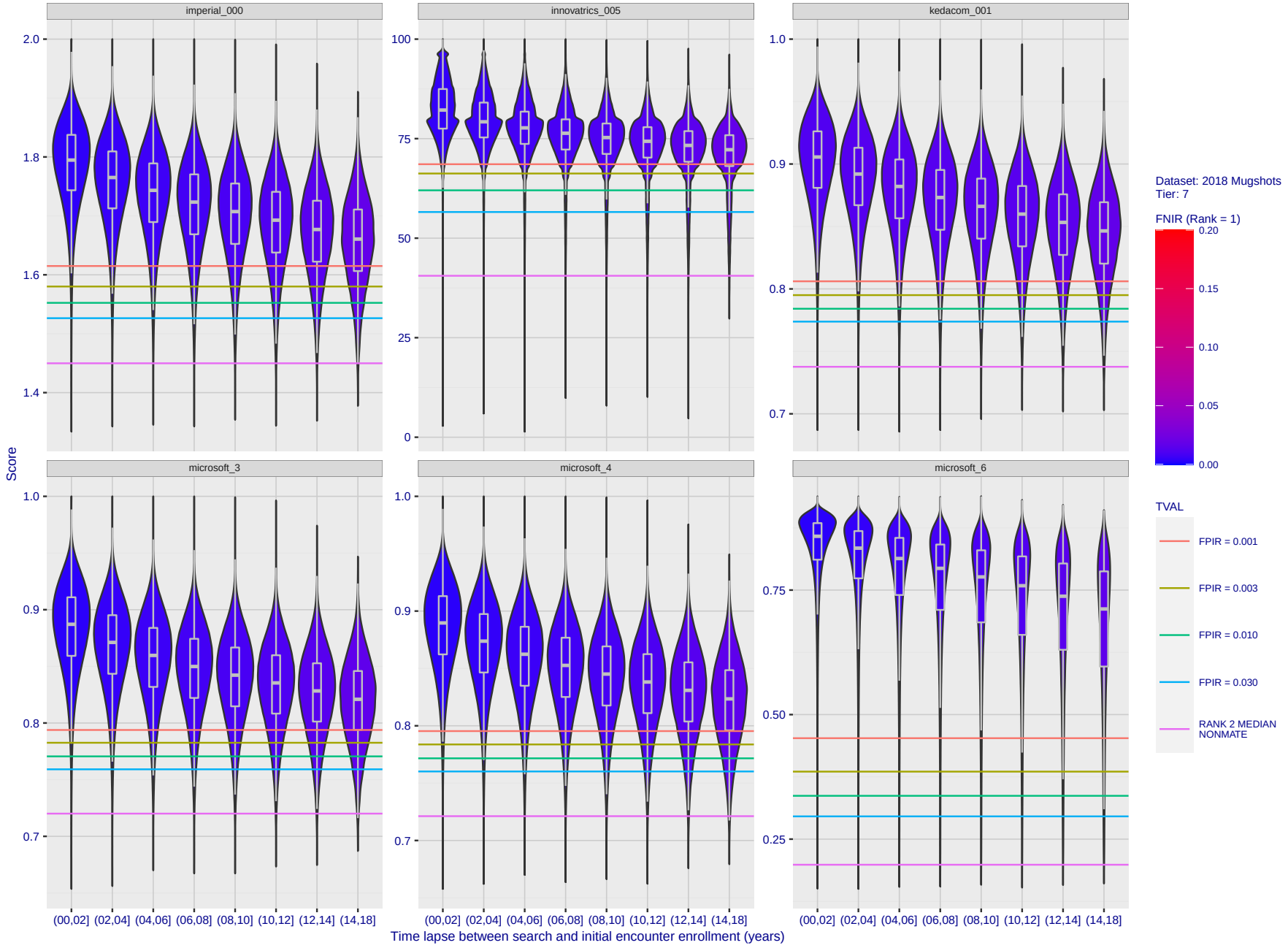

Figure 97: **[FRVT-2018 Mugshot Ageing Dataset] Native mate scores vs. time-elapsed**. *The oldest image of each individual is enrolled. Thereafter, all more recent images are searched. Mated score distributions are computed over all searches noted in row 17 of Table 1 binned by number of years between search and initial enrollment.*

2021/11/22 08:35:53
FNIR(N, R, T) = False neg. identification rate
FPIR(N, T) = False pos. identification rate
N = Num. enrolled subjects
R = Num. candidates examined
T = Threshold
T = 0 → Investigation
T > 0 → Identification

This publication is available free of charge from: https://doi.org/10.6028/NIST.IR.8271

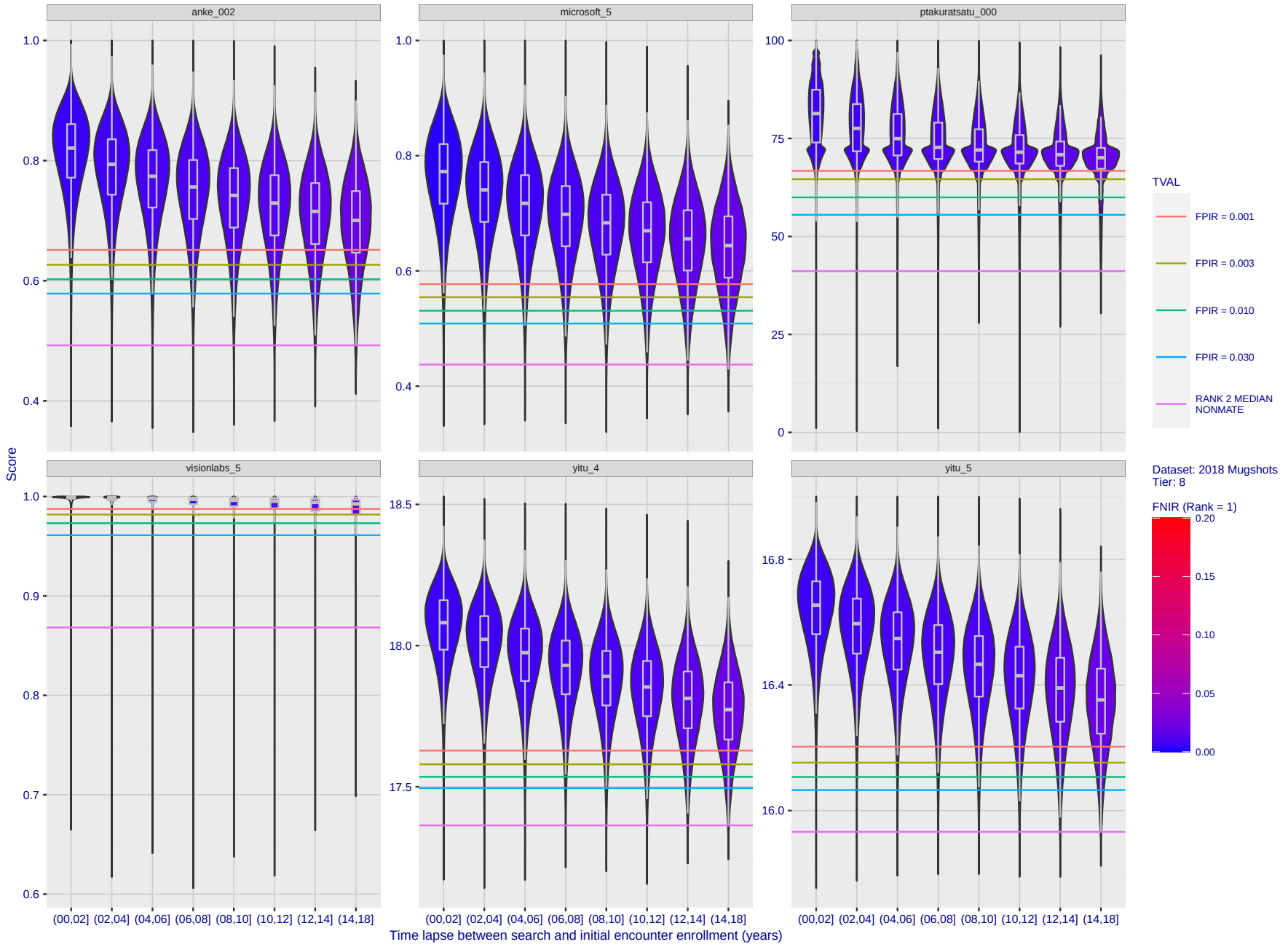

Figure 98: **[FRVT-2018 Mugshot Ageing Dataset] Native mate scores vs. time-elapsed**. *The oldest image of each individual is enrolled. Thereafter, all more recent images are searched. Mated score distributions are computed over all searches noted in row 17 of Table 1 binned by number of years between search and initial enrollment.*

2021/11/22 08:35:53
FNIR(N, R, T) = False neg. identification rate
FPIR(N, T) = False pos. identification rate
N = Num. enrolled subjects
R = Num. candidates examined
T = Threshold
T = 0 → Investigation
T > 0 → Identification

This publication is available free of charge from: https://doi.org/10.6028/NIST.IR.8271

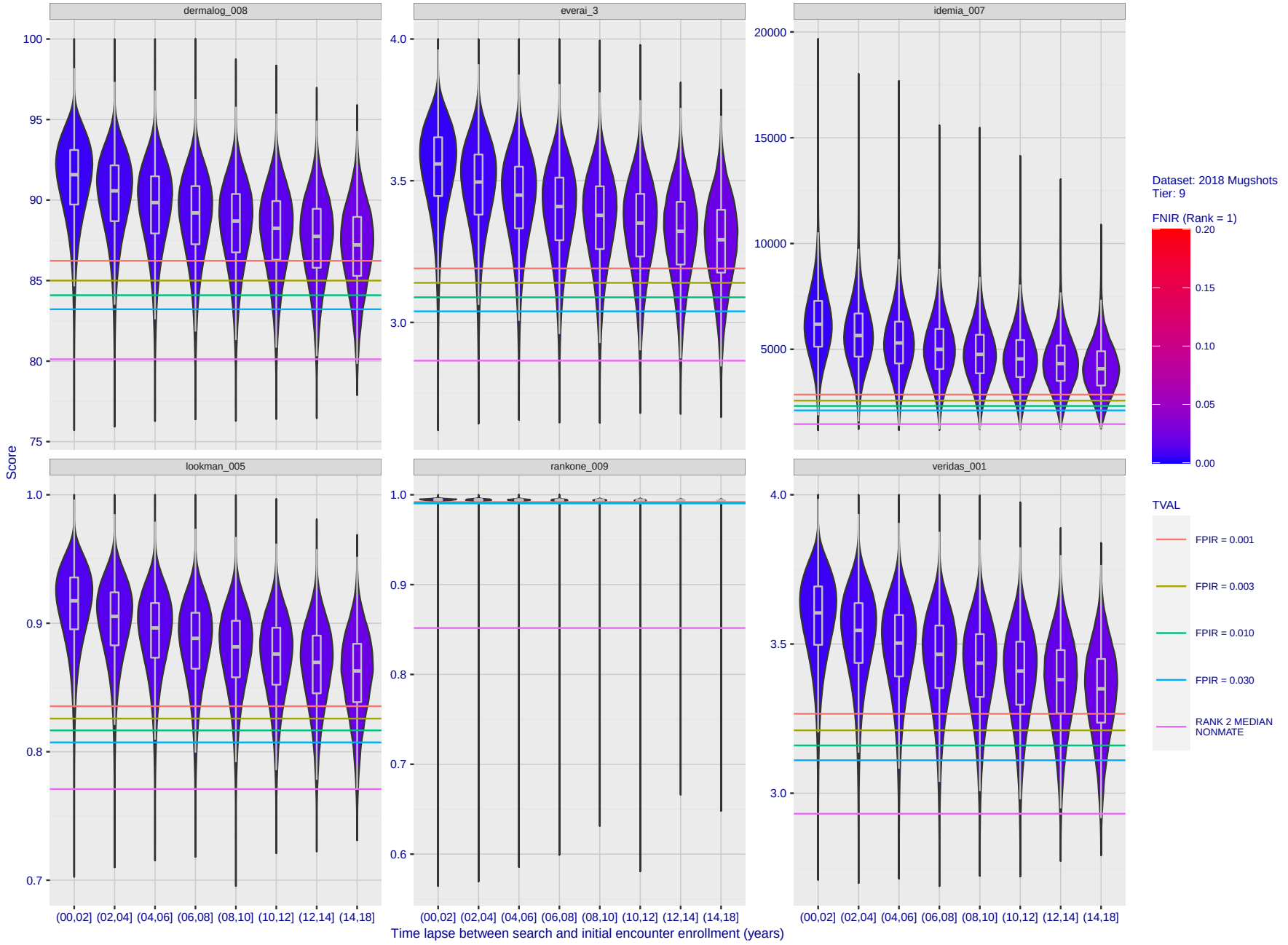

Figure 99: **[FRVT-2018 Mugshot Ageing Dataset] Native mate scores vs. time-elapsed**. *The oldest image of each individual is enrolled. Thereafter, all more recent images are searched. Mated score distributions are computed over all searches noted in row 17 of Table 1 binned by number of years between search and initial enrollment.*

2021/11/22 08:35:53
FNIR(N, R, T) = False neg. identification rate
FPIR(N, T) = False pos. identification rate
N = Num. enrolled subjects
R = Num. candidates examined
T = Threshold
T = 0 → Investigation
T > 0 → Identification

This publication is available free of charge from: https://doi.org/10.6028/NIST.IR.8271

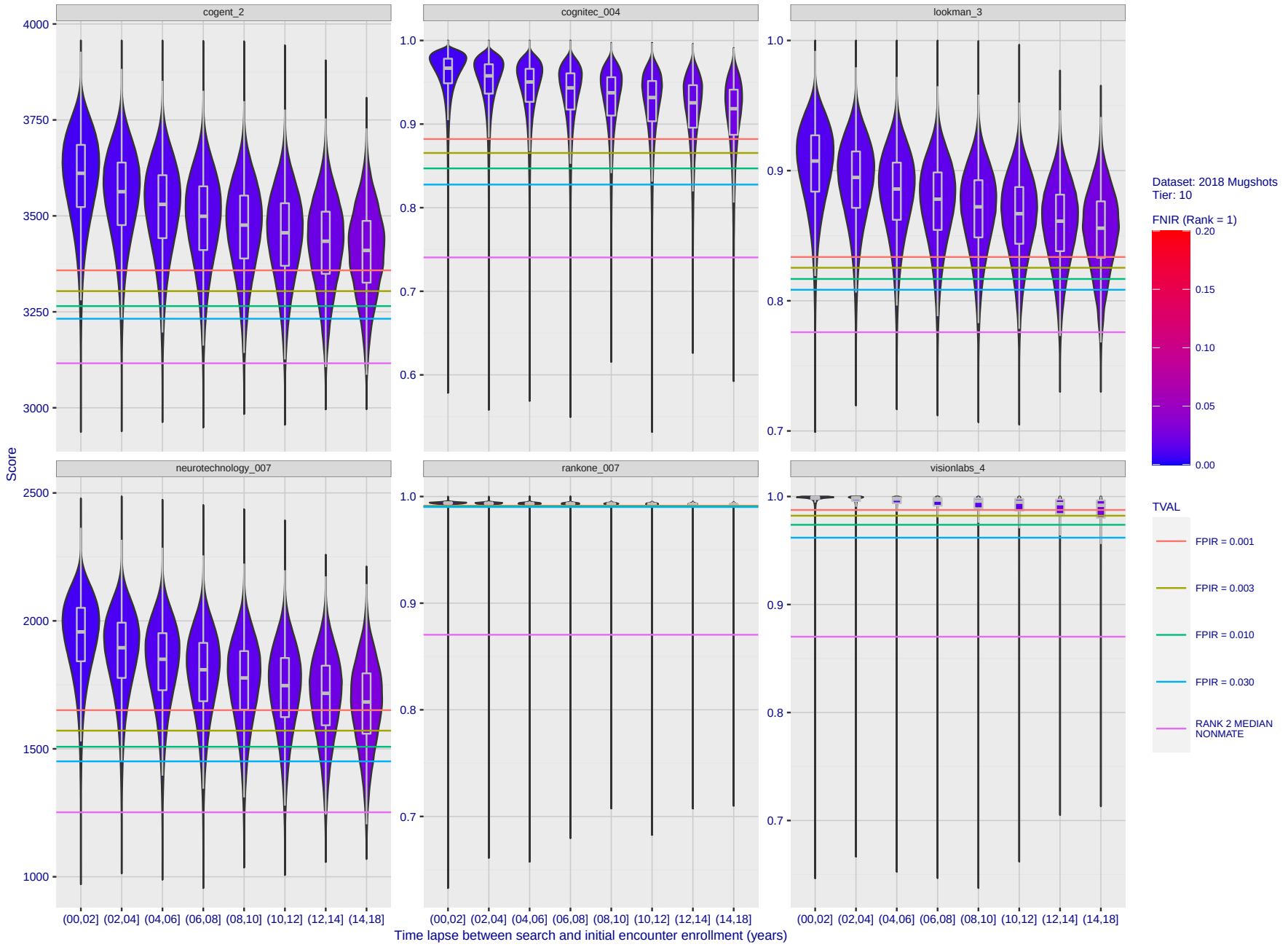

Figure 100: **[FRVT-2018 Mugshot Ageing Dataset] Native mate scores vs. time-elapsed**. *The oldest image of each individual is enrolled. Thereafter, all more recent images are searched. Mated score distributions are computed over all searches noted in row 17 of Table 1 binned by number of years between search and initial enrollment.*

This publication is available free of charge from: https://doi.org/10.6028/NIST.IR.8271

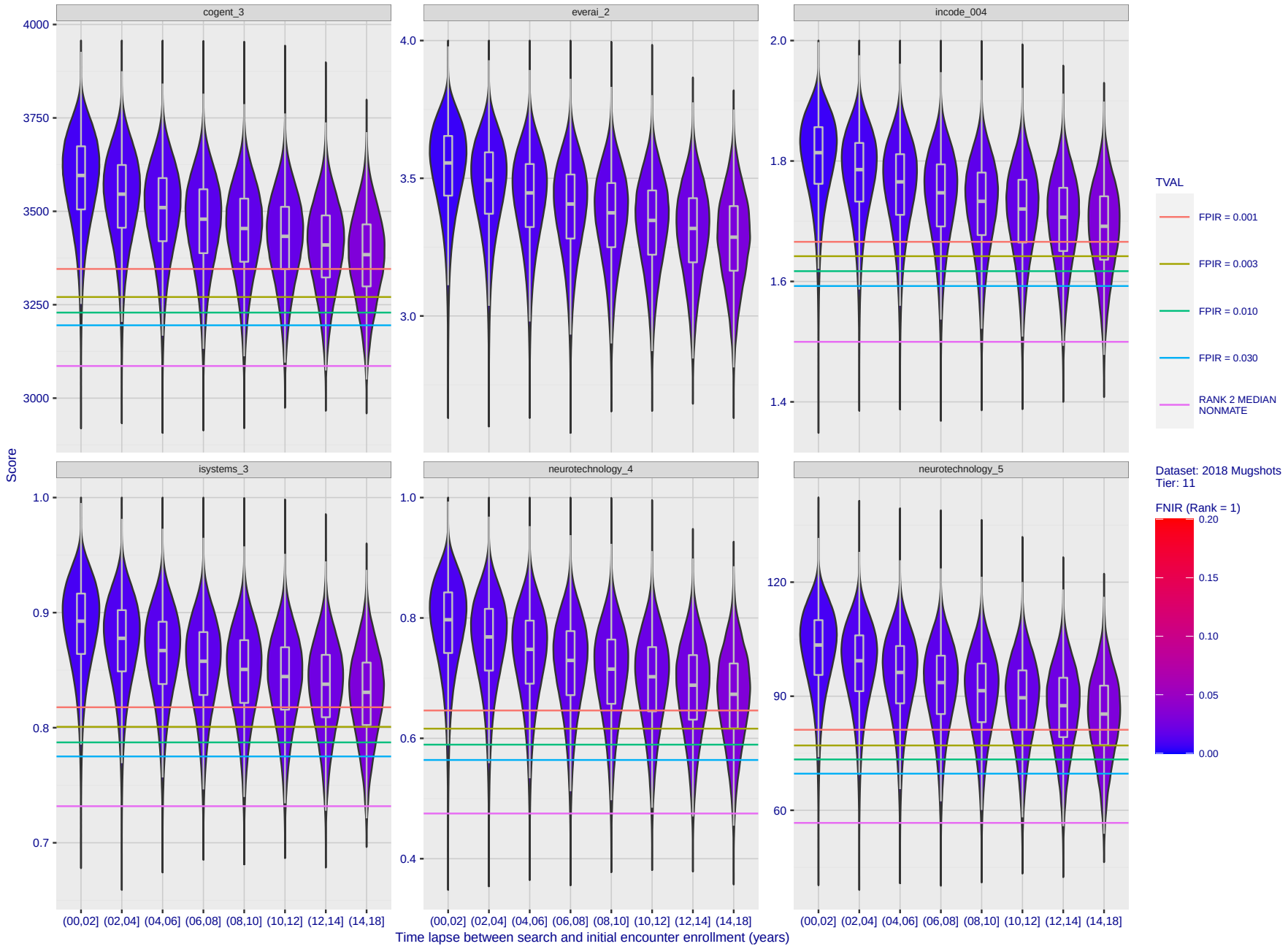

Figure 101: **[FRVT-2018 Mugshot Ageing Dataset] Native mate scores vs. time-elapsed**. *The oldest image of each individual is enrolled. Thereafter, all more recent images are searched. Mated score distributions are computed over all searches noted in row 17 of Table 1 binned by number of years between search and initial enrollment.*

2021/11/22 08:35:53
FNIR(N, R, T) = False neg. identification rate
FPIR(N, T) = False pos. identification rate
N = Num. enrolled subjects
R = Num. candidates examined
T = Threshold
T = 0 → Investigation
T > 0 → Identification

This publication is available free of charge from: https://doi.org/10.6028/NIST.IR.8271

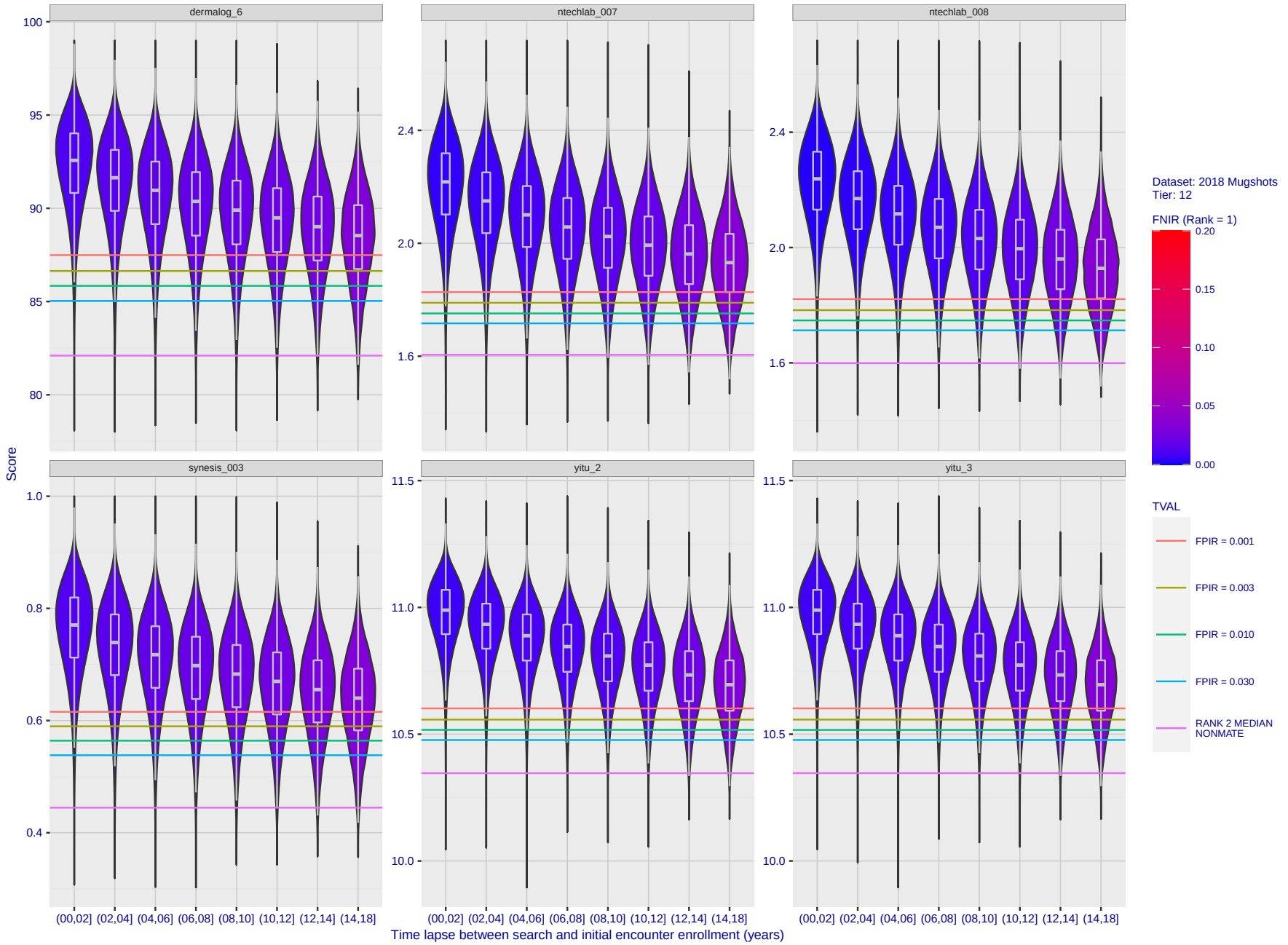

Figure 102: **[FRVT-2018 Mugshot Ageing Dataset] Native mate scores vs. time-elapsed**. *The oldest image of each individual is enrolled. Thereafter, all more recent images are searched. Mated score distributions are computed over all searches noted in row 17 of Table 1 binned by number of years between search and initial enrollment.*

2021/11/22 08:35:53
FNIR(N, R, T) = False neg. identification rate
FPIR(N, T) = False pos. identification rate
N = Num. enrolled subjects
R = Num. candidates examined
T = Threshold
T = 0 → Investigation
T > 0 → Identification

This publication is available free of charge from: https://doi.org/10.6028/NIST.IR.8271

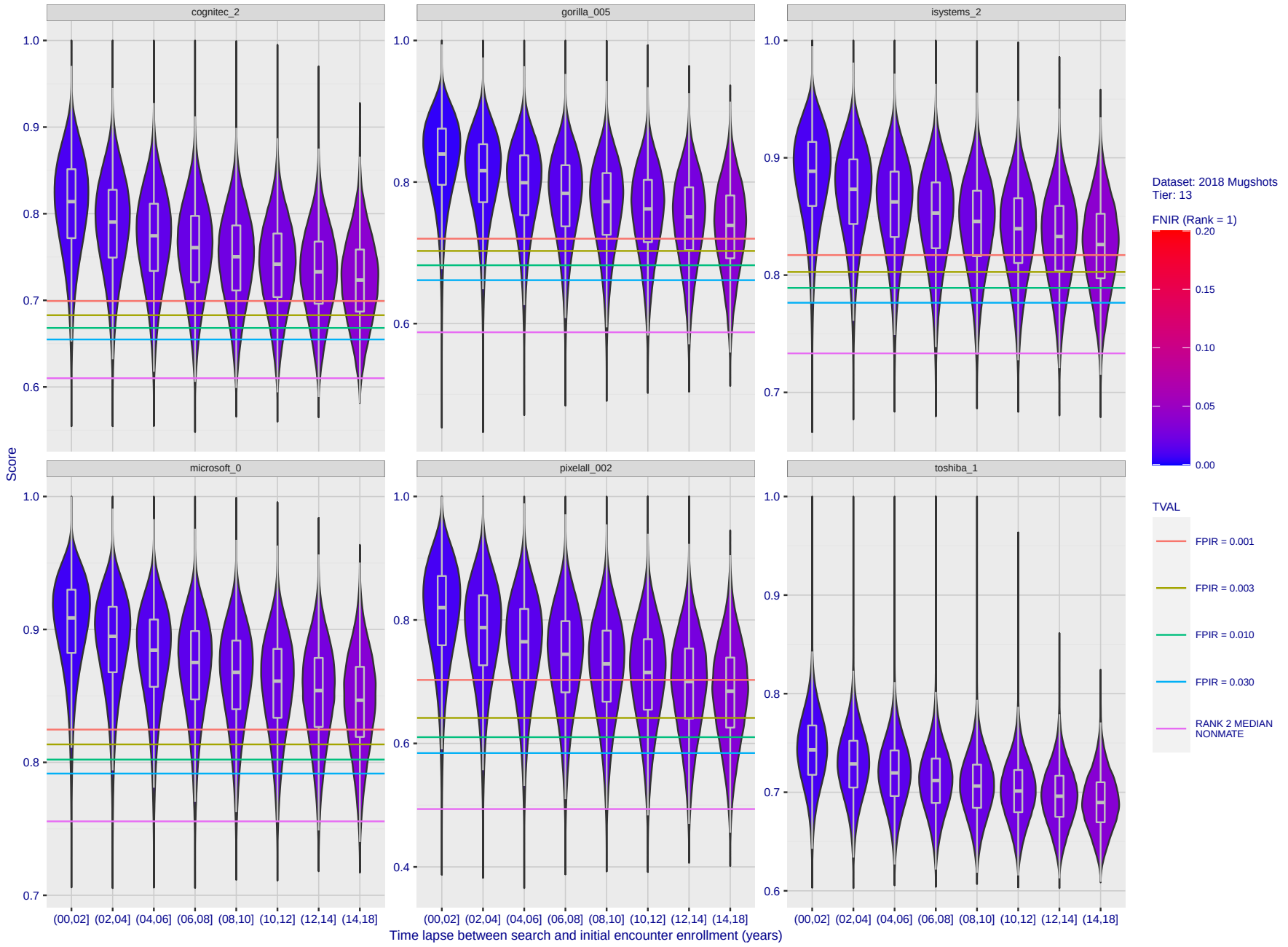

Figure 103: **[FRVT-2018 Mugshot Ageing Dataset] Native mate scores vs. time-elapsed**. *The oldest image of each individual is enrolled. Thereafter, all more recent images are searched. Mated score distributions are computed over all searches noted in row 17 of Table 1 binned by number of years between search and initial enrollment.*

2021/11/22 08:35:53
FNIR(N, R, T) = FPIR(N, T) = False neg. identification rate / False pos. identification rate
N = Num. enrolled subjects
R = Num. candidates examined
T = Threshold
T = 0 → Investigation
T > 0 → Identification

This publication is available free of charge from: https://doi.org/10.6028/NIST.IR.8271

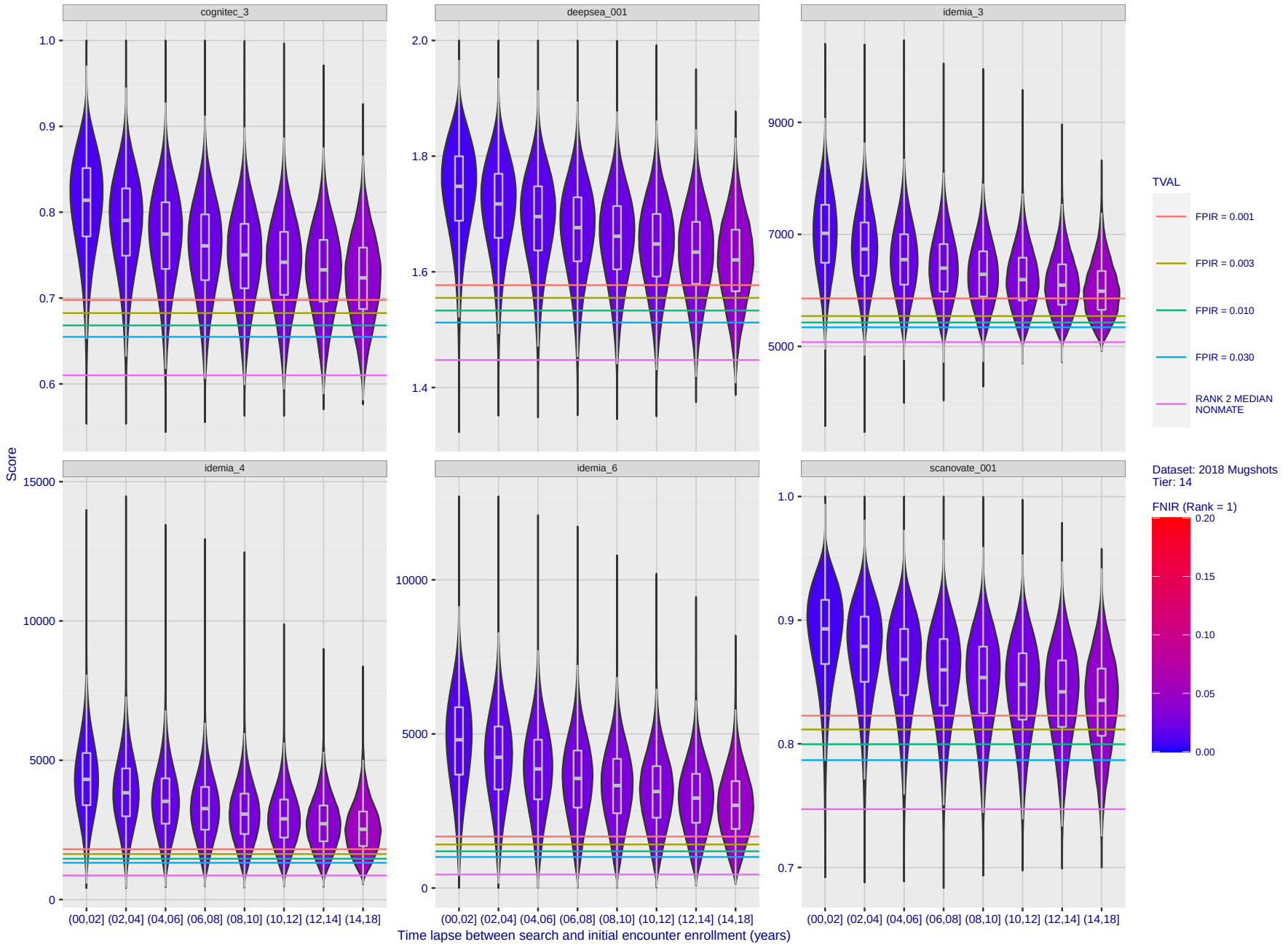

Figure 104: **[FRVT-2018 Mugshot Ageing Dataset] Native mate scores vs. time-elapsed**. *The oldest image of each individual is enrolled. Thereafter, all more recent images are searched. Mated score distributions are computed over all searches noted in row 17 of Table 1 binned by number of years between search and initial enrollment.*

2021/11/22 08:35:53
FNIR(N, R, T) = FPIR(N, T) = False neg. identification rate / False pos. identification rate
N = Num. enrolled subjects
R = Num. candidates examined
T = Threshold
T = 0 → Investigation
T > 0 → Identification

This publication is available free of charge from: https://doi.org/10.6028/NIST.IR.8271

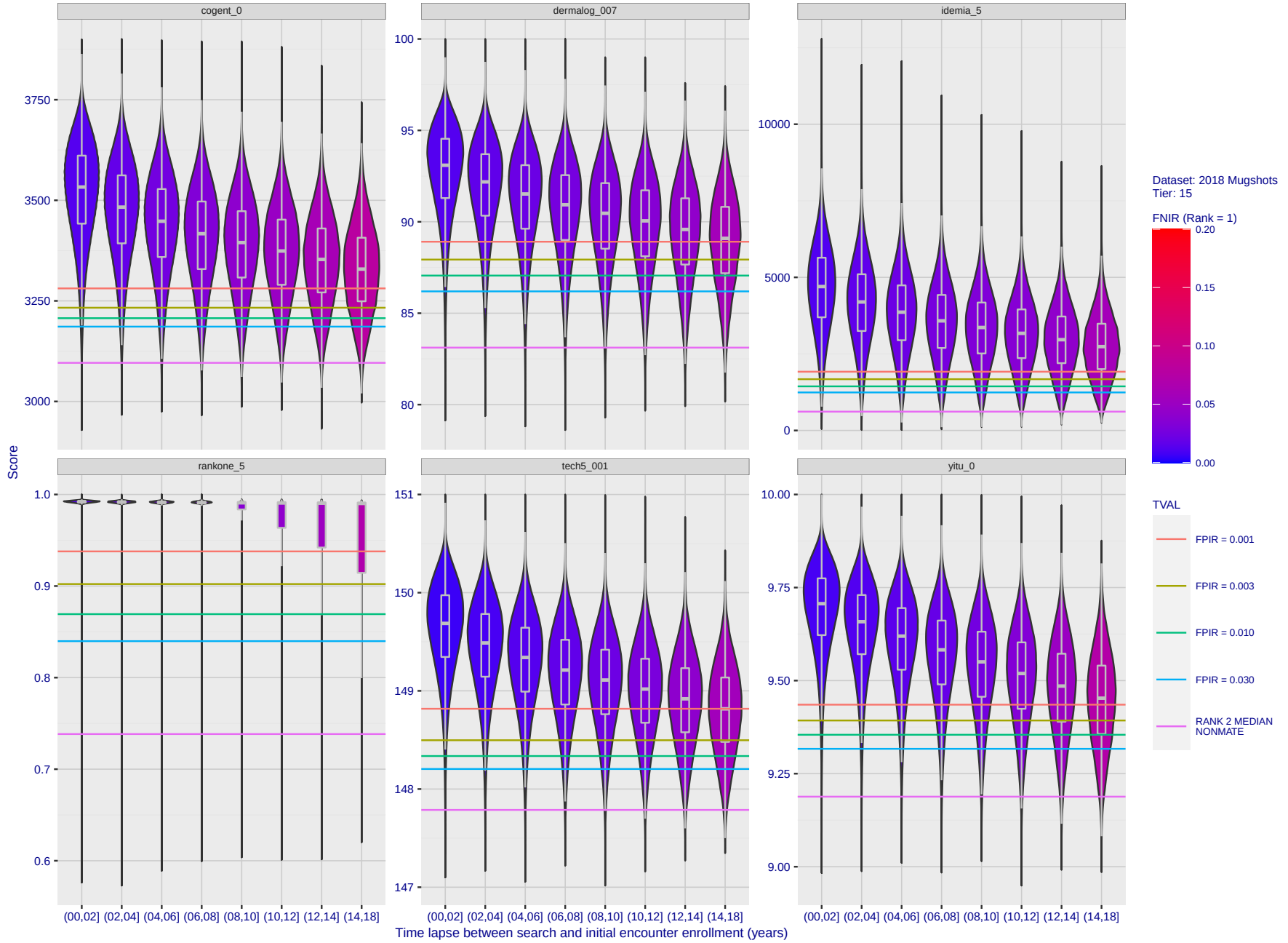

Figure 105: **[FRVT-2018 Mugshot Ageing Dataset] Native mate scores vs. time-elapsed**. *The oldest image of each individual is enrolled. Thereafter, all more recent images are searched. Mated score distributions are computed over all searches noted in row 17 of Table 1 binned by number of years between search and initial enrollment.*

2021/11/22 08:35:53
FNIR(N, R, T) = False neg. identification rate
FPIR(N, T) = False pos. identification rate
N = Num. enrolled subjects
R = Num. candidates examined
T = Threshold
T = 0 → Investigation
T > 0 → Identification

This publication is available free of charge from: https://doi.org/10.6028/NIST.IR.8271

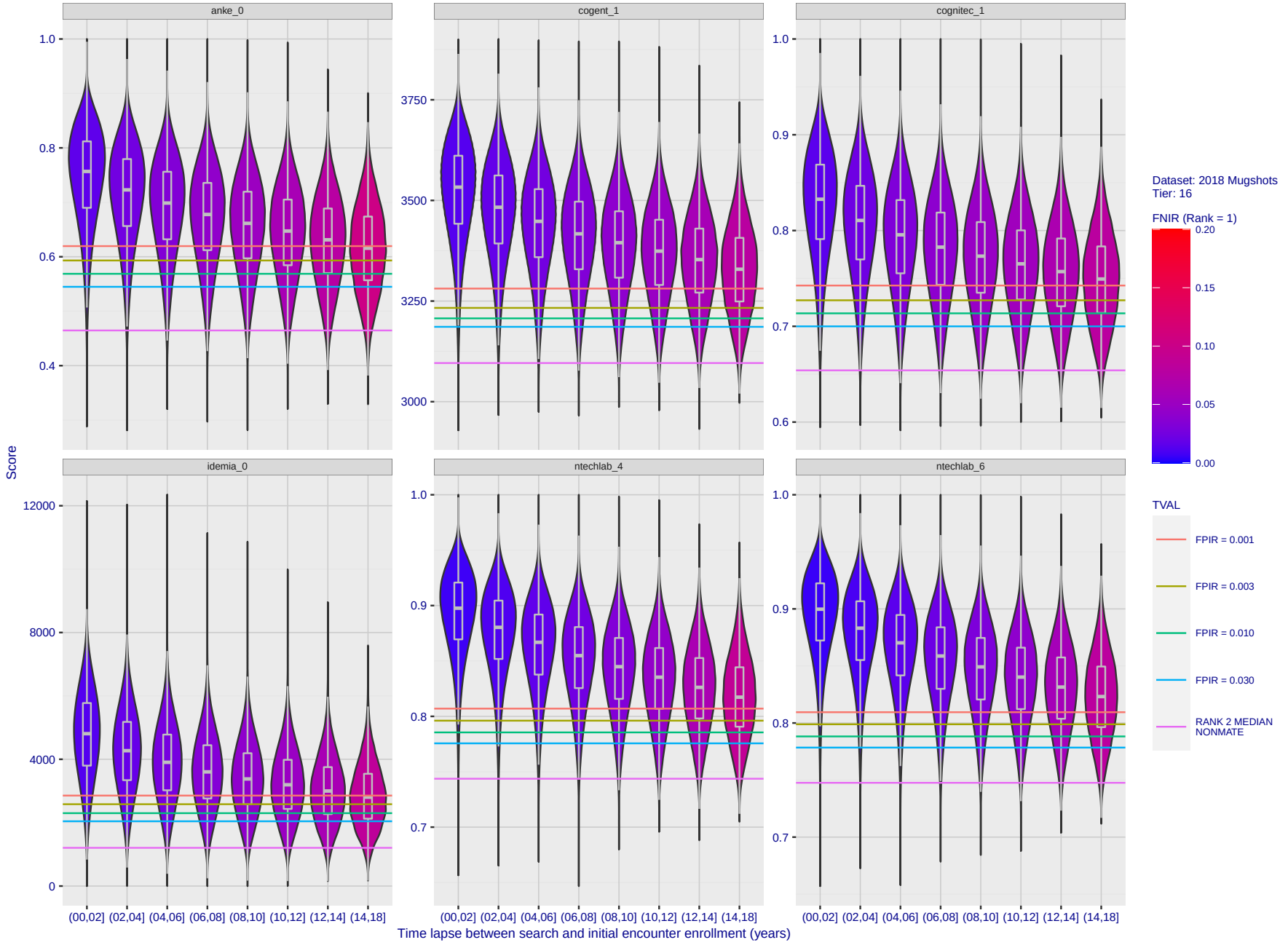

Figure 106: **[FRVT-2018 Mugshot Ageing Dataset] Native mate scores vs. time-elapsed**. *The oldest image of each individual is enrolled. Thereafter, all more recent images are searched. Mated score distributions are computed over all searches noted in row 17 of Table 1 binned by number of years between search and initial enrollment.*

This publication is available free of charge from: https://doi.org/10.6028/NIST.IR.8271

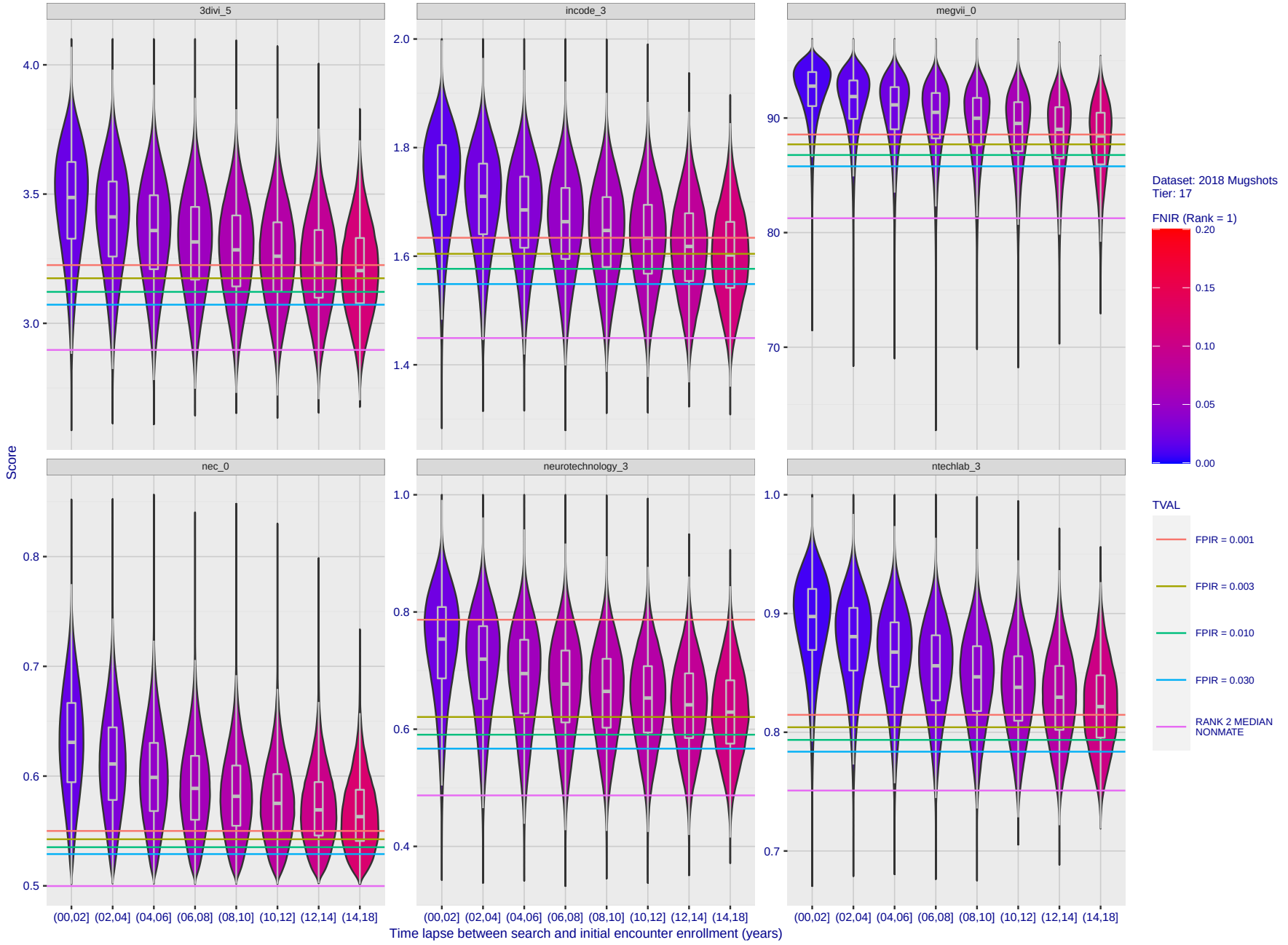

Figure 107: **[FRVT-2018 Mugshot Ageing Dataset] Native mate scores vs. time-elapsed**. *The oldest image of each individual is enrolled. Thereafter, all more recent images are searched. Mated score distributions are computed over all searches noted in row 17 of Table 1 binned by number of years between search and initial enrollment.*

This publication is available free of charge from: https://doi.org/10.6028/NIST.IR.8271

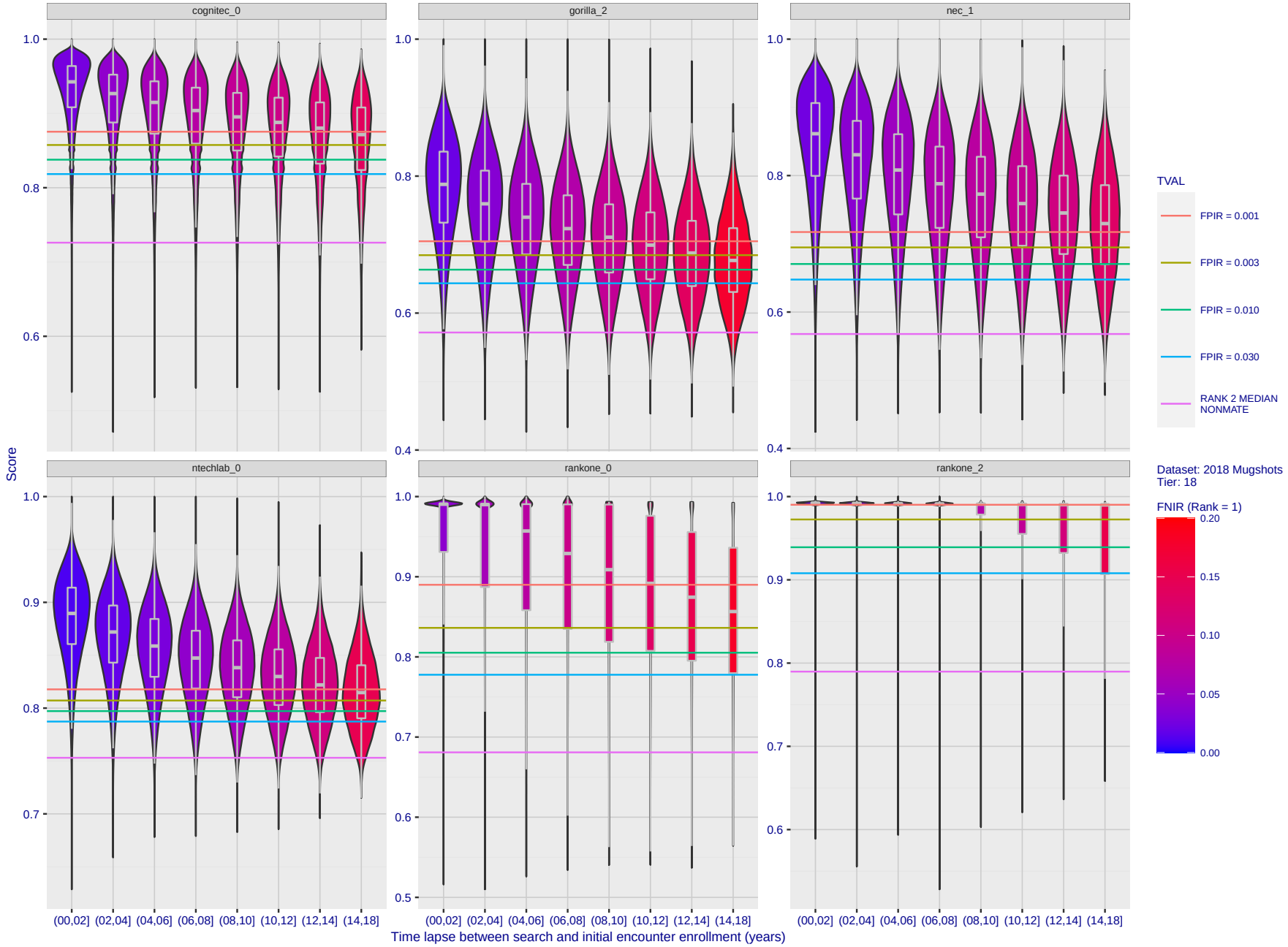

Figure 108: **[FRVT-2018 Mugshot Ageing Dataset] Native mate scores vs. time-elapsed**. *The oldest image of each individual is enrolled. Thereafter, all more recent images are searched. Mated score distributions are computed over all searches noted in row 17 of Table 1 binned by number of years between search and initial enrollment.*

This publication is available free of charge from: https://doi.org/10.6028/NIST.IR.8271

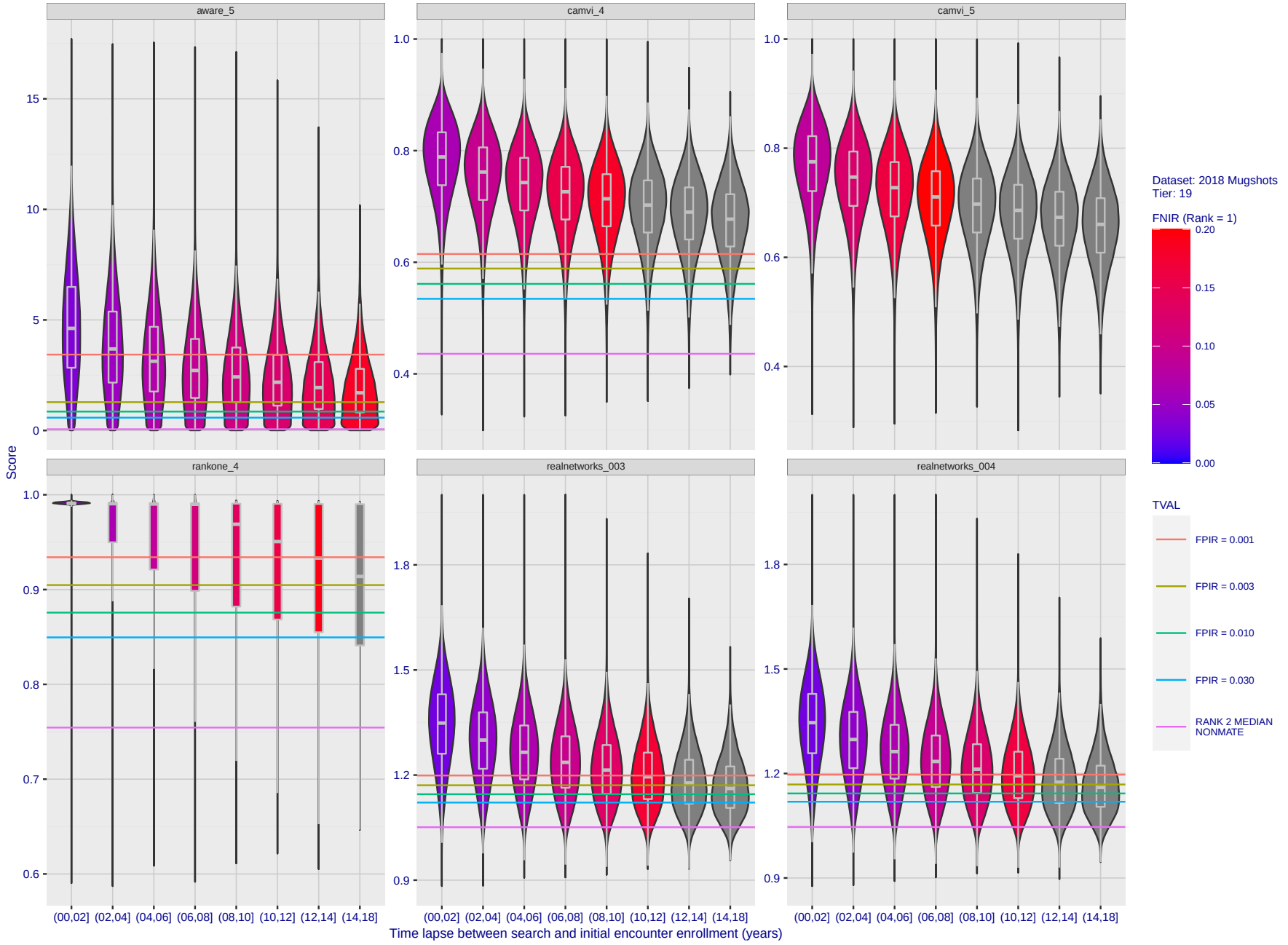

Figure 109: **[FRVT-2018 Mugshot Ageing Dataset] Native mate scores vs. time-elapsed**. *The oldest image of each individual is enrolled. Thereafter, all more recent images are searched. Mated score distributions are computed over all searches noted in row 17 of Table 1 binned by number of years between search and initial enrollment.*

2021/11/22 08:35:53

FNIR(N, R, T) = False neg. identification rate
FPIR(N, T) = False pos. identification rate

N = Num. enrolled subjects
R = Num. candidates examined

T = Threshold

T = 0 → Investigation
T > 0 → Identification

This publication is available free of charge from: https://doi.org/10.6028/NIST.IR.8271

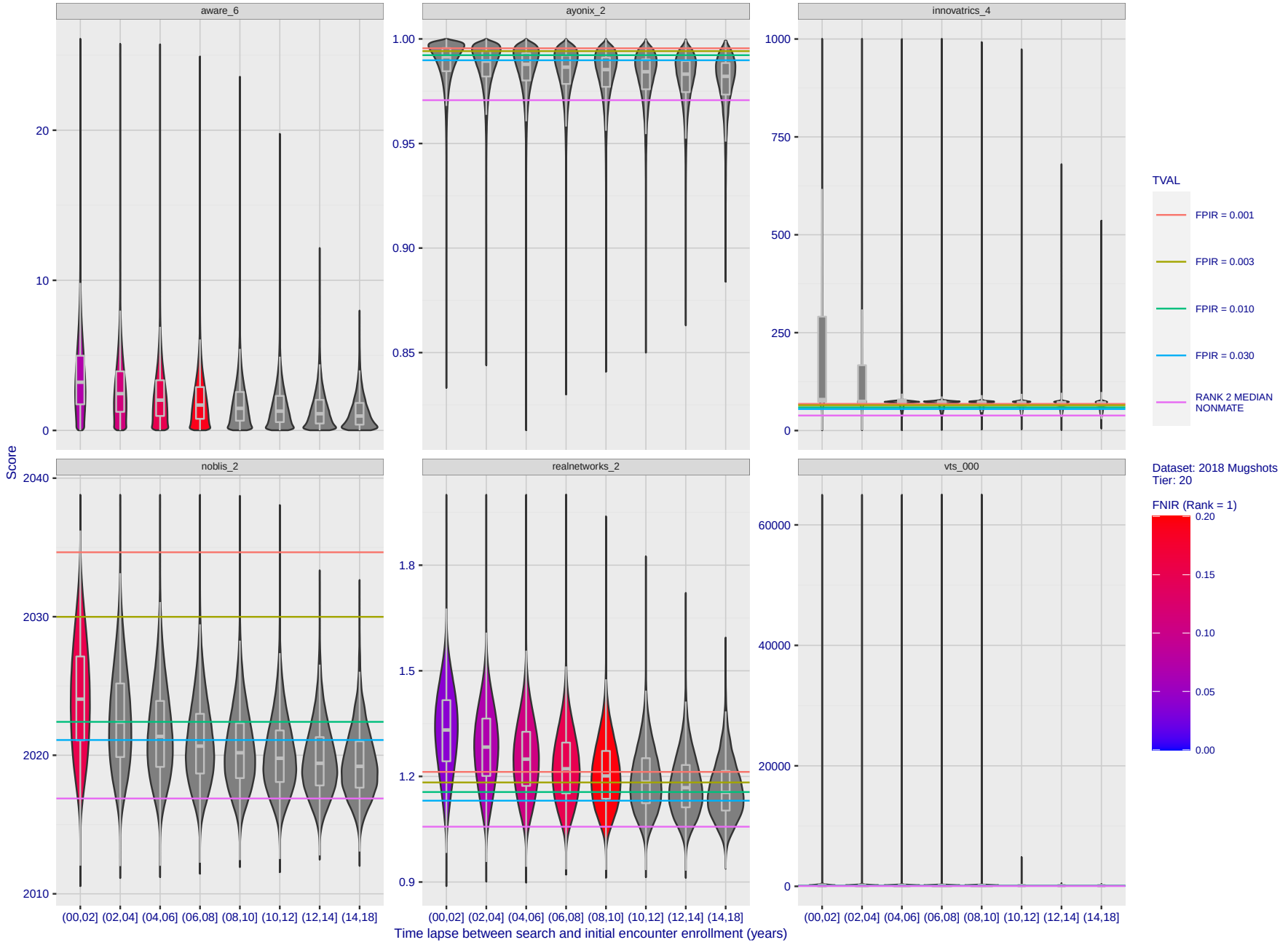

Figure 110: **[FRVT-2018 Mugshot Ageing Dataset] Native mate scores vs. time-elapsed**. *The oldest image of each individual is enrolled. Thereafter, all more recent images are searched. Mated score distributions are computed over all searches noted in row 17 of Table 1 binned by number of years between search and initial enrollment.*

2021/11/22
08:35:53
FNIR(N, R, T) = False neg. identification rate
FPIR(N, T) = False pos. identification rate
N = Num. enrolled subjects
R = Num. candidates examined
T = Threshold
T = 0 → Investigation
T > 0 → Identification

This publication is available free of charge from: https://doi.org/10.6028/NIST.IR.8271

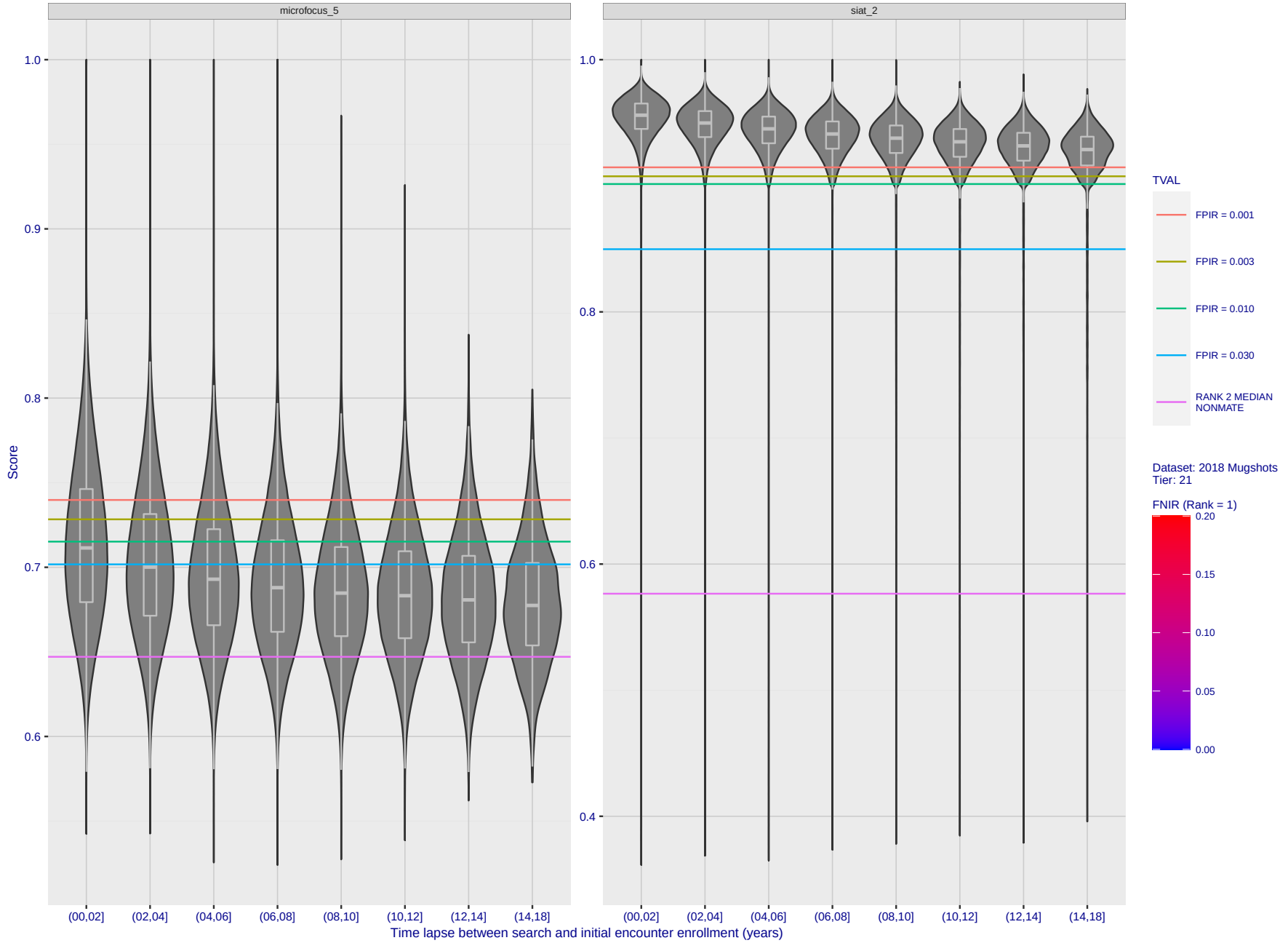

Figure 111: **[FRVT-2018 Mugshot Ageing Dataset] Native mate scores vs. time-elapsed**. *The oldest image of each individual is enrolled. Thereafter, all more recent images are searched. Mated score distributions are computed over all searches noted in row 17 of Table 1 binned by number of years between search and initial enrollment.*

2021/11/22 08:35:53

FNIR(N, R, T) = False neg. identification rate
FPIR(N, T) = False pos. identification rate

N = Num. enrolled subjects
R = Num. candidates examined

T = Threshold

T = 0 → Investigation
T > 0 → Identification

Appendix C Effect of enrolling multiple images

This publication is available free of charge from: https://doi.org/10.6028/NIST.IR.8271

This publication is available free of charge from: https://doi.org/10.6028/NIST.IR.8271

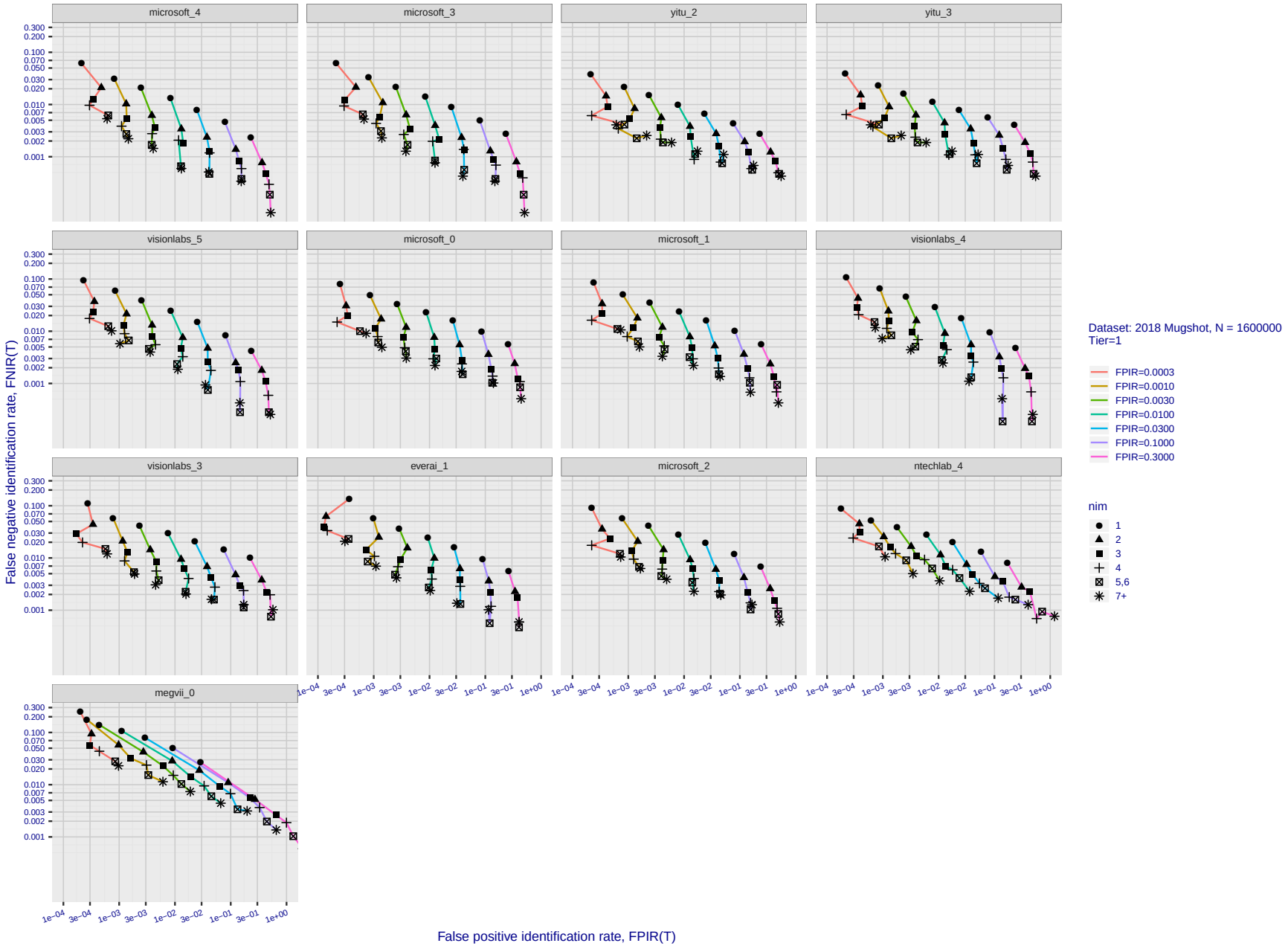

Figure 112: **[FRVT-2018 Mugshot Dataset] Effect of enrolling multiple images for each identity**. *The plot shows an identification miss rates vs. false positive rates, at seven operating thresholds. The enrolled population size is fixed. The images are enrolled with lifetime-consolidation - see section 2.3.*

2021/11/22 08:35:53

FNIR(N, R, T) = False neg. identification rate
FPIR(N, T) = False pos. identification rate

N = Num. enrolled subjects
R = Num. candidates examined

T = Threshold

T = 0 → Investigation
T > 0 → Identification

This publication is available free of charge from: https://doi.org/10.6028/NIST.IR.8271

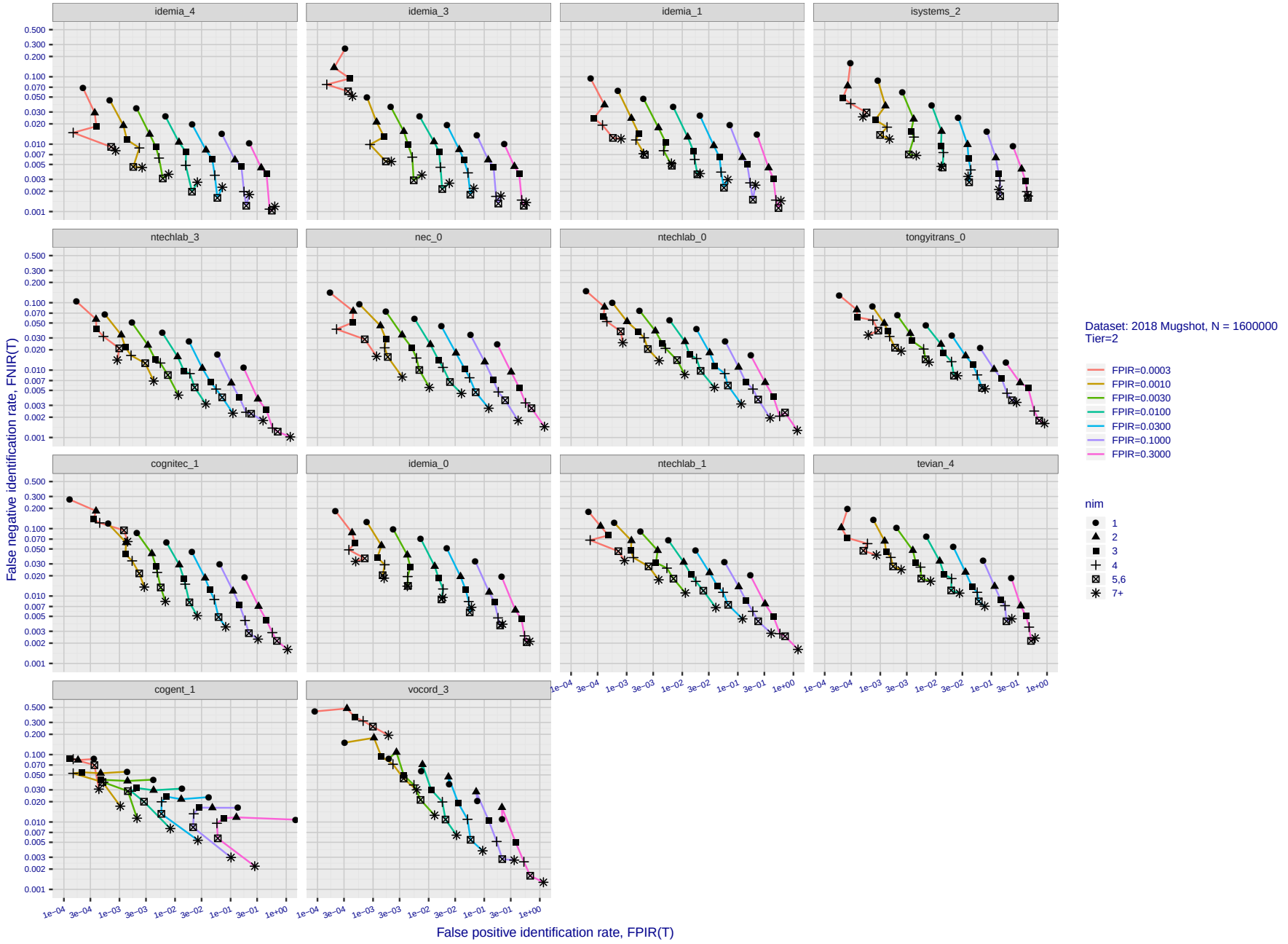

Figure 113: **[FRVT-2018 Mugshot Dataset] Effect of enrolling multiple images for each identity**. *The plot shows an identification miss rates vs. false positive rates, at seven operating thresholds. The enrolled population size is fixed. The images are enrolled with lifetime-consolidation - see section 2.3.*

2021/11/22 08:35:53
FNIR(N, R, T) = False neg. identification rate
FPIR(N, T) = False pos. identification rate
N = Num. enrolled subjects
R = Num. candidates examined
T = Threshold
T = 0 → Investigation
T > 0 → Identification

This publication is available free of charge from: https://doi.org/10.6028/NIST.IR.8271

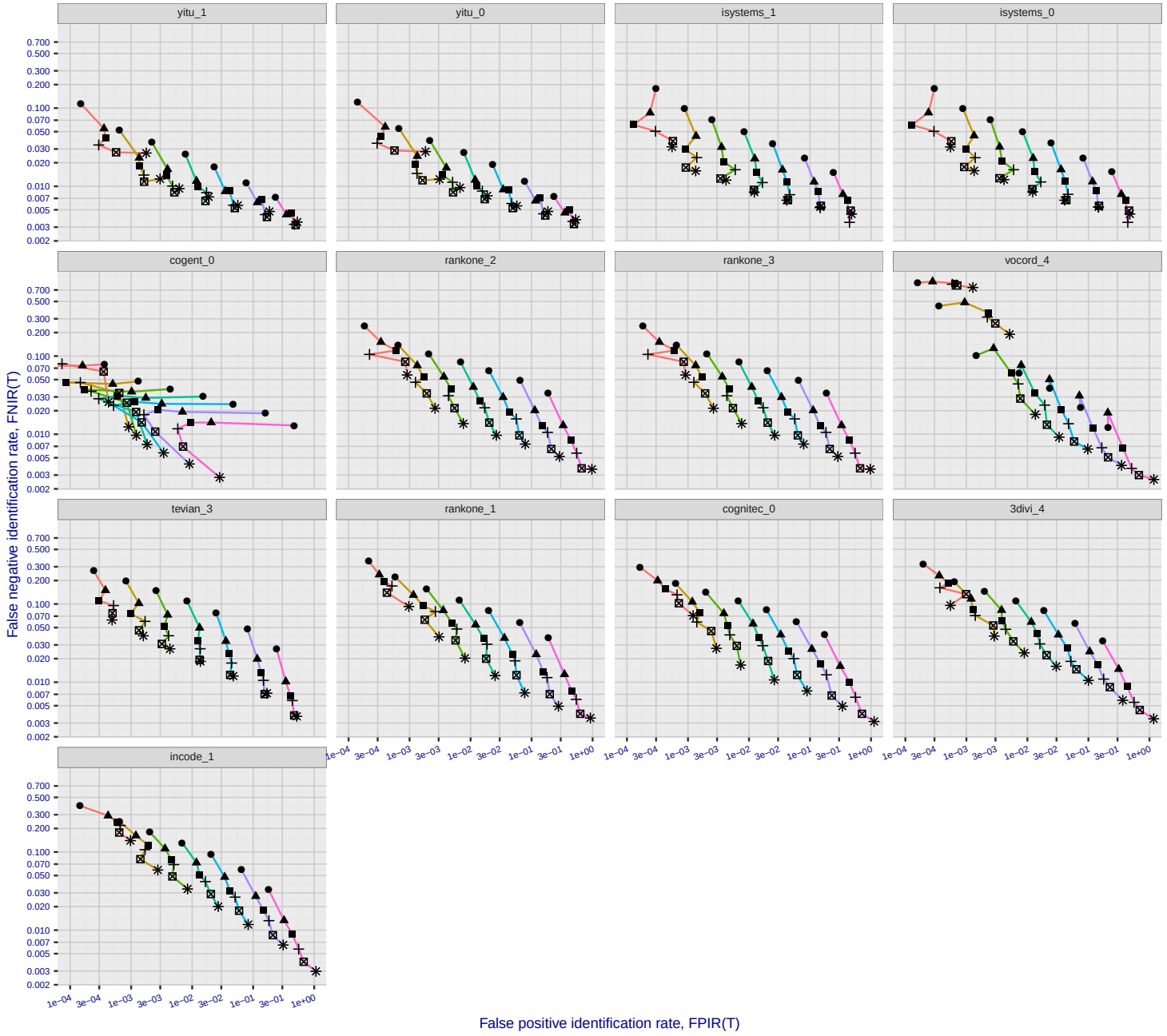

Figure 114: **[FRVT-2018 Mugshot Dataset] Effect of enrolling multiple images for each identity**. *The plot shows an identification miss rates vs. false positive rates, at seven operating thresholds. The enrolled population size is fixed. The images are enrolled with lifetime-consolidation - see section 2.3.*

2021/11/22
08:35:53

FNIR(N, R, T) = False neg. identification rate
FPIR(N, T) = False pos. identification rate

N = Num. enrolled subjects
R = Num. candidates examined

T = Threshold

T = 0 → Investigation
T > 0 → Identification

This publication is available free of charge from: https://doi.org/10.6028/NIST.IR.8271

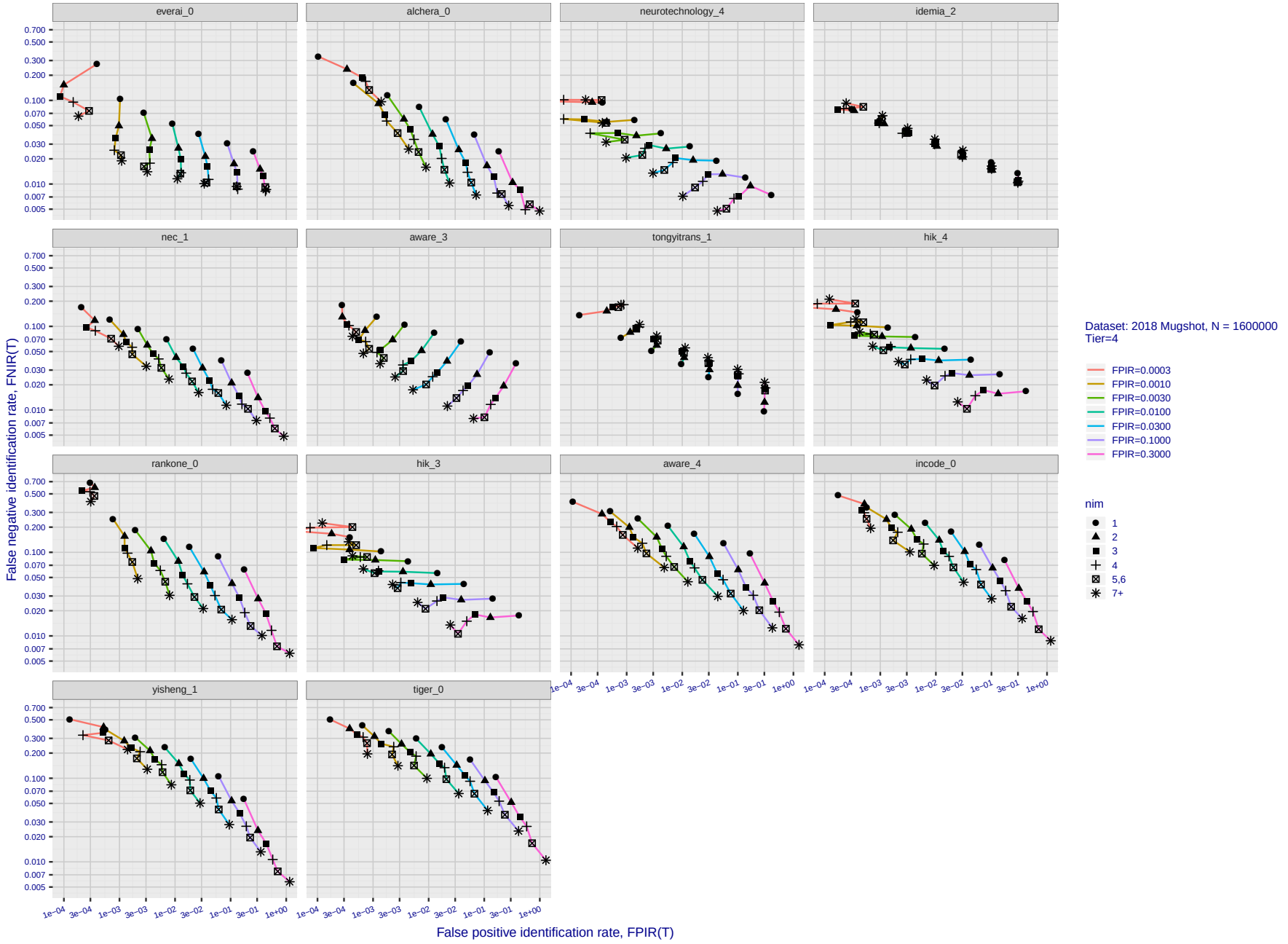

Figure 115: **[FRVT-2018 Mugshot Dataset] Effect of enrolling multiple images for each identity**. *The plot shows an identification miss rates vs. false positive rates, at seven operating thresholds. The enrolled population size is fixed. The images are enrolled with lifetime-consolidation - see section 2.3.*

2021/11/22 08:35:53

FNIR(N, R, T) = False neg. identification rate
FPIR(N, T) = False pos. identification rate

N = Num. enrolled subjects
R = Num. candidates examined

T = Threshold

T = 0 → Investigation
T > 0 → Identification

This publication is available free of charge from: https://doi.org/10.6028/NIST.IR.8271

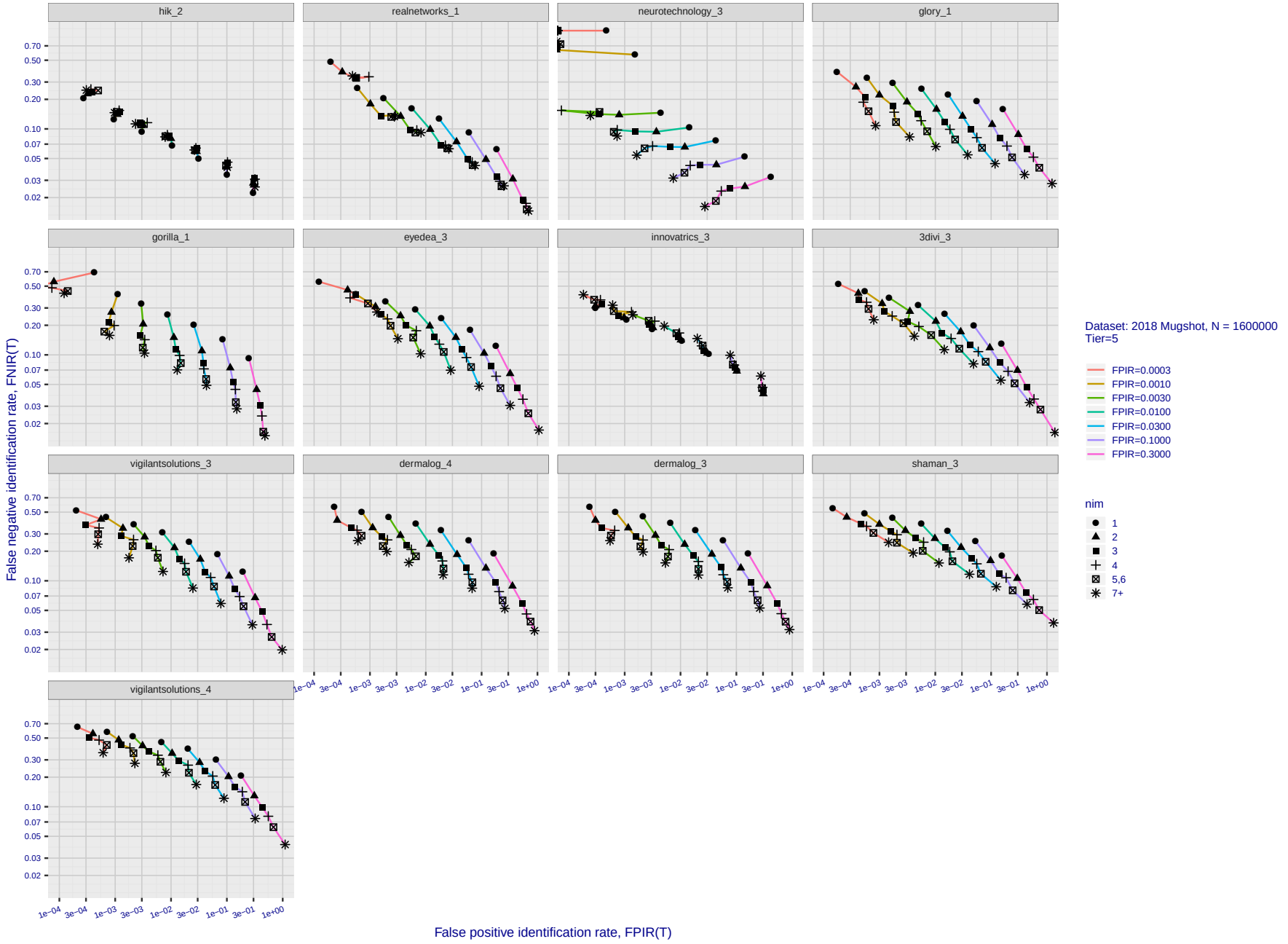

Figure 116: **[FRVT-2018 Mugshot Dataset] Effect of enrolling multiple images for each identity**. *The plot shows an identification miss rates vs. false positive rates, at seven operating thresholds. The enrolled population size is fixed. The images are enrolled with lifetime-consolidation - see section 2.3.*

2021/11/22 08:35:53

FNIR(N, R, T) = False neg. identification rate
FPIR(N, T) = False pos. identification rate
N = Num. enrolled subjects
R = Num. candidates examined
T = Threshold
T = 0 → Investigation
T > 0 → Identification

This publication is available free of charge from: https://doi.org/10.6028/NIST.IR.8271

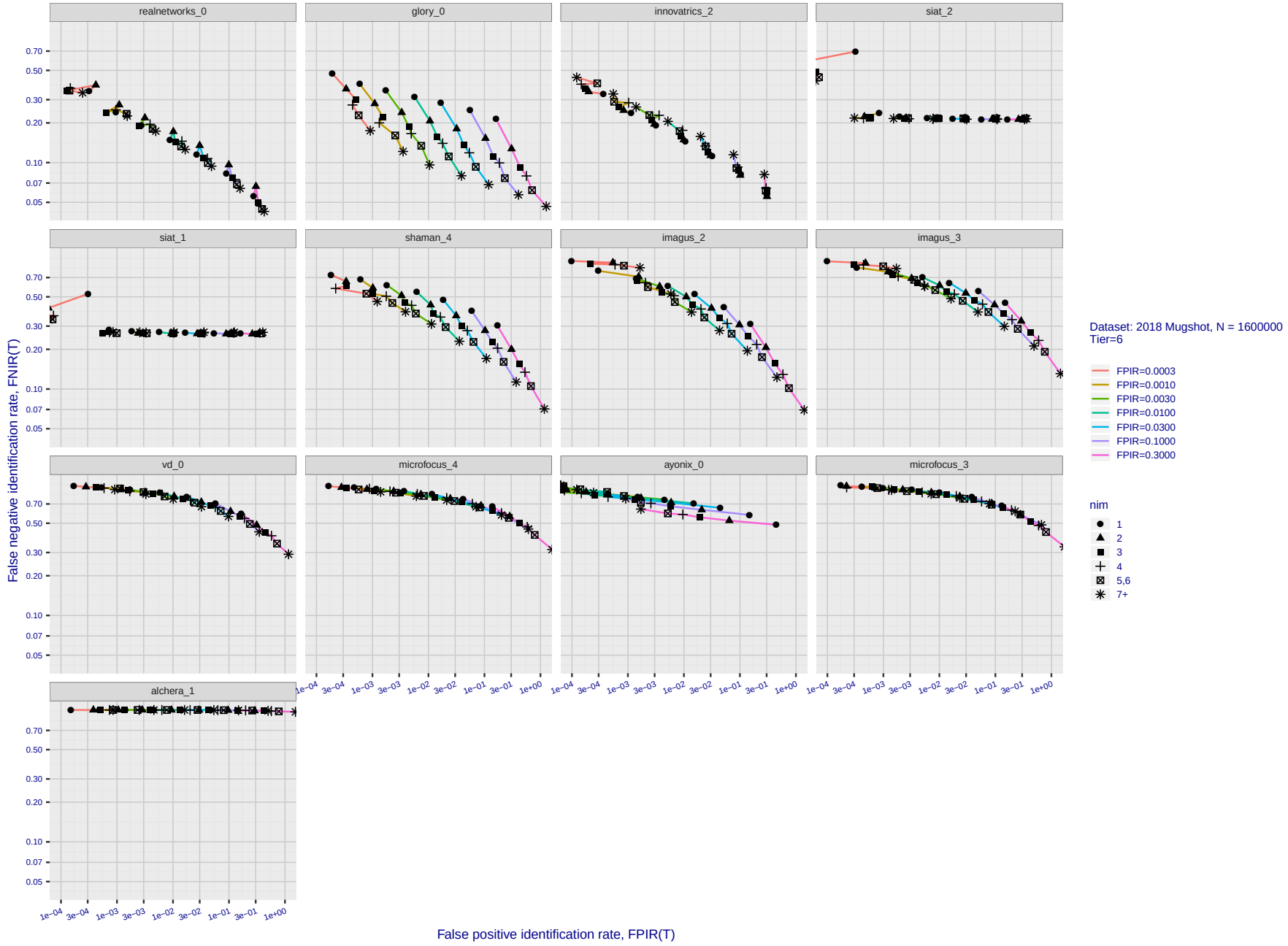

Figure 117: **[FRVT-2018 Mugshot Dataset] Effect of enrolling multiple images for each identity**. *The plot shows an identification miss rates vs. false positive rates, at seven operating thresholds. The enrolled population size is fixed. The images are enrolled with lifetime-consolidation - see section 2.3.*

2021/11/22 08:35:53

FNIR(N, R, T) = False neg. identification rate
FPIR(N, T) = False pos. identification rate
N = Num. enrolled subjects
R = Num. candidates examined
T = Threshold
T = 0 → Investigation
T > 0 → Identification

Appendix D Accuracy with poor quality webcam images

This publication is available free of charge from: https://doi.org/10.6028/NIST.IR.8271

2021/11/22	FNIR(N, R, T) =	False neg. identification rate	N = Num. enrolled subjects	T = Threshold	$T = 0 \rightarrow$ Investigation
08:35:53	FPIR(N, T) =	False pos. identification rate	R = Num. candidates examined		$T > 0 \rightarrow$ Identification

This publication is available free of charge from: https://doi.org/10.6028/NIST.IR.8271

This publication is available free of charge from: https://doi.org/10.6028/NIST.IR.8271

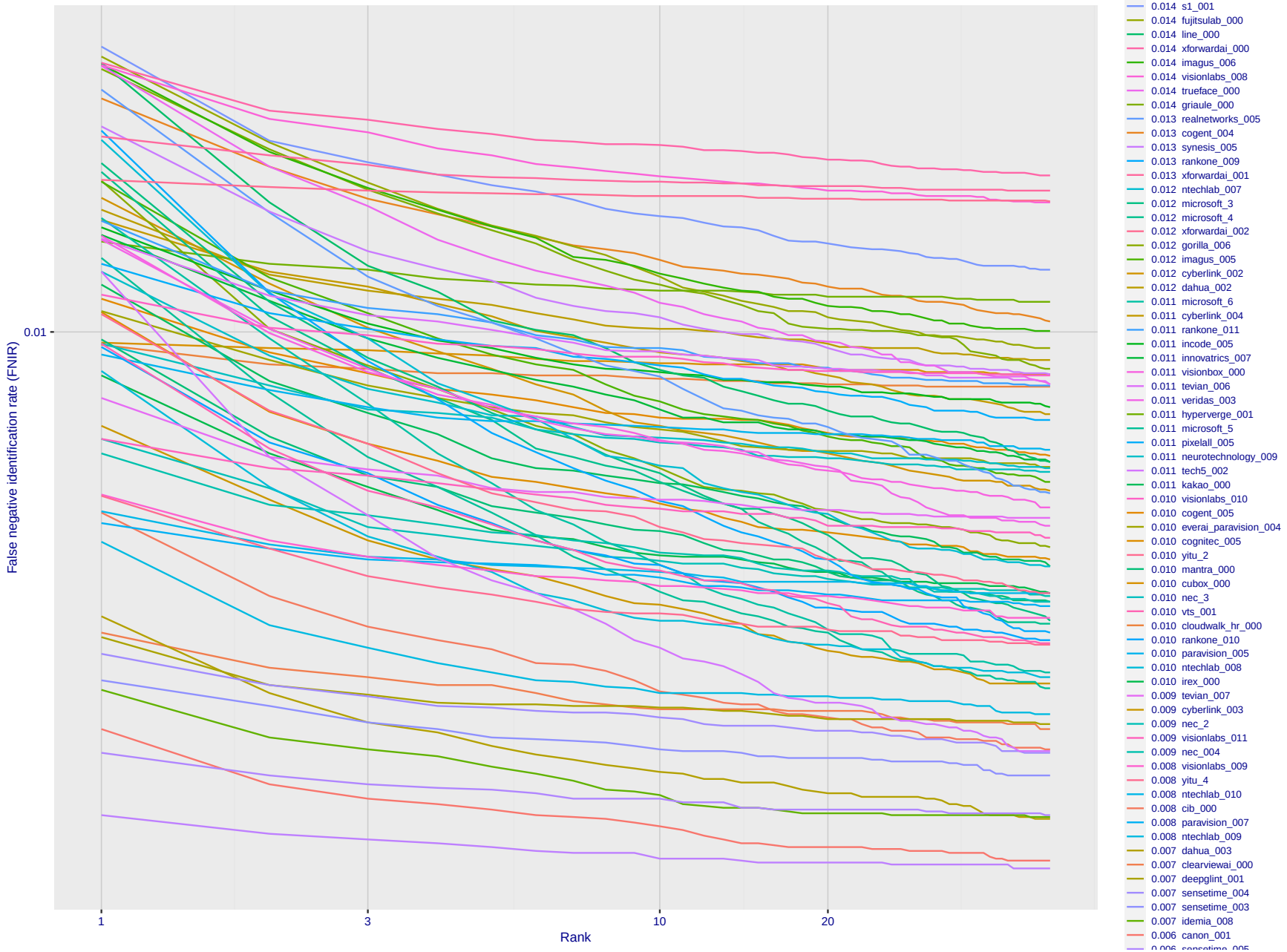

2021/11/22 08:35:53

FNIR(N, R, T) = False neg. identification rate
FPIR(N, T) = False pos. identification rate

N = Num. enrolled subjects
R = Num. candidates examined

T = Threshold

T = 0 → Investigation
T > 0 → Identification

Figure 118: **[Webcam Dataset] Identification miss rates vs. rank**. *The results apply to cross-domain recognition in which webcams are searched against enrolled mugshots. The FNIR values are higher than those for mugshot-mugshot identification due to low image resolution, lighting and less constrained subject pose in webcam images - see Figure 6.*

This publication is available free of charge from: https://doi.org/10.6028/NIST.IR.8271

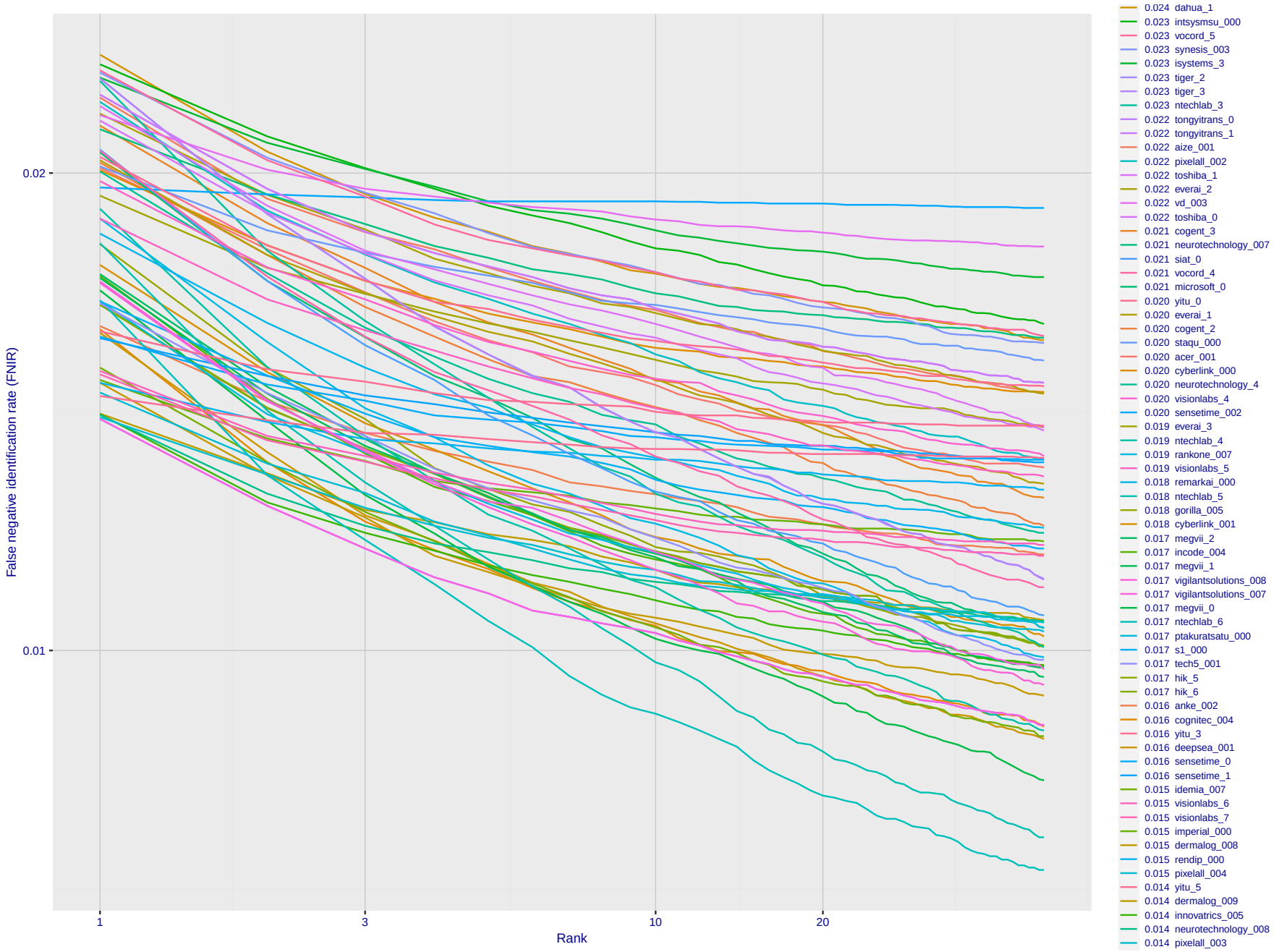

Figure 119: **[Webcam Dataset] Identification miss rates vs. rank**. *The results apply to cross-domain recognition in which webcams are searched against enrolled mugshots. The FNIR values are higher than those for mugshot-mugshot identification due to low image resolution, lighting and less constrained subject pose in webcam images - see Figure 6.*

2021/11/22 08:35:53

FNIR(N, R, T) = FPIR(N, T) =

False neg. identification rate
False pos. identification rate

N = Num. enrolled subjects
R = Num. candidates examined

T = Threshold

T = 0 → Investigation
T > 0 → Identification

This publication is available free of charge from: https://doi.org/10.6028/NIST.IR.8271

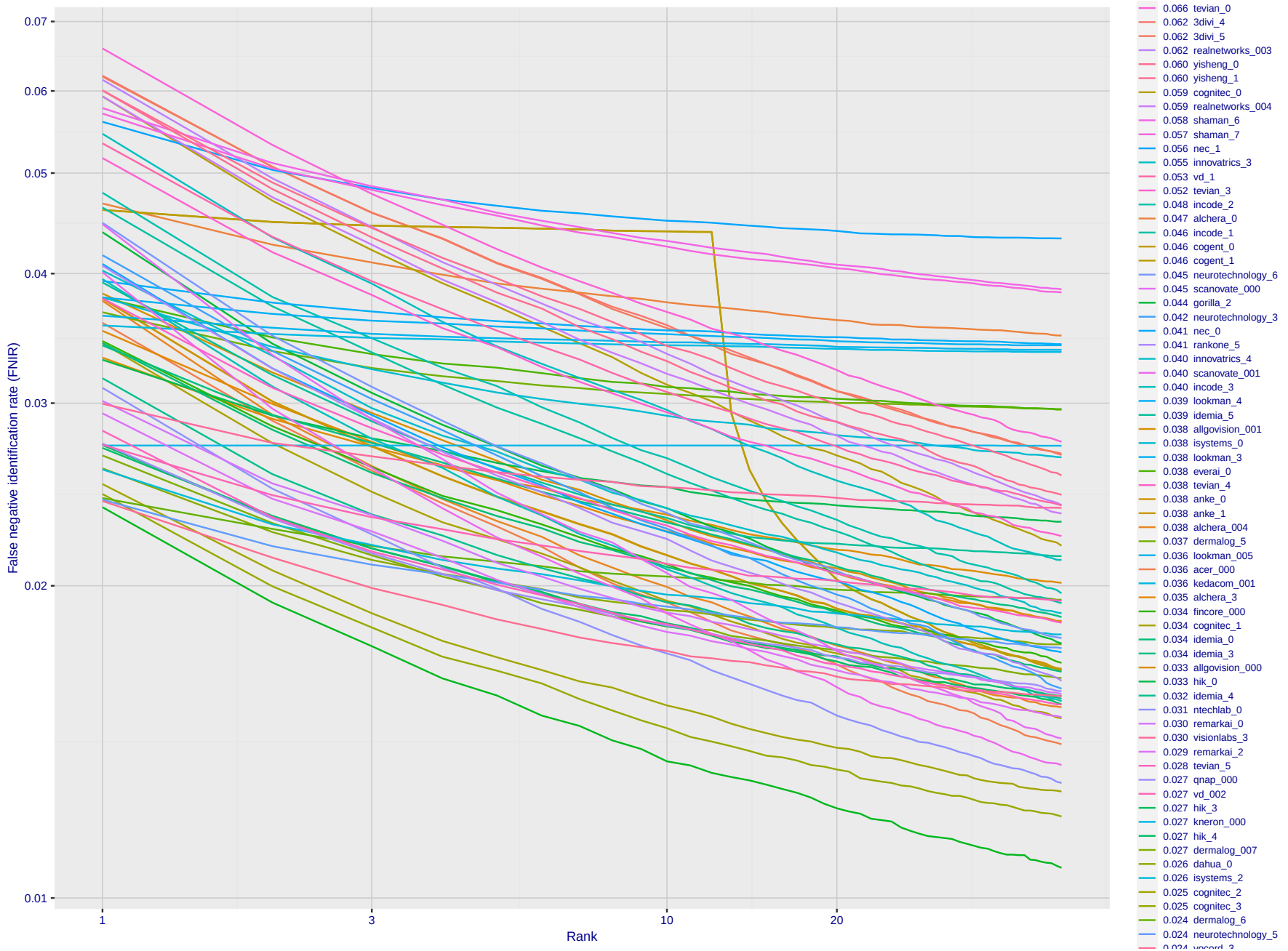

Figure 120: **[Webcam Dataset] Identification miss rates vs. rank**. *The results apply to cross-domain recognition in which webcams are searched against enrolled mugshots. The FNIR values are higher than those for mugshot-mugshot identification due to low image resolution, lighting and less constrained subject pose in webcam images - see Figure 6.*

2021/11/22 08:35:53

FNIR(N, R, T) = False neg. identification rate
FPIR(N, T) = False pos. identification rate

N = Num. enrolled subjects
R = Num. candidates examined

T = Threshold

T = 0 → Investigation
T > 0 → Identification

This publication is available free of charge from: https://doi.org/10.6028/NIST.IR.8271

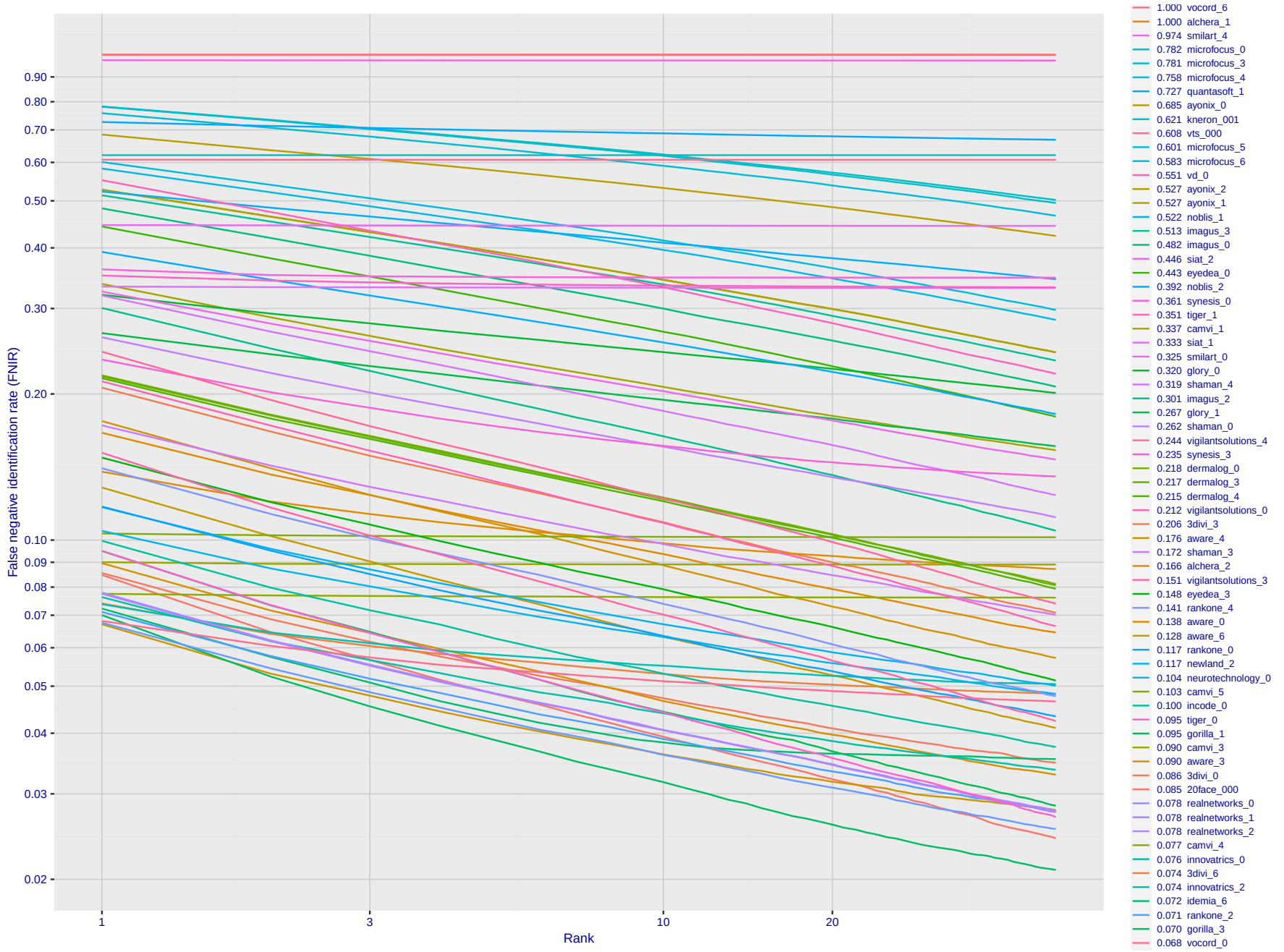

Figure 121: **[Webcam Dataset] Identification miss rates vs. rank**. *The results apply to cross-domain recognition in which webcams are searched against enrolled mugshots. The FNIR values are higher than those for mugshot-mugshot identification due to low image resolution, lighting and less constrained subject pose in webcam images - see Figure 6.*

2021/11/22	FNIR(N, R, T) =	False neg. identification rate	N = Num. enrolled subjects	T = Threshold	$T = 0 \rightarrow$ Investigation
08:35:53	FPIR(N, T) =	False pos. identification rate	R = Num. candidates examined		$T > 0 \rightarrow$ Identification

This publication is available free of charge from: https://doi.org/10.6028/NIST.IR.8271

This publication is available free of charge from: https://doi.org/10.6028/NIST.IR.8271

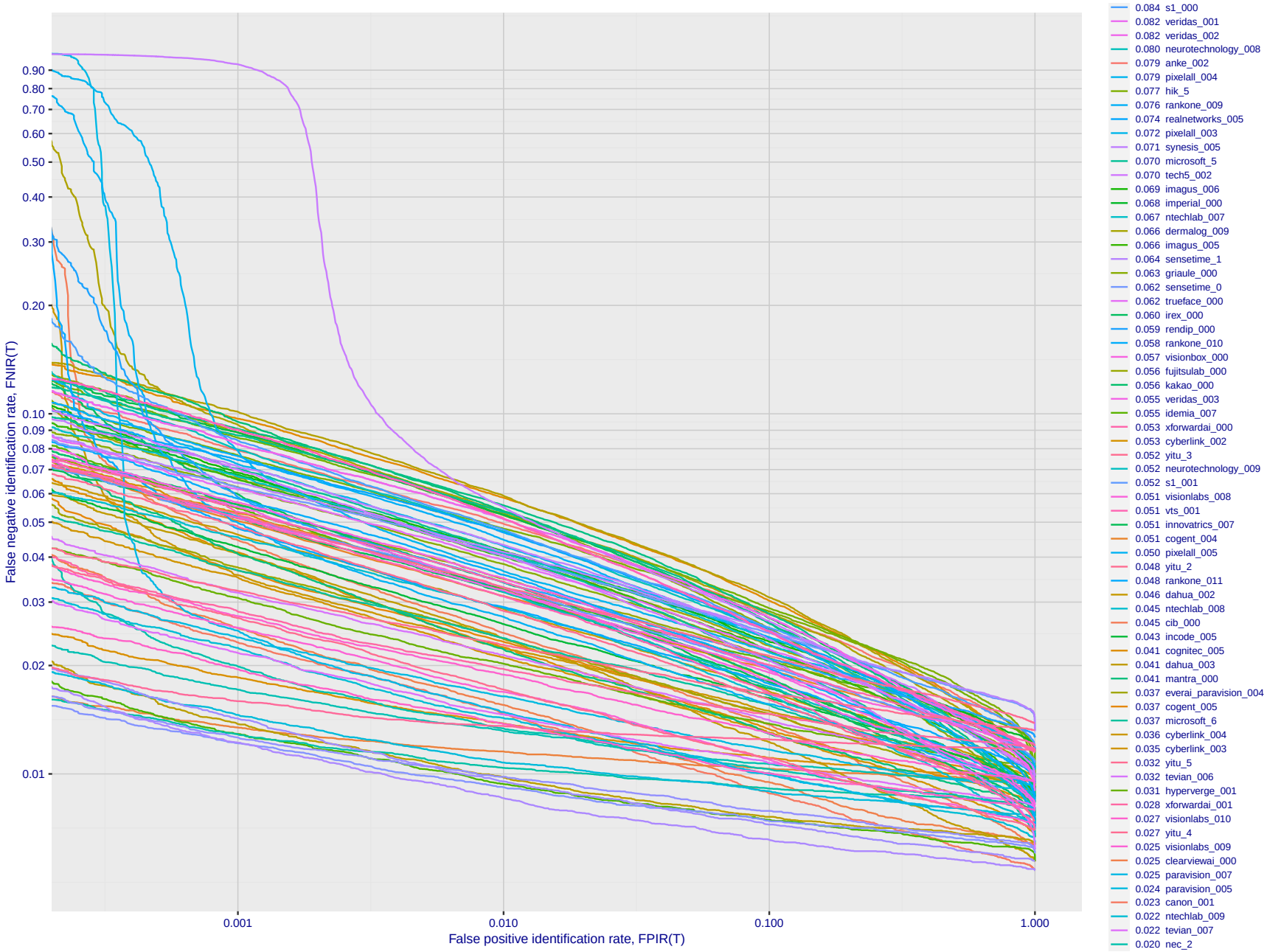

Figure 122: **[Webcam Dataset] Identification miss rates vs. false positive rates**. *The results apply to cross-domain recognition in which webcams are searched against enrolled mugshots. The FNIR values are higher than those for mugshot-mugshot identification due to low image resolution, lighting and less constrained subject pose in webcam images - see Figure 6.*

2021/11/22 08:35:53

FNIR(N, R, T) = FPIR(N, T) =

False neg. identification rate
False pos. identification rate

N = Num. enrolled subjects
R = Num. candidates examined

T = Threshold

T = 0 → Investigation
T > 0 → Identification

This publication is available free of charge from: https://doi.org/10.6028/NIST.IR.8271

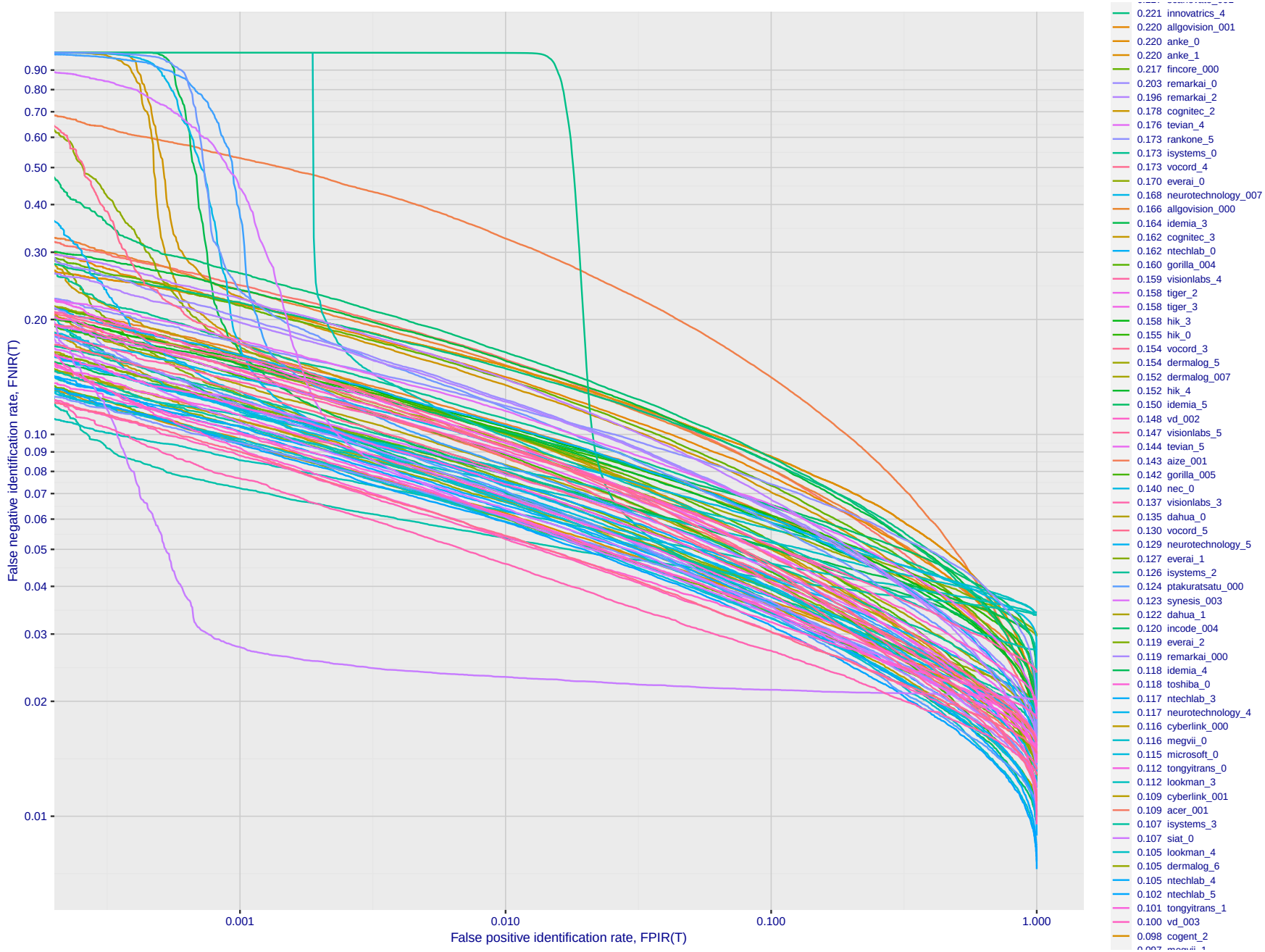

Figure 123: **[Webcam Dataset] Identification miss rates vs. false positive rates**. *The results apply to cross-domain recognition in which webcams are searched against enrolled mugshots. The FNIR values are higher than those for mugshot-mugshot identification due to low image resolution, lighting and less constrained subject pose in webcam images - see Figure 6.*

This publication is available free of charge from: https://doi.org/10.6028/NIST.IR.8271

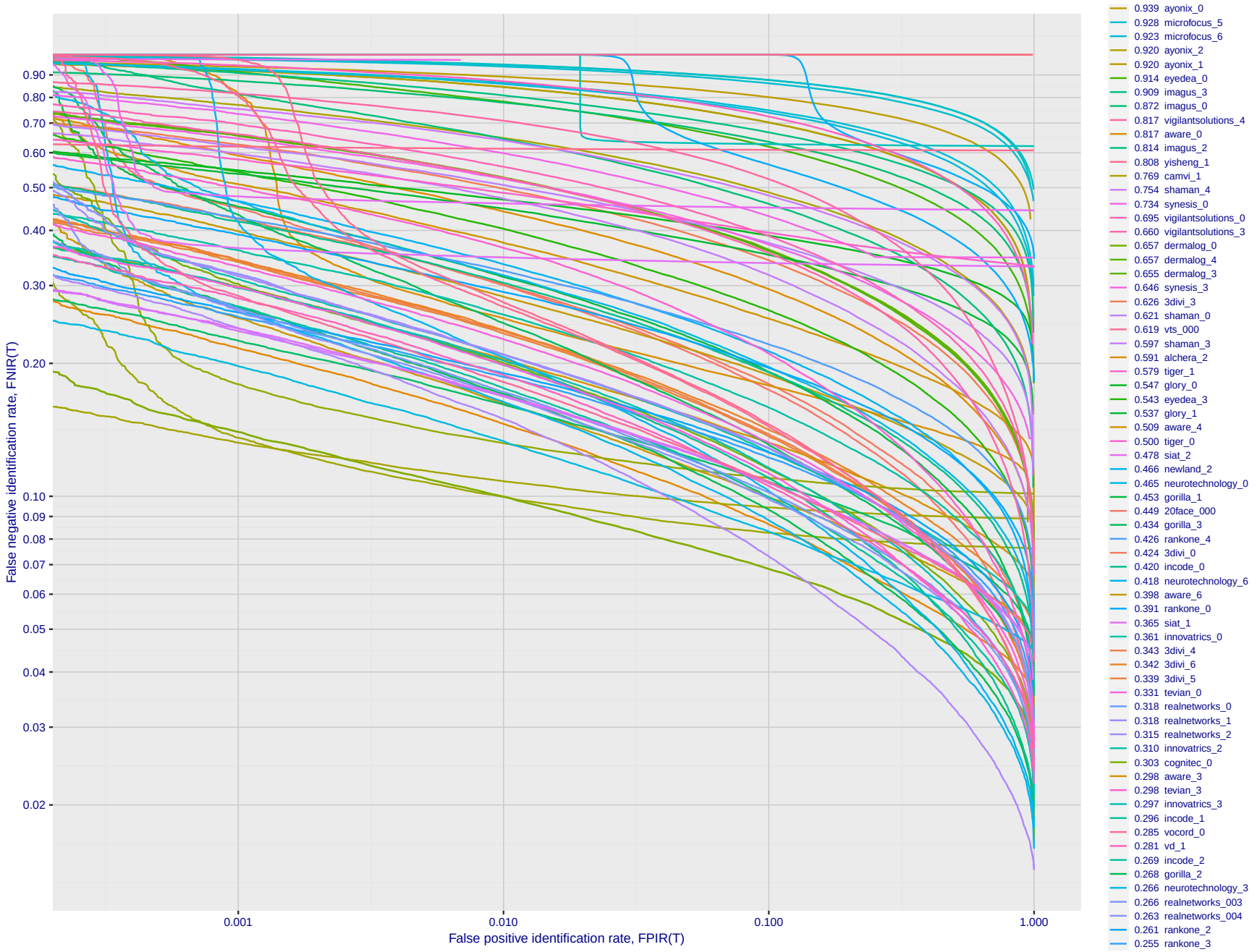

Figure 124: **[Webcam Dataset] Identification miss rates vs. false positive rates**. *The results apply to cross-domain recognition in which webcams are searched against enrolled mugshots. The FNIR values are higher than those for mugshot-mugshot identification due to low image resolution, lighting and less constrained subject pose in webcam images - see Figure 6.*

2021/11/22 08:35:53

FNIR(N, R, T) = FPIR(N, T) =

False neg. identification rate
False pos. identification rate

N = Num. enrolled subjects
R = Num. candidates examined

T = Threshold

T = 0 → Investigation
T > 0 → Identification

Appendix E Accuracy for profile-view to frontal recognition

Figures 125 - 127 gives accuracy results for searching 100 000 mated and 100 000 non-mated profile-view images against the same FRVT 2018 frontal enrollment dataset, N = 1 600 000, used in the main mugshot trials. This experiment corresponds to row-13 of Table 1. An example of profile-view image is given in Figure 7.

This publication is available free of charge from: https://doi.org/10.6028/NIST.IR.8271

This publication is available free of charge from: https://doi.org/10.6028/NIST.IR.8271

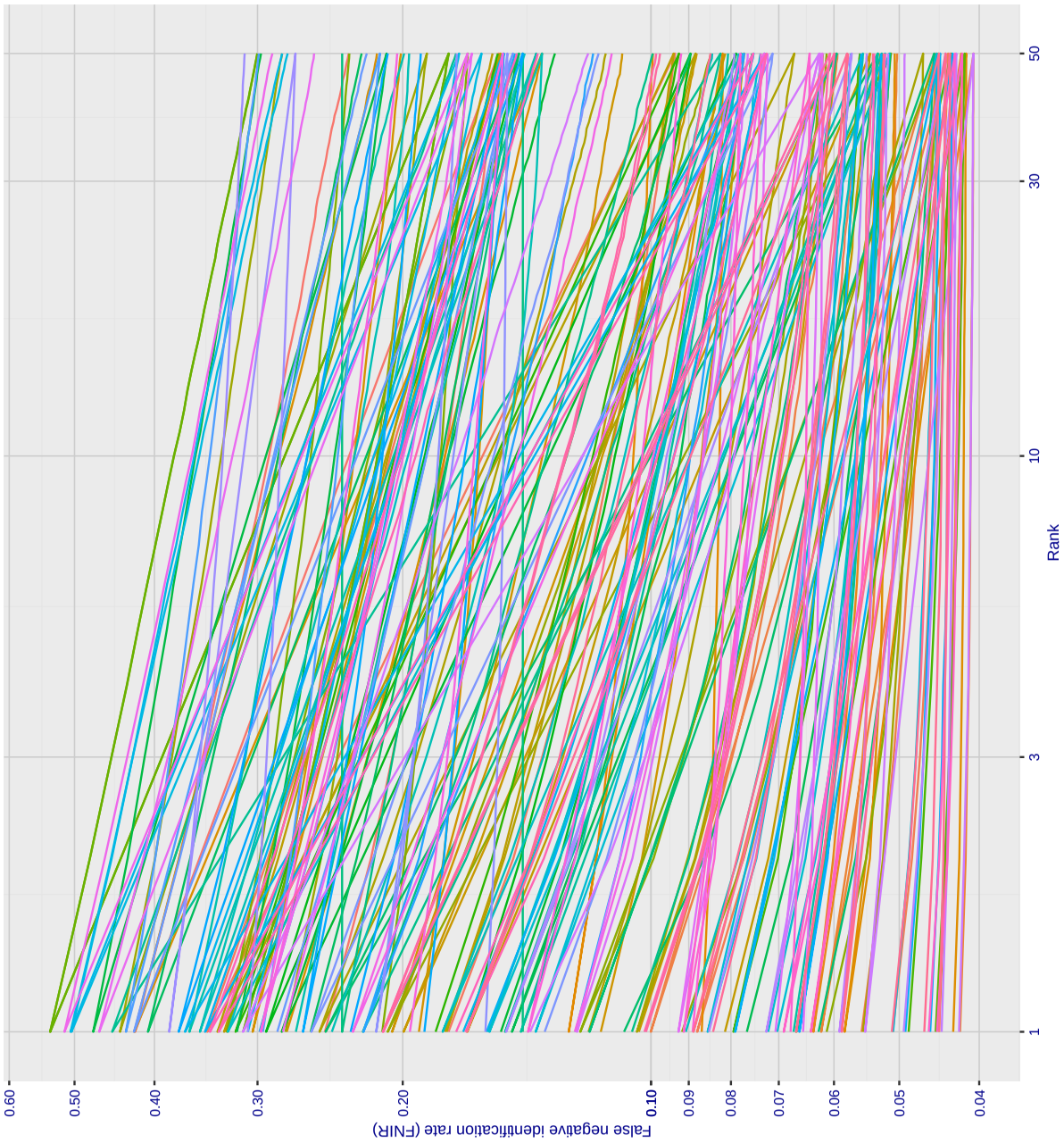

Figure 125: **[Mugshot and profile-view dataset] Rank-based accuracy**. *For some of the more accurate Phase 3 algorithms the figure plots error tradeoff characteristics for frontal and profile-view searches into an enrolled set of $N = 1\,600\,000$ frontal images. Note that some algorithms fail on profile-view images with FNIR → 1 - this evaluation did not ask developers to provide profile-view capability. Some algorithms, on the other hand, give FNIR approaching that for frontal-view searches using c. 2010 algorithms. The best result is that 91% of profile-view searches yield the correct mate at rank 1, and better than 94% in the top-50 candidates.*

This publication is available free of charge from: https://doi.org/10.6028/NIST.IR.8271

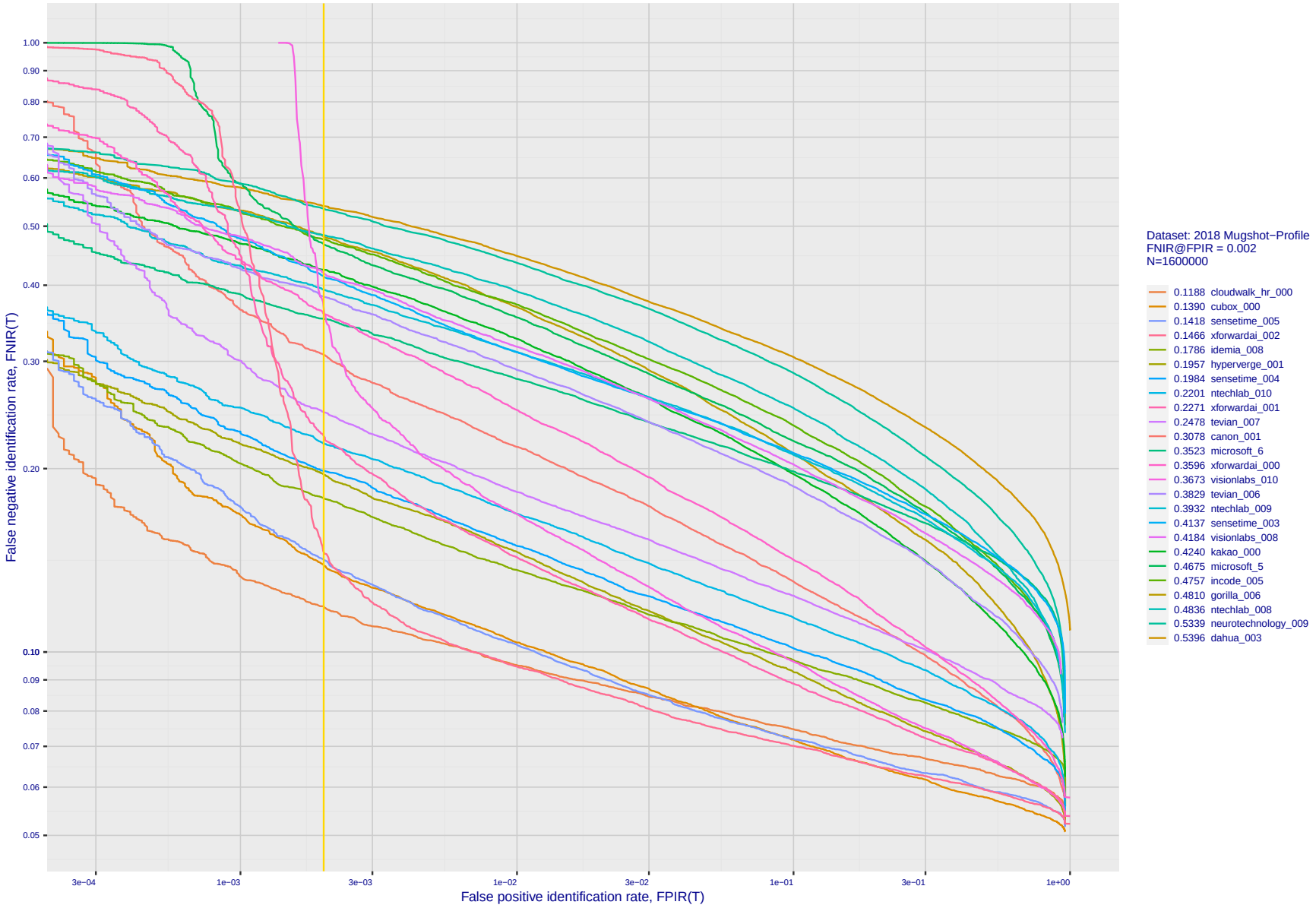

Figure 126: **[Mugshot and profile-view dataset] Threshold-based accuracy**. *For some of the more accurate Phase 3 algorithms the figure plots error tradeoff characteristics for frontal and profile-view searches into an enrolled set of N = 1 600 000 frontal images. Note that some algorithms fail on profile-view images with FNIR → 1 - this evaluation did not ask developers to provide profile-view capability. Some algorithms, on the other hand, give FNIR approaching that for frontal-view searches using c. 2010 algorithms.*

2021/11/22 08:35:53

FNIR(N, R, T) = False neg. identification rate
FPIR(N, T) = False pos. identification rate

N = Num. enrolled subjects
R = Num. candidates examined

T = Threshold

T = 0 → Investigation
T > 0 → Identification

This publication is available free of charge from: https://doi.org/10.6028/NIST.IR.8271

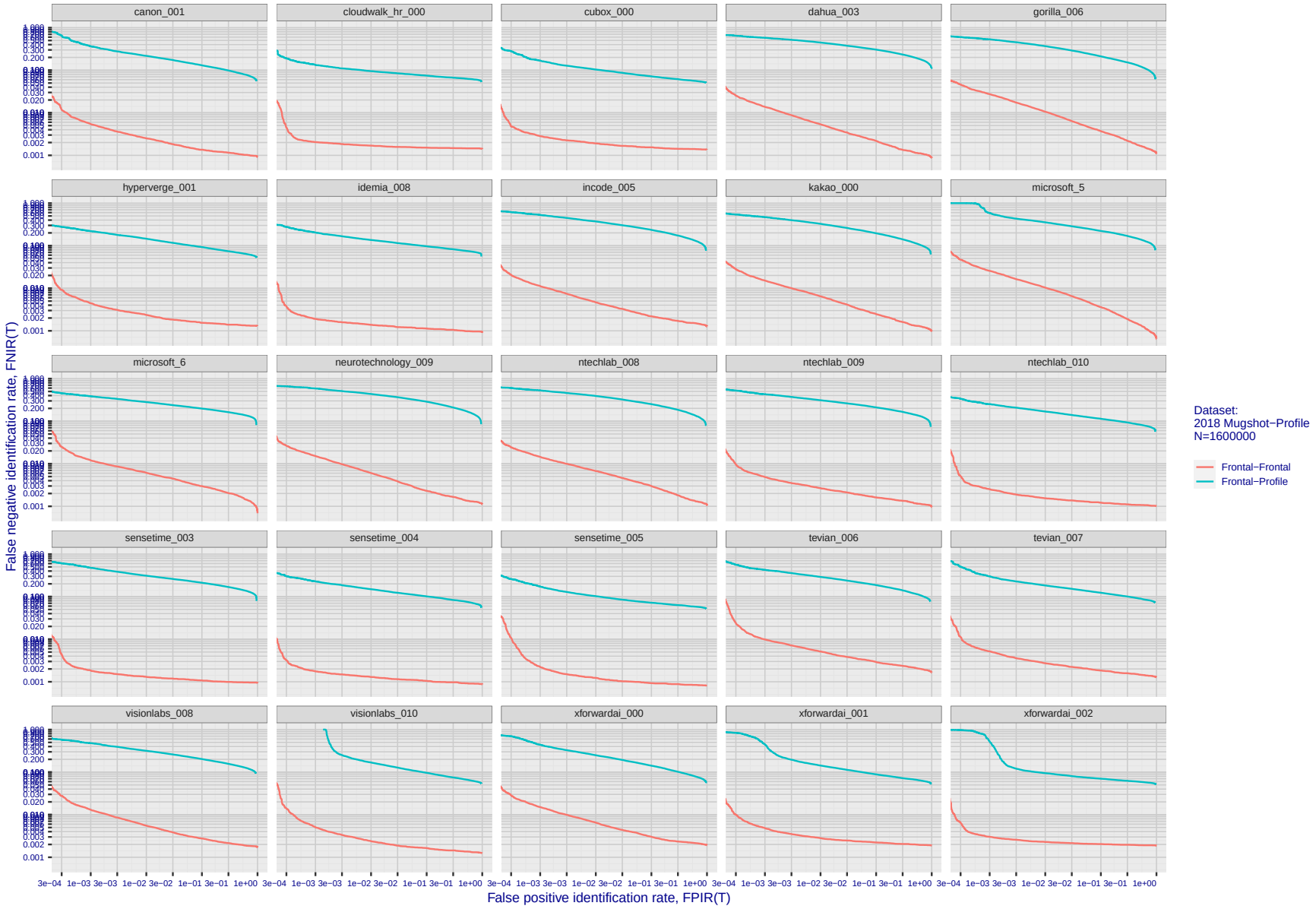

Figure 127: **[Mugshot and profile-view dataset] Speed-accuracy tradeoff**. *For some of the more accurate Phase 3 algorithms the figure plots error tradeoff characteristics for frontal and profile-view searches into an enrolled set of N = 1 600 000 frontal images. Some algorithms fail on profile-view images with FNIR → 1 - this evaluation did not ask developers to provide profile-view capability. Some algorithms, on the other hand, give FNIR approaching that for frontal-view searches using c. 2010 algorithms. Blue lines connect points of equal threshold from which it is evident that some algorithms would give markedly higher false positive outcomes if profile-view images were searched in a system configured for frontal searches. This would be a vulnerability in an access control system.*

2021/11/22 08:35:53

FNIR(N, R, T) = False neg. identification rate
FPIR(N, T) = False pos. identification rate

N = Num. enrolled subjects
R = Num. candidates examined

T = Threshold

T = 0 → Investigation
T > 0 → Identification

Appendix F Search duration

As in and prior tests, this section documents search speeds spanning three orders of magnitude. In applications where search volumes are high enough, this will have implications for hardware requirements especially for large N or when search duration is appreciably larger than the time it takes to prepare a template from the search image(s). Further, given very large (and growing) operational databases, the scalability of algorithms is important. It has been reported previously [8] that search duration can scale sublinearly with enrolled population size N. Further there has been considerable recent research on indexing, exact [13] and approximate nearest neighbor search [1,13] and fast-search [14,16].

Figure 128 charts the search duration measurements presented earlier in Tables 2 - 4.

- Most algorithms scale linearly. For those in that category, there is a wide range in speed with search durations ranging from 82 milliseconds for a 12 million gallery (for NEC-3) to more than 40 seconds (for Yitu-3, Toshiba-2) and even higher for less accurate algorithms.
- Some developers (Camvi, Dermalog, EverAI, Innovatrics, and Visionlabs) provide algorithms whose template search durations grow approimately logarithmically i.e. $T(N)\tilde{a}\log N$ with the constant a varying between implementations. In the figure this model is fit using the point $T(1) = 0$, and $T(640\,000)$. This very sublinear behaviour affords extremely fast search times in very large galleries. One caveat for the sublinear algorithms is that their fast-search data structures can require considerable computation time - on the order of hours - for N in the millions, and this scales mildy super-linearly, i.e. $O(N^b), b > 1$. There are exceptions: the Camvi algorithms take minutes; and Innvovatrics' scale sublinearly.

This publication is available free of charge from: https://doi.org/10.6028/NIST.IR.8271

2021/11/22	FNIR(N, R, T) =	False neg. identification rate	N = Num. enrolled subjects	T = Threshold	$T = 0 \rightarrow$ Investigation
08:35:53	FPIR(N, T) =	False pos. identification rate	R = Num. candidates examined		$T > 0 \rightarrow$ Identification

This publication is available free of charge from: https://doi.org/10.6028/NIST.IR.8271

This publication is available free of charge from: https://doi.org/10.6028/NIST.IR.8271

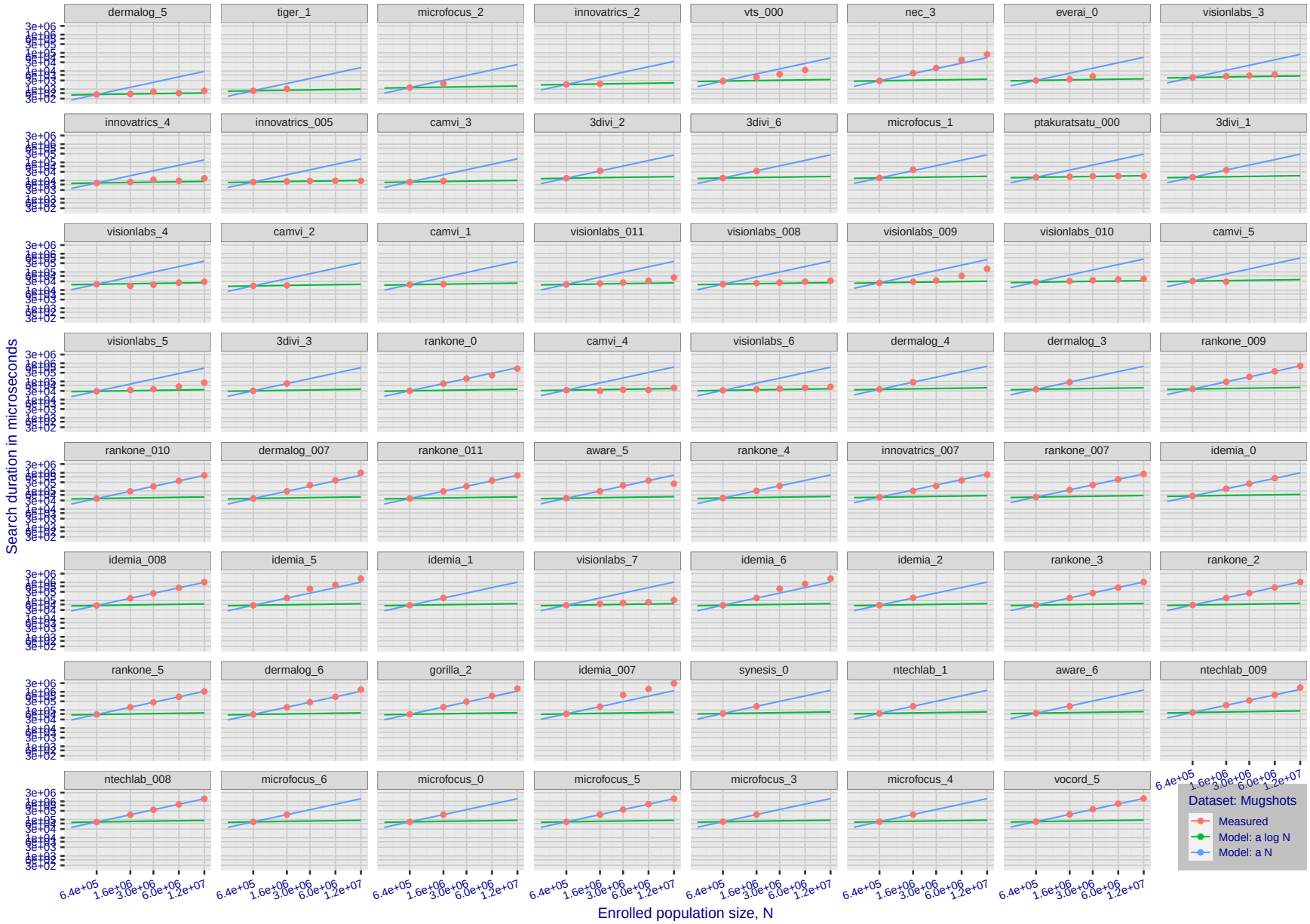

Figure 128: **[Mugshot Dataset] Search duration vs. enrolled population size**. *In red are the actual point durations measured on a single c. 2016 core. The blue shows linear growth from $N = 640\,000$. The green line shows logathmic growth from that point to $N = 1\,600\,000$. Note the sublinear growth from algorithms from Camvi, Dermalog, EverAI, Innovatrics, and Visionlabs. The tiger_1 algorithm is also sublinear, but inaccurate and inoperable at $N \geq 3000000$. This capability sometimes comes at the additional expense of converting a linear gallery data structure into whatever fast-search data structure is used. Note that search times are sometimes dominated by the template generation times shown in Table 21.*

2021/11/22
08:35:53

FNIR(N, R, T) = False neg. identification rate
FPIR(N, T) = False pos. identification rate

N = Num. enrolled subjects
R = Num. candidates examined

T = Threshold

T = 0 → Investigation
T > 0 → Identification

This publication is available free of charge from: https://doi.org/10.6028/NIST.IR.8271

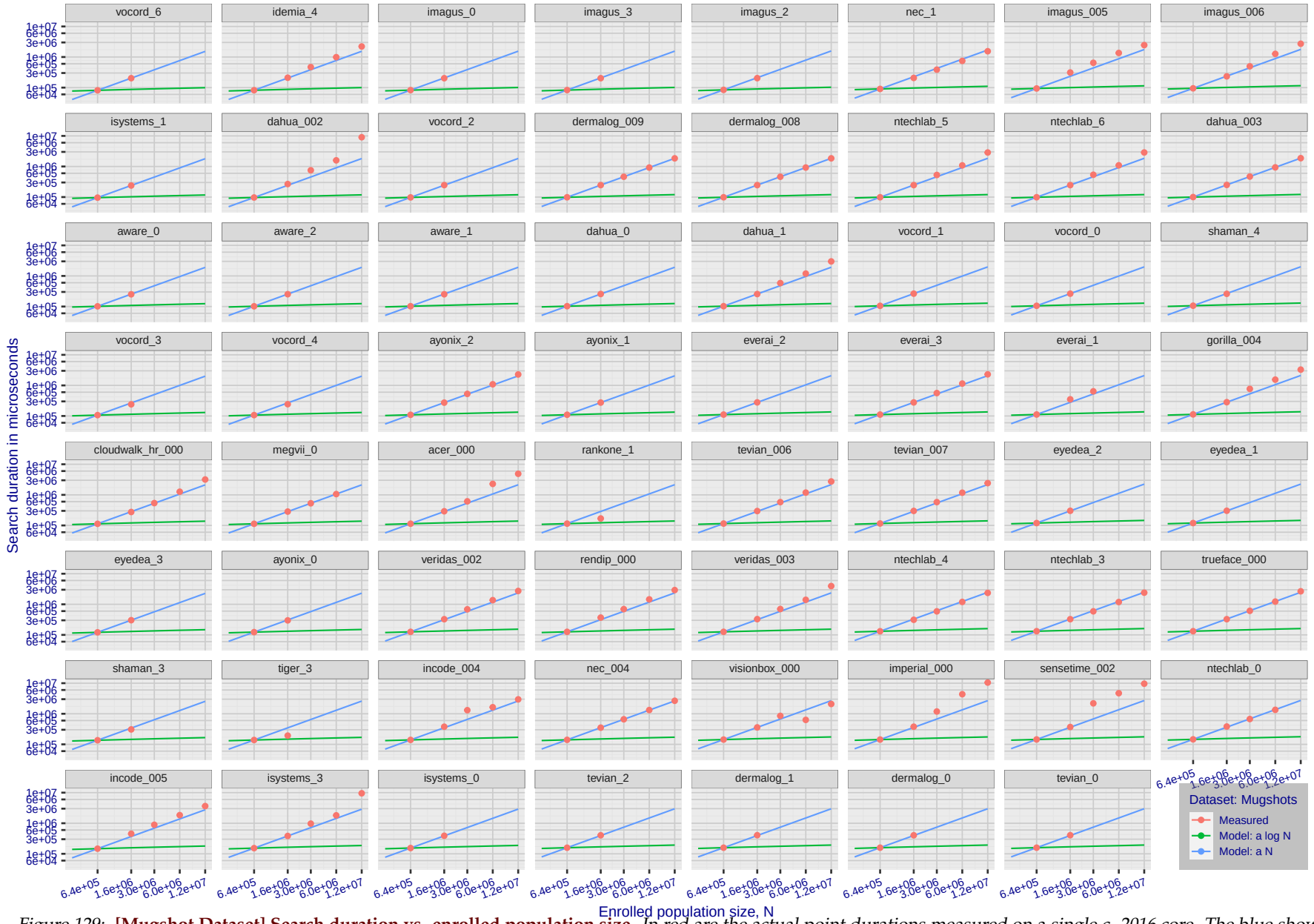

Figure 129: **[Mugshot Dataset] Search duration vs. enrolled population size**. *In red are the actual point durations measured on a single c. 2016 core. The blue shows linear growth from $N = 640\,000$. The green line shows logathmic growth from that point to $N = 1\,600\,000$. Note the sublinear growth from algorithms from Camvi, Dermalog, EverAI, Innovatrics, and Visionlabs. The tiger_1 algorithm is also sublinear, but inaccurate and inoperable at $N \geq 3000000$. This capability sometimes comes at the additional expense of converting a linear gallery data structure into whatever fast-search data structure is used. Note that search times are sometimes dominated by the template generation times shown in Table 21.*

2021/11/22
08:35:53

FNIR(N, R, T) = False neg. identification rate
FPIR(N, T) = False pos. identification rate

N = Num. enrolled subjects
R = Num. candidates examined

T = Threshold

T = 0 → Investigation
T > 0 → Identification

This publication is available free of charge from: https://doi.org/10.6028/NIST.IR.8271

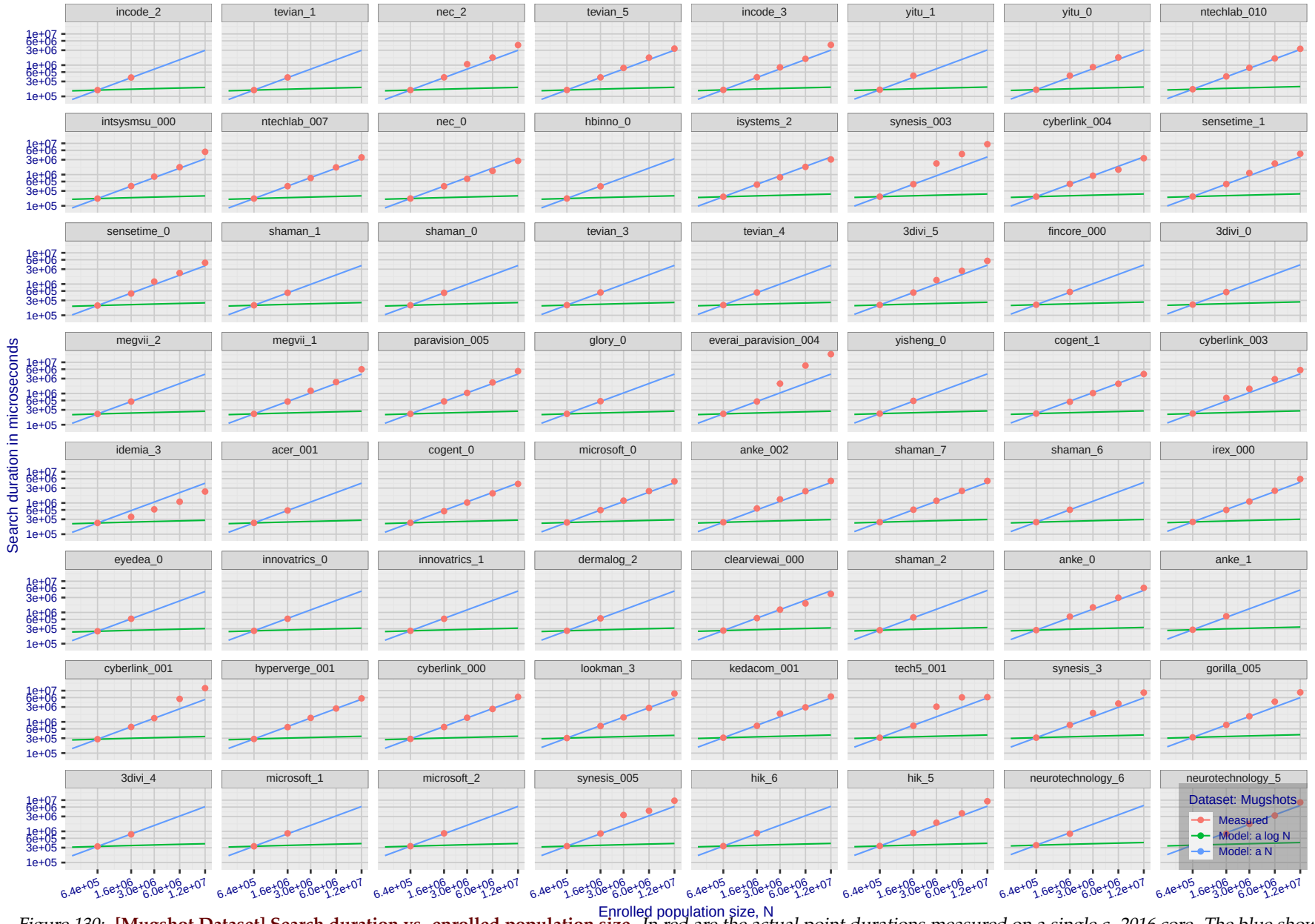

Figure 130: **[Mugshot Dataset] Search duration vs. enrolled population size**. *In red are the actual point durations measured on a single c. 2016 core. The blue shows linear growth from $N = 640\,000$. The green line shows logathmic growth from that point to $N = 1\,600\,000$. Note the sublinear growth from algorithms from Camvi, Dermalog, EverAI, Innovatrics, and Visionlabs. The tiger_1 algorithm is also sublinear, but inaccurate and inoperable at $N \geq 3000000$. This capability sometimes comes at the additional expense of converting a linear gallery data structure into whatever fast-search data structure is used. Note that search times are sometimes dominated by the template generation times shown in Table 21.*

This publication is available free of charge from: https://doi.org/10.6028/NIST.IR.8271

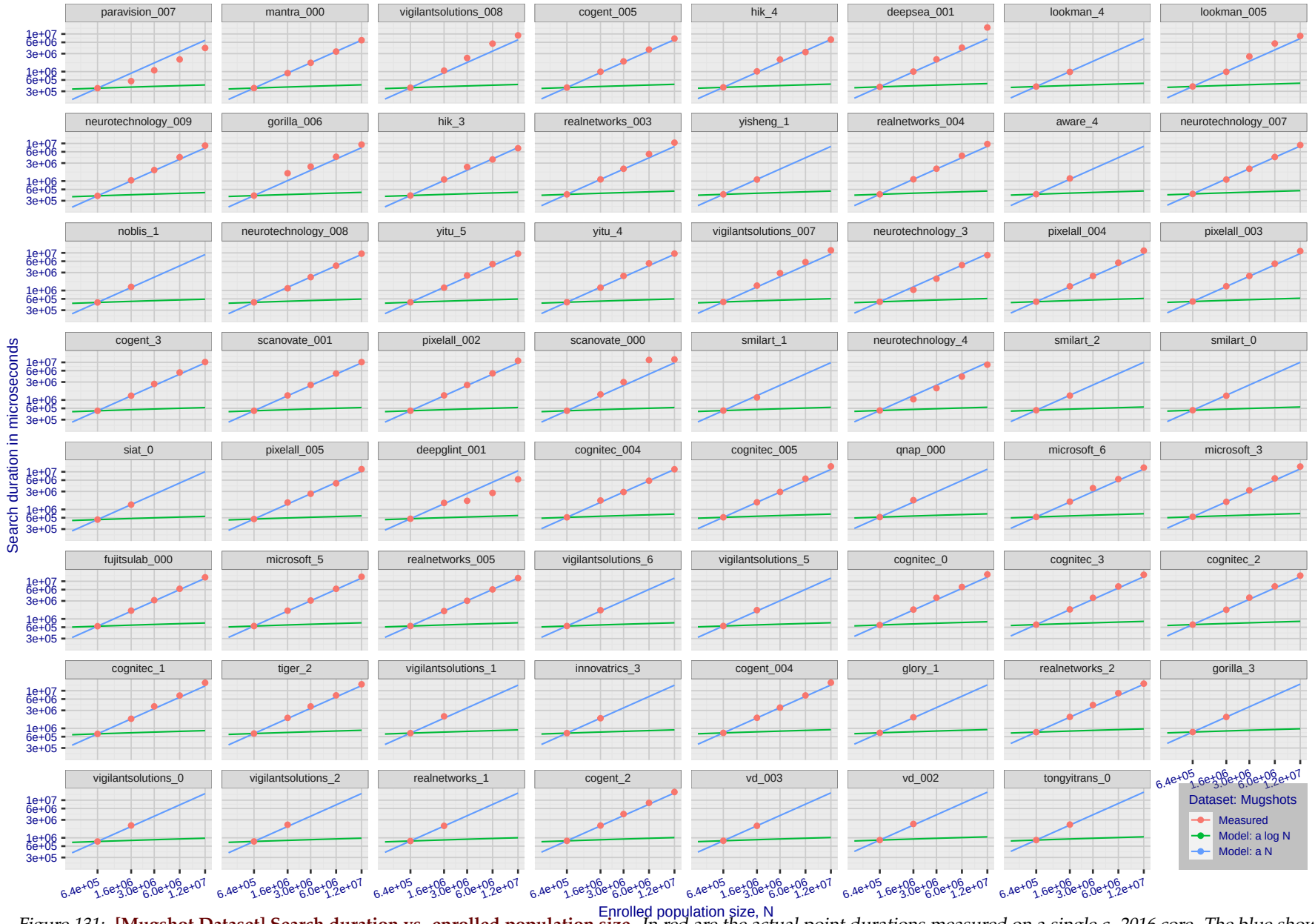

Figure 131: **[Mugshot Dataset] Search duration vs. enrolled population size**. *In red are the actual point durations measured on a single c. 2016 core. The blue shows linear growth from $N = 640\,000$. The green line shows logathmic growth from that point to $N = 1\,600\,000$. Note the sublinear growth from algorithms from Camvi, Dermalog, EverAI, Innovatrics, and Visionlabs. The tiger_1 algorithm is also sublinear, but inaccurate and inoperable at $N \geq 3000000$. This capability sometimes comes at the additional expense of converting a linear gallery data structure into whatever fast-search data structure is used. Note that search times are sometimes dominated by the template generation times shown in Table 21.*

2021/11/22 08:35:53
FNIR(N, R, T) = False neg. identification rate
FPIR(N, T) = False pos. identification rate
N = Num. enrolled subjects
R = Num. candidates examined
T = Threshold
T = 0 → Investigation
T > 0 → Identification

This publication is available free of charge from: https://doi.org/10.6028/NIST.IR.8271

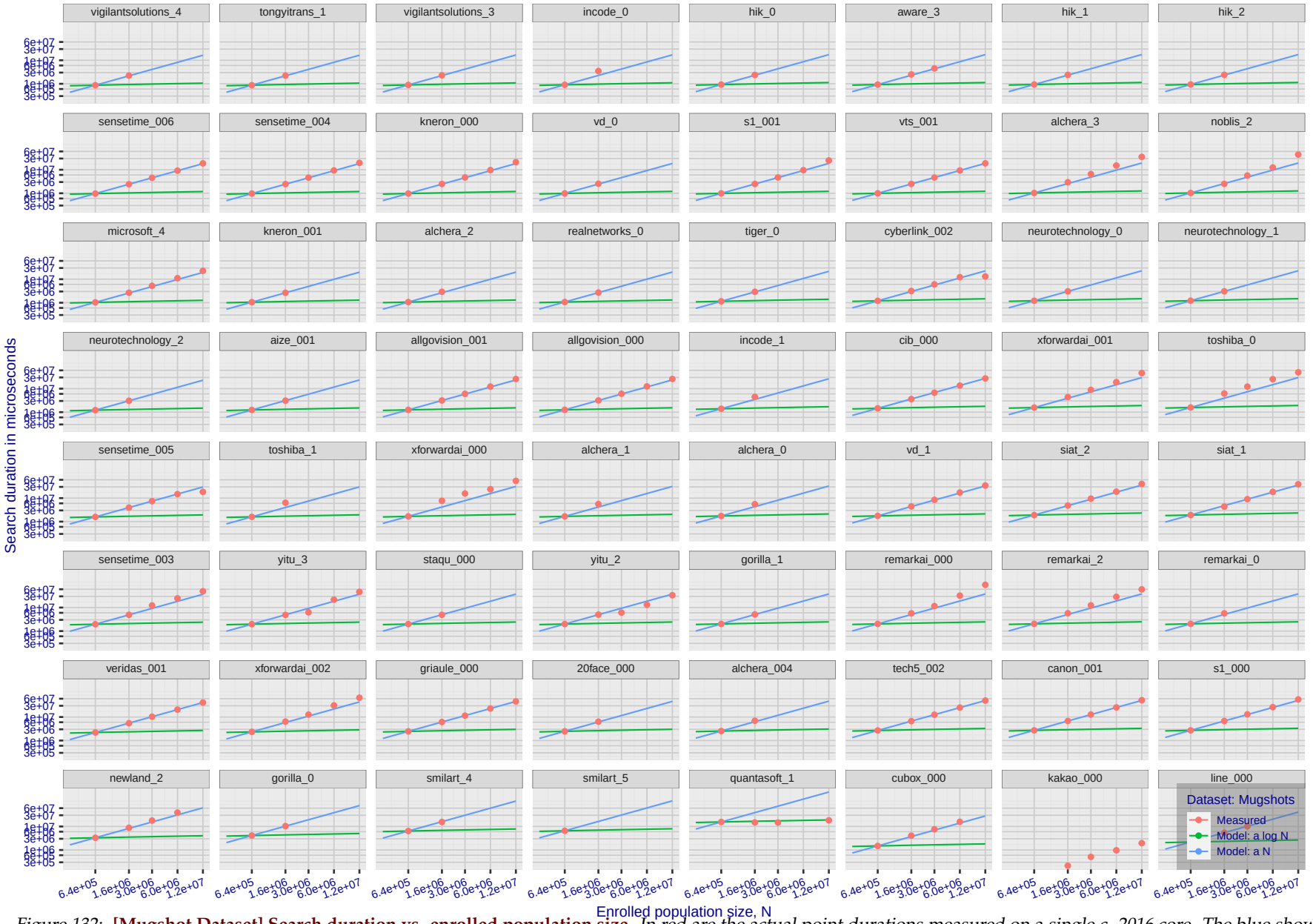

Figure 132: **[Mugshot Dataset] Search duration vs. enrolled population size**. *In red are the actual point durations measured on a single c. 2016 core. The blue shows linear growth from $N = 640\,000$. The green line shows logathmic growth from that point to $N = 1\,600\,000$. Note the sublinear growth from algorithms from Camvi, Dermalog, EverAI, Innovatrics, and Visionlabs. The tiger_1 algorithm is also sublinear, but inaccurate and inoperable at $N \geq 3000000$. This capability sometimes comes at the additional expense of converting a linear gallery data structure into whatever fast-search data structure is used. Note that search times are sometimes dominated by the template generation times shown in Table 21.*

2021/11/22 08:35:53
FNIR(N, R, T) = False neg. identification rate
FPIR(N, T) = False pos. identification rate
N = Num. enrolled subjects
R = Num. candidates examined
T = Threshold
T = 0 → Investigation
T > 0 → Identification

Appendix G Gallery Insertion Timing

This publication is available free of charge from: https://doi.org/10.6028/NIST.IR.8271

This publication is available free of charge from: https://doi.org/10.6028/NIST.IR.8271

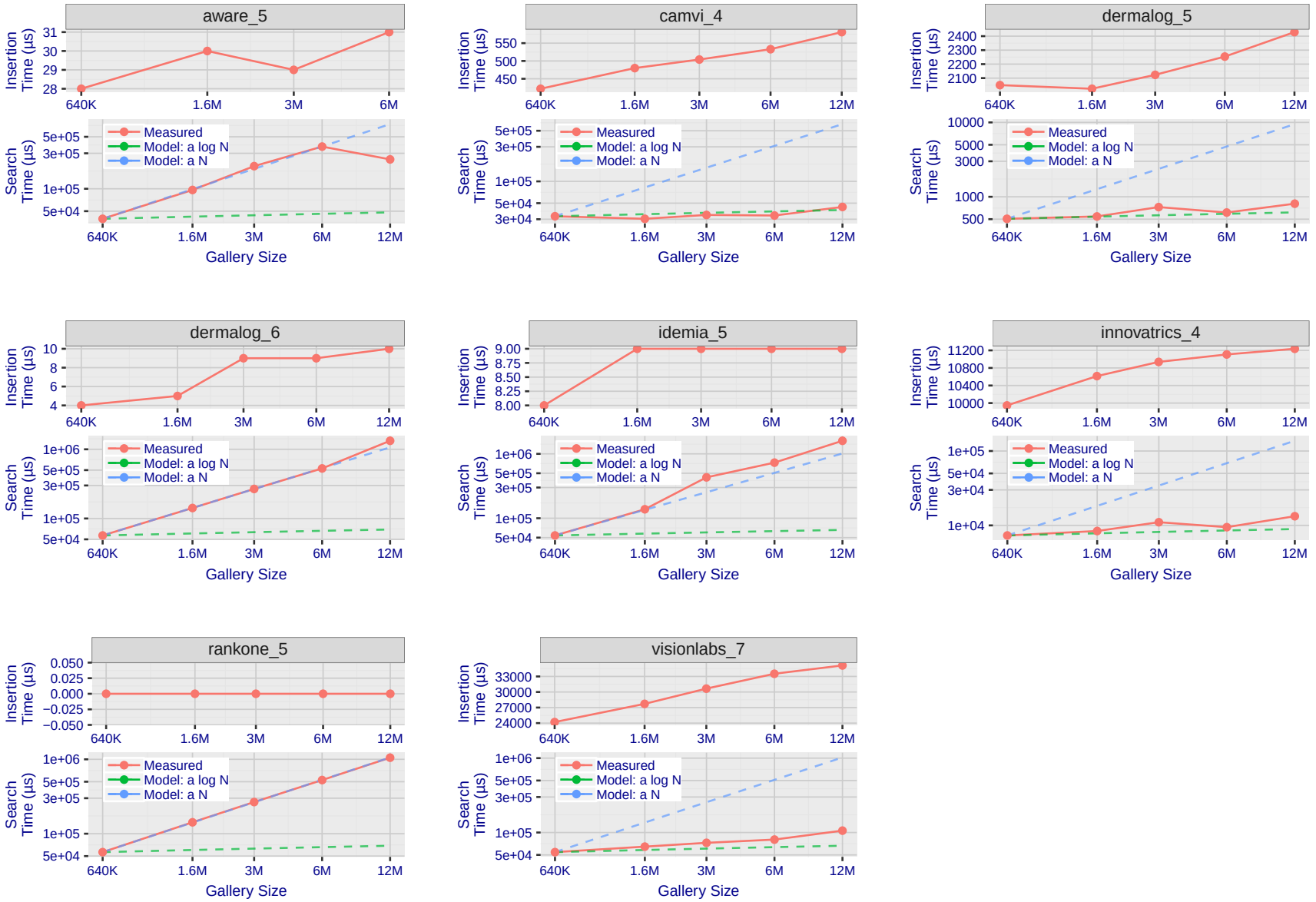

Figure 133: **[Mugshot Dataset] Gallery insertion duration vs. enrolled population size**. *This chart plots the time it takes to insert a single template into a finalized gallery, illustrated over increasing gallery sizes. For reference, search times on finalized galleries of corresponding sizes are plotted right underneath. Gallery insertion time plots were generated on algorithms that 1) successfully implemented gallery insertion with no errors and 2) that were run on galleries with N up to* 12 000 000. *Generally, only the more accurate algorithms were run on galleries with N up to* 12 000 000.

2021/11/22
08:35:53

FNIR(N, R, T) = False neg. identification rate
FPIR(N, T) = False pos. identification rate
N = Num. enrolled subjects
R = Num. candidates examined
T = Threshold
T = 0 → Investigation
T > 0 → Identification

This publication is available free of charge from: https://doi.org/10.6028/NIST.IR.8271

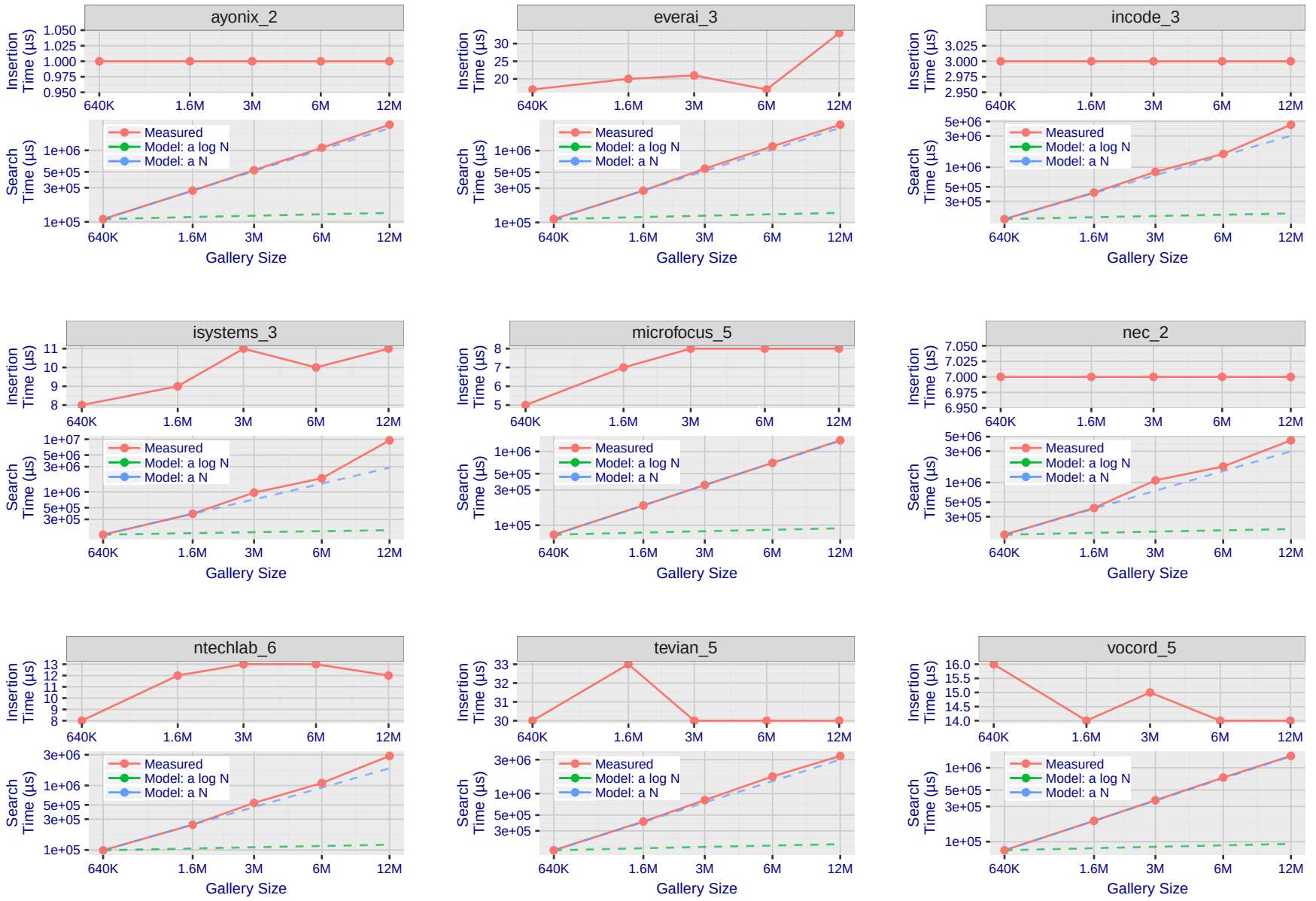

Figure 134: **[Mugshot Dataset] Gallery insertion duration vs. enrolled population size**. *This chart plots the time it takes to insert a single template into a finalized gallery, illustrated over increasing gallery sizes. For reference, search times on finalized galleries of corresponding sizes are plotted right underneath. Gallery insertion time plots were generated on algorithms that 1) successfully implemented gallery insertion with no errors and 2) that were run on galleries with N up to* 12 000 000. *Generally, only the more accurate algorithms were run on galleries with N up to* 12 000 000.

2021/11/22
08:35:53

FNIR(N, R, T) = False neg. identification rate
FPIR(N, T) = False pos. identification rate
N = Num. enrolled subjects
R = Num. candidates examined
T = Threshold
T = 0 → Investigation
T > 0 → Identification

This publication is available free of charge from: https://doi.org/10.6028/NIST.IR.8271

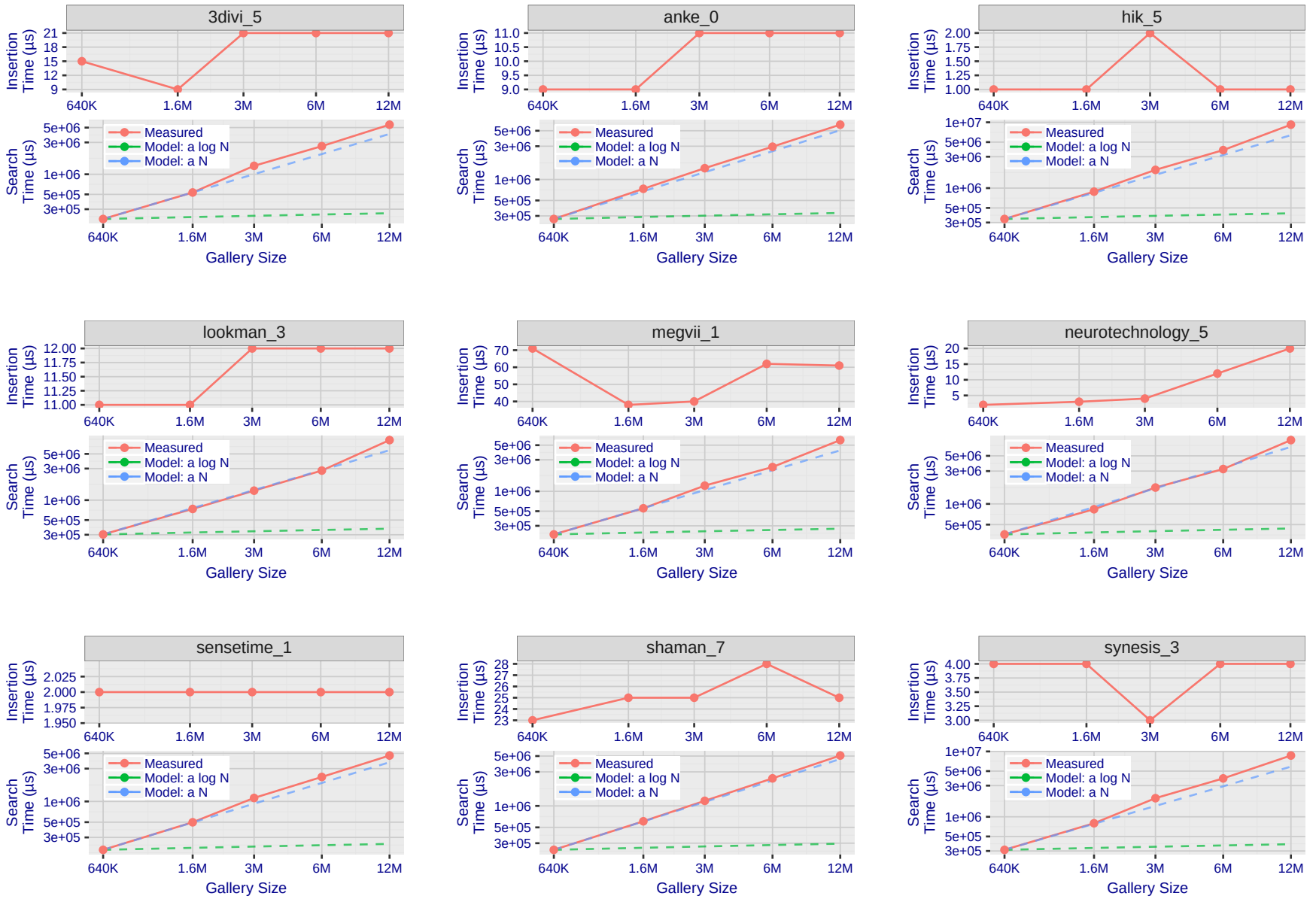

Figure 135: **[Mugshot Dataset] Gallery insertion duration vs. enrolled population size**. *This chart plots the time it takes to insert a single template into a finalized gallery, illustrated over increasing gallery sizes. For reference, search times on finalized galleries of corresponding sizes are plotted right underneath. Gallery insertion time plots were generated on algorithms that 1) successfully implemented gallery insertion with no errors and 2) that were run on galleries with N up to* 12 000 000. *Generally, only the more accurate algorithms were run on galleries with N up to* 12 000 000.

This publication is available free of charge from: https://doi.org/10.6028/NIST.IR.8271

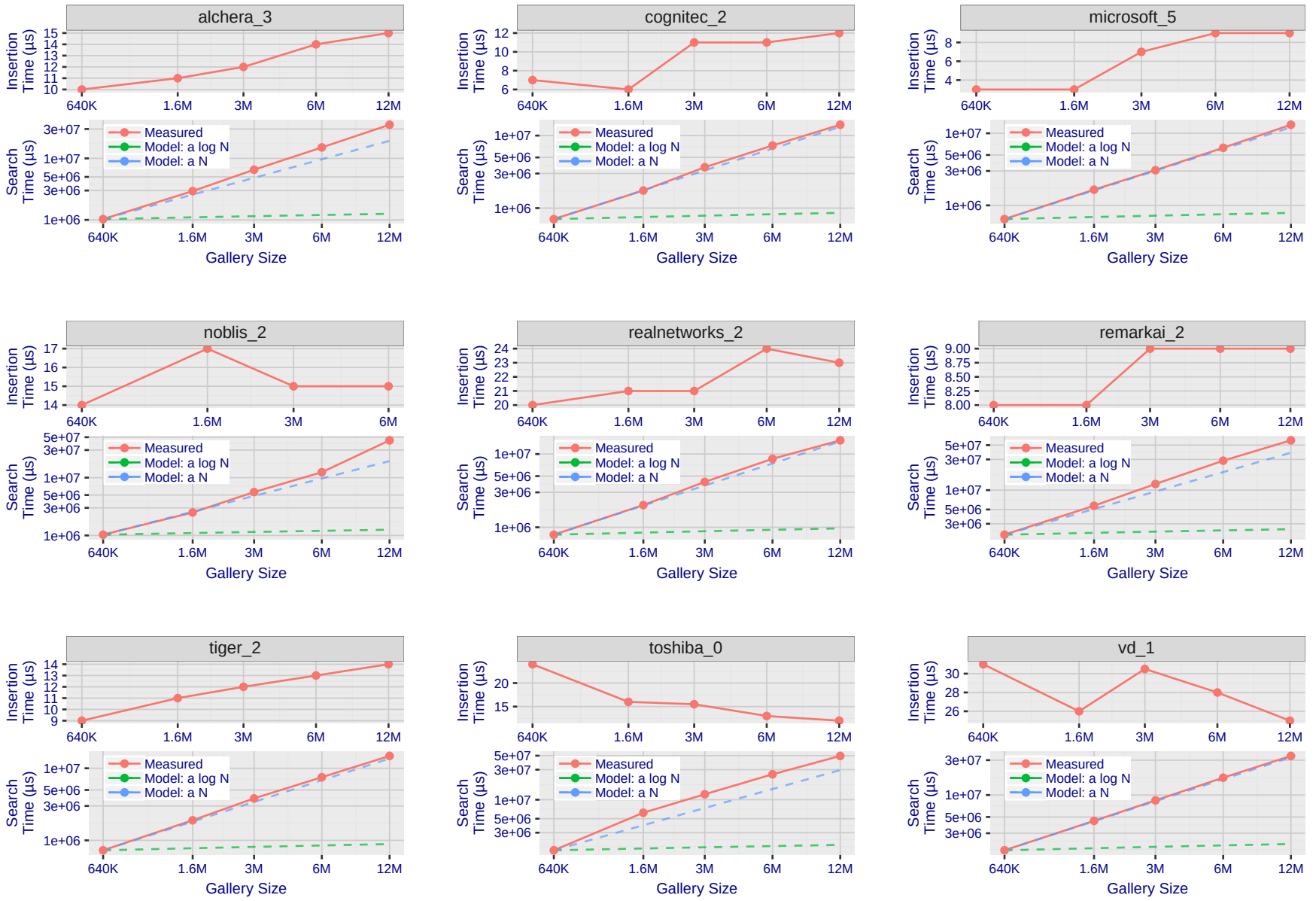

Figure 136: **[Mugshot Dataset] Gallery insertion duration vs. enrolled population size**. *This chart plots the time it takes to insert a single template into a finalized gallery, illustrated over increasing gallery sizes. For reference, search times on finalized galleries of corresponding sizes are plotted right underneath. Gallery insertion time plots were generated on algorithms that 1) successfully implemented gallery insertion with no errors and 2) that were run on galleries with N up to* 12 000 000. *Generally, only the more accurate algorithms were run on galleries with N up to* 12 000 000.

References

[1] Artem Babenko and Victor Lempitsky. Efficient indexing of billion-scale datasets of deep descriptors. In *The IEEE Conference on Computer Vision and Pattern Recognition (CVPR)*, June 2016.

[2] L. Best-Rowden and A. K. Jain. Longitudinal study of automatic face recognition. *IEEE Transactions on Pattern Analysis and Machine Intelligence*, 40(1):148–162, Jan 2018.

[3] Blumstein, Cohen, Roth, and Visher, editors. *Random parameter stochastic models of criminal careers*. National Academy of Sciences Press, 1986.

[4] Thomas P. Bonczar and Lauren E. Glaze. Probation and parole in the united statesm 2007, statistical tables. Technical report, Bureau of Justice Statistics, December 2008.

[5] White D., Kemp R. I., Jenkins R., Matheson M, and Burton A. M. Passport officers' errors in face matching. *PLoS ONE*, 9(8), 2014. e103510. doi:10.1371/journal. pone.0103510.

[6] P. Grother, G. W. Quinn, and P. J. Phillips. Evaluation of 2d still-image face recognition algorithms. NIST Interagency Report 7709, National Institute of Standards and Technology, 8 2010. http://face.nist.gov/mbe as MBE2010 FRVT2010.

[7] P. J. Grother, R. J. Micheals, and P. J. Phillips. Performance metrics for the frvt 2002 evaluation. In *Proceedings of Audio and Video Based Person Authentication Conference (AVBPA)*, June 2003.

[8] Patrick Grother and Mei Ngan. Interagency report 8009, performance of face identification algorithms. *Face Recognition Vendor Test (FRVT)*, May 2014.

[9] Patrick Grother, George Quinn, and Mei Ngan. Face in video evaluation (five) face recognition of non-cooperative subjects. Interagency Report 8173, National Institute of Standards and Technology, March 2017. https://doi.org/10.6028/NIST.IR.8173.

[10] Patrick Grother, George W. Quinn, and Mei Ngan. Face recognition vendor test - still face image and video concept, evaluation plan and api. Technical report, National Institute of Standards and Technology, 7 2013. http://biometrics.nist.gov/cs_links/face/frvt/frvt2012/NIST_FRVT2012_api_Aug15.pdf.

[11] K. He, X. Zhang, S. Ren, and J. Sun. Deep residual learning for image recognition. In *2016 IEEE Conference on Computer Vision and Pattern Recognition (CVPR)*, pages 770–778, June 2016.

[12] Gary B. Huang, Manu Ramesh, Tamara Berg, and Erik Learned-Miller. Labeled faces in the wild: A database for studying face recognition in unconstrained environments. Technical Report 07-49, University of Massachusetts, Amherst, October 2007.

[13] Masato Ishii, Hitoshi Imaoka, and Atsushi Sato. Fast k-nearest neighbor search for face identification using bounds of residual score. In *2017 12th IEEE International Conference on Automatic Face & Gesture Recognition (FG 2017)*, pages 194–199, Los Alamitos, CA, USA, May 2017. IEEE Computer Society.

[14] Jeff Johnson, Matthijs Douze, and Hervé Jégou. Billion-scale similarity search with gpus. *CoRR*, abs/1702.08734, 2017.

This publication is available free of charge from: https://doi.org/10.6028/NIST.IR.8271

[15] Ira Kemelmacher-Shlizerman, Steven M. Seitz, Daniel Miller, and Evan Brossard. The megaface benchmark: 1 million faces for recognition at scale. *CoRR*, abs/1512.00596, 2015.

[16] Yury A. Malkov and D. A. Yashunin. Efficient and robust approximate nearest neighbor search using hierarchical navigable small world graphs. *CoRR*, abs/1603.09320, 2016.

[17] Joyce A. Martin, Brady E. Hamilton, Michelle J.K. Osterman, Anne K. Driscoll, , and Patrick Drake. National vital statistics reports. Technical Report 8, Centers for Disease Control and Prevention, National Center for Health Statistics, National Vital Statistics System, Division of Vital Statistics, November 2018.

[18] O. M. Parkhi, A. Vedaldi, and A. Zisserman. Deep face recognition. In *British Machine Vision Conference*, 2015.

[19] P. Jonathon Phillips, Amy N. Yates, Ying Hu, Carina A. Hahn, Eilidh Noyes, Kelsey Jackson, Jacqueline G. Cavazos, Géraldine Jeckeln, Rajeev Ranjan, Swami Sankaranarayanan, Jun-Cheng Chen, Carlos D. Castillo, Rama Chellappa, David White, and Alice J. O'Toole. Face recognition accuracy of forensic examiners, superrecognizers, and face recognition algorithms. *Proceedings of the National Academy of Sciences*, 115(24):6171–6176, 2018.

[20] Florian Schroff, Dmitry Kalenichenko, and James Philbin. Facenet: A unified embedding for face recognition and clustering. *CoRR*, abs/1503.03832, 2015.

[21] Jeroen Smits and Christiaan Monden. Twinning across the developing world. *PLOS ONE*, 6(9):1–5, 09 2011.

[22] Yaniv Taigman, Ming Yang, Marc'Aurelio Ranzato, and Lior Wolf. Deepface: Closing the gap to human-level performance in face verification. In *Proceedings of the 2014 IEEE Conference on Computer Vision and Pattern Recognition*, CVPR '14, pages 1701–1708, Washington, DC, USA, 2014. IEEE Computer Society.

[23] A. Towler, R. I. Kemp, and D White. *Unfamiliar face matching systems in applied settings*. Nova Science, 2017.

[24] Working Group 3. Ed. M. Werner. *ISO/IEC 19794-5 Information Technology - Biometric Data Interchange Formats - Part 5: Face image data*. JTC1 :: SC37, 2 edition, 2011. http://webstore.ansi.org.

[25] David White, James D. Dunn, Alexandra C. Schmid, and Richard I. Kemp. Error rates in users of automatic face recognition software. *PLoS ONE*, 10:1–14, October 2015.

[26] Bradford Wing and R. Michael McCabe. Special publication 500-271: American national standard for information systems data format for the interchange of fingerprint, facial, and other biometric information part 1. Technical report, NIST, September 2015. ANSI/NIST ITL 1-2015.

[27] Andreas Wolf. Portrait quality - (reference facial images for mrtd). Technical report, ICAO, April 2018.

[28] D. Yadav, N. Kohli, P. Pandey, R. Singh, M. Vatsa, and A. Noore. Effect of illicit drug abuse on face recognition. In *2016 IEEE Winter Conference on Applications of Computer Vision (WACV)*, pages 1–7, Los Alamitos, CA, USA, mar 2016. IEEE Computer Society.

This publication is available free of charge from: https://doi.org/10.6028/NIST.IR.8271